

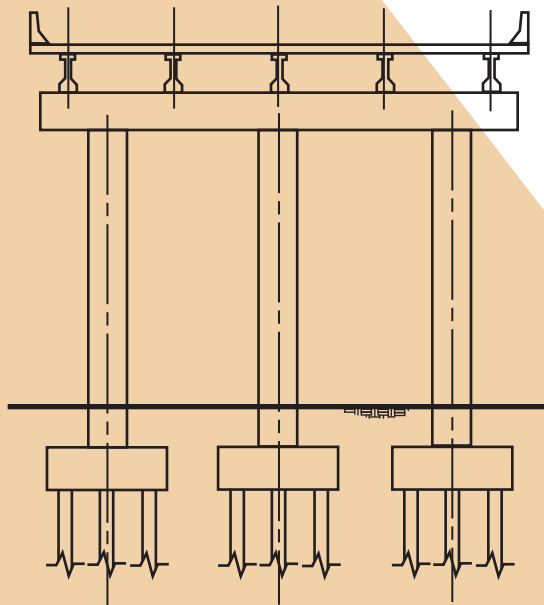
## **ATC/MCEER Joint Venture**

A Partnership of:  
Applied Technology Council and  
Multidisciplinary Center for Earthquake Engineering Research



# **Recommended LRFD guidelines for the seismic design of highway bridges**

## **Part II: Commentary and Appendices**



## **Applied Technology Council**

The Applied Technology Council (ATC) is a nonprofit, tax-exempt corporation established in 1971 through the efforts of the Structural Engineers Association of California. ATC's mission is to develop state-of-the-art, user-friendly engineering resources and applications for use in mitigating the effects of natural and other hazards on the built environment. ATC also identifies and encourages needed research and develops consensus opinions on structural engineering issues in a non-proprietary format. ATC thereby fulfills a unique role in funded information transfer.

ATC is guided by a Board of Directors consisting of representatives appointed by the American Society of Civil Engineers, the National Council of Structural Engineers Associations, the Structural Engineers Association of California, the Western Council of Structural Engineers Associations, and four at-large representatives concerned with the practice of structural engineering. Each director serves a three-year term.

Project management and administration are carried out by a full-time Executive Director and support staff. Project work is conducted by a wide range of highly qualified consulting professionals, thus incorporating the experience of many individuals from academia, research, and professional practice who would not be available from any single organization. Funding for ATC projects is obtained from government agencies and from the private sector in the form of tax-deductible contributions.

## **Multidisciplinary Center for Earthquake Engineering Research**

The Multidisciplinary Center for Earthquake Engineering Research (MCEER) is a national center of excellence in advanced technology applications that is dedicated to the reduction of earthquake losses nationwide. Headquartered at the University at Buffalo, State University of New York, the Center was originally established by the National Science Foundation (NSF) in 1986, as the National Center for Earthquake Engineering Research (NCEER).

Comprising a consortium of researchers from numerous disciplines and institutions throughout the United States, the Center's mission is to reduce earthquake losses through research and the application of advanced technologies that improve engineering, pre-earthquake planning and post-earthquake recovery strategies. Toward this end, the Center coordinates a nationwide program of multidisciplinary team research, education and outreach activities.

Funded principally by NSF, the State of New York and the Federal Highway Administration (FHWA), the Center derives additional support from the Federal Emergency Management Agency (FEMA), other state governments, academic institutions, foreign governments and private industry.

## **ATC/MCEER Joint Venture**

The ATC/MCEER Joint Venture, a partnership of the Applied Technology Council (ATC) and the Multidisciplinary Center for Earthquake Engineering Research (MCEER), was established to conduct the NCHRP 12-49 project, Development of Comprehensive Specifications for the Seismic Design of Bridges, which was funded by the Transportation Research Board of the National Research Council.

### **ATC/MCEER Joint Venture Management Committee**

Christopher Rojahn (ATC representative), Chair and Authorized Representative  
Michel Bruneau (MCEER representative)  
Ian Buckle (MCEER representative)  
Ian Friedland (ATC representative)

## **Notice**

This report was prepared by the Applied Technology Council (ATC) and the Multidisciplinary Center for Earthquake Engineering Research (MCEER) through a contract from the Federal Highway Administration and other sponsors. Neither ATC, MCEER, their associates, sponsors, nor any person acting on their behalf:

- a. makes any warranty, express or implied, with respect to the use of any information, apparatus, method, or process disclosed in this report or that such use may not infringe upon privately owned rights; or
- b. assumes any liabilities of whatsoever kind with respect to the use of, or the damage resulting from the use of, any information, apparatus, method, or process disclosed in this report.

Any opinions, findings, and conclusions or recommendations expressed in this publication are those of the author(s) and do not necessarily reflect the views of ATC, MCEER, Federal Highway Administration or other sponsors. The material presented in this publication should not be used or relied upon for any specific application without competent examination and verification of its accuracy, suitability, and applicability by qualified professionals.

**MCEER/ATC-49**

**Recommended LRFD Guidelines**  
**for the Seismic Design of Highway Bridges**  
**Part II: Commentary and Appendices**

Based on  
NCHRP Project 12-49, FY '98  
“Comprehensive Specification for the Seismic Design of Bridges”  
National Cooperative Highway Research Program

Prepared by  
ATC/MCEER JOINT VENTURE  
A partnership of the  
Applied Technology Council  
([www.ATCouncil.org](http://www.ATCouncil.org))  
and the  
Multidisciplinary Center for Earthquake Engineering Research  
(<http://mceer.buffalo.edu>)

Prepared under the MCEER Highway Project  
Project 094, Task F3-1  
Federal Highway Administration

NCHRP 12-49 PROJECT PARTICIPANTS

*Project Team*

Ian Friedland, Principal Investigator  
Ronald Mayes, Technical Director  
Donald Anderson  
Michel Bruneau  
Gregory Fenves  
John Kulicki  
John Mander  
Lee Marsh  
Geoffrey Martin  
Andrzej Nowak  
Richard Nutt  
Maurice Power  
Andrei Reinhorn

*Project Engineering Panel*

Ian Buckle, Co-Chair  
Christopher Rojahn, Co-Chair  
Serafim Arzoumanidis  
Mark Capron  
Ignatius Po Lam  
Paul Liles  
Brian Maroney  
Joseph Nicoletti  
Charles Roeder  
Frieder Seible  
Theodore Zoli





## PREFACE

In 2003 the ATC/MCEER Joint Venture, a partnership of the Applied Technology Council (ATC) and the Multidisciplinary Center for Earthquake Engineering Research (MCEER), University at Buffalo, published the document, *Recommended LRFD Guidelines for the Seismic Design of Highway Bridges, Part I, Specifications*. As part of the developmental effort for *Part I, Specifications*, the ATC/MCEER Joint Venture also developed this companion document, *Part II, Commentary and Appendices*, which describes the technical basis, optional approaches, and related background information pertaining to the *Specifications*. *Part I* and *Part II* (also known as the MCEER/ATC-49 Report) are reformatted versions of the seismic design provisions (specifications and commentary) for highway bridges developed under NCHRP (National Cooperative Highway Research Program) Project 12-49, a recently completed project to develop seismic design provisions that would be compatible with the American Association of State Highway and Transportation Officials (AASHTO) *LRFD Bridge Design Specifications*. The reformatting effort, which was carried out to facilitate immediate use of the Project 12-49 provisions by bridge design professionals, was funded as a task under the Federal Highway Administration (FHWA) sponsored MCEER Highway Project.

NCHRP Project 12-49 also included companion studies to investigate the effects of liquefaction and an effort to develop design examples using the NCHRP 12-49 provisions. These studies are documented in two companion MCEER/ATC reports: (1) the MCEER/ATC-49-1 Report, *Liquefaction Study Report, Recommended LRFD Guidelines for the Seismic Design of Highway Bridges* (ATC/MCEER, 2003a), and (2) the MCEER/ATC-49-2 Report, *Design Examples, Recommended LRFD Guidelines for the Seismic Design of Highway Bridges* (ATC/MCEER, 2003b).

A broad array of engineering expertise was engaged by the ATC/MCEER Joint Venture to develop the original NCHRP 12-49 seismic design provisions, companion liquefaction study, and design examples. Ian Friedland of ATC

(and formerly MCEER) served as the Project Principal Investigator and Ronald Mayes (Simpson Gumpertz & Heger, Inc.) served as the Project Technical Director. The NCHRP Project 12-49 team consisted of Donald Anderson (CH2M Hill, Inc.), Michel Bruneau (University at Buffalo), Gregory Fenves (University of California at Berkeley), John Kulicki (Modjeski and Masters, Inc.), John Mander (University of Canterbury, formerly University at Buffalo), Lee Marsh (BERGER/ABAM Engineers), Ronald Mayes (Simpson, Gumpertz & Heger, Inc.), Geoffrey Martin (University of Southern California), Andrzej Nowak (University of Michigan), Richard Nutt (bridge consultant), Maurice Power (Geomatrix Consultants, Inc.), and Andrei Reinhorn (University at Buffalo).

The project also included an advisory Project Engineering Panel; Ian Buckle, of the University of Nevada at Reno, co-chaired this committee with Christopher Rojahn of ATC, who also served as the Project Administrative Officer. Other members included Serafim Arzoumanidis (Steinman Engineers), Mark Capron (Sverdrup Civil Inc.), Ignatius Po Lam (Earth Mechanics), Paul Liles (Georgia DOT), Brian Maroney (California DOT), Joseph Nicoletti (URS Greiner Woodward Clyde), Charles Roeder (University of Washington), Frieder Seible (University of California at San Diego), and Theodore Zoli (HNTB Corporation).

NCHRP Project Panel C12-49, under the direction of NCHRP Senior Program Officer David Beal and chaired by Harry Capers of the New Jersey Department of Transportation (DOT), also provided a significant amount of input and guidance during the conduct of the project. The other members of the NCHRP Project Panel were D.W. Dearasaugh (Transportation Research Board), Gongkang Fu (Wayne State University), C. Stewart Gloyd (Parsons Brinckerhoff), Manoucher Karshenas (Illinois DOT), Richard Land (California DOT), Bryan Millar (Montana DOT), Amir Mirmirman (University of Central Florida), Charles Ruth (Washington State DOT), Steven Starkey (Oregon DOT), and Phillip Yen (FHWA).

Three drafts of the Project 12-49 specifications and commentary were prepared and reviewed by the ATC Project Engineering Panel, NCHRP Project Panel 12-49, and the AASHTO Highway Subcom-

mittee on Bridges and Structures seismic design technical committee (T-3), which was chaired by James Roberts of Caltrans.

A subset of the original NCHRP Project 12-49 team, consisting of Donald Anderson, Michel Bruneau, Ronald Mayes, Lee Marsh, Richard Nutt, and Maurice Power, prepared Parts I and II of the *Recommended LRFD Guidelines for the*

*Seismic Design of Highway Bridges* (MCEER/ATC-49 Report). ATC and MCEER staff provided editorial and desktop publishing services during the preparation of *Part II, Commentary and Appendices*.

Michel Bruneau, MCEER  
Christopher Rojahn, ATC

# TABLE OF CONTENTS

<b>PREFACE</b> .....	<b>iii</b>
<b>C1 INTRODUCTION</b> .....	<b>1</b>
<b>C2 DEFINITIONS AND NOTATIONS</b> .....	<b>3</b>
C2.1    DEFINITIONS .....	3
C2.2    NOTATIONS .....	4
<b>C3 GENERAL REQUIREMENTS</b> .....	<b>9</b>
C3.1    APPLICABILITY .....	9
C3.2    SEISMIC PERFORMANCE OBJECTIVES.....	9
C3.3    SEISMIC DESIGN APPROACH.....	12
C3.3.1    Earthquake-Resisting Systems (ERS).....	17
C3.4    DESIGN GROUND MOTION.....	21
C3.4.1    Design Spectra Based on General Procedure.....	22
C3.4.2    Site Effects on Ground Motion .....	23
C3.4.2.1    Site Class Definitions .....	23
C3.4.2.2    Definitions of Site Class Parameters .....	24
C3.4.2.3    Site Coefficients .....	25
C3.4.3    Response Spectra Based on Site-Specific Procedure.....	25
C3.4.4    Acceleration Time Histories .....	25
C3.4.5    Vertical Acceleration Effects.....	27
C3.5    LOAD FACTORS .....	27
C3.6    COMBINATION OF SEISMIC FORCE EFFECTS.....	28
C3.6.1    SRSS Combination Rule.....	28
C3.6.2    100% - 40% Combination Rule .....	28
C3.7    SELECTION OF SEISMIC HAZARD LEVEL (SHL), SEISMIC DESIGN AND ANALYSIS PROCEDURES (SDAP) AND SEISMIC DESIGN REQUIREMENTS (SDR).....	29
C3.8    TEMPORARY AND STAGED CONSTRUCTION.....	29
<b>C4 DESIGN AND ANALYSIS PROCEDURES (SDAP)</b> .....	<b>31</b>
C4.1    SINGLE SPAN BRIDGES .....	31
C4.2    SDAP A1 AND A2.....	31
C4.3    SDAP B – NO SEISMIC DEMAND ANALYSIS.....	32
C4.3.1    No Analysis Approach.....	32
C4.3.2    Limitations.....	32
C4.3.3    Capacity Design and Strength Requirements of Members Framing into Columns .....	33
C4.4    SDAP C – CAPACITY SPECTRUM DESIGN METHOD.....	33
C4.4.1    Capacity Spectrum Design Approach.....	33
C4.4.2    Limitations.....	35
C4.5    SDAP D – ELASTIC RESPONSE SPECTRUM METHOD.....	35
C4.6    SDAP E – ELASTIC RESPONSE SPECTRUM METHOD WITH DISPLACEMENT CAPACITY VERIFICATION .....	35
C4.7    RESPONSE MODIFICATION FACTORS .....	35
C4.8    CAPACITY DESIGN.....	36
C4.8.1    Inelastic Hinging Forces .....	37
C4.9    PLASTIC HINGE ZONES .....	37
C4.10   ELASTIC DESIGN OF SUBSTRUCTURES .....	37
C4.10.1    All Substructure Supports are Designed Elastically .....	37
C4.10.2    Selected Substructure Supports are Designed Elastically .....	37

<b>C5 ANALYSIS REQUIREMENTS .....</b>	<b>39</b>
C5.1 DEFINITION OF PROCEDURES .....	39
C5.1.1 General .....	39
C5.1.2 Selection of Analysis Procedure.....	39
C5.2 SEISMIC LATERAL LOAD DISTRIBUTION .....	40
C5.2.1 Applicability .....	40
C5.2.2 Design Criteria .....	41
C5.2.3 Load Distribution .....	41
C5.3 MODELING REQUIREMENTS .....	41
C5.3.1 General .....	41
C5.3.2 Distribution of Mass .....	42
C5.3.3 Stiffness and Strength.....	42
C5.3.3.1 General .....	42
C5.3.3.2 Substructure .....	42
C5.3.3.3 Superstructure .....	43
C5.3.4 Foundations .....	43
C5.3.5 Abutments .....	43
C5.3.6 Seismic Isolator Units .....	44
C5.3.7 Bearings and Joints.....	44
C5.3.8 Damping .....	44
C5.4 ANALYSIS PROCEDURES .....	44
C5.4.1 Capacity Spectrum Analysis .....	44
C5.4.1.1 Seismic Isolation Systems.....	44
C5.4.2 Elastic Response Spectrum Analysis .....	46
C5.4.2.1 Selection of Analysis Method .....	46
C5.4.2.2 Uniform Load Method .....	46
C5.4.2.3 Multi-Mode Dynamic Analysis Method .....	47
C5.4.3 Seismic Displacement Capacity Verification.....	48
C5.4.4 Nonlinear Dynamic Analysis Procedure .....	48
<b>C6 SEISMIC DESIGN REQUIREMENTS (SDR) 1 AND 2 .....</b>	<b>49</b>
C6.1 GENERAL .....	49
C6.2 DESIGN FORCES .....	49
C6.3 DESIGN DISPLACEMENTS .....	49
C6.4 FOUNDATION DESIGN REQUIREMENTS .....	50
C6.5 ABUTMENT DESIGN REQUIREMENTS .....	50
C6.6 LIQUEFACTION DESIGN REQUIREMENTS .....	50
C6.7 STRUCTURAL STEEL DESIGN REQUIREMENTS .....	50
C6.7.1 SDR 1 .....	50
C6.7.2 SDR 2 .....	50
C6.7.2.1 Ductile Moment-Resisting Frames and Bents.....	50
C6.7.2.1.1 Columns.....	50
C6.7.2.3 Concentrically Braced Frames and Bents with Nominal Ductility .....	50
<b>C7 SEISMIC DESIGN REQUIREMENTS (SDR) 3.....</b>	<b>51</b>
C7.1 GENERAL .....	51
C7.2 DESIGN FORCES .....	51
C7.2.1 Ductile Substructures ( $R > 1$ ) – Flexural Capacity .....	51
C7.2.2 Capacity Protected Elements or Actions .....	51
C7.2.3 Elastically Designed Elements .....	51
C7.2.4 Abutments and Connections.....	51
C7.2.5 Single Span Bridges .....	52

C7.3	DESIGN DISPLACEMENTS .....	52
C7.4	FOUNDATION DESIGN REQUIREMENTS.....	52
C7.4.1	Foundation Investigation .....	52
C7.4.2	Spread Footings .....	52
C7.4.2.1	Moment and Shear Capacity.....	53
C7.4.2.2	Liquefaction Check.....	53
C7.4.3	Driven Piles .....	53
C7.4.3.1	General .....	53
C7.4.3.2	Design Requirements .....	54
C7.4.3.3	Moment and Shear Design .....	54
C7.4.3.4	Liquefaction Check.....	54
C7.4.4	Drilled Shafts .....	55
C7.5	ABUTMENT DESIGN REQUIREMENTS.....	55
C7.5.1	General.....	55
C7.5.2	Longitudinal Direction.....	56
C7.5.3	Transverse Direction.....	56
C7.6	LIQUEFACTION DESIGN REQUIREMENTS.....	56
C7.6.1	General.....	56
C7.6.2	Evaluation of Liquefaction Potential .....	56
C7.6.3	Evaluation of the Effects of Liquefaction and Lateral Ground Movement .....	56
C7.6.4	Design Requirements if Liquefaction and Ground Movement Occurs.....	56
C7.6.5	Detailed Foundation Design Requirements .....	57
C7.6.6	Other Collateral Hazards .....	57
C7.7	STRUCTURAL STEEL DESIGN REQUIREMENTS.....	57
C7.8	REINFORCED CONCRETE DESIGN REQUIREMENTS.....	57
C7.9	BEARING DESIGN REQUIREMENTS .....	57
C7.9.1	Prototype and Quality Control Tests.....	57
C7.10	SEISMIC ISOLATION DESIGN REQUIREMENTS .....	57
<b>C8</b>	<b>SEISMIC DESIGN REQUIREMENTS (SDR) 4, 5 AND 6.....</b>	<b>59</b>
C8.1	GENERAL.....	59
C8.2	DESIGN FORCES.....	59
C8.2.1	Ductile Substructures ( $R > 1$ ) – Flexural Capacity .....	59
C8.2.2	Capacity Protected Elements or Actions.....	59
C8.2.3	Elastically Designed Elements.....	59
C8.2.4	Abutments and Connections .....	59
C8.2.5	Single Span Bridges.....	60
C8.3	DESIGN DISPLACEMENTS .....	60
C8.3.1	General.....	60
C8.3.2	Minimum Seat Width Requirement.....	60
C8.3.3	Displacement Compatibility .....	61
C8.3.4	P- $\Delta$ Requirements .....	61
C8.3.5	Minimum Displacement Requirements for Lateral-Load-Resisting Piers and Bents .....	62
C8.4	FOUNDATION DESIGN REQUIREMENTS.....	62
C8.4.1	Foundation Investigation .....	62
C8.4.1.1	General .....	62
C8.4.1.2	Subsurface Investigations .....	62
C8.4.1.3	Laboratory Testing .....	62
C8.4.2	Spread Footings .....	62
C8.4.2.1	Spring Constants for Footings .....	63

	C8.4.2.2	Moment-Rotation and Shear-Displacement Relationships for Footing .....	64
C8.4.3	Driven Piles .....		66
	C8.4.3.1	General .....	66
	C8.4.3.2	Design Requirements .....	66
	C8.4.3.3	Axial and Rocking Stiffness for Driven Pile/Pile Cap Foundations ....	67
	C8.4.3.4	Lateral Stiffness Parameters for Driven Pile/Pile Cap Foundations ....	68
	C8.4.3.5	Pile Cap Stiffness and Capacity .....	69
	C8.4.3.6	Moment and Shear Design .....	69
	C8.4.3.7	Liquefaction and Dynamic Settlement Evaluations .....	70
C8.4.4	Drilled Shafts.....		71
C8.5	ABUTMENT DESIGN REQUIREMENTS .....		72
	C8.5.1	General .....	72
	C8.5.2	Longitudinal Direction .....	72
		C8.5.2.1 SDAP C.....	73
		C8.5.2.2 SDAP D and E .....	73
	C8.5.3	Transverse Direction .....	73
		C8.5.3.1 SDAP C.....	73
		C8.5.3.2 SDAP D and E .....	73
C8.6	LIQUEFACTION DESIGN REQUIREMENTS .....		74
	C8.6.1	General .....	74
	C8.6.2	Evaluation of Liquefaction Potential.....	74
	C8.6.3	Evaluation of the Effects of Liquefaction and Lateral Ground Movement.....	75
	C8.6.4	Design Requirements if Liquefaction and Ground Movement Occur.....	76
	C8.6.5	Detailed Foundation Design Requirements.....	76
	C8.6.6	Other Collateral Hazards .....	76
C8.7	STRUCTURAL STEEL DESIGN REQUIREMENTS .....		76
	C8.7.1	General .....	76
	C8.7.2	Materials.....	77
	C8.7.3	Sway Stability Effects .....	78
	C8.7.4	Ductile Moment-Resisting Frames and Single Column Structures.....	78
		C8.7.4.1 Columns .....	79
		C8.7.4.2 Beams.....	79
		C8.7.4.3 Panel Zones and Connections .....	79
		C8.7.4.4 Multi-Tier Frame Bents.....	79
	C8.7.5	Ductile Concentrically Braced Frames.....	80
		C8.7.5.1 Bracing Systems.....	80
		C8.7.5.2 Design Requirements for Ductile Bracing Members .....	80
		C8.7.5.3 Brace Connections .....	81
		C8.7.5.4 Columns, Beams and Other Connections.....	81
	C8.7.6	Concentrically Braced Frames with Nominal Ductility .....	81
		C8.7.6.1 Bracing Systems.....	82
		C8.7.6.2 Design Requirements for Nominally Ductile Bracing Members .....	82
		C8.7.6.3 Brace Connections .....	82
		C8.7.6.4 Columns, Beams and Other Connections.....	82
		C8.7.6.5 Chevron Braced and V-Braced Systems .....	82
	C8.7.7	Concrete Filled Steel Pipes.....	83
		C8.7.7.1 Combined Axial Compression and Flexure .....	83
		C8.7.7.2 Flexural Strength.....	83
		C8.7.7.3 Beams and Connections .....	84
	C8.7.8	Other Systems .....	84

	C8.7.8.1	Ductile Eccentrically Braced Frames .....	84
	C8.7.8.2	Ductile End-Diaphragm in Slab-on-Girder Bridge.....	85
	C8.7.8.3	Ductile End Diaphragms in Deck Truss Bridges.....	85
	C8.7.8.4	Other Systems.....	86
	C8.7.9	Plastic Rotational Capacities .....	86
	C8.7.9.1	Life Safety Performance .....	86
	C8.7.9.2	Immediate Use Limit State .....	86
	C8.7.9.3	In-Ground Hinges .....	86
C8.8		REINFORCED CONCRETE DESIGN REQUIREMENTS .....	86
	C8.8.1	General.....	86
	C8.8.2	Column Requirements .....	87
	C8.8.2.1	Longitudinal Reinforcement.....	87
	C8.8.2.2	Flexural Resistance.....	87
	C8.8.2.3	Column Shear and Transverse Reinforcement .....	87
	C8.8.2.4	Transverse Reinforcement for Confinement at Plastic Hinges.....	88
	C8.8.2.5	Transverse Reinforcement for Longitudinal Bar Restraint in Plastic Hinges .....	89
	C8.8.2.6	Spacing for Transverse Reinforcement for Confinement and Longitudinal Bar Restraint .....	90
	C8.8.2.7	Splices.....	90
	C8.8.2.8	Flexural Overstrength.....	90
	C8.8.3	Limited Ductility Requirements for Wall-Type Piers .....	91
	C8.8.4	Moment-Resisting Connection Between Members (Column-Beam and Column-Footing Joints).....	91
	C8.8.4.1	Implicit Approach: Direct Design .....	91
	C8.8.4.2	Explicit Approach: Detailed Design.....	91
		C8.8.4.2.1 Design Forces and Applied Stresses .....	91
		C8.8.4.2.2 Maximum Required Horizontal Reinforcement.....	92
		C8.8.4.2.3 Maximum Allowable Compression Stresses .....	92
	C8.8.4.3	Reinforcement for Joint Force Transfer .....	92
		C8.8.4.3.1 Acceptable Reinforcement Details.....	92
		C8.8.4.3.2 Vertical Reinforcement.....	93
		C8.8.4.3.3 Horizontal Reinforcement.....	93
		C8.8.4.3.4 Hoop or Spiral Reinforcement .....	94
	C8.8.4.4	Structural Strength of Footings.....	94
	C8.8.5	Concrete Piles .....	94
	C8.8.5.1	Transverse Reinforcement Requirements.....	94
	C8.8.6	Plastic Rotation Capacities .....	95
	C8.8.6.1	Life Safety Performance.....	95
	C8.8.6.2	Operational Performance.....	95
	C8.8.6.3	In-Ground Hinges .....	95
C8.9		BEARING DESIGN REQUIREMENTS .....	95
	C8.9.1	Prototype and Quality Control Tests.....	95
C8.10		SEISMIC ISOLATION DESIGN REQUIREMENTS .....	96
C8.11		SUPERSTRUCTURE DESIGN REQUIREMENTS .....	96
	C8.11.1	General.....	96
	C8.11.2	Load Paths .....	96
	C8.11.3	Effective Superstructure Width .....	96
	C8.11.4	Superstructure-To-Substructure Connections.....	97
<b>C15</b>		<b>SEISMIC ISOLATION .....</b>	<b>99</b>

C15.1	SCOPE .....	99
C15.2	DEFINITIONS .....	101
C15.3	NOTATION .....	101
C15.4	ANALYSIS PROCEDURES .....	101
C15.4.1	Capacity Spectrum Method .....	102
C15.4.2	Uniform Load Method .....	104
C15.4.3	Multimode Spectral Method .....	104
C15.4.4	Time-History Method .....	104
C15.5	DESIGN PROPERTIES OF THE ISOLATION SYSTEM .....	105
C15.5.1	Nominal Design Properties .....	105
C15.5.2	System Property Modification Factors .....	105
C15.5.2.1	Minimum and Maximum System Property Modification Factors .....	105
C15.5.2.2	System Property Adjustment Factors .....	105
C15.6	CLEARANCES .....	105
C15.7	DESIGN FORCES FOR SDAP A1 AND A2 .....	105
C15.8	DESIGN FORCES FOR SDAP C, D, AND E .....	105
C15.9	OTHER REQUIREMENTS .....	105
C15.9.1	Non-Seismic Lateral Forces .....	105
C15.9.1.1	Service Force Resistance .....	105
C15.9.1.2	Cold Weather Requirements .....	105
C15.9.2	Lateral Restoring Force .....	106
C15.9.3	Vertical Load Stability .....	106
C15.9.4	Rotational Capacity .....	106
C15.10	REQUIRED TESTS OF ISOLATION SYSTEMS .....	106
C15.10.1	System Characterization Tests .....	107
C15.10.1.1	Low-Temperature Test .....	107
C15.10.1.2	Wear and Fatigue Tests .....	107
C15.10.2	Prototype Tests .....	107
C15.10.3	Determination of System Characteristics .....	107
C15.10.3.1	System Adequacy .....	107
C15.11	ELASTOMERIC BEARINGS .....	108
C15.11.1	General .....	109
C15.11.2	Shear Strain Components for Isolation Design .....	109
C15.11.3	Load Combinations .....	109
C15.12	ELASTOMERIC BEARINGS-CONSTRUCTION .....	109
C15.13	SLIDING BEARINGS – DESIGN .....	109
C15.13.1	General .....	109
C15.13.2	Materials .....	109
C15.13.2.1	PTFE Bearing Liners .....	110
C15.13.2.2	Other Bearing Liner Materials .....	110
C15.13.2.3	Mating Surface .....	110
C15.13.3	Geometry .....	110
C15.13.4	Loads and Stresses .....	110
C15.13.4.1	Contact Pressure .....	110
C15.13.4.2	Coefficient of Friction .....	110
C15.13.4.2.1	Service Coefficient of Friction .....	110
C15.13.4.2.2	Seismic Coefficient of Friction .....	110
C15.13.5	Other Details .....	110
C15.13.6	Materials for Guides .....	110
C15.14	SLIDING BEARINGS – CONSTRUCTION .....	110
C15.15	OTHER ISOLATION SYSTEMS .....	110



C15.15.1	Scope.....	110
C15.15.2	System Characterization Tests.....	110
C15.15.3	Design Procedure.....	110
C15.15.4	Fabrication, Installation, Inspection, and Maintenance Requirements.....	110
C15.15.5	Prototype Tests.....	111
C15.15.6	Quality Control Tests.....	111
<b>APPENDIX A</b>	<b>COMMENTARY ON THE SELECTION OF THE DESIGN EARTHQUAKES .....</b>	<b>113</b>
A.1	INTRODUCTION.....	113
A.2	CURRENT AASHTO MAP (1990 USGS MAP).....	113
A.3	NEW USGS MAPS.....	113
A.4	NATIONAL EARTHQUAKE HAZARD REDUCTION PROGRAM (NEHRP) MAXIMUM CONSIDERED EARTHQUAKE (MCE) MAPS.....	114
A.5	DESIGN EARTHQUAKES.....	116
A.5.1	Rare Earthquake (MCE).....	116
A.5.2	Expected Earthquake.....	119
A.6	IMPACT STUDIES.....	119
<b>APPENDIX B</b>	<b>PROVISIONS FOR SITE CHARACTERIZATION .....</b>	<b>123</b>
B.1/C.B.1	GENERAL.....	123
B.2/C.B.2	SUBSURFACE EXPLORATIONS.....	123
B.2.1/C.B.2.1	In Situ Tests.....	124
B.2.2/C.B.2.2	Exploration for Seismic Studies.....	125
B.2.2.1/ C.B.2.2.1	Liquefaction Potential.....	126
B.2.2.2/ C.B.2.2.2	Site Response Determination.....	129
B.3/C.B.3	LABORATORY TESTING.....	130
B.3.1/C.B.3.1	Standard Laboratory Tests.....	130
B.3.2/C.B.3.2	Special Testing for Seismic Studies.....	131
B.3.3/C.B.3.3	Rock Testing.....	131
<b>APPENDIX C</b>	<b>GUIDELINES FOR CONDUCTING SITE-SPECIFIC GEOTECHNICAL INVESTIGATIONS AND DYNAMIC SITE RESPONSE ANALYSES.....</b>	<b>133</b>
C.1	INTRODUCTION.....	133
C.2	SITE-SPECIFIC GEOTECHNICAL INVESTIGATION.....	133
C.3	DYNAMIC SITE RESPONSE ANALYSIS.....	133
<b>APPENDIX D</b>	<b>PROVISIONS FOR COLLATERAL SEISMIC HAZARDS.....</b>	<b>135</b>
D.1/C.D.1	GENERAL.....	135
D.1.1/C.D.1.1	Evaluation of Collateral Hazards.....	135
D.1.2/C.D.1.2	Designing for Collateral Hazards.....	136
D.2/C.D.2	LIQUEFACTION.....	137
D.2.1/C.D.2.1	Preliminary Screening for Liquefaction.....	138
D.2.2/C.D.2.2	Field Explorations for Liquefaction Hazards Assessment.....	139
D.2.3/C.D.2.3	Ground Motions for Liquefaction Analysis.....	140
D.2.4/C.D.2.4	Evaluation of Liquefaction Hazard.....	141
D.2.4.1/C.D.2.4.1	Simplified Method.....	142
D.2.4.2/C.D.2.4.2	Numerical Modeling Methods.....	145
D.2.5/C.D.2.5	Liquefaction Hazards Assessment.....	147
D.2.5.1/C.D.2.5.1	Lateral Flows.....	148
D.2.5.2/C.D.2.5.2	Lateral Spreading.....	150
D.2.5.3/C.D.2.5.3	Settlement.....	154
D.3/C.D.3	OTHER COLLATERAL HAZARDS.....	157
D.3.1/C.D.3.1	Fault Rupture.....	157

D.3.2/C.D.3.2	Landsliding.....	158
D.3.3/C.D.3.3	Differential Compaction .....	158
D.3.4/C.D.3.4	Flooding or Inundation.....	159
D.4/C.D.4	DESIGNING FOR COLLATERAL HAZARDS .....	159
D.4.1/C.D.4.2	Spread Footing Foundations .....	159
D.4.1.1/C.D.4.1.1	Loss of Bearing Support for Spread Footings .....	160
D.4.1.2/C.D.4.1.2	Settlement of Spread Footing .....	160
D.4.2/C.D.4.2	Deep Foundations .....	161
D.4.2.1/C.D.4.2.1	Loss in Lateral Support for Deep Foundations.....	161
D.4.2.2/C.D.4.2.2	Loads from Lateral Spreading/Flow.....	162
D.4.2.3/C.D.4.2.3	Settlement and Downdrag .....	169
D.4.3/C.D.4.3	Ground Improvement.....	169
D.4.3.1/C.D.4.3.1	Bearing Capacity and Settlement .....	170
D.4.3.2/C.D.4.3.2	Lateral Spreading and Flow.....	171
<b>APPENDIX E</b>	<b>DUCTILE END-DIAPHRAGMS IN GIRDER BRIDGES .....</b>	<b>173</b>
E.1	DESIGN PROCEDURE .....	173
<b>APPENDIX F</b>	<b>DUCTILE END-DIAPHRAGM IN DECK TRUSS BRIDGE .....</b>	<b>179</b>
F.1	DESIGN PROCEDURE .....	179
<b>APPENDIX G</b>	<b>PARAMETRIC STUDY OF COLUMN DESIGNS.....</b>	<b>185</b>
G.1	BACKGROUND AND PURPOSE .....	185
G.2	SCOPE OF THE PARAMETER STUDY .....	185
G.3	DESCRIPTION OF COLUMN DESIGNS.....	185
G.4	DISCUSSION OF RESULTS.....	189
G.4.1	Column Strength Control .....	189
G.4.2	Column Performance .....	189
G.4.3	Column Size Effect .....	197
G.4.4	Column Overstrength.....	197
G.4.5	Cost Impact .....	197
<b>APPENDIX H</b>	<b>LIQUEFACTION EFFECTS AND ASSOCIATED HAZARDS.....</b>	<b>215</b>
H.1	PURPOSE AND SCOPE .....	215
H.2	DESIGN APPROACH.....	216
H.3	SITE SELECTION AND CHARACTERIZATION.....	216
H.4	BRIDGE TYPE.....	217
H.5	DESIGN RESPONSE SPECTRA AND TIME HISTORIES.....	217
H.6	LIQUEFACTION STUDIES .....	222
H.6.1	Simplified Liquefaction Analyses.....	223
H.6.2	DESRA-MUSC Ground Response Studies.....	224
H.6.2.1	Without Embankment Fill .....	227
H.6.2.2	With Embankment Fill.....	227
H.6.3	Lateral Ground Displacement Assessment .....	232
H.6.3.1	Initial Stability Analyses.....	232
H.6.3.2	Lateral Spread Implications from DESRA-MUSC Analyses .....	233
H.6.3.3	Stability Analyses with Mitigation Measures .....	233
H.6.3.4	Displacement Estimates from Simplified Methods .....	236
H.6.3.5	Displacement Estimates Using Site Response Analysis Results .....	236
H.7	STRUCTURAL ANALYSIS AND DESIGN.....	237
H.7.1	Vibration Design .....	237
H.7.2	Lateral Spreading Structural Design/Assessment .....	238
H.7.2.1	Modes of Deformation.....	238

H.7.2.2	Foundation Movement Assessment.....	238
H.7.2.3	Pinning Force Calculation.....	239
H.8	COMPARISON OF REMEDIATION ALTERNATIVES .....	240
H.8.1	Summary of Structural and Geotechnical Options .....	244
H.8.2	Comparisons of Costs.....	244
H.9	MISSOURI EXAMPLE .....	245
H.9.1	Site Characterization and Bridge Type.....	245
H.9.2	Liquefaction Analyses .....	248
H.9.3	Initial Stability Analysis .....	248
H.9.4	Stability Analyses with Mitigation Measures.....	251
H.9.5	Displacement Estimates from Simplified Methods .....	257
H.9.6	Pinning Force Calculations.....	258
H.9.7	Comparison of Remediation Alternatives .....	262
H.10	SUMMARY AND CONCLUSIONS .....	263
<b>APPENDIX I ISOLATION DESIGN PARAMETERS.....</b>		<b>267</b>
I.1/CI.1	SLIDING ISOLATION SYSTEMS .....	267
I.1.1	Factors for Establishing $\lambda_{\min}$ .....	267
I.1.2	Factors for Establishing $\lambda_{\max}$ .....	267
I.1.2.1	$\lambda_{\max,a}$ .....	267
I.1.2.2	$\lambda_{\max,v}$ .....	267
I.1.2.3/CI.1.2.3	$\lambda_{\max,c}$ .....	268
I.1.2.4	$\lambda_{\max,tr}$ .....	268
I.1.2.5	$\lambda_{\max,t}$ .....	268
I.2/CI.2	ELASTOMERIC BEARINGS.....	269
I.2.1	Factors for Establishing $\lambda_{\min}$ .....	269
I.2.2	Factors for Establishing $\lambda_{\max}$ .....	269
I.2.2.1/CI.2.2.1	$\lambda_{\max,a}$ .....	269
I.2.2.2	$\lambda_{\max,v}$ .....	270
I.2.2.3	$\lambda_{\max,c}$ .....	270
I.2.2.4	$\lambda_{\max,tr}$ .....	270
I.2.2.5/CI.2.2.5	$\lambda_{\max,t}$ .....	270
I.2.2.6	$\lambda_{\max,scrag}$ .....	271
<b>REFERENCES.....</b>		<b>273</b>
<b>PROJECT PARTICIPANTS.....</b>		<b>293</b>



## LIST OF FIGURES

Figure C3.3-1	Design Approaches .....	13
Figure C3.3-2	Basis for Conventional Ductile Design .....	14
Figure C3.3-3	Comparison of Elastic and Inelastic Displacements .....	15
Figure C3.3.1-1a	Permissible Earthquake Resisting Systems .....	18
Figure C3.3.1-1b	Permissible Earthquake Resisting Systems .....	19
Figure C3.3.1-2	Permissible Earthquake Resisting Elements that Require Owner's Approval, and Permissible Alternatives Where Owner's Approval Is Not Required (OANR) .....	20
Figure C3.3.1-3	Earthquake Resisting Elements that are not Recommended for New Bridges .....	21
Figure C3.3.1-4	Methods of Minimizing Damage to Abutment Foundation .....	22
Figure C4.7-1	Comparison of Mean Strength-Reduction Factors of Rock and Alluvium Sites with Regression Analysis .....	36
Figure C5.4.2.2-1	Bridge Deck Subjected to Assumed Transverse and Longitudinal Loading .....	47
Figure C8.5.2-1	Trial Wedge Method for Determining Critical Earthquake-Induced Active Forces .....	72
Figure C8.7.4-1	Example of Moment Frame/Bent .....	78
Figure C8.7.4.4-1	Acceptable Plastic Mechanism for Multi-Tier Bent .....	80
Figure C8.7.5.1-1	Examples of (a) Unacceptable and (b) Acceptable Braced Bent Configurations .....	80
Figure C8.7.6.5-1	Plastic Mechanism for a Chevron Braced Bent Configuration that Would Introduce Undesirable Superstructure Damage (Unless This Bridge Has Only Two Girders that are Located Directly over the Columns) .....	82
Figure C8.7.7.1-1	Interaction Curves for Concrete-Filled Pipes .....	83
Figure C8.7.7.2-1	Flexure of Concrete-Filled Pipe; Shaded Area is Concrete in Compression above the Neutral Axis .....	83
Figure C8.7.7.2-2	Free-Body Diagram Used to Calculate Moment Resistance of Concrete-Filled Pipe .....	84
Figure C8.7.7.2-3	Flexure of Concrete-Filled Pipe – Illustrates Approximation Made in Method 2 .....	84
Figure C8.7.8.1-1	Eccentrically Braced Frames Configurations, the Scope of C6.15.5.1 Being Restricted to Split-V Configuration (Case B) .....	85
Figure C8.8.2.4-1	Single Spiral .....	89
Figure C8.8.2.4-2	Column Tie Details .....	89

Figure C8.8.2.4-3	Column Interlocking Spiral Details .....	89
Figure C8.8.2.4-4	Column Tie Details .....	89
Figure C8.8.4.2-1	Effective Joint Width for Shear Stress Calculations .....	92
Figure C8.8.4.3-1	External Vertical Joint Reinforcement for Joint Force Transfer .....	93
Figure C8.8.4.3-2	Locations for Vertical Joint Reinforcement .....	94
Figure C15.1-1	Typical Acceleration Response Curve .....	99
Figure C15.1-2	Typical Displacement Response Curve .....	100
Figure C15.1-3	Response Curves for Increasing Damping .....	100
Figure C15.1-4	Characteristics of Bilinear Isolation Bearings .....	100
Figure C15.1-5	Response Spectrum for Isolated Bridge .....	101
Figure C15.3-1	Definition at Overlap Area .....	101
Figure C15.4-1	Impact Variations on Key Design Variables .....	101
Figure C15.4.1-1	Figure Shows Only One Isolator and One Substructure .....	103
Figure C15.9.2-1	Tangent Stiffness of Isolation System .....	106
Figure C15.9.2-2	Force-Displacement Relation of Systems with Constant Restoring Force .....	106
Figure C15.10.2-1	Definition of Effective Stiffness .....	108
Figure A-1	Procedure for Incorporation of Deterministic Bounds in the Maximum Considered Earthquake (MCE) Ground Motion Map of the 1997 NEHRP <i>Recommended Provisions for Seismic Regulations for New Buildings and Other Structures</i> .....	115
Figure A-2(a)	Ratios of 0.2 Second Spectral Acceleration at Different Return Periods to 0.2-Second Spectral Acceleration At 475-Year Return Period .....	117
Figure A-2(b)	Ratios of 1.0 Second Spectral Acceleration at Different Return Periods to 1.0-Second Spectral Acceleration at 475-Year Return Period .....	118
Figure A-3(a)	Ratios of 0.2-Second Spectral Acceleration at Different Return Periods to 0.2-Second Spectral Acceleration at 108-Year Return Period .....	120
Figure A-3(b)	Ratios of 1.0-Second Spectral Acceleration at Different Return Periods to 1.0-Second Spectral Acceleration at 108-Year Return Period .....	121
Figure D.2.4-1	Simplified Base Curve Recommended for Determination of CRR from SPT Data for Magnitude 7.5 Earthquakes, with Empirical Liquefaction Data .....	143
Figure D.2.4-2	Magnitude Scaling Factors derived by Various Investigators .....	144

Figure D.2.4-3	Curve Recommended for Calculation of CRR from CPT Data, with Empirical Liquefaction Data.....	145
Figure D.2.4-4	Recommended Liquefaction Assessment Chart Based on $V_{s1}$ and CSR for Magnitude 7.5 Earthquakes and Uncemented Soils of Holocene Age.....	146
Figure D.2.4-5	Soil Flexibility Factor ( $r_d$ ) versus Depth Curves Developed by Seed and Idriss (1971) with Added Mean Value Lines .....	147
Figure D.2.5-1	Relationship between Residual Strength ( $S_r$ ) and Corrected “Clean Sand” SPT Blowcount $(N_1)_{60}$ from Case Histories .....	149
Figure D.2.5-2	Martin and Qiu (1994) Simplified Displacement Chart for Velocity-Acceleration Ratio of 30 .....	152
Figure D.2.5-3	Martin and Qiu (1994) Simplified Displacement Charts for Velocity-Acceleration Ratio of 60 .....	153
Figure D.2.5-4	Relationship Between Cyclic Stress Ratio, $(N_1)_{60}$ and Volumetric Strain for Saturated Clean Sands and Magnitude = 7.5 .....	155
Figure D.2.5-5	Schematic Diagram for Determination of $H_1$ and $H_2$ .....	156
Figure D.4.2-1	Flowchart Showing Process for Evaluating the Effects of Lateral Spread and Flows on a Bridge Foundation .....	163
Figure D.4.2-2	Movement of Liquefied Soil Past Pile or Drilled Shaft .....	165
Figure D.4.2-3	Movement of Liquefied Soil with Crust with Pile or Drilled Shaft .....	165
Figure D.4.2-4	$P$ - $\Delta$ Effects to Stub Abutment.....	167
Figure D.4.2-5	$P$ - $\Delta$ Effects for an Intermediate Pier with Piles and Pile Cap .....	167
Figure E.1-1	EBF Ductile Diaphragms .....	173
Figure E.1-2	SPS Ductile Diaphragms .....	173
Figure E.1-3	TADAS Ductile Diaphragms .....	173
Figure E.1-4	Flow Chart of Design Process for Ductile Diaphragm.....	175
Figure F.1-1	Ductile Diaphragm Concept in Deck Trusses .....	179
Figure G-1	SDOF Model for Single-Column Bent Design Study Column Fixed for Moment at Top and Bottom .....	187
Figure G-2	SDOF Model for Multi-Column Bent Design Study Column Fixed for Moment at Bottom Only.....	187
Figure G-3	Column Main Reinforcement Requirements for 4-Foot-Diameter Multi-Column Bents in Seattle Designed with a R-factor of 4 and Various Column Heights (L).....	190

Figure G-4	Column Main Reinforcement Requirements for 4-Foot-Diameter Multi-Column Bents in Seattle Designed with a R-factor of 6 and Various Column Heights (L) .....	190
Figure G-5	Breakdown of Column Main Reinforcement Design Controls for 4-Foot-Diameter 20-Foot-Tall Multi-Column Bents in Seattle .....	191
Figure G-6	Breakdown of Column Main Reinforcement Design Controls for 4-Foot-Diameter 30-Foot-Tall Multi-Column Bents in Seattle .....	191
Figure G-7	Breakdown of Column Main Reinforcement Design Controls for 4-Foot-Diameter 40-Foot-Tall Multi-Column Bents in Seattle .....	192
Figure G-8	Column Main Reinforcement Requirements for 4-Foot-Diameter Multi-Column Bents in Memphis Designed with a R-factor of 4 .....	192
Figure G-9	Breakdown of Column Main Reinforcement Design Controls for 4-Foot-Diameter 20-Foot-Tall Multi-Column Bents in Memphis .....	193
Figure G-10	Breakdown of Column Main Reinforcement Design Controls for 4-Foot-Diameter 30-Foot-Tall Multi-Column Bents in Memphis .....	193
Figure G-11	Breakdown of Column Main Reinforcement Design Controls for 4-Foot-Diameter 40-Foot-Tall Multi-Column Bents in Memphis .....	194
Figure G-12	Column Main Reinforcement Requirements for 4-Foot-Diameter Single-Column Bents in Seattle Designed with a R-factor of 4 .....	194
Figure G-13	Column Main Reinforcement Requirements for 4-Foot-Diameter Single-Column Bents in Seattle Designed with a R-factor of 6 .....	195
Figure G-14	Breakdown of Column Main Reinforcement Design Controls for 4-Foot-Diameter 20-Foot-Tall Single-Column Bents in Seattle .....	195
Figure G-15	Breakdown of Column Main Reinforcement Design Controls for 4-Foot-Diameter 40-Foot-Tall Single-Column Bents in Seattle .....	196
Figure G-16	Column Main Reinforcement Requirements for 4-Foot-Diameter Multi-Column Bents in New York Designed with a R-factor of 4 .....	196
Figure G-17	Column Main Reinforcement Requirements for 5-Foot-Diameter Multi-Column Bents in Seattle Designed with a R-factor of 4 .....	208
Figure G-18	Breakdown of Column Main Reinforcement Design Controls for 3-Foot-Diameter 30-Foot-Tall Multi-Column Bents in New York .....	208
Figure G-19	Breakdown of Column Main Reinforcement Design Controls for 3-Foot-Diameter 40-Foot-Tall Multi-Column Bents in New York .....	209
Figure G-20	Cost Factors (NCHRP 12-49/AASHTO Division 1-A) for 4-Foot-Diameter Single-Column Bents in Seattle Designed with an R-factor of 4 .....	209
Figure G-21	Cost Factors (NCHRP 12-49/AASHTO Division 1-A) for 4-Foot-Diameter Single-Column Bents in Memphis Designed with an R-factor of 4 .....	210



Figure G-22	Cost Factors (NCHRP 12-49/AASHTO Division 1-A) for 4-Foot-Diameter Single-Column Bents in Portland Designed with an R-factor of 4.....	210
Figure G-23	Cost Factors (NCHRP 12-49/AASHTO Division 1-A) for 4-Foot-Diameter Single-Column Bents in St. Louis Designed with an R-factor of 4.....	211
Figure G-24	Cost Factors (NCHRP 12-49/AASHTO Division 1-A) for 4-Foot-Diameter Single-Column Bents in New York Designed with an R-factor of 4.....	211
Figure G-25	Cost Factors (NCHRP 12-49/AASHTO Division 1-A) for 4-Foot-Diameter Multi-Column Bents in Seattle Designed with an R-factor of 4 .....	212
Figure G-26	Cost Factors (NCHRP 12-49/AASHTO Division 1-A) for 4-Foot-Diameter Multi-Column Bents in Memphis Designed with an R-factor of 4 .....	212
Figure G-27	Cost Factors (NCHRP 12-49/AASHTO Division 1-A) for 4-Foot-Diameter Multi-Column Bents in Portland Designed with an R-factor of 4.....	213
Figure G-28	Cost Factors (NCHRP 12-49/AASHTO Division 1-A) for 4-Foot-Diameter Multi-Column Bents in St. Louis Designed with an R-factor of 4.....	213
Figure G-29	Cost Factors (NCHRP 12-49/AASHTO Division 1-A) for 4-Foot-Diameter Multi-Column Bents in New York Designed with an R-factor of 4.....	214
Figure H-1	Simplified Soil Profile for the Western U.S. (Washington State) Site.....	218
Figure H-2	Washington State Department of Transportation Location H-13 CRR Plot .....	219
Figure H-3	Site Profile and Structure Elevation, Washington State Bridge .....	220
Figure H-4	Elevation of an Intermediate Pier, Washington State Bridge .....	221
Figure H-5	Elevations of the Abutment, Washington State Bridge.....	221
Figure H-6	Design Response Spectra Based on Current AASHTO <i>Specifications</i> , Site Class III, and for the MCE and the Expected Earthquake Events in the Recommended NCHRP 12-49 Design Provisions, Site Class E, Washington Site.....	223
Figure H-7a	Liquefaction Potential – 475-Year Return Period (10% PE in 50-Year Ground Motion), Washington State Case Study.....	225
Figure H-7b	Liquefaction Potential – 2,475-Year Return Period (3% PE in 75-Year Ground Motion), Washington State Case Study.....	226
Figure H-8	Input and Output Acceleration Histories and Response Spectra, 475-Year Earthquake (10% in 50-Year PE Ground Motion) Without Fill, Washington State Case Study .....	228
Figure H-9	Maximum Shear Strains Induced as a Function of Depth, 475-Year Earthquake (10% PE in 50-Year Ground Motion) Without Fill, Washington State Case Study .....	229
Figure H-10	Time Histories of Pore Pressure Generation at Various Depths, 475-Year Earthquake (10% PE in 50-Year Ground Motion) Without Fill, Washington State Case Study.....	230

Figure H-11	Shear Stress – Shear Strain Hysteretic Loops at Various Depths, 475-Year Earthquake (10% PE in 50-Year Ground Motion) Without Fill, Washington State Case Study .....	231
Figure H-12	Displacement vs. Time for 2475-Year Earthquake (3% PE in 75-Year Ground Motion), Washington State Case Study .....	234
Figure H-13	Displacement vs. Yield Acceleration for the Deep Sliding Surface of the Washington State Site .....	235
Figure H-14	Plastic Mechanism for an Integral Abutment Supported on Piles, Washington State Case Study .....	239
Figure H-15	Forces Provided by Bridge and Foundation Piling for Resisting Lateral Spreading, Washington State Case Study .....	241
Figure H-16	Piers 5 and 6 Resisting Lateral Spreading – Deep Wedge, Washington State Case Study .....	242
Figure H-17	Pier 6 Resisting Lateral Spreading – Shallow Wedge, Washington State Case Study ...	243
Figure H-18	Elevation and Ground Profile for the Mid-America (Missouri) Bridge .....	246
Figure H-19	Elevation of Intermediate Pier, Missouri Bridge .....	247
Figure H-20	Elevation of Integral Abutment, Missouri Bridge .....	247
Figure H-21	Liquefaction Potential – 475-Year Return Period (10% PE in 50-Year Ground Motion), Missouri Case Study .....	249
Figure H-22	Liquefaction Potential – 2,475-Year Return Period (10% PE in 50-Year Ground Motion), Missouri Case Study .....	250
Figure H-23	Displacement vs. Time for the Missouri Site Failure Surface .....	252
Figure H-24	Input Acceleration History at Base of Liquefiable Layer, 1985 Michoacan Earthquake, Missouri Case Study .....	253
Figure H-25	Displacement vs. Yield Acceleration of the Soil Failure Surface for the Missouri Site .....	254
Figure H-26	Geometry of Toe Failure Wedge for Missouri Site .....	255
Figure H-27	Geometry of Deep Failure Wedge for Missouri Site .....	256
Figure H-28	Pier 4 Structural Forces Resisting Lateral Spreading, Missouri Case Study .....	259
Figure H-29	Pier 3 and Pier 4 Structural Forces Resisting Lateral Spreading, Missouri Case Study .....	260
Figure H-30	Displacement vs. Yield Acceleration of the Soil Failure Surface for the Missouri Site .....	261

## LIST OF TABLES

Table C3.2-1	Geometric Constraints on Service Level .....	10
Table B-1	In-Situ Tests.....	125
Table B-2	Recommended SPT Procedure .....	127
Table G-1	Design Spectral Accelerations and Site Class Coefficients (Soil Class C) NCHRP 12-49 Seismic Provisions (Part I of this document) .....	186
Table G-2	Design Acceleration Coefficients and Soil Type Factors (Soil Type II) AASHTO Division I-A Seismic Provisions.....	186
Table G-3	Example Calculation of Column Design Forces.....	186
Table G-4	Parameter Combinations Used for the Column Design Comparisons.....	188
Table G-5	Column Displacement Summary for 4-Foot-Diameter Single-Column Bents in Seattle Designed with a “R” of 4 .....	198
Table G-6	Column Displacement Summary for 4-Foot-Diameter Single-Column Bents in Portland Designed with a “R” of 4 .....	199
Table G-7	Column Displacement Summary for 4-Foot-Diameter Single-Column Bents in Memphis Designed with a “R” of 4 .....	200
Table G-8	Column Displacement Summary for 4-Foot-Diameter Single-Column Bents in St. Louis Designed with a “R” of 4.....	201
Table G-9	Column Displacement Summary for 4-Foot-Diameter Single-Column Bents in New York Designed with a “R” of 4 .....	202
Table G-10	Column Displacement Summary for 4-Foot-Diameter Multi-Column Bents in Seattle Designed with a “R” of 4 .....	203
Table G-11	Column Displacement Summary for 4-Foot-Diameter Multi-Column Bents in Portland Designed with a “R” of 4 .....	204
Table G-12	Column Displacement Summary for 4-Foot-Diameter Multi-Column Bents in Memphis Designed with a “R” of 4 .....	205
Table G-13	Column Displacement Summary for 4-Foot-Diameter Multi-Column Bents in St. Louis Designed with a “R” of 4.....	206
Table G-14	Column Displacement Summary for 4-Foot-Diameter Multi-Column Bents in New York Designed with a “R” of 4 .....	207



## Section 1: Commentary

### INTRODUCTION

This document contains Commentary and Appendices developed to clarify and explain the technical basis for the *Specifications* provided in *Part I* of the *Recommended LRFD Guidelines for the Seismic Design of Highway Bridges* (ATC/MCEER, 2003a). Commentary are provided for each chapter in Part I except Section I (Introduction), which simply introduces the contents of the document, and Section II (Definitions and Notations), which is a repeat of the material in Part I provided here for the convenience of the reader.

Also included is a complete list of references, including those cited as well as those considered but not cited, and a list of acronyms.



## Section 2: Commentary

### DEFINITIONS AND NOTATIONS

#### C2.1 DEFINITIONS

**Capacity Design** – A method of component design that allows the designer to prevent damage in certain components by making them strong enough to resist loads that are generated when adjacent components reach their overstrength capacity.

**Capacity Protected Element** – Part of the structure that is either connected to a critical element or within its load path and that is prevented from yielding by virtue of having the critical member limit the maximum force that can be transmitted to the capacity protected element.

**Capacity Spectrum Design** – Seismic Design and Analysis Procedure (SDAP) C – A design and analysis procedure that combines a demand and capacity analysis.

**Collateral Seismic Hazard** – Seismic hazards other than direct ground shaking such as liquefaction, fault rupture, etc.

**Complete Quadratic Combination (CQC)** – A statistical rule for combining modal responses from an earthquake load applied in a single direction to obtain the maximum response due to this earthquake load.

**Critical or Ductile Elements** – Parts of the structure that are expected to absorb energy, undergo significant inelastic deformations while maintaining their strength and stability.

**Damage Level** – A measure of seismic performance based on the amount of damage expected after one of the design earthquakes.

**Displacement Capacity Verification** – Seismic Design and Analysis Procedure (SDAP) E – A design and analysis procedure that requires the designer to verify that his or her structure has sufficient displacement capacity. It generally involves a non-linear static (i.e. “pushover”) analysis.

**Ductile Substructure Elements** – See Critical or Ductile Elements

**Earthquake Resisting Element (ERE)** – The individual components, such as columns, connections, bearings, joints, foundation, and abutments, that together constitute the Earthquake Resisting System (ERS).

**Earthquake Resisting System (ERS)** – A system that provides a reliable and uninterrupted load path for transmitting seismically induced forces into the ground and sufficient means of energy dissipation and/or restraint to reliably control seismically induced displacements.

**Expected Earthquake (EE)** – Design earthquake having ground motions with a 50% chance of being exceeded during a 75-year period.

**Life Safety Performance Level** – The minimum acceptable level of seismic performance allowed by this specification. It is intended to protect human life during and following a rare earthquake.

**Liquefaction** – Seismically induced loss of shear strength in loose, cohesionless soil that results from a build up of pore water pressure as the soil tries to consolidate when exposed to seismic vibrations.

**Liquefaction-Induced Lateral Flow.** – Lateral displacement of relatively flat slopes that occurs under the combination of gravity load and excess porewater pressure (without inertial loading from earthquake). Lateral flow often occurs after the cessation of earthquake loading.

**Liquefaction-Induced Lateral Spreading** – Incremental displacement of a slope that occurs from the combined effects of pore water pressure buildup, inertial loads from the earthquake, and gravity loads.

**Maximum Considered Earthquake (MCE)** – The upper level, or rare, design earthquake having ground motions with a 3% chance of being ex-

ceeded in 75 years. In areas near highly-active faults, the MCE ground motions are deterministically bounded to ground motions that are lower than those having a 3% chance of being exceeded in 75 years.

**Minimum Seat Width** – The minimum prescribed width of a bearing seat that must be provided in a new bridge designed according to these specifications.

**Nominal resistance** - Resistance of a member, connection or structure based on the expected yield strength ( $F_{ye}$ ) or other specified material properties, and the nominal dimensions and details of the final section(s) chosen, calculated with all material resistance factors taken as 1.0.

**Operational Performance Level** – A higher level of seismic performance that may be selected by a bridge owner who wishes to have immediate service and minimal damage following a rare earthquake.

**Overstrength Capacity** – The maximum expected force or moment that can be developed in a yielding structural element assuming overstrength material properties and large strains and associated stresses.

**Performance Criteria** – The levels of performance in terms of post earthquake service and damage that are expected to result from specified earthquake loadings if bridges are designed according to this specification.

**Plastic Hinge** – The region of a structural component, usually a column or a pier in bridge structures, that undergoes flexural yielding and plastic rotation while still retaining sufficient flexural strength.

**Pushover Analysis** – See Displacement Capacity Verification

**Plastic Hinge Zone** – Those regions of structural components that are subject to potential plastification and thus must be detailed accordingly.

**Rare Earthquake** – See Maximum Considered Earthquake (MCE).

**Response Modification Factor (R-Factor)** – Factors used to modify the element demands from an

elastic analysis to account for ductile behavior and obtain design demands.

### **Seismic Design and Analysis Procedure (SDAP)**

– One of five defined procedures for conducting seismic design and analysis. Minimum requirements are based on seismic hazard level, performance objective, structural configuration, and the type of ERS and/or ERE's.

**Seismic Design Requirements (SDR)** – One of six categories of minimum design requirements based on the seismic hazard level and the performance objective.

**Seismic Hazard Level** – One of four levels of seismic ground shaking exposure measured in terms of the rare earthquake design spectral accelerations for 0.2 and 1.0 second.

**Service Level** – A measure of seismic performance based on the expected level of service that the bridge is capable of providing after one of the design earthquakes.

**Site Class** – One of six classifications used to characterize the effect of the soil conditions at a site on ground motion.

### **Square Root of the Sum of the Squares (SRSS)**

**Combination** – In this specification, this classical statistical combination rule is used in two ways. The first is for combining forces resulting from two or three orthogonal ground motion components. The second use is for establishing orthogonal moments for biaxial design.

**Tributary Weight** – The portion of the weight of the superstructure that would act on a pier participating in the ERS if the superstructure between participating piers consisted of simply supported spans. A portion of the weight of the pier itself may also be included in the tributary weight.

## **C2.2 NOTATIONS**

$A_{cc}$  = area of column core concrete

$A_g$  = gross cross-sectional area of column

$A_{bh}$  = the area of one spiral bar or hoop in a circular section

$A_{jv}$  = total area of vertical stirrups within a moment resisting connection (joint)



$A_{sh}$	= area of transverse hoops and cross-ties in the direction of applied shear				distance between the outermost layers of bars in a rectangular column in the direction of applied shear
$A'_{sh}$	= total area of transverse reinforcement perpendicular to the direction of applied shear	$D''$	= center-to-center diameter of perimeter hoop or spiral of a circular column OR center-to-center dimension of the transverse hoops of a tied column		
$A_{st}$	= total area of longitudinal column reinforcement entering a moment resisting connection (joint)	$D_p$	= pile dimension about the weak axis at ground line		
$A_v$	= effective shear area of a concrete column	$D_{eff}$	= effective gap width at abutment after passive soil resistance is mobilized (m) (Figures 7.5.2.2-2 and 8.5.2.2-2)		
$B$	= factor that sets the shape of the interaction diagram for concrete-filled steel pipe, as defined in Articles 7.7.7.1 and 8.7.7.1	$D_g$	= gap width at abutment (m) (Figures 7.5.2.2-2 and 8.5.2.2-2)		
$B$	= damping coefficient for isolation systems as defined in Article 5.4.1.1	$d$	= effective depth of a concrete section		
$B$	= width of superstructure in meters as defined in Article 6.3, 7.3.2 and 8.3.2	$d_b$	= longitudinal reinforcing bar diameter		
$B'$	= center-to-center dimension of extreme longitudinal steel reinforcing bars in the direction perpendicular to applied shear	$d_c$	= total thickness of cohesive soil at a site		
$B''$	= center-to-center dimension of the transverse hoops of a tied column in the direction perpendicular to the applied shear	$d_i$	= thickness of soil layer "i"		
$B_L$	= capacity spectrum response reduction factor for constant-velocity portion of design response spectrum curve	$d_s$	= total thickness of cohesionless soil at a site		
$B_s$	= capacity spectrum response reduction factor for short-period portion of design response spectrum curve	$E$	= modulus of elasticity		
$b$	= width of a rectangular plate element in a steel cross section	$EI_{eff}$	= effective flexural rigidity, including the effect of cracking concrete in reinforced concrete members		
$b_f$	= width of the flange in a steel I shaped section	$F_a$	= site coefficient for short-period portion of design response spectrum curve		
$b_w$	= width resisting shear in a rectangular concrete section	$F_v$	= site coefficient for long-period portion of design response spectrum curve		
$c$	= cohesion of soil	$F_{ye}$	= Expected yield strength of steel to be used (MPa)		
$C_c$	= seismic capacity coefficient	$f'_c$	= nominal 28 day concrete strength		
$C_d$	= seismic demand coefficient	$f_h$	= average axial stresses in the horizontal direction within a moment-resisting connection (or joint)		
$C_{sm}$	= elastic seismic response coefficient for the mth mode of vibration	$f_{su}$	= ultimate strength of transverse reinforcement		
$C_v$	= dead load multiplier coefficient for vertical earthquake effects	$f_v$	= average axial stresses in the vertical direction within a moment-resisting connection (or joint)		
$D$	= transverse dimension or diameter of a column or pile	$f_{yh}$	= transverse reinforcement yield stress		
$D'$	= center to center diameter of longitudinal reinforcement in a circular column or the	$g$	= acceleration due to gravity, 32.2 ft/sec <sup>2</sup> or 9.81 m/sec <sup>2</sup>		
		$H$	= height of tallest pier between joints		

$H$	= height of abutment backwall in Articles 7.5.2.2 and 8.5.2.2	$l_{ac}$	= length of embedment of longitudinal column steel into a moment-resisting connection (or joint)
$H_c$	= height of a cap beam joint	$M$	= maximum column moment
$h_c$	= depth of a steel I shaped section	$M_n$	= nominal moment capacity of a column
$K$	= lateral stiffness of bridge in uniform load method	$M_{nx}$	= probable flexural resistance of steel columns
$K_{cr}$	= lateral stiffness of a concrete pier based on the cracked section properties	$M_{po}$	= plastic overstrength capacity of a column
$K_{DED}$	=stiffness of a steel ductile end diaphragm	$M_{px}$	= steel column plastic moment under pure bending calculated using $F_{ye}$
$K_{eff}$	=effective lateral stiffness at design displacement	$M_{rc}$	= factored moment resistance of a concrete filled steel pipe for Articles 7.7.7 and 8.7.7 (kN m)
$K_{eff1}$	=effective initial stiffness of abutment backwall and soil including the initial gap (kN/m) (Figures 7.5.2.2-2 and 8.5.2.2-2)	$M_u$	= factored flexural moment
$K_{eff2}$	= secant stiffness of abutment backwall and soil at maximum EQ displacement (kN/m) (Figures 7.5.2.2-2 and 8.5.2.2-2)	$M_x$	= maximum moment about the “x” axis due to earthquake load applied in all directions
$K_i$	= initial stiffness of abutment backfill based on soil resistance alone (kN/m) (Figures 7.5.2.2-2 and 8.5.2.2-2)	$M_x^L$	= maximum moment about the “x” axis due to earthquake load applied in the longitudinal direction
$K_{srv}$	= rotational spring constant of a pile group (Equation 8.4.3.2-2)	$M_x^{LC1}$	= maximum moment about the “x” axis due to earthquake load case 1
$K_{sv}$	= axial stiffness of a pile group (Equation 8.4.3.2-1)	$M_x^{LC2}$	= maximum moment about the “x” axis due to earthquake load case 2
$K_{vn}$	= axial stiffness of an individual pile (Equation 8.4.3.2-2)	$M_x^T$	= maximum moment about the “x” axis due to earthquake load applied in the transverse direction
$K_{sec}$	= secant stiffness of a column based on the nominal moment capacity and the elastic displacement	$M_y$	= maximum moment about the “y” axis due to earthquake load applied in all directions
$K_{shape}$	=shape factor used in implicit shear design of a concrete column (Articles 7.8.2.3.1 and 8.8.2.3.1)	$M_y^L$	= maximum moment about the “y” axis due to earthquake load applied in the longitudinal direction
$K_{SUB}$	=stiffness of the substructure supporting a steel ductile end diaphragm	$M_y^{LC1}$	= maximum moment about the “y” axis due to earthquake load case 1
$k$	= limiting width-to-thickness ratio in a steel cross section	$M_y^{LC2}$	= maximum moment about the “y” axis due to earthquake load case 2
$L$	= length of bridge	$M_y^T$	= maximum moment about the “y” axis due to earthquake load applied in the transverse direction
$L$	= length of a pile or column from point of fixity to point of zero moment	$\bar{N}$	= average standard penetration test blow count for the top 100 ft (30 m) of a site
$L_g$	= length of isolation gap at an architectural column flare	$\bar{N}_{ch}$	= average standard penetration test blow count for cohesionless layers of top 100 ft (30 m) of a site
$L_p$	= effective plastic hinge length	$N$	= minimum seat width

$N_f$	= number of cycles of loading expected at the maximum displacement amplitude	$r_y$	= minimum radius of gyration of a steel section
$N_i$	= standard penetration test blow count of soil layer “i”	$s$	= center-to-center spacing of hoops or the pitch of spirals
$PI$	= plasticity index of soil	$S_a$	= design response spectral acceleration
$P$	= axial load on a pile or column	$S_{DS}$	= design earthquake response spectral acceleration at short periods
$P_C$	= axial compression capacity of timber pile	$S_{DI}$	= design earthquake response spectral acceleration at 1-second period
$P_e$	= column axial load	$S_s$	= 0.2-second period spectral acceleration on Class B rock from the 1996 USGS national ground motion maps
$p_e$	= uniform load on superstructure for uniform load method for design response spectrum curve	$S_1$	= 1-second period spectral acceleration on Class B rock from the 1996 USGS national ground motion maps
$p_0$	= unit uniform load on superstructure for uniform load method	$\bar{s}_u$	= average undrained shear strength of cohesive soil layers in the top 100 ft (30 m) of a site
$P_e$	= factored axial load including seismic effects	$S_{ui}$	= undrained shear strength of cohesive soil layer “i”
$P_p$	= passive force acting against abutment backwall under earthquake loading (kN) (Articles 7.5.2.2 and 8.5.2.2)	$T$	= period of vibration
$P_r$	= factored axial or tensile resistance of a concrete-filled steel pipe	$T_s$	= period at the end of constant design spectral acceleration plateau
$P_{rc}$	= factored compressive resistance of the concrete core of a concrete-filled steel pipe (Articles 7.7.7.1 and 8.7.7.1) with $\lambda = 0$ (kN)	$T_0$	= period at beginning of constant design spectral acceleration plateau
$P_{ro}$	= factored compressive resistance of concrete-filled steel pipe	$T^*$	= period used to calculate $R$ and $R_d$
$P_u$	= factored applied axial force in a steel compression member	$t$	= thickness of pier wall
$P_y$	= axial yield force of steel pile or column	$t_f$	= thickness of the flange in a steel I-shaped section
$P_c$	= principal compression stress in a moment-resisting connection (or joint)	$t_w$	= thickness of the web in a steel I-shaped section
$P_t$	= principal tension stress in a moment-resisting connection (or joint)	$T_{eff}$	= effective vibration period at design displacement
$Q$	= total factored force effect	$T_m$	= vibration period for uniform load method
$Q_i$	= force effect from specified load	$U_{sf}$	= strain energy capacity of the transverse reinforcement
$R$	= response modification factor	$V$	= equivalent static lateral force for uniform load method or maximum column shear
$R_B$	= base response modification factor	$V_c$	= tensile contribution of concrete to shear resistance
$R_d$	= ratio of estimated actual displacement to displacement determined from elastic analysis	$V_p$	= contribution to shear resistance from the strut action of the column axial load
$R_y$	= ratio of the expected yield strength $F_{ye}$ to the minimum specified yield strength $F_y$		

$V_r$	= factored shear resistance of a concrete pier wall in the strong direction	$\Delta_e$	= displacement obtained from an elastic analysis
$V_s$	= shear resistance of a column provided by transverse reinforcement	$\Delta_m$	= estimated actual displacement at the center of mass
$v_{hv}$	= average shear stress within the plane of a moment-resisting connection (or joint)	$\varepsilon_y$	= yield strain of longitudinal reinforcement
$\bar{v}_s$	= average shear wave velocity for the top 100 ft (30 m) of a site	$\theta$	= principal crack angle in reinforced concrete column
$v_{s,max}$	= maximum displacement of bridge under uniform load	$\theta_p$	= plastic rotation at a plastic hinge
$v_{si}$	= shear wave velocity of soil layer “i”	$\Lambda$	= fixity factor used for the calculation of shear forces
$W$	= weight of bridge	$\lambda_{mo}$	= adjustment factor applied to nominal moment to obtain overstrength moment
$w$	= moisture content (%) of soil	$\lambda_p$	= limiting width-to-thickness ratio for steel cross sections
$Z$	= plastic modulus of a steel section	$\rho_t$	= longitudinal reinforcement ratio of a column or pier
$\alpha$	= skew angle of the bridge as defined in Articles 6.3, 7.3.2 and 8.3.2	$\rho_s$	= volumetric ratio of spiral reinforcement
$\alpha$	= geometric aspect ratio angle of a column as defined in Articles 7.8.2.3.1 and 8.8.2.3.1	$\rho_v$	= ratio of transverse reinforcement required inside the plastic hinge zone
$\alpha_{skew}$	= skew angle of the bridge, (0 degrees being the angle for a right bridge)	$\rho_v^*$	= ratio of transverse reinforcement required outside the plastic hinge zone
$\beta$	= damping ratio in percent	$\phi$	= resistance factor
$\Delta$	= displacement from an elastic seismic analysis	$\phi$	= angle of internal friction of soil
$\Delta_{capacity}$	= maximum displacement capacity in Article 5.4.3		

## Section 3: Commentary

### GENERAL REQUIREMENTS

#### C3.1 APPLICABILITY

No commentary is provided for Article 3.1.

#### C3.2 SEISMIC PERFORMANCE OBJECTIVES

The design earthquake ground motions and forces specified herein are based on the probabilities of exceedance stated in Table 3.2-1 for a nominal life expectancy of a bridge of 75 years. Appendix A provides the background for the selection of these probabilities of exceedance. As a minimum, these specifications are intended to achieve minimal damage to the bridge during expected ground motions during the life of the bridge, and to prevent collapse during rare, high-amplitude ground motions. Bridge owners may choose to mandate higher levels of bridge performance.

For sites close to highly active faults, the upper-level earthquake ground motions (Maximum Considered Earthquake or MCE), defined probabilistically, can reach values that exceed ground motions estimated deterministically for the maximum magnitude earthquake considered capable of occurring on the fault. For such sites, it is considered reasonable to limit or bound the design ground motions to conservative deterministic estimates of the ground motion from the maximum magnitude earthquake. As indicated in the footnote to Table 3.2-1, deterministic bounds on ground motions have been incorporated on MCE maps where applicable (Hamburger and Hunt, 1997; BSSC, 1998; Leyendecker et al., 2000). These bounds were defined as 1.5 times the median ground motions calculated using appropriate attenuation relationships assuming the occurrence of the maximum magnitude earthquake on the fault, but not less than 1.5g for the short-period acceleration plateau ( $S_s$ ) and 0.6g for 1.0-second spectral acceleration ( $S_I$ ). The magnitude of a maximum earthquake is the best estimate of the largest magnitude considered capable of occurring on the fault. On the current MCE maps, (Frankel and Leyendecker, 2001; Frankel et al., 1996, 1997a, b, c, 2000) deterministic bounds are applied only in portions of California, in local areas

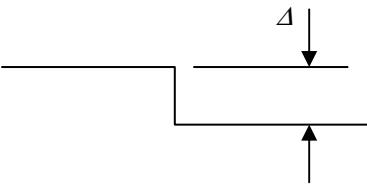
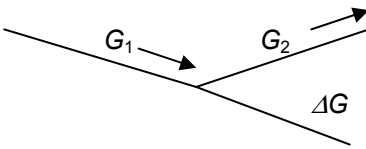
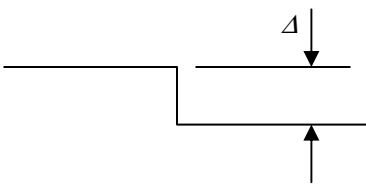
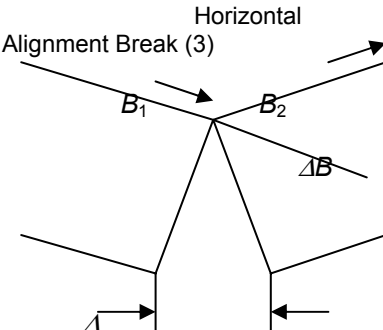
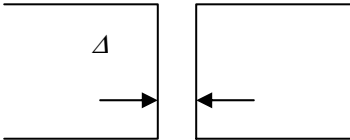
along the California-Nevada border, along coastal Oregon and Washington, and in portions of Alaska and Hawaii.

Probabilistic ground motions developed for MCE ground motion maps by the USGS were calculated for a probability of exceedance of 2% in 50 years. These ground motion values are nearly identical to ground motions for 3% probability of exceedance in 75 years. The corresponding ground motion return periods are nearly the same (2475-year return period for 2% probability of exceedance in 50 years and 2462-year return period for 3% probability in 75 years). Therefore, the map values may be taken as the ground motions for 3% probability of exceedance in 75 years.

Allowable displacements are constrained by geometric, structural and geotechnical considerations. The most restrictive of these constraints will govern displacement capacity. These displacement constraints may apply to either transient displacements as would occur during ground shaking, or permanent displacements as may occur due to seismically induced ground failure or permanent structural deformations or dislocations, or a combination. The extent of allowable displacements depends on the desired performance level of the bridge design. The following paragraphs discuss the geometric constraints that should be considered in establishing displacement capacities. These recommendations are order-of-magnitude values and are not meant to be precise. Structural and geotechnical constraints are discussed in Sections 7 and 8.

Allowable displacements shown in Table C3.2-1 were developed at a Geotechnical Performance Criteria Workshop conducted by MCEER on September 10 and 11, 1999 in support of the NCHRP 12-49 project. The original intent of the workshop was to develop detailed foundation displacement criteria based on geotechnical constraints. The final recommendation of the workshop was that, except in special circumstances, foundations are able to accommodate large structural displacements without strength degradation and that displacement capacities are usually constrained by either structural or geomet-

**Taele C3.2-1 Geometric Constraints on Service Level**

Permanent Displacement Type	Possible Causes	Mitigation Measures	Immediate Service Level	Significant Disruption Service Level
Vertical Offset 	<ul style="list-style-type: none"> <li>Approach fill settlement</li> <li>Bearing failure</li> </ul>	<ul style="list-style-type: none"> <li>Approach slabs</li> <li>Approach fill stabilization</li> <li>Bearing type selection</li> </ul>	0.083 feet (0.03 meters)	0.83 feet (0.2 meters) To avoid vehicle impact
Vertical Grade Break (2) 	<ul style="list-style-type: none"> <li>Interior support settlement</li> <li>Bearing failure</li> <li>Approach slab settlement</li> </ul>	<ul style="list-style-type: none"> <li>Strengthen foundation</li> <li>Bearing type selection</li> <li>Longer approach slab</li> </ul>	Use AASHTO "Green Book" requirements to estimate allowable grade break	None
Horizontal Alignment Offset 	<ul style="list-style-type: none"> <li>Bearing failure</li> <li>Shear key failure</li> <li>Abutment foundation failure</li> </ul>	<ul style="list-style-type: none"> <li>Bearing type selection</li> <li>Strengthen shear key</li> <li>Strengthen foundation</li> </ul>	0.33 feet (0.1 meters) Joint seal may fail	Shoulder Width (To avoid vehicle impact)
Horizontal Alignment Break (3) 	<ul style="list-style-type: none"> <li>Interior support failure</li> <li>Bearing failure</li> <li>Lateral foundation movement</li> </ul>	<ul style="list-style-type: none"> <li>Strengthen interior support</li> <li>Bearing type selection</li> <li>Strengthen foundation</li> </ul>	Use AASHTO "Green Book" requirements to estimate allowable alignment break	None $\Delta = 3.28$ feet (1.0 meters)
Longitudinal Joint Opening 	<ul style="list-style-type: none"> <li>Interior support failure</li> <li>Bearing failure</li> <li>Lateral foundation movement</li> </ul>	<ul style="list-style-type: none"> <li>Strengthen interior support</li> <li>Bearing type selection</li> <li>Strengthen foundation</li> </ul>	0.33 feet (0.1 meters)	3.28 feet (1.0 meters) To avoid vehicle impact

**Table C3.2-1 Geometric Constraints on Service Level (continued)**

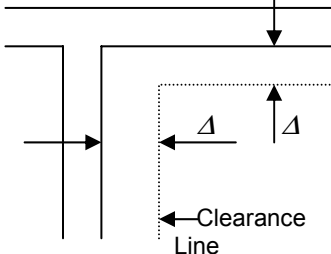
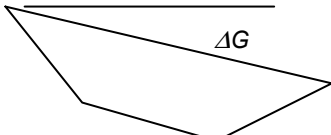
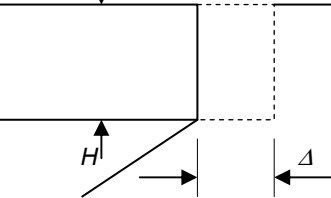
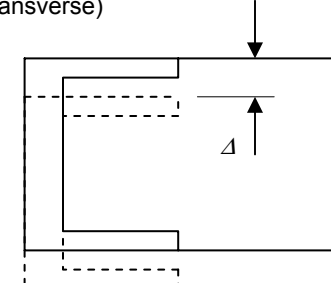
Permanent Displacement Type	Possible Causes	Mitigation Measures	Immediate Service Level	Significant Disruption Service Level
Encroachment on Clearance 	<ul style="list-style-type: none"> <li>Foundation settlement</li> <li>Lateral foundation movement</li> <li>Bearing failure</li> </ul>	<ul style="list-style-type: none"> <li>Strengthen foundation</li> <li>Bearing type selection</li> </ul>	$\Delta$ (Actual Clearance)	Depends on facility being encroached upon
Tilting of Cross-Section 	<ul style="list-style-type: none"> <li>Interior support settlement</li> <li>Bearing failure</li> <li>Approach slab settlement</li> </ul>	<ul style="list-style-type: none"> <li>Strengthen foundation</li> <li>Bearing type selection</li> <li>Longer approach slab</li> </ul>	$\Delta G = .001$ radians	None
Movement into Abutment Fill (Longitudinal) 	<ul style="list-style-type: none"> <li>Engagement of abutment backfill due to horizontal movement of superstructure</li> </ul>	<ul style="list-style-type: none"> <li>Increase gap between superstructure and abutment backwall</li> <li>Stiffen interior supports</li> <li>Increase amount of fill that is engaged</li> </ul>	$\Delta = .02H$	No Constraint Controlled by Adjacent Seat Width
Movement through Abutment Fill (Transverse) 	<ul style="list-style-type: none"> <li>Transverse movement of strengthened or supplemental interior wingwalls through approach fill</li> </ul>	<ul style="list-style-type: none"> <li>Isolate transverse movement with sacrificial shear keys and/or isolation bearings</li> <li>Increase transverse strength and stiffness of abutment</li> </ul>	$\Delta = .02H$	No Constraint

Table notes: Geometric constraints, with the exception of longitudinal and transverse movement through abutment fill, usually apply to permanent displacements which may be difficult to predict accurately. Therefore, the constraints in this table shall be taken as order of magnitude values.

The AASHTO publication "A Policy on Geometric Design of Highways and Streets" (otherwise known as the "Green Book") specifies criteria for determining vertical curve length based on site distance. This criteria, which is based on design speed and whether the curve is a "crest" or a "sag" can be used to determine the allowable change in grade resulting from support settlement. A curve length equal to the sum of adjacent spans may be used in the case of a continuous superstructure or a zero curve length may be used in the case of adjacent simply supported span lengths. Bridge owners may also wish to consider the AASHTO recommendations on appearance and driver comfort in establishing allowable grade changes.

In the case of horizontal curves, minimum curve radius is usually controlled by superelevation and side friction. These radii are specified in the AASHTO "Green Book". When lateral displacement of an interior support results in an abrupt angle break in horizontal alignment a vehicle shall be able to safely achieve the desired turning radius at design speed within the provided lane width minus a margin of safety at each edge of the lane. Consideration shall also be given to the opening of the expansion joint at the edge of the bridge. Joint seals may be damaged at the immediate service level. If no damage at the seal is desired the designer should check the actual longitudinal and transverse capacity or reduce some of the permissible movements.

ric considerations. The values in the table reflect geometric constraints and are based largely on judgment that represents the consensus of the workshop participants.

Geometric constraints generally relate to the usability of the bridge by traffic passing on or under it. Therefore, this constraint will usually apply to permanent displacements that occur as a result of the earthquake. The ability to repair such displacements or the desire not to be required to repair them should be considered when establishing displacement capacities. When uninterrupted or immediate service is desired, the permanent displacements should be small or non-existent, and should be at levels that are within an accepted tolerance for normally operational highways of the type being considered. A guideline for determining these displacements should be the AASHTO publication "A Policy on Geometric Design of Highways and Streets". When limited service is acceptable, the geometric constraints may be relaxed. Constraints may be governed by the geometry of the types of vehicles that will be using the bridge after an earthquake and by the ability of these vehicles to pass through any geometric obstruction. Alternatively, a jurisdiction may simply wish to limit displacements to a certain fraction higher than those allowed for uninterrupted service. A bridge designed to a performance level of no collapse could be expected to be unusable after liquefaction, for example, and geometric constraints would have no influence. However, because life safety is at the heart of the no collapse requirement, jurisdictions may consider establishing some geometric displacement limits for this performance level for important bridges or those with high average daily traffic (ADT). This can be done by considering the risk to highway users in the moments during or immediately following an earthquake. For example, an abrupt vertical dislocation of the highway of sufficient height could present an insurmountable barrier and thus result in a collision that could kill or injure. Usually these types of geometric displacement constraints will be less restrictive than those resulting from structural considerations and for bridges on liquefiable sites it may not be economic to prevent significant displacements from occurring. Table C3.2-1 shows the order of magnitude of suggested displacement limits based on geometric constraints.

### C3.3 SEISMIC DESIGN APPROACH

These provisions provide the designer with a range of performance objectives as shown in Table 3.2-1. Bridges are seismically designed so that inelastic deformation (damage) intentionally occurs in columns in order that the damage can be readily inspected and repaired after an earthquake. Capacity design procedures are used to prevent damage from occurring in foundations and beams of bents and in the connections of columns to foundations and columns to the superstructure. There are two exceptions to this design philosophy. For pile bents and drilled shafts, some limited inelastic deformation is permitted below the ground level, with the owner's approval. The amount of permissible deformation is restricted to ensure that no long-term serviceability problems occur from the amount of cracking that is permitted in the concrete pile or shaft. The second exception is with lateral spreading associated with liquefaction. For the life-safety performance level, significant inelastic deformation is permitted in the piles. It is a costly and difficult problem to achieve a higher performance level from piles. There are a number of design approaches that can be used to achieve the performance objectives. These are given in Figure C3.3-1 and discussed briefly below.

*Conventional Ductile Design* - Caltrans first introduced this design approach in 1973 following the 1971 San Fernando earthquake. It was further refined and applied nationally in the 1983 AASHTO *Guide Specification for Seismic Design of Highway Bridges*, which was adopted directly from the ATC-6 report, *Seismic Design Guidelines for Highway Bridges* (ATC, 1981). These provisions were adopted by AASHTO in 1991 as their standard seismic provisions. The design forces are obtained from an elastic analysis of the bridge using response spectra for the appropriate design event. Component design forces such as column moments ( $M_b$ ) are obtained by dividing the elastic column moment ( $M_e$ ) by a specified  $R$ -factor as shown in Figure C3.3-2. The component's actual strength will be greater than the design strength by an over-strength ratio which will range from 1.3 to 1.6. If the  $R$ -factor for a column is low (i.e.,  $<1.5$ ) then the column should remain essentially elastic for the design event and inelastic deformation (damage) should be avoided. If the  $R$ -factor is high (i.e.,  $R > 3$ ) then significant plastic hinging may occur and the column may not be repairable. If the  $R$ -factor is between 1.5 and 3.0 then the



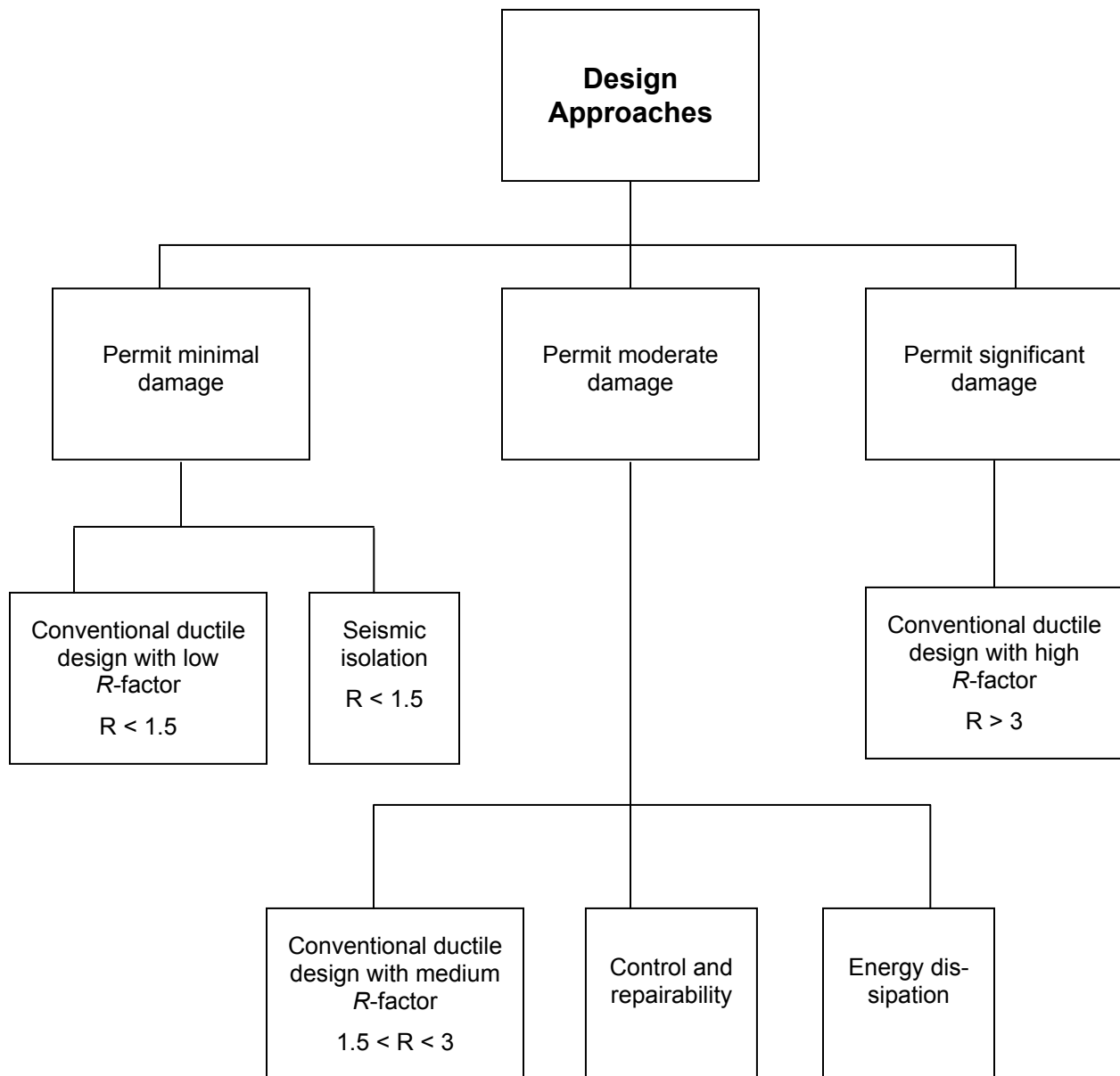


**Figure C3.3-1** Design Approaches

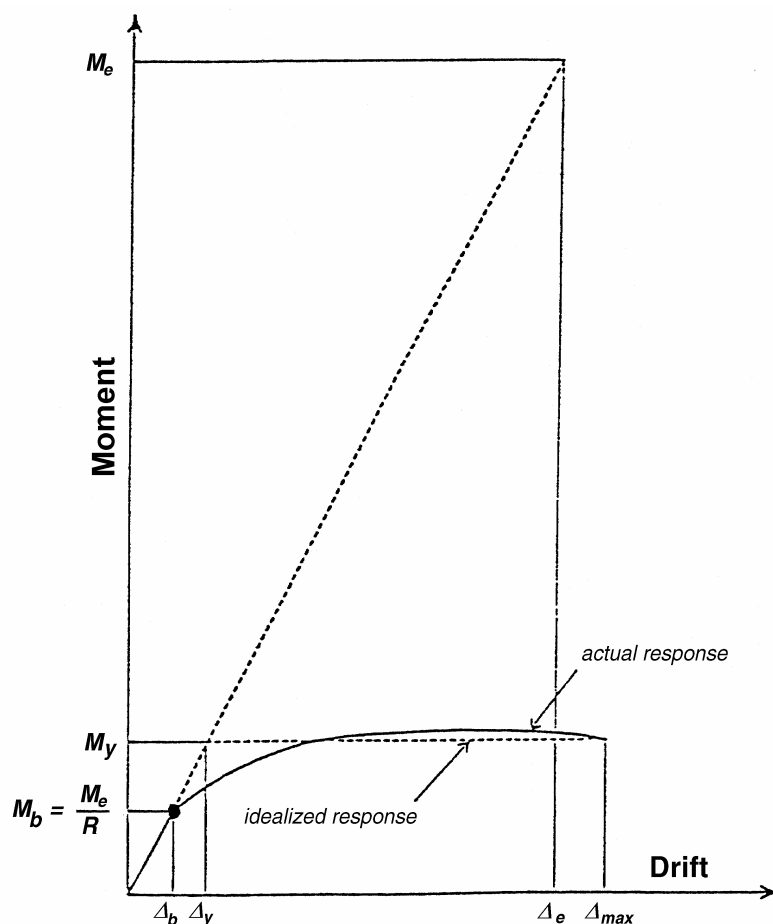


**Figure C3.3-2** Basis for Conventional Ductile Design

column should be repairable. The other key premise of the Part I *Specifications* is that displacements resulting from the inelastic response of a bridge are approximately equal to the displacements obtained from an analysis using the linear elastic response spectrum. As diagrammatically shown in Figure C3.3-2 this assumes that  $\Delta_{max}$  (or  $\Delta_{inelastic}$ ) is equal to  $\Delta_e$  (or  $\Delta_{elastic}$ ). Recent work by Miranda and Bertero (1994a, b) and by Chang and Mander (1994) indicates that this is a reasonable assumption except for short period structures for which it is non-conservative. A correction factor to be applied to elastic displacements to address this issue is given in Article 4.7. A plot of the results from Miranda and Bertero's work is given in Figure C3.3-3. A more detailed discussion on the basis of the conventional design provisions can be found in the ATC-18 report (ATC, 1997).

**Seismic Isolation.** This design approach reduces the seismic forces a bridge must resist by introducing an isolation bearing with an energy dissipation element at the bearing location. The

isolation bearing intentionally lengthens the period of a relatively stiff bridge and this results in lower design forces provided the design is in the decreasing portion of the acceleration response spectrum. This design alternative was first applied in the United States in 1984 and has been extensively reported on at technical conferences and seminars (e.g., the 1989, 1991 and 1993 ASCE Structures Congresses), and in the technical literature (e.g. ATC, 1986 and 1993; EERI, 1990). As of January 1, 1999 there were over 120 bridges constructed in the U.S. and over 300 worldwide using this concept. AASHTO adopted *Guide Specifications for Seismic Isolation Design of Highway Bridges* in 1991 and these were substantially revised in 1997. The 1997 and 2000 revisions are now incorporated in these provisions. Elastic response of the substructure elements is possible with seismic isolation, since the elastic forces resulting from seismic isolation are generally less than the reduced design forces required by conventional ductile design using an  $R$ -factor of 3 to 6.

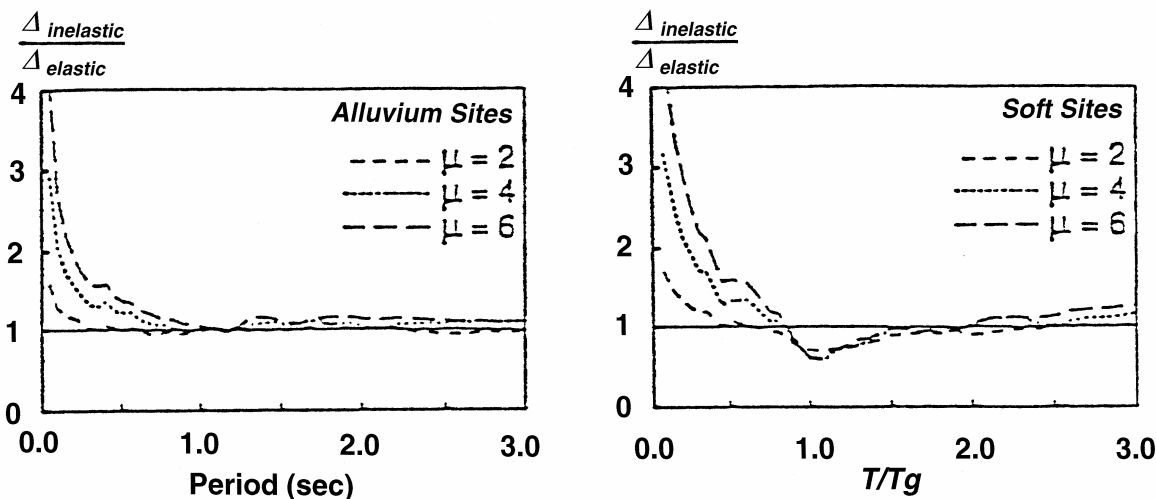


**Figure C3.3-3 Comparison of Elastic and Inelastic Displacements**  
(From Miranda and Bertero, 1994)

**Energy Dissipation.** This design approach adds energy-dissipation elements between the deck and the column, and between the deck and abutment, or in the end diaphragm of a steel girder bridge, with the intent of dissipating energy in these elements. This reduces the energy needing dissipation in the plastic hinge zones of columns. This design approach differs from seismic isolation in that additional flexibility is generally not part of the system and thus the fundamental period of vibration is not changed. If the equivalent viscous damping of the bridge is increased from 5% to 30% then the displacement of the deck will be reduced by a factor of approximately 2. In general the energy dissipation design concept does not result in reduced design forces but it will reduce the ductility demand on columns due to the reduction in deck displacement (ATC, 1993 and EERI, 1998). If the energy dissipation is in the end diaphragm of a steel girder bridge then the diaphragm acts as a force-limiting fuse in the transverse direction.

**Control and Repairability Design.** This design approach is based on the conventional ductile design concept that permits significant inelastic deformation in the plastic hinge zone of a column. The difference from conventional ductile design is that construction details in the hinge zone of reinforced concrete columns provide a replaceable or renewable sacrificial plastic-hinge element. Hinge zones are deliberately weakened with respect to their adjoining elements and all regions outside the hinge zone are detailed to remain elastic and un-

damaged during seismic loading. The concept has been extensively tested but has not been widely used in practice. Cheng and Mander (1997) provide the details for the implementation of this design concept.

The design objectives and performance expectations of the above design approaches are as follows:

*Columns as Primary Energy-Dissipation Mechanisms*

1. The bridge is analyzed to get the elastic design moments in the columns. The elastic moments are reduced by the  $R$ -factor to determine the design moment for the determination of longitudinal column steel. This design value, or the minimum longitudinal steel requirement (0.8%), or the  $P$ - $\Delta$  requirement, may govern the amount of longitudinal steel. The design objective is to minimize the amount of longitudinal steel as this will minimize the foundation and connection costs. Furthermore the more uniform the stiffness of the piers, the better will be the performance of the bridge. Bridges with one or two short stiff columns will find that these columns attract the majority of the seismic loads and this has been the cause of significant failures in past earthquakes. A designer may consider using isolation bearings at the top of short stiff columns or the use of columns in caissons to get more uniform substructure stiffness. For the "no analysis" procedure specified in Article 4.3,

the amount of longitudinal steel required for non-seismic loads is used as the starting point for the capacity design procedure.

2. In order to force inelastic deformation into the columns, the connections of the column to the footing and superstructure are designed for the maximum moments and shears that can be developed by the columns, as described in the capacity design procedures of Article 4.8. The design objective is to force inelastic deformation to occur where it can be readily inspected and repaired.
3. The performance expectation is that inelastic deformation will occur primarily in the columns. If large ductility demands occur, the columns may need to be replaced. Replacement of columns can be avoided with the use of the control and repairability design approach or with the use of a low  $R$ -factor ( $< 3$ ) or with the use of the seismic isolation design alternative to reduce the elastic force demand on the columns.

#### *Abutments as an Additional Energy-Dissipation Mechanism*

1. In the early phases of the development of the *Specifications*, there was serious debate as to whether or not the abutments would be included and relied upon in the earthquake resisting system (ERS). Some states may require the design of a bridge where the substructures are capable of resisting all the lateral load without any contribution from the abutments. In this design approach, the abutments are included in a mechanism to provide an unquantifiable higher level of safety. Rather than mandate this design philosophy here, it was decided to permit two design alternatives. The first is where the ERS does not include the abutments and the substructures are capable of resisting all the lateral loads. In the second alternative the abutments are an important part of the ERS and, in this case, a higher level of analysis is required, for example, the Seismic Design and Analysis Procedure (SDAP) E. Furthermore, this design option requires a continuous superstructure to deliver longitudinal forces to the abutment. If these conditions are satisfied, the abutments can be designed as part of the ERS and become an additional source for dissipating the bridge's earthquake energy. In the longitudinal direction the abutment may be de-

signed to resist the forces elastically utilizing the passive pressure of the backfill. In some cases the longitudinal displacement of the deck will cause larger soil movements in the abutment backfill, exceeding the passive pressures there. This requires a more refined analysis to determine the amount of expected movement. In the transverse direction the abutment is generally designed to resist the loads elastically. In some cases (spread footings) limited movement is permitted and the elastic forces are reduced by 1.5. The design objective when abutments are relied upon to resist either longitudinal or transverse loads is either to minimize column sizes or reduce the ductility demand on the columns, accepting that damage may occur in the abutment.

2. The performance expectation is that inelastic deformation will occur in the columns as well as the abutments. If large ductility demands occur in the columns then the columns may need to be replaced. If large movements of the superstructure occur the abutment back-wall may be damaged and there may be some settlement of the abutment backfill. Large movements of the superstructure can be reduced with use of energy dissipators and isolation bearings at the abutments and at the tops of the columns. Replacement of columns can be avoided with the use of the control and repairability design approach or with the use of a low  $R$ -factor ( $< 3$ ) or with the use of the seismic isolation design alternative to reduce the demand on the columns.

There are several design alternatives available to a designer and these are summarized separately for concrete and steel superstructures.

#### **Concrete Superstructures**

- *Columns monolithic with the superstructure.*  
Energy dissipation occurring in the columns and at times in the abutment soil backfill. The control and repairability concept can be used in conjunction with this design alternative if there is a need to avoid replacing a column after a large earthquake.
- *Superstructure supported on conventional bearings.*  
Energy dissipation will occur in the columns and at times in the abutment soil backfill and to a more limited extent in some types of bear-

ings. Bearings are a critical element in the load path of this design alternative and must be demonstrated by test to be able to resist the MCE forces and displacements in both the longitudinal and transverse directions (Article 7.9 or 8.9). Alternatively, restraint systems may be used to resist the MCE forces. If failure of a bearing is part of this design concept the superstructure must have a level surface on which to slide and this configuration must be analyzed since load redistribution will occur (Article 7.9 or 8.9).

- *Superstructure supported on isolation bearings.*

Energy dissipation will occur in the isolation bearings although some may also occur in the abutment soil backfill. This permits the columns to be designed elastically thus avoiding damage in the columns.

### Steel Superstructures

- *Steel superstructure supported on either conventional or isolation bearings.*

The discussion above for concrete superstructures applies. The control and repair-ability alternative is not applicable for steel substructures.

- *Steel superstructure designed with the ductile end diaphragm concept.*

This concept, when applicable, has the ability to eliminate the ductility demand on columns in the transverse direction only. The columns are capacity-protected in the transverse direction by being designed for the maximum forces generated by the ductile end diaphragm.

### C3.3.1 Earthquake-Resisting Systems (ERS)

Selection of an appropriate ERS is fundamental to achieving adequate seismic performance. To this end, the identification of the lateral-force-resisting concept and the selection of the necessary elements to fulfill the concept should be accomplished in the conceptual design phase, or the type, size and location phase, or the design alternative phase of a project.

Seismic performance is typically better in systems with regular configurations and evenly distributed stiffness and strength. Thus, typical geometric configuration constraints, such as skew, unequal pier heights, and sharp curves, may conflict with seismic design goals. For this reason, it

is advisable to resolve potential conflicts between configuration and seismic performance early in the design effort. For example, resolution may lead to decreased skew angles at the expense of longer end spans. The resulting trade-off between performance and cost should be evaluated in the type, size, and location phase, or design alternative phase, of a project, when design alternatives are viable from a practical viewpoint.

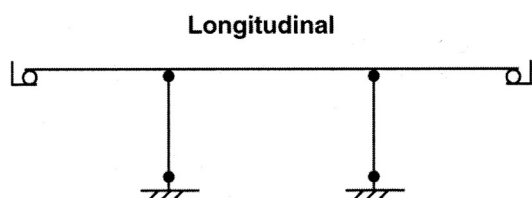
The classification of ERS and ERE into permissible and not recommended categories is meant to trigger due consideration of seismic performance that leads to the most desirable outcome, that is, seismic performance that ensures, wherever possible, post-earthquake serviceability. To achieve such an objective, special care in detailing the primary energy-dissipating elements is necessary. Conventional reinforced concrete construction with ductile plastic-hinge zones can continue to be used, but designers should be aware that such detailing, although providing desirable seismic performance, will leave the structure in a damaged state following a large earthquake. It may be difficult or impractical to repair such damage. Therefore, in order to ensure post-earthquake serviceability of the highway system as a whole, especially on essential routes with high traffic volumes, designers are encouraged to consider the use of seismic isolation devices and systems, replaceable or repairable elements that may consist of plastic hinge zones with fuse bars, and systems with supplemental or sacrificial energy-dissipation devices, such as dampers, or other yielding devices.

Under certain conditions the use of EREs that require owners' approval will be necessary. In previous AASHTO seismic specifications some of the EREs in the owners' approval category were simply not permitted for use (e.g., in-ground hinging of piles and shafts, and foundations permitted to rock beyond  $\frac{1}{2}$  uplift). These elements are now permitted, provided their deformation performance is assessed as part of a pushover analysis (Article 3.3.1). This approach of allowing their use with additional analytical effort was believed to be preferable to an outright ban on their use. Thus, it is not the objective of this specification to discourage the use of systems that require owner approval. Instead, such systems may be used, but additional design effort and consensus between the designer and owner are required to implement such systems.

Common examples from each of the three ERS and ERE categories are shown in Figures C3.3.1-1 through C3.3.1-3.

In general, the soil behind an abutment is capable of resisting substantial seismic forces that may be delivered through a continuous superstructure to the abutment. Furthermore, such soil may also substantially limit the overall movements that a bridge may experience. This is particularly so in the longitudinal direction of a straight bridge with little or no skew and with a continuous deck. The controversy with this design concept is the sce-

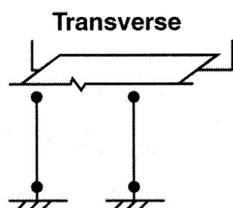
nario of what may happen if there is significant abutment damage early in the earthquake ground-motion duration and if the columns rely on the abutment to resist some of the load. This would be a problem in a long-duration, high-magnitude (greater than magnitude 7), earthquake. Unless shock transmission units (STUs) are used, a bridge composed of multiple simply supported spans cannot effectively mobilize the abutments for resistance to longitudinal force. It is recommended that simply supported spans not rely on abutments for any seismic resistance.



Abutment resistance not required as part of ERS

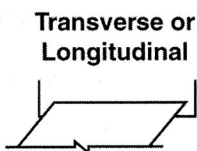
Plastic hinges in inspectable locations or elastic design of columns.

Knock-off backwalls permissible

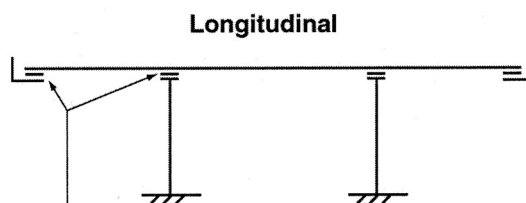


Abutment not required in ERS, breakaway shear keys permissible

Plastic hinges in inspectable locations or elastic design of columns.

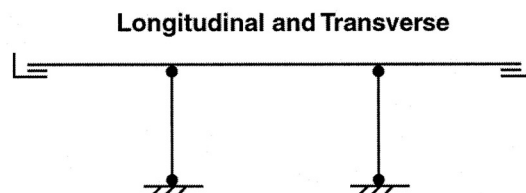


Abutment resistance required, but abutment able to resist Maximum Considered Earthquake elastically and passive soil pressure in longitudinal direction is less than  $0.70 \times$  presumptive value given in 7.5.2 and 8.5.2



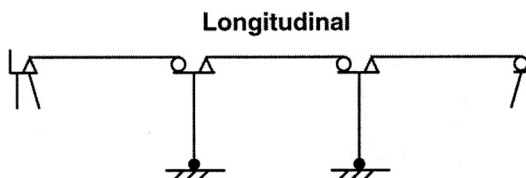
Abutment not required as part of ERS

Isolation bearings accommodate full displacement



Isolation bearings with significant energy dissipation capacity or energy dissipators are used at the abutment to limit overall displacements.

Plastic hinges in inspectable locations or elastic design of columns.



Multiple simply-supported spans with adequate seat widths. Plastic hinges in inspectable location or elastic design of columns.

**Figure C3.3.1-1a Permissible Earthquake Resisting Systems**

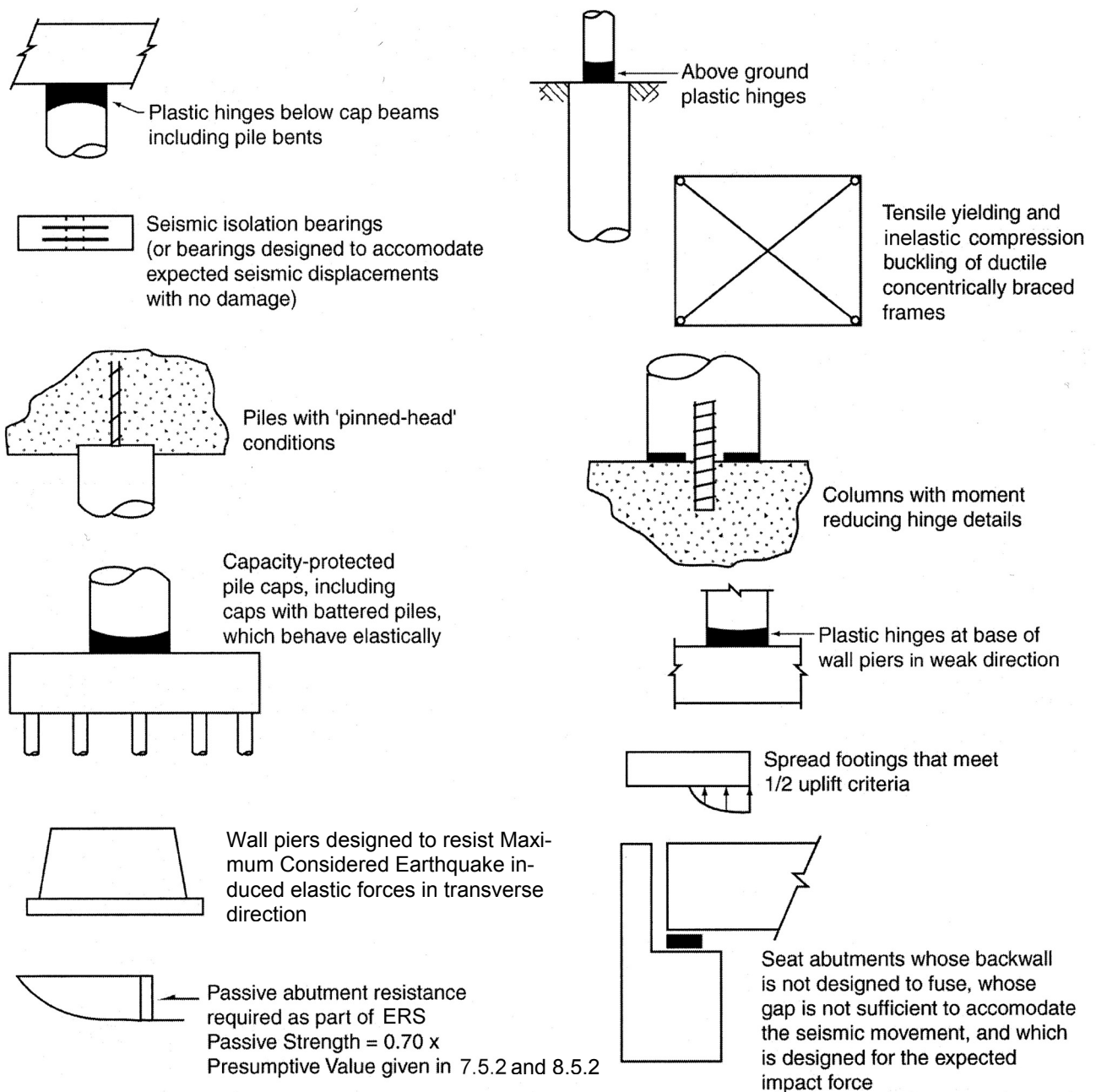


**Figure C3.3.1-1b Permissible Earthquake Resisting Elements**

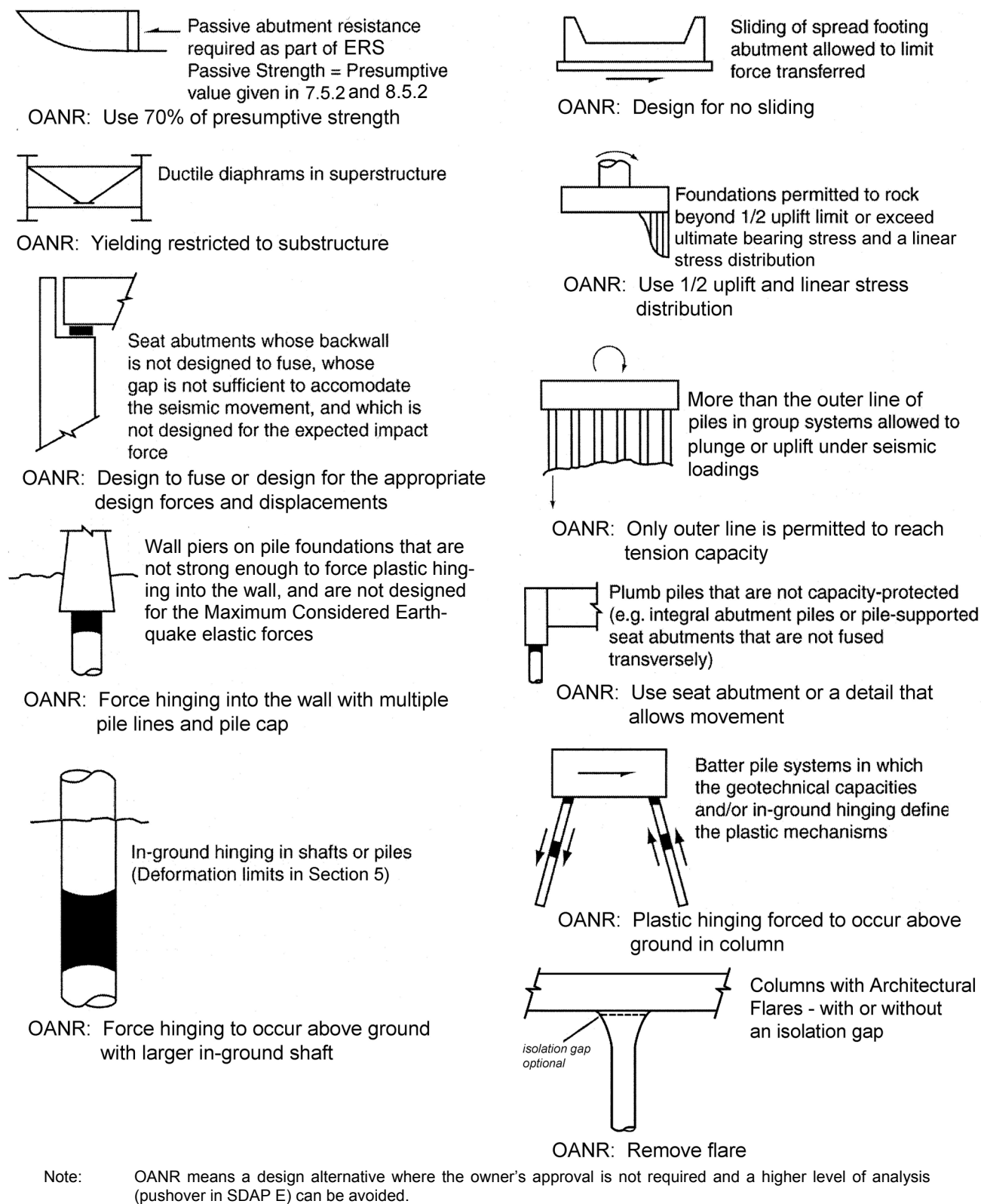


**Figure C3.3.1-2 Permissible Earthquake Resisting Elements that Require Owner's Approval, and Permissible Alternatives Where Owner's Approval Is Not Required (OANR)**



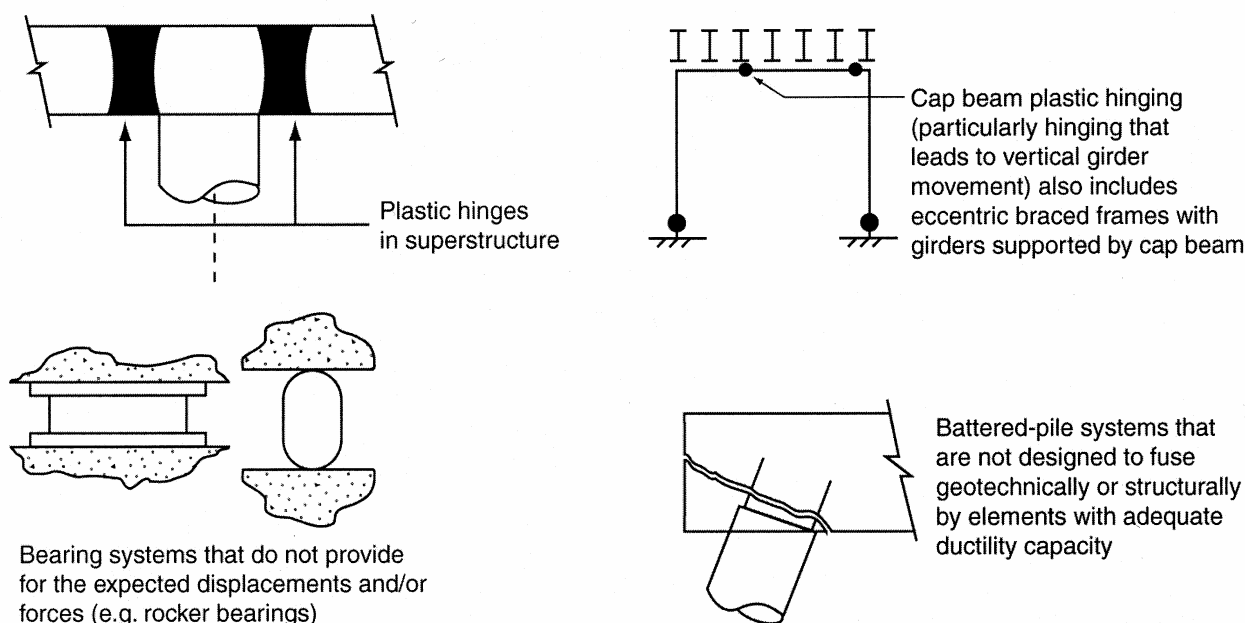


**Figure C3.3.1-3 Earthquake Resisting Elements that are not Recommended for New Bridges**

Because structural redundancy is desirable (Buckle et al., 1987), good design practice dictates the use of the design alternative where the intermediate substructures, between the abutments, are designed to resist all seismic loads, if possible. This ensures that in the event abutment resistance becomes ineffective, the bridge will still be able to resist the earthquake forces and displacements. In such a situation, the abutments provide an increased margin against collapse.

The same arguments can be made for allowing damage in locations that are very difficult to inspect. For instance, the first approach to a design using drilled shafts is to keep plastic hinging above the ground, and some states mandate this design concept. However, situations arise where this is impractical. In such situations, the ERS would require owner approval.

The flow chart in Figure 3.3.1-1 helps facilitate the decision-making process for assessing and accommodating restricted behavior.

The interrelationship between the performance level and the earthquake-resisting system is given in Table 3.3.1-1. Abutment design issues are further amplified in Table 3.3.1-2 and Fig. C3.3.1-4.

#### **C3.4 DESIGN GROUND MOTION**

Using either the general procedure or the site-specific procedure, a decision as to whether the

design motion is defined at the ground surface or some other depth needs to be made as an initial step in the design process. Article C3.4.2 provides a commentary on this issue.

Examples of conditions that could lead to a determination that Site Class F soils would not result in a significantly higher bridge response are (1) localized extent of Site Class F soils and (2) limited depth of these soft soils.

As discussed in Article C3.4.2.2, for short bridges (with a limited number of spans) having earth approach fills, ground motions at the abutments will generally determine the response of the bridge. If Site Class F soils are localized to the intermediate piers and are not present at the abutments, the bridge engineer and geotechnical engineer might conclude that the response of interior piers would not significantly affect bridge response.

Article C3.4.2.2 also describes cases where the effective depth of input ground motion is determined to be in stiffer soils at depth, below a soft surficial layer. If the surficial layer results in a classification of Site Class F and the underlying soil profile classifies as Site Class E or stiffer, a determination might be made that the surficial soils would not significantly increase bridge response.

For purposes of these provisions, an active fault is defined as a fault whose location is known

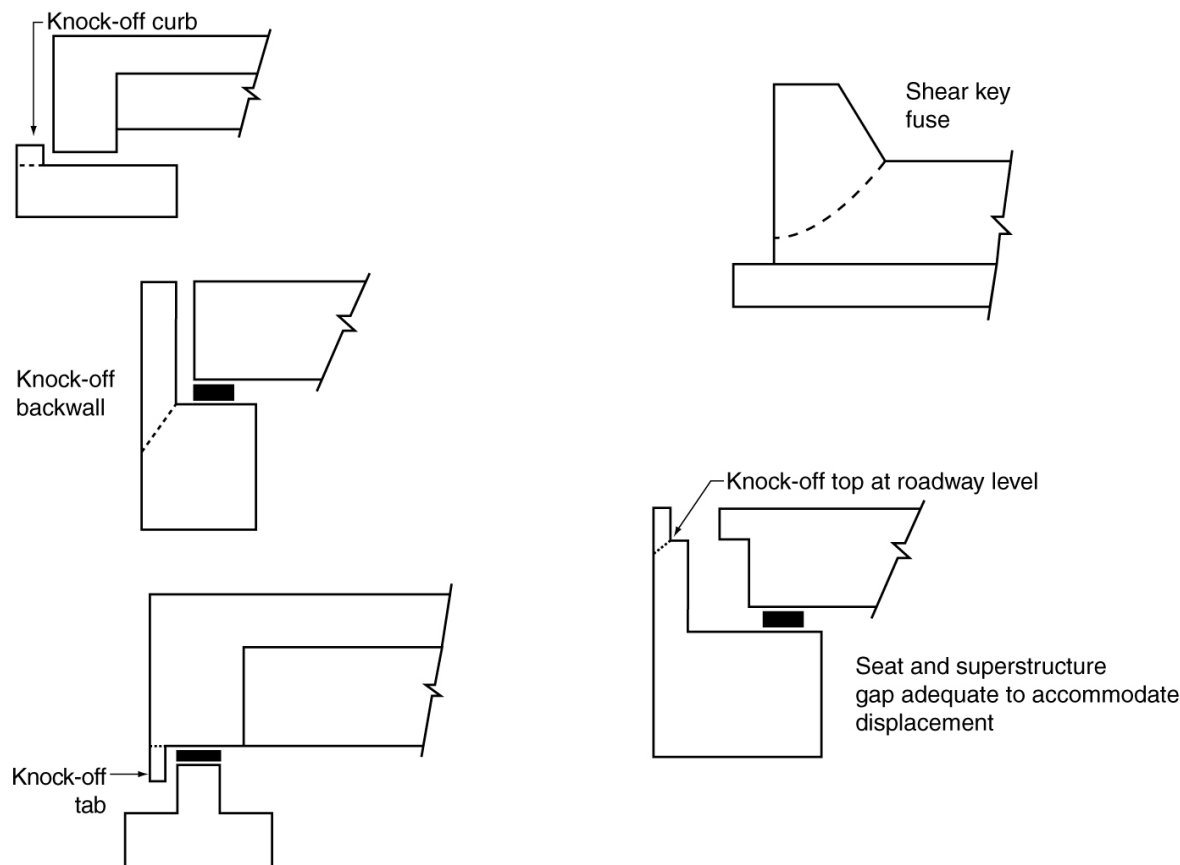


**Figure C3.3.1-4 Methods of Minimizing Damage to Abutment Foundation**

or can reasonably be inferred, and which has exhibited evidence of displacement in Holocene (or recent) time (in the past 11,000 years, approximately). Active fault locations can be found from maps showing active faults prepared by state geological agencies or the U.S. Geological Survey. Article C3.4.3 describes near-fault ground-motion effects that are not included in national ground-motion mapping and could potentially increase the response of some bridges. Normally, site-specific evaluation of these effects would be considered only for major or very important bridges.

#### **C3.4.1 Design Spectra Based on General Procedure**

National ground-motion maps described in the Part I *Specification* are based on probabilistic national ground motion mapping conducted by the U.S. Geological Survey (USGS) and, in California, as a joint effort between the USGS and the California Division of Mines and Geology (CDMG) (Frankel et al., 1996; 1997a; 1997b; 1997c; 2000; Klein et al., 1999; Peterson et al.

1996; Wessen et al., 1999a; 1999b). As described in Commentary to Article 3.2, maps for the rare earthquake (MCE) are for a probability of exceedance of 3% in 75 years but are bounded deterministically near highly active faults. Large scale MCE maps may be obtained from USGS, Golden, Colorado. These maps were originally published in the 1997 edition of the NEHRP Provisions (BSSC, 1998), and subsequently in the 2000 edition of the International Building Code (ICC, 2000). The development of the MCE maps is described in BSSC (1998), Hamburger and Hunt (1997), and Leyendecker et al. (2000b). Ground motions for the expected, or average, earthquake are for a probability of exceedance of 50% in 75 years. Paper maps for the Expected Earthquake as of the date of this printing; however, map values at any location may be obtained by interpolation from the seismic hazard curves on the CD-ROM published by the USGS (Frankel and Leyendecker, 2001).

In lieu of using national ground motion maps referenced in this *Guideline*, ground-motion response spectra may be constructed, based on ap-

proved state ground-motion maps. To be accepted, the development of state maps should conform to the following:

1. The definition of design ground motions should be the same as described in Article 3.2 and Table 3.2-1.
2. Ground-motion maps should be based on a detailed analysis demonstrated to lead to a quantification of ground motion, at a regional scale, that is as accurate or more so, as is achieved in the national maps. The analysis should include: characterization of seismic sources and ground motion that incorporates current scientific knowledge; incorporation of uncertainty in seismic source models, ground motion models, and parameter values used in the analysis; detailed documentation of map development; and detailed peer review. The peer review process should preferably include one or more individuals from the U.S. Geological Survey who participated in the development of the national maps.

Upper bounds of  $1.5g$  on  $S_S$  and  $0.6g$  on  $S_I$  similar to those included in the *International Building Code* (ICC, 2000) for regular structures were incorporated because in areas of high ground motion increasing design force levels may not produce the desired goal of having a bridge that has the best possible deformation capacity to handle the high ground motion that could occur. As a consequence a cap is placed on the design forces, a “pushover” analysis is mandated, and the deformation limits of the pushover analysis are increased.

For a single-mode method of analysis, Equations 3.4.1-1, -2, -4, and -5 may be used to calculate  $C_d$  (i.e.,  $C_d = \frac{S_{D1}}{T} \leq S_{DS}$ ) where  $S_{DS} = S_a = C_d$  for  $T \leq T_S$  (i.e., no reduction in  $S_a$  for  $T < T_0$ , as permitted by Equation 3.4.1-3).

For periods exceeding approximately 3 seconds, depending on the seismic environment, Equation 3.4.1-5 may be conservative because the ground motions may be approaching the constant spectral displacement range for which  $S_a$  decays with period as  $1/T^2$ . Equation 3.4.1-5 should be used unless a more appropriate long-period spectrum decay is determined based on a site-specific study.

### C3.4.2 Site Effects on Ground Motion

The site classes and site factors described in this article were originally recommended at a site response workshop in 1992 (Martin, ed., 1994). Subsequently they were adopted in the seismic design criteria of Caltrans (1999), the 1994 and the 1997 edition of the *NEHRP Recommended Provisions for Seismic Regulations for New Buildings and Other Structures* (BSSC, 1995, 1998), the 1997 *Uniform Building Code* (UBC) and the 2000 *International Building Code* (ICC, 2000). The bases for the adopted site classes and site factors are described by Martin and Dobry (1994), Rinne (1994), and Dobry et al. (2000).

Procedures described in this article were originally developed for computing ground motions at the ground surface for relatively uniform site conditions. Depending on the site classification and the level of the ground motion, the motion at the surface could be different from the motion at depth. This creates some question as to the location of the motion to use in the bridge design. It is also possible that the soil conditions at the two abutments are different or they differ at the abutments and interior piers. An example would be where one abutment is on firm ground or rock and the other is on a loose fill. These variations are not always easily handled by simplified procedures described in this commentary. For critical bridges it may be necessary to use more rigorous numerical modeling to represent these conditions. The decision to use more rigorous numerical modeling should be made after detailed discussion of the benefits and limitations of more rigorous modeling between the bridge and geotechnical engineers.

**Geologic Differences:** If geotechnical conditions at abutments and intermediate piers result in different soil classifications, then response spectra should be determined for each abutment and pier having a different site classification. The design response spectra may be taken as the envelope of the individual spectra. However, if it is assessed that the bridge response is dominated by the abutment ground motions, only the abutment spectra need be enveloped (Article C3.4.2.2).

#### C3.4.2.1 Site Class Definitions

Steps for Classifying a Site (also see Table 3.4.2-1)

Step 1: Check the site against the three categories of Site Class F, requiring site-specific evaluation. If the site corresponds to any of these

categories, classify the site as Site Class F and conduct a site-specific evaluation.

Step 2: Categorize the site using one of the following three methods, with  $\bar{v}_s$ ,  $\bar{N}$ , and  $\bar{s}_u$  computed in all cases as specified by the definitions in Article 3.4.2.2:

Method a:  $\bar{v}_s$  for the top 30 m (100 ft) ( $\bar{v}_s$  method)

Method b:  $\bar{N}$  for the top 30 m (100 ft) ( $\bar{N}$  method)

Method c:  $\bar{N}_{ch}$  for cohesionless soil layers (PI < 20) in the top 30 m (100 ft) and average  $\bar{s}_u$  for cohesive soil layers (PI > 20) in the top 30 m (100 ft) ( $\bar{s}_u$  method)

$\bar{N}_{ch}$  and  $\bar{s}_u$  are averaged over the respective thickness of cohesionless and cohesive soil layers within the upper 30 m (100 ft). Refer to Article 3.4.2.2 for equations for calculating average parameter values for the methods a, b, and c above. If method c is used, the site class is determined as the softer site class resulting from the averaging to obtain  $\bar{N}_{ch}$  and  $\bar{s}_u$  (for example, if  $\bar{N}_{ch}$  were equal to 20 blows/0.30 m (blows/ft) and  $\bar{s}_u$  were equal to 40 kPa (800 psf), the site would classify as E in accordance with Table 3.4.2-1). Note that when using method b,  $\bar{N}$  values are for both cohesionless and cohesive soil layers within the upper 30 m (100 feet).

As described in Article C3.4.2.2, it may be appropriate in some cases to define the ground motion at depth, below a soft surficial layer, if the surficial layer would not significantly influence bridge response. In this case, the Site Class may be determined on the basis of the soil profile characteristics below the surficial layer.

Within Site Class F (soils requiring site-specific evaluation), one category has been deleted in these specifications from the four categories contained in the previously cited codes and documents. This category consists of soils vulnerable to potential failure or collapse under seismic loading, such as liquefiable soils, quick and highly sensitive clays, and collapsible, weakly cemented soils. It was judged that special analyses for the purpose of refining site ground-motion amplifications for these soils was too severe a requirement for ordinary bridge design because such analyses would require utilization of effective stress and strength-degrading nonlinear analyses that are difficult to conduct. Also, limited case-history data and analysis results indicate that liquefaction re-

duces spectral response rather than increases it, except at long periods in some cases. Because of the general reduction in response spectral amplitudes due to liquefaction, the designer may wish to consider special analysis of site response for liquefiable soil sites to avoid excessive conservatism in assessing bridge inertia loads when liquefaction occurs. Site-specific analyses are required for major or very important structures in some cases (Article 3.4), so that appropriate analysis techniques would be used for such structures. The deletion of liquefiable soils from Site Class F only affects the requirement to conduct site-specific analyses for the purpose of determining ground motion amplification through these soils. It is still required to evaluate liquefaction occurrence and its effect on a bridge as a potential site ground-failure hazard as specified in Article 7.6 and 8.6.

#### C3.4.2.2 Definitions of Site Class Parameters

An alternative to applying Equations 3.4.2.2-2, -3, and -4 to obtain values for  $\bar{N}$ ,  $\bar{N}_{ch}$  and  $\bar{s}_u$  is to convert the N-values or  $s_u$  values into estimated shear wave velocities and then to apply Equation 3.4.2.2-1. Procedures given in Kramer (1996) can be used for these conversions.

If the site profile is particularly non-uniform, or if the average velocity computed in this manner does not appear reasonable, or if the project involves special design issues, it may be desirable to conduct shear-wave velocity measurements, using one of the procedures identified in Appendix B. In all evaluations of site classification, the shear-wave velocity should be viewed as the fundamental soil property, as this was used when conducting the original studies defining the site categories.

#### Depth of Motion Determination

For short bridges that involve a limited number of spans, the motion at the abutment will generally be the primary mechanism by which energy is transferred from the ground to the bridge superstructure. If the abutment is backed by an earth approach fill, the site classification should be determined at the base of the approach fill. The potential effects of the approach fill overburden pressure on the shear-wave velocity of the soil should be accounted for in the determination of site classification.

For long bridges it may be necessary to determine the site classification at an interior pier. If

this pier is supported on spread footings, then the motion computed at the ground surface is appropriate. However, if deep foundations (i.e., driven piles or drilled shafts) are used to support the pier, then the location of the motion will depend on the horizontal stiffness of the soil-cap system relative to the horizontal stiffness of the soil-pile system. If the pile cap is the stiffer of the two, then the motion should be defined at the pile cap. If the pile cap provides little horizontal stiffness or if there is no pile cap (i.e., pile extension), then the controlling motion will likely be at some depth below the ground surface. Typically this will be approximately 4 to 7 pile diameters below the pile cap or where a large change in soil stiffness occurs. The determination of this elevation requires considerable judgment and should be discussed by the geotechnical and bridge engineers.

For cases where the controlling motion is more appropriately specified at depth, site-specific ground response analyses can be conducted following guidelines given in Appendix C to establish ground motions at the point of fixity. This approach or alternatives to this approach should be used only with the owner's approval.

#### C3.4.2.3 Site Coefficients

No commentary is provided for Article 3.4.2.3.

#### C3.4.3 Response Spectra Based on Site-Specific Procedure

The intent in conducting a site-specific probabilistic ground motion study is to develop ground motions that are more accurate for the local seismic and site conditions than can be determined from national ground motion maps and the procedure of Article 3.4.1. Accordingly, such studies must be comprehensive and incorporate current scientific interpretations at a regional scale. Because there are typically scientifically credible alternatives for models and parameter values used to characterize seismic sources and ground-motion attenuation, it is important to incorporate these uncertainties formally in a site-specific probabilistic analysis. Examples of these uncertainties include seismic source location, extent and geometry; maximum earthquake magnitude; earthquake recurrence rate; and ground-motion attenuation relationship.

Guidelines are presented in Appendix C for site-specific geotechnical investigations and dynamic site response analyses for Site Class F soils. These guidelines are applicable for site-specific determination of site response for any site class when the site response is determined on the basis of a dynamic site response analysis.

Near-fault effects on horizontal response spectra include: (1) higher ground motions due to the proximity of the active fault; (2) directivity effects that increase ground motions for periods greater than 0.5 second if the fault rupture propagates toward the site; and (3) directionality effects that increase ground motions for periods greater than 0.5 second in the direction normal (perpendicular) to the strike of the fault. If the active fault is included and appropriately modeled in the development of national ground motion maps, then effect (1) is already included in the national ground motion maps. Effects (2) and (3) are not included in the national maps. These effects are significant only for periods longer than 0.5 second and normally would be evaluated only for major or very important bridges having natural periods of vibration longer than 0.5 second. Further discussion of effects (2) and (3) are contained in Somerville (1997) and Somerville et al. (1997). The ratio of vertical-to-horizontal ground motions increases for short-period motions in the near-fault environment. Site-specific vertical response spectra should be developed where required based on Article 3.4.5.

The application of site-specific deterministic limits on response spectra in areas of active faults follows criteria that are similar to the criteria used in constructing deterministic bounds for national ground motion maps for the MCE. However, site-specific deterministic spectra are calculated as median-plus-one-standard-deviation values rather than the nominal 1.5-times-median values used for national ground motion maps (refer to commentary to Article 3.2).

#### C3.4.4 Acceleration Time Histories

Characteristics of the seismic environment of the site to be considered in selecting time-histories include: tectonic environment (e.g., subduction zone; shallow crustal faults in western United States or similar crustal environment; eastern United States or similar crustal environment); earthquake magnitude; type of faulting (e.g., strike-slip; reverse; normal); seismic-source-to-site distance; local site conditions; and design or ex-

pected ground-motion characteristics (e.g., design response spectrum; duration of strong shaking; and special ground-motion characteristics such as near-fault characteristics). Dominant earthquake magnitudes and distances, which contribute principally to the probabilistic design response spectra at a site, as determined from national ground motion maps, can be obtained from deaggregation information on the U.S. Geological Survey website: <http://geohazards.cr.usgs.gov/eq/>.

It is desirable to select time-histories that have been recorded under conditions similar to the seismic conditions at the site listed above, but compromises are usually required because of the multiple attributes of the seismic environment and the limited data bank of recorded time-histories. Selection of time-histories having similar earthquake magnitudes and distances, within reasonable ranges, are especially important parameters because they have a strong influence on response spectral content, response spectral shape, duration of strong shaking, and near-source ground-motion characteristics. It is desirable that selected recorded motions be somewhat similar in overall ground motion level and spectral shape to the design spectrum to avoid using very large scaling factors with recorded motions and very large changes in spectral content in the spectrum-matching approach. If the site is located within 10 km (6.25 miles) of an active fault, then intermediate-to-long-period ground-motion pulses that are characteristic of near-source time-histories should be included if these types of ground motion characteristics could significantly influence structural response. Similarly, the high short-period spectral content of near-source vertical ground motions should be considered.

Ground-motion modeling methods of strong-motion seismology are being increasingly used to supplement the recorded ground-motion database. These methods are especially useful for seismic settings for which relatively few actual strong-motion recordings are available, such as in the central and eastern United States. Through analytical simulation of the earthquake rupture and wave-propagation process, these methods can produce seismologically reasonable time series.

Response-spectrum-matching approaches include methods in which time series adjustments are made in the time domain (Lilhanand and Tseng, 1988; Abrahamson, 1992) and those in which the adjustments are made in the frequency domain (Gasparini and Vanmarcke, 1976; Silva and Lee, 1987; Bolt and Gregor, 1993). Both of

these approaches can be used to modify existing time-histories to achieve a close match to the design response spectrum while maintaining fairly well the basic time-domain character of the recorded or simulated time-histories. To minimize changes to the time-domain characteristics, it is desirable that the overall shape of the spectrum of the recorded or simulated time-history not be greatly different from the shape of the design response spectrum and that the time-history initially be scaled so that its spectrum is at the approximate level of the design spectrum before spectrum matching.

When developing three-component sets of time histories by simple scaling rather than spectrum matching, it is difficult to achieve a comparable aggregate match to the design spectra for each component of motion when using a single scaling factor for each time-history set. It is desirable, however, to use a single scaling factor to preserve the relationship between the components. Approaches for dealing with this scaling issue include: (1) use of a higher scaling factor to meet the minimum aggregate match requirement for one component while exceeding it for the other two; (2) use of a scaling factor to meet the aggregate match for the most critical component with the match somewhat deficient for other components; (3) compromising on the scaling by using different factors as required for different components of a time-history set. While the second approach is acceptable, it requires careful examination and interpretation of the results and possibly dual analyses for application of the horizontal higher horizontal component in each principal horizontal direction.

The requirements for the number of time histories to be used in nonlinear inelastic dynamic analysis and for the interpretation of the results take into account the dependence of response on the time domain character of the time histories (duration, pulse shape, pulse sequencing) in addition to their response spectral content.

Additional guidance on developing acceleration time histories for dynamic analysis may be found in publications by the Caltrans Seismic Advisory Board Adhoc Committee (CSABAC) on Soil-Foundation-Structure Interaction (1999) and the U.S. Army Corps of Engineers (2000). CSABAC (1999) also provides detailed guidance on modeling the spatial variation of ground motion between bridge piers and the conduct of seismic soil-foundation-structure interaction (SFSI) analy-

ses. Both spatial variations of ground motion and SFSI may significantly affect bridge response. Spatial variations include differences between seismic wave arrival times at bridge piers (wave passage effect), ground motion incoherence due to seismic wave scattering, and differential site response due to different soil profiles at different bridge piers. For long bridges, all forms of spatial variations may be important. For short bridges, limited information appears to indicate that wave passage effects and incoherence are, in general, relatively unimportant in comparison to effects of differential site response (Shinozuka et al., 1999; Martin, 1998). Somerville et al. (1999) provide guidance on the characteristics of pulses of ground motion that occur in time histories in the near-fault region.

### C3.4.5 Vertical Acceleration Effects

The most comprehensive study (Button et al., 1999) performed to date on the impact of vertical acceleration effects indicates that for some design parameters (superstructure moment and shear, column axial forces) and for some bridge types the impact can be significant. The study was based on vertical response spectra developed by Silva (1997) from recorded western United States ground motions. Until more information is known about the characteristics of vertical ground motions in the central and eastern United States and those areas impacted by subductions zones in the Pacific, this Guideline does *not* provide specific recommendations. However, it is advisable for designers to be aware that vertical acceleration effects may be important (Button et al., 1999) and, for more important bridges, should be assessed.

Recent studies (e.g. Abrahamson and Silva, 1997; Silva, 1997; Campbell and Bozorgnia, 2000) have shown that the ratio of the vertical response spectrum to the horizontal response spectrum of ground motions can differ substantially from the nominal two-thirds ratio commonly assumed in engineering practice. These studies show that the ratios of vertical to horizontal response spectral values are functions of the tectonic environment, subsurface soil or rock conditions, earthquake magnitude, earthquake-source-to-site distance, and period of vibration. Whereas the two-thirds ratio may be conservative for longer periods of vibration (say greater than 0.3 second) in many cases, at shorter periods, the ratio of vertical to horizontal response spectra may exceed two-thirds and even substantially exceed unity for close earthquake

source-to-site distances and periods less than 0.2 second. At present, detailed procedures have not been developed for constructing vertical spectra having an appropriate relationship to the horizontal spectra constructed using the general procedure of Article 3.4.1. When developed, these procedures could be used in conjunction with deaggregation information on dominant earthquake source-to-site distance and earthquake magnitude from the USGS national map Internet website [<http://geohazards.cr.usgs.gov/eq/>] to construct vertical spectra at any location.

At present, this guideline recommends explicit consideration of vertical acceleration effects in design only as a function of the distance of a bridge site from an active fault. As such, these requirements would generally not be applied to sites in the central and eastern United States because few active faults meeting the definition in Article 3.2 have been accurately located in that part of the country. Also, because the characteristics of vertical ground motions in subduction zones have been the subject of only limited studies, the guideline does not at present impose requirements for vertical acceleration effects as a function of distance from subduction zone faults.

For use in Tables 3.4.5-1 and 3.4.5-2, earthquake magnitude is taken as the largest (maximum) magnitude, based on the moment magnitude scale (rather than the Richter, or local, magnitude), of an earthquake considered capable of occurring on the active fault. Usually, maximum magnitude is estimated on the basis of the longest rupture length or the largest rupture area assessed as achievable during an earthquake on the fault (e.g., Wells and Coppersmith, 1994). Maximum magnitude should be estimated by a knowledgeable geologist or seismologist.

### C3.5 LOAD FACTORS

Extreme Event-I limit state includes water loads, WA. The probability of a major flood and an earthquake occurring at the same time is small. Therefore, basing water loads and scour depths on mean discharges may be warranted. Live load coincident with an earthquake is only included for bridges with heavy truck traffic (i.e., high ADTT) and for elements particularly sensitive to gravity loading.

Because of the difficulty in predicting the partial live load to be applied with earthquake loads, and the probability that this live load will be significantly below the AASHTO design live load, it

is acceptable to use  $\gamma_{EQ}$  values with AASHTO live-load envelopes. Universally acceptable methods for determining values for  $\gamma_{EQ}$  have not been established, but values between 0.25 and 0.40 have been suggested for use in design when live load is included.

### C3.6 COMBINATION OF SEISMIC FORCE EFFECTS

The combination of seismic forces computed from a response spectrum analysis has three aspects.

The first is the combination of the vibration modes due to ground motion in one direction (longitudinal, transverse, or vertical). The CQC method ("complete quadratic combination") provides a good estimate of the maximum force, including the correlation of modal responses closely spaced in frequency.

The second is the contribution of two or three orthogonal ground motion components to a single force effect. The SRSS rule ("square root sum of the squares") is the most appropriate rule for combining the contribution of orthogonal, and uncorrelated, ground motion components to a single seismic force. The SRSS method is recommended particularly for seismic analysis including vertical ground motion (Button et. al. 1999). Prior AASHTO seismic provisions were based on a 100% - 30% combination. It was decided to modify this and permit a 100% - 40% combination rule as an alternative to the SRSS combination rule. The 100%-40% combination of forces provides results similar to the SRSS combination when the same response spectrum is used in two orthogonal directions (Clough and Penzien, 1993).

For three components of ground motions the combination rules of a bending moment are as follows.

SRSS Combination:

$$M_x = \sqrt{(M_x^T)^2 + (M_x^L)^2 + (M_x^V)^2}$$

100% - 40% Combination:

$$M_x^{LC1} = 1.0M_x^T + 0.4M_x^L + 0.4M_x^V$$

$$M_x^{LC2} = 0.4M_x^T + 1.0M_x^L + 0.4M_x^V$$

$$M_x^{LC3} = 0.4M_x^T + 0.4M_x^L + 1.0M_x^V$$

Third is the combination of two force quantities when biaxial design of a member is important (e.g. circular column). This is the most difficult consideration since the maxima of the three com-

ponents (axial force  $P$ , and bending moments about two local axes  $M_x$  and  $M_y$ ) are not likely to occur at the same time. A sophisticated approach to determine the critical combination is difficult to justify for design. Instead a simpler approach is adopted.

For the SRSS combination and a regular bridge the two components to be combined,  $M_x$  and  $M_y$ , utilize the 100% - 40% rule prior to obtaining the vector sum, which is then used with the positive or negative value of the maximum axial force in the design of the column. If the bridge has any significant skew or curvature, the vector sum is applied to the maximum moments. This is because the 100% - 40% rule as applied in biaxial design can be non-conservative when significant skew and curvature exist.

For the 100% - 40% combination rule the  $M_x$  and  $M_y$  components from each load case are combined to obtain the vector sum and the maximum moment of the two load cases is used with the maximum axial load in the design of the column. The combination rules are as follows:

SRSS Combination for Biaxial Design:

- For bridges with skew or curvature less than 10 degrees - Maximum of  $\sqrt{M_x^2 + (0.4M_y)^2}$  and  $\sqrt{(0.4M_x)^2 + M_y^2}$  with the maximum axial load  $\pm P$
- For bridges with skew or curvature greater than 10 degrees-  $\sqrt{M_x^2 + M_y^2}$  with the maximum axial load  $\pm P$

100%- 40% Combination for Biaxial Design:

- Maximum of  $\sqrt{(M_x^{LC1})^2 + (M_y^{LC1})^2}$  and  $\sqrt{(M_x^{LC2})^2 + (M_y^{LC2})^2}$  and  $\sqrt{(M_x^{LC3})^2 + (M_y^{LC3})^2}$  with the maximum axial load  $\pm P$

#### C3.6.1 SRSS Combination Rule

No commentary is provided for Article 3.6.1.

#### C3.6.2 100% - 40% Combination Rule

No commentary is provided for Article 3.6.2.



**C3.7 SELECTION OF SEISMIC HAZARD LEVEL (SHL), SEISMIC DESIGN AND ANALYSIS PROCEDURES (SDAP) AND SEISMIC DESIGN REQUIREMENTS (SDR)**

The Seismic Hazard Level is defined as a function of the magnitude of the ground surface shaking as expressed by  $F_v S_I$  and  $F_a S_s$ . Bridges with a period greater than 1 second would be more appropriately governed by the  $F_v S_I$  definition whereas bridges with a period less than 0.7 second would be more appropriately governed by the  $F_a S_s$  definition. Since the period of the bridge is not known at an early stage in the design process both criteria are therefore used to define the Seismic Hazard Level. The two footnotes to Table 3.7-1 effectively limit boundaries for Soil Types E and F in Hazard Levels I and II to those of Soil Type D. This decision was made in part because of the

greater uncertainty in the values of  $F_v$  and  $F_a$  for Type E and F soils when ground shaking is relatively low ( $S_I < 0.10$  and  $S_s < 0.25$ ) and in part to not extend the boundaries beyond those of Soil Type D until the impact of this major revision of the specification is better understood.

Seismic design and analysis procedures (SDAP) and seismic design requirements (SDR) reflect the variation in seismic risk across the country and are used to permit different requirements for methods of analysis, minimum support lengths, column design details, and foundation and abutment design procedures.

**C3.8 TEMPORARY AND STAGED CONSTRUCTION**

The option to use a reduced acceleration coefficient is provided to reflect the limited exposure period.



## Section 4: Commentary

### DESIGN AND ANALYSIS PROCEDURES (SDAP)

#### C4.1 SINGLE SPAN BRIDGES

Requirements for single span bridges are not as rigorous as for multi-span bridges because of their favorable response to seismic loads in past earthquakes. As a result, single span bridges need not be analyzed for seismic loads, regardless of the SDR, and design requirements are limited to minimum seat widths and connection forces. Adequate seat widths must be provided in both the transverse and longitudinal directions. Connection forces are based on the premise that the bridge is stiff and that the fundamental period of response is short. This assumption acknowledges the fact that the period of vibration is difficult to calculate because of significant interaction with the abutments.

These reduced requirements are also based on the assumption that there are no vulnerable substructures (i.e., no columns) and that a rigid (or near rigid) superstructure is in place to distribute the in-plane loads to the abutments. If, however, the superstructure is not able to act as a stiff diaphragm and sustains significant in-plane deformation during horizontal loading, it should be analyzed for these loads and designed accordingly. Single span trusses may be sensitive to in-plane loads and the designer may need to take additional precautions to ensure the safety of truss superstructures.

#### C4.2 SDAP A1 AND A2

In areas of low seismicity, only minimum seat widths (Article 6.3), minimum connection design forces for bearings, and minimum shear reinforcement in concrete columns and piles in SDR 2, are deemed necessary for the life-safety performance level. These default values are used as minimum design forces in lieu of rigorous analysis. The division of SDAP A1 and A2 at a short-period spectral response acceleration of 0.10 is an arbitrary expedient intended to provide some relief to parts of the country with very low seismicity.

This article describes the minimum connection force that must be transferred from the superstructure to its supporting substructures through the bearings. It does not apply if the connection is a

monolithic structural joint. Similarly, it does not apply to unrestrained bearings or in the unrestrained directions of bearings that are free to move (slide) in one direction but fixed (restrained) in an orthogonal direction. The minimum force is simply 0.1 or 0.25 times the weight that is effective in the restrained direction. The calculation of the effective weight requires care and may be thought of as a tributary weight. It is calculated from the length of superstructure that is tributary to the bearing in the direction under consideration. For example, in the longitudinal direction at a fixed bearing, this length will be the length between expansion joints and may include more than one span if it is a continuous girder. But in the transverse direction at the same bearing, this length may be as little as one-half of the span if the bearing is located at an expansion joint. This is because the expansion bearings at the adjacent piers will generally be transversely restrained and able to transfer these transverse loads to the substructure.

It is important that not only the bearing but also the details that fasten the bearing to the sole and masonry plates (including the anchor bolts which engage the supporting members), have sufficient capacity to resist the above forces. At a fixed bearing, it is necessary to consider the simultaneous application of the longitudinal and transverse connection forces when checking these capacities.

The primary purpose of this requirement is to ensure that the connections between the superstructure and its supporting substructures remain intact during the design earthquake and thus protect the girders from being unseated. The failure of these connections has been observed in many earthquakes and imposing minimum strength requirements is considered to be a simple but effective strategy to minimize the risk of collapse. However, in areas of low seismic hazard it is not necessary to design the substructures or their foundations for these forces since it is expected that if a column does yield it will have sufficient inherent ductility to survive without collapse. Even though bridge columns in SDR 2 are not required to be designed for seismic loads, minimum

shear reinforcement requirements will provide a minimum level of capacity for ductile deformations which is considered to be adequate for the magnitude and duration of the ground motion expected in SDR 2.

The magnitude of live load assumed to exist at the time of the earthquake should be consistent with the value of  $\gamma_{eq}$  used in conjunction with Table 3.5-1.

#### **C4.3 SDAP B — NO SEISMIC DEMAND ANALYSIS**

The option for no seismic demand analysis is an important new addition to the provisions because it applies in the expanded areas now requiring more detailed seismic design. These provisions provide the designers of regular bridges (that comply with certain restrictions) with the ability to design a structure without the need to undertake a dynamic analysis. The bridge is designed for all non-seismic requirements and capacity design procedures are then used to determine shear reinforcement and confining reinforcement requirements. Capacity design principles are also used for the connection forces of the columns to the pile cap or spread footing, and of the columns to the superstructure or bent cap. There are no seismic design requirements for abutments except that integral abutments need to be designed for passive pressure. The superstructure displacements anticipated in these low seismicity zones are expected to be relatively modest and significant abutment contribution to the response of the bridge is not anticipated but if it occurs it will reduce substructure displacements. The design forces for the soil and pile aspects of foundation design are the overstrength forces from the columns but using an overstrength ratio of 1.0 as specified in Article 4.8.1. The use of the lower overstrength ratio for SDR 3 implies that there will be some limited ductility demand on the piles in the event of the Maximum Considered Earthquake (MCE). Since shear and confining reinforcement are also required at the top of the piles, for a depth of  $3D$ , this reduction in foundation design forces was believed to be prudent in the lower seismic risk areas. Current AASHTO Division I-A requirements (SPC B) do not require capacity design of the foundation; instead, the foundations are designed for twice the column design forces. Converting to a capacity design approach with an overstrength ratio of 1.0 will lead to a more uniform level of seismic resistance in these lower seismic areas.

##### **C4.3.1 No Analysis Approach**

No commentary is provided for Article 4.3.1.

##### **C4.3.2 Limitations**

The restrictions on the application of this procedure were developed to ensure that the bridge had a reasonably regular configuration and that unusually high loads would not be present. Furthermore, it is important that most of the substructures contribute to resisting both the transverse and longitudinal lateral loads. A multi-pier bridge, in which only one pier resists longitudinal loads, needs to be analyzed prior to its detailed design. The restrictions on the method were based on engineering judgment and should be refined as research on this design approach progresses.

Structures with low axial loads or strong columns (i.e., more steel and large column and pile sizes) have a greater intrinsic strength and are able to resist the design ground motions with less damage. However, ductile detailing still needs to be provided in accordance with Articles 7.7 and 7.8.

The no-analysis option is not applicable to steel braced-frame substructures. In the case of a cantilever column, in a pile bent configuration, the length  $L$  in the  $L/b < 10$  criteria would be equal to the length above ground to the top of the bent plus 3 pile bent diameters.

These provisions do not apply for bridges whose piers have different heights because one or more piers will attract significantly more lateral load. Designers are encouraged to design the portion of piers participating in a seismic mechanism to have similar column lengths.

Variable span lengths can also create uneven loading conditions on the piers resulting from unusual modal behavior and are therefore not permitted.

For highly skewed and curved bridges, biaxial loadings on the piers have problems from a design point of view and hence this method is not applicable. Moreover, extra care needs to be taken in assessing the displacement demands at joints and bearings.

Designers are actively discouraged from using one pier to resist all longitudinal inertia loads when using this analysis method. The further limit on  $F_v S_1$  due to a lesser number of bents participating is a first attempt to limit this type of configuration. Its use is most appropriate when all supporting bents participate in the ERS.

Careful and site-specific analysis of soil-structure interaction is needed at sites with liquefaction or lateral-spreading potential and hence this is another limit on the method.

### C4.3.3 Capacity Design and Strength Requirements of Members Framing into Columns

The principles of capacity design require that the strength of those members that are not part of the primary energy-dissipating system be stronger than the overstrength capacity of the primary energy-dissipating members—that is, the columns with hinges at their member ends.

The geotechnical features of foundations (i.e. soil bearing, and side friction and end bearing on piles) possess inherent ductility. At low to moderate levels of seismic input this manifests itself as minor rocking of the foundation or nominal permanent settlements which do not significantly affect the service level of the bridge.

Full capacity protection of the geotechnical features of the foundation in SDAP B is not required. Should the rare, large, earthquake occur, some limited ductility demand may occur in the piles and some minor rocking and permanent settlement may occur. This trade-off, compared to current practice for SPC B in the existing AASHTO provisions, is considered prudent.

## C4.4 SDAP C — CAPACITY SPECTRUM DESIGN METHOD

### C4.4.1 Capacity Spectrum Design Approach

The capacity spectrum design method is conceptually the same as the Caltrans displacement-based design method. The primary difference is that the capacity spectrum approach begins with the existing nonseismic capacity of the columns and then assesses the adequacy of the resulting displacements. The Caltrans procedure uses methods to estimate the maximum displacement that can be tolerated and then assesses the minimum strength requirements for the column.

The key equation used in the capacity spectrum method is the relationship between the seismic capacity coefficient,  $C_c$ , and displacement,  $\Delta$ :

$$C_c \Delta = \left( \frac{F_v S_1}{2\pi B_L} \right)^2 g \quad \text{C.4.4-1}$$

in which  $S_1$  is the spectral acceleration coefficient at 1-second period,  $F_v$  is the site factor for the earthquake event, and  $g$  is the acceleration due to gravity ( $32.2 \text{ ft/sec}^2$  or  $9.8 \text{ m/sec}^2$ ). The factor  $B_L$  reduces the demand to account for inelastic deformation capacity of the earthquake resisting elements; Table 5.4.1-1 gives  $B_L$  for the two earthquake events and two performance levels. This equation is valid in the velocity-sensitive region of the response spectrum and is applicable to most bridges of a regular configuration that respond essentially as single-degree-of-freedom system. The complete design procedure includes steps for shorter period bridges, such as those with pier walls, but such cases are not discussed in this commentary.

Bridges that have elastomeric or sliding bearings at each pier shall be designed as isolated structures using all of the provisions of Article 15 because it is essential that the columns remain essentially elastic (i.e.,  $R = 1.5$ ).

The following detailed summary of this method expands on the procedure outlined in the Guidelines. It focuses on conservative estimates of strength and displacement. More refined techniques may be used which still satisfy the capacity spectrum method, but for most cases the simple approach described herein provides efficient designs that will satisfy the performance requirements defined in the *Specifications*, Part I.

#### Step 1

During design for all non-seismic requirements, determine if the configuration and component requirements for a regular bridge are satisfied. If so, the capacity spectrum procedure may be used.

#### Step 2

Determine  $F_v$  and  $S_1$  for the Expected Earthquake event. In the longitudinal and transverse direction, perform the following sub steps:

- 2-1: Compute the yield displacement,  $\Delta_y$ , for each participating bent or pier and set  $\Delta_y$  to 1.3 times the smallest value. Note that a participating pier or bent is one whose fixity conditions permit it to resist horizontal lateral loads. It is possible a pier may participate transversely but not longitudinally due to a bearing that has transverse fixity and longitudinal movement.
- 2-2: Compute the lateral strength of each participating pier or bent, and sum the strengths to

give the lateral strength of the bridge,  $V_n$ . The seismic capacity coefficient for the bridge is  $C_c = V_n/W$ , in which  $W$  is the weight of the bridge responding to earthquake ground motion (generally the superstructure and a portion of the substructure).

- 2-3: If the following equation is satisfied for the Expected Earthquake values of  $F_v$  and  $S_1$ ,

$$C_c \Delta_y \geq \left( \frac{F_v S_1}{2\pi} \right)^2 g \quad \text{C4.4-2}$$

the bridge is expected to meet the performance requirement for the Expected Earthquake event.

#### Step 3

If the equation in *Step 2-3* is not satisfied, increase the strength of the participating piers or reconfigure the bridge so more piers participate such that  $V_n$  and  $C_c$  satisfy *Step 2-3*.

#### Step 4

Determine  $F_v$  and  $S_1$  for the MCE event. For the strength of the bridge in *Step 3*, determine if the bridge has sufficient deformation capacity according to the following substeps in the longitudinal and transverse directions:

- 4-1: Using the strength from *Step 3*, determine the maximum displacement from:

$$\Delta = \frac{1}{C_c} \left( \frac{F_v S_1}{2\pi B_L} \right)^2 g \quad \text{C4.4-3}$$

where  $B_L$  is obtained from Table 5.4.1-1.

- 4-2: Check that the maximum displacement is less than the deformation capacity for the shortest pier, with height  $H$ :

$$\Delta \leq \theta_p H \quad \text{C4.4-4}$$

for reinforced concrete columns satisfying the requirements of Article 7.8 or 8.8, the plastic rotation capacity  $\theta_p$  may be taken as 0.035 or as given in Article 7.8.6 or 8.8.6. A similar value is applicable for steel columns that satisfy the requirements of Article 7.7 or 8.7 or as given in Article 7.7.9 or 8.7.9.

- 4-3: Check that the  $P$ - $\Delta$  requirement is met using the height of the shortest participating pier:

$$\Delta \leq 0.25 C_c H \quad \text{C4.4-5}$$

If the displacement limits in *Steps 4-2* and *4-3* are met, the design is satisfactory for the MCE event.

#### Step 5

If the displacement limits in *Step 4* are not satisfied, the strength of the participating piers must be increased or additional piers must participate. For reinforced concrete columns it is necessary to increase the longitudinal reinforcement. If the reinforcement ratio exceeds 2.5%, the column size may need to be increased. The new strength can be determined as follows, in the longitudinal and transverse directions:

- 5-1: If *Step 4-2* is not satisfied, set the maximum displacement to  $\Delta = \theta_p H$ , where  $H$  is the height of the shortest participating column. Determine the required seismic coefficient from,

$$C_c = \frac{1}{\Delta} \left( \frac{F_v S_1}{2\pi B_L} \right)^2 g \quad \text{C4.4-6}$$

- 5-2: If *Step 4-3* is not satisfied, determine the required seismic coefficient from,

$$C_c = 4 \frac{\Delta}{H} \quad \text{C4.4-7}$$

where  $H$  is the height of the shortest column.

- 5-3: The required lateral strength is  $V_n = C_c W$ , where  $W$  is the total weight of the bridge, and  $C_c$  is a seismic capacity coefficient which is the ratio between the strength of the lateral-load system and the inertial weight resisted by the lateral-load system. Distribute  $V_n$  to the individual piers participating in resisting lateral loads in proportion to the tributary mass for the pier. Redesign the piers to provide the required strength.

Bridges that satisfy *Steps 4* and *5* are expected to have satisfactory performance in the MCE event for each performance level.

#### Step 6

Capacity design procedures of Article 4.8 are used to determine the shear and confinement reinforcement requirements, the column connection forces and the foundation design forces. The bridge is designed so it can resist the MCE event without any contribution from the abutment and hence there are no seismic design requirements for the abutments.

#### C4.4.2 Limitations

The configuration requirements for capacity spectrum analysis restrict application to individual frames or units that can be reasonably assumed to respond as a single-degree-of-freedom system in the transverse and longitudinal directions. When abutments do not resist significant seismic forces, the superstructure will respond as a rigid-body mass. The lateral-load-resisting piers or bents must be uniform in strength and stiffness to justify the assumption of independent translational response in the longitudinal and transverse directions. Abutments are assumed not to participate in the lateral resisting system and therefore are not part of the stiffness or strength limitations. All the lateral load is resisted by the piers.

SDAP C may be appropriate for pier wall substructures in the longitudinal direction but will not work in the transverse direction if bearings are fixed. If bearings permit movement transversely, then the capacity spectrum method for isolation bearings (Article 15.4) shall be used.

The restrictions are similar to the ones for no-analysis in Article 4.3.2.

#### C4.5 SDAP D — ELASTIC RESPONSE SPECTRUM METHOD

This is essentially a two-level analysis procedure. However, in many parts of the United States, and in the eastern United States in particular, the Expected Earthquake event will rarely govern. In most cases designers will be able to assess quickly which of the two events will produce the maximum column moments by dividing the ground response spectra for each event by the respective  $R$ -factors and comparing the resulting values. Only when the two spectra are relatively close will two analyses be required.

#### C4.6 SDAP E — ELASTIC RESPONSE SPECTRUM METHOD WITH DISPLACEMENT CAPACITY VERIFICATION

This design procedure is a key element in the philosophic development of these Guidelines. The pushover method of analysis has seen increasing use throughout the 1990s, especially in Caltrans' seismic retrofit program. This analysis method provides additional information on the expected deformation demands of columns and foundations and as such provides the designer with a greater

understanding of the expected performance of the bridge. The use of the pushover method of analysis is used in two ways. First, it encouraged designers to be as liberal as possible with the  $R$ -factor for preliminary column design, because there is an additional limit on the column plastic rotations that must be obtained from a pushover analysis.

Second, it provides a mechanism to allow EREs that need the owner's approval (Article 3.3.1). The trade-off was the need for a more sophisticated analysis in order that the expected deformations in critical elements could be assessed. Provided the appropriate limits (i.e., plastic rotations for in-ground hinges) are met, the EREs requiring the owner's approval can be used. This method applies to all the EREs shown in Figure C3.3.1.1(b).

Early drafts of these Guidelines used stress and strain limits for the deformations resulting from the pushover analysis. The difficulty in translating plastic rotations that result from most nonlinear analysis programs to element stresses and strains led to the decision to provide limits on plastic rotations as given in Articles 7.7.9 and 7.8.6 or 8.7.9 and 8.8.6.

#### C4.7 RESPONSE MODIFICATION FACTORS

These Guidelines recognize that it is uneconomical to design a bridge to resist rare, large, earthquakes elastically. Columns are assumed to deform inelastically when the actual seismic forces first exceed their design levels. These are established by dividing the elastically computed forces by the appropriate  $R$ -factor. Most other elements of the ERS are designed by capacity design procedures for the maximum forces that can be developed by plastic hinges in the columns or the elastic forces from the analysis.

The most important  $R$ -factor is that of the supporting substructure. Since a bridge closely approximates a single-degree-of-freedom (SDOF) system, the design process is schematically shown in Figure C3.3-2 and discussed in Article C3.3. There has been a considerable amount of research over the past ten years on the relationship between the ductility demand of a SDOF system and its design strength. For example, if we assume an element has a displacement ductility capacity  $\mu$  at a given value, we would like to know the design force necessary to ensure that this ductility is not exceeded. A good overview of this issue can be found in ATC-18 (ATC, 1997), which summarizes

the work of Miranda and Bertero (1996), Nasser and Krawinkler (1991) and Chang and Mander (1994a; 1994b). Figure C4.7-1 shows a smoothed relationship (Miranda and Bertero, 1996) between the ductility factor  $\mu$  and  $R$  for two sites. Note that  $R$  is less than  $\mu$  for periods less than one second and hence the need for the short-period modifier on  $R$  given by Equation 4.7-1.

The short-period modifier should be applied separately in the transverse and longitudinal directions if there is a significant difference in the fundamental periods in the two directions (e.g., for pier walls). If there is significant coupling in the fundamental modes in the two directions then the lowest period should be used to determine the  $R$ -factor for both directions.

If the abutments are dominating the period of the structure and causing a low  $R$ -factor an engineer could evaluate the option of assuming all lateral loads are taken by the columns. This will result in a longer period structure and hence a higher  $R$ -factor but will be offset by the columns taking more load.

The  $R$ -factors of Table 4.7-1 were based on an evaluation of existing test data of structural components, parametric studies that were performed in conjunction with the development of these provisions, and engineering judgment. Test data on reinforced concrete columns (Hose, Silvan and Sieble, 2000) was reviewed to establish the range of ductility capacity that could be relied upon. This was in the range of 6 to 10 for well-detailed columns, depending on the range of design pa-

rameters (e.g., axial load, and longitudinal and confinement reinforcement). The parameter study associated with the development of this criteria showed that there were only a limited number of instances where use of an  $R$ -factor greater than 6 would not be limited either by the minimum longitudinal steel requirement of 0.8% in concrete columns or the  $P$ - $\Delta$  requirements of Article 7.3.4 or 8.3.4. As a consequence the  $R$ -factor for concrete and steel columns was set at 6 for SDAP E with a provision that the design forces could be further reduced (but not lower than 70%) provided the displacement capacity of the element was satisfied in the pushover analysis.

Wall-type piers may be treated as wide columns in the strong direction, provided the appropriate  $R$ -factor in this direction is used.

#### C4.8 CAPACITY DESIGN

The objective of these Guidelines for conventional design is that inelastic deformation (plastic hinging) occurs at the location in the columns (top or bottom or both) where they can be readily inspected and repaired. To achieve this objective, all members connected to the columns, the shear capacity of the column and all members in the load path from the superstructure to the foundation, shall be capable of transmitting the maximum (overstrength) force effects developed by plastic hinges in the columns. The exceptions to the need for capacity design of connecting elements is when all substructure elements are designed elasti-

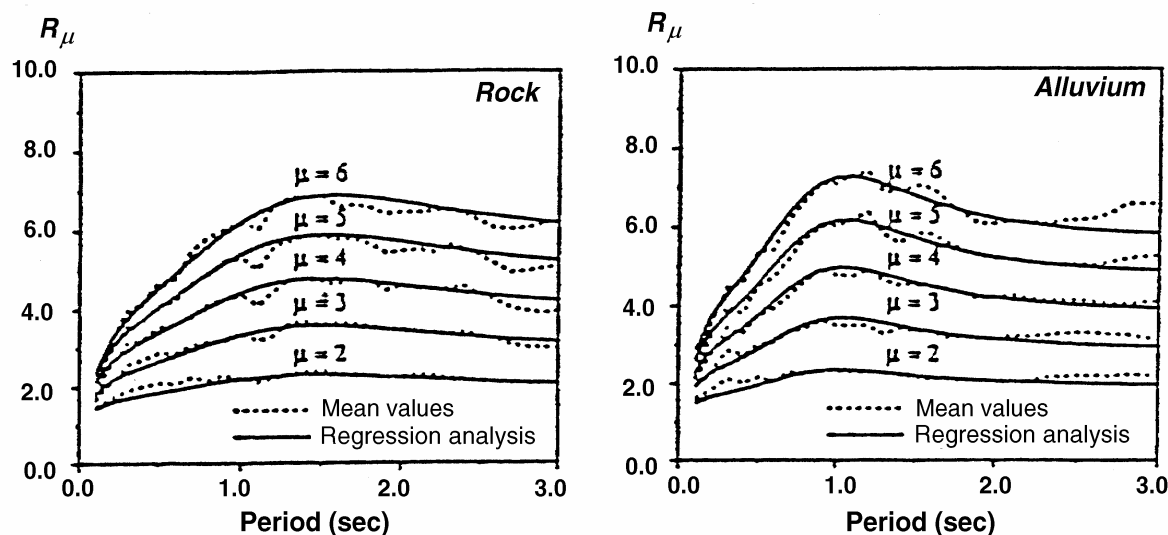


Figure C4.7-1 Comparison of Mean Strength-Reduction Factors of Rock and Alluvium Sites with Regression Analysis



cally (Article 4.10), seismic isolation design (Article 7.10 or 8.10) and in the transverse direction of columns when a ductile diaphragm (Article 7.7.8 or 8.7.8) is used.

#### C4.8.1 Inelastic Hinging Forces

The principles of capacity design require that the strength of those members that are not part of the primary energy-dissipating system should be stronger than the overstrength capacity of the primary energy-dissipating members—that is, the columns with hinges at their member ends.

This clause permits three approaches of increasing sophistication (but also of increasing effort) for assessing the overstrength capacity of reinforced concrete columns. (See Article 4.3.3 for foundation design in SDR 3.)

1. Overstrength factors applied to nominal moment capacities are a simplified method for determining flexural overstrength. For reinforced concrete columns, detailed calculations of overstrength factors for a variety of column properties ranged from 1.25 to 1.50 (Mander, Dutta and Goel, 1998). A conservative default value of 1.5 is specified for the first approach but a designer can calculate a more precise value using one of the other two approaches.
2. The flexural moment overstrength capacity ( $M_{po}$ ) of reinforced concrete columns, piers, and piles that form part of the primary mechanism resisting seismic loads may be assessed using the simplified plastic moment – axial load interaction formula method (Mander, Dutta and Goel, 1997). It is recommended that for this approach  $f'_{co}$  for concrete be assumed to be  $1.7f'_c$  and  $f_{yo}$  of steel be  $1.3f_y$ .
3. When assessing overstrength capacity of flexural members using compatibility section analysis (i.e., the moment-curvature method), it is important to differentiate between overstrength resulting from the response of the section to high curvature demands, and overstrength resulting from upper-bound material properties.

For example, for reinforced concrete columns, confined concrete will have enhanced capacity and reinforcing steel will strain-harden at high plastic curvatures. This will result in increased flexural capacity of the column that will be captured by a moment-curvature analysis that considers these factors. In addition, reinforcing steel can have a

higher than nominal yield point, and concrete is likely to be stronger than specified and will gain strength with age beyond the 28-day specified strength. It has been recommended that for the purpose of a rigorous calculation that  $f'_{co}$  for concrete be assumed to be  $1.7f'_c$  and  $f_{yo}$  of steel be  $1.3f_y$ . In this case the overstrength moment is taken at the design curvature from the moment-curvature analysis (ATC, 1996).

For structural steel,  $f_{yo}$  may be taken as  $1.2F_{ye}$  where  $F_{ye}$  is the expected yield strength, considering the likelihood that higher-than-nominal-strength steel will be used. The plastic section modulus should be used in overstrength moment calculations for steel members.

The guidelines require the calculation of capacity design shear forces for columns, pile bents, and drilled shafts at the mud or ground surface. If, however, a concrete traffic barrier or other structural element is added between these members, which effectively shortens them, then only the height above the barrier should be considered in the shear force calculation.

#### C4.9 PLASTIC HINGE ZONES

No commentary is provided for Article 4.9.

#### C4.10 ELASTIC DESIGN OF SUBSTRUCTURES

##### C4.10.1 All Substructure Supports are Designed Elastically

If all the supporting substructure elements (columns, piers, pile bents) are designed elastically for the Maximum Considered Earthquake event, there will be no redistribution of lateral loads due to plastic hinges developing in one or more columns. As a consequence the elastic analysis results are appropriate for design. The recommended provisions attempt to prevent any brittle modes of failure from occurring.

##### C4.10.2 Selected Substructure Supports are Designed Elastically

If only one or a selected number of supporting substructure elements are designed elastically, there will be a significant redistribution of lateral loads when one or more of the columns develop plastic hinges. Generally, the elastically designed elements will attract more lateral load. Hence the

need to use either capacity design principles for all elements connected to the elastically designed column, or an  $R$ -factor of 0.67 with the elastic force for any element that could result in a brittle mode of failure. If this is not practical, the complete

bridge needs to be reanalyzed using the secant stiffness of any columns in which plastic hinges will form, in order to capture the redistribution of lateral loads that will occur.

## Section 5: Commentary

### ANALYSIS REQUIREMENTS

#### C5.1 DEFINITION OF PROCEDURES

##### C5.1.1 General

Seismic analysis encompasses a demand analysis and a displacement capacity verification. The objective of a demand analysis is to estimate the forces and displacements induced by the seismic excitation. Depending on the design procedure, a verification of displacement capacity of piers or bents may be required. The objective of a displacement capacity verification is to determine the displacement of an individual pier when its deformation capacity (that of the inelastic earthquake resisting element) is reached. The displacement capacity must be greater than the displacement demand. The accuracy of the demand and capacity analyses depend on the assumption of the model related to the geometry, boundary conditions, material properties, and energy-dissipation incorporated in the model. It is the responsibility of the designer to assess the reasonableness of a model in representing the behavior of the structure at the level of forces and deformations expected for the seismic excitation.

Very flexible bridges, e.g., suspension and cable-stayed bridges, shall be analyzed accounting for the nonlinear geometry. The need for modeling of foundations and abutments depends on the sensitivity of the structure to foundation flexibility and associated displacements. This in turn depends on whether the foundation is a spread footing, pile footing with pile cap, a pile bent, or drilled shaft. Article 5.3.4 defines the requirements for the foundation modeling in the seismic analysis.

When gross soil movement or liquefaction is determined to be possible, the model shall represent the change in support conditions and additional loads on the substructure associated with soil movement.

For structures whose response is sensitive to the support conditions, such as in a fixed-end arch, the model of the foundation shall account for the conditions present.

##### C5.1.2 Selection of Analysis Procedure

Bridges are designed to remain essentially elastic when subjected to earthquakes with a high-probability of occurrence (Expected Earthquake ground motions, which have a 50% probability of being exceeded in 75 years). For low-probability earthquakes (Maximum Considered Earthquake ground motions, which have a 3% probability of being exceeded in 75 years, but are capped in some areas), and depending on the desired performance level, bridges are designed to dissipate energy through inelastic deformation in earthquake-resisting elements. Depending on the type of analysis, the demand and capacity may be expressed in terms of forces (bending moments in the plastic hinge zones or shear forces in isolation bearings) and displacements of the structure at the centroid of the mass.

In specifying the minimum Seismic Design and Analysis Procedure (SDAP), two principles are followed. First, as the seismic hazard increases, improved modeling and analysis for seismic demands is necessary because the behavior may be sensitive to the maximum demands. Second, as the complexity of the bridge increases, more sophisticated models are required for seismic demand and displacement capacity evaluation. No seismic analysis is required for regular bridges in SDAP B because minimum ductile detailing and capacity design principles provide sufficient displacement capacity for the hazard levels and performance requirements in which SDAP B is permitted. For bridges with a regular configuration, a single-degree-of-freedom model is sufficiently accurate to represent the seismic response. For these types of bridges, the capacity spectrum method in SDAP C combines the demand and capacity evaluation. The capacity spectrum method is appropriate for most structures with seismic isolation systems.

For structures that do not satisfy the requirements for a capacity spectrum analysis, an elastic response spectrum analysis, SDAP D, must be used to determine the displacement demands and the forces in the plastic hinge of structural components. Two elastic response spectrum analyses

methods are permitted: either the uniform load method, or the multi-mode response spectrum method, depending on the configuration of the structure.

The uniform load method is suitable for short to medium span structures with regular configuration. Long bridges, or those with significant skew or horizontal curvature, have dynamic characteristics that should be assessed in a multi-mode dynamic analysis.

The model for an elastic response spectrum analysis is linear, and as such it does not represent the inelastic behavior of earthquake-resisting elements under strong ground motion. However, with the proper representation of the inelastic elements and interpretation of responses, an elastic analysis provides reasonable estimates of seismic demands. The model must be based on cracked section properties for concrete components, and on secant stiffness coefficients for the foundations, abutments, and seismic isolation components. All must be consistent with the expected levels of deformation of the components. The only forces that are meaningful from an elastic response spectrum analysis are the forces in the earthquake-resisting substructure elements, such as the bending moment at a plastic hinge in a column. The elastic forces in the earthquake-resisting elements are reduced by a factor that accounts for ductility of the earthquake-resisting system. The displacements at the center of mass, generally the superstructure, can be used to estimate the displacement demand of the structure including the effect of inelastic behavior in the earthquake-resisting elements as discussed in Article C3.3.

For SDAP E, a displacement capacity evaluation is required. The displacement capacity evaluation involves determining the displacement at which the first component reaches its inelastic deformation capacity. All nonductile components shall be designed using capacity design principles to avoid brittle failure. For simple piers or bents, the displacement capacity can be evaluated by simple calculations using the geometry of displaced shapes, and forces and deformations at the plastic hinges. For more complicated piers or bents, particularly when foundations and abutments are included in the model, a nonlinear static (“pushover”) analysis may be used to evaluate the displacement capacity. It is recommended that the nonlinear static analysis continue beyond the displacement at which the first component reaches its inelastic deformation capacity in order to under-

stand the behavior beyond the displacement capacity.

The displacement capacity is compared to the displacement demand determined from an elastic response-spectrum analysis. The displacement capacity must exceed the demand by at least 50%. There are several reasons for this requirement. First, while, on average, the displacement of the elastic model, using a design response spectrum, should be approximately equal to the inelastic displacement, a significant difference is possible because of variability of the ground motion and its effect on inelastic behavior. Second, the demand analysis is performed on a three-dimensional model, whereas the displacement capacity verification is performed for individual bents or piers in the longitudinal and transverse directions separately. In Article 7.3.5 or 8.3.5, the displacement demand is multiplied by 1.5 to account for ground motion variability and the differences in the demand models, capacity models, and analysis methods.

A nonlinear dynamic analysis is the most general analysis method because the effect of inelastic behavior is included in the demand analysis. Depending on the mathematical model, the deformation capacity of the inelastic elements may or may not be included in the dynamic analysis. A nonlinear dynamic analysis requires a suite of time-histories (Article 3.4.4) of earthquake ground motion that is representative of the hazard and conditions at the site. Because of the complexity involved with nonlinear dynamic analysis, it is best used in conjunction with SDAP E.

Seismically isolated structures with long periods or large damping ratios require a nonlinear dynamic analysis because the analysis procedures using an effective stiffness and damping may not properly represent the effect of isolation units on the response of the structure. The model for nonlinear analysis shall represent the hysteretic relationships for the isolator units.

## **C5.2 SEISMIC LATERAL LOAD DISTRIBUTION**

### **C5.2.1 Applicability**

No commentary is provided for Article 5.2.1.

### C5.2.2 Design Criteria

If the forces from the substructure corresponding to the overstrength condition are used to design the superstructure, the distribution of these forces may not be the same as that of the elastic demand analysis forces. The Engineer may calculate a more refined distribution of the inertial forces present when a full inelastic mechanism has developed in the EREs. However, in lieu of such a calculation, the simpler linear distribution may be used, as long as the applied forces are in equilibrium with the substructure's plastic-moment forces. The vertical spatial relationship between location of the substructure plastic resistance and the location of the superstructure inertia force application shall also be considered in this analysis.

Diaphragms, cross-frames, lateral bracing, bearings, and substructure elements are part of an earthquake-resisting system in which the lateral loads and performance of each element are affected by the strength and stiffness characteristics of the other elements. Past earthquakes have shown that when one of these elements responded in a ductile manner or allowed some movement, damage was limited. In the strategy followed herein, it is assumed that ductile plastic hinging in substructure or seismic isolator units are the primary source of energy dissipation.

Even if a component does not participate in the load path for seismic forces it must deform under the seismic loads. Such components must be checked that they have deformation capacity sufficient to maintain their load resistance under seismic-induced deformations.

### C5.2.3 Load Distribution

A continuous path is necessary for the transmission of the superstructure inertia forces to the substructure. Concrete decks have significant rigidity in their horizontal plane, and in short-to-medium slab-on-girder spans, their response approaches rigid body motion. Therefore, the lateral loading of the intermediate diaphragms is minimal, consisting primarily of local tributary inertia forces from the girders themselves.

All bearings in a bridge do not usually resist load simultaneously, and damage to only some of the bearings at one end of a span is not uncommon. When this occurs, high load concentrations can result at the location of the other bearings, and this effect shall be taken into account in the design of the end diaphragms and pier diaphragms. Also,

a significant change in the load distribution between end and pier diaphragm members may occur.

## C5.3 MODELING REQUIREMENTS

### C5.3.1 General

Depending on the chosen seismic analysis method, different types of approximations may be used for modeling the strength, stiffness, and energy-dissipation mechanisms. One-dimensional beam-column elements are sufficient for dynamic analysis of structures due to earthquake ground motion (referred to as "spine" models or "stick" models). For seismic analyses, grid or finite-element analyses are generally not necessary. They greatly increase the size of the model and complicate the understanding of the force and deformation distribution through the substructure because of the large number of vibration modes.

The geometry of skew, horizontal curvature, and joint size shall be included in the model. However, two-dimensional models are adequate for bridges with skew angle less than 30 degrees and a subtended angle of horizontal curvature less than 20 degrees. When skew is included in a three-dimensional model, the geometry and boundary conditions at the abutments and bearings shall be represented in order to determine the forces and displacements at these locations. Short columns or piers may be modeled with a single element, but tall columns may have two or more elements, particularly if they have significant mass (in the case of concrete), or are modeled as framed substructures.

For bridges with multiple frames, which are separated by expansion bearings or hinges, it is unnecessary to model and analyze the entire bridge for seismic loads. Each frame shall have sufficient strength to resist inertia loads from the mass of the frame. However, when adjacent frames have large differences in vibration period, the frame with the longer period may increase the seismic load on the frame with the shorter period by impact across the bearing or hinge, or by transverse forces through shear keys. To account for these effects, the number of frames included in a model depends on the ratio of vibration period of the frames. For bridges in which the period ratio of adjacent frames is less than 0.70 (shortest period frame divided by longest period frame), it is recommended to limit a model to five frames. The first and fifth frames in the model are considered

to be boundary frames, representing the interaction with the remainder of the structure. The response of the three interior frames can be used for design of those frames. For a bridge with more than five frames, several different models are then used in the design.

For bridges with period ratios of frames between 0.70 and 1.0, fewer than five frames may be used in a model.

A common practice is to define the “longitudinal direction” of a curved bridge as that of the chord connecting the ends of the bridge, and the transverse direction as orthogonal to the longitudinal direction.

Bridges within 10 km of an active fault require a site-specific study and inclusion of vertical ground motion in the seismic analysis. For bridges located more than 10 km from an active fault, the procedures in Article 3.4.5 are used to account for the response to vertical ground motion in lieu of including the vertical component in the seismic analysis. If the vertical ground motion component is not included in the dynamic analysis, the forces from the analysis must be modified to account for the effect. For bridges with long, flexible spans, C-bents, or other large eccentricity in the load path for vertical loads, it is recommended to include vertical ground motion in the dynamic analysis.

### C5.3.2 Distribution of Mass

The distributions of stiffness and mass are included in the model for dynamic analysis. The discretization of the model shall account for geometric and material variation in stiffness and mass. Most of the mass of a bridge is in the superstructure. Four to five elements per span are generally sufficient to represent the mass and stiffness distribution of the superstructure. For spine models of the superstructure, the line of elements shall be located at the locus of the mass centroid. Rigid links can be used to represent the geometric location of mass relative to the spine elements in the model.

For single-column piers, C-bents, or unusual pier configurations, the rotational mass moment of inertia of the superstructure about the longitudinal axis shall be included.

The inertia of live loads need not be included in the seismic analysis. However, the probability of a large live load being on the bridge during an earthquake shall be considered when designing bridges with high live-to-dead-load ratios that are

located in metropolitan areas where traffic congestion is likely to occur.

### C5.3.3 Stiffness and Strength

#### C5.3.3.1 General

For elastic analysis methods, there is a significant approximation in representing the force-deformation relationship of inelastic structural elements by a single linearized stiffness. For inelastic columns or other inelastic earthquake-resisting elements, the common practice is to use an elastic stiffness for steel elements and a cracked stiffness for reinforced concrete elements. However, the stiffness of seismic isolator units, abutments, and foundation soils are represented by a secant stiffness consistent with the maximum deformation. The designer shall consider the distribution of displacements from an elastic analysis to verify that they are consistent with the inelastic behavior of the earthquake-resisting elements.

#### C5.3.3.2 Substructure

Seismic design procedures have been calibrated using stiffness that is representative of deformations close to the yield deformations. At these levels of deformation, reinforced concrete elements will have cracked. The effects of cracking on the stiffness depend on the cross-section, longitudinal reinforcement ratio, axial load, and amount of bond slip. The cracked flexural stiffness of a reinforced concrete member can be obtained by a moment-curvature analysis of the cross section, with modifications for bond-slip. In lieu of a moment-curvature analysis, the cracked section stiffness may be estimated by:

$$EI_{eff} = \frac{M_n}{(2\varepsilon_y/D')}$$

where  $M_n$  is the nominal flexural strength of the section considering axial load,  $\varepsilon_y$  is the yield strain of the reinforcement, and  $D'$  is the effective depth of the column. If the flexural strength has not been selected, the effective stiffness may be approximated by  $EI_{eff} = 0.50EI_g$  for columns and pier walls (in the weak direction), where  $EI_g$  is the cross-sectional stiffness based on gross geometry and nominal material properties.

Where the load path depends on torsion of a reinforced concrete column or substructure ele-

ment, the cracked torsional stiffness may be taken as 20% of the uncracked torsional stiffness.

The objective of the nonlinear displacement capacity verification is to determine the displacement at which the inelastic components reach their deformation capacity. The deformation capacity is the sum of elastic and plastic deformations. The plastic deformation is expressed in terms of the rotation of the plastic hinges. A nonlinear analysis using nominal strengths of the components gives larger plastic deformations than an analysis including overstrength. Hence, it is appropriate to use the nominal strength of the components when estimating the displacement capacity.

The stiffness of pier caps shall be included in the model. Pile caps and joints in reinforced concrete substructures may be assumed to be rigid. The strength of capacity-protected elements need not be included in the model.

#### C5.3.3.3 Superstructure

For a spine or stick model of the superstructure, the stiffness is represented by equivalent section properties for axial deformation, flexure about two axes, torsion, and possibly shear deformation in two directions. The calculation of the section stiffness shall represent reasonable assumptions about the three-dimensional flow of forces in the superstructure, including composite behavior.

The effects of skew can be neglected in the model of the superstructure. However, for large skew angles, the geometry of the piers with respect to the superstructure and connections between them must be included in the model.

For reinforced box girders the effective stiffness may be based on 75% of the gross stiffness to account for cracking. For prestressed box girders, the full gross stiffness shall be used. The torsional stiffness may be based on a rational shear flow without reduction due to cracking.

The flexural stiffness of the superstructure about a transverse axis is reduced near piers when there is a moment transfer between the superstructure and pier because of shear lag effects. The reduced stiffness shall be represented in the model of the superstructure.

#### C5.3.4 Foundations

A wide range of methods for modeling foundations for seismic analysis is available. Generally a refined model is unnecessary for seismic analysis. For many cases the assumption of a rigid

foundation is adequate. Flexibility of a pile bent or shaft can be estimated using an assumed point of flexibility associated with the stiffness estimate of the pile (or shaft) and the soil. Spread footings and piles can be modeled with rotational and translational springs.

The requirement for including soil springs for Foundation Modeling Method II depends on the contribution of the foundation to the elastic displacement of the pier. Foundation springs for a pier are required when the foundation increases the elastic displacement of the pier by more than 20%. This may be calculated for individual piers using estimates of the pier stiffness with hand calculations. If the contributions exceeds 15% for a majority of piers in a bridge, then it is recommended that foundation springs be included in all piers for the seismic analysis.

This approach is based on judgment that the forces and displacements from a seismic analysis, with or without foundation springs, that contribute less than 20% of the displacement of a pier will be comparable for design. More flexible spread and pile footings should be modeled and included in the seismic analysis.

If foundation springs are included in the multi-mode dynamic analysis, they must be included in the pushover analysis so the two models are consistent for the displacement comparison.

For most spread footings and piles with pile caps a secant stiffness for the soil springs is adequate. If the design limits for spread or pile footings are exceeded, according to the requirements in Articles 7.4 or 8.4, bi-linear soil springs are required for the pushover analysis.

For pile bents and drilled shafts, an estimated depth to fixity is generally adequate for representing the relative flexibility of the soil and pile or shaft. Soil springs with secant stiffness may be used to provide a better representation based on P-y curves for the footing and soil. Bi-linear springs may be used in the pushover analysis if there is particular concern with depth of the plastic hinge and effective depth of fixity.

If bilinear springs are used in a pushover analysis, a secant stiffness, typical of the expected level of soil deformation, is used in the multi-mode dynamic analysis for a valid comparison of displacement demand and capacity.

#### C5.3.5 Abutments

Articles 7.5.2.2, 7.5.3.2, 8.5.2.2 and 8.5.3.2 provide requirements for the modeling of abut-

ments in the longitudinal and transverse directions. The iterative procedure with secant stiffness coefficients defined in those articles are included in the mathematical model of the bridge to represent the resistance of the abutments in an elastic analysis. The load-displacement behavior of the abutment may be used in a static nonlinear analysis when the resistance of the abutment is included in the design of the bridge.

### C5.3.6 Seismic Isolator Units

The requirements for analysis of bridges with seismic isolation systems are specified in Article 15.4 and are based on the 1999 AASHTO *Guide Specifications for Seismic Isolation Design*, which provide requirements for modeling seismic isolator units, including the use of property modification factors as given in Article 15.5.

The force-deformation characteristics can be idealized as a bilinear relationship with two key variables: second slope stiffness and characteristic strength. The area under the bilinear curve is equal to the energy dissipated by hysteretic work during cyclic loading. For design, the force-deformation relationship can be represented by an effective stiffness based on the secant stiffness, and a damping coefficient.

The requirements for determining the upper-bound and lower-bound properties are provided in Article 15.4.

### C5.3.7 Bearings and Joints

The use of compression and tension models is expected to provide a reasonable bound on forces (compression model) and displacements (tension model).

### C5.3.8 Damping

Damping may be neglected in the calculation of natural frequencies and associated modal displacements. The effects of damping shall be considered when the dynamic response for seismic loads is considered. The specified ground motion spectra are for 5% viscous damping and this is a reasonably conservative value.

Suitable damping values may be obtained from field measurement of induced free vibration or by forced vibration tests. In lieu of measurements, the following values may be used for the equivalent viscous damping ratio of time-history analysis:

- Concrete construction: 5%
- Welded and bolted steel construction: 2%
- Timber: 5%

For single-span bridges or two-span continuous bridges with abutments designed to activate significant passive pressure in the longitudinal direction, a damping ratio of up to 10% may be used for longitudinal vibration modes.

Equivalent viscous damping may be considered to represent the energy dissipation due to cyclic loading of yielding members. Equivalent damping shall only be used with a secant stiffness estimate for the entire structure. For single-degree-of-freedom models the equivalence can be established within a satisfactory degree of accuracy. For bridges with seismic isolation or other seismic protection components, the equivalence is established in an approximate manner. Equivalent viscous damping shall not be used to represent inelastic energy dissipation for any other model or method of dynamic analysis.

## C5.4 ANALYSIS PROCEDURES

### C5.4.1 Capacity Spectrum Analysis

Capacity spectrum analysis may be used for bridges that are designed to respond to earthquake ground motion as a single-degree-of-freedom system in the longitudinal and transverse direction with the columns being the primary energy-dissipation mechanism. Regular bridges that satisfy the special requirements are expected to respond as a single-degree-of-freedom system and the capacity spectrum approach may be used for such cases.

Bridges that have elastomeric or sliding bearings at each pier shall be designed as an isolated structure using the provisions of Article 5.4.1.2 and Article 15. The  $B_S$  and  $B_L$  factors of Table 5.4.1-1 are for configurations where the columns are the primary dissipation elements.

The capacity spectrum analysis uses the elastic response spectrum defined in Article 3.4.1. The elastic spectrum is reduced to account for dissipation of energy in the inelastic earthquake-resisting elements. The reduced elastic spectrum is evaluated at the effective vibration period, which is based on an effective stiffness equal to the design strength divided by the maximum displacement. An advantage of the capacity spectrum method is that the vibration period does not need to be calcu-



lated because it is implicit in equations 5.4.1-1 and 5.4.1-2. Equation 5.4.1-1 will govern for most bridges, and as a result the designer has several choices in selecting the lateral strength and maximum displacement as described in Article C4.4.

For stiff bridges, the maximum displacement may give a seismic capacity coefficient  $C_c$  greater than required by Equation 5.4.1-1. In such cases the strength need not be greater than the value defined by Equation 5.4.1-2.

The basis of the capacity spectrum method is to linearize nonlinear structural behavior by determining a "secant" period and effective damping factor based on hysteretic response. This approach was originally proposed by Gulkan and Sozen (1974) and called the "Substitute Structure Method."

Assuming the peak response of the nonlinear structure is equal to the displacement of an equivalent (substitute) SDOF system, the effective period is given by

$$T_{eff} = 2\pi \sqrt{\frac{m}{K_{eff}}} = 2\pi \sqrt{\frac{W/g}{F_y/\Delta_{max}}} = 2\pi \sqrt{\frac{\Delta_{max}}{C_c g}} \quad (C5.4.1-1)$$

in which  $m$  = structure mass;  $W$  = seismic structure weight;  $F_y$  and  $D_{max}$  are the idealized response force and maximum displacement shown in Figure C3.3-2 as  $M_y$  and  $\Delta_{max}$ ;  $C_c$  = normalized base shear capacity given by  $F_y/W$ ; and  $g$  = gravitational acceleration.

The seismic demand coefficient ( $C_d = F_{elastic}/W$  where  $F_{elastic}$  = elastic design force) can be expressed in terms of the design spectrum with the appropriate damping as used for seismic isolation such that the lesser of the following governs

$$C_d = \frac{F_a S_s}{B_s} \quad (C5.4.1-2)$$

$$C_d = \frac{F_v S_1}{T_{eff} B_L} \quad (C5.4.1-3)$$

in which  $F_a S_s$  and  $F_v S_1$  are obtained from Article 3.4, and  $B_s$  and  $B_L$  are modification factors for the short and long-period portions of the design spectra that account for hysteretic damping effects, given by

$$B_s = \left( \frac{\xi_{eff}}{0.05} \right)^{0.5} \quad \text{and} \quad B_L = \left( \frac{\xi_{eff}}{0.05} \right)^{0.3} \quad (C5.4.1-4)$$

where for an equivalent elasto-plastic system

$$\xi_{eff} = 0.05 + \frac{2}{\pi} \eta \left( 1 - \frac{1}{\mu} \right) \quad (C5.4.1-5)$$

in which  $\mu$  = displacement ductility factor;  $\eta$  = energy absorption efficiency factor.

Based on extensive experimental calibration,  $\eta$  may be taken as follows:

- For seismically detailed reinforced concrete elements,

$$\eta = 0.35 - 0.4$$

- For poorly detailed (nonductile) reinforced concrete,

$$\eta = 0.25$$

- For timber structures,

$$\eta = 0.1 - 0.15$$

- For steel structures,

$$\eta = 0.70$$

Assuming the capacity is equal to the reduced demand and taking equation (C5.4.1-1) and substituting it into (C5.4.1-3) and rearranging, gives for long-period structures:

$$F_v S_1 = 2\pi B_L \sqrt{\frac{C_c^* \Delta^*}{g}} \quad (C5.4.1-6)$$

and for short-period structures:

$$F_a S_s = C_c B_s \quad (C5.4.11-7)$$

The greater of the above two equations governs.

In the above,  $C_c^* = C_c / \alpha_2$  and  $\Delta^* = \Delta / \alpha_1$  where  $\alpha_1$  and  $\alpha_2$  are transformation factors that account for converting a MDOF system into a substitute SDOF structure. These are defined as

$$\alpha_1 = \phi_{mn} \frac{\sum_{i=1}^N w_i \phi_{im}}{\sum_{i=1}^N w_i \phi_{im}^2} \quad (C5.4.1-8)$$

$$\alpha_2 = \frac{\left[ \sum_{i=1}^N w_i \phi_{im} \right]^2}{\sum_{i=1}^N w_i \sum_{i=1}^N w_i \phi_{im}^2} \quad (C5.4.1-9)$$

where  $\sum_{i=1}^N w_i = W$  = total seismic weight;  $w_i$  = tribu-

tary weight at location  $i$ ; and  $\phi_{mn} = m^{\text{th}}$  mode shape at the  $n^{\text{th}}$  location.

If the bridge has a simple configuration, such that the deck is subjected to pure translation (that is, there is no substantial deck bending due to favorable support conditions), then the structure will behave in a single-degree-of-freedom fashion. Thus  $\alpha_1$  and  $\alpha_2$  are set to unity. Such a condition can be orchestrated by design, particularly when all the piers have similar stiffnesses and the deck is uncoupled from the abutments through the use of low-stiffness bearing supports as required for the application of this analysis method.

The maximum displacement of the superstructure for the Maximum Considered Earthquake (MCE) is limited by the plastic deformation capacity of the substructure, taken as  $\Delta = \theta_p H$ , with  $\theta_p = 0.035$  for reinforced concrete and the P- $\Delta$  limitation in Article 7.3.4 or 8.3.4. The maximum displacement of the superstructure for the Expected Earthquake is limited to 1.3 times the elastic displacement of the substructure.

#### C5.4.1.1 Seismic Isolation Systems

The requirements of Article 15.4 govern the analysis procedures for seismic isolation. Commentary on the capacity spectrum method follows. Using the capacity spectrum equation in the velocity-controlled region of the spectrum (5.4.1-1), the maximum displacement is

$$\Delta = \left( \frac{F_v S_1}{2\pi B} \right)^2 g \frac{1}{C_c} \quad (\text{C5.4.1.2-1})$$

In the capacity spectrum method, the effective period is defined by the maximum displacement and seismic coefficient:

$$T_{\text{eff}} = 2\pi \sqrt{\frac{\Delta}{C_c g}} \quad (\text{C5.4.1.2-2})$$

With the effective stiffness expressed as  $K_{\text{eff}} = C_c W / \Delta$ , the effective period is

$$T_{\text{eff}} = 2\pi \sqrt{\frac{W}{K_{\text{eff}} g}} \quad (\text{C5.4.1.2-3})$$

Solving (C5.4.1.2-2) for the seismic capacity coefficient and substituting into (C5.4.1.2-1) and simplifying gives

$$\Delta = \frac{g}{(2\pi)^2} \frac{F_v S_1 T_{\text{eff}}}{B} \quad (\text{C5.4.1.2-4})$$

When in meters, the coefficient for the expression is 0.25, and when in inches, the coefficient is 10. This is the same as (3a) and (3b) in the 1999 *Guide Specifications for Seismic Isolation Design* with  $AS_i$  replaced by  $F_v S_1$  for the Maximum Considered Earthquake loading. In Part I (*Specifications*), the reduction factor  $B$  is defined for the long-period range as is  $B$  in this article.

Alternatively, the seismic capacity coefficient evaluated at the effective period and reduced for the effects of energy dissipation is:

$$C_c = \frac{F_v S_1}{T_{\text{eff}} B} \quad (\text{C5.4.1.2-5})$$

This is the same as equation (2a) in the 1999 *Guide Specifications for Seismic Isolation Design* with  $AS_i$  replaced by  $F_v S_1$  for the Maximum Considered Earthquake loading and the  $B$  values from the 1999 *Guide Specifications* are given in Table 5.4.2-1.

### C5.4.2 Elastic Response Spectrum Analysis

#### C5.4.2.1 Selection of Analysis Method

No commentary is provided for Article 5.4.2.1.

#### C5.4.2.2 Uniform Load Method

The Uniform Load Method, described in the following steps, may be used for both transverse and longitudinal earthquake motions. It is essentially an equivalent static method of analysis that uses a uniform lateral load to approximate the effect of seismic loads. The method is suitable for regular bridges that respond principally in their fundamental mode of vibration. The capacity spectrum analysis is similar to the uniform load method, in that they are both appropriate for bridges whose dynamic response can be represented by an equivalent single-degree-of-freedom system. Capacity spectrum analysis may only be used for bridges in which abutments do not resist significant longitudinal or transverse seismic forces. For such bridges, the vibration mode shape is essentially a rigid body displacement of the superstructure, providing a uniform lateral load.

Whereas displacements are calculated with reasonable accuracy, the method can overestimate the transverse shears at the abutments by up to 100%. Consequently, the columns may have inadequate lateral strength because of the overestimate of abutment forces. A multi-mode dynamic analysis is recommended to avoid unrealistic distributions of seismic forces.

The steps in the uniform load method are as follows:

1. Calculate the static displacements  $v_s(x)$  due to an assumed uniform load  $p_o$ , as shown in Figure C5.4.2.2-1. The uniform loading  $p_o$  is applied over the length of the bridge; it has dimension of force/unit length and may be arbitrarily set equal to 1.0. The static displacement  $v_s(x)$  has the dimension of length.
2. Calculate the bridge lateral stiffness,  $K$ , and total weight,  $W$ , from the following expressions:

$$K = \frac{p_o L}{V_{s,MAX}} \quad (C5.4.2.2-1)$$

$$W = \int_0^L w(x) dx \quad (C5.4.2.2-2)$$

where:

$L$  = total length of the bridge

$v_{s,MAX}$  = maximum value of  $v_s(x)$

$w(x)$  = nominal, unfactored dead load of the bridge superstructure and tributary substructure.

The weight shall take into account structural elements and other relevant loads including, but not limited to, pier caps, abutments, columns, and footings. Other loads, such as live loads, may be

included.

3. Calculate the period of the bridge,  $T_m$ , using the expression:

$$T_m = 2\pi \sqrt{\frac{W}{Kg}} \quad (C5.4.2.2-3)$$

where:

$g$  = acceleration of gravity

4. Calculate the equivalent static earthquake loading  $p_e$  from the expression:

$$p_e = \frac{C_d W}{L} \quad (C5.4.2.2-4)$$

where:

$C_d$  = the dimensionless elastic seismic response demand coefficient obtained from Article C3.4.1 with the coefficient taken as  $S_{DS}$  for short periods.

$p_e$  = equivalent uniform static seismic loading per unit length of bridge applied to represent the primary mode of vibration.

5. Calculate the displacements and member forces for use in design either by applying  $p_e$  to the structure and performing a second static analysis or by scaling the results of the first step above by the ratio  $p_e/p_o$ .

#### C5.4.2.3 Multi-Mode Dynamic Analysis Method

Vibration modes are convenient representations of dynamic response for response spectrum analysis. Enough modes should be included to provide sufficient participation for bending moments in columns, or other components with inelastic deformation. Dynamic analysis programs,

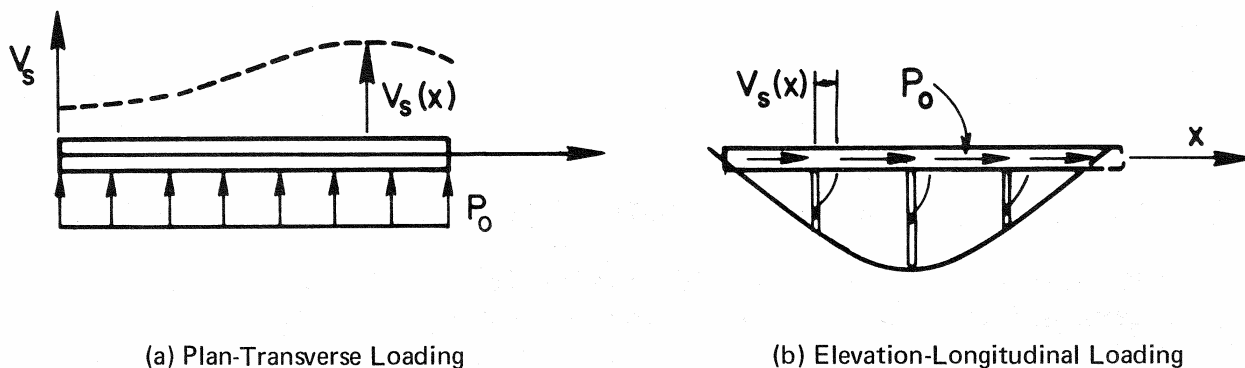


Figure C5.4.2.2-1 Bridge Deck Subjected to Assumed Transverse and Longitudinal Loading

however, usually compute participation factors only for base shear, often expressed as a percentage of total mass. For regular bridges the guideline of including 90% of the modal mass for horizontal components generally provides a sufficient number of modes for accurate estimate of forces in lateral-load-resisting components. For irregular bridges, or large models of multiple-frame bridges, the participating mass may not indicate the accuracy for forces in specific components. It is for this reason that the models of long bridges are limited to five frames.

The response spectrum in Article 3.4.1 is based on 5% damping. For bridges with seismic isolation the additional damping from the seismic isolator units applies only to the isolated vibration modes. Other vibration modes have 5% damping.

A suitable modification of the 5% response spectrum is to divide the spectrum by:

$$\left(\frac{\beta}{5}\right)^{0.3}$$

for vibration periods greater than  $T_s$ , and divide by

$$\left(\frac{\beta}{5}\right)^{0.5}$$

for vibration periods less than or equal to  $T_s$ , where  $\beta\%$  is the damping ratio, capped at 30%.

Member forces and displacements obtained using the CQC combination method are generally adequate for most bridge systems.

If the CQC method is not readily available, alternative methods include the square root of the sum of the squares method (SRSS), but this method is best suited for combining responses from modes with well-separated frequencies. For closely spaced modes, the absolute sum of the modal responses shall be used.

#### **C5.4.3 Seismic Displacement Capacity Verification**

The objective of the displacement capacity verification analysis is to determine the displacement at which the earthquake-resisting elements achieve their inelastic deformation capacity. Damage states are defined by local deformation limits, such as plastic hinge rotation, footing settlement or uplift, or abutment displacement. Dis-

placement may be limited by loss of capacity from either degradation of strength under large inelastic deformations or  $P-\Delta$  effects.

For simple piers or bents, the maximum displacement capacity can be evaluated by hand calculations using the defined mechanism and the maximum allowable deformations of the plastic hinges. If interaction between axial force and moment is significant, iteration is necessary to determine the mechanism.

For more complicated piers or foundations, displacement capacity can be evaluated using a nonlinear static analysis procedure (pushover analysis).

Displacement capacity verification is required for individual piers or bents. Although it is recognized that force redistribution may occur as the displacement increases, particularly for frames with piers of different stiffness and strength, the objective of the capacity verification is to determine the maximum displacement capacity of each pier. The displacement capacity is to be compared with an elastic demand analysis, which considers the effects of different stiffness and is specified in Article 7.3.5 or 8.3.5.

Nominal inelastic capacities are used for the displacement capacity verification. Although the displacement capacity verification considers a monotonically increasing displacement, the effects of cyclic loading must be considered when selecting an appropriate model and establishing a maximum inelastic deformation. This includes strength and stiffness degradation and low-cycle fatigue.

Generally, the center of mass is at the elevation of the mass centroid of the superstructure.

#### **C5.4.4 Nonlinear Dynamic Analysis Procedure**

The nonlinear dynamic analysis procedure is normally only used for the Maximum Considered Earthquake. The structure is expected to remain essentially elastic for the Expected Earthquake. Hence a multi-mode response spectrum analysis is adequate.

The results of a nonlinear dynamic analysis should be compared with a multi-mode response spectrum analysis to check the nonlinear model is reasonable.

## Section 6: Commentary

### SEISMIC DESIGN REQUIREMENTS (SDR) 1 AND 2

#### C6.1 GENERAL

No commentary is provided for Article 6.1.

#### C6.2 DESIGN FORCES

In areas of low seismicity only (1) minimum seat widths (Article 6.3) and connection design forces for bearings and (2) minimum shear reinforcement in concrete columns and piles (in SDR 2) are deemed necessary for the life-safety performance objective. These default values are used as minimum design criteria in lieu of rigorous analysis. The division of SDAP A1 and A2 at a short-period spectral response acceleration of 0.10 is an arbitrary expedient intended to provide some relief to parts of the country with low seismicity.

This article describes the minimum connection force that must be transferred from the superstructure to its supporting substructures through the bearings. It does not apply if the connection is a monolithic structural joint. Similarly, it does not apply to unrestrained bearings or in the unrestrained directions of bearings that are free to move (slide) in one direction but fixed (restrained) in an orthogonal direction. If a bridge has all elastomers or all sliders then either these minimums apply to all bearing connections or the forces shall be determined using the provisions of Article 6.10. The minimum force is simply 0.1 or 0.25 times the weight that is effective in the restrained direction. The calculation of the effective weight requires care and may be thought of as a tributary weight. It is calculated from the length of superstructure that is tributary to the bearing in the direction under consideration. For example, in the longitudinal direction at a fixed bearing, this length will be the length of the segment and may include more than one span if it is a continuous girder (i.e. it is the length from one expansion joint to the next). However, in the transverse direction at the same bearing, this length may be as little as one-half of the span if the beam is located at an expansion joint. This is because the expansion bearings at the adjacent piers will generally be transversely restrained and able to transfer lateral loads to the substructure.

It is important that not only the bearing but also the details that fasten the bearing to the sole and masonry plates (including the anchor bolts which engage the supporting members), have sufficient capacity to resist the above forces. At a fixed bearing, it is necessary to consider the simultaneous application of the longitudinal and transverse connection forces when checking these capacities.

Note that the primary purpose of this requirement is to ensure that the connections between the superstructure and its supporting substructures remain intact during the design earthquake and thus protect the superstructure's girders from being unseated. The failure of these connections has been observed in many earthquakes, and imposing minimum strength requirements is considered to be a simple but effective strategy to minimize the risk of collapse. However, in low seismic zones it is not necessary to design the substructures or their foundations for these forces since it is expected that if a column does yield it will have sufficient inherent ductility to survive without collapse. Even though bridge columns in SDR 2 are not required to be designed for seismic loads, shear reinforcement requirements will provide a minimum level of capacity for ductile deformations. This level is considered to be adequate for the magnitude and duration of the ground motion expected in SDR 2.

The magnitude of live load assumed to exist at the time of the earthquake should be consistent with the value of  $\gamma_{eq}$  used in conjunction with Table 3.4.1-1.

#### C6.3 DESIGN DISPLACEMENTS

Unseating of girders at abutments and piers must be avoided in all circumstances. The current AASHTO Division I-A requirement for minimum seat width is:

$$N = 0.20 + 0.0017L + 0.0067H$$

for seismic performance categories A and B. The seat width is multiplied by 1.5 for SPC C and SPC D. The seat width is further multiplied by  $1/\cos\alpha$  to account for skew effects. The Division I-A ex-

pression gives reasonable minimum seat widths, but it is modified herein for higher seismic zones.

The requirement for minimum seat width accounts for (1) relative displacement due to out-of-phase ground motion of the piers, (2) rotation of pier footings, and (3) longitudinal and transverse deformation of the pier. The Division I-A expression provides reasonable estimates of the first two effects, but underestimates the third. The maximum deformation demand is given by the P- $\Delta$  limitation because P- $\Delta$  generally controls the displacement of the piers. The capacity spectrum gives:

$$C_c \Delta = \left( \frac{F_v S_1}{2\pi B} \right)^2 g$$

and the P- $\Delta$  limitation is:

$$C_c > 4 \frac{\Delta}{H}$$

Combining the two expressions gives the maximum displacement when P- $\Delta$  controls:

$$\Delta = \frac{\sqrt{g}}{4\pi B} \sqrt{H} \cdot F_v S_1$$

Assuming  $B=1.4$ , with moderate ductility capacity, the longitudinal displacement limit in meter units is  $\Delta_s = 0.18\sqrt{H} \cdot F_v S_1$ .

Transverse displacement of a pier supporting both a span with fixed bearings and a span with a longitudinal release will result in additional seat displacement. The seat displacement at the edge of the span with the longitudinal release is  $2\Delta_s B / L$ . Combining the seat displacement due to longitudinal and transverse displacement of the pier using the SRSS combination rule gives the pier displacement contribution to seat width as:

$$N = 0.18\sqrt{H} \sqrt{1 + \left( 2 \frac{B}{L} \right)^2} \cdot F_v S_1$$

for  $F_v S_1 = 0.40$  the coefficient is 0.072. Because transverse displacement of a pier is limited by "arching" of the superstructure, the maximum of  $B/L=3/8$  is reasonable for determining the seat displacement.

Using this approach, the minimum seat width in Equation 6.3-1 is a linear function of the seismic hazard,  $F_v S_1$ . The factor on seat width varies from unity for  $F_v S_1 = 0$  to 1.5 for  $F_v S_1 = 0.40$ . The factor for  $F_v S_1 = 0.80$  is 2.0. The coefficient for the

pier deformation term provides a contribution to the seat width for  $F_v S_1 = 0.40$  of:

$$N = 0.075\sqrt{H} \sqrt{1 + \left( 2 \frac{B}{L} \right)^2}$$

which is close to the value from the P- $\Delta$  analysis. The constant term is reduced from 0.20 to 0.10 because the pier deformation is included directly.

Equation 6.3-1 provides seat widths that are slightly larger than the Division I-A requirement for low seismic zones, and larger seat widths, for  $F_v S_1 = 0.80$ , by a factor of 1.5 to 1.8.

#### **C6.4 FOUNDATION DESIGN REQUIREMENTS**

No commentary is provided for Article 6.4.

#### **C6.5 ABUTMENT DESIGN REQUIREMENTS**

No commentary is provided for Article 6.5.

#### **C6.6 LIQUEFACTION DESIGN REQUIREMENTS**

No commentary is provided for Article 6.6.

#### **C6.7 STRUCTURAL STEEL DESIGN REQUIREMENTS**

##### **C6.7.1 SDR 1**

No commentary is provided for Article 6.7.1.

##### **C6.7.2 SDR 2**

##### **C6.7.2.1 Ductile Moment-Resisting Frames and Bents**

###### **C6.7.2.1.1 Columns**

This provides an increase in the permitted maximum axial load, due to the lower ductility demands expected in SDR 2.

##### **C6.7.2.3 Concentrically Braced Frames and Bents with Nominal Ductility**

This provides an increase in the permitted maximum axial load, due to the lower ductility demands expected in SDR 2.

## Section 7: Commentary

### SEISMIC DESIGN REQUIREMENTS (SDR) 3

#### C7.1 GENERAL

No commentary is provided for Article 7.1.

#### C7.2 DESIGN FORCES

##### C7.2.1 Ductile Substructures ( $R > 1$ ) — Flexural Capacity

The key element in the design procedure is the flexural capacity of the columns. Philosophically, the lower the flexural capacity of the column the more economic will be the seismic design provisions, because the overstrength flexural capacity of a column drives the cost and capacity of both the foundations and the connections to the superstructure. For SDAP B the capacity of the column designed for nonseismic loads is considered to be acceptable for the lower seismic hazard levels.

For SDAP C the design procedure provides a trade-off between acceptable design displacements and minimum flexural capacities of columns. For SDAP D and E the flexural capacity of a column must meet the maximum of the moments from either the Expected Earthquake or the MCE event divided by the appropriate  $R$ -factor. For SDAP C, D, and E there are additional strength limitations based on  $P$ - $\Delta$  considerations.

##### C7.2.2 Capacity Protected Elements or Actions

The objective of these provisions for conventional design is that inelastic deformation (plastic hinging) occurs at the location in the columns (top or bottom or both) where they can be readily inspected and repaired. To achieve this objective, all members connected to the columns, the shear capacity of the column, and all members in the load path from the superstructure to the foundation, shall be capable of transmitting the maximum (overstrength) force effects developed by plastic hinges in the columns. The exceptions to the need for capacity design of connecting elements are (1) when all substructure elements are designed elastically (Article 4.10), (2) seismic isolation design (Article 7.10) and (3) in the transverse direction of

columns when a ductile diaphragm is used (Article 7.7.8.2)

#### C7.2.3 Elastically Designed Elements

If all of the supporting substructure elements (columns, piers, pile bents) are designed elastically, there will be no redistribution of lateral loads due to plastic hinges developing in one or more columns. As a consequence the elastic analysis results are appropriate for design. The recommended provisions attempt to prevent any brittle modes of failure from occurring.

If only one or a selected number of supporting substructure elements are designed elastically, there will be a significant redistribution of lateral loads when one or more of the columns develops plastic hinges. Generally, the elastically designed elements will attract more lateral load. Hence the need to use capacity design principles for all elements connected to the elastically designed column. If this is not practical, the complete bridge needs to be reanalyzed using the secant stiffness of any columns in which plastic hinges will form, in order to capture the redistribution of lateral loads that will occur.

##### C7.2.4 Abutments and Connections

In general the connections between the superstructure and substructure should be designed for the maximum forces that could be developed. In the spirit of capacity design, this implies that the forces corresponding to the full plastic mechanism (with yielding elements at their overstrength condition) should be used to design the connections. In cases where the full plastic mechanism might not develop during the Maximum Considered Earthquake, the elastic forces for this event are permitted. However, it is still good practice to design the connections to resist the higher forces corresponding to the full plastic mechanism. It is also good practice to design for the best estimate of forces that might develop in cases such as pile bents with battered piles. In such bents the connections should be stronger than the expected forces, and these forces may be large and may

have large axial components. In such cases, the plastic mechanism may be governed by the pile geotechnical strengths, rather than the pile structural strengths.

### **C7.2.5 Single Span Bridges**

Requirements for single-span bridges are not as rigorous as for multi-span bridges because of their favorable response to seismic loads in past earthquakes. As a result, single-span bridges need not be analyzed for seismic loads regardless of the SDR, and design requirements are limited to minimum seat widths and connection forces. Adequate seat widths must be provided in both the transverse and longitudinal directions. Connection forces are based on the premise that the bridge is very stiff and that the fundamental period of response will be short. This assumption acknowledges the fact that the period of vibration is difficult to calculate because of significant interaction with the abutments.

These reduced requirements are also based on the assumption that there are no vulnerable substructures (i.e., no columns) and that a rigid (or near-rigid) superstructure is in place to distribute the in-plane loads to the abutments. If, however, the superstructure is not able to act as a stiff diaphragm and sustains significant in-plane deformation during horizontal loading, it should be analyzed for these loads and designed accordingly. Single-span trusses may be sensitive to in-plane loads and the designer may need to take additional precautions to ensure the safety of truss superstructures.

## **C7.3 DESIGN DISPLACEMENTS**

See Article C8.3 for the commentary to this section.

### **C7.4 FOUNDATION DESIGN REQUIREMENTS**

#### **C7.4.1 Foundation Investigation**

Refer to C8.4.1 for the commentary to this section.

#### **C7.4.2 Spread Footings**

During a seismic event, the inertial response of the bridge deck results in a transient horizontal force at the abutments and central piers. This iner-

tial force is resisted by (1) the abutments, (2) the interior piers, or (3) some combination of the two. Forces imposed on the interior columns or piers result in both horizontal shear force and an overturning moment being imposed on the footing. The footing responds to this load by combined horizontal sliding and rotation. The amount of sliding and rotation depends on the magnitude of imposed load, the size of the footing, and the characteristics of the soil.

For seismic design of spread footings, the responses of the footing to shear forces and moment are normally treated independently, i.e., the problem is de-coupled. The overturning component of the column load results in an increase in pressures on the soil. Since the response to moment occurs as a rotation, pressure is highest at the most distant point of the footing, referred to as the toe. This pressure can temporarily exceed the ultimate bearing capacity of the soil. As the overturning moment continues to increase, soil yields at the toe and the heel of the footing can separate from the soil, which is referred to as liftoff of the footing. This liftoff is temporary. As the inertial forces from the earthquake change direction, pressures at the opposite toe increase and, if moments are large enough, liftoff occurs at the opposite side. Bearing failure occurs when the force induced by the moment exceeds the total reactive force that the soil can develop within the area of footing contact. Soil is inherently ductile, and therefore, yielding at the toe and liftoff at the heel of the footing are acceptable phenomena, as long as (1) global stability is preserved and (2) settlements induced by the cyclic loading are small.

The shear component of column load is resisted by two mechanisms: (1) the interface friction between the soil and the footing along the side and at the base of the footing, and (2) the passive resistance at the face of the footing. These resistances are mobilized at different deformations. Generally, it takes more displacement to mobilize the passive pressure. However, once mobilized, it normally provides the primary resistance to horizontal loading.

Inertial response of a bridge deck results in a horizontal shear force and a moment at the connection of the column to the footing. The footing should not undergo permanent rotation, sliding, or appreciable settlement under these loads. Any permanent displacement that occurs should be constrained by the limits required to preserve the service level of the bridge as suggested in Table C3.2-1.



#### C7.4.2.1 Moment and Shear Capacity

The shear component of loading should not be included during the overturning check; i.e., a de-coupled approach should be used in treating the two loads. Experience has shown that use of inclination factors to represent the combined horizontal load and moment in simplified bearing capacity equations can result in unreasonably sized footings for seismic loading.

Unfactored resistance is used for the moment capacity check for two reasons: (1) the potential for the design seismic load is very small, and (2) the peak load will occur for only a short duration. The distribution and magnitude of bearing stress, as well as liftoff of the footing, are limited to control settlement of the footing from the cycles of load.

Nontriangular stress distributions or greater than 50% liftoff are allowed if studies can show that soil settlement from cyclic shakedown does not exceed amounts that result in damage to the bridge or unacceptable movement of the roadway surface. By limiting stress distribution and the liftoff to the specified criteria, the amount of shakedown will normally be small under normal seismic loading conditions.

No special check is required for the shear component of column loads for SDR 3 because the maximum horizontal load induced by the seismic event will normally be less than the friction mobilized at the base of the footing for this seismic category.

#### C7.4.2.2 Liquefaction Check

Liquefaction below a spread footing foundation can result in three conditions that lead to damage or failure of a bridge:

- loss in bearing support which causes large vertical downward movement,
- horizontal forces on the footing from lateral flow or lateral spreading of the soil, and
- settlements of the soil as porewater pressures in the liquefied layers dissipate.

Most liquefaction-related damage during past earthquakes has been related to lateral flow or spreading of the soil. In these cases ground movements could be a meter or more. If the spread footing foundation is located above the

water table, as is often the case, it will be very difficult to prevent the footing from being displaced with the moving ground. This could result in severe column distortion and eventual loss of supporting capacity.

In some underwater locations, it is possible that the lateral flow could move past the footing without causing excessive loading; however, these cases will be limited. For these situations special studies are required to evaluate the magnitude of forces that will be imposed on the foundation and to confirm that these forces will not result in large lateral movement of the footing.

Additional discussion of the consequences of liquefaction is provided in Appendix D to these *Guidelines*. A flow chart showing the methodology for addressing the moving soil case is given in Figure D.4.2-1.

### C7.4.3 Driven Piles

#### C7.4.3.1 General

To meet uplift loading requirements during a seismic event or during ship impact, the depth of penetration may have to be greater than minimum requirements for compressive loading to mobilize sufficient uplift resistance. This uplift requirement can impose difficult installation conditions at locations where very hard bearing layers occur close to the ground surface. In these locations ground anchors, insert piles, and H-pile stingers can be used to provide extra uplift resistance in these situations.

If batter piles are used in SDR 3 and above, consideration must be given to (1) downdrag forces caused by dissipation of porewater pressures following liquefaction, (2) the potential for lateral displacement of the soil from liquefaction-induced flow or lateral spreading, (3) the ductility at the connection of the pile to the pile cap, and (4) the buckling of the pile under combined horizontal and vertical loading. These studies will have to be more detailed than those described elsewhere within Article 8.4. As such, use of batter piles should be handled on a case-by-case basis. Close interaction between the geotechnical engineer and the structural engineer will be essential when modeling the response of the batter pile for seismic loading.

For drained loading conditions, the vertical effective stress,  $\sigma'_{vs}$ , is related to the groundwater level and thus affects pile capacity. Seismic design

loads have a low probability of occurrence. This low probability normally justifies not using the highest groundwater level during seismic design.

#### C7.4.3.2 Design Requirements

Shear forces and overturning moments developing within this design category will normally be small. Except in special circumstances, the load and resistance factors associated with Strength Limit State will control the number and size of the pile foundation system. A capacity check for the overturning moment is, however, required to confirm that the specific features of the bridge design and soil condition do not result in instability or excessive uplift of the foundation system. Checks should also be made to confirm that unacceptable displacements from flow slides or loss of bearing support from liquefaction do not occur.

The flexibility of pile bents is included because it is relatively easy to include and it is generally more significant than that of spread and piled foundations. For pile bents the estimated depth of fixity can be determined in one of the following ways: (1) using the simplified relationships shown in Figure 10.7.4-1 of the 1998 AASHTO LRFD provisions and Figure 10.7.4-2 of the AASHTO LRFD provisions, (2) using relationships given in FHWA (1997) and DM7 (1982), or (3) conducting lateral pile analyses using a beam-column approach.

#### C7.4.3.3 Moment and Shear Design

Unfactored resistance and uplift are permitted for the foundation design for two reasons: (1) the design seismic load is likely to be small, and (2) the peak load will occur for only a short duration. By allowing uplift in only the most distant row of piles, the remaining piles will be in compression. Normally piles designed for the Strength Limit State will have a capacity reserve of 2.0 or more, resulting in adequate capacity for vertical loads. The moment capacity check determines whether adequate capacity exists in rotation. If rotational capacities are not satisfied, longer piles or additional piles may be required to meet seismic requirements.

#### C7.4.3.4 Liquefaction Check

The design of a pile foundation for a liquefied soil condition involves careful consideration on

the part of the designer. General cases occur for liquefaction with and without lateral flow or spreading.

#### *Liquefaction without Lateral Flow or Spreading*

Pile foundations should be designed to extend below the maximum depth of liquefaction by at least 3 pile diameters or to such a depth that axial and lateral capacity are not affected by liquefaction of any overlying layer. Porewater pressures in a liquefied zone can result in increases in porewater pressure within layers below the liquefied zone. Porewater pressure increases can also occur in a zone where the factor of safety for liquefaction is greater than 1.0, as discussed in Appendix D. These increases in porewater pressure will temporarily reduce the strength of the material from its pre-earthquake (static) strength. The potential for this decrease should be evaluated, and the capacity of the foundation evaluated for the lower strength. Alternatively, the toe of the pile should be founded at a depth where the effects of porewater pressure changes are small. Normally, the static design of the pile will include a resistance factor of 0.6 or less. This reserve capacity allows an increase in porewater pressure by 20% without significant downward movement of the pile.

As porewater pressures dissipate following liquefaction, drag loads will develop on the side of the pile. The drag loads occur between the pile cap and the bottom of the liquefied layer. The side friction used to compute drag loads will increase with dissipation in porewater pressure from the residual strength of the liquefied sand to a value approaching the static strength of the sand. The maximum drag occurs when the porewater pressures are close to being dissipated. Simultaneously relative movement between the pile and the soil decrease as the porewater pressure decreases, resulting in the drag load evaluation being a relatively complex soil-pile interaction problem. For simplicity, it can be conservatively assumed that the drag load used in the settlement estimate is determined by the pre-liquefied side resistance along the side of the pile between the bottom of the pile cap and the bottom of the liquefied zone.

#### *Liquefaction with Lateral Flow or Spreading*

Lateral flow and spreading have been common occurrences during liquefaction at bridge sites involving an approach fill or at a river or stream crossing. The amount of movement can range from a few millimeters to over a meter. This

amount of movement is generally sufficient to develop full passive pressures on pile or pile cap surfaces exposed to the moving soil. If the system of piles and pile cap is not strong enough to resist these movements, the pile cap system will displace horizontally under the imposed load.

Procedures for estimating either the forces or displacements of the pile from the moving ground are discussed in Appendix D. If these forces or displacements are large, some type of ground remediation might be used to reduce these displacements. These ground remediation methods can include vibro densification, stone columns, pressure grouting, or in-place soil mixing. Costs of these improvements can range from \$10/m<sup>3</sup> to in excess of \$40/m<sup>3</sup> (in year-2000 dollars). Depending on the specific conditions and design requirements for a site, the use of ground improvement could increase construction costs by 10% or more. In view of these costs, the owner needs to be made aware of the potential risks and the costs of remediation methods as soon as these conditions are identified.

Appendix D provides a more detailed discussion of the process to follow when designing for lateral flow or spreading ground.

#### **C7.4.4 Drilled Shafts**

Lam et al. (1998) provides a detailed discussion of the seismic response and design of drilled shaft foundations. Their discussion includes a summary of procedures to determine the stiffness matrix required to represent the shaft foundation in most dynamic analyses.

Drilled shaft foundations will often involve a single shaft, rather than a group of shafts. This is not the case for driven piles. In single shaft configuration the relative importance of axial and lateral response changes. Without the equivalent of a pile cap, lateral-load displacement of the shaft becomes more critical than the (axial) load-displacement relationships discussed above for driven piles.

Many drilled-shaft foundation systems consist of a single shaft supporting a column. Compressive and uplift tensile loads on these shafts during seismic loading will normally be within the limits of the load factors used for gravity loading. However, checks should be performed to confirm that any changes in axial load do not exceed ultimate capacities in uplift or compression. In contrast to driven piles in a group, no reserve capacity exists

for a single shaft; i.e., if ultimate capacity is exceeded, large deformations can occur.

Special design studies can be performed to demonstrate that deformations are within acceptable limits if axial loads approach or exceed the ultimate uplift or compressive capacities if the drilled shaft is part of a group. These studies can be conducted using computer programs, such as APILE Plus (Reese, et al., 1997). Such studies generally will require rigorous soil-structure interaction modeling.

Various studies (Lam et al., 1998) have found that conventional p-y stiffnesses derived for driven piles are too soft for drilled shafts. This stiffer response is attributed to a combination of (1) higher unit side friction, (2) base shear at the bottom of the shaft, and (3) the rotation of the shaft. The rotation effect is often implicitly included in the interpretation of lateral load tests, as most lateral load tests are conducted in a free-head condition. A scaling factor equal to the ratio of shaft diameter to 600 mm is generally applicable, according to Lam et al. (1998). The scaling factor is applied to either the linear subgrade modulus or the resistance value in the p-y curves. This adjustment is dependent on the construction method.

Base shear can also provide significant resistance to lateral loading for large diameter shafts. The amount of resistance developed in shear will be determined by conditions at the base of the shaft during construction. For dry conditions where the native soil is relatively undisturbed, the contributions for base shear can be significant. However, in many cases the base conditions result in low interface strengths. For this reason the amount of base shear to incorporate in lateral analyses will vary from case to case.

### **C7.5 ABUTMENT DESIGN REQUIREMENTS**

#### **C7.5.1 General**

One of the most frequent observations of damage during past earthquakes has been damage to the abutment wall. This damage has been due to two primary causes: (1) the approach fill has moved outward, carrying the abutment with it, and (2) large reactive forces have been imposed on the abutment as the bridge deck has forced it into the approach fill. This latter cause of damage has often resulted from a design philosophy that assumed that the abutment wall had to survive only active seismic earth pressures, and that gaps between the bridge deck and abutment wall would

never be forced to close. In many cases the gap was not sufficient to remain open, and large loads were imposed by the deck. The passive reaction from the soil was as much as 30 times the forces used for active pressure design, resulting in overloading and damage of the wall.

These LRFD *Guidelines* have been prepared to acknowledge specifically the potential for this higher load on the abutment wall. If designed properly, the reactive capacity of the approach fill can provide significant benefit to the bridge-foundation system.

### **C7.5.2 Longitudinal Direction**

Refer to Article C8.5.2 for the commentary to this subsection.

### **C7.5.3 Transverse Direction**

Refer to Article C8.5.3 for the commentary to this subsection.

## **C7.6 LIQUEFACTION DESIGN REQUIREMENTS**

### **C7.6.1 General**

Liquefaction has been perhaps the single most significant cause of damage to bridge structures during past earthquakes. Most of the damage has been related to lateral movement of soil at the bridge abutments. However, cases involving the loss in lateral and vertical bearing support of foundations for central piers of a bridge have also occurred.

The threat of liquefaction requires careful attention to the determination of the potential for liquefaction and its consequences. For earthquake magnitudes less than 6.0, liquefaction develops slowly at most sites, and results in minimal effects to the structure during dynamic shaking, and therefore the effects of liquefaction on dynamic response can be neglected. If the mean magnitude of the Maximum Considered Earthquake is less than 6.0, then the discussion above with regard to duration is applicable. For the magnitude interval of 6.0 to 6.4, a liquefaction analysis is not required when the combination of ground shaking and blow count are below values that would cause liquefaction. This transition interval is based on both an assessment of available data from past earthquakes and on engineering judgment.

The mean magnitudes shown in Figures 7.6.1-1 to 7.6.1-4 are based on deaggregation information, which can be found on the USGS website (<http://geohazards.cr.usgs.gov/eq/>). A site-specific determination of the mean magnitude can be obtained from this website using the coordinates of the project site.

If liquefaction is expected to occur in the Expected Earthquake, then the performance criteria for piles will need to be operational for the life-safety performance level as per Article 7.8.6.

### **C7.6.2 Evaluation of Liquefaction Potential**

Refer to Article C8.6.2 for the commentary to this subsection.

### **C7.6.3 Evaluation of the Effects of Liquefaction and Lateral Ground Movement**

Refer to Article C8.6.3 for the commentary to this subsection.

### **C7.6.4 Design Requirements if Liquefaction and Ground Movement Occurs**

If liquefaction with no lateral flow occurs for SDR 3 bridges, then the only additional design requirements are those reinforcement requirements specified for the piles and spread foundation. Additional analyses are not required, although for major or important bridges the additional analyses specified in Article 4.6 may be considered in order to assess the impact on the substructures above the foundation.

If liquefaction and lateral flow are predicted to occur for SDR 3, a detailed evaluation of the effects of lateral flow on the foundation should be performed. Lateral flow is one of the more difficult issues to address because of the uncertainty in the movements that may occur. The design steps to address lateral flow are given in Appendix D. Liberal plastic rotation of the piles is permitted. This plastic rotation does imply that the piles and possibly other parts of the bridge will need to be replaced if these levels of deformation do occur. Design options range from (a) an acceptance of the movements with significant damage to the piles and columns if the movements are large, to (b) designing the piles to resist the forces generated by lateral spreading. Between these options are a range of mitigation measures to limit the amount of movement to tolerable levels for the desired

performance objective. Pile group effects are not significant for liquefied soil.

#### **C7.6.5 Detailed Foundation Design Requirements**

Refer to the appropriate subsections of Article C7.4 for the commentary.

#### **C7.6.6 Other Collateral Hazards**

The assessment of these collateral hazards will normally be limited to bridges located in SDR 3, 4, 5, and 6 as the potential for any of these hazards in SDR 1 and 2 will generally be small.

### **C7.7 STRUCTURAL STEEL DESIGN REQUIREMENTS**

Refer to Article C8.7 for the commentary to all of the subsections of this article.

### **C7.8 REINFORCED CONCRETE DESIGN REQUIREMENTS**

Refer to Article C8.8 for the commentary to all of the subsections of this article.

### **C7.9 BEARING DESIGN REQUIREMENTS**

One of the significant issues that arose during the development of these recommended *Guidelines* was the critical importance of bearings as part of the overall bridge load path. The 1995 Kobe earthquake, and others that preceded it or have occurred since, clearly showed poor performance of some recent bearing types and the disastrous consequences that a bearing failure can have on the overall performance of a bridge. A consensus was developed that some testing of bearings would be desirable provided a designer had the option of providing restraints or permitting the bearing to fail if an adequate surface for subsequent movement is provided. An example occurred in Kobe where a bearing failed. The steel diaphragm and steel girder were subsequently damaged because the girder became jammed on the failed bearing and could not move.

There have been a number of studies performed when girders slide either on specially designed bearings or concrete surfaces. A good summary of the range of the results that can be anticipated from these types of analyses can be found in Dicleli and Bruneau (1995).

#### **C7.9.1 Prototype and Quality Control Tests**

The types of tests that are required by these *Guidelines* are similar to but significantly less extensive than those required for seismically isolated bridges. Each manufacturer is required to conduct a prototype qualification test to qualify a particular bearing type and size for its design forces or displacements. This series of tests only needs to be performed once to qualify the bearing type and size, whereas for seismically isolated bridges, prototype tests are required on every project. The quality control tests required on 1 out of every 10 bearings is the same as that required for every isolator on seismic isolation bridge projects. The cost of the much more extensive prototype and quality control testing of isolation bearings is approximately 10 to 15% of the total bearing cost, which is of the order of 2% of the total bridge cost. The testing proposed herein is much less stringent than that required for isolation bearings and is expected to be less than 0.1% of the total bridge cost. However, the benefits of testing are considered to be significant since owners would have a much higher degree of confidence that each new bearing will perform as designed during an earthquake. The testing capability exists to do these tests on full-size bearings.

### **C7.10 SEISMIC ISOLATION DESIGN REQUIREMENTS**

The commentary on this subject is given in C15, which will become a new section in the AASHTO LRFD provisions.



## Section 8: Commentary

### SEISMIC DESIGN REQUIREMENTS (SDR) 4, 5 AND 6

#### C8.1 GENERAL

No commentary is provided for Article 8.1.

#### C8.2 DESIGN FORCES

##### C8.2.1 Ductile Substructures ( $R > 1$ ) — Flexural Capacity

The key element in the design procedure is the flexural capacity of the columns. Philosophically, the lower the flexural capacity of the column the more economic will be the seismic design provisions because the overstrength flexural capacity of a column drives the cost and capacity of both the foundations and the connections to the superstructure. For SDAP B the capacity of the column designed for nonseismic loads is considered to be acceptable for the lower seismic hazard levels.

For SDAP C the design procedure provides a trade-off between acceptable design displacements and minimum flexural capacities of columns. For SDAP D and E the flexural capacity of a column must meet the maximum of the moments from either the Expected Earthquake or the MCE event divided by the appropriate  $R$ -factor. For SDAP C, D, and E there are additional strength limitations based on  $P$ - $\Delta$  considerations.

##### C8.2.2 Capacity Protected Elements or Actions

The objective of these provisions for conventional design is that inelastic deformation (plastic hinging) occurs at the location in the columns (top or bottom, or both) where they can be readily inspected and repaired. To achieve this objective, all members connected to the columns, the shear capacity of the column, and all members in the load path from the superstructure to the foundation, shall be capable of transmitting the maximum (overstrength) force effects developed by plastic hinges in the columns. The exceptions to the need for capacity design of connecting elements are (1) when all substructure elements are designed elastically (Article 4.10), (2) seismic isolation design (Article 8.10) and (3) in the transverse direction of

columns when a ductile diaphragm is used (Article 8.7.8.2).

##### C8.2.3 Elastically Designed Elements

If all of the supporting substructure elements (columns, piers, pile bents) are designed elastically, there will be no redistribution of lateral loads due to plastic hinges developing in one or more columns. As a consequence the elastic analysis results are appropriate for design. The recommended provisions attempt to prevent any brittle modes of failure from occurring.

If only one or a selected number of supporting substructure elements are designed elastically, there will be a significant redistribution of lateral loads when one or more of the columns develops plastic hinges. Generally, the elastically designed elements will attract more lateral load. Hence the need to use capacity design principles for all elements connected to the elastically designed column. If this is not practical, the complete bridge needs to be reanalyzed using the secant stiffness of any columns in which plastic hinges will form, in order to capture the redistribution of lateral loads that will occur.

##### C8.2.4 Abutments and Connections

In general the connections between the superstructure and substructure should be designed for the maximum forces that could be developed. In the spirit of capacity design, this implies that the forces corresponding to the full plastic mechanism (with yielding elements at their overstrength condition) should be used to design the connections. In cases where the full plastic mechanism might not develop during the Maximum Considered Earthquake, the elastic forces for this event are permitted. However, it is still good practice to design the connections to resist the higher forces corresponding to the full plastic mechanism. It is also good practice to design for the best estimate of forces that might develop in cases such as pile bents with battered piles. In such bents the connections should be stronger than the expected forces, and these forces may be large and may have large axial components. In such cases, the

plastic mechanism may be governed by the pile geotechnical strengths, rather than the pile structural strengths.

### C8.2.5 Single Span Bridges

Requirements for single-span bridges are not as rigorous as for multi-span bridges because of their favorable response to seismic loads in past earthquakes. As a result, single-span bridges need not be analyzed for seismic loads regardless of the SDR, and design requirements are limited to minimum seat widths and connection forces. Adequate seat widths must be provided in both the transverse and longitudinal directions. Connection forces are based on the premise that the bridge is very stiff and that the fundamental period of response will be short. This assumption acknowledges the fact that the period of vibration is difficult to calculate because of significant interaction with the abutments.

These reduced requirements are also based on the assumption that there are no vulnerable substructures (i.e., no columns) and that a rigid (or near-rigid) superstructure is in place to distribute the in-plane loads to the abutments. If, however, the superstructure is not able to act as a stiff diaphragm and sustains significant in-plane deformation during horizontal loading, it should be analyzed for these loads and designed accordingly. Single-span trusses may be sensitive to in-plane loads and the designer may need to take additional precautions to ensure the safety of truss superstructures.

## C8.3 DESIGN DISPLACEMENTS

### C8.3.1 General

No commentary is provided for Article 8.3.1.

### C8.3.2 Minimum Seat Width Requirement

Unseating of girders at abutments and piers must be avoided in all circumstances. The current Division I-A requirement for minimum seat width is:

$$N = 0.20 + 0.0017L + 0.0067H$$

for seismic performance categories A and B. The seat width is multiplied by 1.5 for SPC C and D. The seat width is further multiplied by  $1/\cos\alpha$  to account for skew effects. The current expression

gives reasonable minimum seat widths, but it is modified herein for larger seismic zones.

The requirement for minimum seat width accounts for (1) relative displacement due to out-of-phase ground motion of the piers, (2) rotation of pier footings, and (3) longitudinal and transverse deformation of the pier. The current expression provides reasonable estimates of the first two effects, but underestimates the third. The maximum deformation demand is given by the  $P-\Delta$  limitation because  $P-\Delta$  generally controls the displacement of the piers. The capacity spectrum gives:

$$C_c \Delta = \left( \frac{F_v S_1}{2\pi B} \right)^2 g$$

and the  $P-\Delta$  limitation is:

$$C_c > 4 \frac{\Delta}{H}$$

Combining the two expressions gives the maximum displacement when  $P-\Delta$  controls:

$$\Delta = \frac{\sqrt{g}}{4\pi B} \sqrt{H} \cdot F_v S_1$$

Assuming  $B=1.4$ , with moderate ductility capacity, the longitudinal displacement limit in meter units is  $\Delta_s = 0.18\sqrt{H} \cdot F_v S_1$ .

Transverse displacement of a pier supporting both a span with fixed bearing and a span with a longitudinal release, will result in additional seat displacement. The seat displacement at the edge of the span with the longitudinal release is  $2\Delta_s B/L$ . Combining the seat displacement due to longitudinal and transverse displacement of the pier using the SRSS combination rule gives the pier displacement contribution to seat width as:

$$N = 0.18\sqrt{H} \sqrt{1 + \left( 2 \frac{B}{L} \right)^2} \cdot F_v S_1$$

for  $F_v S_1 = 0.40$  the coefficient is 0.072. Because transverse displacement of a pier is limited by "arching" of the superstructure, the maximum of  $B/L=3/8$  is reasonable for determining the seat displacement.

Using this approach, the minimum seat width in Equation 8.3.2-1 is a linear function of the seismic hazard,  $F_v S_1$ . The factor on seat width varies from unity for  $F_v S_1 = 0$  to 1.5 for  $F_v S_1 = 0.40$ . The factor for  $F_v S_1 = 0.80$  is 2.0. The



coefficient for the pier deformation term provides a contribution to the seat width for  $F_v S_1 = 0.40$  of:

$$N = 0.075\sqrt{H} \sqrt{1 + \left(2\frac{B}{L}\right)^2}$$

which is close to the value from the  $P$ - $\Delta$  analysis. The constant term is reduced from 0.20 to 0.10 because the pier deformation is included directly.

Equation (8.3.2-1) provides seat widths that are slightly larger than the Division I-A requirement for low seismic zones, whereas larger seat widths for  $F_v S_1 = 0.80$  are larger by a factor of 1.5 to 1.8.

### C8.3.3 Displacement Compatibility

Certain components may be designed to carry only dead and live loads (e.g., bearings, non-participating bents). Other components are non-structural, but their failure would be unacceptable or could result in structural problems (e.g., large-diameter water pipes that could erode soils away if they failed). Under seismic loads these components must deform to remain compatible with their connections. The purpose of this section is to require a check that the non-seismic-load-resisting components have sufficient deformation capacity under seismically induced displacements of the bridge.

### C8.3.4 P- $\Delta$ Requirements

Structures subject to earthquake ground motion may be susceptible to instability from  $P$ - $\Delta$  effects. Inadequate strength can result in "ratcheting" of structural displacements, with large residual deformation, and eventually, instability. The intent of this section is to provide a minimum strength, or a maximum displacement, for which  $P$ - $\Delta$  effects will not significantly affect seismic behavior of a bridge.

$P$ - $\Delta$  produces a negative slope in a structures' force-displacement relationship equal to  $P/H$ .

The basis for the requirement in Equation 8.3.4-1 is that the maximum displacement is such that the reduction in resisting force is limited to a 25% reduction from the lateral strength assuming no post yield stiffness:

$$\Delta \frac{P}{H} < 0.25V \quad (\text{C8.3.4-1})$$

where  $P$  is the gravity load on the substructure. Stating a limitation on displacement in terms of lateral strength is justified from dynamic analysis of SDOF systems with various hysteretic relationships. The requirement of Equation C8.3.4-1 will avoid "ratcheting" in structures with typical post-yield stiffness. The requirement has been shown to limit  $P$ - $\Delta$  effects from dynamic analysis of single-degree-of-freedom systems (Mahin and Boroschek, 1991, MacRae 1994).

The lateral strength can be expressed in terms of the seismic coefficient,  $C_c = V/W$ , which upon substitution into Equation C8.3.4-1 gives:

$$\Delta \leq 0.25C_c \left( \frac{W}{P} \right) H \quad (\text{C8.3.4-2})$$

where  $W$  is the weight of the bridge responding to horizontal earthquake ground motion. For bridges in which the weight responding to horizontal ground motion is equal to the gravity load on the substructure, Equation C8.3.4-2 gives Equation 8.3.4-1.

However, bridges with abutments may have a  $W/P$  ratio greater than unity if the abutments do not deform significantly, thus reducing  $P$ - $\Delta$  effects because a portion of the gravity load is resisted by the abutments. The designer may consider using Equation C8.3.4-2 with  $W/P \leq 2$  when such an assumption is documented.

Equation 8.3.4-1 can also be stated as a minimum seismic coefficient to avoid  $P$ - $\Delta$  effects.

$$C_c > 4 \frac{\Delta}{H} \quad (\text{C8.3.4-3})$$

In the short period range, the equal displacement rule does not apply. Inelastic displacement will be greater than the elastic displacement according to:

$$\Delta_{inelastic} = \frac{R_B}{R} \Delta \quad (\text{C8.3.4-4})$$

in which  $R_B$  is the target reduction factor and  $R$  is the ratio of the lateral strength to the elastic force according to Article 4.7. Substitution of Equation 4.7-1 into C8.3.4-4 gives Equations 8.3.4-2 and 8.3.4-3.

### **C8.3.5 Minimum Displacement Requirements for Lateral-Load-Resisting Piers and Bents**

The requirement in this section is based on the “equal displacement rule”, that is, the maximum displacement from dynamic analysis with a linear model using cracked section properties is approximately equal to the maximum displacement for the yielding structure – Figure C3.3-2.

The factor of 1.5 on the displacement demand recognizes the approximations in the modeling for the seismic analysis. Furthermore, the demand analysis is performed for a model of the entire bridge including three-dimensional effects. However, the displacement capacity verification is done using a two-dimensional pushover analysis on individual bents. Since the relationship between the two methods of analysis is not well-established, the factor of 1.5 represents a degree of conservatism to account for the lack of a rigorous basis for comparing displacement demand and capacity.

For regular bridges satisfying the requirements for SDAP C in Article 4.4, the displacement requirement implied in the capacity spectrum approach does not include the 1.5 factor.

## **C8.4 FOUNDATION DESIGN REQUIREMENTS**

### **C8.4.1 Foundation Investigation**

#### **C8.4.1.1 General**

The conduct of the subsurface exploration program is part of the process of obtaining information relevant for the design and construction of substructure elements. Information from the subsurface exploration is particularly critical in areas of high seismicity as information from the exploration will determine the Site Classification for seismic design and the potential for geologic hazards, such as liquefaction and slope stability.

The elements of the process that should precede the actual exploration program include search and review of published and unpublished information at and near the site, a visual site inspection, and design of the subsurface exploration program. Refer to *AASHTO Manual on Subsurface Investigations* (1988) for general guidance regarding the planning and conduct of subsurface exploration programs.

#### **C8.4.1.2 Subsurface Investigations**

The exploration phase of the project should be conducted early enough that geologic conditions that could have a significant effect on project costs are identified. If subsurface information is not available from previous work in the area, it may be desirable to conduct a limited exploration program before the Type, Size, and Location (TSL) phase of the project, to identify conditions that may change either the location or type of bridge.

A variety of subsurface exploration methods is available. The most common methods involve drilling methods or cone penetrometer soundings. In some cases geophysical methods can be used to provide information relevant to the design of the substructure system. Appendix B provides a discussion of these methods. As noted in Appendix B, each of these methods has limitations. A geotechnical engineer or engineering geologist should be involved in the selection of the most appropriate exploration method.

#### **8.4.1.3 Laboratory Testing**

The equipment and methods used during laboratory testing will depend on the type of soil or rock, as well as the state of disturbance of the sample to be tested. Therefore, the need for certain types of samples should be considered when planning the field exploration phase of the project.

The number and type of laboratory tests should be determined after reviewing boring logs developed from the field exploration plan relative to the range in substructures that will be possibly used for the bridge. Additional details regarding laboratory testing are presented in Appendix B.

### **C8.4.2 Spread Footings**

During a seismic event, the inertial response of the bridge deck results in a transient horizontal force at the abutments and central piers. This inertial force is resisted by (1) the abutments, (2) the interior piers, or (3) some combination of the two. Forces imposed on the interior columns or piers result in both horizontal shear force and an overturning moment being imposed on the footing. The footing responds to this load by combined horizontal sliding and rotation. The amount of sliding and rotation depends on the magnitude of imposed load, the size of the footing, and the characteristics of the soil.

For seismic design of spread footings, the responses of the footing to shear forces and moment are normally treated independently, i.e., the problem is de-coupled. The overturning component of the column load results in an increase in pressures on the soil. Since the response to moment occurs as a rotation, pressure is highest at the most distant point of the footing, referred to as the toe. This pressure can temporarily exceed the ultimate bearing capacity of the soil. As the overturning moment continues to increase, soil yields at the toe and the heel of the footing can separate from the soil, which is referred to as liftoff of the footing. This liftoff is temporary. As the inertial forces from the earthquake change direction, pressures at the opposite toe increase and, if moments are large enough, liftoff occurs at the opposite side. Bearing failure occurs when the force induced by the moment exceeds the total reactive force that the soil can develop within the area of footing contact. Soil is inherently ductile, and therefore, yielding at the toe and liftoff at the heel of the footing are acceptable phenomena, as long as (1) global stability is preserved and (2) settlements induced by the cyclic loading are small.

The shear component of column load is resisted by two mechanisms: (1) the interface friction between the soil and the footing along the side and at the base of the footing, and (2) the passive resistance at the face of the footing. These resistances are mobilized at different deformations. Generally, it takes more displacement to mobilize the passive pressure. However, once mobilized, it normally provides the primary resistance to horizontal loading.

Various approaches are available to evaluate the response of the bridge-footing system during the design event. In most cases the bridge designer will use equivalent linear springs to represent the soil-footing system. Guidance provided in these Specifications focuses on these simple procedures.

For critical or irregular bridges more rigorous modeling is sometimes used. These methods can involve use of two- and three-dimensional finite element or finite difference modeling methods. This approach to modeling involves considerable expertise in developing a model that represents the soil-structure system. Close cooperation is required between the structural engineer and the geotechnical engineer when developing the model; each discipline has to be familiar with the limitations associated with the development of the model. Without this cooperative approach, it is very easy to obtain very precise results that have

little relevance to likely performance during the design earthquake.

Liquefaction represents a special design problem for spread footings because of the potential for loss in bearing support, lateral movement of the soil from flow or lateral spreading, and settlements following an earthquake as porewater pressures in liquefied soil dissipate. Nonlinear, effective-stress methods are normally required to replicate adequately these conditions in computer models. Such modeling methods are limited in number and require significant expertise. They are usually applicable for bridge design projects only in special circumstances.

#### C8.4.2.1 Spring Constants for Footings

A Winkler spring model is normally used to represent the vertical stiffness and moment-rotation relationship in the analysis. A uniformly distributed rotational stiffness can be calculated by dividing the total rotational stiffness of the footing by the moment of inertia of the footing in the direction of loading. Similar methods are used for vertical stiffness.

#### *Strain and Liftoff Adjustment Factors*

Equations given in Tables 8.4.2.1-1 and 8.4.2.1-2 are based on elastic halfspace theory. These equations were originally developed for low levels of dynamic loading associated with machine foundations. For these levels of loading, it is possible to use the low-strain shear modulus ( $G_{\max}$ ) of the soil, and the footing remains in full contact with the soil. During seismic loading, at least two different phenomena occur which are inconsistent with the assumptions used in the original development of these equations. These differences involve (1) the nonlinear response of the soil from both free-field earthquake wave propagation and from local strain amplitude effects and (2) the liftoff of the footing.

- *Strain Amplitude Effects:* The strain amplitude effects reflect the inherent nonlinearity of soil, even at low shear strain amplitudes. As the seismic wave propagates through the soil, the soil softens, resulting in a reduced shear modulus. Both field measurements and numerical modeling have shown this softening, as discussed by Kramer (1996). A second source of soil nonlinearity also must be considered. As the footing responds to inertial loading from the bridge column, local soil

nonlinearities occur around the footing as the soil is subjected to stress from the shear forces and overturning moments. While various procedures exist for estimating the free-field effects of wave propagation, simple methods for estimating the local strain effects have yet to be developed. Nonlinear finite-element or finite-difference methods can be used to evaluate these effects; however, for most bridge studies such modeling cannot be justified. In recognition of the need for simple guidelines,  $G/G_{max}$  adjustment factors were estimated. This approach for dealing with soil nonlinearity involves considerable judgment, which may warrant modification on a case-by-case basis.

- *Liftoff Effects:* The consequence of uplift during seismic loading will be that the effective area of the footing will be less than if full contact were to occur. The amount of uplift is expected to be larger in a higher seismic zone and during an event with a long return period. The area adjustments for liftoff were made by recognizing that the maximum liftoff allowed under the extreme loading condition will usually be one-half uplift of the footing. It was also recognized that the maximum uplift would only occur for a short period of time, and that during most of the earthquake, the maximum loading might be from 50 to 70% of the peak value. For this reason the effective uplift would not be as much as the peak uplift. Values shown were selected after discussing the potential values of effective area that might occur and then applying considerable engineering judgment.

#### *Uncertainty in Spring Constant Determination*

Stiffness constants developed in the manner described in this Article involve uncertainty. A prudent design will account for this uncertainty by evaluating stiffness for upper and lower-bound modulus values, in addition to the best-estimate shear modulus. The upper and lower-bound values are used to account for (1) the variability of shear modulus that is likely to occur in the field, (2) the uncertainty in adjustments being used for shearing strain and geometric nonlinearities, and (3) limitations in the equation for determining stiffness.

The range of modulus variation used in a sensitivity evaluation is expected to change, depending on the characteristics of the site, the details of the site characterization process, and the type of

analysis. Common practice is often to assume that the lower bound shear modulus is approximately 50% of the best estimate and the upper bound is approximately 100% greater than the best estimate. If the resulting upper and lower-bound values of stiffness are such that significant differences in bridge response are possible, then consideration should be given to either (1) evaluating bridge response for the range of stiffness values or (2) performing additional site characterization studies to reduce the range used in defining the upper and lower bound.

#### *Geometric or Radiation Damping*

The conventional approach during the use of elastic halfspace methods accounts for energy loss within the foundation system through a spectral damping factor. The spectral damping factor is typically defined as 5%, and is intended to represent the damping of the structure-foundation system. This damping differs from the geometric or radiation damping of a foundation. For translational modes of loading, the foundation damping can be in excess of 20%. The 5% spectral damping used in the modal analysis procedures is intended to account for the geometric damping within the foundation system, as well as damping in the bridge structure. While it may be possible to increase the spectral damping of the overall system to a higher level to account for the high geometric damping within the foundation, in view of the liftoff that is allowed to occur during the design earthquake, it is generally not prudent to count on the high levels of foundation damping, at least without special studies that properly account for the liftoff of the foundation.

#### C8.4.2.2 Moment-Rotation and Shear-Displacement Relationships for Footings

The foundation capacity requires an evaluation of the soil to resist the overturning moment and the shear force from the column. Vertical loading to the footing will also change during seismic loading, and this change also needs to be considered.

The initial slope of the moment-rotation curve should be established using the best-estimate rotational spring constant defined in the previous article. Checks can be performed for the upper and lower bound of the initial slope; however, these variations will not normally be important to design.

It is critical, during determination of the moment capacity, for the moment-rotation curve to use the ultimate bearing capacity for the footing without use of a resistance factor (i.e., use  $\phi = 1.0$ ). The determination of ultimate bearing capacity should not be limited by settlement of the footing, as is often done for static bearing capacity determination. The ultimate capacity for the moment-rotation relationship should be defined for the best-estimate soil conditions.

For important bridges, the design should consider use of upper and lower bounds for bearing capacity to account for uncertainties. The range for the upper and lower bound will depend on the variability of soils at the site and the extent of field explorations and laboratory testing. Common practice is often to assume that the lower bound capacity is approximately 50% of the best estimate and the upper bound is approximately 100% greater than the best estimate.

### *Shear-Displacement*

During horizontal shear loading, the resisting force comprises the resistance developed along the base and the sides of the footing and from the passive pressure at the face of the footing. The passive pressure will often provide most of the reaction during a seismic event. For simplicity it can be assumed that the maximum resistance (passive + base + two sides) is developed at a deformation equal to 2% of the footing thickness.

The shear resistance on the base and side of the footing should be determined using an interface shear strength. For most cast-in-place concrete foundations, a value of interface friction of 0.8 times the friction angle of the soil will be appropriate. Displacements to mobilize this resistance will normally be less than 10 to 20 mm. The passive pressure at the face of the footing should be computed assuming an interface friction angle equal to 50% of the friction angle of the backfill material. The log spiral or Caquot-Kerisel (1948) methods should be used for determining the ultimate passive pressure. If the backfill material changes within twice the height of the footing, the effects of the second material should be included in the computation of the passive pressure. A method of slices similar to a slope stability analysis offers one method of accomplishing this computation.

Deformations needed to mobilize the ultimate passive resistance of the face of a footing could easily exceed 25 mm for a typical footing thick-

ness. The potential consequences of this movement relative to column behavior will usually be evaluated during the soil-structure interaction analysis. The uncertainty in computing deformations associated with ultimate passive resistance determination is such that a variation of -50% and +100% would not be unusual. If this variation has a significant effect on, say, the push-over-analysis, the designer may want to modify the foundation or the soil conditions to reduce the uncertainty or limit the deformations.

As discussed by Kramer (1996), evidence exists that the available ultimate passive resistance during seismic loading could be reduced by the seismic response of the ground. This condition occurs if the direction of loading from the inertial response of the bridge structure is the same as the motions in the ground. These two loadings normally occur at different frequencies, and therefore, the coincidence of the directions of loading is usually for only a moment in time. When the movements are out of phase, the loading increases. It was felt that reducing the passive ultimate resistance for the short periods of coincidence would underestimate the effective passive capacity of the foundation (i.e., low ultimate resistance), and therefore the approach taken in these *Specifications* is to ignore this potential effect. This approach clearly involves considerable judgment, and therefore, an alternative approach that includes the reduction in passive resistance could be used, subject to the Owner's approval.

### *Vertical Load Capacity*

For most designs it is unnecessary to consider increases in vertical forces on the footing during seismic loading, as these forces will normally be a fraction of the gravity load. However, if the bridge site is located in proximity to an active fault, vertical accelerations could become important, as discussed in Article 3.4.5. For these situations the potential displacement should be checked using the spring constants given in Table 8.4.2.1-1 together with the increase in vertical column load. The potential consequences of reduction in vertical loads through inertial response should also be considered. This effect could temporarily decrease lateral resistance and moment capacity.

Liquefaction below a spread footing foundation located in SDR 4 and above could be significant because of the combination of higher ground accelerations and larger earthquake magnitudes. As the potential for liquefaction increases, the po-

tential for damage or failure of a bridge from loss in bearing support, lateral flow or lateral spreading of the soil, or settlements of the soil as porewater pressures in the liquefied layers dissipate also increases.

Additional discussion of the consequences of liquefaction is provided in Article 8.6 and Appendix D. A flow chart showing the methodology for addressing the moving soil case is given in Figure D.4.2-1.

#### C.8.4.2.3 Liquefaction and Dynamic Settlement

No commentary is provided for Article 8.4.2.3.

### C8.4.3 Driven Piles

#### C8.4.3.1 General

If batter piles are used, consideration must be given to (1) downdrag forces caused by dissipation of porewater pressures following liquefaction, (2) the potential for lateral displacement of the soil from liquefaction-induced flow or lateral spreading, (3) the ductility at the connection of the pile to the pile cap, and (4) the buckling of the pile under combined horizontal and vertical loading. These studies will have to be more detailed than those described elsewhere within Article 8.4. As such, use of batter piles should be handled on a case-by-case basis. Close interaction between the geotechnical engineer and the structural engineer will be essential when modeling the response of the batter pile for seismic loading.

For drained loading conditions, the vertical effective stress,  $\sigma'_v$ , is related to the groundwater level and thus affects pile capacity. Seismic design loads will have a low probability of occurrence. This low probability normally justifies not using the highest groundwater level during seismic design.

#### C8.4.3.2 Design Requirements

During a seismic event, the inertial response of the bridge deck results in a transient horizontal force. This inertial force is resisted by (1) the abutments, (2) the interior piers, or (3) some combination of the two. Forces imposed on the interior columns or piers result in both horizontal shear force and overturning moments being imposed on the pile foundation. The pile foundation responds to this load by combined horizontal deflection and

rotation. The amount of horizontal deflection and rotation depends on the magnitude of imposed load, the size and type of the foundation system, and the characteristics of the soil.

For seismic design of driven pile foundations, the response of the foundation system to shear forces and moment is normally treated independently; i.e., the problem is de-coupled. If the driven pile is part of a group of piles, as normally occurs, the overturning component of the column load results in an increase in vertical loading on the piles in the direction of loading and a reduction in load in the other direction. Since the response to moment occurs as a rotation, load increase is highest at the most distant pile. This load can temporarily exceed the bearing capacity of the soil. As the overturning moment continues to increase, soil yields at the leading edge of the pile group and the pile begins to plunge. At the trailing edge, uplift loads occur, possibly, resulting in separation between the pile tip and the soil. This uplift is temporary. As the inertial forces from the earthquake change direction, loads at the opposite side increase and, if moments are large enough, uplift occurs at the opposite end. Plunging failure of the pile group occurs only when the force induced by the moment exceeds the total reactive force that the soil can develop for the entire group of piles. Soil is inherently ductile, and therefore, yielding of the forward pile and uplift at the trailing pile are acceptable phenomena, as long as global stability is preserved.

The shear component of column load is resisted by the passive pressure at the face of each pile. Normally, this resistance is mobilized in the upper 5 to 10 pile diameters. If the foundation system includes a pile cap, the reaction to the shear load results from the resistance of the piles and the resistance of the pile cap. The cap develops resistance from (1) the interface friction between the soil and the cap along the side of the cap and (2) the passive resistance at the face of the cap. These resistances are mobilized at different deformations. Generally, it takes more displacement to mobilize the passive pressure. However, once mobilized, it can provide the primary resistance of the foundation system.

For some sites the potential occurrence of scour around the pile is possible. If scour occurs the effective length of the pile could change, which could in turn affect the seismic response of the bridge-foundation system. If a potential for scour around the piles exists during the design life of the bridge, the seismic analysis should be made

considering the likely, but not necessarily maximum, depth of scour. In this situation, the maximum depth of scour may not be required because of the low probability of both cases occurring at the same time. If the assumptions on scour depth have (or could have) a significant effect on seismic response, the designer should meet with the owner and establish a strategy for addressing this issue. This strategy could involve conducting a series of parametric studies to bracket the range of possible responses.

Similar to the discussion in Article C8.4.2, various approaches are available to evaluate the response of the bridge-foundation system during the design event. In most cases the designer will use equivalent linear springs to represent the soil-foundation system. Guidance provided in these *Specifications* focuses on these simple procedures. Comments provided in Article C8.4.2 regarding more rigorous modeling methods are equally valid for pile foundation systems.

Most recent research on seismic response of pile-supported foundations has focused on lateral pile loading. Lam et al. (1998) report that many pile-supported foundations are more sensitive to variations in axial pile stiffness, and therefore, the axial pile-load stiffness problem warrants more consideration. Moment demand on a pile group also generally should govern foundation design, which is determined by axial response of the group, rather than lateral loading for most soil conditions.

Characterization of the stiffness of an individual pile or pile group involves an evaluation of the pile load-displacement behavior for both axial and lateral loading conditions. The overall pile-soil stiffness can be estimated in a number of ways, and the method used should reflect the soil characteristics (e.g., type, strength, and nonlinearity) and the structural properties of the pile or pile group (e.g., type, axial and bending stiffness, diameter, length, and structural constraints). If a stiffness matrix is used, it is critical that it be positive-definite and symmetric for it to be suitable for implementation in a global response analyses. This will require p-y curves to be linearized prior to assembly of the stiffness components of the matrix. Such a procedure has been adopted in the charts shown in Article 8.4.3. If the stiffness matrix is used in a computer program to determine foundation loading demands, then programs such as LPILE or GROUP should be used to determine bending moments and shear forces for design, with nonlinear p-y curves used as appropriate.

The seismic displacement capacity verification step described in Article 5.4.3 requires development of moment-rotation and lateral load-displacement relationships. These relationships are normally assumed to be uncoupled because the lateral loads are mobilized in the upper portion of the pile while the axial load is mobilized at deep levels. For most push-over analyses a secant stiffness can be used to represent soil springs. If design uplift or plunging limits are exceeded, nonlinear springs should be used. In most cases a bi-linear spring will be an acceptable model of the nonlinear behavior of the soil.

#### C8.4.3.3 Axial and Rocking Stiffness for Driven Pile/Pile Cap Foundations

Axially loaded piles transfer loads through a combination of end bearing and side resistance along the perimeter of the pile. Their true axial stiffness is a complex nonlinear interaction of the structural properties of the pile and the load-displacement behavior of the soil for friction and end bearing (Lam et al., 1998). Both simplified and more rigorous computer methods are used for evaluating axial stiffness. In most cases simplified methods are sufficient for estimating the axial stiffness of piles. However, at sites where the soil profile changes appreciably with depth or where the effects of group action occur, computer models will often provide a better representation of soil-pile interaction.

##### *Use of Simplified Methods*

The axial stiffness value in the simplified equation,  $K_{sv} = \Sigma 1.25AE/L$ , represents an average value that accounts for uncertainties in the determination of soil properties, the mechanism for developing resistance (i.e., side resistance versus end bearing), and the simplified computational method being used. The basis of this equation is summarized as follows:

- If the pile develops reaction from purely end bearing, the tip bearing stiffness must be relatively large compared with the side resistance stiffness of the soil and the axial stiffness properties of the pile. If the tip displacement is assumed to be zero, the resulting axial stiffness is

$$K_{sv} = \Sigma AE/L$$

- At the other extreme, a purely friction pile implies that the force at the tip is zero. For

zero tip force and a uniform total transfer to the soil by side resistance along the pile, the axial stiffness of the pile approximates:

$$K_{sv} = \Sigma 2AE/L$$

- Allowing for some tip displacements and recognizing the inherent complexity of the problem, a reasonable range is from  $0.5AE/L$  to  $2AE/L$ .

Other methods of estimating the axial stiffness of the pile are also available. Lam et al. (1998) present a simplified graphical procedure that uses the average between a rigid and flexible pile solution.

#### *Nonlinear Computer Methods*

In the above discussion simplified methods are used to define the axial stiffness of a single pile. More rigorous computer methods that accommodate the nonlinear behavior of the soil and structure are also available. These more rigorous methods involve more effort on the part of the Designer. In many cases the increased accuracy of the more rigorous method is limited by the uncertainty associated with selection of input parameters for the analyses.

A number of computer programs are available for conducting more rigorous determination of the axial stiffness of the soil-pile system (e.g., Lam and Law, 1994). These programs are analogous to the program used to estimate the lateral load-displacement response of piles. Rather than p-y curves, they use t-z curves and q-z curves to represent the side resistance and end bearing load-displacement relationships, respectively.

These same procedures can be used to determine uplift stiffness values. For these determinations the end bearing component of the load-displacement relationship is deleted, and the resistance in uplift is assumed to be the same as that in compression.

Computer programs such as APILE Plus (Reese et al., 1998) provide recommendations for load-transfer relationships in end bearing and side resistance for driven piles. Typical amounts of displacement to mobilize side resistance are on the order of a few millimeters in sands and up to 2% of the pile diameter in clay. According to Reese et al. (1997), up to 10% of the pile diameter can be required to mobilize the full end bearing of a pile, whether it is in clay or sand. Actual determination of the deformations to mobilize either end bearing or side resistance involves considerable judgment.

While the computer programs often make the material property selection and the analysis procedure easy, the uncertainty of the analysis can still be high. For this reason it is important to involve a person knowledgeable in soil properties and pile loading in the selection of the soil parameters used to model the load-displacement relationship.

The effects of group action for axial loading can be modeled in some computer programs by modification of “t-z” and “q-z” curves. The modifications to these curves will depend on the soil type, with cohesionless soils showing increasing stiffness as the spacing decreases and cohesive soils softening with decreasing spacing. In contrast to lateral loading, explicit relationships for modifying the “t-z” and “q-z” curves are not provided. However, in the limit the adjusted curves should result in an ultimate capacity similar to ultimate capacity of a group determined by static methods (i.e.,  $Q_g = nQ_s \cdot \eta$  where  $Q_g$  is the capacity of the group,  $n$  is the number of piles in the group,  $Q_s$  is the capacity of an isolated pile, and  $\eta$  is an efficiency factor that will vary with pile spacing and soil type. In the user’s manual for GROUP (Reese and Wang, 1996), the authors indicate that the efficiency of pile groups in sands is greater than 1 and by implication the stiffness of a closely spaced group will be greater. They also show that the efficiency of pile groups in clays is less than 1, with the implication that the stiffness of a closely spaced group will be lower.

#### **C8.4.3.4 Lateral Stiffness Parameters for Driven Pile/Pile Cap Foundations**

As with axial stiffness, a variety of methods are available for determining the lateral stiffness of a pile or group of piles. Generally, these methods involve the use of simplified charts or the use of more rigorous computer models. The simplified methods normally provide a convenient method for initial design of a pile-supported bridge and may be sufficient for final design if earthquake loads are small. Computer models allow the user to explicitly account for variations in soil stiffness along the embedded depth of the pile, and to account for the effects of group action and changes in the flexural stiffness of the pile during loading. For these reasons, the computer models are often used in final design, particularly where significant changes in soil profile occur with depth or where earthquake loads are large.



### *Use of Simplified Linear Charts*

The charts developed by Lam and Martin (1986) and presented as Figures 8.4.3.4-1 through 8.4.3.4-6 require that an "f" value be defined for the soil. Lam et al. (1998) recommend that the "f" value be selected at a depth of approximately 5 pile diameters. The charts assume no pile top embedment, but yield reasonable stiffnesses for shallow embedment of no more than 1.5 m. Lateral pile stiffness increases quickly with depth for most piles, and therefore, if greater embedment occurs, nonlinear computer methods should be used, as the charts will potentially result in a considerable underestimation of stiffness.

These charts are applicable for pile-head deflections between 5 and 50 mm. The charts also assume that the piles are sufficiently long to achieve full fixity.

### *Use of Computer Methods*

Procedures for conducting nonlinear lateral pile analyses are described by Lam and Martin (1986). Lam and Martin's discussion includes procedures for developing p-y curves in both sands and clays. Reese et al. (1997), as well as a number of other technical papers, also discuss the development of p-y curves.

A number of these methods identify a factor for cyclic loading. Generally, this factor is not applicable to seismic loading conditions. It was developed for problems involving wave loading to offshore structures, where thousands of cycles of load were being applied. For earthquake problems, the non-cyclic p-y curves are most applicable.

Group interaction should usually be considered in the evaluation of lateral response of closely spaced piles. Interaction results when the lateral stress developed during loading of one pile interacts with the adjacent pile. Group reduction curves are usually used to represent this interaction. Early studies suggested significant reduction in stiffness for pile spacings of 8 diameters or less. More recent studies indicate that the group effects are not normally as significant as once thought. A reduction factor of 50% is recommended by Lam et al. (1998) as being appropriate for most seismic loading situations. According to Lam et al. (1998), this reduction accounts for the effects of gapping, local porewater pressure effects, and the interaction of the stress field from individual piles. Alternatively, p-multiplier methods suggested by Brown et al. (1988) provide a systematic method of introducing

group effects for various pile group configurations.

Another consideration in the use of computer programs is whether a cracked or uncracked section modulus should be used in the representation of concrete piles. This modulus will have a significant influence on the resulting load-deformation response calculation, and therefore requires careful consideration by the person performing the analyses. Programs such as FLPIER and LPILE can explicitly account for the transition from uncracked to cracked section modulus during the loading sequence.

### C8.4.3.5 Pile Cap Stiffness and Capacity

The response of the pile-supported footing differs in one important respect from a spread footing foundation: resistance at the base of the footing is not included in the response evaluation. The base resistance is neglected to account for likely separation between the base of the foundation and soil, as soil settlement occurs.

As noted in Article C8.4.2.2, the pile cap will have to deform by as much as 2% of the pile cap thickness to mobilize the passive pressure of the cap. If this displacement is significantly greater than the design displacement, it may be possible to neglect the contribution of the pile cap without significant effects on the total stiffness calculation. At these low displacements, the stiffness of the pile will govern response.

### C8.4.3.6 Moment and Shear Design

The stiffness of the pile in axial loading is limited by the plunging capacity of the pile. Side resistance and end bearing soil springs should be limited by the unfactored axial capacity at large deformations. Similarly, moment capacity checks are normally made with the unfactored axial capacity of the pile. Resistance factors are not applied to enable the designer to obtain a better understanding of pile performance under seismic loading. By using unfactored capacities, a best-estimate of the displacement for a given force in the bridge structure can be obtained. If factored capacities are used, the deformation could be greater than the deformation under best-estimate conditions, resulting in design decisions that may not be appropriate.

It is recognized that uncertainty exists even with the best-estimate capacity. Although it may not be economical to evaluate these uncertainties

in all bridges, uncertainty should be considered during evaluations of stiffness and capacity and should be evaluated for more important bridges. To account for uncertainty, upper and lower bound capacities and stiffnesses can be determined, allowing the designer to assess the potential effects on the design if higher or lower capacities occur for the site.

The range for the upper and lower bound evaluation will depend on the characteristics of the site, the type of analysis used to estimate capacity, and whether or not a field load test is conducted (e.g., using a pile driving analyzer, static load test with head measurements only, or fully instrumented pile-load test). Common practice is to use an upper bound that is 100% greater than the unfactored stiffness and capacity and a lower bound that is 50% of the unfactored stiffness and capacity.

The range of uncertainty is normally higher than the uncertainty implied by the resistance factor used for static design for several reasons: (1) there is greater uncertainty in the seismic resistance of the pile in seismic loading than static loading, (2) there is a greater potential for cyclic degradation of resistance properties during seismic loading, and (3) there are rate of loading effects.

The designer can reduce the range of uncertainty by conducting more detailed site explorations to fully characterize the soil, by performing more rigorous analyses that treat the full load-deformation process, and by conducting pile-load test to quantify the load-displacement response of the pile. Even with a full-scale field load test, some uncertainty exists as discussed in the previous paragraph. For this reason, a range of values to represent upper and lower bound response may be warranted even under the best circumstances.

#### C8.4.3.7 Liquefaction and Dynamic Settlement Evaluations

The design of a pile foundation for a liquefied soil condition involves careful engineering considerations. Two general cases occur: liquefaction with and without lateral flow or spreading.

##### *Liquefaction without Lateral Flow or Spreading*

Pile foundations should be designed to extend below the maximum depth of liquefaction by at least 3 pile diameters or to such a depth that axial and lateral capacity are not affected by liquefaction of any overlying layer. Porewater pressures in

a liquefied zone can result in increases in porewater pressure within layers below the liquefied zone. Porewater pressures increases can also occur in a zone where the factor of safety for liquefaction is greater than 1.0, as discussed in Appendix D. These increases in porewater pressures will temporarily reduce the strength of the material from its pre-earthquake (static) strength. The potential for this decrease should be evaluated, and the capacity of the foundation evaluated for the lower strength. Alternatively, the toe of the pile should be founded at a depth where the effects of porewater pressure changes are small. Normally, the static design of the pile will include a resistance factor of 0.6 or less. This reserve capacity allows an increase in porewater pressures by 20% without significant downward movement of the pile.

As porewater pressures dissipate following liquefaction, drag loads will develop on the side of the pile. The drag loads occur between the pile cap and the bottom of the liquefied layer. The side friction used to compute drag loads will increase with dissipation in porewater pressure from the residual strength of the liquefied sand to a value approaching the static strength of the sand. The maximum drag occurs when the porewater pressures are close to being dissipated. Simultaneously relative movement between the pile and the soil decrease as the porewater pressure decreases, resulting in the drag load evaluation being a relatively complex soil-pile interaction problem. For simplicity, it can be conservatively assumed that the drag load used in the settlement estimate is determined by the pre-liquefied side resistance along the side of the pile between the bottom of the pile cap and the bottom of the liquefied zone.

##### *Liquefaction with Lateral Flow or Spreading*

Lateral flow and spreading have been common occurrences during liquefaction at bridge sites involving an approach fill or at a river or stream crossing. The amount of movement can range from a few millimeters to over a meter. This amount of movement is generally sufficient to develop full passive pressures on pile or pile cap surfaces exposed to the moving soil. If the system of piles and pile cap is not strong enough to resist these movements, the pile cap system will displace horizontally under the imposed load.

Procedures for estimating either the forces or displacements of the pile from the moving ground are discussed in Appendix D. If these forces or displacements are large, some type of ground

remediation might be used to reduce these displacements. These ground remediation methods can include vibro densification, stone columns, pressure grouting, or in-place soil mixing. Costs of these improvements can range from \$10/m<sup>3</sup> to in excess of \$40/m<sup>3</sup> (in year-2000 dollars). Depending on the specific conditions and design requirements for a site, the use of ground improvement could increase construction costs by 10% or more. In view of these costs, the owner needs to be made aware of the potential risks and the costs of remediation methods as soon as these conditions are identified.

Appendix D provides a more detailed discussion of the process to follow when designing for lateral flow or spreading ground.

For SDR 4 and above, the change in lateral stiffness of the pile resulting from liquefaction is also determined. This change in stiffness is usually accomplished by defining the liquefied zone as a cohesive soil layer with the ultimate strength in the p-y curve being equal to the residual strength of the liquefied soil. Appendix D identifies procedures for making these adjustments.

#### **C8.4.4 Drilled Shafts**

Lam et al. (1998) provides a detailed discussion of the seismic response and design of drilled shaft foundations. Their discussion includes a summary of procedures to determine the stiffness matrix required to represent the shaft foundation in most dynamic analyses.

Drilled shaft foundations will often involve a single shaft, rather than a group of shafts. This is not the case for driven piles. In single shaft configuration the relative importance of axial and lateral response changes. Without the equivalent of a pile cap, lateral-load displacement of the shaft becomes more critical than the (axial) load-displacement relationships discussed above for driven piles.

Many drilled-shaft foundation systems consist of a single shaft supporting a column. Compressive and uplift tensile loads on these shafts during seismic loading will normally be within the limits of the load factors used for gravity loading. However, checks should be performed to confirm that any changes in axial load do not exceed ultimate capacities in uplift or compression. In contrast to driven piles in a group, no reserve capacity exists for a single shaft; i.e., if ultimate capacity is exceeded, large deformations can occur.

Special design studies can be performed to demonstrate that deformations are within acceptable limits if axial loads approach or exceed the ultimate uplift or compressive capacities if the drilled shaft is part of a group. These studies can be conducted using computer programs, such as APILE Plus (Reese, et al., 1997). Such studies generally will require rigorous soil-structure interaction modeling.

Various studies (Lam et al., 1998) have found that conventional p-y stiffnesses derived for driven piles are too soft for drilled shafts. This stiffer response is attributed to a combination of (1) higher unit side friction, (2) base shear at the bottom of the shaft, and (3) the rotation of the shaft. The rotation effect is often implicitly included in the interpretation of lateral load tests, as most lateral load tests are conducted in a free-head condition. A scaling factor equal to the ratio of shaft diameter to 600 mm is generally applicable, according to Lam et al. (1998). The scaling factor is applied to either the linear subgrade modulus or the resistance value in the p-y curves. This adjustment is dependent on the construction method.

Base shear can also provide significant resistance to lateral loading for large diameter shafts. The amount of resistance developed in shear will be determined by conditions at the base of the shaft during construction. For dry conditions where the native soil is relatively undisturbed, the contributions for base shear can be significant. However, in many cases the base conditions result in low interface strengths. For this reason the amount of base shear to incorporate in lateral analyses will vary from case to case.

Typically it is necessary to embed shafts to between 2 diameters in rock to 3 or 5 shaft diameters in soil to achieve stable conditions. This depth for stable conditions will depend on the stiffness of the rock or soil. Shorter embedment is acceptable if the embedment length and the strength of the drilled shaft provide sufficient lateral stiffness with adequate allowances for uncertainties in soil stiffness. Generally, it will be necessary to conduct a lateral load analysis using a program such as COM624 or LPILE to demonstrate that shorter embedment is acceptable.

Section properties of the drilled shaft should be consistent with the deformation caused by the seismic loading. In many cases it is necessary to use the cracked section modulus in the evaluation of lateral load-displacement relationships. In the absence of detailed information regarding reinforcing steel and applied load, an equivalent

cracked section can be estimated by reducing the stiffness of the uncracked section by half. In general the cracked section is a function of the reinforcement ratio (i.e., volume of steel reinforcement to that of concrete), but is often adequate to assume as one-half of the uncracked section.

## C8.5 ABUTMENT DESIGN REQUIREMENTS

### C8.5.1 General

One of the most frequent observations of damage during past earthquakes has been damage to the abutment wall. This damage has been due to two primary causes: (1) the approach fill has moved outward, carrying the abutment with it, and (2) large reactive forces have been imposed on the abutment as the bridge deck has forced it into the approach fill. This latter cause of damage has often resulted from a design philosophy that assumed that the abutment wall had to survive only active seismic earth pressures, and that gaps between the bridge deck and abutment wall would never be forced to close. In many cases the gap was not sufficient to remain open, and large loads were imposed by the deck. The passive reaction from the soil was as much as 30 times the forces used for active pressure design, resulting in overloading and damage of the wall.

These LRFD *Guidelines* have been prepared to acknowledge specifically the potential for this higher load on the abutment wall. If designed properly, the reactive capacity of the approach fill can provide significant benefit to the bridge-foundation system.

### C8.5.2 Longitudinal Direction

Common practice is to use the Mononobe-Okabe equations to estimate the magnitude of seismic earth pressures, for both active and passive pressure conditions. Current editions of AASHTO LRFD specifications specifically discuss these methods and present equations for making these estimates. These equations have, however, been found to have significant limitations.

For the case of seismic active earth pressures, the Mononobe-Okabe equations are based on the Coulomb failure wedge assumption and a cohesionless backfill. For high accelerations or for backslopes, the equations lead to excessively high pressures that asymptotically approach infinity at critical acceleration levels or backslope angles. For the latter conditions, no real solutions to the

equations exist, implying equilibrium is not possible (Das, 1999). For horizontal backfills for example, for a friction angle for sand of  $40^\circ$ , a wall friction angle of  $20^\circ$  and a peak acceleration of  $0.4g$ , the failure surface angle is  $20^\circ$  to the horizontal. For a peak acceleration of  $0.84g$ , the active pressure becomes infinite, implying a horizontal failure surface.

Clearly, for practical situations, cohesionless soil is unlikely to be present for a great distance behind an abutment wall and consequently encompass the entire failure wedge under seismic conditions. In some cases, free-draining cohesionless soil may only be placed in the static active wedge (say at a 60 degree angle) with the remainder of the soil being cohesive embankment fill ( $c, \phi$  soil) or even rock. Under these circumstances, the maximum earthquake-induced active pressure should be determined using trial wedges (Figure C8.5.2-1), with the strength on the failure planes determined from the strength parameters for the soils through which the failure plane passes. This approach will provide more realistic estimates of active pressure.

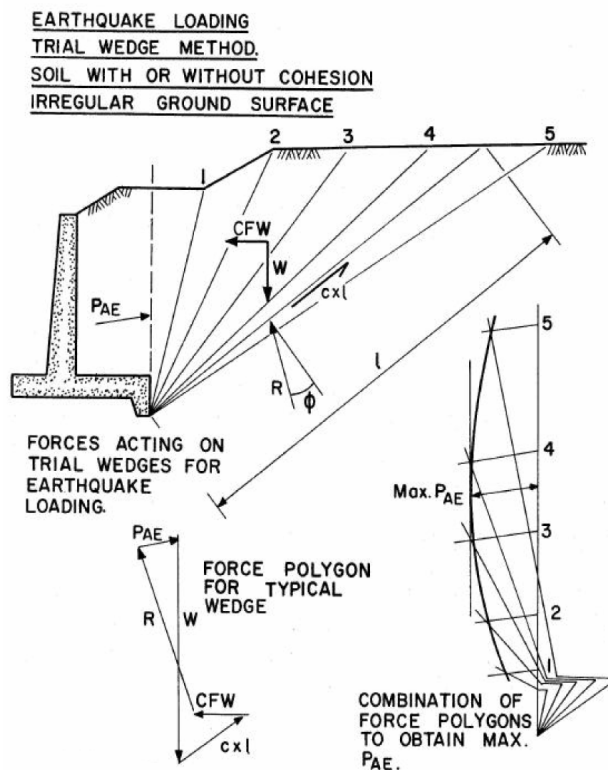


**Figure C8.5.2-1 Trial Wedge Method for Determining Critical Earthquake-Induced Active Forces**

### C8.5.2.1 SDAP C

No seismic provisions are required for bridges covered by these SDAPs because increased earth pressures from the approach fill and bridge displacements will normally be within tolerable levels. In the case of seismically induced active earth pressures, the static design of the wall will usually result in the controlling load case, if normal load and resistance factors are used. In the case of integral abutments, the designs based on static at-rest pressures will also be sufficiently conservative to meet seismic demand. For cases where the abutment is engaged and high passive forces could develop, the preferred approach is to design a fuse into the system to protect against damage. Alternatively, the Owner could decide to accept some level of damage, given the low likelihood of occurrence of the design earthquake.

### C8.5.2.2 SDAP D and E

The determination of stiffness and capacity is a key step during the design of many bridges by these SDAPs. Procedures for calculating passive force,  $P_p$ , and abutment stiffness are described below. These procedures should use best-estimate soil properties. The approach is based upon using a uniform distribution of passive soil pressure against the abutment backwall. The uniform pressure approach is a simplification of more complex distribution patterns, which are functions of wall friction and deformation patterns (i.e., translation or tilting).

## C8.5.3 Transverse Direction

To meet the performance criteria, abutments shall experience essentially no damage in the Expected Earthquake, and this may be achieved if the abutments are designed to resist the elastic forces for the Expected Earthquake. For the larger, MCE event, the elastic forces may be large enough that they cannot be resisted without some abutment damage. In general, the design of the abutment should attempt to restrict damage to locations that are inspectable and which can be reasonably accessed for repair.

Two preferred strategies may be considered. One is to use isolation, elastomeric or other bearings that accommodate the full seismic movement at the abutment and thereby significantly reduce the likelihood of damage to the abutment itself.

The second strategy is to use fuse elements (isolation bearings with a high yield level or shear keys) that are intended to yield or breakaway thereby limiting the forces transferred to the abutment. It should be noted that it is difficult to predict the capacity of a concrete shear key and hence this is a less reliable concept when compared to isolation elements with a high yield force. Such fuse elements should be designed to restrict damage to inspectable locations. In situations where neither of these strategies is practical, then damage may be incurred in the foundation of the abutment, but such a design approach shall only be undertaken with the approval of the owner.

The calculation of stiffness may require the estimation of effective secant stiffnesses based on both ultimate strength and estimates of yield displacements. The approach will be similar to that used in calculating longitudinal abutment stiffness. Alternatively, bounding analyses may be used wherein a resisting element is completely released. Where a complete loss of resistance may occur, for example breakaway shear keys or blocks, a small nominal spring resistance may be necessary to obtain reasonable and stable results from a multimode dynamic analysis.

### C8.5.3.1 SDAP C

For abutments of bridges in these lower seismic design categories, the abutment, as typically designed for service loads, should be adequate for resisting the seismic effects. Where lateral restraint is provided at the abutment, for example with shear keys, minimum design forces are specified to provide a reasonable amount of strength to resist the forces that are likely to develop in an earthquake.

Abutments designed for non-seismic loads and for the connection forces outlined in Article 4.2 for SDAP A1 and A2 or in Article 4.3 for SDAP B should resist earthquakes with minimal damage. Bridges designed using SDAP C are proportioned such that the abutments are not required to resist inertial forces. Therefore some damage may occur in abutments of such bridges, particularly for the higher Seismic Hazard Levels.

### C8.5.3.2 SDAP D and E

For SDAP D and E, seismic design and analysis is required and the actual restraint conditions at the abutments will determine the amount of force that is attracted to the abutments. These forces

shall either be resisted elastically or fuse elements may be used.

Short bridges that have abutments that can continuously provide soil resistance under cyclic deformations will exhibit damping that likely exceeds the normal 5% value. Therefore for shorter bridges that have small skew and only small horizontal curvatures, a 1.4 reduction value is allowed for all the elastic forces and displacements resulting from transverse earth-quake motion. This provision only applies to shorter bridges with a continuous superstructure where the effects of the transverse abutment response extend throughout the entire bridge. To rely on this reduction, the soil must be able to provide continuous resistance under cyclic loading. Friction against the base of foundations not supported on piles or shafts may be considered sustained resistance, as may be friction against vertical surfaces not subject to gapping as described below. The force reduction is not permitted for other types of abutment resistance, for instance, passive mobilization of backfill where a gap may form between the soil and the backwall. These provisions have been adapted from the "short bridge" provisions outlined by Caltrans in their Seismic Design Criteria and Memo 20-4.

Wingwalls, in general, should not be relied upon to resist significant transverse forces. Typical configurations of wingwalls are normally inadequate to resist large forces corresponding to the passive resistance of the soil retained by the wingwalls. The wingwalls' yield resistance may, however, be counted in the resistance, even though this value will likely not contribute significantly to the lateral resistance.

In cases where the backfill may be displaced passively, whether intended to be part of the ERS or not, the possibility of a gap opening in the backfill should be considered when calculating the transverse lateral capacity of an abutment. If a gap could open between the backfill soil and the abutment, the transverse resistance provided by the wingwalls may be compromised. Specifically, cohesion in the backfill may produce such a situation. If this occurs, reduction of the transverse resistance may be necessary.

## **C8.6 LIQUEFACTION DESIGN REQUIREMENTS**

### **C8.6.1 General**

Liquefaction has been perhaps the single most significant cause of damage to bridge structures during past earthquakes. Most of the damage has been related to lateral movement of soil at the bridge abutments. However, cases involving the loss in lateral and vertical bearing support of foundations for interior piers of a bridge have also occurred.

The threat of liquefaction requires careful attention to the determination of the potential for liquefaction and its consequences. For earthquake magnitudes less than 6.0, liquefaction develops slowly at most sites, and results in minimal effects to the structure during dynamic shaking, and therefore the effects of liquefaction on dynamic response can be neglected. If the mean magnitude of the Maximum Considered Earthquake is less than 6.0, then the discussion above with regard to duration is applicable. For the magnitude interval of 6.0 to 6.4, a liquefaction analysis is not required when the combination of ground shaking and blow count are below values that would cause liquefaction. This transition interval is based on both an assessment of available data from past earthquakes and on engineering judgment.

The mean magnitudes shown in Figures 8.6.1-1 to 8.6.1-4 are based on deaggregation information, which can be found on the USGS website (<http://geohazards.cr.usgs.gov/eq/>). A site-specific determination of the mean magnitude can be obtained from this website using the coordinates of the project site.

If liquefaction is expected to occur in the Expected Earthquake event then the performance criteria for piles will need to be Operational for the Life Safety performance level addressed in Article 8.8.6.

### **C8.6.2 Evaluation of Liquefaction Potential**

A site is considered potentially susceptible to liquefaction if one or more of the following conditions exists (SCEC, 1999):

- Liquefaction has occurred at the site during historical earthquakes.
- The site consists of uncompacted or poorly compacted fills containing liquefaction-susceptible materials that are saturated, nearly

saturated, or may be expected to become saturated.

- The site has sufficient existing geotechnical data, and analyses indicate that the soils are potentially susceptible to liquefaction.

For sites where geotechnical data are lacking or insufficient, the potential for liquefaction can be delineated using one or more of the following criteria:

- The site consists of soil of late Holocene age (less than 1,000 years old, current river channels and their historical flood plains, marshes, and estuaries) where the groundwater is less than 12 m below the surface and the anticipated earthquake ground shaking  $F_a S_s$  is greater than 0.375 (peak ground acceleration (PGA) greater than 0.15g.)
- The site consists of soils of Holocene age (less than 11,000 years old) where the ground water is less than 10 m below the surface and  $F_a S_s$  is greater than 0.50 (PGA is greater than 0.2g.)
- The site consists of soils of latest Pleistocene age (11,000 to 15,000 years old) where the ground water is less than 5 m below the surface and  $F_a S_s$  is greater than 0.75 (PGA is greater than 0.3g).

### C8.6.3 Evaluation of the Effects of Liquefaction and Lateral Ground Movement

The design of bridge structures for liquefaction effects generally has two components.

- *Vibration Effects:* The first is that the bridge must perform adequately with just the liquefaction-induced soil changes alone. This means that the mechanical properties of the soil that liquefy are changed to reflect their liquefied conditions (i.e., “p-y” curves or modulus of subgrade reaction for lateral stiffness are reduced). Design for these cases is in reality a design for structural vibration effects, and these are the effects that the code-based procedures typically cover for design.
- *Permanent Displacement Effects:* The second component of the design is the consideration of liquefaction-induced ground movements. These can take several forms: lateral spreading, lateral flow, and dynamic settlement. Lateral spreading is a lateral movement that is induced by the ground shaking and develops

in an incremental fashion as shaking occurs. Flow, on the other hand, is movement that occurs due to the combined effects of sustained pore pressure and gravity without the inertial loading from the earthquake. Flows can occur several minutes following an earthquake when porewater pressures redistribute to form a critical combination with gravity loading. Dynamic settlement occurs following an earthquake as porewater pressures dissipate.

Vibration and permanent movement occur simultaneously during a seismic event. Their simultaneous occurrence is a complicated process that is difficult to represent without the use of very complex computer modeling. For most bridges the complexity of the modeling doesn’t warrant performing a combined analysis. In these cases the recommended methodology is to consider the two effects independently, i.e., de-coupled. The reasoning behind this is that it is not likely that the peak vibrational response and the peak spreading or flow effect will occur simultaneously. For many earthquakes the peak vibration response occurs somewhat in advance of maximum ground movement loading. For very large earthquakes where liquefaction may occur before peak ground accelerations occur, the peak vibration response is like to be significantly attenuated and, hence, inertial loading reduced from peak design values. In addition, peak displacement demands arising from lateral ground spreading are likely to generate maximum pile moments at depths well below depths of peak moments arising from inertial loading. Finally, the de-coupling of response allows the flexibility to use separate and different performance criteria for design to accommodate the two phenomena. Two detailed case studies on the application of the recommended design methods for both liquefaction and lateral flow design are given in ATC/MCEER (2003).

While the de-coupled method is recommended for most bridges, more rigorous approaches are sometimes necessary, such as when a critical bridge might be involved. Coupled approaches are available to represent the large-strain, pore-water pressure buildup mechanisms that occur during liquefaction. However, these methods are difficult to use, and should only be considered after detailed discussions between the owner and the designer regarding the capabilities and limitations of these methods.

If lateral flow occurs, significant movement of the abutment and foundation systems can result.

Inelastic deformation of the piles is permitted for this condition (e.g., plastic rotation of 0.05 radians). The geometric constraints of Table C3.2-1 provide guidance for meeting the desired performance objective. The range of design options includes designing the piles for the flow forces to an acceptance of the predicted lateral flow movements realizing the bridge may need to be replaced. Structural and soil mitigation measures may be used to minimize the amount of movement to meet higher performance objectives.

#### **C8.6.4 Design Requirements if Liquefaction and Ground Movement Occur**

Spread footings are not normally used if liquefiable soils are present. Spread footings can be considered if the spread footing is located below the bottom of the liquefiable layer, the ground will be improved to eliminate the potential for liquefaction, or special studies are conducted to demonstrate that the spread footing will perform adequately during and following liquefaction. In most situations these requirements will result in the use of either driven pile foundations or drilled shaft foundations.

The approach used to design the foundation first involves designing to accommodate the non-seismic load conditions and the vibration case of seismic loading without liquefaction. This structure and foundation system should then be assessed for its capability to resist the inertial loads when the soil layers have liquefied. In general this second case will only impact the design of the structure above the foundation system when the upper layers of soil have liquefied.

Lateral flow is one of the more difficult issues to address because of the uncertainty in the movements that may occur. The design steps to address lateral flow are given in Appendix D. A liberal plastic rotation of the piles is permitted, but this does imply that the piles and possibly other parts of the bridge will need to be replaced if these deformation levels do occur. One suggestion is to use a tube in the center of a few piles so that the amount of subsurface deformation could be measured after an earthquake. Design options range from an acceptance of the movements with significant damage to the piles and columns if the movements are large to designing the piles to resist the forces generated by lateral spreading. Between these options is a range of mitigation measures to limit the amount of movement to tolerable

levels for the desired performance objective. Pile group effects are not significant for liquefied soil.

Because the foundation will typically possess some lateral resistance capable of reducing the magnitude of spreading, this capacity should be utilized. If the lateral displacements are too great for the structure to accommodate adequately, then geotechnical improvements will be necessary, unless the performance objective under spreading loads is to accept a severely damaged bridge that likely will need to be replaced. Therefore the most cost-effective approach is to account for the beneficial restraint action of the existing (as-designed for non-spreading effects) foundation.

Additionally, if the foundation can provide significant restraint, but not fully adequate restraint, then additional piles may be considered. Depending on the soil profile and the manner in which spreading develops, simple “pinch” piles provided in addition to the foundation may prove effective. The cost trade-off between pinch piles and geotechnical remediation should be assessed to determine the most effective means of achieving appropriate soil restraint.

#### **C8.6.5 Detailed Foundation Design Requirements**

See Article C8.4 for the commentary.

#### **C8.6.6 Other Collateral Hazards**

No commentary is provided for Article 8.6.6.

### **C8.7 STRUCTURAL STEEL DESIGN REQUIREMENTS**

#### **C8.7.1 General**

Most components of steel bridges are not expected to behave in a cyclic inelastic manner during an earthquake. The provisions of Article 8.7 are only applicable to the limited number of components (such as specially detailed ductile substructures or ductile diaphragms) whose stable hysteretic behavior is relied upon to ensure satisfactory bridge seismic performance. The seismic provisions of Article 8.7 are not applicable to the other steel members expected to remain elastic during seismic response. In most steel bridges, the steel superstructure is expected (or can be designed) to remain elastic.

Recently, the number of steel bridges seriously damaged in earthquakes has risen dramatically.



One span of the San Francisco-Oakland Bay Bridge collapsed due to loss of support at its bearings during the 1989 Loma Prieta earthquake, and another bridge suffered severe bearing damage (EERI, 1990). The end diaphragms of some steel bridges suffered damage in a subsequent earthquake in northern California (Roberts, 1992). During the 1994 Northridge earthquake some steel bridges, located close to the epicenter, sustained damage to either their reinforced concrete abutments, connections between concrete substructures and steel superstructures, steel diaphragms or structural components near the diaphragms (Astaneh-Asl et al., 1994). Furthermore, a large number of steel bridges were damaged by the 1995 Hyogoken-Nanbu (Kobe) earthquake. The concentration of steel bridges in the area of severe ground motion was considerably larger than for any previous earthquake and some steel bridges collapsed. Many steel piers, bearings, seismic restrainers and superstructure components suffered significant damage (Bruneau, Wilson and Tremblay, 1996). This experience emphasizes the importance of ductile detailing in the critical elements of steel bridges.

Research on the seismic behavior of steel bridges (e.g. Astaneh-Asl, Shen and Cho, 1993; Dicleli and Bruneau, 1995a, 1995b; Dietrich and Itani, 1999; Itani et al., 1998a; McCallen and Astaneh-Asl, 1996; Seim, Ingham and Rodriguez, 1993; Uang et al., 2000; Uang et al., 2001; Zahrai and Bruneau 1998) and findings from recent seismic evaluation and rehabilitation projects (e.g. Astaneh and Roberts, 1993, 1996; Ballard et al., 1996; Billings et al., 1996; Dameron et al., 1995; Donikian et al., 1996; Gates et al., 1995; Imbsen et al., 1997; Ingham et al., 1996; Jones et al., 1997; Kompfner et al., 1996; Maroney 1996; Prucz et al., 1997; Rodriguez and Ingham, 1996; Schamber et al., 1997; Shirolé and Malik, 1993; Vincent et al., 1997) further confirm that seismically induced damage is likely in steel bridges subjected to large earthquakes and that appropriate measures must be taken to ensure satisfactory seismic performance.

The intent of Article 8.7 is to ensure the ductile response of steel bridges during earthquakes. First, effective load paths must be provided for the entire structure. Following the concept of capacity design, the load effect arising from the inelastic deformations of part of the structure must be properly considered in the design of other elements that are within its load path.

Second, steel substructures must be detailed to ensure stable ductile behavior. Note that the term

“substructure” here refers to structural systems exclusive of bearings (Article 8.9) and articulations, which are considered in other sections. Steel substructures, although few, need ductile detailing to provide satisfactory seismic performance.

Third, Article 8.7 introduces considerations for other special ductile systems which are described in this Commentary.

Special consideration may be given to slip-critical connections that may be subjected to cyclic loading. Some researchers have expressed concern that the Poisson effect may cause steel plate thickness to reduce, when yielding on a component's net section occurs during seismic response, which may translate into a reduced clamping action on the faying surfaces after the earthquake. This has not been experimentally observed, nor noted in post-earthquake inspections, but the impact of such a phenomenon would be to reduce the slip-resistance of the connection, which may have an impact on fatigue resistance. This impact is believed to be negligible for a Category C detail for finite life, and a Category D detail for infinite life. Design to prevent slip for the Expected Earthquake should be also considered.

#### C8.7.2 Materials

To ensure that the objective of capacity design is achieved, Grade 250 steel is not permitted for the components expected to respond in a ductile manner. Grade 250 is difficult to obtain and contractors often substitute it with a Grade 345 steel. Furthermore it has a wide range in its expected yield and ultimate strength and large overstrength factors to cover the anticipated range of property variations. The common practice of dual-certification for rolled shapes, recognized as a problem from the perspective of capacity design following the Northridge earthquake, is now becoming progressively more common also for steel plates. As a result, only Grade 345 steels are allowed within the scope of Article 8.7.2, with a  $R_y$  of 1.1.

In those instances when Grade 250 must be used, capacity design must be accomplished assuming a Grade 345 steel (i.e., with a  $R_y$  of 1.5 applied to the  $F_y$  of 250 Mpa), but  $R$ -factor design and deformation limits shall be checked using Grade 250's yield strength of 250 Mpa.

The use of A992 steel is explicitly permitted. Even though this ASTM grade is currently designated for “shapes for buildings”, there is work currently being done to expand applicability to any

shapes. ASTM 992 steel, recently developed to ensure good ductile seismic performance, is specified to have both a minimum and maximum guaranteed yield strength, and may be worthy of consideration for ductile energy-dissipating systems in steel bridges.

Since other steels may be used, provided that they are comparable to the approved Grade 345 steels, High Performance Steel (HPS) Grade 345 would be admissible, but not HPS Grade 485 (or higher). This is not a detrimental restriction for HPS steel, as the scope of Article 8.7 encompasses only a few steel members in a typical steel bridge. (Based on limited experimental data available, it appears that HPS Grade 485 has a lower rotational ductility capacity and may not be suitable for "ductile fuses" in seismic applications).

When other steels are used for energy dissipation purposes, it is the responsibility of the designer to assess the adequacy of material properties available and design accordingly.

Other steel members expected to remain elastic during earthquake shall be made of steels conforming to Article 6.4 of the AASHTO LRFD provisions.

Steel members and weld materials shall have adequate notch toughness to perform in a ductile manner over the range of expected service temperatures. The A709/A709M S84 "Fracture-Critical Material Toughness Testing and Marking" requirement, typically specified when the material is to be utilized in a fracture-critical application as defined by AASHTO, is deemed to be appropriate to provide the level of toughness sought for seismic resistance. For weld metals, the AASHTO/AWS D1.5 Bridge Welding Code requirement for Zone III, familiar to the bridge engineering community, is similar to the 20 ft-lbs at -20F requirement proposed by the SAC Joint Venture for weld metal in welded moment frame connections in building frames.

The capacity design philosophy and the concept of capacity-protected element are defined in Article 4.8.

### C8.7.3 Sway Stability Effects

No commentary is provided for Article 8.7.3.

### C8.7.4 Ductile Moment-Resisting Frames and Single Column Structures

It is believed that properly detailed fully welded column-to-beam or beam-to-column con-

nections in the moment-resisting frames that would typically be used in bridges (See Figure C8.7.4-1) can exhibit highly ductile behavior and perform adequately during earthquakes (contrary to what was observed in buildings following Northridge). As a result, strategies to move plastic hinges away from the joints are not required in the *Specifications*.

However, the designer may still elect to provide measures (such as haunches at the end of yielding members) to locate plastic hinges some distance away from the welded beam-to-column or column-to-beam joint (SAC, 1995, 1997, 2000).

Although beams, columns and panel zones can all be designed, detailed and braced to undergo severe inelastic straining and absorb energy, the detailing requirements of Article 8.7 address common bridge structures with deep non-compact beams much stiffer in flexure than their supporting steel columns, and favor systems proportioned so that plastic hinges form in the columns. This is consistent with the philosophy adopted for concrete bridges.

Even though some bridges could be configured and designed to develop stable plastic hinging in beams without loss of structural integrity, the large gravity loads that must simultaneously be resisted by those beams also make plastic hinging at mid-span likely as part of the plastic collapse mechanism. The resulting deformations can damage the superstructure (for example, the diaphragms or deck).

The special case of multi-tier frames is addressed in Article 8.7.4.4.

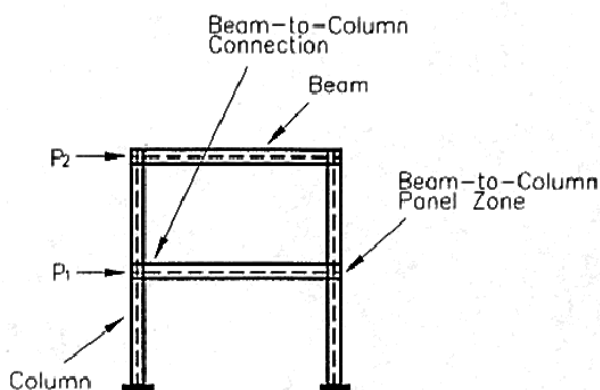


**Figure C8.7.4-1 Example of Moment Frame/Bent**

### C8.7.4.1 Columns

At plastic hinge locations, members absorb energy by undergoing inelastic cyclic bending while maintaining their resistance. Therefore, plastic design rules apply, namely, limitations on width-to-thickness ratios, web-to-flange weld capacity, web shear resistance, and lateral support.

Axial load in columns is also restricted to avoid early deterioration of beam-column flexural strengths and ductility when subject to high axial loads. Tests by Popov et al. (1975) showed that W-shaped columns subjected to inelastic cyclic loading suffered sudden failure due to excessive local buckling and strength degradation when the maximum axial compressive load exceeded  $0.50A_gF_y$ . Tests by Schneider et al. (1992) showed that moment-resisting steel frames with hinging columns suffer rapid strength and stiffness deterioration when the columns are subjected to compressive load equal to approximately  $0.25A_gF_y$ . Most building codes set this limit at  $0.30A_gF_y$ .

The requirement for lateral support is identical to Equation 6.10.4.1.7-1 of the AASHTO LRFD provisions with a moment  $M_1$  of zero at one end of the member, but modified to ensure inelastic rotation capacities of at least four times the elastic rotation corresponding to the plastic moment (resulting in a coefficient of 17250 instead of the approximately 25000 that would be obtained for Equation 6.10.4.1.7-1 of the AASHTO LRFD provisions). Consideration of a null moment at one end of the column accounts for changes in location of the inflexion point of the column moment diagram during earthquake response. Figure 10.27 in Bruneau et al. (1997) could be used to develop other unsupported lengths limits.

Built-up columns made of fastened components (e.g., bolted or riveted) are beyond the scope of these Guidelines.

### C8.7.4.2 Beams

Since plastic hinges are not expected to form in beams, beams need not conform to plastic design requirements.

The requirement for beam resistance is consistent with the outlined capacity-design philosophy. The beams should either resist the full elastic loads or be capacity-protected. In the extreme load situation, the capacity-protected beams are required to have nominal resistances of not less than the combined effects corresponding to the plastic hinges in the columns attaining their probable ca-

capacity and the probable companion permanent load acting directly on the beams. The columns' probable capacity should account for the over-strength due to higher yield than specified yield and strain hardening effects. The value specified in Article 6.9.2.2 of the AASHTO LRFD provisions, used in conjunction with the resistance factor  $\phi_f$  for steel beams in flexure of 1.00, (Article 6.5.4.2 of the AASHTO LRFD provisions) is compatible with the AISC (1997)  $1.1R_y$  used with a resistance factor  $\phi$  of 0.9 (here  $R_y$  is embedded in  $F_{ye}$ ).

### C8.7.4.3 Panel Zones and Connections

The panel zone should either resist the full elastic load (i.e.,  $R=1.0$ ) or be capacity-protected.

Column base connections should also resist the full elastic loads ( $R=1.0$ ) or be capacity-protected, unless they are designed and detailed to dissipate energy.

Panel zone yielding is not permitted.

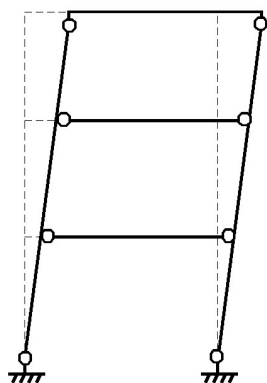
There is a concern that doubler plates in panel zones can be an undesirable fatigue detail. For plate-girder sections, it is preferable to specify a thicker web plate, if necessary, rather than use panel zone doubler plates.

### C8.7.4.4 Multi-Tier Frame Bents

Multi-tier frame bents are sometimes used, mostly because they are more rigid transversely than single-tier frame bents. In such multi-tier bents, the intermediate beams are significantly smaller than the top beam as they are not supporting the gravity loads from the superstructure.

As a result, in a multi-tier frame, plastic hinging in the beams may be unavoidable, and desirable, in all but the top beam. In fact, trying to ensure strong-beam weak-column design at all joints in multi-tier bents may have the undesirable effect of concentrating all column plastic hinging in one tier, with greater local ductility demands than otherwise expected in design.

Using capacity design principles, the equations and intent of Article 8.7.4 may be modified by the designer to achieve column plastic hinging only at the top and base of the column, and plastic hinging at the ends of all intermediate beams, as shown in Figure C8.7.4.4-1.



○ = Schematic plastic hinge location

**Figure C8.7.4.4-1 Acceptable Plastic Mechanism for Multi-Tier Bent**

### C8.7.5 Ductile Concentrically Braced Frames

Concentrically braced frames are those in which both ends of diagonal braces attach at beam-column joints, and the centerlines of braces, beams, and columns are approximately concurrent with little or no joint eccentricity. Inelastic straining must take place in bracing members subjected principally to axial load. Compression members can absorb considerable energy by inelastic bending after buckling and in subsequent straightening after load reversal but the amount is small for slender members. Local buckling or buckling of components of built-up members also limit energy absorption.

#### C8.7.5.1 Bracing Systems

This requirement ensures some redundancy and also similarity between the load-deflection characteristics in the two opposite directions. A significant proportion of the horizontal shear is carried by tension braces so that compression brace buckling will not cause a catastrophic loss in overall horizontal shear capacity. Alternative wording sometimes encountered to express the same intent includes:

- Diagonal braces shall be oriented such that, at any level in any planar frame, at least 30% of the horizontal shear carried by the bracing system shall be carried by tension braces and at

least 30% shall be carried by compression braces.

- Along any line of bracing, braces shall be deployed in alternate directions such that, for either direction of force parallel to the bracing, at least 30% but no more than 70% of the total horizontal force is resisted by tension braces.

This ensures that structural configurations that depend predominantly on the compression resistance of braces (such as case (a) in Figure C8.7.5.1-1) are avoided. Case (b) in that same figure is a better design that meets the above criteria.

This article also excludes bracing systems that have not exhibited the ductile behavior expected for ductile concentrically braced frames, such as:

- Chevron bracing or V-bracing, in which pairs of braces are located either above or below a beam and meet the beam at a single point within the middle half of the span;
- K-bracing, in which pairs of braces meet a column on one side near its mid-height; or
- Knee-bracing.

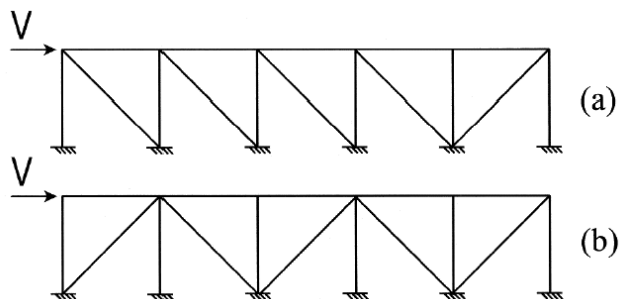


**Figure C8.7.5.1-1 Examples of (a) Unacceptable and (b) Acceptable Braced Bent Configurations**

#### C8.7.5.2 Design Requirements for Ductile Bracing Members

In the ductile design of concentrically braced frames in buildings, the slenderness ratio limits for braces, up until the late 1990s, were approximately 75% of the value specified here. The philosophy was to design braces to contribute significantly to the total energy dissipation when in compression. Member slenderness ratio was restricted because the energy absorbed by plastic bending of braces in compression diminishes with increased slenderness. To achieve these more stringent  $KL/r$  limits,

particularly for long braces, designers have almost exclusively used tubes or pipes for the braces. This is unfortunate as these tubular members are most sensitive to rapid local buckling and fracture when subjected to inelastic cyclic loading (in spite of the low width-to-thickness limits prescribed). Recent reviews of this requirement revealed that it may be unnecessary, provided that connections are capable of developing at least the member capacity in tension. This is partly because larger tension brace capacity is obtained when design is governed by the compression brace capacity, and partly because low-cycle fatigue life increases for members having greater  $KL/r$ . As a result, seismic provisions for buildings (AISC, 1997; CSA, 2001) have been revised to permit members having greater  $KL/r$  values. The proposed relaxed limits used here are consistent with the new recently adopted philosophy for buildings. The limit for back-to-back legs of double-angle bracing members is increased from the value of Table 8.7.4-1 to  $200/\sqrt{F_y}$ .

Early local buckling of braces prohibits the braced frames from sustaining many cycles of load reversal. Both laboratory tests and real earthquake observations have confirmed that premature local buckling significantly shortens the fracture life of high-strength steel (HSS) braces. The more stringent requirement on the  $b/t$  ratio for rectangular tubular sections subjected to cyclic loading is based on tests (Tang and Goel, 1987; Uang and Bertero, 1986). The  $D/t$  limit for circular sections is identical to that in the AISC plastic design specifications (AISC, 1993; Sherman, 1976).

#### C8.7.5.3 Brace Connections

Eccentricities that are normally considered negligible (for example at the ends of bolted or welded angle members) may influence the failure mode of connections subjected to cyclic load (Astaneh, Goel and Hanson, 1986).

A brace which buckles out-of-plane will form a plastic hinge at mid-length and hinges in the gusset plate at each end. When braces attached to a single gusset plate buckle out-of-plane, there is a tendency for the plate to tear if it is restrained by its attachment to the adjacent frame members (Astaneh, Goel and Hanson, 1982). Provision of a clear distance, approximately twice the plate thickness, between the end of the brace and the adjacent members allows the plastic hinge to form in the plate and eliminates the restraint. When in-plane buckling of the brace may occur, ductile rotational behavior should be possible either in the

brace or in the joint. Alternatively, the system could be designed to develop hinging in the brace, and the connections shall then be designed to have a flexural strength equal to or greater than the expected flexural strength  $1.2R_yM_p$  of the brace about the critical buckling axis.

Buckling of double-angle braces (legs back-to-back) about the axis of symmetry leads to transfer of load from one angle to the other, thus imposing significant loading on the stitch fastener (Astaneh, Goel and Hanson, 1986).

#### C8.7.5.4 Columns, Beams and Other Connections

Columns and beams that participate in the lateral-load-resisting system must also be designed to ensure that a continuous load path can be maintained.

A reduced compressive resistance must be considered for this purpose. This takes into account the fact that, under cyclic loading, the compressive resistance of a bracing member rapidly diminishes. This reduction stabilizes after a few cycles to approximately 30% of the nominal compression capacity.

The unreduced brace compressive resistance must be used if it leads to a more critical condition, as it will be attained in the first cycle. However, redistributed loads resulting from the reduced buckled compressive brace loads must be considered in beams and columns as well as in connections, if it leads to a more critical condition.

Other connections that participate in the lateral-load-resisting system must also be designed to ensure that a continuous load path can be maintained. Therefore, they should

- a. resist the combined load effect corresponding to the bracing connection loads and the permanent loads that they must also transfer; and
- b. resist load effect due to load redistribution following brace yielding or buckling.

#### C8.7.6 Concentrically Braced Frames with Nominal Ductility

Detailing requirements are relaxed for concentrically braced frames having nominal ductility (a steel substructure having less stringent detailing requirements). They are consequently being designed to a greater force level.

### C8.7.6.1 Bracing Systems

This requirement ensures some redundancy. It also ensures similarity between the load-deflection characteristics in two opposite directions. A significant proportion of the horizontal shear is carried by tension braces so that compression-brace buckling will not cause a catastrophic loss in overall horizontal shear capacity.

Tension-only systems are bracing systems in which braces are connected at beam-to-column intersections and are designed to resist in tension 100% of the seismic loads.

Systems in which all braces are oriented in the same direction and may be subjected to compression simultaneously shall be avoided.

K-braced frames, in which pairs of braces meet a column near its mid-height, and knee-braced frames shall not be considered in this section.

Analytical and experimental research, as well as observations following past earthquakes, have demonstrated that K-bracing systems are poor dissipators of seismic energy. The members to which such braces are connected can also be adversely affected by the lateral force introduced at the connection point of both braces on that member due to the unequal compression buckling and tension yielding capacities of the braces.

Knee-braced systems in which the columns are subjected to significant bending moments are beyond the scope of this article.

### C8.7.6.2 Design Requirements for Nominally Ductile Bracing Members

Nominally ductile braced frames are expected to undergo limited inelastic deformations during earthquakes. Braces yielding in tension are relied upon to provide seismic energy dissipation. While frames with very slender braces (i.e. tension-only designs) are generally undesirable for multistoried frames in buildings, this is mostly because energy dissipation in such frames tend to concentrate in only a few stories, which may result in excessive ductility demands on those braces. However, nonlinear inelastic analyses show that satisfactory seismic performance is possible for structures up to 4 stories with tension-only braces, provided that connections are capable of developing at least the member capacity in tension and that columns are continuous over the frame height (CSA, 2001). The width-to-thickness ratios for the compression elements of columns can be relaxed for braces

having  $KL/r$  approaching 200, as members in compression do not yield at that slenderness.

### C8.7.6.3 Brace Connections

The additional factor of 1.10 for tension-only bracing systems is to ensure, for the slender members used in this case, that the impact resulting when slack is taken up, does not cause connection failure. Details leading to limited zones of yielding, such as occur at partial joint penetration groove welds should be avoided.

### C8.7.6.4 Columns, Beams and Other Connections

No commentary is provided for Article 8.7.6.4.

### C8.7.6.5 Chevron Braced and V-Braced Systems

Lateral bracing at the beam-brace intersection in chevron and inverted-chevron frames is crucial to prevent lateral torsional buckling of the beam at that location (see Figure C8.7.6.5-1). Effective lateral bracing requires structural elements framing transversely to the frame bent, which may be only possible in 4-column tower piers where horizontal members can be introduced to tie and brace all four faces of the tower pier. Alternatively, lateral bracing could be provided by a connection to the superstructure if proper consideration is given to fatigue and deformation compatibility.

Furthermore, geometry of the braced system must be chosen to preclude beam deformations that could translate into undesirable superstructure damage.

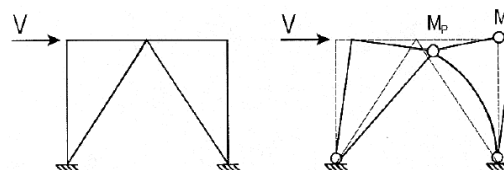


**Figure C8.7.6.5-1** Plastic Mechanism for a Chevron Braced Bent Configuration that Would Introduce Undesirable Superstructure Damage (Unless This Bridge Has Only Two Girders that are Located Directly over the Columns)

### C8.7.7 Concrete-Filled Steel Pipes

This article is only applicable to concrete-filled steel pipes without internal reinforcement, and connected in a way that allows development of their full composite strength. It is not applicable to design a concrete-filled steel pipe that relies on internal reinforcement to provide continuity with another structural element, or for which the steel pipe is not continuous or connected in a way that enables it to develop its full yield strength. When used in pile bent, the full composite strength of the plastic hinge located below ground can only be developed if it can be ensured that the concrete fill is present at that location.

Recent research (e.g., Alfawahkiri, 1998; Bruneau and Marson, 1999) demonstrates that the AASHTO equations for the design of concrete-filled steel pipes in combined axial compression and flexure (Articles 6.9.2.2, 6.9.5, and 6.12.2.3.2 of the AASHTO LRFD provisions), provide a conservative assessment of beam-column strength. Consequently, the calculated strength of concrete-filled steel pipes that could be used as columns in ductile moment-resisting frames or pile-bents, could be significantly underestimated. This is not surprising given that these equations together are deemed applicable to a broad range of composite member types and shapes, including concrete-encased steel shapes. While these equations may be perceived as conservative in a non-seismic perspective, an equation that more realistically captures the plastic moment of such columns is essential in a capacity design perspective. Capacity-protected elements must be designed with adequate strength to withstand elastically the plastic hinging in the columns. Underestimates of this hinging force translate into under-design of the capacity-protected elements; a column unknowingly stronger than expected will not yield before damage develops in the foundations or at other undesirable locations in the structure. This can have severe consequences, as the capacity-protected elements are not detailed to withstand large inelastic deformations. The provisions of Article 8.7.7 are added to prevent this behavior.

Note that for analysis, as implied by Article 6.9.5 of the AASHTO LRFD provisions, flexural stiffness of the composite section can be taken as  $E_s I_s + 0.4 E_c I_c$ , where  $I_c$  is the gross inertia of the concrete ( $\pi D^4/16$ ),  $I_s$  is the inertia of the steel pipe, and  $E_s$  and  $E_c$  are respectively the steel and concrete moduli of elasticity.

#### C8.7.7.1 Combined Axial Compression and Flexure

This equation is known to be reliable up to a maximum slenderness limit  $D/t$  of  $28000/F_y$ , underestimating the flexural moment capacity by 1.25, on average (see Figure C8.7.7.1-1). It may significantly overestimate columns strength having greater  $D/t$  ratios.

This new equation is only applicable to concrete-filled steel pipes. Other equations may similarly be needed to replace those of Article 6.9.2.2 of the AASHTO LRFD provisions for other types of composite columns (such as concrete-encased columns).

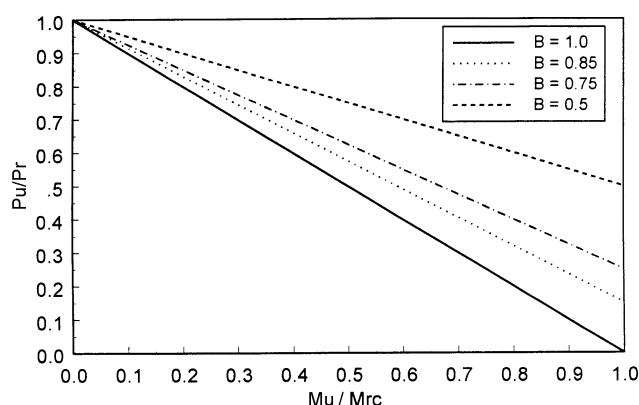


**Figure C8.7.7.1-1 Interaction Curves for Concrete-Filled Pip**

#### C8.7.7.2 Flexural Strength

When using these equations to calculate the forces acting on capacity-protected members as a result of plastic hinging of the concrete-filled pipes,  $F_y$  should be replaced by  $F_{ye}$ , for consistency with the capacity design philosophy.

Figure C8.7.7.2-1 illustrates the geometric parameters used in this Article.

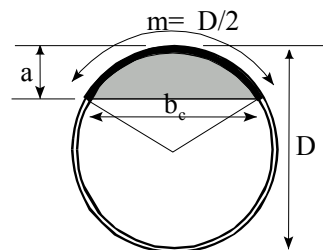


**Figure C8.7.7.2-1 Flexure of Concrete-Filled Pipe; Shaded Area is Concrete in Compression above the Neutral Axis**

Moment resistance is calculated assuming the concrete in compression at  $f'_c$ , and the steel in tension and compression at  $F_y$ . The resulting free-body diagram is shown in Figure C8.7.7.2-2, where  $e$  is equal to  $y_{sc} + y_{st}$ ,  $e'$  is equal to  $y_c + y_{st}$ , and  $y_c$  is the distance of the concrete compressive force ( $C_r'$ ) from the center of gravity, and  $y_{st}$  and  $y_{sc}$  are the respective distances of the steel tensile ( $T_r$ ) and compressive forces ( $C_r$ ) from the center of gravity.

In Method 2, a geometric approximation is made in calculating the area of concrete in compression by subtracting the rectangular shaded area shown in Figure C8.7.7.2-3 from the total area enclosed by the pipe (and dividing the result by 2). Neutral axis is at height  $h_n$ .

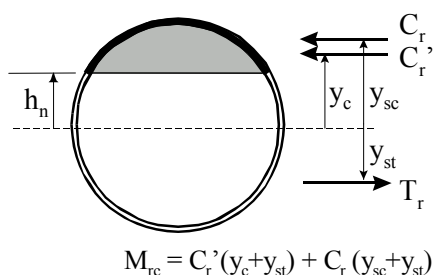


**Figure C8.7.7.2-2 Free-Body Diagram Used to Calculate Moment Resistance of Concrete-Filled Pipe**

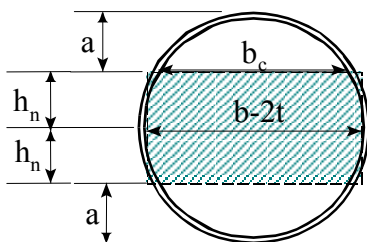


**Figure C8.7.7.2-3 Flexure of Concrete-Filled Pipe – Illustrates Approximation Made in Method 2**

Method 2 (using approximate geometry) gives smaller moments than Method 1 (exact geometry). The requirement to increase the calculated moment by 10% for capacity design when using the approximate method was established from the ratio of the moment calculated by both methods for a  $D/t$  of 10. That ratio decreases as  $D/t$  increases.

### C8.7.7.3 Beams and Connections

Recent experimental work by Bruneau and Marson (1999), Shama et al. (2001), Azizinamini et al. (1999), provide examples of full fixity connection details. In some instances, full fixity may not be needed at both ends of columns. Concrete-filled steel pipes, when used in pile bents, only require full moment connection at the pile-cap.

### C8.7.8 Other Systems

Article 8.7.8, Other Systems, contains systems less familiar to bridge engineers. Eccentrically braced substructures are included in this section partly for that reason, but also because most configurations of this system would introduce beam deformations that are undesirable in bridges as this could translate into superstructure damage. Furthermore, bracing of the links may be a difficult design issue that requires special consideration in bridge bents.

The designer must take the necessary steps to ensure that special systems will provide a level of safety comparable to that provided in these *Specifications*. This may require review of published research results, observed performance in past earthquakes, or special investigations.

#### C8.7.8.1 Ductile Eccentrically Braced Frames

The scope of Article 8.7.8.1 is for eccentrically braced frames used as ductile substructure, not as part of ductile diaphragms.

Eccentrically braced frames have been extensively tested and implemented in numerous buildings, but, at the time of this writing, few new bridges have been built relying on shear links for seismic energy dissipation. An obvious difficulty in bridge applications arises because the eccentric link cannot easily be laterally braced to prevent movement out of the plane of the braced bent. Nonetheless, the bents of the Richmond-San Raphael bridge near San Francisco have been retrofitted using eccentrically braced frames. For that bridge, the multiple adjacent frames were used to provide proper bracing of the shear links. Large-scale testing was conducted to validate the retrofit concept (Vincent, 1996; Itani et al., 1998b). Furthermore, the tower of the new east-bay crossing of the Bay Bridge between San Francisco and Oakland is connected by shear links, although not in an eccentrically braced frame configuration (Tang et al., 2000).



While effective eccentrically braced bents are possible, component details that have been tested with the same lateral bracing considerations as in the prototype must be used. Other details must be experimentally validated. Size effects have not been fully investigated. Although it is preferable to use links with sizes no greater than those validated by full-scale tests, in some instances, this may not be possible.

Extensive detailing requirements are not provided within these *Specifications*. However, the designer could follow the detailing practice used for buildings, modified to address the above concerns regarding lateral bracing.

The scope of this article is restricted to eccentrically braced frames of split-V configuration. Eccentrically braced frame (EBF) configurations in which the ductile link is adjacent to a beam-column connection are prohibited, unless it can be demonstrated, by tests of specimens greater or equal in size to the prototype, that the connection can develop the required strength and hysteretic ductility.

Furthermore, the geometry of the eccentrically braced system must be chosen to preclude beam deformations that could translate into undesirable superstructure damage. As such, the configurations shown in Figure C8.7.8.1-1 would introduce undesirable superstructure damage, unless this bridge has only two girders that are located directly over the columns. In most cases, alternative configurations would be required.

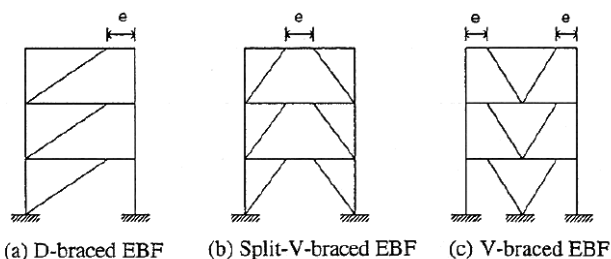


**Figure C8.7.8.1-1** Eccentrically Braced Frames Configurations, the Scope of C6.15.5.1 Being Restricted to Split-V Configuration (Case B).

For eccentrically braced frames, all references to “inelastic hinging of the column” in other seismic requirements elsewhere in the *Specifications* should be interpreted as “yielding of the eccentric link”.

### C8.7.8.2 Ductile End-Diaphragm in Slab-on-Girder Bridge

The ductile diaphragm strategy is not effective when the substructure is significantly more flexible than the superstructure. This is addressed by Article 8.7.8.2. Bridges having wide piers, wall-piers, or other substructure elements of similar limited ductility, would be good candidates for the implementation of the ductile diaphragm system. In these examples, the ductile diaphragms could also be designed to yield instead of the bridge piles, thus preventing the development of damage below ground level where it may not be able to be inspected following an earthquake.

The contribution of girders can be significant and cannot be neglected, as indicated in Article 8.7.8.2. For that reason, ductile diaphragms are generally more effective in long-span bridges, and may be of limited benefit for short-span bridges.

The inertia forces attributable to the mass of the pier-cap will be resisted by the substructure, in spite of the presence of ductile diaphragms. Refined analyses should consider this condition if that mass is a significant portion of the total superstructure mass.

For ductile end-diaphragms, all references to “inelastic hinging of the column” in other seismic requirements elsewhere in the Guidelines should be interpreted as “yielding of the ductile diaphragm”.

A detailed procedure for the design of ductile diaphragms in slab-on-girder bridges is presented in Appendix E, along with illustrations of systems that would satisfy the restrictions of Article 8.7.8.2.

### C8.7.8.3 Ductile End-Diaphragms in Deck Truss Bridges

Articles 8.7.8.2 and 8.7.8.3 share many conceptual similarities, but seismic forces in deck-trusses follow a more complex and redundant load-path. This requires the use of ductile diaphragms vertically over the supports as well as horizontally in the last lower horizontal cross-frame before each support.

For ductile end-diaphragms, all references to “inelastic hinging of the column” in other seismic requirements elsewhere in the Guidelines should be interpreted as “yielding of the ductile diaphragm.”

Further research may allow to relax the limits imposed by Article 8.7.8.3.

A detailed procedure for the design of ductile diaphragms in deck truss bridges is presented in Appendix F.

#### C8.7.8.4 Other Systems

Other "special systems" may emerge in the future, such as friction-braced frames, shock transmission units, other approaches of superstructure plastic hinging, and marine bumpers.

#### C8.7.9 Plastic Rotational Capacities

A moment-curvature analysis based on strain compatibility and nonlinear stress-strain relations can be used to determine plastic limit states. From this, a rational analysis is used to establish the rotational capacity of plastic hinges.

##### C8.7.9.1 Life Safety Performance

No commentary is provided for Article 8.7.9.1.

##### C8.7.9.2 Immediate Use Limit State

No commentary is provided for Article 8.7.9.2.

##### C8.7.9.3 In-Ground Hinges

In-ground hinges are necessary for certain types of bridge substructures. These may include, but are not restricted to:

- Pile bents
- Pile foundations with strong pier walls
- Drilled shafts
- Piled foundations with oversized columns

It is necessary to restrict these plastic hinge rotations in order to limit plastic strains. This limit is expected to reduce plastic strains to less than 10% of their above-ground counterpart (with  $\theta_p = 0.035$  radians), due to the increased plastic hinge length of in-ground hinges.

## C8.8 REINFORCED CONCRETE DESIGN REQUIREMENTS

### C8.8.1 General

High-strength reinforcement reduces congestion and cost as demonstrated by Mander and Cheng (1999), and Dutta, Mander and Kokorina, (1999). However it is important to ensure that the cyclic fatigue life is not inferior when compared to ordinary mild steel reinforcing bars. Mander, Panthaki, and Kasalanati, (1994) have shown that modern high-alloy prestressing threadbar steels can have sufficient ductility to justify their use in seismic design.

The Modulus of Toughness is defined as the area beneath the monotonic tensile stress-strain curve from initial loading (zero stress) to fracture.

Designers working with sites subjected to Seismic Hazard Levels III and IV are encouraged to avail themselves of current research reports and other literature to augment these Specifications.

The 1989 Loma Prieta and 1994 Northridge earthquakes confirmed the vulnerability of columns with inadequate transverse reinforcement and inadequate anchorage of longitudinal reinforcement. Also of concern are:

- lack of adequate reinforcement for positive moments that may occur in the superstructure over monolithic supports when the structure is subjected to longitudinal dynamic loads;
- lack of adequate shear strength in joints between columns and bent caps under transverse dynamic loads;
- inadequate reinforcement for torsion, particularly in outrigger-type bent caps; and
- inadequate transverse reinforcement for shear and for restraint against global buckling of longitudinal bars ("bird caging").

The purpose of the additional design requirements of this article is to increase the probability that the design of the components of a bridge are consistent with the principles of "Capacity Design", especially for bridges located in Seismic Hazard Levels II to IV, and that the potential for failures observed in past earthquakes is minimized. The additional column design requirements of this article for bridges located in Seismic Hazard Levels III and IV are to ensure that a column is provided with reasonable ductility and is forced to yield in flexure and that the potential for

a shear, compression failure due to longitudinal bar buckling, or loss of anchorage mode of failure is minimized. See also Articles 3.3 and 4.8 for further explanation. The actual ductility demand on a column or pier is a complex function of a number of variables, including:

- Earthquake characteristics, including duration, frequency content and near-field (or pulse) effects,
- Design force level,
- Periods of vibration of the bridge,
- Shape of the inelastic hysteresis loop of the columns, and hence effective hysteretic damping,
- Elastic damping coefficient,
- Contributions of foundation and soil conditions to structural flexibility, and
- Spread of plasticity (plastic hinge length) in the column.

The damage potential of a column is also related to the ratio of the duration of strong ground shaking to the natural period of vibration of the bridge. This ratio will be an indicator of the low-cycle fatigue demand on the concrete column hinge zones.

### C8.8.2 Column Requirements

The definition of a column in this article is provided as a guideline to differentiate between the additional design requirements for a wall-type pier and the requirements for a column. If a column or pier is above or below the recommended criterion, it may be considered to be a column or a pier, provided that the appropriate  $R$ -factor of Article 4.7 and the appropriate requirements of either Articles 8.8.2 or 8.8.3 are used. For columns with an aspect ratio less than 2.5, the forces resulting from plastic hinging will generally exceed the elastic design forces; consequently, the forces of Article 8.8.3 would not be applicable.

Certain oversize columns exist for architectural or aesthetic reasons. These columns, if fully reinforced, place excessive demands of moment, shear, or both, on adjoining elements. The designer should strive to “isolate structurally” those architectural elements that do not form part of the primary energy dissipation system that are located either within or in close proximity to plastic hinge zones. Nevertheless, the architectural elements

must remain serviceable throughout the life of the structure. For this reason, minimum steel for temperature and shrinkage should be provided. When architectural flares are not isolated, Article 4.8 requires that the design shear force for a flared column be the worst case calculated using the overstrength moment of the oversized flare or the shear generated by a plastic hinge at the bottom of the flare.

#### C8.8.2.1 Longitudinal Reinforcement

This requirement is intended to apply to the full section of the columns. The 0.8% lower limit on the column reinforcement reflects the traditional concern for the effect of time-dependent deformations as well as the desire to avoid a sizable difference between the flexural cracking and yield moments. The 4% maximum ratio is to avoid congestion and extensive shrinkage cracking and to permit anchorage of the longitudinal steel, but most importantly, the smaller the amount of longitudinal reinforcement, the greater the ductility of the column.

#### C8.8.2.2 Flexural Resistance

Columns are required to be designed biaxially and to be investigated for both the minimum and maximum axial forces. Resistance factors of unity may be used wherever moments and axial loads are derived from a plastic mechanism.

#### C8.8.2.3 Column Shear and Transverse Reinforcement

The implicit method is conservative and is most appropriate when a shear demand has not been calculated, e.g., SDR 2 and piles. The explicit method should result in less reinforcement and is recommended if the shear demand is available.

This implicit shear detailing approach assumes that

$$\phi V_u = V_c + V_p + V_s \geq \frac{\Lambda M_p^o}{H_c}$$

in which  $V_c = 0$  (the contribution of shear carried by the concrete tensile section). This shear demand at plastic overstrength ( $M_p^o$ ) is implicitly resisted by arch action ( $V_p$ ) which is carried by a corner-to-corner diagonal strut in the concrete, and truss action ( $V_s$ ), which is resisted by the trans-

verse reinforcement. The overstrength demand for the transverse steel comes solely from the presence of the longitudinal reinforcement. It is for this reason the transverse steel ( $\rho_v$ ) is directly proportional to the longitudinal steel ( $\rho_l$ ). Thus, if steel congestion results for a chosen column size, one viable solution is to enlarge the column and reduce the longitudinal steel volume.

For a derivation of the implicit shear detailing approach, refer to the recent research by Dutta and Mander (1998).

The requirements for shear outside the hinge zones assumes the concrete is capable of sustaining a concrete stress of  $v_c = 0.17\sqrt{f'_c} \cot \theta$ .

The basis of equation (8.8.2.3-5) follows.

Shear in end zones = shear outside end zones

$$V_s = V_s^* + V_c$$

where  $V_s^*$  = shear carried by the transverse steel outside the plastic hinge zone. Expanding both sides gives

$$\rho_v A_v f_{yh} \cot \theta = \rho_v^* A_v f_{yh} \cot \theta + 0.17\sqrt{f'_c} \cot \theta A_v$$

Solving for  $\rho_v^*$ , the required amount of transverse reinforcement outside the potential plastic hinge zone, gives equation (8.8.2.3-5). If  $\rho_v^*$  is negative, the concrete alone is theoretically adequate for strength, although the minimum steel is still required if this occurs.

The shear-strength model is based on the concept that the total shear strength is given by the following design equation:

$$V_u < V_s + V_p + V_c$$

The concrete tensile contribution to shear,  $V_c$ , is assumed to diminish significantly under high ductilities and cyclic loading.

The requirements of this article are intended to avoid column shear failure by using the principles of "capacity protection". The design shear force is specified as a result of the actual longitudinal steel provided, regardless of the design forces. This requirement is necessary because of the potential for superstructure collapse if a column fails in shear.

A column may yield in either the longitudinal or transverse direction. The shear force corresponding to the maximum shear developed in either direction for noncircular columns should be used for the determination of the transverse reinforcement.

For a noncircular pile, this provision may be applied by substituting the larger cross-sectional dimension for the diameter.

As a starting point for initial design, assume  $\theta = 35^\circ$ . The actual crack angle should be estimated based on the provided transverse reinforcement using equation 8.8.2.3-13. From this the shear strength should be checked based on the provided steel.

The explicit shear approach defined herein is similar to the shear model of Priestley, Verma and Xiao (1994). Based on a survey of empirical observations, Priestley et al. recommended that the crack angle be taken as  $\theta = 35^\circ$  and  $30^\circ$  for design and analysis, respectively.

The crack angle computed in equation 8.8.2.3-13 is more general. The associated theory is based on research by Kim and Mander (1999). In their approach an energy minimization of shear-flexure deflections was used on a truss model of a beam-column element to find an analytical expression for the crack angle. This theoretical crack angle equation was then validated against a wide variety of experimental observations.

#### C8.8.2.4 Transverse Reinforcement for Confinement at Plastic Hinges

Plastic hinge regions are generally located at the top and bottom of columns and pile bents.

These requirements and equations govern the transverse reinforcement for confinement at plastic hinges. They are not in addition to those of Article 8.8.2.3.

These equations ensure that the concrete is adequately confined so that the transverse hoops will not prematurely fracture as a result of the plastic work done on the critical column section. For typical bridge columns with low levels of axial load, these equations rarely govern, but must be checked. The equations were developed by Dutta and Mander (1998), with experiments demonstrating that they work well for both regular mild steel spirals as well as high strength steel in the form of wire rope (see Dutta et al, 1999). The latter should not be used for hoops, ties or stirrups with bent hooks.

Preventing the loss of concrete cover in the plastic hinge zone as a result of spalling requires careful detailing of the confining steel. It is clearly inadequate to simply lap the spiral reinforcement. If the concrete cover spalls, the spiral will be able to unwind. Similarly, rectangular

hoops should be anchored by bending ends back into the core.

Examples of transverse column reinforcement are shown in Figures C8.8.2.4-1 to C8.8.2.4-4. Figures C8.8.2.4-1 through C8.8.2.4-4 also illustrate the use of Equations 8.8.2.4-1 and 8.8.2.4-2. The required total area of hoop reinforcement should be determined for both principal axes of a rectangular or oblong column, and the greater value should be used.

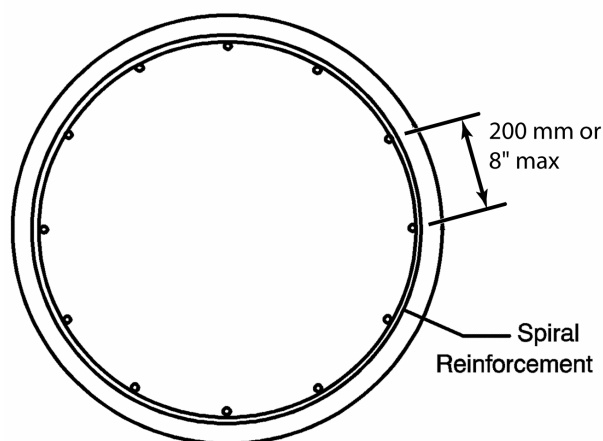


**Figure C8.8.2.4-1 Single Spiral**

While these Guidelines allow the use of spirals, hoops or ties for transverse column reinforcement, the use of spirals is recommended as the most effective and economical solution. Where more than one spiral cage is used to confine an oblong column core, the spirals should be interlocked with longitudinal bars as shown in Figure C8.8.2.4-3. Spacing of longitudinal bars of a maximum of 200 mm center-to-center is also recommended to help confine the column core.

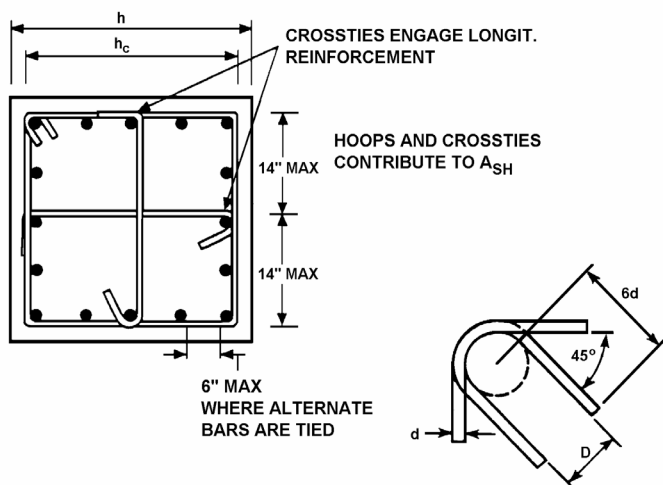


**Figure C8.8.2.4-2 Column Tie Details**

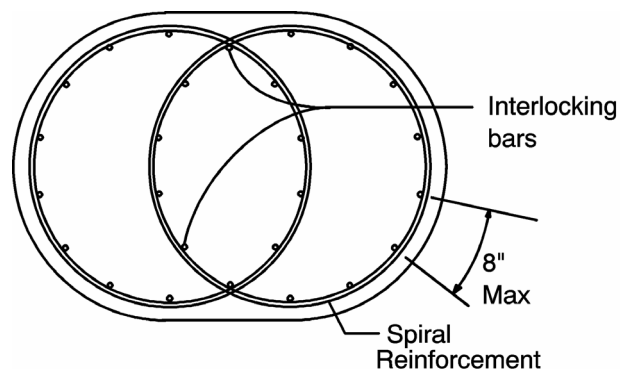


**Figure C8.8.2.4-3 Column Interlocking Spiral Details**

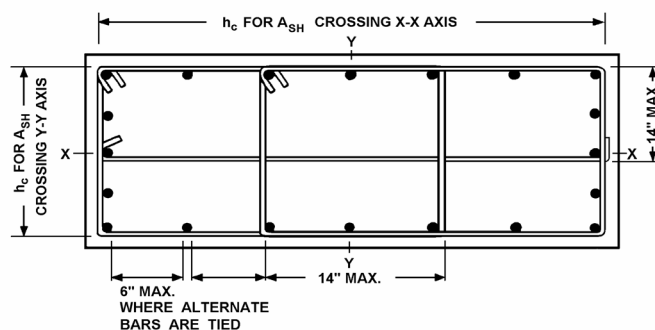


**Figure C8.8.2.4-4 Column Tie Details**

#### C8.8.2.5 Transverse Reinforcement for Longitudinal Bar Restraint in Plastic Hinges

Longitudinal reinforcing bars in potential plastic hinge zones may be highly strained in compression to the extent that they may buckle. Buckling may either be

- local between two successive hoop sets or spirals, or
- global and extend over several hoop sets or spirals.

Condition (a) is prevented by using the maximum vertical spacing of transverse reinforcement given by Equation 7.8.2.5-1 or 8.8.2.5-1 of the *Specifications*.

Although research has been conducted to determine the amount of transverse reinforcement required to prevent condition (b), this research has not been fully peer reviewed, and thus has not been included as part of the *Specifications*. However, designers should not ignore the possibility of condition (b) and should take steps to prevent it.

The following tentative criteria for transverse reinforcement to prevent condition (b) have been proposed:

- i. For circular sections confined by spirals or circular hoops:

$$\rho_s = 0.016 \left( \frac{D}{s} \right) \left( \frac{s}{d_b} \right) \rho_t \frac{f_y}{f_{yh}}$$

- ii. For rectangular sections confined by transverse hoops and/or cross ties the area of the cross tie or hoop legs ( $A_{bh}$ ) shall be:

$$A_{bh} = 0.09 A_b \frac{f_y}{f_{yh}}$$

where

$\rho_s$  = ratio of transverse reinforcement

$$\rho_s = \frac{4A_{bh}}{sD'}$$

$D$  = diameter of circular column

$d_b$  = diameter of longitudinal reinforcing bars being restrained by circular hoop or spiral

$A_b$  = area of longitudinal reinforcing bars being restrained by rectilinear hoops and/or cross ties

$A_{bh}$  = bar area of the transverse hoops or ties restraining the longitudinal steel

$\rho_t$  = volumetric ratio of longitudinal reinforcement

$f_y$  = yield stress of the longitudinal reinforcement

$f_{yh}$  = yield stress of the transverse reinforcing bars

Trial applications have shown that the above equations result in excessive transverse reinforcement in some cases. This is usually associated with high amounts of column longitudinal reinforcement, and so it may be prudent for a designer to limit the volumetric ratio of longitudinal reinforcement.

Criteria (i) and (ii) of Article 8.8.2.5 (above) are intended to ensure that the yield capacity of the longitudinal reinforcement is maintained. This is a life-safety requirement. If global buckling of the longitudinal reinforcing is to be inhibited only to ensure postearthquake repairability, then it has been proposed that the following be used:

$$\rho_s = 0.024 \left( \frac{D}{d_b} \right) \rho_t \frac{f_y}{f_{yh}}$$

and

$$A_{bh} = 0.25 A_b \frac{f_y}{f_{yh}}$$

Criteria (i) and the above recommendation for postearthquake repairability may lead to congestion of hoops or spirals in circular columns with large amounts of longitudinal reinforcement. One way to overcome this is to use wire rope or prestressing strands with a high yield strain as transverse reinforcement. However, this is another reason for not mandating the global anti-buckling criteria since it would require a major change in construction practice that needs to be more thoroughly evaluated from the standpoint of constructability.

An alternative approach to relieve transverse reinforcement congestion arising from these anti-buckling requirements is to use two concentric rings of longitudinal steel. The antibuckling requirements need only apply to the outer ring of longitudinal bars.

#### C8.8.2.6 Spacing for Transverse Reinforcement for Confinement and Longitudinal Bar Restraint

This requirement ensures all inelastic portions of the column are protected by confining steel.

#### C8.8.2.7 Splices

It is often desirable to lap longitudinal reinforcement with dowels at the column base. This is undesirable for seismic performance because:

- The splice occurs in a potential plastic hinge region where requirements for bond are critical, and
- Lapping the main reinforcement will tend to concentrate plastic deformation close to the base and reduce the effective plastic hinge length as a result of stiffening of the column over the lapping region. This may result in a severe local curvature demand.

#### C8.8.2.8 Flexural Overstrength

The simplified method for calculating an overstrength moment-axial-load interaction diagram

(Mander, et. al, 1998) involves a parabolic curve fit to  $(M_{bo}, P_b)$  and  $(0, P_{to})$  given by Equation C8.8.2.8-1.

$$\frac{M_{po}}{f'_c A_g D} = \left( \frac{M_{bo}}{f'_c A_g D} \right) \left[ 1 - \left( \frac{\frac{P_e}{f'_c A_g} - \frac{P_b}{f'_c A_g}}{\frac{P_{to}}{f'_c A_g} - \frac{P_b}{f'_c A_g}} \right)^2 \right] \quad (C8.8.2.8-1)$$

where:

$\frac{P_e}{f'_c A_g}$  = axial stress ratio on the column based on gravity load and seismic (framing) actions

$\frac{P_{to}}{f'_c A_g} = -\rho_t \frac{f_{su}}{f'_c}$  = normalized axial tensile capacity of the column

$\frac{P_b}{f'_c A_g} = 0.425\beta_1$  = normalized axial load capacity at the maximum nominal (balanced) moment on the section where  $\beta_1$  = stress block factor ( $\leq 0.85$ )

$$\frac{M_{bo}}{f'_c A_g D} = \left( K_{shape} \rho_t \frac{f_{su}}{f'_c} \frac{D'}{D} + \frac{P_b}{f'_c A_g} \frac{1 - \kappa_o}{2} \right) \quad (C8.8.2.8-2)$$

$D'$  = pitch circle diameter of the reinforcement in a circular section, or the out-to-out dimension of the reinforcement in a rectangular section, this generally may be assumed as  $D' = 0.8D$ .

$f_{su}$  = ultimate tensile strength of the longitudinal reinforcement.

$K_{shape}$  should be taken defined in Article 8.8.2.3.

$\kappa_o$  = a factor related to the stress block centroid which should be taken as 0.6 and 0.5 for circular and rectangular sections, respectively.

### C8.8.3 Limited Ductility Requirements for Wall-Type Piers

The requirements of this article are based on limited data available on the behavior of piers in the inelastic range. Consequently, the R-factor of 2.0 for piers is based on the assumption of minimal inelastic behavior.

The requirement that  $\rho_v \geq \rho_h$  is intended to avoid the possibility of having inadequate web

reinforcement in piers which are short in comparison to their height. Splices should be staggered to avoid weak sections.

### C8.8.4 Moment-Resisting Connection Between Members (Column-Beam and Column-Footing Joints)

#### C8.8.4.1 Implicit Approach: Direct Design

Shear steel will often govern in connections due to the increased shear demand at flexural overstrength arising from a smaller shear span within the joint compared to the columns framing into the connection. If this results in considerable congestion, particularly when large volumes of longitudinal steel exist, then detailed design in accordance with the explicit approach of Article 8.8.4.2 might give some relief. This is because this explicit approach permits some of the joint reinforcement to be placed outside the joint in the adjacent cap beam.

#### C8.8.4.2 Explicit Approach: Detailed Design

The designer may consider the following means to improve constructability:

- prestressing the joint as a means of reducing reinforcing steel,
- placing vertical shear reinforcement within the joint or in the cap beam adjacent to the joint region, or both.

#### C8.8.4.2.1 Design Forces and Applied Stresses

The stresses  $f_h$  and  $f_v$  in Equations 8.8.4.2-1 and 8.8.4.2-2 are nominal compression stresses in the horizontal and vertical directions, respectively. In a typical joint  $f_v$  is provided by the column axial force  $P_e$ . An average stress at midheight of the cap beam, or mid-depth of the footing, should be used, assuming a 45° spread away from the boundaries of the column in all directions. The horizontal axial stress  $f_h$  is based on the mean axial force at the center of the joint, including effects of cap beam prestress, if present.

The joint shear stress  $v_{hv}$  can be estimated with adequate accuracy from the expression

$$v_{hv} = \frac{M_p}{h_b h_c b_{ji}} \quad (8.8.4.2-1)$$

where

- $M_p$  = the maximum plastic moment  
 $h_b$  = the cap beam or footing depth  
 $h_c$  = the column lateral dimension in the direction considered (i.e.,  $h_c = D$  for a circular column)  
 $b_{je}$  = the effective joint width, found using a 45-degree spread from the column boundaries.

Figure C8.8.4.2-1 (Priestley, Seible and Calvi, 1996) clarifies the quantities to be used in this calculation.

#### C8.8.4.2.2 Maximum Required Horizontal Reinforcement

The need to include spiral reinforcement to aid in joint force transfer has become obvious as a result of the poor performance of moment-resisting connections in recent earthquakes and in large-scale tests. Theoretical considerations (Priestley, Seible and Calvi, 1996) and experimental observation (Sriharan and Priestley et al., 1994a; Sriharan and Priestley, 1994b; Priestley et al. 1992), indicate that unless the nominal principal tension stress in the connection (joint region) exceeds  $0.29\sqrt{f'_c}$  MPa, diagonal cracking in the connection will be minimal. Equation 8.8.4.2-3 requires placement of sufficient hoop reinforcement to carry 50% of the tensile force at  $0.29\sqrt{f'_c}$  MPa, nominal tensile stress, resolved into the horizontal plane. This is the minimum level of reinforcement.

#### C8.8.4.2.3 Maximum Allowable Compression Stresses

The principal compression stress in a connection is limited to  $0.25 f'_c$ . This limits the shear stress to less than  $0.25 f'_c$ . It is felt that the level of nominal principal compression stress is a better indicator of propensity for joint crushing than is the joint shear stress.

#### C8.8.4.3 Reinforcement for Joint Force Transfer

##### C8.8.4.3.1 Acceptable Reinforcement Details

A "rational" design is required for joint reinforcement when principal tension stress levels ex-

ceed  $0.29\sqrt{f'_c}$  MPa. The amounts of reinforcement required are based on the mechanism shown in Figure C8.8.4.3-1 which primarily uses external reinforcement for joint resistance to reduce joint congestion.

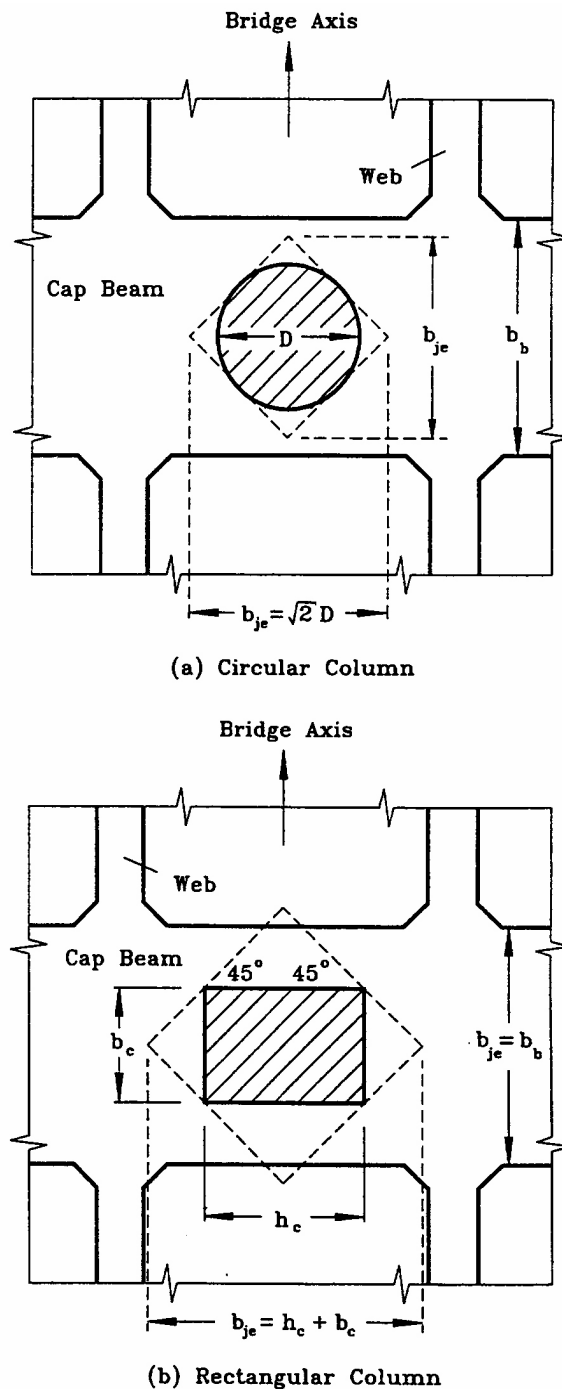
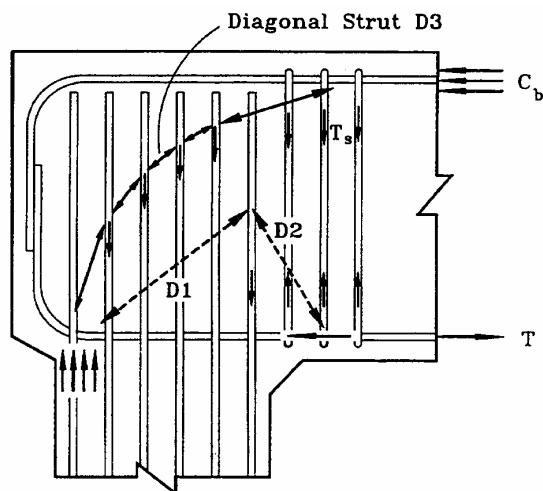


Figure C8.8.4.2-1 Effective Joint Width for Shear Stress Calculations





**Figure C8.8.4.3-1 External Vertical Joint Reinforcement for Joint Force Transfer**

#### C8.8.4.3.2 Vertical Reinforcement

##### *Stirrups*

Figure C8.8.4.3-1 is intended to clarify this clause.  $A_{ST}$  is the total area of column reinforcement anchored in the joint. Reinforcement  $A_{jv}$  is required to provide the tie force  $T_s$  resisting the vertical component of strut D2 in Figure C8.8.4.3-1. This reinforcement should be placed close to the column cage for maximum efficiency.

##### *Clamping Reinforcement*

In addition, it will be recognized that the cap beam top reinforcement or footing bottom reinforcement may have severe bond demands, since stress levels may change from close to tensile yield on one side of the joint to significant levels of compression stress on the other side. The required  $0.08 A_{ST}$  vertical ties inside the joint are intended to help provide this bond transfer by clamping the cap-beam rebar across possible splitting cracks. Similar restraint may be required for superstructure top longitudinal rebar. Cap beam widths one foot greater than column diameter are encouraged so that the joint shear reinforcement is effective.

When the cap-beam, superstructure, or both, are prestressed, the bond demands will be much less severe and the clamping requirement can be relaxed. It can also be shown theoretically (Priestley, Seible and Calvi, 1996) that the volu-

metric ratio of hoop reinforcement can be proportionately reduced to zero as the prestress force approaches  $0.25T_c$ .

Figure C8.8.4.3-2 shows each of the areas within which the reinforcement required by this clause must be placed. For an internal column of a multi-column bent, there will be four such areas, overlapping, as shown in Figure C8.8.4.3-2a). For an exterior column of a multi-column bent, there will be three such areas (Figure C8.8.4.3-2b). For a single-column bent with monolithic column-to-cap-beam connection, there will be two such areas corresponding to longitudinal response (Figure C8.8.4.3-2c). Where these areas overlap, vertical joint reinforcement within the overlapping areas may be considered effective for both directions of response. Where shear reinforcement exists within a given area and is not fully utilized for shear resistance in the direction of response considered, that portion not needed for shear resistance may be considered to be vertical joint reinforcement. Since cap-beam shear reinforcement is normally dictated by conditions causing cap beam negative moment (gravity and seismic shear are additive) while the external joint reinforcement discussed in this section applies to cap beam positive moment (when gravity and seismic shear are in opposition), it is normal to find that a considerable portion of existing cap beam shear reinforcement adjacent to the joint can be utilized.

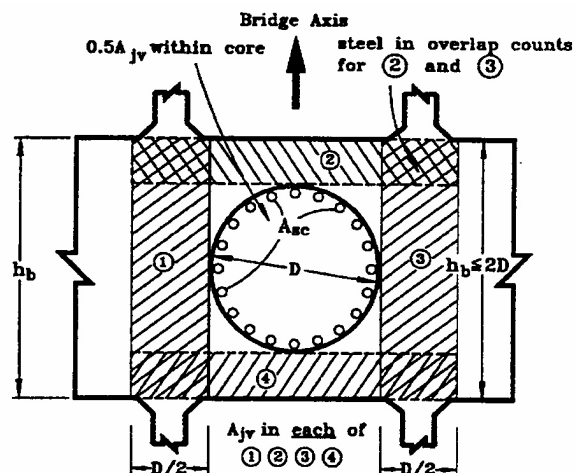
#### C8.8.4.3.3 Horizontal Reinforcement

Additional cap-beam bottom reinforcement of area  $0.08 A_{ST}$  is required to provide the horizontal resistance of the strut D2 in Figure C8.8.4.3-1.

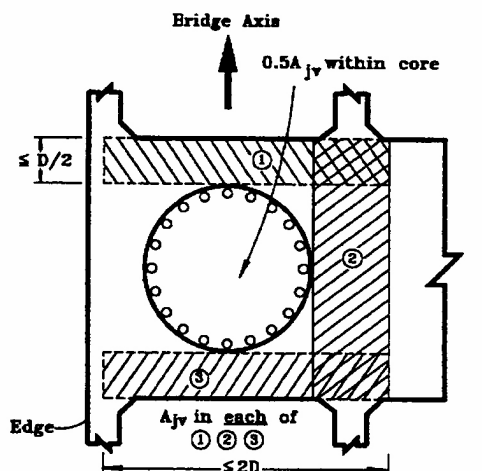
Special care is needed for knee joints as represented by Figure C8.8.4.3-2(b). For moment tending to close the joint, force transfer must be provided between the top cap beam reinforcement and the column outer reinforcement. When the cap beam does not extend significantly past the column, this is best effected by making the cap beam top and bottom reinforcement into a continuous loop outside the column cage, as shown in Figure C8.8.4.3-1.

If a cap-beam cantilever is provided, with cap-beam reinforcement passing beyond the joint, additional vertical shear reinforcement outside the joint, as for Figure C8.8.4.3-2, will be required.

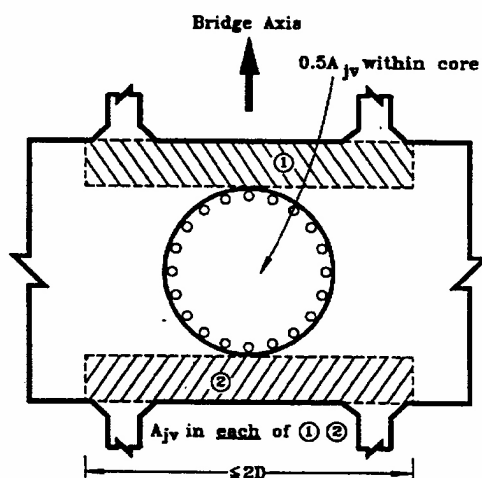
Moment-resisting connections designed according to these requirements have performed well in experiments (Seible et al., 1994; Sritharan and Priestley, 1994a; Sritharan and Priestley, 1994b).



(a) Internal Column: Multicolumn Bent



(b) Exterior Column: Multicolumn Bent



(c) Single Column Bent

Figure C8.8.4.3-2 Locations for Vertical Joint Reinforcement

This reinforcement may be omitted in prestressed or partially prestressed cap beams if the prestressed design force is increased by the amount needed to provide an equivalent increase in cap-beam moment capacity to that provided by this reinforcement.

#### C8.8.4.3.4 Hoop or Spiral Reinforcement

The hoop or spiral reinforcement of Equation 8.8.4.3-1 is required to provide adequate confinement of the joint, and to resist the net outward thrust of struts D1 and D2 in Figure C8.8.4.3-1.

#### C8.8.4.4 Structural Strength of Footings

Under extreme seismic loading, it is common for the footing to be subjected to positive moments on one side of the column and negative moments on the other. In this case, shear lag considerations show that it is unrealistic to expect footing reinforcement at lateral distances greater than the footing effective depth to participate effectively in footing flexural strength. Tests on footings (Xiao et al., 1994) have shown that a footing effective width complying with this clause will produce a good prediction of maximum footing reinforcement stress. If a larger effective width is adopted in design, shear lag effects will result in large inelastic strains developing in the footing reinforcement adjacent to the column. This may reduce the shear strength of the footing and jeopardize the footing joint force transfer mechanisms. Since the reinforcement outside the effective width is considered ineffective for flexural resistance, it is permissible to reduce the reinforcement ratio in such regions to 50% of that within the effective width unless more reinforcement is required to transfer pile reactions to the effective sections.

Arguments similar to those for moment apply to the effective width for shear strength estimation.

### C8.8.5 Concrete Piles

#### C8.8.5.1 Transverse Reinforcement Requirements

Note the special requirements for pile bents given in Article 8.8.2.

**C8.8.5.2 Volumetric Ratio of Transverse Reinforcement**

No commentary is provided for Article 8.8.5.2.

**C8.8.5.3 Cast-in-Place and Precast Concrete Piles**

No commentary is provided for Article 8.8.5.3.

**C8.8.6 Plastic Rotation Capacities**

A moment-curvature analysis based on strain compatibility and nonlinear stress-strain relations can be used to determine plastic limit states. From this a rational analysis is used to establish the rotational capacity of plastic hinges.

**C8.8.6.1 Life Safety Performance**

If a section has been detailed in accordance with the transverse reinforcement requirement of these provisions, then the section is said to be 'capacity protected' against undesirable modes of failure such as shear, buckling of longitudinal bars, and concrete crushing due to lack of confinement. The one remaining failure mode is low-cycle fatigue of the longitudinal reinforcement. The fatigue life depends on the fatigue capacity (Chang and Mander, 1994a) versus demand (Chang and Mander, 1994b).

This rotational capacity ensures a dependable fatigue-life for all columns, regardless of the period-dependent cyclic demand.

**C8.8.6.2 Operational Performance**

No commentary is provided for Article 8.8.6.2.

**C8.8.6.3 In-Ground Hinges**

In-ground hinges are necessary for certain types of bridge substructures. These may include, but are not restricted to:

- Pile bents
- Pile foundations with strong pier walls
- Drilled shafts
- Piled foundations with oversized columns.

It is necessary to restrict these plastic hinge rotations in order to limit the crack width and plastic strains, so as to avoid long-term corrosion problems after an earthquake has occurred. This limit is expected to reduce plastic strains to less than 40% of their above-ground counterpart (with  $\theta_p = 0.035$  rad.) This is because the plastic hinge length of in-ground hinges is typically two pile diameters due to the reduced moment gradient in the soil.

**C8.9 BEARING DESIGN REQUIREMENTS**

One of the significant issues that arose during the development of these recommended *Guidelines* was the critical importance of bearings as part of the overall bridge load path. The 1995 Kobe earthquake, and others that preceded it or have occurred since, clearly showed poor performance of some recent bearing types and the disastrous consequences that a bearing failure can have on the overall performance of a bridge. A consensus was developed that some testing of bearings would be desirable provided a designer had the option of providing restraints or permitting the bearing to fail if an adequate surface for subsequent movement is provided. An example occurred in Kobe where a bearing failed. The steel diaphragm and steel girder were subsequently damaged because the girder became jammed on the failed bearing and could not move.

There have been a number of studies performed when girders slide either on specially designed bearings or concrete surfaces. A good summary of the range of the results that can be anticipated from these types of analyses can be found in Dicleli and Bruneau (1995).

**C8.9.1 Prototype and Quality Control Tests**

The types of tests that are required by these *Guidelines* are similar to but significantly less extensive than those required for seismically isolated bridges. Each manufacturer is required to conduct a prototype qualification test to qualify a particular bearing type and size for its design forces or displacements. This series of tests only needs to be performed once to qualify the bearing type and size, whereas for seismically isolated bridges, prototype tests are required on every project. The quality control tests required on 1 out of every 10 bearings is the same as that required for every isolator on seismic isolation bridge projects. The cost of the much more extensive prototype and quality

control testing of isolation bearings is approximately 10 to 15% of the total bearing cost, which is of the order of 2% of the total bridge cost. The testing proposed herein is much less stringent than that required for isolation bearings and is expected to be less than 0.1% of the total bridge cost. However, the benefits of testing are considered to be significant since owners would have a much higher degree of confidence that each new bearing will perform as designed during an earthquake. The testing capability exists to do these tests on full size bearings.

### **C8.10 SEISMIC ISOLATION DESIGN REQUIREMENTS**

The commentary on this subject is given in C15 which will become a new section in the AASHTO LRFD specifications.

### **C8.11 SUPERSTRUCTURE DESIGN REQUIREMENTS**

#### **C8.11.1 General**

Capacity-protection or elastic design of the superstructure is required to reduce the possibility of earthquake-induced damage in the superstructure. It is generally felt that such damage is not easily repairable and may jeopardize the vertical-load-carrying capability of the superstructure.

The elastic forces from the MCE event may be used in lieu of capacity-protecting the superstructure, because their use will typically satisfy the performance objective for the design level ground motion.

When the superstructure can effectively span transversely between abutments as a diaphragm, then the resistance of the intermediate piers may not contribute significantly to the lateral resistance. In such cases, the elastic forces for the design earthquake should be used for the design of the superstructure lateral capacity. However, when designed in this manner, the superstructure could be vulnerable in earthquakes that produce shaking at the site that is larger than the design ground motion. If the maximum resistances of the abutments are defined, then they may be used to define the maximum forces in the superstructure, as an alternative to the use of the elastic seismic forces.

#### **C8.11.2 Load Paths**

The path of resistance for the seismic loads should be clearly defined, and the mechanisms for resistance engineered to accommodate the expected forces. In general, the seismic forces in the superstructure should be those corresponding to a plastic mechanism (yielding elements at their respective overstrength conditions) or the elastic demand analysis forces. The load path in the superstructure should be designed to accommodate these forces elastically.

Where nonseismic constraints preclude the use of certain connection elements, alternative positive connections should be made. For instance, non-composite action is often used in the negative moment regions of continuous steel plate girders. Consequently, studs are not present to transfer inertial loads from the deck to the diaphragm. In such cases, the girder pad portion of the deck slab could be extended beside the girder flange to provide a bearing surface.

Longitudinal forces may only be transferred to the abutment by a continuous superstructure. If a series of simple spans are used the seismic loads must be resisted at each substructure location.

#### **C8.11.3 Effective Superstructure Width**

In the case of longitudinal seismic force resistance, the piers will receive loads at the connection points between the superstructure and substructure. For longitudinal loading the primary load path from the superstructure to the pier is along the girder or web lines. To transfer these forces effectively to the substructure, connections to the piers should be made close to the girder or web lines. This requires that the cap beam of the pier in a single- or multi-column bent should be capable of resisting the effects of these forces, including shears, moments, and torsion.

In the case of longitudinal moment (moment about the superstructure transverse axis) transferred between super- and substructure, significant torsion may develop in the cap beam of the pier. The designer may choose to resist the longitudinal moment directly at the column locations and avoid these torsions. However, in a zone adjacent to the column, the longitudinal moment in the superstructure must then be transferred over an effective superstructure width, which accounts for the concentration of forces at the column location. The provisions specifying the effective width are based on Caltrans' *Seismic Design Criteria* (1999). On

the other hand, if the cap beam is designed for the longitudinal moments applied at the girder lines, no effective width reduction of the superstructure is required.

#### **C8.11.4 Superstructure-To-Substructure Connections**

In general the connections between the superstructure and substructure should be designed for the maximum forces that could be developed. In the spirit of capacity design, this implies that the forces corresponding to the full plastic mechanism (with yielding elements at their overstrength condition) should be used to design the connections. In cases where the full mechanism might not develop during the Maximum Considered Earthquake, it is still good practice to design the connections to resist the higher forces corresponding to the full plastic mechanism. It is also good practice to design for the best estimate of forces that might develop in cases such as pile bents with battered piles. In such bents the connections should be stronger than the expected forces, and these

forces may be large and may have large axial components. In such cases, the plastic mechanism may be governed by the piles' geotechnical strengths, rather than the piles' structural strengths.

Elements that fuse to capacity-protect attached elements should be treated similarly to elements that form a plastic hinge. The overstrength force from the fusing element may be used to design the adjacent elements and connections. Just as with plastic hinging, the designer should attempt to control the failure mechanism, as much as is possible. This implies that some modes of failure may be suppressed by adding strength, and others promoted by reducing strength. In general, the upper bound strength of the fuse should be about 75% of capacity of the elements being protected. For instance, strength of a fusible shear key at a pile-supported abutment might be sized to be 75% of the lateral strength of the pile group. The connections of adjacent elements to the abutment would then be designed to provide at least this capacity.



## Section 15: Commentary

### SEISMIC ISOLATION

#### C15.1 SCOPE

Isolating structures from the damaging effects of earthquakes is not a new idea. The first patents for base isolation schemes were obtained in the 1870s, but until the 1970s, few structures were built using these ideas. Early concerns were focused on the displacements at the isolation interface. These have been largely overcome with the successful development of mechanical energy dissipators. When used in combination with a flexible device such as an elastomeric bearing, an energy dissipator can control the response of an isolated structure by limiting both the displacements and the forces. Interest in seismic isolation, as an effective means of protecting bridges from earthquakes, was revived in the 1970s. To date there are several hundred bridges in New Zealand, Japan, Italy, and the United States using seismic isolation principles and technology for their seismic design.

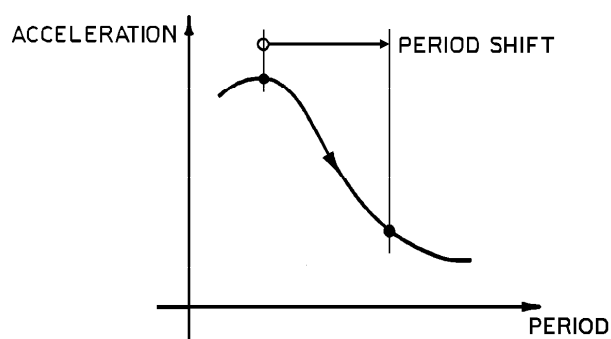
Seismically isolated buildings such as the University of Southern California Hospital in Los Angeles, and the West Japan Postal Savings Computer Center in Kobe, Japan, performed as expected in the 1994 Northridge and 1995 Kobe earthquakes, respectively. Records from these seismically isolated structures show good correlation between analytical prediction and recorded performance.

The basic intent of seismic isolation is to increase the fundamental period of vibration such that the structure is subjected to lower earthquake forces. However, the reduction in force is accompanied by an increase in displacement demand that must be accommodated within the isolation system. Furthermore, flexible bridges can be lively under service loads.

The three basic elements in seismic isolation systems that have been used to date are:

- a. a vertical-load-carrying device that provides lateral flexibility so that the period of vibration of the total system is lengthened sufficiently to reduce the force response,
- b. a damper or energy dissipator so that the relative deflections across the flexible mounting can be limited to a practical design level, and
- c. a means of providing rigidity under low (service) load levels, such as wind and braking forces.

*Flexibility* – Elastomeric and sliding bearings are two ways of introducing flexibility into a structure. The typical force response with increasing period (flexibility) is shown schematically in the typical acceleration response curve in Figure C15.1-1. Reductions in base shear occur as the period of vibration of the structure is lengthened. The extent to which these forces are reduced depends primarily on the nature of the earthquake ground motion and the period of the fixed-base structure. However, as noted above, the additional flexibility needed to lengthen the period of the structure will give rise to relative displacements across the flexible mount. Figure C15.1-2 shows a typical displacement response curve from which displacements are seen to increase with increasing period (flexibility).



ACCELERATION RESPONSE SPECTRUM

**Figure C15.1-1 Typical Acceleration Response Curve**

*Energy Dissipation* – Relative displacements can be controlled if additional damping is introduced into the structure at the isolation level. This is shown schematically in Figure C15.1-3.

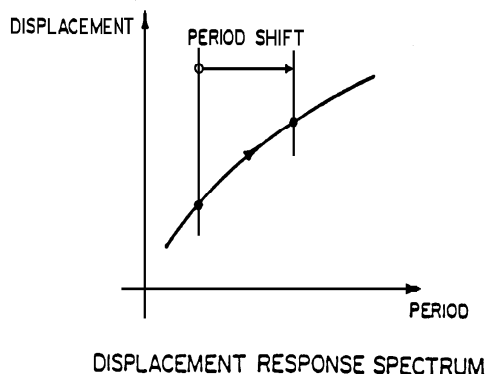


**Figure C15.1-2 Typical Displacement Response Curve**

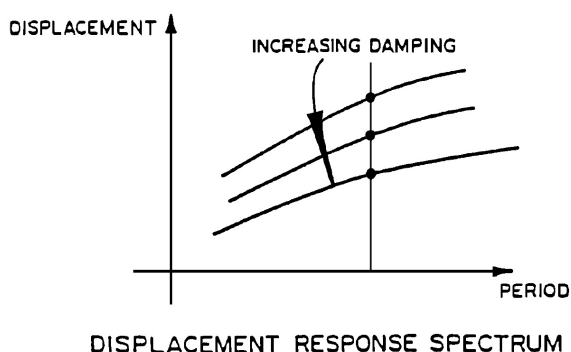
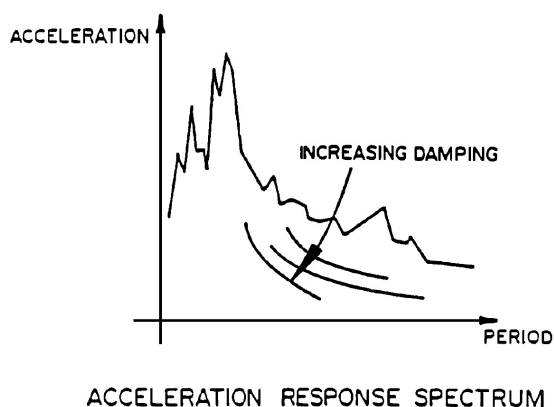
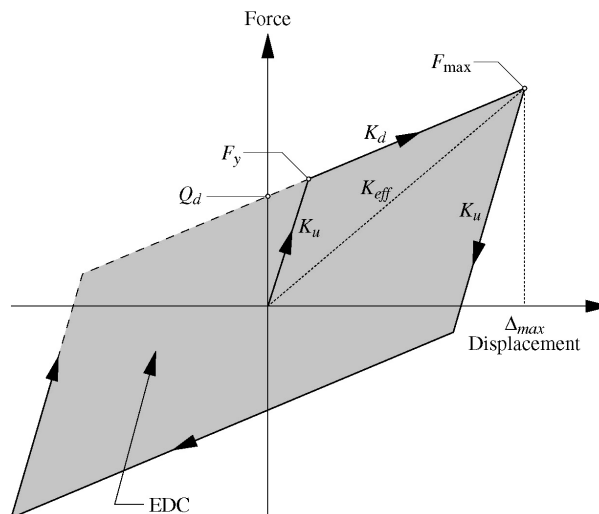


**Figure C15.1-3 Response Curves for Increasing Damping**

Two effective means of providing damping are hysteretic energy dissipation and viscous energy dissipation. The term *viscous* refers to energy dissipation that is dependent on the magnitude of the velocity. The term *hysteretic* refers to the offset between the loading and unloading curves under cyclic loading. Figure C15.1-4 shows an ideal-

ized force-displacement hysteresis loop where the enclosed area is a measure of the energy dissipated during one cycle (EDC) of motion.



- $Q_d$  = Characteristic strength
- $F_y$  = Yield force
- $F_{max}$  = Maximum force
- $K_d$  = Post-elastic stiffness
- $K_u$  = Elastic (unloading) stiffness
- $K_{eff}$  = Effective stiffness
- $\Delta_{max}$  = Maximum bearing displacement
- EDC = Energy dissipated per cycle = Area of hysteresis loop (shaded)

**Figure C15.1-4 Characteristics of Bilinear Isolation Bearings**

*Rigidity Under Low Lateral Loads* – While lateral flexibility is desirable for high seismic loads, it is clearly undesirable to have a bridge that will vibrate perceptibly under frequently occurring loads, such as wind or braking. External energy dissipators and modified elastomers may be used to provide rigidity at these service loads by virtue of their high initial elastic stiffness ( $K_u$  in Figure C15.1-4). As an alternative, friction in sliding isolation bearings may be used to provide the required rigidity.

*Example* – The principles for seismic isolation are illustrated by Figure C15.1-5. The dashed line is the elastic ground response spectrum as specified in Article 3.4.1. The solid line represents the composite response spectrum for an isolated bridge. The period shift provided by the flexibility of the isolation system reduces the spectral acceleration from  $A_1$  to  $A_2$ . The increased damping provided by the isolation system further reduces the spectral



acceleration from  $A_2$  to  $A_3$ . Note that spectral acceleration  $A_1$  and  $A_3$  are used to determine forces for the design of conventional and isolated bridges, respectively.

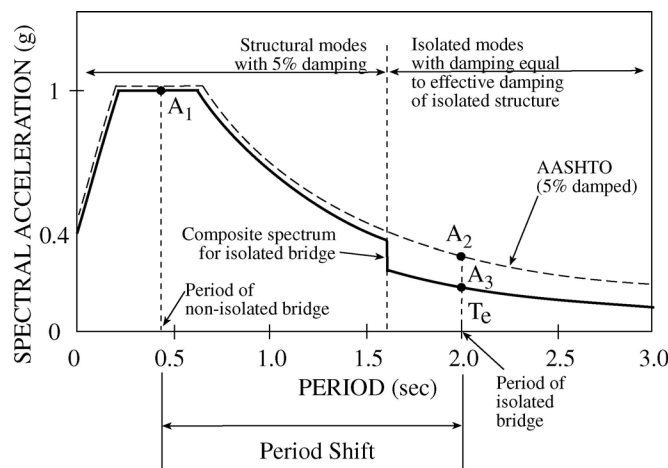


**Figure C15.1-5 Response Spectrum for Isolated Bridge**

## C15.2 DEFINITIONS

### Isolation System

The isolation system does not include the substructure and deck.

### Offset Displacement

The offset displacement is used for prototype testing and designing the isolator units.

## C15.3 NOTATION

$A_r$  is defined as the overlap area between the top-bonded and bottom-bonded elastomer areas of a displaced bearing, as shown in Figure C15.3-1.

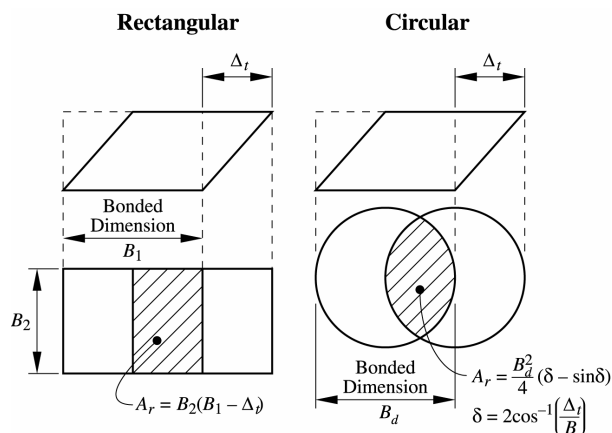


**Figure C15.3-1 Definition at Overlap Area**

$\bar{k}$  = Material constant related to hardness. (Refer to Roeder, Stanton, and Taylor 1987 for values.)

$LL_s$ , the seismic live load, shall be determined by the engineer as a percentage of the total live load considered applicable for the design.

## C15.4 ANALYSIS PROCEDURES

The basic premise for the analysis (consistent with those for buildings and hospitals) is twofold. First, the energy dissipation of the isolation system can be expressed in terms of equivalent viscous damping; and second, the stiffness of the isolation system can be expressed as an effective linear stiffness. These two basic assumptions permit both the single and multimodal methods of analysis to be used for seismic isolation design.

The force-deflection characteristics of a bilinear isolation system (Figure C15.1-4) are controlled by several variables, some of which are influenced by environmental and temperature effects. The key variables, however, are  $K_d$ , the stiffness of the second slope of the bilinear curve, and  $Q_d$ , the characteristic strength. The area of the hysteresis loop, EDC, and hence the damping coefficient, are affected primarily by  $Q_d$ . The effective stiffness  $K_{eff}$  is influenced by  $Q_d$  and  $K_d$ .

The two important design variables of an isolation system are  $K_{eff}$  and  $B$ , the damping coefficient, since they affect the period (Equation 15.4.1-4), the displacement (Equation 15.4.1-3), and the base shear forces (Equation 15.4.1-2). Since  $K_{eff}$  and the damping coefficient  $B$  are affected differently by  $K_d$  and  $Q_d$ , the impact of variations in  $K_d$  and  $Q_d$  on the key design variables, needs to be assessed (Figure C15.4-1). Article 15.5 provides a method to determine  $\lambda_{min}$  and  $\lambda_{max}$  values for both  $K_d$  and  $Q_d$ .

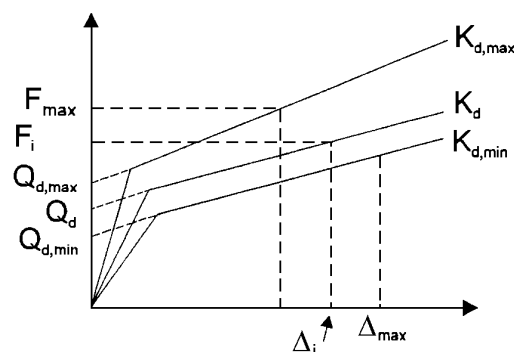


**Figure C15.4-1 Impact Variations on Key Design Variables**

The design forces on the columns and abutments generally will be at their maximum value when both  $K_d$  and  $Q_d$  are their maximum values. Therefore, an analysis is required using  $Q_{d,max}$  and  $K_{d,max}$  to determine the maximum forces that will occur on the substructures. The design displacements will be at their maximum value when both  $Q_d$  and  $K_d$  are at their minimum values. Therefore, an analysis is required using  $Q_{d,min}$  and  $K_{d,min}$  to determine the maximum displacements that will occur across the isolator units.

Using the design properties of the isolator units,  $Q_d$  and  $K_d$  (Figures C15.1-4 and C15.4-1), the design forces  $F_i$ , where  $F_i = K_{eff} \times \Delta$ , and displacements  $\Delta$  are first calculated with Equations 15.4.1-1, 15.4.1-2, and 15.4.1-3. The design properties  $K_d$  and  $Q_d$  are then multiplied by  $\lambda_{max,K_d}$ ,  $\lambda_{min,K_d}$ ,  $\lambda_{max,Q_d}$ , and  $\lambda_{min,Q_d}$  as prescribed in Article 15.5.1 to obtain upper- and lower-bound values of  $K_d$  and  $Q_d$ . The analyses are then repeated using the upper-bound values,  $K_{d,max}$  and  $Q_{d,max}$  to determine  $F_{max}$ , and the lower-bound values  $K_{d,min}$  and  $Q_{d,min}$  to determine  $\Delta_{max}$ . These upper- and lower-bound values account for all anticipated variations in the design properties of the isolation system resulting from temperature, aging, scragging, velocity, wear or travel, and contamination. The exception is that only one analysis is required using the design properties, provided that the maximum and minimum values of the forces and displacements are within  $\pm 15\%$  of the design values.

The  $\lambda_{max}$  and  $\lambda_{min}$  factors for each of the six variables are to be determined by the system characterization tests prescribed in Article 15.10.1, or the default values given in Appendix I.

The prototype tests of Article 15.10.2 are required to validate the design properties of the isolation system. Prototype tests do not include any of the variables from the characterization tests that affect the design properties of the isolation system, because they are incorporated in the design process through the use of system property modification factors.

In order to provide guidance on some of the available systems, potential variations in the key parameters are as follows:

- *Lead-Rubber Isolator Unit* – The value of  $Q_d$  is influenced primarily by the lead core. In cold temperatures, however, natural rubber will cause the most significant increase in  $Q_d$ . The value of  $K_d$  depends on the properties of the rubber. Rubber properties are affected by

aging, frequency of testing, strain, and temperature.

- *High-Damping Rubber Isolator Unit* – The value of  $Q_d$  is a function of the additives to the rubber. The value of  $K_d$  is also a function of the additives to the rubber. High-damping rubber properties are affected by aging, frequency of testing, strain, temperature, and scragging.
- *Friction Pendulum System®* – The value of  $Q_d$  is a function primarily of the dynamic coefficient of friction and axial load. The value of  $K_d$  is a function of the curvature of the sliding surface. The dynamic coefficient of friction is affected by aging, temperature, velocity of testing, contamination, and length of travel or wear.
- *Eradiquake®* – The value of  $Q_d$  is a function of the dynamic coefficient of the disc bearing and the preload friction force, when it is used. The value of  $K_d$  is a function of whatever springs are incorporated in the device. The dynamic coefficient of friction is affected by aging, temperature, velocity of testing, contamination, and length of travel or wear. The variations in spring properties depend on the materials used.
- *Viscous Damping Devices* – These can be used in conjunction with either elastomeric bearings or sliders. The value of  $Q_d$  is a function of both the viscous damper and the bearing element. The value of  $K_d$  is primarily a function of the bearing element.

#### C15.4.1 Capacity Spectrum Method

The capacity spectrum method of Article 4.4 and Article 5.4.1 is based on the same principles used in the original derivation of the simplified seismic isolation design approach. The only difference is the sequence in which it is applied. For non-isolated bridges, it is recommended that a designer sum the strength of the columns to obtain  $C_c$  and then determine if the displacement capacity of the columns is adequate using Equation 5.4.1-1. If not, the columns must be strengthened. In an isolation design the bridge achieves its single degree of freedom response characteristics by virtue of using flexible isolation bearings rather than having columns of similar stiffness characteristics. The design procedure uses the stiffness characteristics of the isolation bearings, sized to resist the

non-seismic loads, to determine the design displacement (Equation 15.4.1-3). The lateral force that the substructure must resist is then calculated using Equation 15.4.1-2 where  $K_{eff}$  is the sum of the effective linear stiffnesses of all bearings and substructures supporting the superstructure; and  $C_d$  is the lateral force demand coefficient. The derivation of the isolation design equations follows.

For the design of conventional bridges, the form of the elastic seismic demand coefficient in the longer period segment of the spectra is

$$C_d = \frac{F_v S_1}{T}$$

For seismic isolation design, the elastic seismic demand coefficient is directly related to the elastic ground-response spectra and damping of the isolation system.

$$C_d = \frac{F_v S_1}{T_{eff} B}$$

where  $B$  is the damping coefficient given in Table 15.4.1-1. For 5% damping,  $B = 1.0$ .

The quantity  $C_d$  is a dimensionless design coefficient, which when multiplied by  $g$  produces the spectral acceleration. This spectral acceleration ( $S_A$ ) is related to the spectral displacement ( $S_D$ ) by the relationship

$$S_A = \omega^2 S_D$$

where  $\omega$  is the circular natural frequency and is given by  $2\pi/T_{eff}$ . Therefore, since  $S_A = C_d \cdot g$

$$S_A = \frac{F_v S_1}{T_{eff} B} g$$

and

$$\begin{aligned} S_D &= \frac{1}{\omega^2} \frac{F_v S_1}{T_{eff} B} g \\ &= \frac{T_{eff}^2 F_v S_1}{(2\pi)^2 T_{eff} B} (9.81) \frac{\text{m}}{\text{sec}^2}; \frac{T_{eff}^2 F_v S_1}{(2\pi)^2 T_{eff} B} (386.4) \frac{\text{inches}}{\text{sec}^2} \\ &= \frac{0.249 F_v S_1 T_{eff}}{B} \text{m}; \frac{9.79 F_v S_1 T_{eff}}{B} \text{inches} \end{aligned}$$

Denoting  $S_D$  as  $\Delta$  (Article 15.4), which is the deck displacement relative to the ground, the above is approximated by

$$\Delta = \frac{0.25 F_v S_1 T_{eff}}{B} \text{m}; \frac{10 F_v S_1 T_{eff}}{B} \text{inches}$$

An alternative form for  $C_d$  is possible. The quantity  $C_d$  is defined by the relationship

$$F = C_d W$$

where  $F$  is the earthquake design force and  $W$  is the weight of the structure. Therefore,

$$C_d = \frac{F}{W} = \frac{K_{eff} \times \Delta}{W}$$

where  $K_{eff}$  is defined below. The equivalence of this form to the previous form is evident by observing that  $K_{eff} = \omega^2 W/g$ , from which

$$C_d = \frac{\omega^2 W}{g} \times \frac{\Delta}{W} = \frac{(2\pi)^2}{T_{eff}^2} \times \frac{1}{9.81} \times \frac{0.25 F_v S_1 T_{eff}}{B} = \frac{F_v S_1}{B T_{eff}}$$

$$C_d = \frac{\omega^2 W}{g} \times \frac{\Delta}{W} = \frac{(2\pi)^2}{T_{eff}^2} \times \frac{1}{386.4} \times \frac{9.79 F_v S_1 T_{eff}}{B}$$

In calculating the effective stiffness, the configuration, flexibility, and individual stiffnesses of the isolator units ( $k_{iso}$ ) (see Figure C15.4.1-1) and substructure ( $k_{sub}$ ) shall be taken into account:

$$K_{eff} = \sum_j \left( \frac{k_{sub} k_{iso}}{k_{sub} + k_{iso}} \right) = \sum_j K_{eff,j}$$

where the sum  $\Sigma$  extends over all substructures.

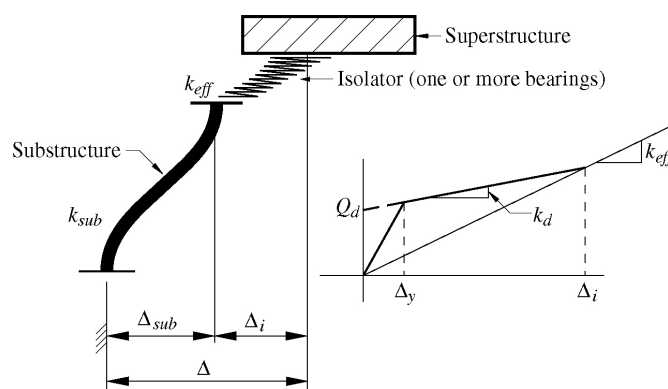


**Figure C15.4.1-1** Figure Shows Only One Isolator and One Substructure

The corresponding equivalent viscous damping may be calculated as follows:

$$\beta = \frac{\text{Energy Dissipated}}{2\pi K_{eff} \Delta^2} = \frac{\text{Total Dissipated Energy}}{2\pi \sum_j (K_{eff,j} \Delta^2)}$$

$$\beta = \frac{2Q_d(\Delta_i - \Delta_y)}{\pi(\Delta_i + \Delta_{sub})^2 K_{eff}} = \frac{2 \sum_j [Q_d(\Delta_i - \Delta_y)]}{\pi \sum_j [K_{eff,j}(\Delta_i + \Delta_{sub})^2]}$$

Hysteretic Energy Dissipated at Isolator =  $4Q_d(\Delta_i - \Delta_y)$

Note: These equations exclude contribution to damping from the substructure.

If damping is truly linear viscous, then the damping coefficient in Table 15.4.1-1 may be extended to 50% ( $B=2$ ).

If damping exceeds 30%, and a  $B$  of 1.7 is used, then a time-history analysis is not required.

Equations 15.4.1-1 and 15.4.1-2 are strictly applicable to hysteretic systems, that is, systems having no added damping of a truly viscous nature, such as viscous dampers.

For systems with added viscous damping, as in the case of elastomeric or sliding systems with viscous dampers, Equations 15.4.1-3a and 15.4.1-3b are valid, provided that the damping coefficient  $B$  is based on the energy dissipated by all elements of the isolation system, including the viscous dampers. Equivalent damping shall be determined by Equation 15.10.3-2. The seismic force shall be determined in three distinct stages as follows:

1. At the stage of maximum bearing displacement. The seismic force shall be determined by Equation 15.4.1-1. At this stage, the viscous damping forces are zero.
2. At the stage of maximum velocity and zero bearing displacement. The seismic force shall be determined as the combination of characteristic strength of the isolation bearings and the peak viscous damper force. The latter shall be determined at a velocity equal to  $2\pi d_d / T_{eff}$ , where  $d_d$  is the peak damper displacement. (Displacement  $d_d$  is related to bearing displacement  $\Delta_i$ ).
3. At the stage of maximum total inertia force (that is, the maximum superstructure acceleration), the seismic force shall be determined by:

$$F = (f_1 + 2\beta_d f_2) C_d W$$

where  $C_d$  is determined by Equation 15.4.1-2;  $K_{eff}$  is determined from the contribution of all elements of the isolation system other than viscous damp-

ers;  $\beta_d$  is the portion of the effective damping ratio of the isolated bridge contributed by the viscous dampers and

$$f_1 = \cos [\tan^{-1} (2\beta_d)]$$

$$f_2 = \sin [\tan^{-1} (2\beta_d)]$$

The modified equation provides an estimate of the maximum total inertia force on the bridge superstructure. The distribution of this force to elements of the substructure shall be based on bearing displacements equal to  $f_1 \Delta_i$ , and substructure displacements equal to  $f_1 \Delta_{sub}$ , and damper velocities equal to  $f_2 (2\pi d_d / T_{eff})$  where  $d_d$  is the peak damper displacement.

#### C15.4.2 Uniform Load Method

The uniform load method of analysis given in Article 5.4.2.2 is appropriate for seismic isolation design.

#### C15.4.3 Multimode Spectral Method

The guidelines given in Article 5.4.2.3 are appropriate for the response spectrum analysis of an isolated structure with the following modifications:

- a. The isolation bearings are modeled by use of their effective stiffness properties determined at the design displacement  $\Delta_i$  (when  $\Delta_{max}$  in Figure C15.1-4 is  $\Delta_i$ ).
- b. The ground response spectrum is modified to incorporate the effective damping of the isolated structure (Figure C15.1-5).

The response spectrum required for the analysis needs to be modified to incorporate the higher damping value of the isolation system. This modified portion of the response spectrum should only be used for the isolated modes of the bridge and will then have the form shown in Figure C15.1-5.

The effective damping of the structure system shall be used in the multimode spectral analysis method. Structure system damping shall include all structural elements and be obtained by rational methods as discussed in C15.4.1.

#### C15.4.4 Time-History Method

When a time-history analysis is required, the ground-motion time histories may be frequency-scaled so they closely match the appropriate ground-response spectra for the site.

A two-dimensional nonlinear analysis may be used on normal structures without skews or curves.

## **C15.5 DESIGN PROPERTIES OF THE ISOLATION SYSTEM**

### **C15.5.1 Nominal Design Properties**

For an explanation of the system property modification factors concept, see Constantinou et al. (1999).

### **C15.5.2 System Property Modification Factors**

#### **C15.5.2.1 Minimum and Maximum System Property Modification Factors**

All  $\lambda_{min}$  values are unity at this time. The Task Group that developed these provisions determined that available test data for  $\lambda_{min}$  values would produce forces and displacements that are within 15% of the design values. If the engineer believes a particular system may produce displacements outside of the  $\pm 15\%$  range, then a  $\lambda_{min}$  analysis should be performed.

#### **C15.5.2.2 System Property Adjustment Factors**

The opinion of the Task Group that developed these provisions is that only operational bridges need to consider all maximum  $\lambda$  factors at the same time. The reduction factor for other bridges is based on engineering judgment.

Example:

$$\lambda_{max,c} = 1.2 \text{ without adjustment factor}$$

$$\lambda_{max,c} = 1 + (1.2 - 1) 0.67 = 1.13 \text{ for adjustment factor of } 0.67$$

## **C15.6 CLEARANCES**

Adequate clearance shall be provided for the displacements resulting from the seismic isolation analysis in either of two orthogonal directions. As a design alternative in the longitudinal direction, a knock-off abutment detail (Figure C3.3.1-4) may be provided for the seismic displacements between the abutment and deck slab. Adequate clearance for the seismic displacement must be provided between the girders and the abutment. In addition, the design rotation capacity of the bearing shall exceed the maximum seismic rotation.

The purpose of the minimum clearance default value is to guard against analysis procedures that produce excessively low clearances.

Displacements in the isolators resulting from longitudinal forces, wind loads, centrifugal forces, and thermal effects will be a function of the force-deflection characteristics of the isolators. Adequate clearance at all expansion joints must be provided for these movements.

### **C15.7 DESIGN FORCES FOR SDAP A1 AND A2**

This section permits utilization of the real elastic force reduction provided by seismic isolation. It should be noted, however, that  $F_v S_I$  has a maximum value of 0.25 for SDAP A bridges and is specified to have a minimum value of 0.25 if seismic isolation is used.

### **C15.8 DESIGN FORCES FOR SDAP C, D, AND E**

No commentary is provided for Article 15.8

## **C15.9 OTHER REQUIREMENTS**

### **C15.9.1 Non-Seismic Lateral Forces**

Since a measure of flexibility is an essential part of an isolation system, it is also important that the isolation system provide sufficient rigidity to resist frequently occurring wind and service loads. The displacements resulting from non-seismic loads need to be checked.

#### **C15.9.1.1 Service Force Resistance**

No commentary is provided for Article 15.9.1.1.

#### **C15.9.1.2 Cold Weather Requirements**

Low temperatures increase the coefficient of friction on sliding systems and increase the shear modulus and characteristic strength of elastomeric systems. These changes increase the effective stiffness of the isolation system.

The test temperatures used to determine low-temperature performance in Article 15.10.1 represent 75% of the difference between the base temperature and the extreme temperature in Table 14.7.5.2-2 of the 1998 AASHTO LRFD Specifications.

### C15.9.2 Lateral Restoring Force

The basic premise of these seismic isolation design provisions is that the energy dissipation of the system can be expressed in terms of equivalent viscous damping and the stiffness by an effective linear stiffness. The requirement in Article 15.9.2 provides the basis upon which this criteria is founded.

The purpose for the lateral restoring force requirement is to prevent permanent cumulative displacements and to accommodate isolator installation imperfections, such as imperfect leveling.

The lateral restoring force requirements are applicable to systems with a restoring force that is dependent on displacement, that is, a spring-like restoring force. However, it is possible to provide constant restoring force that is independent of displacement. There are two known means for providing constant restoring force: (a) using compressible fluid springs with preload and (b) using sliding bearings with a conical surface. Figure C15.9.2-2 illustrates the typical force-displacement relation of these devices.

The requirement for lateral restoring force in these cases is that the combined constant lateral restoring force of the isolation system is at least equal to 1.05 times the combined characteristic strength of the isolation system under service conditions. For example, when constant restoring force devices are combined with frictional elements (e.g., sliding bearings), the restoring force must be at least equal to 1.05 times the static friction force. This requirement ensures that the restoring force is sufficiently large to overcome the characteristic strength and, thus, provide re-centering capability.

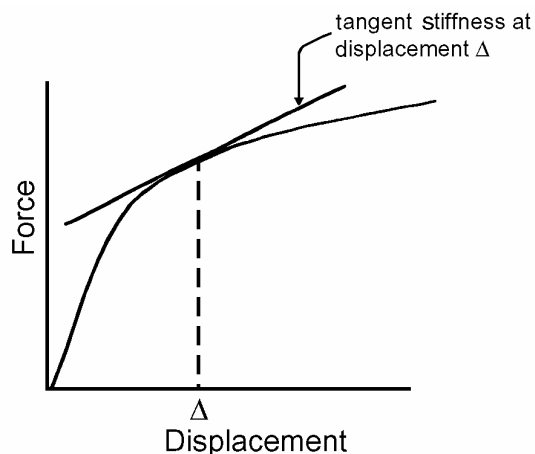


**Figure C15.9.2-1 Tangent Stiffness of Isolation System**

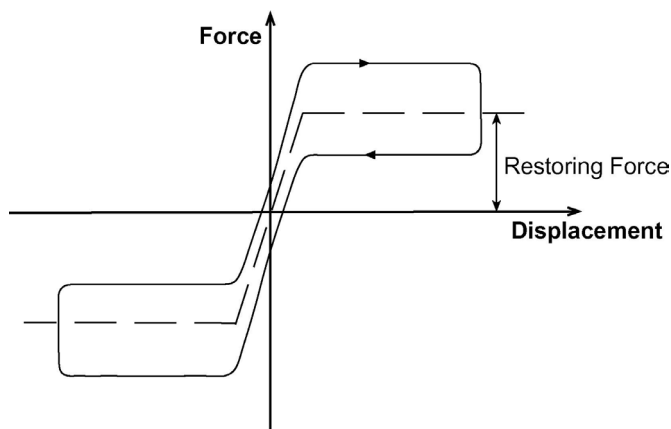


**Figure C15.9.2-2 Force-Displacement Relation of Systems with Constant Restoring Force**

### C15.9.3 Vertical Load Stability

This section provides minimum requirements for the design of the isolation system. The detailed design requirements of the system will be dependent on the type of system. The 1.2 factor accounts for vertical acceleration effects and uncertainty in the dead load.

### C15.9.4 Rotational Capacity

Larger construction rotations may be allowed, provided that they do not damage the isolator unit.

## C15.10 REQUIRED TESTS OF ISOLATION SYSTEMS

In general, the code requirements are predicated on the fact that the isolation system design is based on tested properties of isolator units. This section provides a comprehensive set of prototype tests to confirm the adequacy of the isolator properties used in the design. Systems that have been previously tested with this specific set of tests on similar type and size of isolator units do not need to have these tests repeated. Design properties must therefore be based on manufacturers' preapproved or certified test data. Extrapolation of design properties from tests of similar type and size of isolator units is permissible.

Isolator units used for the system characterization tests (except shaking table tests), prototype tests, and quality control tests shall have been manufactured by the same manufacturer with the same materials.

### C15.10.1 System Characterization Tests

These tests are usually not project-specific. They are conducted to establish the fundamental properties of individual isolator units as well as the behavior of an isolation system. They are normally conducted when a new isolation system or isolator unit is being developed or a substantially different version of an existing isolation system or isolator unit is being evaluated.

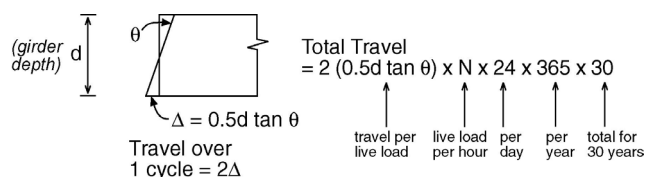
Several guidelines for these tests have been developed. The NIST (1996) Guidelines are currently being developed into the ASCE (1996) Standard for Testing Seismic Isolation Systems, Units, and Components. This new standard currently exists in draft form. Testing guidelines (ASCE CERF, 1996) have also been developed and used for the HITEC evaluation of seismic isolation and energy dissipation devices.

#### C15.10.1.1 Low-Temperature Test

The test temperatures represent 75% of the difference between the base temperature and the extreme temperature in Table 14.7.5.2-2 of the 1998 AASHTO LRFD Specifications. Prior to testing, the core temperature of the isolator unit shall reach the specified temperature.

#### C15.10.1.2 Wear and Fatigue Tests

The movement that is expected from live load rotations is dependent on structure type, span length and configuration, girder depth, and average daily traffic. The total movement resulting from live load rotations can be calculated as follows:



### C15.10.2 Prototype Tests

**Test 1, Thermal** – This test verifies the lateral force exerted by the isolation system at maximum thermal displacement.

**Test 2, Wind and Braking** – This test verifies the resistance of the isolation system under service load conditions.

**Test 3, Seismic** – This test verifies the dynamic response of the isolation system for various displacements.

The sequence of fully reversed cycles is important in developing hysteresis loops at varying displacements. By starting with a multiple of 1.0 times the total design displacement, the performance of the unscragged and scragged bearing may be directly compared.

**Test 4, Seismic** – This verifies the survivability of the isolator after a major earthquake. The test is started from a displaced position to reflect the uncertainty of the starting position when an earthquake occurs. The seismic displacements shall be superimposed on the offset load displacement so that the peak displacements will be asymmetric.

**Test 5, Wind and Braking** – This test verifies service load performance after a seismic event.

**Test 6, Seismic Performance Verification** – The seismic performance verification test verifies the performance of the bearing after the sequence of tests has been completed.

**Test 7, Stability Verification** – Stability is demonstrated if the isolator shows a positive incremental force carrying capacity satisfying the requirements of Article 15.4.

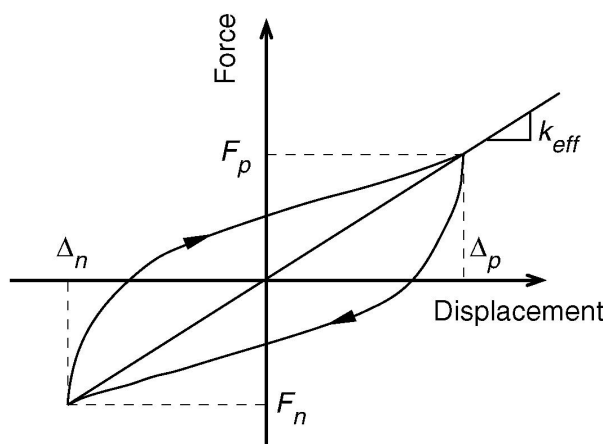
An isolation system needs a positive incremental force-carrying capability to satisfy the requirements of Article 15.9.2 (see Figure C15.10.2-1). The purpose of this requirement is to ensure that the hysteretic elements of the system are stable. A viscous damper will have a negative incremental force-carrying capacity toward the point of maximum displacement. Since this is acceptable performance, it needs to be deleted from the other components prior to their stability evaluation.

### C15.10.3 Determination of System Characteristics

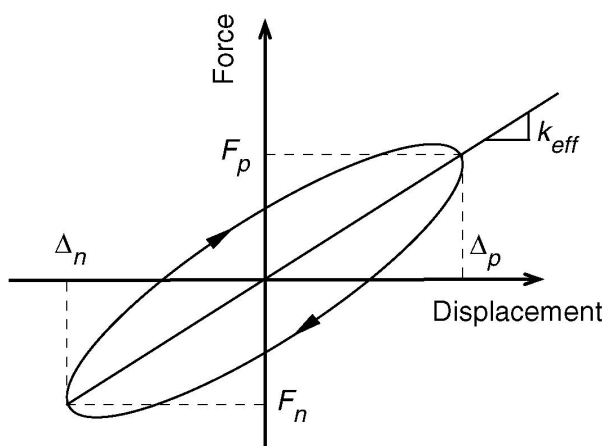
#### C15.10.3.1 System Adequacy

For Test 4, if the change in effective stiffness is greater than 20%, the minimum effective stiffness value should be used to calculate the system displacements, and the maximum effective stiffness values should be used to calculate the structure forces and isolation system forces.

A decrease in stiffness during cyclic testing may occur in some systems and is considered acceptable if the degradation is recoverable within a time frame acceptable to the engineer. That is, the



Hysteretic behavior



Viscoelastic behavior

**Figure C15.10.2-1 Definition of Effective Stiffness**

bearing will return to its original stiffness after a waiting period.

For Test 4, a decrease in energy dissipated per cycle (EDC) during cyclic testing may occur in some systems and is considered acceptable if the degradation is recoverable within a time frame acceptable to the engineer.

At the conclusion of testing, the test specimens shall be externally inspected or, if applicable, disassembled and inspected for the following faults, which shall be cause for rejection:

1. Lack of rubber-to-steel bond.
2. Laminate placement fault.

3. Surface cracks on rubber that are wider or deeper than 2/3 of the rubber cover thickness.
4. Material peeling.
5. Lack of polytetrafluoroethylene (PTFE)-to-metal bond.
6. Scoring of stainless steel plate.
7. Permanent deformation.
8. Leakage.

### C15.11 ELASTOMERIC BEARINGS

Elastomeric bearings used for seismic isolation will be subjected to earthquake-induced displacements ( $\Delta_i$ ) and must therefore be designed to carry safely the vertical loads at these displacements. Since earthquakes are infrequently occurring events, the factors of safety required under these circumstances will be different from those required for more frequently occurring loads.

Since the primary design parameter for earthquake loading is the displacement ( $\Delta_i$ ) of the bearing, the design procedures must be capable of incorporating this displacement in a logical, consistent manner. The requirements of Article 14.7.5.3 of the 1998 AASHTO LRFD Specifications limit vertical loads by the use of a limiting compressive stress, and therefore do not have a mechanism for including the simultaneous effects of seismic displacements. The shear displacement is also limited to half of the elastomer thickness. The British Specifications BE 1/76 (Department of Environment, 1976) and BS 5400 (BSI, 1983) recognize that shear strains are induced in reinforced bearings by compression, rotation, and shear deformations. In BE 1/76, the sum of these shear strains is limited to a proportion of the elongation-at-break of the rubber. The proportion (1/2 or 1/3 for service load combinations and 3/4 for seismic load combinations) is a function of the loading type. In BS 5400 and the 1995 draft Eurocode EN 1337 (CEN, 1995), the limit is a constant 5.0.

Since the approach used in BE 1/76 and BS 5400 incorporates shear deformation as part of the design criteria, it can be readily modified for seismic isolation bearings. The design requirements given are based on the appropriate modifications to BE 1/76 and BS 5400.

In the extensive testing conducted for NCHRP Report No. 298 (Roeder, Stanton, and Taylor 1987), no correlation was found between the elongation-at-break and the ability of the elastomers to



resist shearing strain without debonding from the steel reinforcement. Furthermore, the French code UIC772R and the BS 5400 also imply no dependence on  $\epsilon_u$ , but rather use a single limit of 5.0 for the sum of the strains, regardless of the elastomer type.

#### **C15.11.1 General**

No commentary is provided for Article 15.11.1.

#### **C15.11.2 Shear Strain Components for Isolation Design**

The allowable vertical load on an elastomeric bearing is not specified explicitly. The limits on vertical load are governed indirectly by limitations on the equivalent shear strain in the rubber due to different load combinations and to stability requirements.

The effects of creep of the elastomer shall be added to the instantaneous compressive deflection, when considering long-term deflections. They are not to be included in the calculation of Article 15.11.3. Long-term deflections shall be computed from information relevant to the elastomer compound used, if it is available. If not, the values given in Article 14.7.5.3.3 of the 1998 AASHTO LRFD Specifications govern.

For incompressible isotropic material  $E = 3G$ . However, this is not true for rubber. For rubber,  $E = (3.8 \text{ to } 4.4)G$  depending on its hardness, which indicates anisotropy in rubber. Accordingly, Equation 15.11.2-1 is based on Equation 8 of the 1991 AASHTO Guide Specifications with  $E$  replaced by  $4G$ . The quantity  $4G(1 + 2\bar{k}S^2)$  is the compression modulus of the bearing, as calculated on the assumption of incompressible rubber. For bearings with large shape factors, the assumption of incompressible rubber leads to significant overestimation of the compression modulus and, thus, underestimation of the shear strain due to compression. Equation 15.11.2-2 is introduced to account for the effects of rubber compressibility. It is based on the empirical relation that the compression modulus is given by  $[1/(8G\bar{k}S^2) + 1/K]^{-1}$ .

The shear modulus  $G$  shall be determined from the secant modulus between 25% and 75% shear strain in accordance with ASTM D 4014, published by the American Society of Testing and Materials.

The design rotation is the maximum rotation of the top surface of the bearing relative to the bot-

tom surface. Any negative rotation due to camber will counteract the DL and LL rotation and should be included in the calculation.

#### **C15.11.3 Load Combinations**

Tests for NCHRP at the University of Washington, Seattle, have shown that static rotation is significantly less damaging than dynamic rotation.

#### **C15.12 ELASTOMERIC BEARINGS-CONSTRUCTION**

No commentary is provided for Article 15.12.

#### **C15.13 SLIDING BEARINGS – DESIGN**

##### **C15.13.1 General**

The sliding bearing is typically made from two dissimilar materials that slide against each other. Low friction is achieved when a softer material, usually PTFE and herein called the bearing liner, slides against a hard, smooth surface that is usually stainless steel and is herein called the mating surface. Lubrication may be used.

The restoring force may be provided either by gravity acting through a curved sliding surface or by a separate device such as a spring.

##### **C15.13.2 Materials**

Certain combinations of materials have been found to promote severe corrosion and are strongly discouraged (British Standards Institution 1979; 1983). Examples are

- structural steel and brass,
- structural steel and bronze,
- structural steel and copper,
- structural steel and aluminum, and
- chromium on structural steel (chrome plating of steel).

Chrome is porous, so structural steel is exposed to oxygen.

Other combinations of materials known to promote additional but not severe corrosion are

- stainless steel and brass,
- stainless steel and bronze, and
- stainless steel and copper.

**C15.13.2.1 PTFE Bearing Liners**

No commentary is provided for Article 15.13.2.1.

**C15.13.2.2 Other Bearing Liner Materials**

No commentary is provided for Article 15.13.2.2.

**C15.13.2.3 Mating Surface**

Higher grades of stainless steel such as type 316, conforming to ASTM A 240, should be considered for applications in severe corrosive environments.

Measurements of surface roughness need to be reported together with information on profilometer stylus tip radius, traversing length and instrument cutoff length. It is recommended that the stylus tip radius not be more than 200 micro inches (5 micro meters) and the cutoff length be 0.03 inches (0.8 mm).

**C15.13.3 Geometry**

No commentary is provided for Article 15.13.3.

**C15.13.4 Loads and Stresses****C15.13.4.1 Contact Pressure**

In Table 15.13.4.1-1, Allowable Average Contact Stresses for PTFE, the rotation-induced edge stresses must be calculated by a rational method that accounts for the rotational stiffness and rotational demand of the bearing.

**C15.13.4.2 Coefficient of Friction****C15.13.4.2.1 Service Coefficient of Friction**

Table 15.13.4.2.1-1, Service Coefficients of Friction, contains service coefficients of friction for various types of PTFE determined at a test speed of 2.5 inches/min (63.5 mm/min) on a mirror finish (no. 8) stainless steel mating surface with scaled samples (Stanton, Roeder, and Campbell 1993).

**C15.13.4.2.2 Seismic Coefficient of Friction**

Typically the maximum seismic coefficient of friction for PTFE based material is reached at a testing velocity of 2 to 8 inches/sec (50 to 200 mm/sec).

**C15.13.5 Other Details**

No commentary is provided for Article 15.13.5.

**C15.13.6 Materials for Guides**

No commentary is provided for Article 15.13.6.

**C15.14 SLIDING BEARINGS – CONSTRUCTION**

No commentary is provided for Article 15.14.

**C15.15 OTHER ISOLATION SYSTEMS****C15.15.1 Scope**

Article 15.15 is intended to cover new isolation systems that are not addressed in the preceding Articles 15.11 to 15.14.

**C15.15.2 System Characterization Tests**

The purpose of these tests is to demonstrate that the principles on which the system is intended to function are realized in practice. The number and details of tests must be approved by the engineer.

**C15.15.3 Design Procedure**

No commentary is provided for Article 15.15.3.

**C15.15.4 Fabrication, Installation, Inspection, and Maintenance Requirements**

The maintenance requirements must be known at the time of submission of the design procedure in order that the engineer may assess their impact on the reliability and life-cycle costs of the system.

#### **C15.15.5 Prototype Tests**

The purpose of the prototype testing is to verify that the as-built bearing system satisfies the design requirements for the particular size and configuration used in the job in question.

#### **C15.15.6 Quality Control Tests**

No commentary is provided for Article 15.15.6.



## Appendix A

# COMMENTARY ON THE SELECTION OF THE DESIGN EARTHQUAKES

### A.1 INTRODUCTION

This appendix describes the design earthquakes and associated ground motions that have been adopted for the proposed revisions to the AASHTO LRFD Bridge Seismic Design Specifications.

For applicability to most bridges, the objective in selecting design earthquakes and developing the design provisions of the specifications is to (1) preserve life safety and prevent bridge collapse during rare earthquakes and (2) provide immediate (except for inspections) post-earthquake serviceability of bridges with minimal damage during expected earthquakes. For applicability to certain bridges of special importance as determined by the bridge owner, performance objectives may be higher than stated above.

This appendix is organized as follows: Section A.2 provides a brief description of the design earthquake ground motion map in the current AASHTO LRFD Provisions. Sections A.3 and A.4 describe earthquake ground motion maps that are proposed for these revised LRFD Specifications. Section A.5 describes the proposed design earthquakes and associated ground motions utilizing the new USGS ground motion maps. Finally, Section A.6 introduces and briefly summarizes the results of studies conducted to evaluate the impacts of the proposed revised specifications on bridge construction costs.

### A.2 CURRENT AASHTO MAP (1990 USGS MAP)

The national earthquake ground motion map in the current AASHTO LRFD Bridge Seismic Design Specifications is a probabilistic map of peak ground acceleration (PGA) on rock developed by the U.S. Geological Survey (USGS, 1990). The map provides contours of PGA for a probability of exceedance of 10% in 50 years. The PGA map is used with rules contained in the AASHTO Specifications for obtaining seismic response coefficients or response spectral accelerations.

### A.3 NEW USGS MAPS

In 1993, the USGS embarked on a major project to prepare updated national earthquake ground motion maps. In California, the mapping project was a joint effort between USGS and the California Division of Mines and Geology (CDMG). The result of that project was a set of probabilistic maps published in 1996 for the conterminous United States and subsequently for Alaska and Hawaii that cover several rock ground motion parameters and three different probability levels or return periods (Frankel et al., 1996, 1997a, 1997b, 1997c, 2000; Frankel and Leyendecker, 2000; Klein et al., 1999; Peterson et al., 1996; Wessen et al., 1999a, 1999b). The maps are available as large-scale paper maps, as small-scale paper maps obtained via the Internet, and as digitized values obtained from the Internet or a CD-ROM published by the USGS (Frankel and Leyendecker, 2001), which is provided with Part I, *Specifications*.

Parameters of rock ground motions that have been contour mapped by USGS include peak ground acceleration (PGA) and response spectral accelerations for periods of vibration of 0.2, 0.3, and 1.0 second. Contour maps for these parameters have been prepared for three different probabilities of exceedance (PE): 10% PE in 50 years, 5% PE in 50 years, and 2% PE in 50 years (approximately equal to 3% PE in 75 years), corresponding, respectively, to approximate ground motion return periods of 500 years, 1000 years, and 2500 years. In addition to these contour maps, the ground motion values at locations specified by latitude and longitude can be obtained via the Internet for the aforementioned three probability levels for PGA and spectral accelerations for periods of vibration of 0.2, 0.3, and 1.0 seconds. The CD-ROM published by the USGS also provides spectral accelerations at additional periods of 0.1, 0.5, and 2.0 seconds. In addition, the CD-ROM contains not only the PGA and spectral acceleration values at three probability levels but also the complete hazard curves (i.e., relationships between the amplitude of a ground motion parameter and

its annual frequency of exceedance [annual frequency of exceedance is the reciprocal of return period]) for specified latitudes and longitudes. Therefore, ground motion values can be obtained for any return period or probability of exceedance from the hazard curves on the CD-ROM.

The effort to develop the new USGS national ground motion maps incorporated inputs for seismic source models and ground motion attenuation models that represent major improvements over the models used for the current AASHTO maps with regard to capturing the state of scientific knowledge. Some of the key areas of incorporation of updated scientific knowledge for the new USGS maps include:

1. Much more extensive inclusion of identified discrete active faults and geologic slip rate data. Approximately 500 faults were incorporated in the mapping. Geologic slip rates for these faults were utilized to determine earthquake recurrence rates for the faults.
2. Improved and updated seismicity catalogs were utilized in determining earthquake recurrence rates for seismic sources not identified as discrete faults. In the central and eastern United States (CEUS), these catalogs utilized updated assessments of magnitudes of pre-instrumental older earthquakes (originally characterized by their maximum, or epicentral, Modified Mercalli Intensity). These assessments had the effect of reducing the estimated rate of larger earthquakes in the CEUS (equal to or greater than approximately magnitude 5).
3. In the Pacific Northwest (Washington, Oregon, and northwest California), the Cascadia subduction zone seismic source was explicitly included. Geologic/paleo-seismic data were utilized to characterize the recurrence rate of very large earthquakes (magnitude 8 to 9) occurring in the coastal and offshore regions of the Pacific Northwest.
4. Geologic/paleoseismic data were utilized to characterize the recurrence rates of large earthquakes occurring in the New Madrid seismic zone (in the vicinity of New Madrid, Missouri) and the Charleston seismic zone (in the vicinity of Charleston, South Carolina).
5. Updated, recently developed ground motion attenuation relationships were utilized. These relationships incorporated the developing knowledge of differences in ground motion at-

tenuation relationships in different regions and tectonic environments of the United States. As a result, different attenuation relationships were used in the CEUS, shallow-crustal faulting regions of the western United States (WUS), and subduction zone regions of the Pacific Northwest and Alaska.

The new probabilistic maps developed by the USGS have been widely accepted as providing a greatly improved scientific portrayal of probabilistic ground motions in the United States compared to earlier maps. These maps were assessed for possible utilization for seismic design of bridges and other highway facilities by the 1997 FHWA/MCEER workshop on the National Characterization of Seismic Ground Motion for New and Existing Highway Facilities (Friedland et al., 1997). The workshop concluded that "...these new maps represent a major step forward in the characterization of national seismic ground motion. The maps are in substantially better agreement with current scientific understanding of seismic sources and ground motion attenuation throughout the United States than are the current AASHTO maps. ...the new USGS maps should provide the basis for a new national seismic hazard portrayal for highway facilities..."

The USGS has in place a systematic process for periodically updating the maps to reflect continuing advances in knowledge of earthquake sources and ground motions. Therefore organizations using these maps (or maps adapted from the USGS maps as described below) have the opportunity to update the maps in their seismic criteria documents as appropriate.

#### **A.4 NATIONAL EARTHQUAKE HAZARD REDUCTION PROGRAM (NEHRP) MAXIMUM CONSIDERED EARTHQUAKE (MCE) MAPS**

The Building Seismic Safety Council (BSSC) adopted a modified version of the new USGS Maps for 2% PE in 50 years to define the recommended ground motion basis for the seismic design of buildings in the 1997 *NEHRP Recommended Provisions for Seismic Regulations for New Buildings and Other Structures* (BSSC, 1998; Leyendecker et al., 2000, 2001). These maps are termed the Maximum Considered Earthquake (MCE) maps and are presented in these *Specifications* in Figures 3.4.1-2(a) through 3.4.1-2(l). The maps are for 0.2-second and 1.0-second response

spectral accelerations. Map values for locations specified by latitude and longitude may be obtained from the CD-ROM published by USGS (Leyendecker et al., 2001).

The 1997 NEHRP MCE maps are identical to the new USGS maps for a probability of ground motion exceedance of 2% in 50 years (return period of approximately 2500 years), except that in areas close to highly active faults, “deterministic bounds” are placed on the ground motions with the intent that ground motions are limited to levels calculated assuming the occurrence of maximum magnitude earthquakes on the faults. The deterministic bounds are defined as 1.5 times the median ground motions calculated using appropriate ground motion attenuation relationships (the same relationships as used in the USGS probabilistic mapping), assuming the occurrence of maximum magnitude earthquakes on the faults, but not less than 1.5g for 0.2-second spectral acceleration and 0.6g for 1.0-second spectral acceleration. Multi-

plying the median ground motions by 1.5 results in ground motions that are approximately at a median-plus-standard-deviation level (actually somewhat lower, in general, because the ratio of median-plus-standard-deviation ground motions to median ground motions usually exceeds 1.5). Figure A-1 conceptually illustrates the procedure for incorporating deterministic bounds on the MCE maps. The deterministic bounds limit ground motions to values that are lower than those for 2% PE in 50 years in areas near highly active faults in California, western Nevada, coastal Oregon and Washington, and parts of Alaska and Hawaii.

MCE maps are also used in the *NEHRP Guidelines for the Seismic Rehabilitation of Buildings* (ATC/BSSC, 1997), and its successor document, *Prestandard and Commentary for the Seismic Rehabilitation of Buildings* (ASCE, 2000).

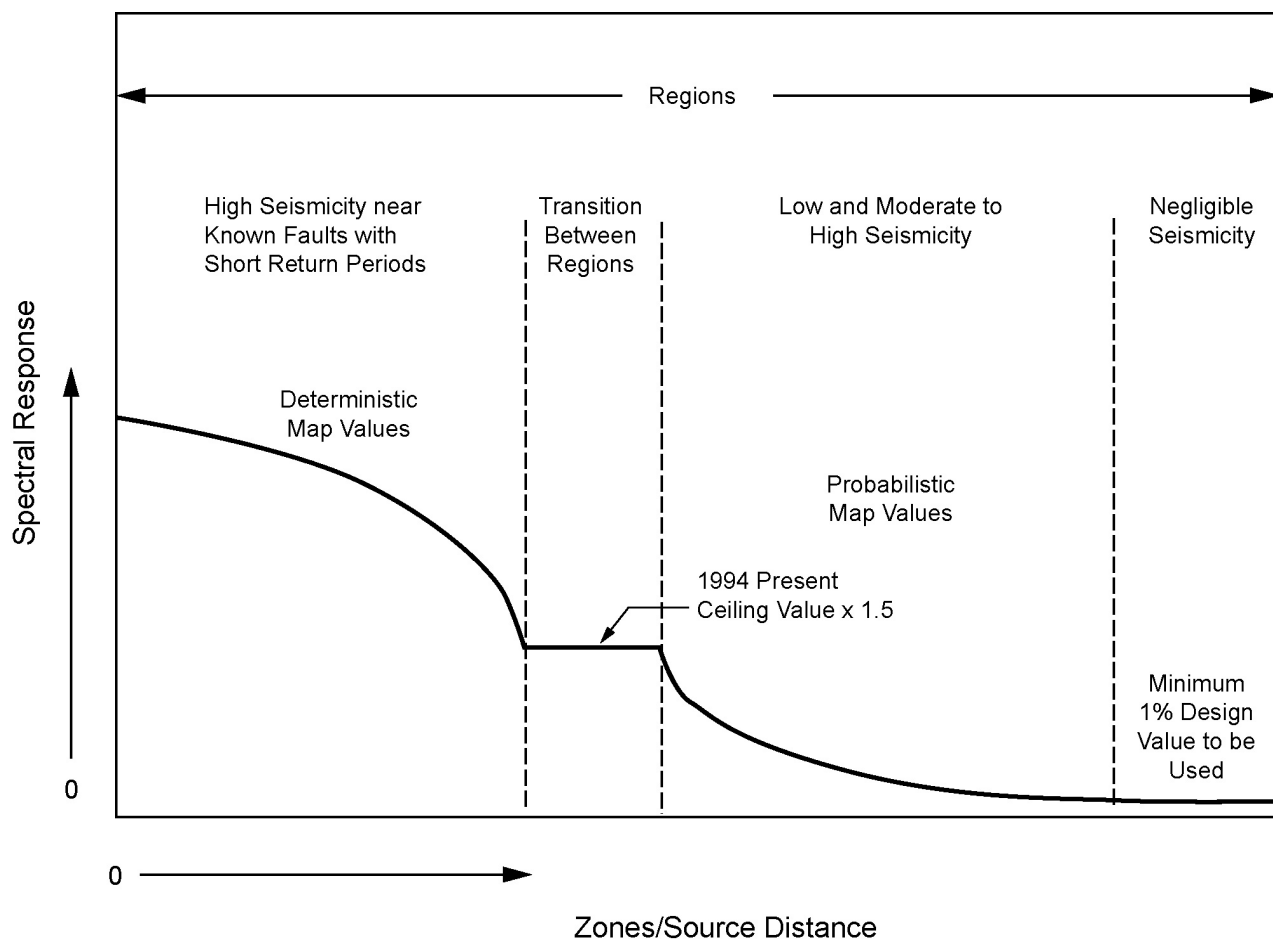


**Figure A-1** Procedure for Incorporation of Deterministic Bounds in the Maximum Considered Earthquake (MCE) Ground Motion Map of the 1997 *NEHRP Recommended Provisions for Seismic Regulations for New Buildings and Other Structures* (BSSC, 1998)

## A.5 DESIGN EARTHQUAKES

Two design earthquakes are defined for these *Specifications*. The upper level earthquake is the “rare” earthquake and is defined as the MCE described in the preceding section. For a bridge design life of 75 years, the ground motions for the MCE correspond to 3% PE in 75 years, except that lower ground motions are defined in areas of deterministic bounds as described above. The lower level earthquake is the Expected Earthquake and is defined as ground motions corresponding to 50% PE in 75 years.

### A.5.1 Rare Earthquake (MCE)

The intent of the MCE is to reasonably capture the maximum earthquake potential and ground motions throughout the United States. As summarized in Section A.1, the design objective is to preserve life safety and prevent collapse of the bridge, although some bridges may suffer considerable damage and may need to be replaced following the MCE.

In the current AASHTO LRFD specifications, a 10% probability of exceedance in 50 years, or approximately a 500-year return period, is used. However, based on a detailed analysis of the new USGS maps, the ground motions over much of the United States increase substantially for probability levels lower than 10% in 50 years or return period longer than 500 years. The increase in ground motions with return period is illustrated in Figures A-2(a) and A-2(b). In these figures, ratios of 0.2-second and 1.0-second spectral accelerations for given return periods to 0.2-second and 1.0-second spectral accelerations for an approximate 500-year return period are plotted versus return period for selected cities in three regions of the conterminous United States: central and eastern United States (CEUS); western United States outside California (WUS); and California. In California and coastal Oregon and Washington, the effects of deterministic bounds described in Section A.4 on the ground motion ratios are included where applicable. The curves in Figures A-2(a) and A-2(b) illustrate that MCE ground motions in areas of deterministic bounds in highly seismically active areas of California do not greatly exceed 500-year ground motions, with ratios of MCE to 500-year ground motions typically in the range of about 1.2 to 1.5. However in other parts of the WUS and in the CEUS, ratios of MCE ground motions (i.e. approximately 2500-year ground motions except

where deterministically bounded) to 500-year ground motions typically range from about 2 to 2.5 in the WUS and 2.5 to 3.5 in the CEUS. Even higher ratios are obtained for some areas exposed to large magnitude characteristic earthquakes having moderately long recurrence intervals defined by paleoseismic data, such as Charleston, New Madrid, Wasatch Front, and coastal Oregon and Washington. These results motivate the recommendation to adopt MCE ground motions as a design basis for a “no collapse” performance criterion for bridges during rare but credible earthquakes.

Analysis of 1996 USGS map ground motions in the Charleston, South Carolina and New Madrid, Missouri regions also indicate that 500-year return period ground motions within 75 km of the source region of the 1811-1812 New Madrid earthquakes and the 1886 Charleston earthquake are far below the ground motions that are likely to have occurred during these historic earthquakes. However, 2500-year return period ground motions are in much better agreement with ground motions estimated for these earthquakes. If deterministic estimates of ground motions are made for the historic New Madrid earthquake of estimated moment magnitude 8.0 using the same ground motion attenuation relationships used in the USGS probabilistic ground motion mapping, then the 500-year mapped ground motions are at or below the deterministic median-minus-standard-deviation ground motions estimated for the historic events within 75 km of the earthquake sources, whereas 2500-year ground motions range from less than median to less than median-plus-standard-deviation ground motions. Similarly, 500-year ground motions range from less than median-minus-standard-deviation to less than median ground motions deterministically estimated for the 1886 Charleston earthquake of estimated moment magnitude 7.3 within 75 km of the earthquake source. The 2500-year ground motions range from less than median to slightly above median-plus-standard-deviation ground motions for this event. It is desirable that design ground motions reasonably capture the ground motions estimated for historically occurring earthquakes.

Adoption of the MCE as a design earthquake for a collapse-prevention performance criteria is consistent with the adoption of the MCE in the 1997 and 2000 *NEHRP Recommended Provisions for Seismic Regulations for New Buildings and Other Structures* (BSSC, 1998; BSSC, 2001), the 2000 *International Building Code* (ICC, 2000),



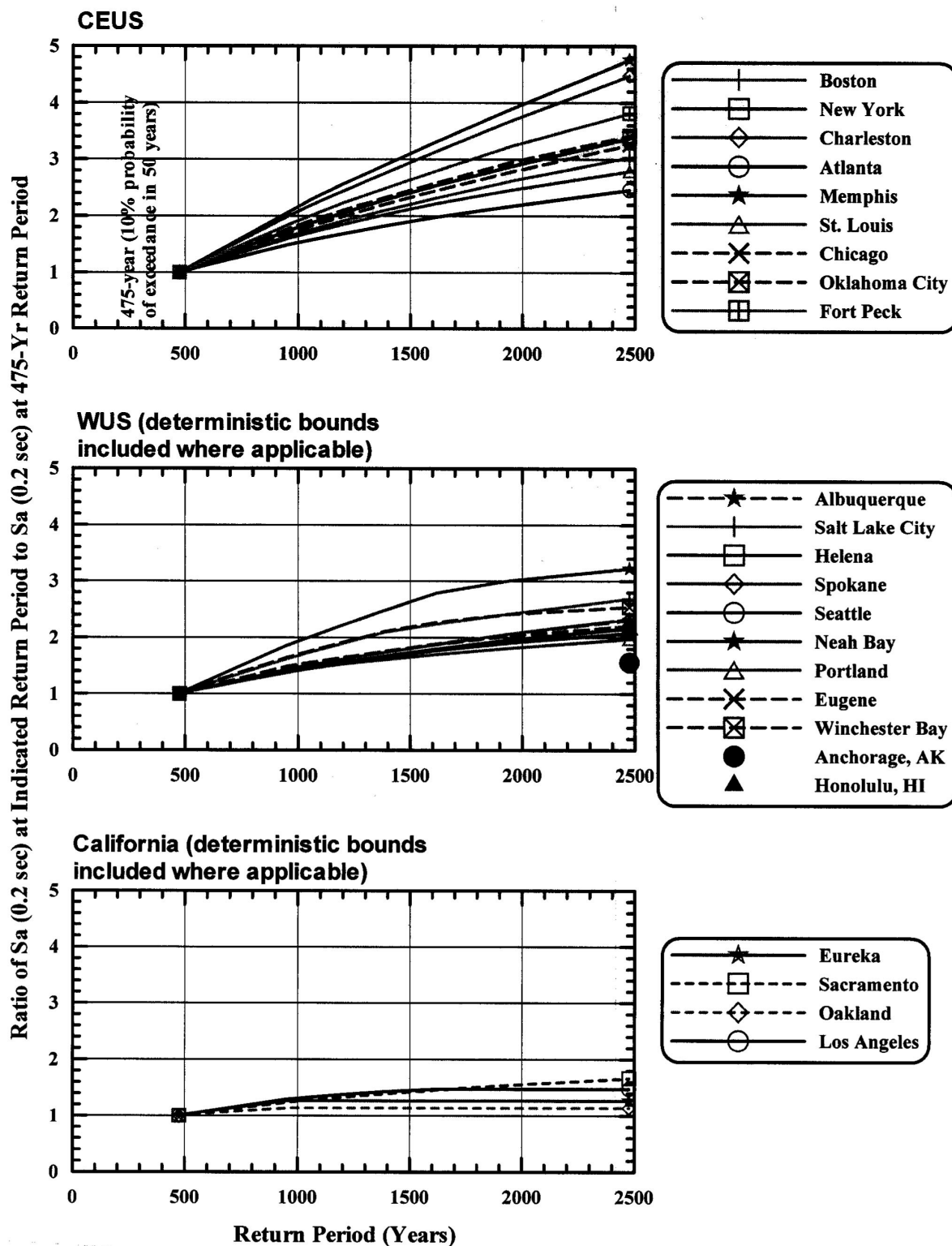


Figure A-2(a) Ratios of 0.2 Second Spectral Acceleration at Different Return Periods to 0.2-Second Spectral Acceleration At 475-Year Return Period

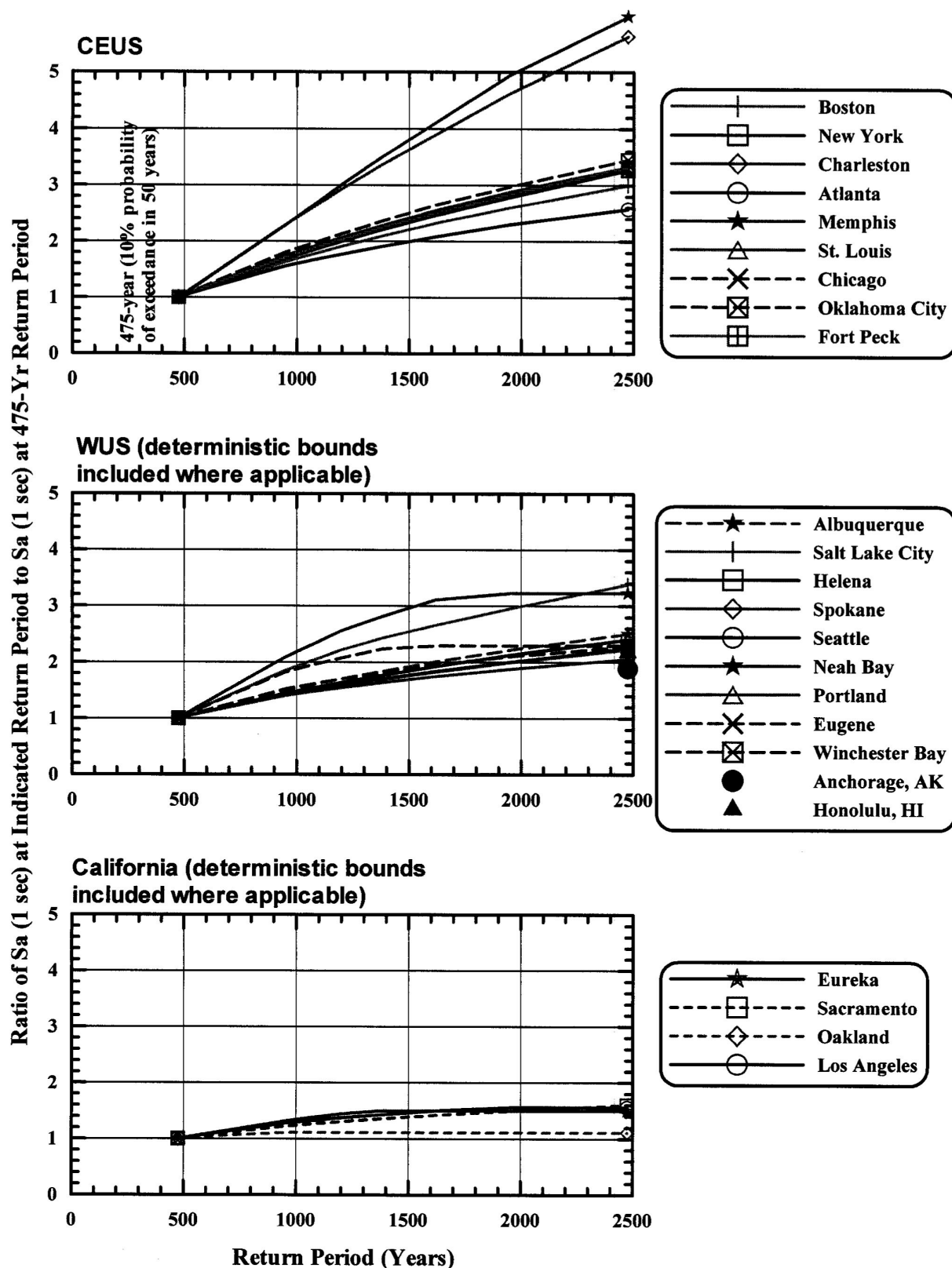


Figure A-2(b) Ratios of 1.0 Second Spectral Acceleration at Different Return Periods to 1.0-Second Spectral Acceleration at 475-Year Return Period

and the NEHRP *Guidelines for the Seismic Rehabilitation of Buildings* (ATC/BSSC, 1997). In the 1997 and 2000 NEHRP *Recommended Provisions for Seismic Regulations for New Buildings and Other Structures* and the 2000 *International Building Code*, the MCE ground motions are defined as collapse prevention motions but design is conducted for two-thirds of the MCE ground motions on the basis that the design provisions in those documents (including the *R*-factors) would provide a minimum margin of safety of 1.5 against collapse. On the other hand, in the NEHRP *Guidelines for Seismic Rehabilitation of Buildings*, the MCE ground motions are performance criterion directly used in the collapse prevention performance check. The approach proposed for these specifications is similar to that of the NEHRP *Guidelines for the Seismic Rehabilitation of Buildings* in that the design provisions for the MCE have been explicitly developed for a collapse-prevention performance criterion.

The decision to use the 3% PE in 75 year event with deterministic bounds rather than 2/3 of this event (as used in the 2000 NEHRP *Recommended Provisions for Seismic Regulations for New Buildings and Other Structures*) was to directly address and incorporate design displacements associated with the MCE event. Displacements are much more important in bridge design because they govern the seat width of girders supported by columns and thus are critically important in preventing collapse.

### A.5.2 Expected Earthquake

The intent of the Expected Earthquake is to describe ground motions that are expected to occur during a 75-year bridge life (with a 50% probability of being exceeded during the bridge life). Design is for minimal damage and normal service following postearthquake inspection. Expected Earthquake ground motions are defined by the new USGS probabilistic ground motion mapping described in Section A.3.

Figures A-3(a) and A-3(b) illustrate ratios of 0.2-second and 1.0-second response spectral accelerations at various return periods to 0.2-second and 1.0-second spectral accelerations at 108-year return period (corresponding to 50% PE in 75 years) for selected cities in California, WUS outside California, and CEUS based on new USGS mapping. Deterministic bounds on ground motions for long return periods have been incorporated where applicable in the curves in Figures A-

3(a) and A-3(b). The curves indicate that ratios of MCE to Expected Earthquake ground motions in highly seismically active regions of California are typically equal to or less than 3 but typically exceed 4 to 5 in other parts of the WUS and 7 to 10 in the CEUS. As shown, in some locales of low seismicity and environments of characteristic large-magnitude earthquakes having moderately long recurrence intervals, MCE-to-Expected Earthquake spectral ratios may exceed 10 to 20.

The decision to incorporate explicit design checks for this lower level design event was to get some parity between wind, flood and earthquake loads. The AASHTO LRFD provisions require essentially elastic design for the 100 year flood and the 100 mph wind, which in many parts of the country is close to a 100 year wind load. Although the 50% PE in 75 year earthquake (108 year return period) only controls column design in parts of the western United States, this recommendation provides for the first time some consistency in the expected performance of 100 year return period design events. The significant difference in the magnitude of earthquake loads with longer return periods is another reason why seismic design must consider much longer return period events. Both wind and flood loads tend to asymptotic values as the return period increases and in fact the ratio of a 2000 year/ 50 year wind load is in the range of 1.7 to 2.1 (Whalen and Simiu 1998).

## A.6 IMPACT STUDIES

Current AASHTO design uses a 500-year return period for defining the design earthquake. A more meaningful way to express design ground motions for this earthquake is in terms of probability of exceedance. Ground motions for a 500-year earthquake would be those for which there is a 15% chance of exceedance in the 75 year life of the bridge. In other words there is a 15% chance that earthquake ground motions larger than the design earthquake ground motions will occur in the life of the bridge. Whether this risk is acceptable or not depends on the probability of occurrence of the event, the consequences of the larger ground motions, and the cost of reducing the consequences. A 15% PE in 75 years is by most standards a high chance of exceeding the design load. But to know if one should act to reduce the probability of exceedance, the consequences of exceedance must be known. To answer this question one needs to know two things: (1) by how much will the design earthquake ground motions be

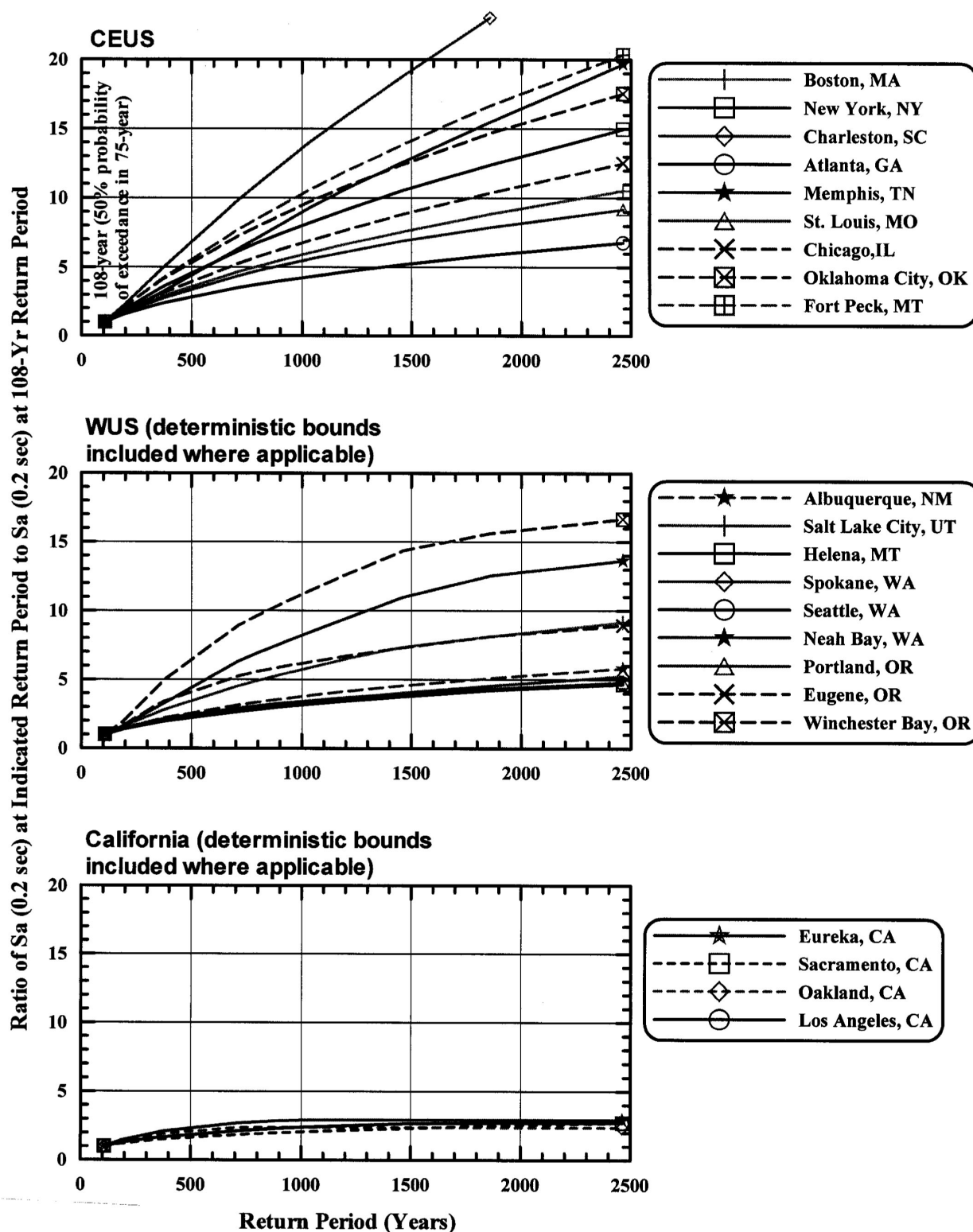


Figure A-3(a) Ratios of 0.2-Second Spectral Acceleration at Different Return Periods to 0.2-Second Spectral Acceleration at 108-Year Return Period

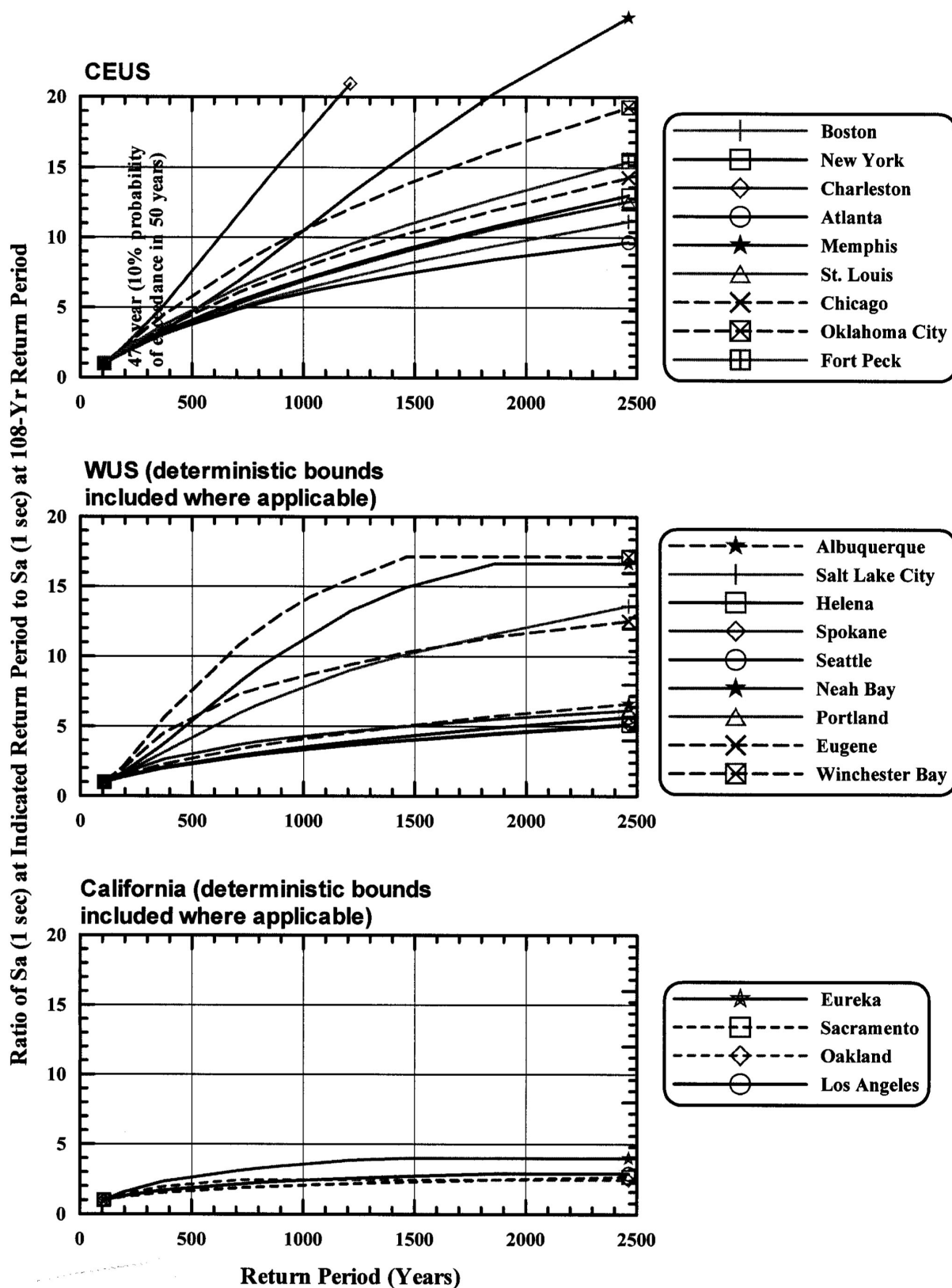


Figure A-3(b) Ratios of 1.0-Second Spectral Acceleration at Different Return Periods to 1.0-Second Spectral Acceleration at 108-Year Return Period

exceeded and (2) the reserve capacity in the bridge due to conservative design provisions.

Most bridges have at least some capacity in reserve for extreme events. The present AASHTO LRFD specification uses low  $R$ -factors, a spectral shape based on  $1/T^{2/3}$ , generous seat widths, uncracked sections for analysis, low  $\phi$  factors, and Mononabe-Okabe coefficients for abutment wall design. These criteria are based on engineering judgment and provide a measure of protection against large but infrequent earthquakes. But the degree of protection is unknown and the consequences of the larger events are uncertain and may be considerable. If ground motions during the actual event are only 20% larger than ground motions during the design event, damage will be slight, the consequences tolerable and the risk acceptable. On the other hand if ground motions during the actual event are two to five times as large, the reserve capacity may be exceeded, and damage and loss of access will likely be extensive. Here the risk may be unacceptable. If one uses the 0.2-second and 1.0 second value of the spectral acceleration shown in Figures A-2(a) and A-2(b) as a measure of earthquake ground shaking, actual forces may exceed the design 500-year forces by factors that range from 1.5 (in Los Angeles) to 4.5 (in Charleston). Figures A-2(a) and A-2(b) illustrate this range for a number of cities in the US. Similar ratios to the 108 year forces are shown in Figures A-3(a) and A-3(b) and are approximately 3 for Los Angeles and exceeding 20 for Charleston. Reserve capacities as high as 4.5 are not explicitly embodied in the current AASHTO LRFD specifications and no assurance should be given regarding damage and access in these situations.

With this as background there were two options for the development of these new seismic design provisions. (1) Design explicitly for ground motions associated with a larger event (3% PE in 75 year) but refine the provisions to reduce the

conservatism and thus keep the costs about the same as the current provisions. Under this scenario, the degree of protection against larger earthquakes is quantified and based on scientific principles and engineering experience. (2) Design for ground motions associated with a moderate sized event (15% PE in 75 year), and maintain the current conservative provisions as a measure of protection against larger events. In this scenario, the degree of protection is unknown and depends on intuition and engineering judgment.

The project team selected the first option and as part of the development of the provisions performed a series of parameter studies to assess the cost impact of designing for the higher-level event ground motions. These studies are summarized in Appendix G. In brief, they show that the net effect on the cost of a column and spread footing system is on the average 2% less than the current Division I-A provisions for multi-column bents and 16% less than Division I-A provisions for single column bents. These cost comparisons are based on the use of the more refined method for calculating overstrength factors and 2400 different column configurations, including the seismic input of five different cities.

Another cost concern that arose during the development of the provisions was the impact of the longer return period on liquefaction. Two detailed case studies were performed using the new and existing provisions and these are summarized in Appendix H. These examples demonstrated that application of the new provisions, with the inclusion of inelastic deformation in the piles as a result of lateral flow, would not be significantly more costly than the application of the current provisions. Hence the objective of having a quantifiable degree of protection against larger earthquakes for similar costs was achieved.

## **Appendix B**

### **PROVISIONS FOR SITE CHARACTERIZATION**

#### **B.1 GENERAL**

Site characterization shall be performed for each substructure element, as appropriate, to provide the necessary information for the design and construction of foundations. The type and extent of site characterization shall be based on subsurface conditions, structure type, and project requirements. The site characterization program shall be extensive enough to reveal the nature and types of soil deposits and/or rock formations encountered, the engineering properties of the soils and/or rocks, the potential for liquefaction, and the groundwater conditions.

#### **B.2 SUBSURFACE EXPLORATIONS**

Subsurface explorations shall be made to competent material of suitable bearing capacity or to a depth where added stresses due to the estimated footing load is less than 10% of the existing effective soil overburden stress, whichever is the greater. If bedrock is encountered at shallow depths, the exploration shall advance a minimum of 3 m into the bedrock or to 1 m beyond the proposed foundation depth, whichever is greater.

#### **C.B.1 GENERAL**

Site characterization normally includes subsurface explorations and laboratory testing of samples of soil/rock recovered during the exploration work. Subsurface exploration can include drilling and sampling of the soil or rock, as well as in situ testing.

#### **C.B.2 SUBSURFACE EXPLORATIONS**

As a minimum, the subsurface exploration and testing program should obtain information to analyze foundation stability and settlement with respect to:

- Geological formation(s);
- Location and thickness of soil and rock units;
- Engineering properties of soil and rock units, including density, shear strength and compressibility;
- Groundwater conditions;
- Ground surface topography;
- Local considerations, such as expansive or dispersive soil deposits, collapse potential of soil in arid regions, underground voids from solution weathering or mining activity, or slope instability potential; and
- Behavior under seismic loading, including liquefaction, seismic-induced ground settlement, lateral flow and spreading (e.g., sloping ground underlain by very loose saturated soil and the presence of a free face), and ground motion amplification or attenuation.

Issues related to the constructibility of the foundation system should also be identified during the subsurface investigation process. These issues can include the drivability of piles, the excavability/stability of holes for drilled shafts and similar bored systems (e.g., Cast-in-Drill Hole (CIDH) piles), occurrence of boulders and rocks that could affect pile or retaining wall construction, need for and ability to de-water soils or control groundwater flow.

### B.2.1 In Situ Tests

In situ tests may be performed to obtain deformation and strength parameters of foundation soils or rock for the purposes of design and/or analysis. The tests shall be performed in accordance with the appropriate standards recommended by ASTM or AASHTO and may include the following in-situ soil tests and in-situ rock tests:

#### *In Situ Soil Tests*

- Standard Penetration Test - AASHTO T 206 (ASTM D 1586)
- Static Cone Test - ASTM D 3441
- Field Vane Test - AASHTO T 223 (ASTM D 2573)
- Pressuremeter Test - ASTM D 4719
- Plate Bearing Test - AASHTO T 235 (ASTM D 1194)
- Well Test (Permeability) - ASTM D 4750

#### *In Situ Rock Tests*

- Deformability and Strength of Weak Rock by an In-Situ Uniaxial Compressive Test - ASTM D 4555
- Determination of Direct Shear Strength of Rock Discontinuities - ASTM D 4554
- Modulus of Deformation of Rock Mass Using the Flexible Plate Loading Method - ASTM D 4395
- Modulus of Deformation of Rock Mass Using a Radial Jacking Test - ASTM D 4506
- Modulus of Deformation of Rock Mass Using the Rigid Plate Loading Method - ASTM D 4394

### C.B.2.1 In Situ Tests

The most suitable type of exploration method will depend on the type of soil/rock encountered, the type and size of the foundation, and the requirements of design. Often a combination of one or more methods is required. In nearly every situation at least one boring with soil/rock sampling should be planned. Results of other soil exploration methods, such as the cone penetrometer or field vane, should be compared to information recovered in the soil boring. Table B-1 provides a summary of the suitability and information that can be obtained from different in situ testing methods.

Parameters derived from field tests, such as standard penetration, cone penetrometer, dynamic penetrometer, and pressuremeter tests, can often be used directly in design calculations based on empirical relationships. These are sometimes found to be more reliable than analytical calculations, especially in familiar ground conditions for which the empirical relationships are well established.



- Stress and Modulus of Deformation Determination Using the Flatjack Method - ASTM D 4729
- Stress in Rock Using the Hydraulic Fracturing Method - ASTM D 4645

If so requested by the owner or required by permitting agencies, boring and penetration test holes shall be plugged to prevent water contamination.

**Table B-1 In-Situ Tests**

Type of Test	Best Suited To	Not Applicable To	Properties That Can Be Determined
Standard Penetration Test (SPT)	Sand	Coarse Gravel	Qualitative evaluation of compactness. Qualitative comparison of subsoil stratification.
Dynamic Cone Test	Sand and Gravel	Clay	Qualitative evaluation of compactness. Qualitative comparison of subsoil stratification.
Static Cone Test	Sand, Silt, and Clay	Coarse Gravel, Cemented Soil, Rock	Continuous evaluation of density and strength of sands. Continuous evaluation of undrained shear strength in clays.
Field Vane Test	Clay	All Other Soils	Undrained shear strength.
Pressuremeter Test	Soft Rock, Sand, Gravel, and Till	Soft Sensitive Clays	Bearing capacity and compressibility.
Plate Bearing Test and Screw Plate Test	Sand and Clay	-	Deformation modulus. Modulus of subgrade reaction. Bearing capacity.
Flat Plate Dilatometer Test	Sand and Clay	Gravel	Empirical correlation for soil type, $K_e$ , overconsolidation ratio, undrained shear strength, and modulus.
Permeability Test	Sand and Gravel	-	Evaluation of coefficient of permeability.

### B.2.2 Explorations for Seismic Studies

In areas of high seismic activity (e.g., Seismic Detailing Requirement (SDR) 3 and above), spe-

### C.B.2.2 Explorations for Seismic Studies

Subsurface exploration methods in areas of high seismicity are generally the same as those

cial consideration shall be given to the seismic response of the site during the planning of field explorations. The planning process shall consider the potential for liquefaction and the requirement to determine the Site Class Definition, as required for establishing the Seismic Hazard Level and SDR. Article 3.7 provides definitions Seismic Hazards Level (SHL), SDAP and SDR.

#### B.2.2.1 Liquefaction Potential

Field explorations shall be performed to evaluate the potential for liquefaction in SDR 3, 4, 5, and 6 at those sites potentially susceptible to liquefaction. For sites that are potentially liquefiable, it is important to obtain an accurate determination of soil stratigraphy, the groundwater location, and the density of cohesionless soil. Of particular importance is the identification of thin layers that, if liquefied, could result in lateral flows or spreading of the soil above the liquefied layers.

used for standard subsurface explorations. However, the empirical correlations used to estimate the potential for liquefaction or the shear wave velocity of the soil normally require use of equipment that has been calibrated according to certain standards. The geotechnical engineer or engineering geologist responsible for having the subsurface explorations carried out should become familiar with these methods and confirm during the exploration program that correct methods and calibrated equipment are being used. If incorrect methods or un-calibrated equipment are used, it is possible to predict overly conservative or unconservative ground response for a design seismic event.

#### C.B.2.2.1 Liquefaction Potential

A potential for liquefaction exists if the following conditions are present: (1) the peak horizontal acceleration at the ground surface is predicted to be greater than 0.15g (g = acceleration of gravity); (2) the soil consists of loose to medium dense non-plastic silts, sands, and in some cases gravels; and (3) the permanent groundwater location is near the ground surface. Appendix D provides specific guidance on the determination and evaluation of liquefaction.

##### *Depth of Exploration*

The potential depth of liquefaction is an important decision. Normally, liquefaction is assumed to be limited to the upper 15 to 20 m of soil profile. However, it appears that this limiting depth is based on the observed depth of liquefaction rather than the maximum depth of liquefaction that is physically possible. For this reason an exploration program should extend at least to 25 m or until a competent bearing layer (with no underlying loose layers) is encountered, whichever occurs first.

##### *Methods of Exploration*

Several different exploration methods can be used to identify soils that could be susceptible to liquefaction. These include the Standard Penetration Test (SPT), the cone penetration test (CPT), and certain types of shear wave velocity measurements (e.g., crosshole, downhole, and Spectral Analysis of Surface Wave methods). ASTM standards exist for conducting SPTs, CPTs (see Article B.2.1), and certain types of shear wave velocity measurement. These methods should be followed. If standards are not available, then it is essential to have testing completed by experienced individuals, who understand the limitations of the test

methods and who understand the level of accuracy needed by the designer for Site Class Definition or liquefaction determination.

*Standard Penetration Test (SPT) Method:* The SPT is currently the most common field exploration method for liquefaction studies. It is critical that if SPTs are conducted to obtain information for liquefaction assessments, procedures follow those recommended by Youd and Idriss (1997). These procedures have strict requirements for hammer energy, sampler size, and drilling method. If these methods are not followed, the value of the blow count determined from the SPT can vary by 100%, resulting in great uncertainty in any liquefaction assessment based on the SPT results. Recommended SPT procedures are summarized in Table B-2.

**Table B-2 Recommended SPT Procedure**

Borehole size	66 mm < Diameter < 115 mm
Borehole support	Casing for full length and/or drilling mud
Drilling	Wash boring; side discharge bit Rotary boring; side or upward discharge bit Clean bottom of borehole*
Drill rods	A or AW for depths of less than 15 m N or NW for greater depths
Sampler	Standard 51 mm Outer Diameter +/- 1 mm 35 mm Inner Diameter +/- 1 mm >457 mm length
Penetration resistance	Record number of blows for each 150 mm; N = number of blows from 150 to 450 mm penetration
Blow count rate	30 to 40 blows per minute

\* Maximum soil heave within casing <70 mm

An automatic trip hammer should be used wherever possible; hammer energy calibrations should be obtained for the hammer, whether it is a donut hammer or an automatic hammer. Records should also be available that indicate whether the SPT sampler used liners or not, and the type of drilling method that was used. It will usually be necessary to conduct the SPTs at close depth intervals, rather than the conventional 1.5-m interval, because thin liquefiable layers could be important in design.

Sites with gravel deposits require special consideration when performing SPTs. Because of the coarse size of gravel particles, relative to the size of the sampler, these deposits can result in mis-

leadingly high blow counts. Three procedures can be considered for these sites:

- If a site has only a few gravel layers or if the gravel is not particularly abundant or large, it may be possible to obtain an equivalent SPT blow count if “incremental” blow counts are measured. To perform “incremental” blow count measurements, the number of blows for each 25 mm of penetration is recorded, rather than the blows for 150 mm. By plotting the blow counts per 25 mm versus depth, it is sometimes possible to distinguish between the blow count obtained in the matrix material and blow counts affected by large gravel particles. The equivalent blow count for 150 mm can then be estimated by summing and extrapolating the number of blows for the representative 25 mm penetrations that appear to be uninfluenced by coarse gravel particles. This procedure is described in Vallee and Skryness (1980).
- Andrus and Youd (1987) describe an alternate procedure for determining blow counts in gravel deposits. They suggest that the penetration per blow be determined and the cumulative penetration versus blow count be plotted. With this procedure, changes in slope can be identified when gravel particles interfere with penetration. From the slope of the cumulative penetration, estimates of the penetration resistance can be made where the gravel particles did or did not influence the penetration resistance.
- An alternative in gravel deposits is to obtain Becker Hammer blow counts, which have been correlated to the standard penetration test blow count (Youd and Idriss, 1997).

*Cone Penetrometer Test (CPT) Method:* For many locations the CPT is the preferred method of determining liquefaction potential. This method is preferred because it is able to provide an essentially continuous indication of soil consistency and type with depth. It is also less susceptible to operator-related differences in measurements. The CPT method may not be applicable at sites where cobbles and gravels overlie looser sandy soils. At these sites it may be impossible to push the CPT rod and sensor through the gravel. For these sites it is sometimes possible to auger through the gravel materials to provide access for the cone penetrometer rod and sensor.

Most CPT equipment are not capable of ob-

taining soil samples. Empirical correlations can, however, be used to estimate soil type and grain size. Although these correlations often provide very good indirect estimations of soil type and grain size, it is generally desirable to perform a limited number of SPTs at the site to obtain soil samples for laboratory determination of grain size, to confirm soil descriptions, and to provide a comparison to SPT blow counts.

Procedures for interpreting liquefaction resistance from the CPT measurement are given in Youd and Idriss (1997).

*Shear Wave Velocity Methods:* Shear wave velocity can also be used for both liquefaction evaluations and the determination of soil shear modulus, which is required when establishing spring constants for spread footing foundations. The shear wave velocity of the soil is also fundamental to the determination of Site Class Definition, as discussed in Article 3.4.2.1.

A variety of methods are available for making shear wave velocity measurements. They include downhole and crosshole methods, which are performed in boreholes, seismic-cone methods, which are conducted in conjunction with a CPT, and Spectral Analysis of Surface Wave (SASW) methods, which are conducted from the ground surface without a borehole. Experienced individuals should perform these methods, as the collection and interpretation of results requires considerable skill. In the absence of this experience, it is possible to obtain misleading results. Surface wave refraction procedures should not be used, as they are generally not able to obtain information in low-velocity layers. Additional information about the shear wave velocity can be found in Kramer (1996).

Procedures for interpreting liquefaction resistance from shear wave velocity data are discussed in Youd and Idriss (1997).

#### B.2.2.2 Site Response Determination

The field exploration shall provide sufficient information to determine the Site Class Definition (see Article 3.4.2.1), which is used to determine the Seismic Hazard Level.

#### C.B.2.2.2 Site Response Determination

The Site Class Definition is used to determine whether amplification or de-amplification of ground motions occurs as earthquake-induced motions propagate from depth to the ground surface. Five general site classes have been defined (Article 3.4.2.1) for seismic studies. These categories generally require determination of soil properties in the upper 30 m of soil profile. Procedures for establishing the soil properties include the SPT, the shear wave velocity, and the strength of the material. It is important when planning the field

### B.3 LABORATORY TESTING

Laboratory tests shall be performed to determine the strength, deformation, and flow characteristics of soils and/or rocks and their suitability for the foundation selected. In areas of higher seismicity (e.g., SDR 3, 4, 5, and 6), it may be appropriate to conduct special dynamic or cyclic tests to establish the liquefaction potential or stiffness and material damping properties of the soil at some sites if unusual soils exist or if the foundation is supporting a critical bridge.

#### B.3.1 Standard Laboratory Tests

Laboratory soil tests may include:

- Water Content - ASTM D 4643
- Specific Gravity - AASHTO T 100 (ASTM D 854)
- Grain Size Distribution - AASHTO T 88 (ASTM D 422)
- Soil Compaction Testing – ASTM D 698 or D 1557
- Liquid Limit and Plastic Limit - AASHTO T 90 (ASTM D 4318)
- Direct Shear Test - AASHTO T 236 (ASTM D 3080)
- Unconfined Compression Test - AASHTO T 208 (ASTM D 2166)
- Unconsolidated-Undrained Triaxial Test - ASTM D 2850
- Consolidated-Undrained Triaxial Test - AASHTO T 297 (ASTM D 4767)
- Consolidation Test - AASHTO T 216 (ASTM D 2435 or D 4186)
- Permeability Test - AASHTO T 215 (ASTM D 2434)

explorations to recognize that this information could be important to a site and make explorations plans accordingly.

### C.B.3 LABORATORY TESTING

An understanding of the engineering properties of soils is essential to the use of current methods for the design of foundations and earth structures. The purpose of laboratory testing is to provide the basic data with which to classify soils and to measure their engineering properties. The design values selected from the laboratory tests should be appropriate to the particular limit state and its corresponding calculation model under consideration.

For the value of each parameter, relevant published data together with local and general experience should be considered. Published correlations between parameters should also be considered when relevant.

#### CB.3.1 Standard Laboratory Tests

Standard laboratory tests of soils may be grouped broadly into two general classes:

- Classification tests. These can be performed on either disturbed or undisturbed samples.
- Quantitative tests for permeability, compressibility, and shear strength. These tests are generally performed on undisturbed samples, except for materials to be placed as controlled fill or materials that do not have an unstable soil structure. In these cases, tests should be performed on specimens prepared in the laboratory.

A certain number of classification tests should be conducted at every bridge site; the number of quantitative tests will depend on the types of soils encountered. In many cases disturbance associated with the soil sampling process can limit the usefulness of quantitative test results. This is particularly the case for cohesionless soil. It can also occur for cohesive soil if high quality Shelby tube samples are not obtained. High quality sampling also requires careful sampling and careful soil setup once the sample is retrieved from the ground.

**B.3.2 Special Testing for Seismic Studies**

For some important projects it may be necessary or desirable to conduct special soil laboratory tests to establish the liquefaction strength or stiffness and material damping properties of the soil. These tests can include resonant column, cyclic triaxial, and cyclic simple shear tests. Only a limited number of academic and consulting organizations are currently conducting these types of tests; therefore, special care is required when selecting a testing laboratory for these tests. Kramer (1996) provides a summary of the laboratory testing for determination of dynamic properties of soil.

**B.3.3 Rock Testing**

Laboratory rock tests may include:

- Determination of Elastic Moduli - ASTM D 3148
- Triaxial Compression Test - AASHTO T 266 (ASTM D 2664)
- Unconfined Compression Test - ASTM D 2938
- Splitting Tensile Strength Test - ASTM D 3967

**C.B.3.2 Special Testing for Seismic Studies**

For liquefaction assessments it is generally preferable to rely on in situ methods for determining the liquefaction strength of the soil, because of difficulties associated with sample disturbance. The exception to this general rule is for non-plastic silty soil, where the database for in situ-based correlations is not as well established. For these soils cyclic laboratory test may be necessary to estimate liquefaction strengths.

Empirical correlations have also been developed to define the effects of shearing strain amplitude and confining pressure on shear modulus and material damping of cohesionless and cohesive soils. Laboratory determination of these properties may be warranted where special soil conditions exist or where the stress state on the soil could change. Kramer (1996) provides a summary of the available methods for estimating shear modulus and material damping as a function of shearing strain amplitude and confining pressure.

**C.B.3.3 Rock Testing**

Laboratory testing of rock has very limited applicability for measuring significant rock properties, such as:

- Compressive strength,
- Shear strength,
- Hardness,
- Compressibility, and
- Permeability.

Rock samples small enough to be tested in the laboratory are usually not representative of the entire rock mass. Laboratory testing of rock is used primarily for classification of intact rock samples, and, if performed properly, serves a useful function in this regard.

Laboratory tests on intact samples provide upper bounds on strength and lower bounds on compressibility. Frequently, laboratory tests can be used in conjunction with field tests to give reasonable estimates of rock mass behavioral characteristics.





## Appendix C

# GUIDELINES FOR CONDUCTING SITE-SPECIFIC GEOTECHNICAL INVESTIGATIONS AND DYNAMIC SITE RESPONSE ANALYSES

### C.1 INTRODUCTION

As indicated in Article 3.4.2.3 and Tables 3.4.2.3-1 and 3.4.2.3-2, site coefficients  $F_a$  and  $F_v$  are not provided for Site Class F soils, and site-specific geotechnical investigations and dynamic site response analyses are required for these soils. Guidelines are provided below for conducting site-specific investigations and site response analyses for Site Class F soils. These guidelines are also applicable if it is desired to conduct dynamic site response analyses for other soil types. Additional guidance on the topics addressed below is presented in a report by the Caltrans Seismic Advisory Board Ad Hoc Committee on Soil-Foundation-Structure-Interaction (CSABAC, 1999).

### C.2 SITE-SPECIFIC GEOTECHNICAL INVESTIGATION

For purposes of obtaining data to conduct a site response analysis, site-specific geotechnical investigations should include borings with sampling, standard penetration tests (SPTs), cone penetrometer tests (CPTs), and/or other subsurface investigative techniques and laboratory soil testing to establish the soil types, properties, and layering and the depth to rock or rock-like material. It is desirable to measure shear wave velocities in all soil layers. Alternatively, shear wave velocities may be estimated based on shear wave velocity data available for similar soils in the local area or through correlations with soil types and properties. A number of such correlations are summarized by Kramer (1996).

### C.3 DYNAMIC SITE RESPONSE ANALYSIS

Components of a dynamic site response analysis include: (1) modeling the soil profile; (2) selecting rock motions to input into the soil profile; and (3) conducting a site response analysis and interpreting the results.

1. *Modeling the soil profile:* Typically, a one-dimensional soil column extending from the ground surface to bedrock is adequate to capture first-order site response characteristics. However, two- to three-dimensional models may be considered for critical projects when two or three-dimensional wave propagation effects may be significant (e.g., in basins). The soil layers in a one-dimensional model are characterized by their total unit weights, shear wave velocities from which low-strain (maximum) shear moduli may be obtained and by relationships defining the nonlinear shear stress-strain relationships of the soils. The required relationships for analysis are often in the form of curves that describe the variation of shear modulus with shear strain (modulus reduction curves) and by curves that describe the variation of damping with shear strain (damping curves). In a two- or three-dimensional model, compression wave velocities or moduli or Poissons ratios are also required. In an analysis to estimate the effects of liquefaction on soil site response, the nonlinear soil model must also incorporate the buildup of soil pore water pressures and the consequent effects on reducing soil stiffness and strength. Typically, modulus reduction curves and damping curves are selected on the basis of published relationships for similar soils (e.g., Seed and Idriss, 1970; Seed et al., 1986; Sun et al., 1988; Vucetic and Dobry, 1991; Electric Power Research Institute, 1993; Kramer, 1996). Site-specific laboratory dynamic tests on soil samples to establish nonlinear soil characteristics can be considered where published relationships are judged to be inadequate for the types of soils present at the site. The uncertainty in soil properties should be estimated, especially the uncertainty in the selected maximum shear moduli and modulus reduction and damping curves.

2. *Selecting input rock motions:* Acceleration time histories that are representative of horizontal rock motions at the site are required as input to the soil model. Unless a site-specific analysis is carried out to develop the rock response spectrum at the site, the Maximum Considered Earthquake (MCE) rock spectrum for Site Class B rock can be defined using the general procedure described in Article 7.4.1 or 8.4.1. For hard rock (Site Class A), the spectrum may be adjusted using the site factors in Tables 3.4.2.3-1 and 3.4.2.3-2. For profiles having great depths of soil above Site Class A or B rock, consideration can be given to defining the base of the soil profile and the input rock motions at a depth at which soft rock or very stiff soil of Site Class C is encountered. In such cases, the design rock response spectrum may be taken as the spectrum for Site Class C defined using the site factors in Tables 3.4.2.3-1 and 3.4.2.3-2. Several acceleration time histories, typically at least four, recorded during earthquakes having magnitudes and distances that significantly contribute to the site seismic hazard should be selected for analysis. The U.S. Geological Survey results for deaggregation of seismic hazard (website address: <http://geohazards.cr.usgs.gov/eq/>) can be used to evaluate the dominant magnitudes and distances contributing to the hazard. Prior to analysis, each time history should be scaled so that its spectrum is at the approximate level of the design rock response spectrum in the period range of interest. It is desirable that the average of the response spectra of the suite of scaled input time histories be approximately at the level of the design rock response spectrum in the period range of interest. Because rock response spectra are defined at the ground surface rather than at depth below a soil deposit, the rock time histories should be input in the analysis as outcropping rock motions rather than at the soil-rock interface.
3. *Site response analysis and results interpretation:* Analytical methods may be equivalent linear or nonlinear. Frequently used computer programs for one-dimensional analysis include the equivalent linear program SHAKE (Schnabel et al., 1972; Idriss and Sun, 1992) and nonlinear programs DESRA-2 (Lee and Finn, 1978), MARDES (Chang et al., 1991), SUMDES (Li et al., 1992), D-MOD (Matasovic, 1993), TESS (Pyke, 1992), and DESRAMUSC (Qiu, 1998). If the soil response is highly nonlinear (e.g. high acceleration levels and soft clay soils), nonlinear programs are generally preferable to equivalent linear programs. For analysis of liquefaction effects on site response, computer programs incorporating pore water pressure development (effective stress analyses) must be used (e.g., DESRA-2, SUMDES, D-MOD, DESRAMUSC and TESS). Response spectra of output motions at the ground surface should be calculated and the ratios of response spectra of ground surface motions to input outcropping rock motions should be calculated. Typically, an average of the response spectral ratio curves is obtained and multiplied by the design rock response spectrum to obtain a soil response spectrum. This response spectrum is then typically adjusted to a smooth design soil response spectrum by slightly decreasing spectral peaks and slightly increasing spectral valleys. Sensitivity analyses to evaluate effects of soil property uncertainties should be conducted and considered in developing the design response spectrum.

## Appendix D

### PROVISIONS FOR COLLATERAL SEISMIC HAZARDS

#### COLLATERAL SEISMIC HAZARDS

The term collateral seismic hazards refers to earthquake-caused movement of the earth that either results in loads being imposed on a bridge foundation system or causes changes in the resistance of the earth that affects the response of a bridge-foundation system. These effects can be either dynamic or static in form. Liquefaction is one of the most well-known examples of a collateral hazard. This Appendix provides an overview of methods used to evaluate and design for these collateral hazards. This overview includes

- a general discussion of the term collateral hazards and the implication of these hazards on design of bridge foundations (Article D.1)
- a summary of methods used to screen for and evaluate liquefaction and associated hazards, such as lateral flows, lateral spreading, settlement, and differential settlement (Article D.2)
- an overview of other collateral hazards such as faulting, landsliding, differential compaction, and flooding and inundation (Article D.3), and
- a review of methods for designing spread footings and deep foundations for the most common collateral hazards, liquefaction (Article D.4)

The design of a bridge structure should consider the potential for these collateral hazards during the initial type, size, and location (TS&L) phase of the project, as significant cost can be incurred to design for, mitigate, or avoid these hazards.

#### D.1 GENERAL

The most common of the collateral hazards is liquefaction. During liquefaction, saturated granular soil loses stiffness and strength, which can affect the vertical or lateral bearing support of a foundation. Under normal circumstances, these losses in support can be handled during design. The more serious consequences of liquefaction are permanent lateral ground movements and settlement of the soil, both of which can damage a bridge foundation system.

Several other types of hazards associated with seismic-related ground behavior also can lead to damage of a bridge. These hazards include ground faulting, landsliding, differential compaction, and inundation and flooding resulting from earthquake-induced failures of dams or reservoirs, and tsunami..

##### D.1.1 Evaluation of Collateral Hazards

Various procedures have been developed over

#### CD.1 GENERAL

The term collateral hazards has been selected to differentiate loads that are imposed on a structure by displacement of soil from loads developed within a structure due to the inertial response of the bridge deck and abutments. These hazards are also called geologic or geotechnical hazards by those practicing in the areas of geology and geotechnical engineering. In this Appendix the terms geologic hazards and collateral hazards are used interchangeably.

Displacement associated with these collateral hazards can be very large, often being on the order of a meter and sometimes being as large as several meters. In some cases such as liquefaction-induced flow failures or landsliding, it will be difficult to prevent or limit displacement without significant expenditure of project funds. In the case of faulting the displacement cannot be prevented; all that can be done is to design the structure to withstand or avoid the movement.

##### C.D.1.1 Evaluation of Collateral Hazards

As time passes and more is learned about seis-

the past 20 years for quantifying the potential for and the consequences of these geologic hazards. The discussions in this Appendix summarize procedures and approaches commonly employed within the profession. The applicability of these procedures will depend on the soil conditions at the site, the complexity of the structure, and the risk that the owner is prepared to assume.

#### D.1.2 Designing for Collateral Hazards

The design of bridge structures for collateral hazards must consider the movement of the earth and the changes in soil properties resulting from this movement. In the case of liquefaction both effects must be considered in design. The first is that the bridge must perform adequately with just the liquefaction-induced soil changes alone. This means that the mechanical properties of the soil that liquefy are changed to reflect their post-liquefaction values (e.g., properties such as “p-y curves” and modulus of subgrade reaction values used to evaluate the lateral stiffness of a pile foundation are reduced). The second component of the design is the consideration of liquefaction-related ground movements. These can take several forms: lateral spreading, lateral flow, and ground settlement.

- Lateral spreading is a lateral movement that is induced by the ground shaking and develops in an incremental fashion as shaking occurs.
- Lateral flow is movement that occurs due to

mic response of soil, methods for identifying and dealing with collateral seismic hazards will likely change. For this reason this Appendix is intended to provide guidance and not be prescriptive.

Much of the following discussion will focus on the evaluation of liquefaction and its related hazards. Procedures given in this Appendix for the assessment of liquefaction are based on a consensus document prepared after a workshop sponsored by the National Center for Earthquake Engineering Research (NCEER) in 1996 (Youd and Idriss, 1997). The workshop was attended by a group of leading professionals working or conducting research in the area of liquefaction. The NCEER Workshop participants were not always in complete agreement in all areas dealing with liquefaction or design for liquefaction; however, the participants did agree that the NCEER Workshop report would form a minimum basis for conducting liquefaction evaluations. It was expected that the profession would build on these methods as more information became available.

The dilemma that an owner will face is deciding when methods advocated by an individual or group of individuals should be used to upgrade the procedures developed during the consensus NCEER Workshop. There is no simple process of making these decisions, a situation that is common to any evolving technology.

#### CD.1.2 Designing for Collateral Hazards

The focus of this Appendix is the design for liquefaction and liquefaction-related hazards, as liquefaction has been perhaps the single most significant cause of damage to bridge structures during past earthquakes. Most of the damage has been related to lateral movement of soil at the bridge abutments. However, cases involving the loss in lateral and vertical bearing support of foundations for central piers of a bridge have also occurred.

Loss in lateral support and permanent ground movement can occur simultaneously during a seismic event. Their simultaneous occurrence is a complicated process that is difficult to represent without the use of very complex computer modeling. For most bridges the complexity of the modeling does not warrant performing a combined analysis. In these cases the recommended methodology is to consider these effects independently, i.e., de-coupled. The reasoning behind this is that it is not likely that the peak vibrational response and the peak spreading or flow effect will occur simultaneously. For many earthquakes the peak vibration response occurs somewhat in advance of

the combined effects of sustained porewater pressure and gravity loads without the inertial loading from the earthquake. Flows can occur several minutes following an earthquake, when porewater pressures redistribute to form a critical combination with gravity loading.

- Dynamic settlement occurs following an earthquake as porewater pressures dissipate.

These liquefaction-related effects are normally considered separately as uncoupled events.

## D.2 LIQUEFACTION<sup>1</sup>

The need for an evaluation of liquefaction and liquefaction-related hazards depends on the level of ground shaking and the magnitude of the earthquake that could occur at a site. In areas of very low seismicity (SDR 1 and SDR 2), no specific seismic design requirements occur. On the other hand, the potential for liquefaction at sites should be determined for sites located in SDR 3, 4, 5, and 6.

The evaluation of liquefaction potential should follow procedures given in Youd and Idriss (1997) and SCEC (1999). These procedures are summarized in Article D.2.

maximum ground movement loading. For very large earthquakes where liquefaction may occur before peak ground accelerations occur, the peak vibration response is likely to be significantly attenuated and, hence, inertial loading reduced from peak design values. In addition peak displacements demands arising from lateral ground spreading are likely to generate maximum pile moments at depths well below peak moments arising from inertial loading. Finally, the de-coupling of response allows the flexibility to use separate and different performance criteria for design to accommodate these phenomena.

Two detailed case studies on the application of the recommended design methods for both liquefaction and lateral flow design are given in the companion Liquefaction Study Report (ATC/MCEER, 2003a) and summarized in Appendix H of this document.

## CD.2 LIQUEFACTION

In SDR's 1 and 2 the potential for liquefaction is generally low. In some cases the peak ground acceleration in these SDR's may exceed 0.15g. While this level of peak ground acceleration is sufficient to cause liquefaction, the magnitude of the earthquake causing liquefaction in these categories will generally be less than 6. For this earthquake magnitude liquefaction develops slowly for most soils, and results in minimal effects other than ground settlement.

The potential for liquefaction in SDR's 3, 4, 5, and 6 is much higher, and therefore careful attention to the determination of the potential for and consequences of liquefaction is needed for sites with these classifications. At some locations it may be necessary to use ground improvement methods to mitigate the potential effects of liquefaction. As these methods are often expensive, detailed consideration of the potential for liquefaction is warranted.

<sup>1</sup> Much of the contents of this discussion of liquefaction was taken from a report titled "Recommended Procedures for Implementation of DMG Special Publication 117, Guideline for Analyzing and Mitigating Liquefaction in California" and referenced as SCEC (1999). The SCEC report was prepared by a group of consultants and government agency staff led by G.R. Martin of the University of Southern California and M. Lew of Law/Crandall. Funding for the report was provided by the City of Los Angeles, the County of Los Angeles, the California Division of Mines and Geology, the Federal Emergency Management Agency, as well as the Counties of Riverside, San Bernadino, San Diego, Orange, and Ventura. The intent of the SCEC report was to provide practical guidance to design engineers in the implementation of liquefaction prediction and hazards evaluation methods. The SCEC report represented the current state-of-the-practice at the time that these Guidelines were being prepared. Where appropriate, the SCEC report recommendations have been updated or augmented in this Appendix to be more consistent with requirements for bridge design or new developments in liquefaction assessment methodologies.

### D.2.1 Preliminary Screening for Liquefaction

An evaluation of liquefaction hazard potential may not be required if the following conditions occur at a site:

- The estimated maximum-past-, current-, and maximum-future-groundwater-levels (i.e., the highest groundwater level applicable for liquefaction analyses) are determined to be deeper than 15 m below the existing ground surface or proposed finished grade, whichever is deeper.
- “Bedrock” or similar lithified formational material underlies the site. In many areas glacially overridden (till) deposits fall in this classification.
- The corrected standard penetration blow count,  $(N_1)_{60}$ , is greater than or equal to 30 in all samples with a sufficient number of tests. If cone penetration test soundings are made, the corrected cone penetration test tip resistance,  $q_{cIN}$ , should be greater than or equal to 160 in all soundings in sand materials.
- The soil is clayey. For purposes of this screening, clayey soils are those that have a clay content (i.e., particle size  $<0.005$  mm) greater than 15%. However, based on the so-called “Chinese Criteria,” (Seed and Idriss, 1982) clayey soils having all of the following characteristics may be susceptible to severe strength loss:
  - Percent finer than 0.005 mm: less than 15 %
  - Liquid Limit: less than 35
  - Water Content: greater than 0.9 of the Liquid Limit

If the screening investigation clearly demonstrates the absence of liquefaction hazards at a project site and the owner concurs, the screening investigation will satisfy the site investigation report requirement for liquefaction hazards. If not, a quantitative evaluation will be required to assess the liquefaction hazards.

### CD.2.1 Preliminary Screening for Liquefaction

Liquefaction will generally occur in loose, saturated granular materials. These granular materials can include silts, sands, and in some cases loose gravels. Liquefaction of loose gravels has been observed during several earthquakes when cohesive soils overlying the gravel prevented drainage of porewater pressures.

Geologically young cohesionless materials are more susceptible than geologically old cohesionless soils, as a result of cementation and other similar aging effects that tend to occur in geologically old materials. Common geologic settings for liquefaction-susceptible soils include unlithified sediments in coastal regions, bays, estuaries, river floodplains and basins, areas surrounding lakes and reservoirs, and wind-deposited dunes and loess. In many coastal regions, liquefiable sediments occupy back-filled river channels that were excavated during Pleistocene low stands of sea level, particularly during the most recent glacial stage. Among the most easily liquefiable deposits are beach sand, dune sand, and clean alluvium that were deposited following the rise in sea level at the start of the Holocene age, about 11,000 years ago.

Preliminary screening can often be used to eliminate a site from further liquefaction consideration. The screening investigation should include a review of relevant topographic, geologic, and soils engineering maps and reports, aerial photographs, groundwater contour maps, water well logs, agricultural soil survey maps, the history of liquefaction in the area, and other relevant published and unpublished reports. The purpose of the screening investigations for sites within zones of required study is to filter out sites that have no potential or low potential for liquefaction.

No specific limitation is placed on the depths of liquefiable soils in the screening process. As discussed in a following section of this Appendix, liquefaction can occur to depths of 25 m or more.

### D.2.2 Field Explorations for Liquefaction Hazards Assessment

Two field exploration methods are normally used during the evaluation of liquefaction potential, Standard Penetration Test (SPT) methods and Cone Penetrometer Test (CPT) methods. Appendix B gives a brief discussion of these methods. Shear wave velocity methods have also been found to be advantageous for evaluating liquefaction potential at some sites. The SPT and CPT methods should be regarded as the minimum requirement for evaluating site liquefaction potential. A geologic reconnaissance and review of the available geotechnical information for the site should supplement any field investigation.

#### *SPT Method*

Procedures for evaluating liquefaction potential using SPT methods are described in detail by Youd and Idriss (1997) and by SCEC (1999). These procedures include consideration of correction factors for drilling method, hole diameter, drive-rod length, sampler type, energy delivery, and spatial frequency of tests.

Information presented in Youd and Idriss (1997) and in SCEC (1999) indicate that the results of SPT explorations are affected by small changes in measurement method; therefore, it is critical for these tests that standard procedures are followed and that all information regarding the test method and equipment used during the field work be recorded. The energy of the SPT hammer system should also be established for the equipment, as this energy directly affects the determination of liquefaction potential. The variation in hammer energy can be as much as a factor of 2, which can easily cause a liquefiable site to be identified as being nonliquefiable, if a correct hammer calibration factor is not introduced.

#### *CPT Method*

The CPT is gaining recognition as the preferred method of evaluating liquefaction potential in many locations. Methods for assessing liquefaction potential from CPT results are given in Youd and Idriss (1997). The primary advantages of the CPT method are:

- The method provides an almost continuous penetration resistance profile that can be used for stratigraphic interpretation, which is particularly important in determining the poten-

### CD.2.2 Field Explorations for Liquefaction Hazards Assessment

A number of factors must be considered during the planning and conduct of the field exploration phase of the liquefaction investigation.

#### *Location of Liquefiable Soils*

During the field investigation, the limits of unconsolidated deposits with liquefaction potential should be mapped within and beyond the footprint of the bridge. Typically, this will involve investigations at each pier location and at enough locations away from the approach fill to establish the spatial variability of the material. The investigation should establish the thickness and consistency of liquefiable deposits from the ground surface to the depth at which liquefaction is not expected to occur. The “zone of influence” where liquefaction could affect a bridge approach fill will generally be located within a 2H:1V (horizontal to vertical) projection from the bottom of the approach fill.

#### *Location of Groundwater Level*

The permanent groundwater level should be established during the exploration program. Shallow groundwater may exist for a variety of reasons, of natural or man-made origin. Groundwater may be shallow because the ground surface is only slightly above the elevation of the ocean, a nearby lake or reservoir, or the sill of a basin. Another concern is man-made lakes and reservoirs that may create a shallow groundwater table in young sediments that were previously unsaturated. If uncertainty exists in the location of the groundwater level, piezometers should be installed during the exploration program. The location of the groundwater level should be monitored in the piezometers over a sufficient duration to establish seasonal fluctuations that may be due to rainfall, river runoff, or irrigation.

Usually, soils located below the groundwater level are fully saturated; however, at locations where fluctuations in groundwater occur, soil can be in a less than fully saturated condition. The liquefaction resistance of the soil is affected by the degree of saturation, with the resistance increasing significantly as the degree of saturation decreases. If the groundwater level fluctuates due to tidal action or seasonal river fluctuations, then the zone of fluctuation will often have a lower degree of saturation, making the soil more resistant to liquefac-

tial for lateral spreading, lateral flows, and significant differential post-liquefaction settlements.

- The repeatability of the test is very good.
- The test is fast and economical compared to drilling and laboratory testing of soil samples.

The limitations of the method are:

- The method does not routinely provide soil samples for laboratory tests.
- The method provides approximate, interpreted soil behavior types and *not* the actual soil types according to ASTM Test Methods D 2488 (Visual Classification) or D 2487 (USCS Classification) [ASTM, 1998].
- The test cannot be performed in gravelly soils and sometimes the presence of hard/dense crusts or layers at shallow depths makes penetration to desired depths difficult.

The CPT method should be performed in accordance with ASTM D 3441 (ASTM, 1998). Generally, it is recommended that at least one boring be drilled to confirm soil types and obtain samples for laboratory testing if the CPT method is used for evaluating liquefaction potential.

#### *Shear Wave Velocity Method*

Correlations have also been developed between liquefaction potential and shear wave velocity, as reported in Youd and Idriss (1997). The shear wave velocity method offers a rapid screening of liquefiable sites, if velocities are obtained by the Spectral Analysis of Surface Wave (SASW) procedure. Procedures involving the use of boreholes, such as downhole and crosshole methods, can be used as a comparison with liquefaction potential obtained by SPT or CPT methods. The shear wave velocity method also provides an estimate of liquefaction potential in soils where SPT and CPT methods are not usually successful, such as in gravels. Limitations of the shear wave velocity method include its limited database and its inability to measure thin layers that could serve as sliding surfaces for flow failures.

### **D.2.3 Ground Motions for Liquefaction Analysis**

To perform an analysis of liquefaction triggering, liquefaction settlement, seismically induced

tion. Unless the seasonal fluctuation is in place for an extended period of time, say weeks at a higher level, it is usually acceptable to use a long-term groundwater level as a basis for design.

#### *Depth of Liquefaction*

The field exploration should be conducted to the maximum depth of liquefiable soil. A depth of about 15 m has often been used as the depth of analysis for the evaluation of liquefaction. However, the Seed and Idriss (1982) EERI Monograph on "Ground Motions and Soil Liquefaction During Earthquakes" does not recommend a minimum depth for evaluation, but notes 12 m as a depth to which some of the numerical quantities in the "simplified procedure" can be estimated reasonably. Liquefaction has been known to occur during earthquakes at deeper depths than 15 m given the proper conditions such as low-density granular soils, presence of groundwater, and sufficient cycles of earthquake ground motion. For example, liquefaction occurred to depths in excess of 25 m during the 1964 Alaska earthquake.

For this reason it is recommended that a minimum depth of 25 m below the existing ground surface or lowest proposed finished grade (whichever is lower) be investigated for liquefaction potential. For deep foundations (e.g., shafts or piles), the depth of investigation should extend to a depth that is a minimum of 6 m below the lowest expected foundation level (e.g., shaft bottom or pile toe) or 25 m below the existing ground surface or lowest proposed finished grade, whichever is deeper.

If, during the investigation, the indices to evaluate liquefaction indicate that the liquefaction potential may extend below that depth, the exploration should be continued until a significant thickness (e.g., at least 3 m, to the extent possible) of nonliquefiable soils is encountered.

### **CD.2.3 Ground Motions for Liquefaction Analysis**

The peak ground acceleration used in the simplified liquefaction evaluation is defined at the



settlement, and lateral spreading, a peak horizontal ground acceleration and a mean earthquake magnitude must be established for the site:

- *Peak Ground Acceleration (PGA)*: The PGA may be determined from  $0.40 S_{DS}$  as defined in Article 3.4.1 or from the seismic hazard maps described in Article 3.4 or a site-specific probabilistic seismic hazard analysis (PSHA). Appropriate adjustments must be made to correct the firm-ground motion (obtained from the map or from the PSHA) for local site effects. This adjustment is included in  $S_{DS}$ .
- *Earthquake Magnitude*: The magnitude required in the liquefaction analysis can be determined from magnitude-distance deaggregation information for PGA given in the USGS Website ([http:// geohazards.cr.usgs.gov/eq/](http://geohazards.cr.usgs.gov/eq/)) or as part of the site-specific PSHA. The mean magnitude of the deaggregation will be applicable for most locations; however, if a single or few magnitude-distance peaks dominate the distribution (e.g., characteristic earthquake on a seismic source), the peak or the mean of the few peaks should be used to define the magnitude. In locations where bi- or tri-modal magnitude-distance distributions occur, each magnitude and an associated acceleration level should be considered.

Although for most analyses, information in the USGS Website will be sufficient for determining the PGA and the earthquake magnitude, a site-specific PSHA may provide better estimation of the ground motions at some locations. The decision to perform a PSHA should be made after detailed discussions with the owner.

#### D.2.4 Evaluation of Liquefaction Hazard

Two basic procedures are used to evaluate the potential for liquefaction at a site. These involve

- a simplified procedure that is based on empirical correlations to observations of liquefaction, or
- more rigorous numerical modeling.

The decision between the two procedures should be made after careful review of conditions at the site and the risks associated with liquefaction, and with the concurrence of the owner.

ground surface. Maps and most site-specific hazard evaluations also define the PGA at the ground surface; however, the soil conditions used to develop the PGA maps or the attenuation relationships in the PSHA are relatively stiff (Site Classification B/C) as defined in Article 3.4.2 of the companion *Guidelines*. It is necessary to adjust these accelerations for local site effects. This adjustment can be made by either using the factors given in Table 3.4.2.3-1 or by conducting site-specific ground response studies with a computer program such as SHAKE (Idriss and Sun, 1992) or DESRA 2 (Lee and Finn, 1978).

When Table 3.4.2.3-1 is used to estimate site factors, the amplification or attenuation factor is determined on the basis of the site class before liquefaction and the spectral acceleration at short periods ( $S_s$ ), where  $S_s$  is equal to  $2.5 \times \text{PGA}$ .

#### CD.2.4 Evaluation of Liquefaction Hazard

For most projects the simplified procedure will be acceptable. However, for critical projects, more rigorous modeling using equivalent linear and nonlinear computer codes may be appropriate. Conditions warranting use of more rigorous methods include (1) sites where liquefiable soils extend to depths greater than 25 m, (2) sites that have significant interlayering, particularly where interlayers comprise highly permeable soils or soft clay layers, and (3) sites where the cost of ground remediation methods to mitigate liquefaction is great. Most site-specific ground response analyses result in lower estimations of ground acceleration and shearing stresses within the soil profile be-

#### D.2.4.1 Simplified Method

The most basic procedure used in engineering practice for assessment of site liquefaction potential is that of the “Simplified Procedure” originally developed by Seed and Idriss (1971, 1982) with subsequent refinements by Seed et al. (1983), Seed et al. (1985), Seed and De Alba (1986), and Seed and Harder (1990). The procedure essentially compares the cyclic resistance ratio (CRR) [the cyclic stress ratio required to induce liquefaction for a cohesionless soil stratum at a given depth] with the earthquake-induced cyclic stress ratio (CSR) at that depth from a specified design earthquake (defined by a peak ground surface acceleration and an associated earthquake magnitude).

##### *Cyclic Resistance Ratio*

Values of CRR for the Simplified Method were originally established from databases for sites that did or did not liquefy during past earthquakes and where values of the normalized SPT value,  $(N_1)_{60}$ , could be correlated with liquefied strata. The current version of the baseline chart defining values of CRR as a function of  $(N_1)_{60}$  for magnitude 7.5 earthquakes is shown on Figure D.2.4-1. This chart was established by a consensus at a 1996 NCEER Workshop, which convened a group of experts to review current practice and new developments in the area of liquefaction evaluations (Youd and Idriss, 1997). Magnitude adjustment factors are presented in Figure D.2.4-2. The CRR value can also be obtained using CPT, Becker Hammer Tests (BHT), or shear wave velocity methods, as discussed by Youd and Idriss (1997). The determination of CRR must consider the fines content of the soil, the energy of the hammer for the SPT and BHT methods, the effective overburden pressure, and the magnitude of the earthquake. Figures D.2.4-3 and D.2.4-4 show the liquefaction potential (i.e., CRR values) for the CPT and shear wave velocity methods.

##### *Cyclic Stress Ratio*

For estimating values of the earthquake-induced cyclic shearing stress ratio, CSR, the NCEER Workshop recommended essentially no change to the original simplified procedure (Seed and Idriss, 1971), where the use of a mean  $r_d$  fac-

cause the energy dissipative mechanisms occurring during liquefaction are explicitly considered in this approach.

#### CD.2.4.1 Simplified Method

Adjustments for changes in water table and overburden condition should be made during the simplified analyses. The following guidance can be used in making these adjustments.

##### *Overburden Corrections for Differing Water Table Conditions*

To perform analyses of liquefaction triggering, liquefaction settlement, seismically induced settlement, and lateral spreading, it is necessary to develop a profile of SPT blow counts, CPT  $q_c$ -values or shear wave velocities that have been normalized using the effective overburden pressure.

This normalization should be performed using the effective stress profile that existed at the time the SPT, CPT or shear wave velocity testing was performed. Then, those normalized values are held constant throughout the remainder of the analyses, regardless of whether or not the analyses are performed using higher or lower water-table conditions. Although the possibility exists that softening effects due to soil moistening can influence CRR results if the water table fluctuates, it is commonly assumed that the only effect that changes in the water table have on the results is due to changes in the effective overburden stress.

Raw, field N-values (or  $q_c$ -values) obtained under one set of groundwater conditions should not be input into an analysis where they are then normalized using  $C_N$  correction factors based on a new (different) water table depth.

##### *Overburden Corrections for Differing Fill Conditions*

Approach fills and other increases in overburden pressure should be handled similar to that described above for changes in groundwater location. It is necessary to develop a profile of SPT blow counts or CPT  $q_c$ -values that have been normalized using the effective overburden pressure existing before the fill is placed. Then, these normalized values are held constant throughout the remainder of the analyses, regardless of whether or not the analyses are performed using a deeper fill.

Although the overburden effects of the fill will modify the effective stress condition and could change the SPT, CPT or shear wave velocity re-

sults, it is commonly assumed that these effects will be minor.

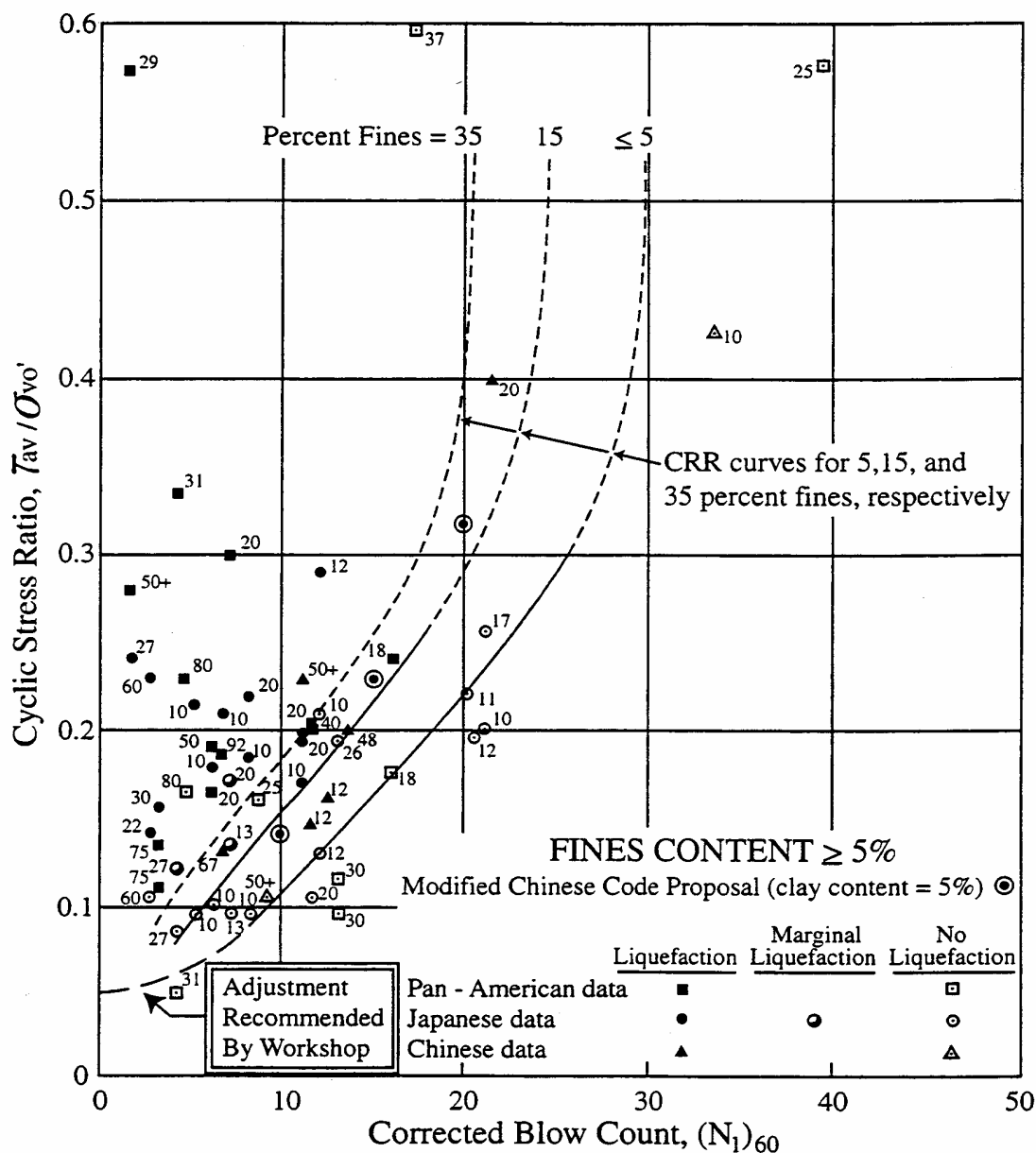


**Figure D.2.4-1 Simplified Base Curve Recommended for Determination of CRR from SPT Data for Magnitude 7.5 Earthquakes, with Empirical Liquefaction Data (after Youd and Idriss, 1997)**

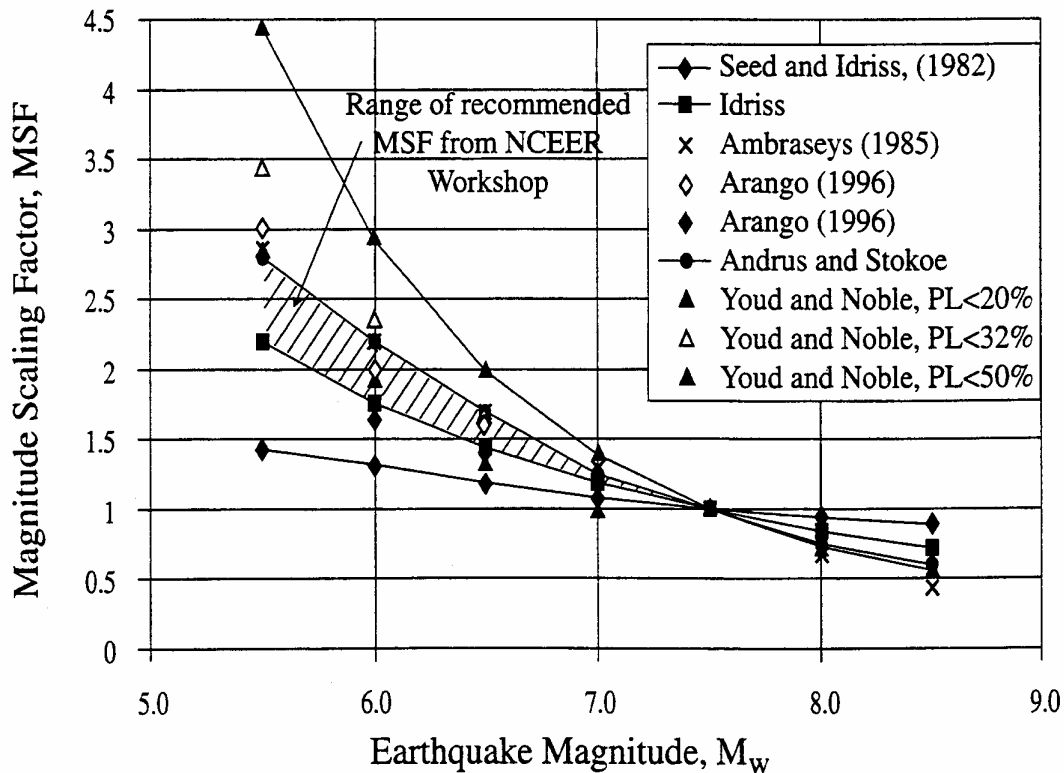


**Figure D.2.4-2** Magnitude Scaling Factors derived by Various Investigators (after Youd and Idriss, 1997)

CSR is calculated using the following equation:

$$CSR = (\tau_{av}/\sigma'_{vo}) = 0.65(a_{max}/g)(\sigma_{vo}/\sigma'_{vo})r_d$$

where  $\tau_{av}/\sigma'_{vo}$  is the earthquake-induced shearing stress,  $a_{max}/g$  is the PGA at the ground surface,  $\sigma_{vo}/\sigma'_{vo}$  is the ratio of total overburden stress to effective overburden stress, and  $r_d$  is a soil flexibility number.

#### *Liquefaction Potential*

Once values of CRR and CSR are established for a soil stratum at a given depth, the factor of safety against liquefaction (i.e.,  $FS = CRR/CSR$ ) can be computed. The ratio of CRR to CSR should be greater than 1.0 to preclude the development of liquefaction. As the ratio drops below 1.0, the potential for liquefaction increases. Even when the ratio of CRR to CSR is as high as 1.5, increases in porewater pressure can occur. The potential consequences of these increases should be considered during design.

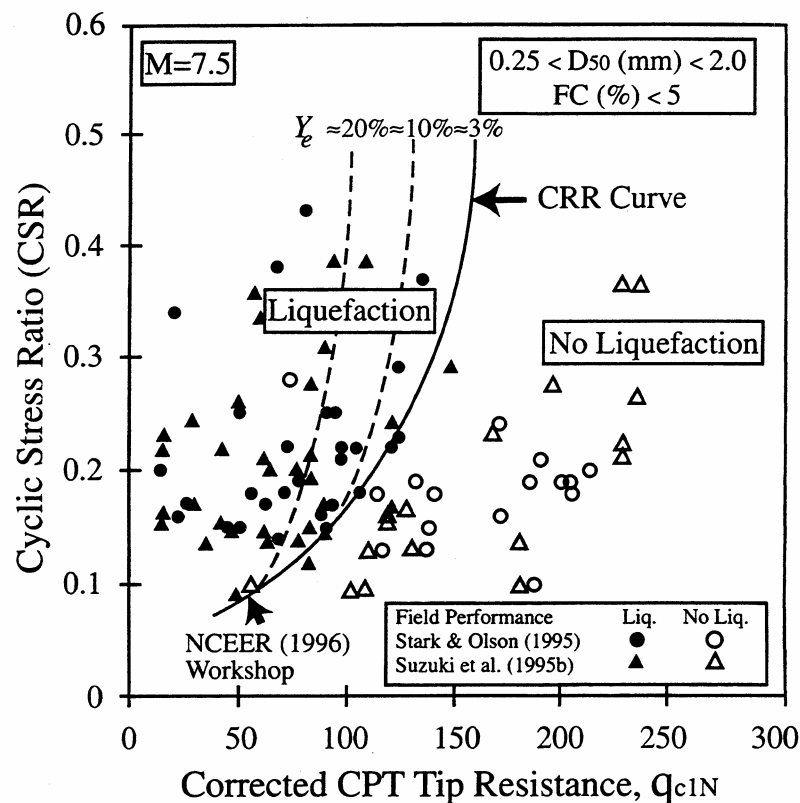


**Figure D.2.4-3** Curve Recommended for Calculation of CRR from CPT Data, with Empirical Liquefaction Data

#### D.2.4.2 Numerical Modeling Methods

For critical projects, the use of equivalent linear or non-linear site specific, one-dimensional ground response analyses may be warranted to assess the liquefaction potential at a site. For these analyses, acceleration time histories representative of the seismic hazard at the site are used to define input ground motions at an appropriate firm-ground interface at depth.

One common approach is to use the equivalent linear total stress computer program SHAKE (Idriss and Sun, 1992) to determine maximum earthquake-induced shearing stresses at depth for use with the simplified procedure described above, in lieu of using the mean values of  $r_d$  shown in Figure D.2.4-5. Another alternative involves the use of nonlinear, effective stress methods, such as with the computer program DESRA 2 (Lee and Finn, 1978) or DESRA-MUSC (Martin and Qiu, 2000), a modified version of DESRA 2.

#### CD.2.4.2 Numerical Modeling Methods

In general, equivalent linear analyses are considered to have reduced reliability as ground shaking levels increase to values greater than about 0.4g in the case of softer soils, or where maximum shearing strain amplitudes exceed 1 to 2%. For these cases, true non-linear site response programs should be used, where non-linear shearing stress-shearing strain models (including failure criteria) can replicate the hysteric soil response over the full time history of earthquake loading. The computer program DESRA 2, originally developed by Lee and Finn (1978), was perhaps the first of the widely recognized non-linear, one-dimensional site response program. Since the development of DESRA 2, a number of other non-linear programs have been developed, including MARDES (Chang et al., 1991), D-MOD (Matasovic, 1993) and SUMDES (Li et al., 1992), and DESRA-MUSC (Martin and Qiu, 2000).

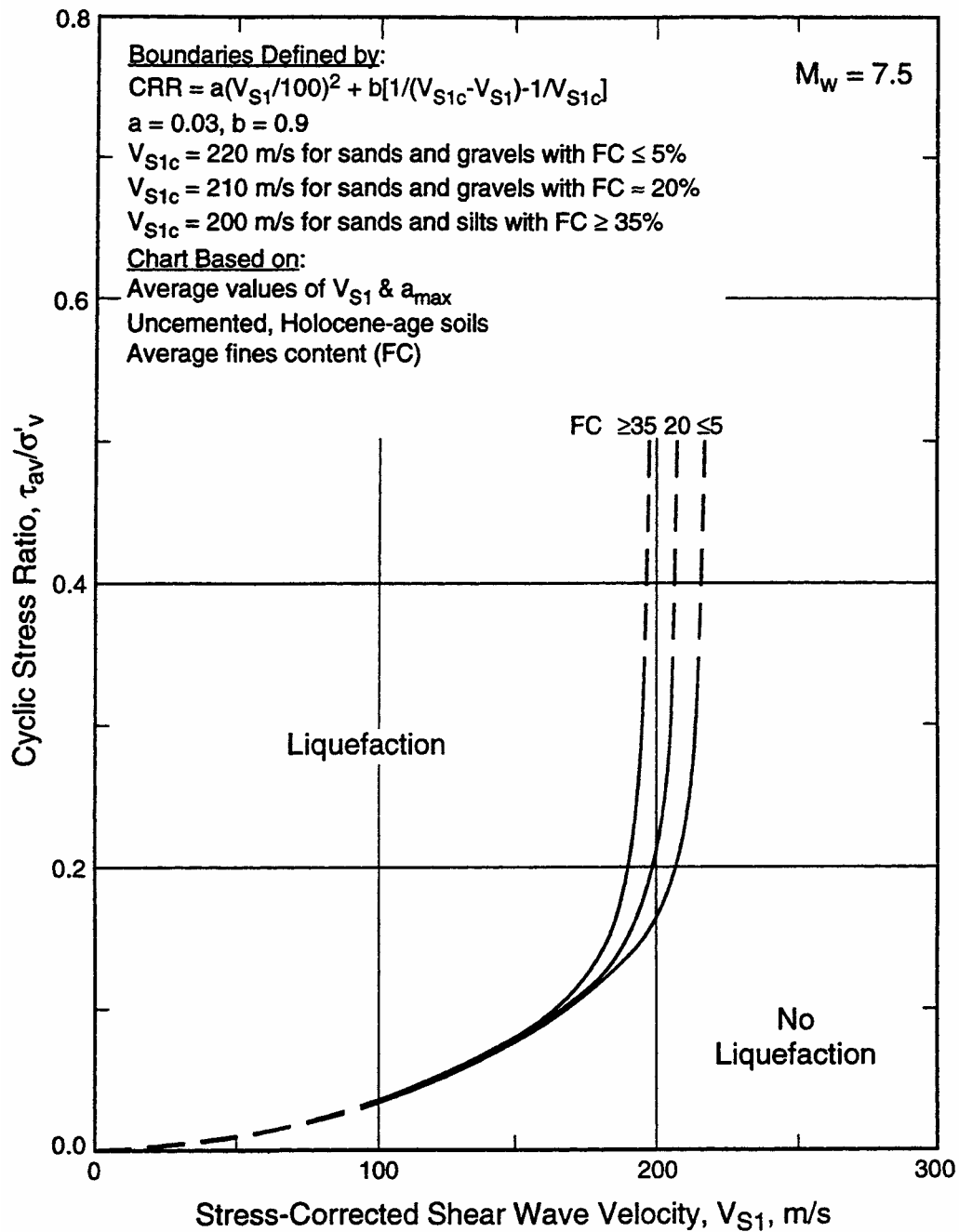
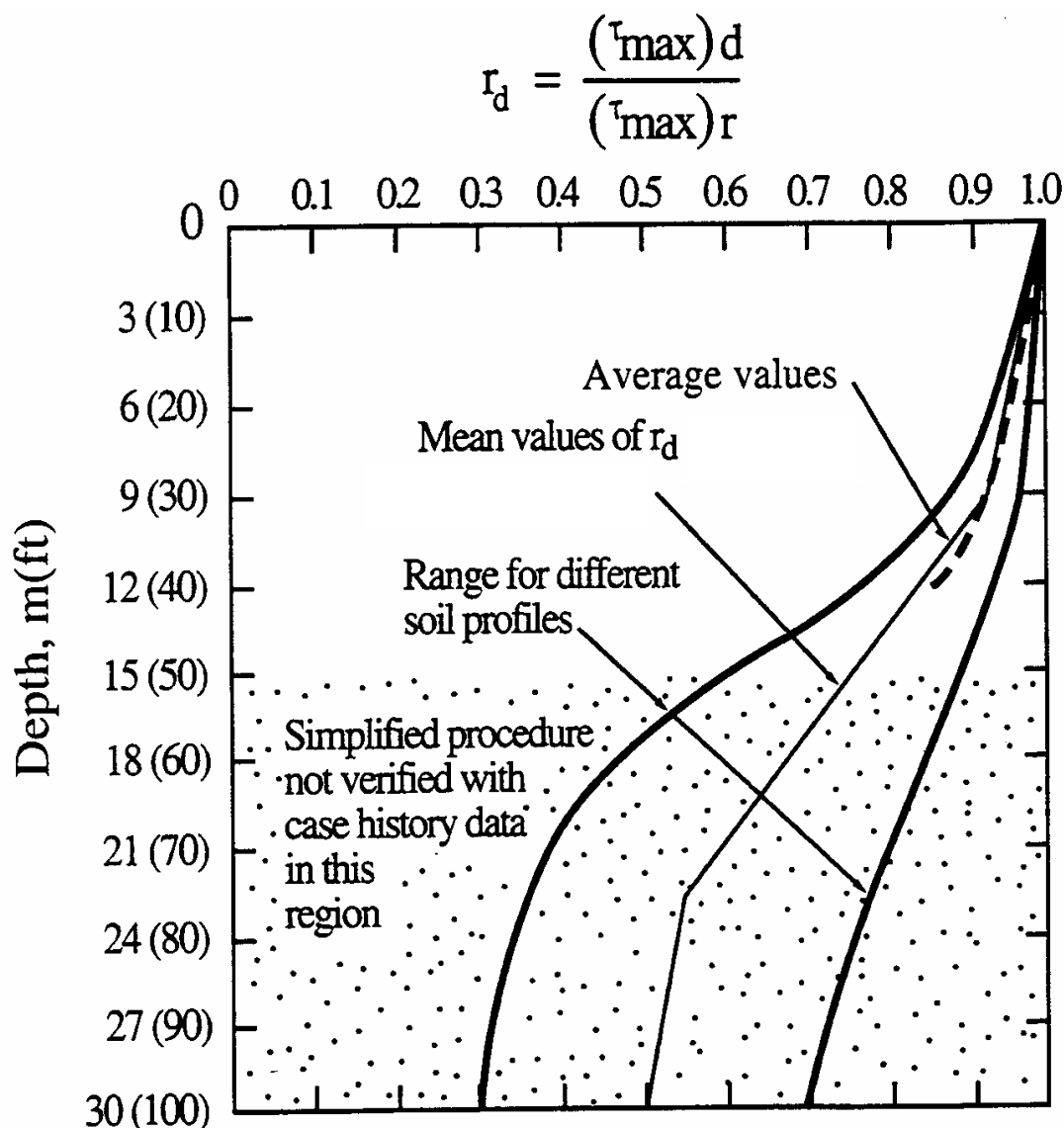


Figure D.2.4-4 Recommended Liquefaction Assessment Chart Based on  $V_{S1}$  and CSR for Magnitude 7.5 Earthquakes and Uncemented Soils of Holocene Age



**Figure D.2.4-5 Soil Flexibility Factor ( $r_d$ ) versus Depth Curves Developed by Seed and Idriss (1971) with Added Mean Value Lines (after Youd and Idriss, 1997)**

### D.2.5 Liquefaction Hazards Assessment

Results of the liquefaction assessment are used to evaluate the potential severity of three liquefaction-related hazards to the bridge:

- Flow failures that involve large translational or rotational slope failures mobilized by existing static stresses (i.e., the site static factor of safety drops below 1.0 due to low strengths of liquefied soil layers).
- Limited lateral spreads that involve a progressive accumulation of deformations during

### CD.2.5 Liquefaction Hazards Assessment

The factor of safety from the liquefaction analysis can be used to determine if a more detailed evaluation of these hazards is warranted. No single factor of safety value can be cited in a guideline, as considerable judgment is needed in weighing the many factors involved in the decision. A number of those factors are noted below:

- The type of structure and its vulnerability to damage. Structural mitigation solutions may be more economical than ground remediation.

ground shaking with eventual deformations that can range from a fraction of a meter to several meters.

- Ground settlement.

The potential for these hazards can be determined initially on the basis of the factor of safety calculated from the ratio of CRR to CSR. If the ratio is less than 1.0 to 1.3, the hazard should be evaluated following the guidelines given below, unless agreed otherwise by the owner.

- Levels of risk accepted by the owner regarding design for life safety, limited structural damage, or essentially no damage.
- Damage potential associated with the particular liquefaction hazards. Flow failures or major lateral spreads pose more damage potential than differential settlement. Hence, factors of safety could be adjusted accordingly.
- Damage potential associated with design earthquake magnitude. A magnitude 7.5 event is potentially far more damaging than a 6.5 event.
- Damage potential associated with SPT values, i.e., low blow counts have a greater cyclic strain potential than higher blow counts.
- Uncertainty in SPT- or CPT- derived liquefaction strengths used for evaluations. Note that a change in silt content from 5 to 15% could change a factor of safety from say 1.0 to 1.25.
- For high levels of design ground motion, factors of safety may be indeterminate. For example, if  $(N_I)_{60} = 20$ ,  $M = 7.5$  and fines content = 35% liquefaction strengths cannot be accurately defined due to the vertical asymptote on the empirical strength curve.

In addition a change in the required factor of safety from 1.0 to 1.25 often only makes minor differences in the extent of liquefiable zones, albeit it would increase the blow count requirements for ground remediation. However, for the example cited, the additional costs of remediation from  $(N_I)_{60} = 20$  to  $(N_I)_{60} = 25$  say, could be small.

The final choice of an appropriate factor of safety must reflect the particular conditions associated with a specific site and the vulnerability of site-related structures.

#### D.2.5.1 Lateral Flows

Flow failures are the most catastrophic form of ground failure that may be triggered when liquefaction occurs. These large translational or rotational flow failures are mobilized by existing static stresses when average shearing stresses on potential failure surfaces exceed the average residual strength developing in the liquefied soil.

To assess the potential for flow failure, the static strength properties of the soil in a liquefied layer is replaced with the residual strength determined from Figure D.2.5-1. A conventional slope stability check is then conducted. No seismic coef-

#### CD.2.5.1 Lateral Flows

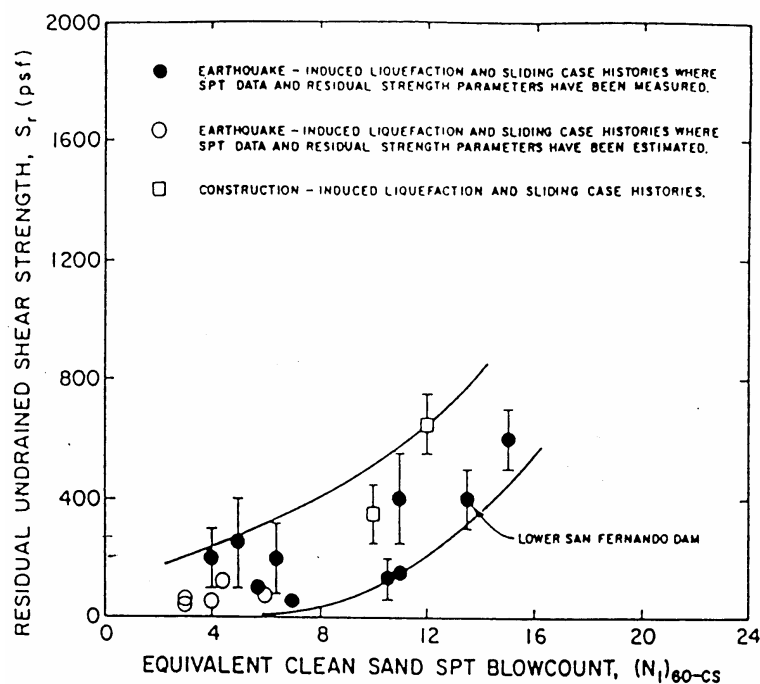
Valuable commentary on this problem may be found, for example, in publications by NRC (1985), Seed (1987), Seed and Harder, (1990), Dobry (1995), and Kramer (1996). The topic of Post-Liquefaction Shear Strength of Granular Soils was also the subject of an NSF-sponsored NCEER Workshop at the University of Illinois in 1997, a summary of which has been published by Stark et al. (1998). The complexities of the problem have also been illustrated in centrifuge tests, as described by Arulandan and Zeng (1994) and Fiegel and Kutter (1994).



ficient is used during this evaluation, thus representing conditions after the completion of the earthquake. The resulting factor of safety defines the potential for flow failures. If the factor of safety is less than 1.0, lateral flow is predicted.

The estimation of deformation associated with lateral flow cannot be easily made. The deformations can be in excess of several meters, depending on the geometry of the flowing ground and the types and layering of soil. In the absence of reliable methods for predicting deformations, it is usually necessary to assume that the soil will undergo unlimited deformations. If the loads imposed by these movements exceed those that can be tolerated by the structure, some type of ground remediation will likely be required. This situation should be brought to the attention of the owner and a strategy for dealing with the flow problem agreed upon.

The most difficult step in the flow analysis is the determination of the residual strength of the soil. The most common procedure for evaluating the residual strength involves an empirical correlation between SPT blow counts and apparent residual strength back-calculated from observed flow slides. This relationship is shown in Figure D.2.5-1. Mean or lower-bound values in the data range shown are often adopted. Some experimental work suggests that residual strength is related to confining pressure (Stark and Mesri, 1992). Steady state undrained shear strength concepts based on laboratory tests have also been used to estimate post liquefaction residual strengths (Poulos et al., 1985; Kramer, 1996). Due to the difficulties of test interpretation and corrections for sample disturbance, empirically based correlations are normally used.



RECOMMENDED FINES CORRECTION FOR  $S_r$  EVALUATION USING SPT DATA

Percent Fines	$N_{cor}$ (blows/ft)
10%	1
25%	2
50%	4
75%	5

**Figure D.2.5-1** Relationship between Residual Strength ( $S_r$ ) and Corrected "Clean Sand" SPT Blowcount  $(N_1)_{60}$  from Case Histories (after Seed and Harder, 1990)

### D.2.5.2 Lateral Spreading

The degradation in undrained shearing resistance arising from liquefaction can lead to limited lateral spreads induced by earthquake inertial loading. Such spreads can occur on gently sloping ground or where nearby drainage or stream channels can lead to static shearing stress biases on essentially horizontal ground (Youd, 1995).

Four general approaches can be used to assess the magnitude of the lateral spread hazard:

- *Youd Empirical Approach:* Using regression analyses and a large database of lateral spread case histories from past earthquakes, Bartlett and Youd (1992) developed empirical equations relating lateral-spread displacements to a number of site and source parameters. A refined version of this approach was recently presented by Youd et al. (1999). Generally, this approach should be used only for screening of the potential for lateral spreading, as the uncertainty associated with this method of estimating displacement is generally assumed to be too large for bridge design.
- *Newmark Time History Analyses:* The simplest of the numerical methods is the so called Newmark sliding block analysis, (Newmark, 1965; Kramer, 1996), where deformation is assumed to occur on a well-defined failure plane and the sliding mass is assumed to be a rigid block. This approach requires (1) an initial pseudo-static stability analysis to determine the critical failure surface and associated yield acceleration coefficient ( $k_y$ ) corresponding to a factor of safety of 1.0, and (2) a design earthquake acceleration record at the base of the sliding mass. Cumulative displacements of the sliding mass generated when accelerations exceed the yield acceleration are computed using computer programs such as described by Houston et al. (1987). These methods are most appropriate when local site effects modify the ground motion as it propagates through the soil profile and when the database for the chart method described below is not adequate. This latter consideration generally involves sites where the source mechanism will be from a magnitude 8 or higher event.
- *Simplified Newmark Charts:* Charts have been developed by a number of individuals

### CD.2.5.2 Lateral Spreading

The lateral spreading mechanism is a complex process involving the post-liquefaction strength of the soil, coupled with the additional complexities of potential porewater pressure redistribution and the nature of earthquake loading on the sliding mass. At larger cyclic shearing strains, the effects of dilation can also significantly increase post-liquefaction undrained shearing resistance of the liquefied soil. Incremental permanent deformations will still accumulate during portions of the earthquake load cycles when low residual resistance is available. Such low resistance will continue even while large permanent shearing deformations accumulate through a ratcheting effect. These effects have recently been demonstrated in centrifuge tests to study liquefaction-induced lateral spreads, as described by Balakrishnan et al. (1998). Once earthquake loading has ceased, the effects of dilation under static loading can mitigate the potential for a flow slide.

The four methods available for estimating deformations from lateral spreading account for this complex process in varying degrees.

#### *The Youd Empirical Approach*

The Youd empirical approach uses a variety of earthquake parameters, including magnitude, geometry, and soil grain size in an empirical equation to estimate displacement. Two cases, a sloping ground model and a free-face model, are used. This prediction method is the least reliable in the small displacement range with the level of accuracy probably no better than 1 m. However, it does allow a relatively straightforward screening to be accomplished to identify the potential severity of lateral spreads. Several research projects are also presently in progress to enhance these empirical prediction models by improvements in approaches used in the regression analysis and the use of a larger database.

#### *Newmark Time History Analyses*

The Newmark method has been used extensively to study earthquake-induced displacements in dams (e.g., Makdisi and Seed, 1978) and natural slopes (e.g., Jibson, 1993). This approach involves the double integration of earthquake records above the yield acceleration. The yield acceleration ( $k_y$ ) is determined by finding the seismic coefficient that causes the factor of safety in a slope stability assessment to be 1.0. During the stability analyses,

(Franklin and Chang, 1977; Hynes and Franklin, 1984; Wong and Whitman, 1982; and Martin and Qiu, 1994) using large databases of earthquake records and the Newmark Time History Analysis method. These charts allow deformations during seismic loading to be estimated using relationships between the acceleration ratio (i.e., ratio of yield acceleration ( $k_y$ ) to the peak ground acceleration ( $k_{max}$ ) occurring at the base of the sliding mass) to ground displacement. The Martin and Qiu (1994) charts are recommended in this Appendix, as they include peak ground acceleration and peak ground velocity as additional regression parameters. This method does not include earthquake magnitude. Martin and Qiu note that magnitude was not a statistically significant parameter for the range of magnitudes (M6 to M7.5) used in their evaluation.

- *Numerical Modeling:* The most rigorous approach to assessing liquefaction-induced lateral spread or slope deformations entails the use of dynamic finite element / finite difference programs coupled with effective stress based soil constitutive models. However, the use of such programs is normally beyond the scope of routine bridge design projects. Finn (1991) gives a summary of such approaches, and a recent case history has been described by Elgamel et al. (1998).

The decision between use of the Youd empirical approach and any one of several charts or numerical models will depend on a number of factors, including the level of seismic loading and the consequences of failure. Normally, the Youd empirical approach should be used only for screening of the potential for lateral spreading, as the uncertainty associated with this method of estimating displacements is generally assumed to be large. Although charts and numerical methods offer the capability of estimating displacements more accurately, these methods are often limited by the methods of characterizing the boundary conditions for the problem and on the selection of material properties. Extreme care must be exercised when any of these methods are used.

If lateral spreading is anticipated at a site, the geotechnical engineer should meet with the owner and decide what approach offers the most appropriate method of estimating the magnitude of lateral spread.

the liquefied layer is modeled with the residual strength of the soil. Other layers with partial buildup in porewater pressure can also be degraded in strength during the evaluation.

The earthquake records must be selected from the available catalogue of records, such that they are representative of the source mechanism, magnitude, and distance for the site. A minimum of three records from three independent earthquakes should be selected for the Newmark analyses. Often it is necessary to modify these records for local site effects, as the ground motion propagates through soil to the base of the sliding block.

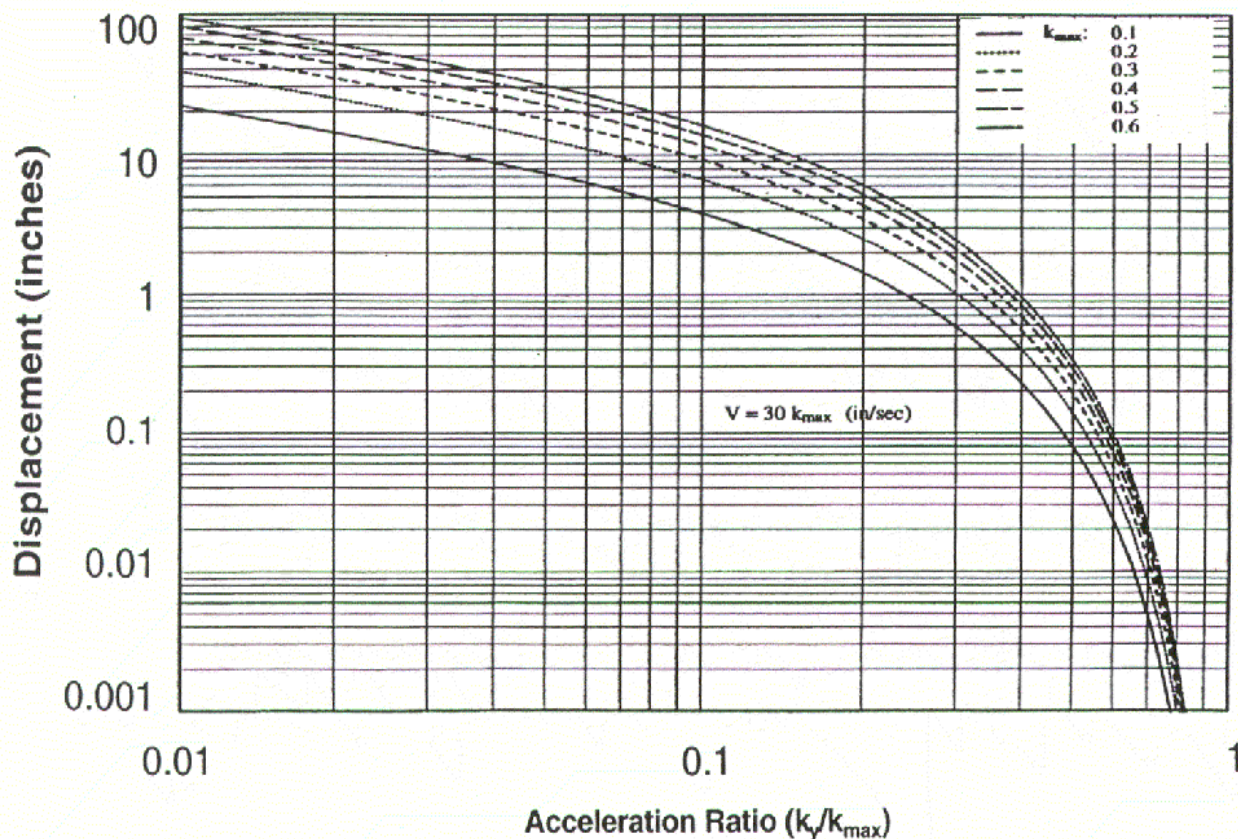
A number of uncertainties are inherent in this approach due to the assumptions involved. In particular, for liquefaction-induced lateral spreads, uncertainties include:

- The point in the time history when cyclic strength degradation or liquefaction is triggered.
- The magnitude of the apparent post-liquefaction residual resistance as discussed above.
- The influence of the thickness of liquefied soil on displacement.
- Changes in values of yield acceleration ( $k_y$ ) as deformations accumulate.
- The influence of a non-rigid sliding mass.
- The influence of ground motion incoherence over the length of the sliding mass.

#### *Simplified Newmark Charts*

The simplified chart correlations were developed by conducting Newmark analyses on a large number of earthquake records and then statistically analyzing the results. Of the various chart methods, the Martin and Qiu (1994) method is recommended for use on bridge design projects. Figure D.2.5-2 and Figure D.2.5-3 show the relationships developed by Martin and Qiu (1994). A velocity-to-acceleration ratio of 60 is used if the epicentral distance is less than 15 km; a velocity-to-acceleration ratio of 30 is used for distances greater than 30 km; and values are interpolated between these distances. These figures are appropriate for magnitudes between 6 and 7.5. If magnitudes exceed 7.5, the deformation should be determined using other methods, such as by conducting Newmark time history analyses or 2-dimensional numerical modeling.

The Franklin and Chang (1977) procedure,

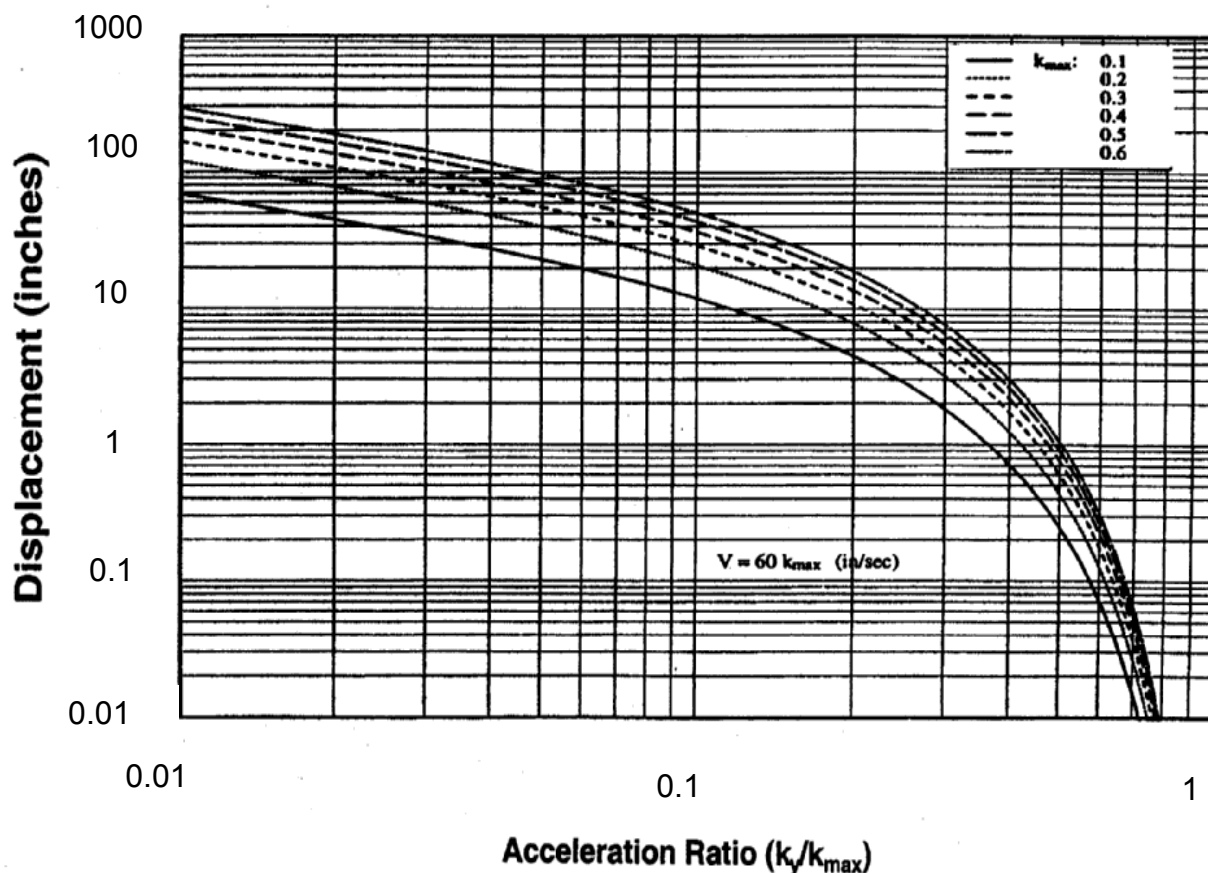


Note: Displacements less than several inches are shown for presentation purposes only. The accuracy of the predictive method is such that predicted deformations less than several inches should not be used.

**Figure D.2.5-2** Martin and Qiu (1994) Simplified Displacement Chart for Velocity-Acceleration Ratio of 30

which was given in earlier editions of the *AASHTO Standard Specifications for Highway Bridges*, is now thought to overestimate displacements, partly because it was developed by bounding all data and partly because the database had some artificially high records. The Hynes and Franklin (1984) charts used the same database as did Martin and Qiu, and therefore the mean values from the Hynes and Franklin chart are normally similar to the values estimated by the Martin and Qiu method. Wong and Whitman (1982) provides the smallest estimate of displacements, and appears to be unconservative at times.

To use these charts, the yield acceleration is determined by finding the seismic coefficient that causes the factor of safety in a slope stability assessment to be 1.0. As noted for the Newmark Time History Analyses, the liquefied layer is modeled with the residual strength of the soil.



Note: Displacements less than several inches are shown for presentation purposes only. The accuracy of the predictive method is such that predicted deformations less than several inches should not be used.

Figure D.2.5-3 Martin and Qiu (1994) Simplified Displacement Charts for Velocity-Acceleration Ratio of 60

Other layers with partial buildup in porewater pressure can also be degraded in strength during the evaluation. With the yield acceleration and the peak ground acceleration at the base of the failure surface ( $k_{max}$ ), it is a simple matter to enter the chart and determine the estimated amount of displacement.

These simplified chart methods are limited by the database used in their development. Typically few records greater than magnitude 7.5 were available for analysis, and therefore, use of the methods for larger magnitudes must be done with caution. Other limitations are similar to those presented for the Newmark Time History Analyses.

#### Numerical Modeling

Various two-dimensional, nonlinear computer programs have been used to perform these analyses.

For realistic modeling, these programs must be able to account for large displacements, nonlinear soil properties, and changes in effective stress during seismic modeling. One computer program seeing increasing use for this type of modeling is FLAC (Itasca, 1998). This program has been used on a number of bridge-related projects, including the Alaskan Way Viaduct in downtown Seattle, Washington (Kramer et al., 1995).

As with any rigorous modeling method, considerable experience and judgment are required when using a program such as FLAC to model soil-pile-structure interaction during earthquake-induced liquefaction. Good practice when using these methods is to compare the results to results of empirically-based simplified methods or to laboratory experimental data, such as produced in the centrifuge.

#### D.2.5.3 Settlement

Another consequence of liquefaction resulting from an earthquake is the volumetric strain caused by the excess porewater pressures generated in saturated granular soils by the cyclic ground motions. The volumetric strain, in the absence of lateral flow or spreading, results in settlement. Liquefaction-induced settlement could lead to collapse or partial collapse of a structure, especially if there is significant differential settlement between adjacent structural elements. Even without collapse, significant settlement could result in damage.

In addition to the settlement of saturated deposits, the settlement of dry and/or unsaturated granular deposits due to earthquake shaking should also be considered in estimating the total seismically induced settlements.

#### CD.2.5.3 Settlement

The Tokimatsu and Seed (1987) procedures for both saturated and dry (or unsaturated) sands is the most common of the procedures currently used to estimate the magnitude of settlement. Figure D.2.5-4 shows the relationship between the cyclic stress ratio ( $\tau_{av}/\sigma'_o$ ) and volumetric strain for different values of  $(N_1)_{60}$ . It should also be noted that the settlement estimates are valid only for level-ground sites that have no potential for lateral spreading. If lateral spreading is likely at a site and is not mitigated, the settlement estimates using the Tokimatsu and Seed method will likely be less than the actual values.

The settlement of silty sand and silt requires adjustments of the cyclic strength for fines content. Ishihara (1993) recommends increasing the cyclic shear strength of the soils if the Plasticity Index (PI) of the fines is greater than 10. This increases the factor of safety against liquefaction and decreases the seismically-induced settlement estimated using the Ishihara and Yoshimine procedure. Field data suggest that the Tokimatsu and Seed procedure without correcting the SPT values for fines content could result in overestimation of seismically-induced settlements (O'Rourke et al., 1991; Egan and Wang, 1991). The use of an appropriate fines-content correction will depend on whether the soil is dry/unsaturated or saturated and if saturated whether it is completely liquefied (i.e., post-liquefaction), on the verge of becoming liquefied (initial liquefaction), or not liquefied. SCEC (1999) suggests that for 15% fines, the SPT correction value ranges from 3 to 5 and for 35% fines

it ranges from 5 to 9.

Although the Tokimatsu and Seed procedure for estimating liquefaction- and seismically-induced settlements in saturated sand is applicable for most level-ground cases, caution is required when using this method for stratified subsurface conditions. Martin et al. (1991) demonstrated that for stratified soil systems, the SPT-based method of liquefaction evaluation outlined by Seed et al. (1983) and Seed et al. (1985) could over-predict (conservative) or under-predict (unconservative) excess porewater pressures developed in a soil layer depending on the location of the soil layer in

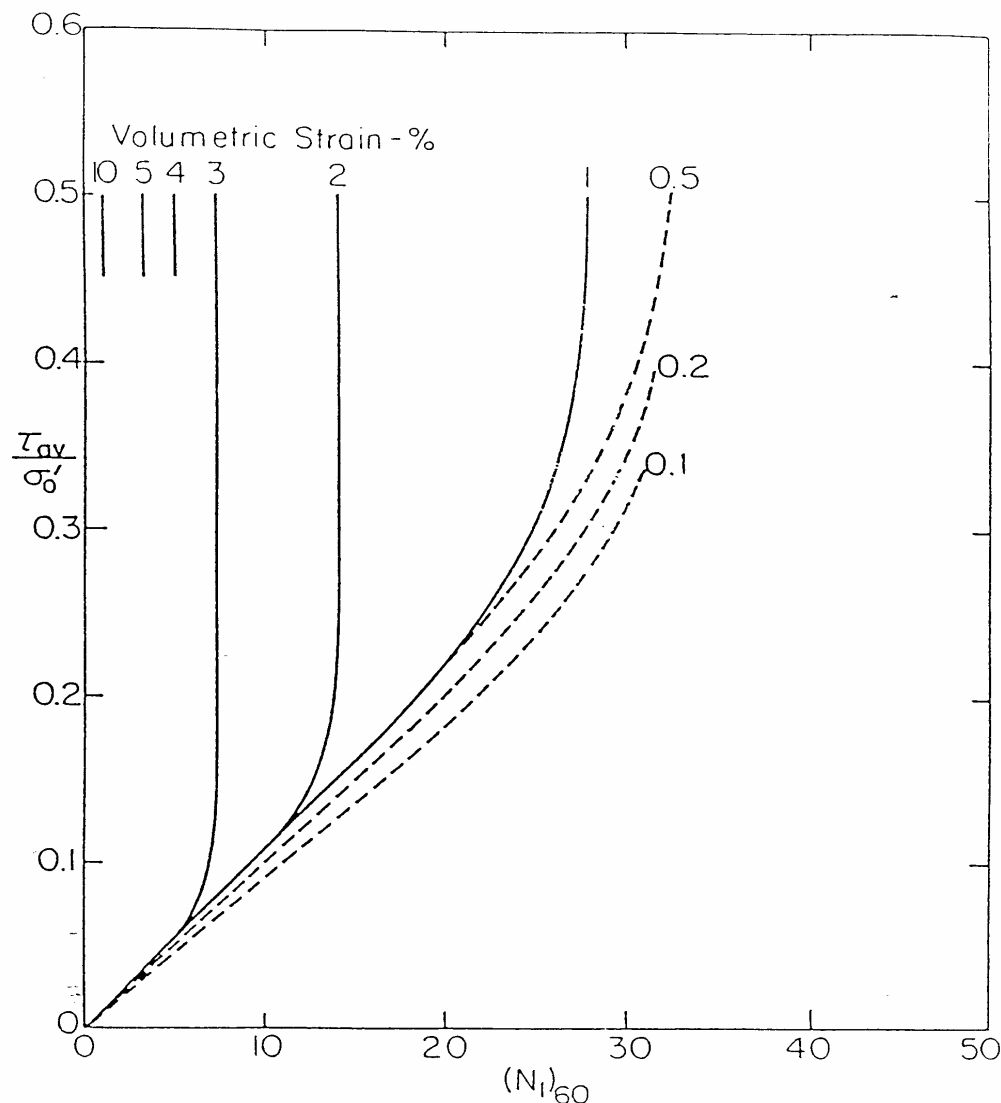


**Figure D.2.5-4 Relationship Between Cyclic Stress Ratio,  $(N_1)_{60}$  and Volumetric Strain for Saturated Clean Sands and Magnitude = 7.5 (after Tokimatsu and Seed, 1987)**

the stratified system. Given the appropriate boundary conditions, Martin et al. (1991) shows that thin, dense layers of soils could liquefy if sandwiched between liquefiable layers. For this situation the estimated settlement using the Tokimatsu and Seed procedure (which is based on the SPT values and excess porewater pressures generated in the individual sand layers) therefore, may be over-predicted or under-predicted.

The Tokimatsu and Seed (1987) method can be used to estimate settlement in layered deposits by accounting for settlement of non-liquefiable layers. One approach to estimate the settlement of such a non-liquefiable soil layer is to use Figure D.2.5-4 in combination with Figure D.2.5-5 to determine if the layer will be affected by the layer

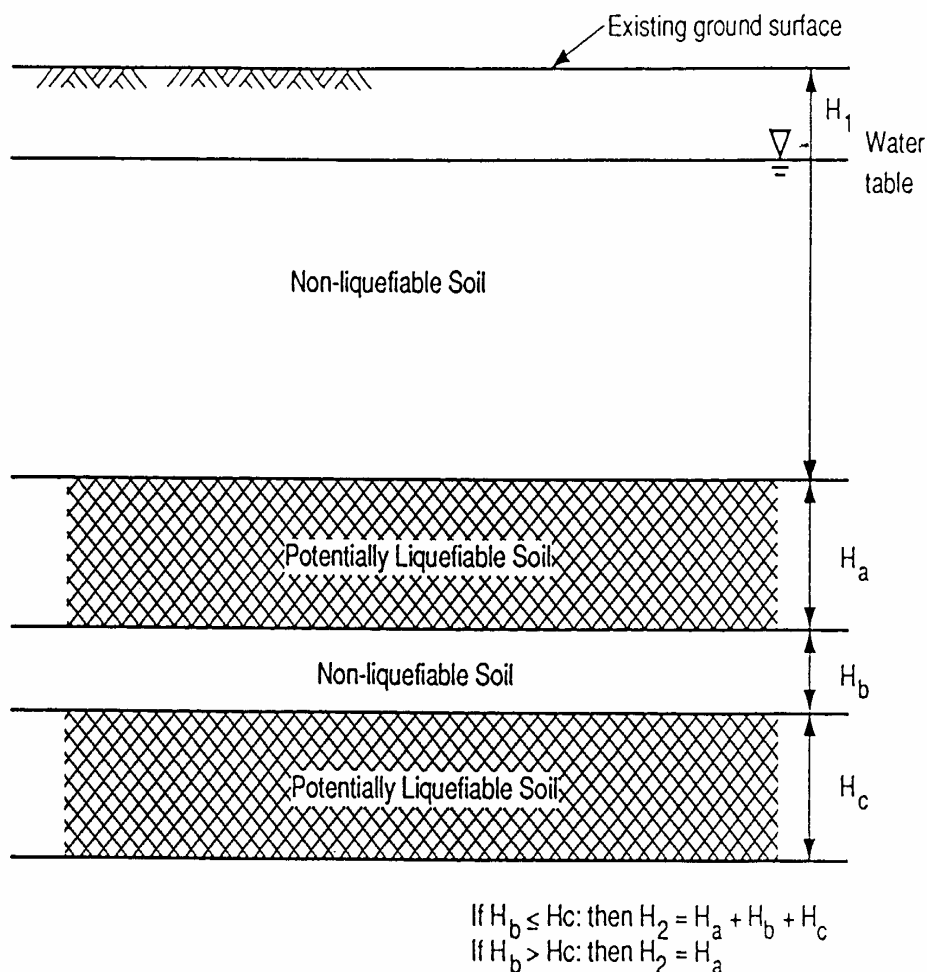


**Figure D.2.5-5 Schematic Diagram for Determination of  $H_1$  and  $H_2$  (after Ishihara, 1985)**



below. If  $H_c > H_b$ , then the settlement of the nonliquefied layer can be estimated by assuming that the volumetric strain in the layer will be approximately 1.0% (1.0% seems to be the volumetric strain corresponding to initial liquefaction), given that the non-liquefiable layer ( $H_b$ ) meets all of the following criteria:

- Thickness of the layer is less than or equal to 1.5 m.
- Corrected SPT value  $(N_f)_{60}$  less than 30 or CPT tip resistance normalized to 100 kPa ( $q_{cIN}$ ) less than 160.
- Soil type is sand or silty sand with fines content less than or equal to 35%.
- Magnitude of design earthquake is greater than or equal to 7.0.

The logic for using these four criteria is that the migration of porewater pressure and subsequent settlement of the non-liquefiable layer depends on factors such as the thickness, density (SPT or CPT tip value), and permeability (soil type) of the layer and the duration of earthquake shaking (magnitude). It should be noted that the criteria are only guidelines to allow the Designer to be aware of the potential settlement contributions from certain non-liquefiable soil layers present in a layered system.

### D.3 Other Collateral Hazards

The potential risk to bridges located in SDR 3 and higher from collateral hazards not associated with liquefaction must also be considered. These other collateral hazards include fault rupture, landsliding, differential compaction, and flooding or inundation.

If the risk of the ground displacement hazard from one or more of these sources is determined to be unacceptable by the owner for the desired performance level, then the hazard should be mitigated through use of ground improvement methods or by selecting an alternative bridge location.

#### D.3.1 Fault Rupture

Ground displacements generally are expected to reoccur along preexisting fault traces. The development of a new fault or reactivation of a very old (pre-Quaternary) fault is uncommon and gen-

### CD.3 Other Collateral Hazards

With the exception of flooding and inundation, these other collateral hazards involve ground displacements. These ground displacement hazards can sometimes be very large, on the order of meters, and quantification of the amount of displacement can be difficult. Detailed geotechnical explorations and analyses are usually required to identify the potential for these displacement hazards and their consequences.

#### CD.3.1 Fault Rupture

To evaluate the potential hazards of surface fault rupture, a number of evaluations are necessary, including determination of the location of fault traces, the nature and amount of near-surface

erally does not need to be considered for typical bridges. Faults are generally considered active and present a potential risk to a bridge if they have displaced in the past 11,000 years. Bridges should not be constructed across active faults, unless specialized studies are performed to quantify the amount of potential fault movement and to determine the consequences of this movement to the bridge.

### **D.3.2 Landsliding**

Earthquake-induced landsliding represents a significant hazard to roadways in seismically active areas, and can be a hazard to bridges. Damage can be in the form of ground movement either at the abutment or extending to the central piers of a bridge. Sites that are most susceptible to earthquake-induced landslides include locations with slopes of 18 degrees or greater, or a history of rock falls, avalanches, or debris torrents.

### **D.3.3 Differential Compaction**

Loose cohesionless soil above the water table will tend to densify during the period of earthquake ground shaking. This potential should be considered when evaluating the potential for dif-

formations, and the history of deformations. Maps showing the location of active faults have been developed by many state geological agencies and by the United States Geological Survey. The potential amount of movement can be estimated from empirical relationships between magnitude of the seismic event on the fault and displacement (e.g., Wells and Coppersmith, 1994).

The evaluation of fault displacement involves skills and techniques not commonly used in geotechnical or geologic investigations, and therefore should be done by an individual or organization with specific expertise in making these estimates. The owner must consider the uncertainty in these estimates and the consequences of incorrect estimates when deciding whether to locate a bridge across a fault.

### **CD.3.2 Landsliding**

Pseudo-static stability methods are often used to evaluate the potential for landsliding at soil sites (in the absence of liquefaction). These methods involve conducting slope stability analyses using a seismic coefficient equal to two-thirds to one-half the predicted peak ground acceleration. Conditions are normally considered acceptable if the computed factor of safety under the imposed loads is 1.0 or higher. If the factor of safety is less than 1.0, a sliding block analysis using the Newmark (1965) method, as discussed in Article D.2.5.2, is conducted to estimate the magnitude of displacement during the landslide. A detailed discussion of seismic-induced landslides is presented in MCEER (2000).

Where cliffs or steep slopes occur, earthquake-induced rock fall hazards may exist. The Colorado Rock Fall Simulation Program (Pfeiffer and Higgins, 1991) can be used to evaluate the potential danger from this mechanism.

Numerous more rigorous two- and three-dimensional computer methods, which model the nonlinear response of the soil or rock, can be used to investigate the potential for landsliding, pending the owner's approval. In some cases these more rigorous methods may be the only reasonable method for making the evaluation.

### **CD.3.3 Differential Compaction**

Procedures describe by Tokimatsu and Seed (1987) can be used to estimate the amount of settlement. The Tokimatsu and Seed procedure for estimating seismically-induced settlements in dry

ferential displacement between the bridge abutment and the closest central pier or between central piers in a multi-pier bridge.

#### **D.3.4 Flooding or Inundation**

Tsunamis and seiches can be triggered by earthquakes, causing wave impact and inundation. Failure of reservoirs or aqueducts, and canals located upslope of the bridge can also result in flooding. With the exception of coastal areas in the western United States, the risk associated with these mechanisms is low for most bridge sites.

### **D.4 DESIGNING FOR COLLATERAL HAZARDS**

Collateral hazards discussion described in previous paragraphs identify methods for quantifying the occurrence of collateral hazards. In most cases it is also possible to quantify the amount of displacement associated with the hazards. These estimates are normally made assuming free-field conditions, and therefore don't consider the effects on or from a bridge structure located on the hazards. In some cases the foundations of the structure will either limit or prevent the amount of predicted displacement. Procedures for evaluating the effects of soil movement are summarized in the following paragraphs. Additional requirements for foundations and abutments are presented in Sections 7 and 8 of these *Guidelines*.

#### **D.4.1 Spread Footing Foundations**

Spread footing foundations located above liquefiable layers must consider the potential for loss in bearing support and for liquefaction-induced settlement if liquefaction is predicted below the foundation. Either of these occurrences can result in displacements of the bridge support system that lead to damage of the structure.

(and unsaturated) sand requires that the settlement estimates be multiplied by a factor of 2.0 to account for the effect of multidirectional shaking.

#### **CD.3.4 Flooding or Inundation**

For some performance levels in SDR 3, 4, 5, and 6, it may be desirable to confirm that flooding and inundation will not jeopardize the bridge. Maps have been developed for some areas, such as the west coast of the United States, showing areas where tsunami danger exists. Most states also have identified possible areas of inundation from failure of reservoirs.

### **CD.4 DESIGNING FOR COLLATERAL HAZARDS**

The occurrence of a collateral hazard is normally determined by an engineering geologist and a geotechnical engineer. Often results are presented in terms of a factor of safety or an estimated amount of deformation. The bridge designer is then left with the decision on how this information should be used in the selection and design of the bridge foundation system. Too often, little communication occurs between the geotechnical engineer/geologist and the bridge designer regarding the uncertainties and implications associated with the prediction and quantification of the hazard. This approach to seismic design is undesired and not recommended. The best and most efficient design for handling the collateral seismic hazards described above will be achieved only if the geotechnical and bridge engineers work as a team.

#### **CD.4.1 Spread Footing Foundations**

The state-of-the-practice for predicting the consequences of liquefaction, whether it is loss in bearing support or settlement, is one of the least precise of the predictions made by geotechnical engineers. This imprecision reflects the complexity of the overall liquefaction mechanisms and the uncertainties on how these will affect a spread footing foundation. For this reason spread footing foundations are normally discouraged if liquefaction is predicted below the footing.

If liquefaction is predicted to occur below a planned spread footing foundation, this potential should be brought to the attention of the owner, and a decision made as to the appropriateness of the spread footing foundation in this particular situation.

#### D.4.1.1 Loss of Bearing Support for Spread Footings

Liquefaction can cause the loss of bearing capacity beneath spread footing foundations supported on “stable” strata above the liquefiable soils. In view of the possible loss in support, spread footing foundations for bridge structures are not recommended above liquefiable soil layers, except in SDR 1 and SDR 2. For SDR 3 and above the liquefiable layer should be at least two foundation widths below the bottom of the footing. At this depth the induced vertical stress in the soil from the footing is less than 10% of the bearing pressure imposed at the base of the foundation. Even with the low overburden stress increase, the potential for settlement should be determined.

Spread footing foundations typically should not be used when lateral spreading or flow failures that would load the foundations are predicted. In most cases the spread footing will move with the soil, resulting in excessive bending and possible collapse of the column supported by the footing.

#### D.4.1.2 Settlement of Spread Footing

Settlement of spread footings located above loose granular soils should be quantified using the procedures identified in D.3.3. These evaluations should be made whenever liquefaction is predicted to occur below the footing or, in the case of dry or unsaturated soils that are not expected to liquefy, if the  $(N_1)_{60}$  value is less than 30.

Where there are relatively uniform conditions at a site with deep sediments (if demonstrated by the field program), minimum differential settle-

#### CD.4.1.1 Loss of Bearing Support for Spread Footings

Spread footings supporting bridge structures should not normally be used above layers that will liquefy in SDR 3, 4, 5, and 6 because of the potential for loss in bearing capacity and post-earthquake settlement as porewater pressures dissipate. As bearing pressure is lost the foundation will displace downward, likely resulting in differential settlement between column supports. While numerical methods can be used to predict the amount of settlement, the accuracy of the numerical prediction is not usually sufficient to make accurate estimates of distortion between columns. At least part of the difficulty in making these predictions, either numerically or by simple methods, is the inherent variability of soils.

For non-critical spread footing foundations, it is possible to design the footing for the occurrence of liquefaction. For these situations, Ishihara's method of analysis (Ishihara, 1993) for surface manifestation can be used for shallow footings, using the elevation of the bottom of the footing as the top of the surface layer. If Ishihara's criteria cannot be met, consideration should be given to alternative mitigation methods. In the event that an explicit bearing capacity analysis is performed, the undrained residual strength of liquefied layers can be used in assessing the bearing capacity.

If spread footing foundations must be used above liquefiable layers, whether it is for an SDR 3 or an SDR 6 site, another alternative to consider is to improve the ground below the footing using stone columns, compaction grouting, or a similar improvement procedure. The area improved should extend a distance from the footprint of the footing such that liquefaction of surrounding soils will not cause loss in bearing capacity for the footing. Mitchell et al. (1998) provide guidance in designing liquefaction mitigation methods.

#### CD.4.1.2 Settlement of Spread Footing

The differential settlement between adjacent columns, or distortion, is normally needed by the structural designer to evaluate effects of settlement on the structure. While differential settlement estimates based on one-half to two-thirds of the total settlement provide an indication of the differential settlement, this approach does not account for location specific soil conditions.

For a location specific estimate, total settlement must be determined at each support location. This

ment of less than one-half of the total settlement may be used in the design. When the subsurface condition varies significantly in lateral directions and/or the thickness of soil deposit (Holocene deposits and artificial fills) varies within the site, a minimum value of one-half to two-thirds of the total settlement is suggested. Once again, it should be noted that the settlement and differential settlement estimates are valid only for level-ground sites that have no potential for lateral spread. If lateral spreading is likely at a site and is not mitigated, the differential settlements could be much greater than the above-suggested values.

#### **D.4.2 Deep Foundations**

Deep foundations extending through liquefiable soils will require special consideration. The lateral capacities of piles or drilled shafts may be reduced if the surrounding soils liquefy. Lateral spreading or flow slides can also result in the imposition of significant additional lateral demands on the deep foundations. Liquefaction also can result in settlement of the liquefied strata and the strata above the liquefied strata. This settlement will cause down-drag or negative friction to be imposed on the deep foundations. The potential for these must be addressed for bridges located in SDR 3, 4, 5, and 6.

##### **D.4.2.1 Loss in Lateral Support for Deep Foundations**

A well-designed deep foundation should extend beyond the deepest depth of liquefaction. Liquefaction of a layer above the toe of the pile or drilled shaft may have limited effects on the axial capacity of the foundation but can result in loss of lateral support of the pile or drilled shaft. This can reduce the lateral stiffness of the soil-pile system if the loss in lateral support occurs within 10 pile diameters of the bottom of the pile cap or the ground surface. The effects of this loss should be quantified in accordance with procedures given in Article 7.4 or 8.4 of these *Guidelines*.

determination would require a soil boring to establish thickness of layers that could settle, thereby adding to the exploration costs. In the absence of this approach it is suggested that the differential settlement estimates from the one-half to two-thirds factor be used as representative of the minimum differential settlement between adjacent supports. If these settlements are approaching unacceptable levels, a more detailed site investigation should be performed to obtain location specific estimates.

#### **CD.4.2 Deep Foundations**

If the effects of liquefaction cannot be adequately accommodated in deep foundation design, consideration should be given to alternative mitigation methods. Liquefaction effects on deep foundations can be mitigated by the implementation of ground improvement techniques prior to, or after deep foundation installation.

##### **CD.4.2.1 Loss in Lateral Support for Deep Foundations**

The change in stiffness of a pile or drilled shaft extending through liquefied soil can be determined by conducting a lateral pile analysis using a beam-column-type computer software. Common examples of these software are LPILE+ and COM624. These programs allow modeling of individual layers within the soil profile. Liquefied layers are assigned a residual strength and treated as a cohesive soil. The strain necessary to mobilize 50% of ultimate resistance ( $\epsilon_{50}$ ) is assumed to be 0.02.

If a cohesionless layer does not liquefy but the factor of safety against liquefaction is less than 1.5, a reduced soil friction angle and a reduced subgrade modulus should be used. It is suggested that the reduced friction angle be taken as 10 degrees for FS of 1.0 and should be interpolated for FS between 1.0 and 1.5. Modulus of subgrade reaction values are reduced in a similar manner with the modulus at FS of 1.0 equal to the modulus of a soft clay.

## D.4.2.2 Loads from Lateral Spreading/Flow

If lateral flow or spreading of the ground is predicted during a seismic event, deep foundations that would be loaded by the deforming ground need to be designed to withstand the loads from the moving soil. The recommended design approach for evaluating this condition involves the following four steps:

1. Slope stability analyses are conducted to determine the yield acceleration. This step may include the pinning effects of the deep foundation or the increased resistance of soil that has been improved by some type of ground improvement method.
2. Newmark sliding block analyses are performed to estimate displacements of the soil-deep foundation system.
3. The passive force that can ultimately develop ahead of a pile or foundation as soil movement occurs is estimated, and
4. The likely plastic mechanisms that may develop in the foundations and substructure are evaluated.

The rationale behind the proposed method is to determine the likely magnitude of lateral soil movement and assess the ability of the structure to both accommodate this movement and/or potentially limit the movement.

The concept of considering a plastic mechanism in the foundation under the action of spreading forces is tantamount to accepting substantial damage in the foundation. This is a departure from seismic design for vibration alone, and the departure is believed to be reasonable because it is unlikely that the formation of a mechanism in the foundation will lead to structure collapse. The reasoning behind this is that lateral spreading is essentially a displacement-controlled process. Thus the estimated soil displacements represent a limit on the structure displacement, excluding the phenomena of buckling of the piles or shafts below grade and the continued displacement that could be produced by large  $P-\Delta$  effects. Buckling should be checked, and methods that include the soil residual resistance should be used. Meyer-sohn, et al. (1992) provide a method for checking buckling as an example. The effects of  $P-\Delta$  amplification are discussed in this section.

## CD.4.2.2 Loads from Lateral Spreading/Flow

A flowchart of the proposed methodology for evaluating spreading is given in Figure D.4.2-1. Key components of this methodology are numbered in the flowchart, and this chart along with the following commentary provide a 'roadmap' to the recommended procedure for lateral spreading resistance design. The primary feature of the proposed methodology is the use of passive piles to restrict the movement of soil and foundations to levels that are tolerable by the structure.

- *Step 1:* The soil layers that are likely to liquefy are identified.
- *Step 2:* A stability analysis is conducted to determine the likelihood of soil movements, and to determine the extent of such movements. This would include the depths of soil likely to move and the plan extent of the likely soil failure block. Assessment of the impacts to a bridge structure can then be made by considering the proximity of the failure block to the foundation system.
- *Step 3:* The maximum displacement of the soil is estimated. This can be accomplished using the simplified Newmark charts or the Newmark Time History Analysis described in Article D.2.5.2. The Designer is permitted to apply more advanced techniques if the benefits justify the additional engineering costs and with the concurrence of the owner. In some cases, substantial improvements and reduction in overall estimated displacements can be achieved.
- *Step 4:* An assessment is made whether soil moves past the foundation, (i.e., foundation is relatively fixed) or movement of the foundation occurs. The assessment requires a comparison between the estimated passive soil forces that can be exerted on the foundation system and the ultimate structural resistance that can be developed by the structure, itself. This assessment requires estimating the forces that can develop if soil is to actually flow around the foundation system and comparing them with the likely resistance the structure will provide. In cases where a crust of non-liquefied material exists at or near the ground surface, the full structural resistance is likely to be less than the movement-induced passive

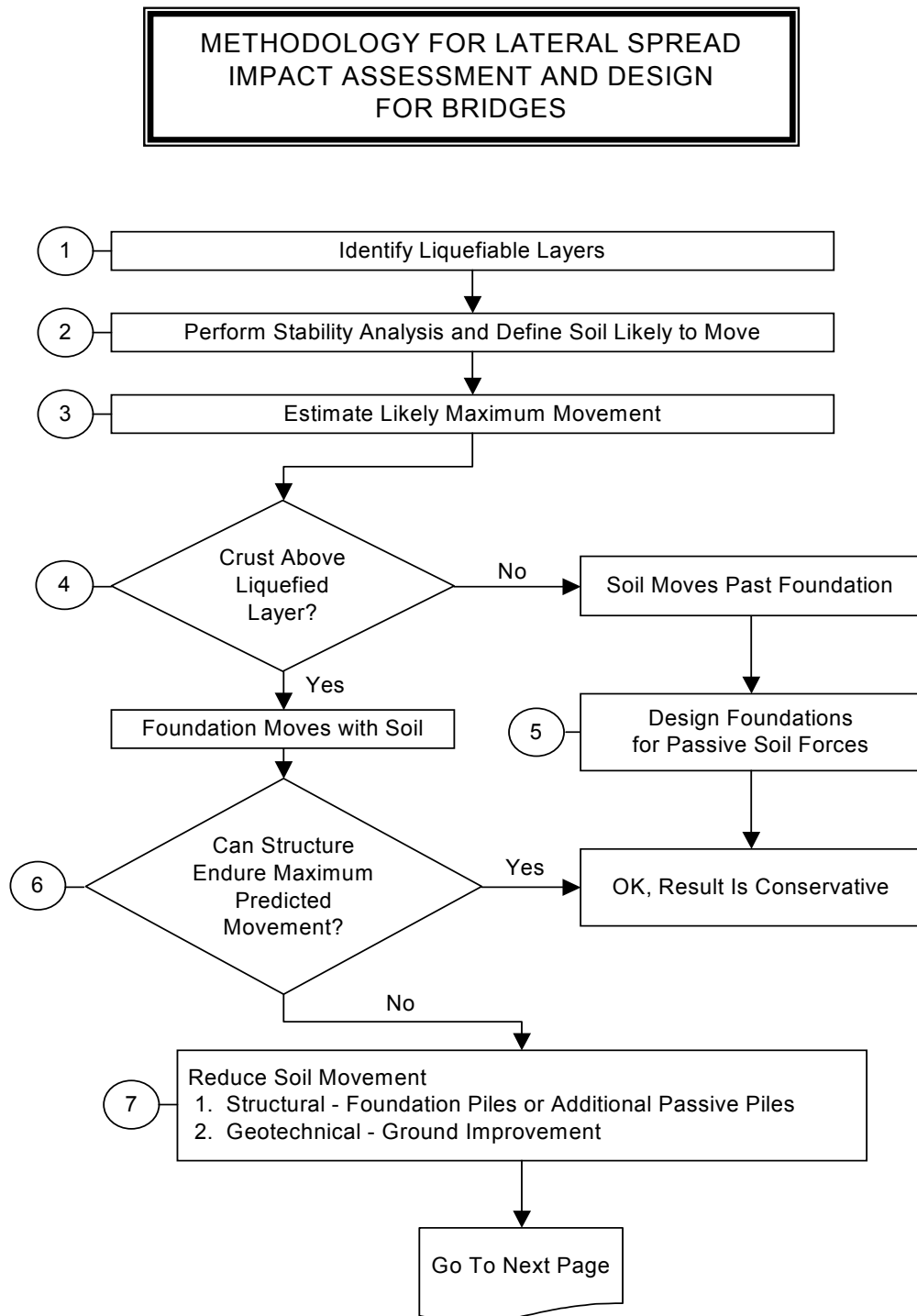


**Figure D.4.2-1** Flowchart Showing Process for Evaluating the Effects of Lateral Spread and Flows on a Bridge Foundation

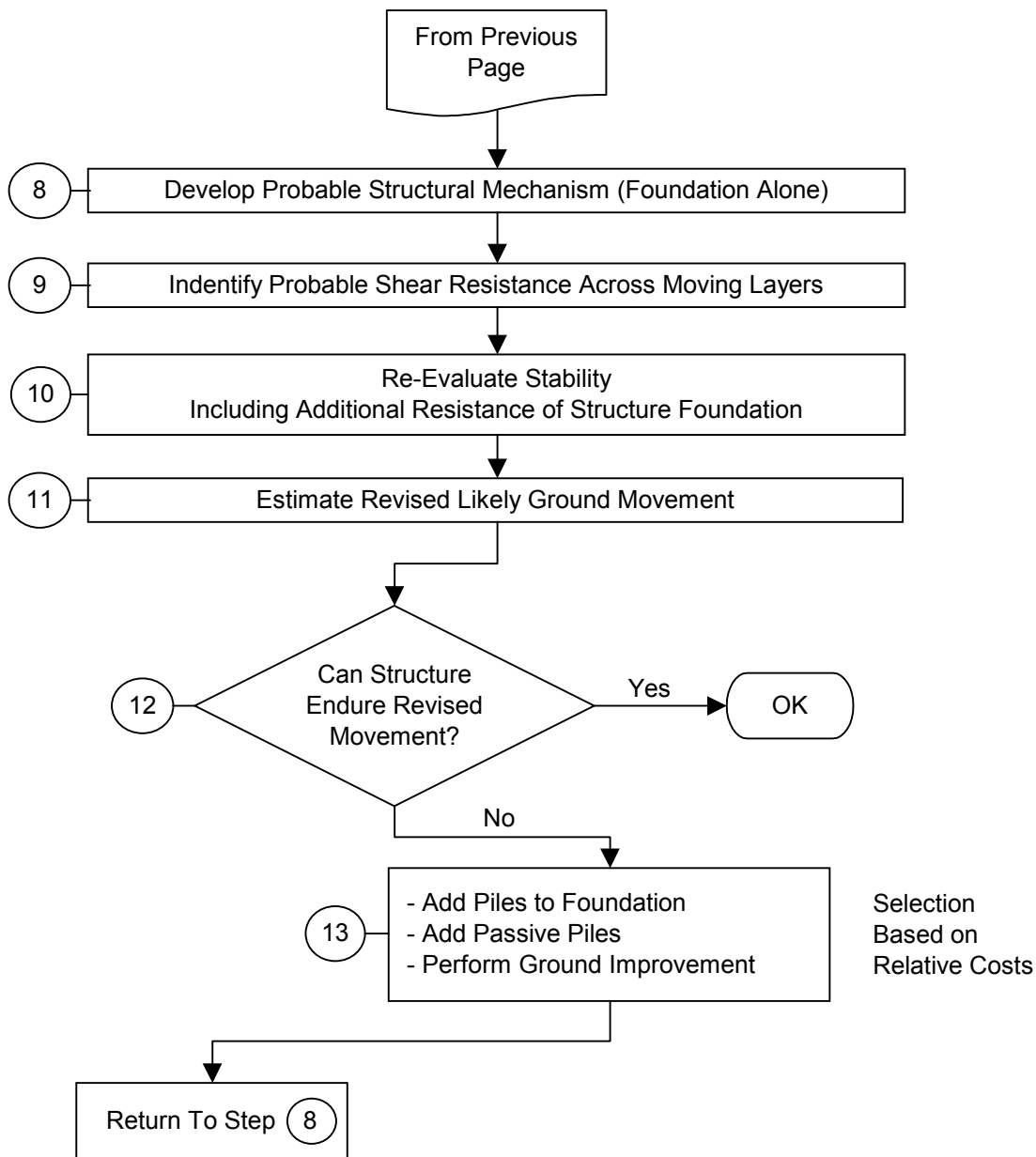


**Figure D.4.2-1** Flowchart Showing Process for Evaluating the Effects of Lateral Spread and Flows on a Bridge Foundation (cont.)



forces, and in such cases the foundation is likely to move with the soil. In many cases, it may be immediately obvious which condition, soil or foundation movement, is more likely. Qualitative illustrations of the two scenarios are given in Figure D.4.2-2 and Figure D.4.2-3.

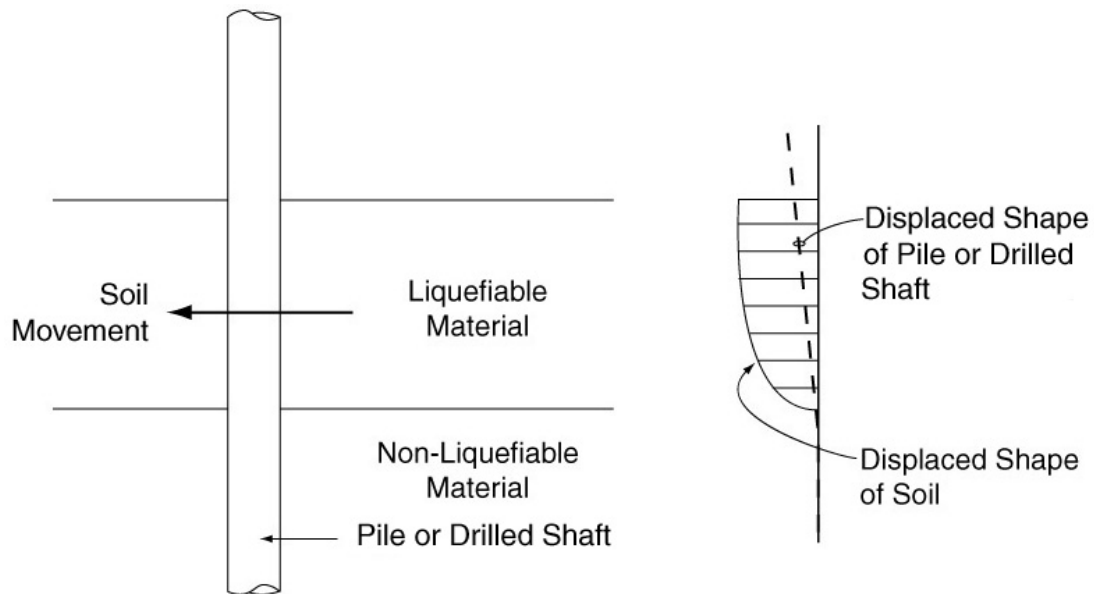


**Figure D.4.2-2 Movement of Liquefied Soil Past Pile or Drilled Shaft**

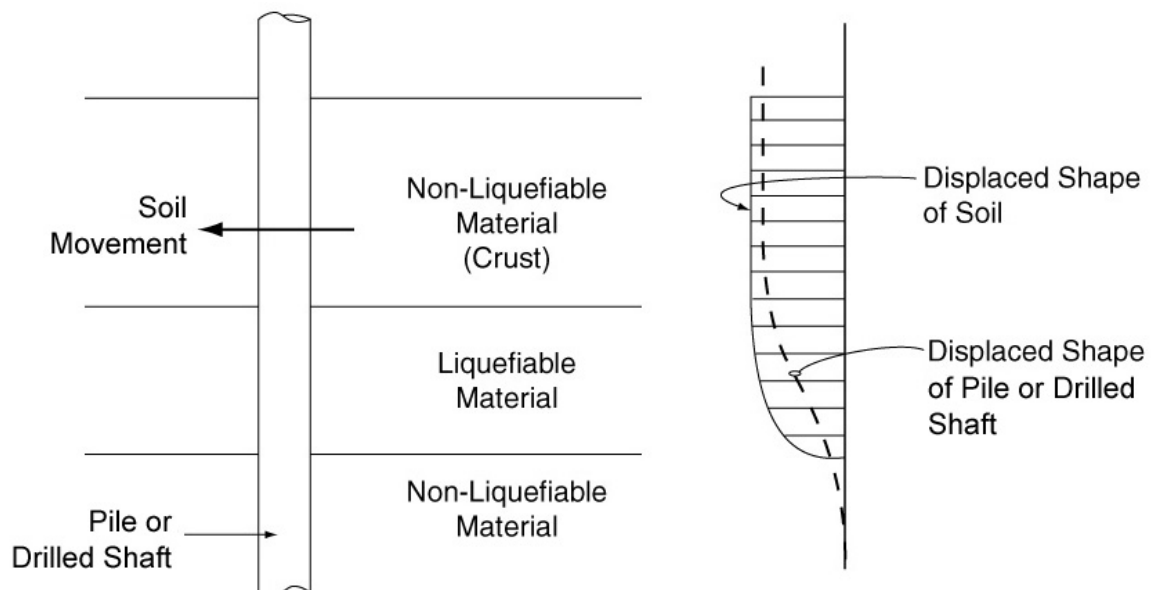


**Figure D.4.2-3 Movement of Liquefied Soil with Crust with Pile or Drilled Shaft**

- *Step 5:* If movement of soil around the structure is indicated, then the foundation is designed to withstand the passive pressures created by the soil moving around the structure. The induced forces are effectively the largest forces that the structure will experience, and for this reason it is conservative to design a structure for such forces.
- *Step 6:* If on the other hand, the assessment indicates that movement of the foundation is likely, then the structure must be evaluated at the maximum expected displacement. This check is shown in Step 6. The implication of this assessment is that for relatively large ground movements, soil displacements are likely to induce similar magnitude movements of the foundation. In this context, “large” is taken relative to the structural yield resistance. The resulting induced movements of the foundations may produce substantial plasticity in the foundations, and may induce relatively large reactions in the superstructure. Guidelines for the acceptable rotation are provided in Articles 7.7.9, 7.8.6, 8.7.9, and 8.8.6 of these *Guidelines*. For an upper level event, the recommended acceptance criterion is a plastic rotation of 0.05 radians. The allowance of plasticity in the foundation is believed to be reasonable, even though plasticity may occur below grade, because damage in the foundation is not likely to pose a collapse hazard.

*Step 7:* If deformations are not acceptable, there are realistically only two ways to restrict the foundation and substructure forces to acceptable values. The first method is to design the foundations to resist the full passive pressure forces that would accompany passive movement of the soil around the foundations. The other method would be to limit the ground movement by providing either ground or structural remediation. It is the structural option that provides the simplest first option, and this makes use of the “pinning” or dowel action that pile or shaft foundations contribute as they cross the potential failure plane of the moving soil mass.

- *Step 8:* The determination of the plastic mechanism that is likely to occur in the presence of spreading should be done in a reasonable manner. Due to the range of inherent uncertainties, great precision in the determina-

tion may not produce more accuracy. Thus a simple estimate of the mechanism and its corresponding lateral resistance capability is often adequate. For instance, one method is to use the upper bound method of plasticity and postulate potential mechanisms, then using judgment assess the mechanism that is likely to control. The acceptance criteria are basically the structural deformation criteria for SDAP E, which uses the push-over method. In fact, the piles are the elements that limit the acceptable displacements of the system.

The lateral shear that produces the plastic mechanism can be adjusted downward to account for the driving effect of the  $P$ - $\Delta$  effect. The lateral soil force that produces a plastic mechanism in the foundation/substructure system is required; therefore, the reduction in shear required to produce a mechanism due to  $P$ - $\Delta$  should be considered. Figure D.4.2-4 and Figure D.4.2-5 illustrate first-order corrections for  $P$ - $\Delta$  effects for a stub abutment and for an

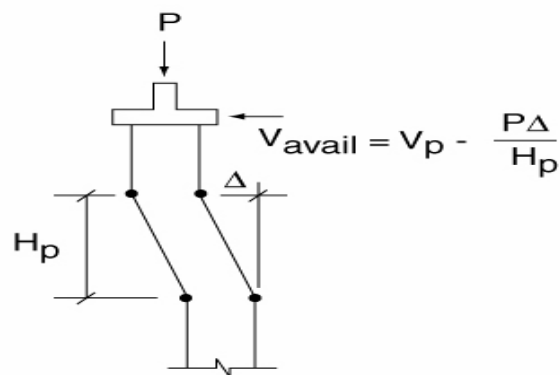


Figure D.4.2-4  $P$ - $\Delta$  Effects to Stub Abutment

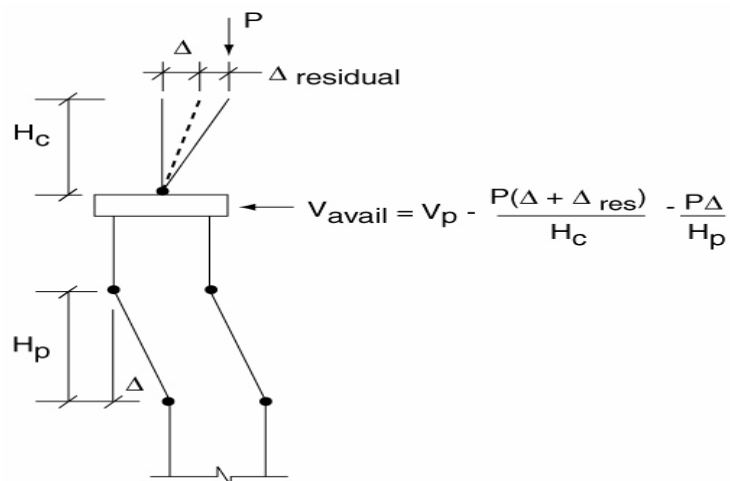


Figure D.4.2-5  $P$ - $\Delta$  Effects for an Intermediate Pier with Piles and Pile Cap

intermediate pier with piles and pile cap, respectively.

A more precise method of determining the plastic mechanism would be to use an approach that ensures compatibility of deformations between the soil and piles (e.g., similar to that incorporated in LPILE) and which accounts for plastic deformations in the piles themselves. This second requirement could be satisfied by using software that is capable of performing push-over-analysis, then using p-y curves from a program such as LPILE to produce boundary support elements that ensure compatibility.

- *Step 9:* The system then must be assessed for a prescribed displacement field to represent the likely soil spreading deformation. From this analysis, an estimate of the likely shear resistance the foundation will provide is estimated and this shear can then be incorporated back into the stability analysis.
- *Step 10:* If substantial resistance is provided, then its effect on limiting the instability driven movement of the soil block should be introduced into the stability analysis. This step is typically not included in current assessments of potential foundation movements, although inclusion of this resistance could improve the expected performance of the structure.
- *Step 11 and 12:* The overall displacement is re-calculated with the revised resistance levels considered. Once a realistic displacement is calculated, then the foundation and structural system can be assessed for this movement. It is at this point that more permissive displacements than for substructure design can be relied upon. This implies that plastic rotations, and potentially large ones, may be allowed to occur in the foundation under such conditions.
- *Step 13:* If the behavior of the structure is acceptable then the design is complete; if not, then the Designer must assess whether to try to produce adequacy either through additional piles or shafts, and these may not need to connect to the foundation (passive piles). Alternately ground improvement approaches may be considered, for instance stone columns. The selection of structural or geotechnical remediation methods is based on the relative economy of the system being used.

The process is repeated by returning to *Step 8* and modifying the available resistance until the slope is stabilized. The fact that inelastic deformations may occur below grade during the upper level seismic event and that these may be difficult to detect and inspect should be considered. However, typically the presence of large ground movements induced by earthquake motions is discernible. Thus it should be possible to postulate whether inelastic deformations have occurred from the post-earthquake inspection information. Additionally, inclinometer tubes could be installed in selected elements of deep foundations to allow quantitative assessment of pile or shaft movement following an earthquake.

#### D.4.2.3 Settlement and Downdrag

Deep foundations should also be designed for settlement that occurs during the seismic event. The settlement can be estimated based on settlement below the neutral plane of the pile or drilled shaft. Procedures given in Section 10 of the AASHTO LRFD Bridge Design Specifications can be used to estimate the location of the neutral plane. The Tokimatsu and Seed (1987) method described in Article D.2.5.3 can be used to estimate the settlement.

Vertical drag loads will be imposed on a deep foundation as liquefied layers settle. These loads should be used to estimate the total settlement of the deep foundation (i.e., added to the settlement estimated by the Tokimatsu and Seed (1987) method) and the structural capacity of the pile under the drag loads.

#### D.4.3 Ground Improvement

Ground improvement methods can be implemented to mitigate the effects of liquefaction. A number of these methods are available, including grouting (compaction, permeation, and jet), vibro systems (vibratory probe, vibro-compaction, vibro-replacement), surcharge and buttress fills, reinforcement and containment (root piles, mixed-in-place walls and columns) and drains. Cooke and Mitchell (1999) provide detailed guidelines for mitigating the effects of liquefaction at bridge sites. The suitability of these methods will depend on the soil conditions at the site, the location of the ground water, and project logistics.

A critical phase in any ground improvement method is confirmation that the ground improve-

#### CD.4.2.3 Settlement and Downdrag

The drag load will develop along the side of the deep foundation from settlement of all layers above the bottom of the liquefied layer. The drag load in non-liquefied layers will be the same as the ultimate side resistance developed under compressive loading. The drag load along the portion of the deep foundation that is in liquefied soil will initially be the residual strength of the liquefied soil, but will then increase gradually as porewater pressures dissipate. For design purposes it is conservative to assume that maximum drag occurs at the end of porewater pressure dissipation, when the soil strength has returned to its initial condition.

#### CD.4.3 Ground Improvement

Two of the more common procedures for accomplishing this remediation are described below:

- *Vibro-Replacement:* The most widely used densification method is the vibro-replacement technique. This method involves the repeated insertion and withdrawal of a large vibrating probe in the soil, to the desired depth of densification. As vibration-induced liquefaction occurs, crushed stone backfill is placed around the vibrator leading to the development of a stone column approximately 1 m in diameter. The stone column provides for an increased effectiveness of vibration transmission, and facilitates drainage of excess pore water pressures as densification occurs. The procedure is

ment goals have been achieved. Pre- and post-field explorations are required using SPT or CPT methods to confirm that required ground improvements have been achieved. In many cases it will be desirable to conduct a test program before the actual ground improvement program to confirm that the proposed improvement methods will work in the particularly conditions occurring at the project site.

repeated at grid spacing of 2 to 3 feet. Relative densities of the order of 80%, can be accomplished by the method. The method has been shown to be effective if sands to be densified contain less than 15 to 20% fines, although the use of wick drains placed at the midpoints of stone column grid points to aid drainage, can potentially lead to densification of sandy silts (Luehring et al., 1998). Details on design information and equipment applications can be found in many publications such as Baez (1995, 1997), Hayden and Baez (1994), and Martin (1998).

- *Compaction Grouting:* This method involves pumping a stiff mix of soil, cement, and water into the ground under high pressure to compress or densify the soil. For sites where vibratory techniques may be impractical, compaction grouting can be used. Typically, a very stiff (25 to 50 mm slump) soil-cement-water mixture is injected into the soil, forming grout bulbs which displace and potentially densify the surrounding ground, without penetrating the soil pores. A grid or network of grout columns formed by bottom up grouting, results in improved liquefaction resistance over a required areal extent, similar to the use of a network of stone columns described above for vibro-replacement. An overview of this approach is documented by Boulanger and Hayden (1995).

#### D.4.3.1 Bearing Capacity and Settlement

Ground improvement methods can be used to limit settlements of approach fills and improve bearing capacity or lateral capacity of soil that is predicted to liquefy. The amount of improvement is determined by the type and extent of improvement. Cooke and Mitchell (1999) provide guidance on evaluating these improvement methods.

#### CD.4.3.1 Bearing Capacity and Settlement

When used to improve the bearing capacity for spread footings or the lateral capacity of deep foundations, the ground is usually improved to a level where it will not liquefy during the seismic event. However, material beyond the improved zone will likely liquefy. Porewater pressures in these liquefied zones can migrate into the improved area, reducing the capacity of the improved zone. Similarly, loss in strength in the liquefied zone can lead to loss in either vertical or lateral support within the improved ground, due to loss of soil reaction in the liquefied zone. This loss in capacity can lead to increased vertical or lateral displacements. The placement of a zone with a radius of 1.5 to 2 times the thickness of the liquefiable layer can be used to eliminate post liquefaction downdrag on a pile, and the potential effects of cyclic ground lurch (progressive unidirectional movement of soil due to high ground accelerations).

The improved ground will also propagate ground motions more effectively than will the liquefied zone. Site conditions following ground improvement will likely be stiffer than what existed before ground improvement. This increased stiffness should be considered when defining the site category for determining peak ground and spectral accelerations.

These factors must be considered during the design process.

#### D.4.3.2 Lateral Spreading and Flow

Ground improvement methods can be used to control or limit the amount of lateral flow or spreading. The approach used in design is to increase the strength of the ground enough that it either causes the liquefied soil to flow around the improved ground or provides sufficient resistance to stop the lateral spread or flow. In most bridge designs one goal will be to prevent movement of the approach fill, either transverse or in line with the bridge alignment. Conventional slope stability methods are used to make these assessments. Initially, the potential for flow failure should be evaluated, with the improved ground characterized by a higher strength. If the resulting factor of safety is less than 1.0, then either the Newmark Charts or the Newmark Time History Analyses can be conducted to determine the amount of ground deformation. Procedures described in Article D.4.2.2 can then be used to evaluate whether the resulting deformations meet design criteria for the bridge structure and foundation.

#### CD.4.3.2 Lateral Spreading and Flow

A Newmark approach can be used to determine the buttress width that leads to acceptable displacement performance of abutment or bridge pier piles in the failure zone. This involves determining the yield acceleration for slope movement through the improved ground, and then using the simplified charts, equations, or integrated earthquake records to revise the displacement procedure. As the width of the improved zone increases, the amount of deformation will decrease. This relationship allows a cost-benefit study to be conducted to determine the minimum area of improved ground (minimum costs) that will result in deformations that can be tolerated by the bridge structure-foundation system.





## Appendix E

### DUCTILE END-DIAPHRAGMS IN GIRDER BRIDGES

#### E.1 DESIGN PROCEDURE

A seismic design strategy that relies on ductile end-diaphragms inserted in the steel superstructure can be, in some instances, an effective alternative to energy dissipation in the substructure. This could be the case, for example, when stiff wall-piers that can, with difficulty, be detailed to have a stable ductile response are used as substructure elements. The ductile diaphragms considered in this Appendix are therefore those that can be specially designed and calibrated to yield before the strength of the substructure is reached (substructural elements, including foundations and bearings are referred to generically as “substructure” here). Many types of systems capable of stable passive seismic energy dissipation could be used for this

purpose. Among these, eccentrically braced frames (EBF) (e.g. Malley and Popov, 1983; Kasai and Popov, 1986), shear panel systems (SPS) (Fehling et al., 1992; Nakashima, 1995), and steel triangular-plate added damping and stiffness devices (TADAS) (Tsai et al., 1993), popular in building applications, have been studied for bridge applications (Zahrai and Bruneau, 1999a, 1999b). These are illustrated in Figures E.1-1 to E.1-3. Although concentrically braced frames can also be ductile, they are not admissible in Article 7.7.8.2 or 8.7.8.2 because they can often be stronger than calculated, and their hysteretic curves can exhibit pinching and some strength degradation.

The plate girders can also contribute to the lateral load resistance, making the end-diaphragm

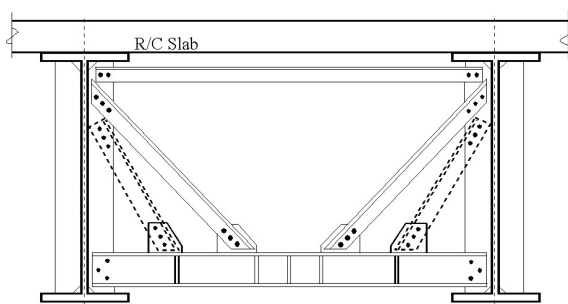


**Figure E.1-1 EBF Ductile Diaphragms**

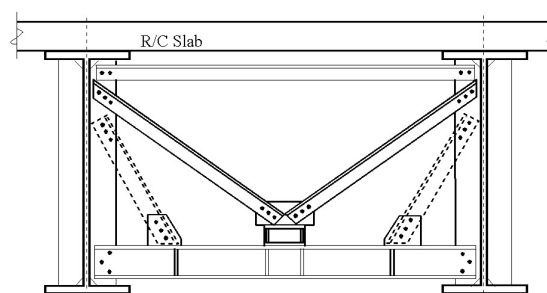


**Figure E.1-2 SPS Ductile Diaphragms**

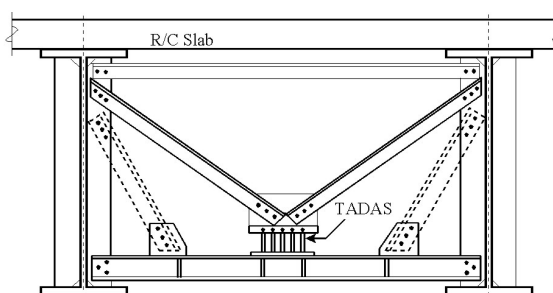


**Figure E.1-3 TADAS Ductile Diaphragms**

behave as a dual system. Therefore, the lateral stiffness of the stiffened girders,  $\Sigma K_g$ , must be added to the stiffness of the ductile diaphragms,  $\Sigma K_{DD}$  (usually much larger than the former), to obtain the lateral stiffness of the bridge end-diaphragms (adding the stiffnesses of both ends of the span),  $K_{ends}$ , i.e:

$$K_{ends} = \Sigma K_{DD} + \Sigma K_g \quad (E.1-1)$$

The stiffness contribution of a plate girder is obviously a function of the fixity provided to its top and bottom flanges by the deck slab and bearing respectively. If full fixity is provided at both flanges of the plate girder,

$$K_g = \frac{12EI_g}{h_g^3} \quad (E.1-2)$$

where  $I_g$  is the moment of inertia of the stiffened stub-girder (mainly due to the bearing web stiffeners) in the lateral direction, and  $h_g$  is its height. If one end is fully fixed, the other one pinned,

$$K_g = \frac{3EI_g}{h_g^3} \quad (E.1-3)$$

If both ends effectively behave as pin supports,  $K_g=0$ . Full fixity at the deck level in composite bridges is possible if shear studs are closely spaced and designed to resist the pull-out forces resulting from the moments developed at the top of the girders under lateral seismic forces. As for fixity at the bearing level, it obviously depends on the type of bearings present. However, even when infinitely rigid bearings are present, full fixity is still difficult to ensure due to flexibility of the girder flanges, as revealed by finite element analyses of subassemblies at the girder-to-bearing connection point.

It is the engineer's responsibility to determine the level of fixity provided at the ends of the girders. However, contrary to conventional design, the most conservative solution is not obtained when zero fixity is assumed because fixity also adds strength to the diaphragms, and the role of the ductile diaphragms is to limit the magnitude of the maximum forces that can develop in the substructure.

The lateral stiffness of the ductile diaphragms,  $K_{DD}$ , depends on the type of ductile device implemented. For example, if a ductile SPS is used, the stiffness of one such end-diaphragm in a slab-on-girder bridge,  $K_{SPS}$ , can be obtained by:

$$K_{SPS} = \frac{E}{\left[ \frac{l_b}{2A_b \cos^2 \alpha} + \frac{L_s}{4A_{bb}} + \left( \frac{h_l^3}{3I_l} + \frac{2.6h_l}{A_{s,l}} \right) + \frac{L_s(h_l + d_{bb}/2)^2}{12I_{bb}} + \frac{H \tan^2 \alpha}{2A_g} \right]} \quad (E.1-4)$$

where  $E$  is the modulus of elasticity,  $l_b$  and  $A_b$  are the length and area of each brace,  $\alpha$  is the brace's angle with the horizontal,  $L_s$  is the girder spacing,  $d_{bb}$ ,  $A_{bb}$  and  $I_{bb}$  are the depth, cross sectional area and moment of inertia for the bottom beam,  $h_l$ ,  $I_l$  and  $A_{s,l}$  are the length, moment of inertia and shear area of the link, and  $H$  and  $A_g$  are the height and area of the stiffened girders.

Similarly, lateral stiffness of the EBF and TADAS implemented as end-diaphragms of slab-on-girder bridges,  $K_{EBF}$  and  $K_{TADAS}$ , can be computed as follows:

$$K_{EBF} = \frac{E}{\left[ \frac{l_b}{2A_b \cos^2 \alpha} + \frac{a}{2A_l} + \frac{e^2 H^2}{12L_s I_l} + \frac{1.3eH^2}{aL_s A_{s,l}} + \frac{H \tan^2 \alpha}{2A_g} \right]} \quad (E.1-5)$$

$$K_{TADAS} = \frac{E}{\left[ \frac{l_b}{2A_b \cos^2 \alpha} + \frac{L_s}{4A_{bb}} + \frac{6h_T^3}{Nb_T t_T^3} + \frac{L_s(h_T + d_{bb}/2)^2}{12I_{bb}} + \frac{H \tan^2 \alpha}{2A_g} \right]} \quad (E.1-6)$$

where  $a$  is the length of the beam outside the link,  $e$ ,  $I_l$ ,  $A_l$  and  $A_{s,l}$  are the length, moment of inertia, cross sectional and shear areas of the link,  $N$ ,  $h_T$ ,  $b_T$ , and  $t_T$  are the number, height, width and thickness of the TADAS plates, and all other parameters are as defined previously. Note that of the five terms in the denominator of Equations E.1-4 to E.1-6, the second and fifth which account for axial deformations of bottom beam and stiffened girders could be ignored, and the fourth (accounting for the rotation of bottom beam at midspan in SPS and TADAS) could have a small impact if the bottom beam was a deep and stiff beam, which is not, however, always the case.

For a bridge having a given number of girders,  $n_g$ , number of end-diaphragms implemented at each support,  $n_d$ , and girder spacing,  $L_s$ , the design procedure for a ductile diaphragm consists of the following steps illustrated in Figure E.1-4.

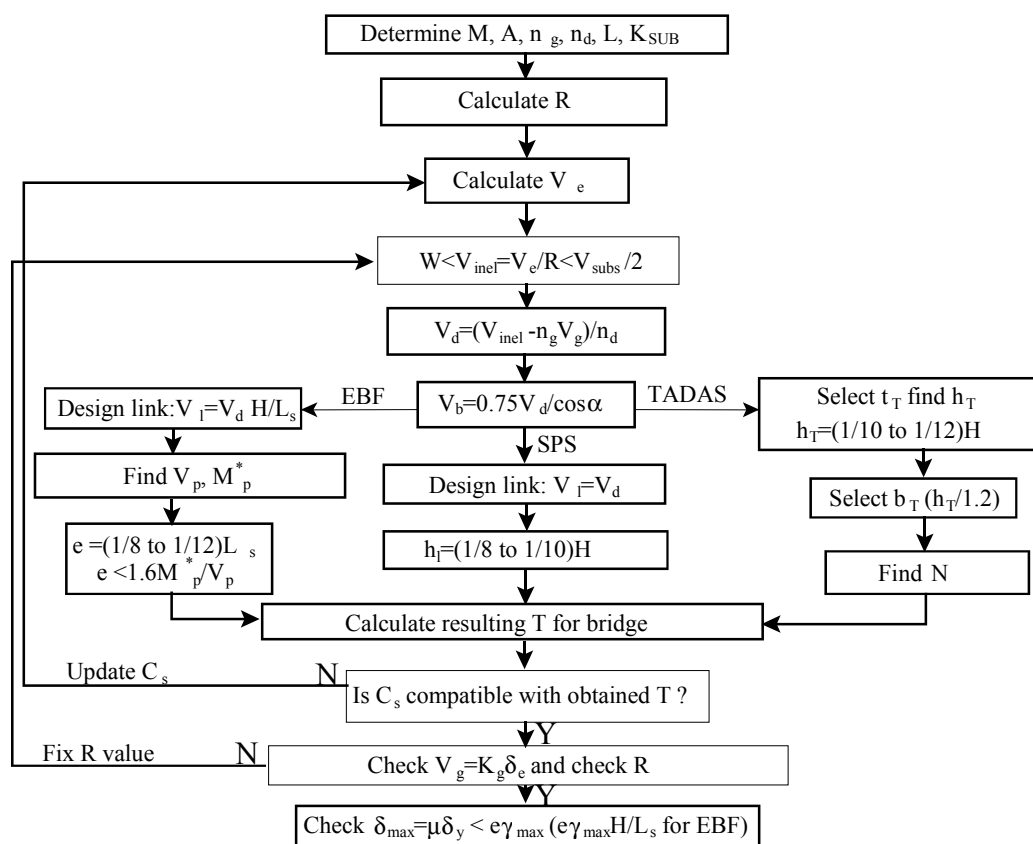


**Figure E.1-4 Flow Chart of Design Process for Ductile Diaphragm**

1. Determine the elastic seismic base shear resistance,  $V_e$ , for one end of the bridge (half of equivalent static force).
2. Calculate  $V_{inel} = V_e / R$ , where  $V_{inel}$  is the inelastic lateral load resistance of the entire ductile diaphragm panel at the target reduction factor, and  $R$  is the force reduction factor calculated as indicated in Article 7.7.8.2 or 8.7.8.2. Note that  $\mu$  in Equations (7.7.8.2-1), (8.7.8.2-1), represents the ductility capacity of the ductile diaphragm as a whole, not the local ductility of the ductile device that may be implemented in that diaphragm.
3. Determine the design lateral load,  $V_d$ , to be resisted by the energy dissipation device (e.g. link beam or TADAS) at the target ductility level, by:

$$V_d = \frac{V_{inel} - n_g V_g}{n_d} \quad (\text{E.1-7})$$

where  $V_g$  is the lateral load resistance of one stiffened girder. Note that in short bridges,  $V_g$  can be a dominant factor that could overwhelm the resistance contribution provided by the special ductile diaphragm elements. In that perspective, it is recommended in this procedure that the bearing stiffeners at the support of these girders be trimmed to the minimum width necessary to satisfy the strength and stability requirements. Ideally, the braced diaphragm assembly should also be 5 to 10 times stiffer than the girders with bearing web stiffeners (even though ductility demand tends to be larger in stiffer structures) to prevent, or at least minimize, yielding in the main girders under transverse displacements. Note that in longer bridges, particularly those with a lesser number of girders

per cross-section, the contribution of the girders to lateral load resistance is nearly insignificant.

4. Design all structural members and connections of the ductile diaphragm, with the exception of the seismic energy dissipation device, to be able to resist forces corresponding to  $1.5V_d$  to account for potential overstrength of the ductile device due to strain hardening, strain rate effects and higher than specified yield strength. For example, braces should be designed to resist an axial compression force,  $V_b$ , equal to:

$$V_b = 1.5 \left( \frac{V_d}{2 \cos \alpha} \right) = 0.75 \frac{V_d}{\cos \alpha} \quad (\text{E.1-8})$$

Likewise, for the SPS and TADAS systems, the bottom beam should be designed to resist a moment equal to  $1.5 V_d h_l$  or  $1.5 V_d h_T$ . Moreover, for a given SPS or TADAS device, it is also advantageous to select a flexurally stiff bottom beam to minimize rigid-body rotation of the energy dissipating device and thus maximize hysteretic energy at a given lateral deck displacement.

5. Design the energy dissipating device. For the link beam in an EBF end-diaphragm, the shear force  $V_l$  in the link is:

$$V_l = \frac{H}{L_s} V_d \quad (\text{E.1-9})$$

The plastic shear capacity  $V_p$  of a wide flange steel beam is given by Equation E.1-10:

$$V_p = 0.58 F_y t_w d_l \quad (\text{E.1-10})$$

where  $F_y$  is the yield stress of steel,  $t_w$  is the web thickness, and  $d_l$  is the depth of the beam. The moment simultaneously applied to the link must be less than the reduced moment capacity,  $M_p^*$ , of the link yielding in shear (Malley and Popov, 1983):

$$M_p^* = t_f b_f F_y (d_l - t_f) \quad (\text{E.1-11})$$

Since shear links are more reliable energy dissipators than flexural links (Kasai and Popov, 1986; AISC, 1992), shear links are favored and their length is therefore limited by the equation below:

$$e < e_{\max} = 1.6 \frac{M_p^*}{V_p} \quad (\text{E.1-12})$$

A link length,  $e$ , of  $1/8$  to  $1/12$  of the girder spacing,  $L_s$ , is recommended for preliminary design, the less restrictive value preferred for practical reasons (i.e. detailing constraints) in presence of closely spaced girders. Deeper link beams are also preferred as the resulting larger flexural stiffness enhances the overall stiffness of the ductile device, ensuring that its yield displacement is reached much before onset of yielding of the stiffened girders.

For a SPS, the above procedure would be followed with the obvious exception that  $V_l = V_d$  and the height of panel should be limited to half of the value obtained by the above equation since the yielding link is only in single curvature, as opposed to double curvature for the EBF. A link height of  $1/8$  to  $1/10$  of the girder depth is recommended for preliminary design. However, for a TADAS system, replace *Step 5* with *Step 6*:

6. Select a small plate thickness,  $t_T$ , based on available plate size. The shear strength,  $V_T$ , and the stiffness,  $K_T$ , of a TADAS device can be determined from (Tsai et al., 1993):

$$V_T = \frac{N b_T t_T^2 F_y}{4 h_T} \quad (\text{E.1-13})$$

$$K_T = \frac{N E b_T t_T^3}{6 h_T^3} \quad (\text{E.1-14})$$

where  $N$ ,  $b_T$ ,  $t_T$  and  $h_T$  are the number, base width, thickness and height of the triangular steel plates. The ratio of the above equations directly provides a relationship between  $h_T$  and  $t_T$ :

$$h_T = \sqrt{\frac{2 E t_T V_T}{3 F_y K_T}} \quad (\text{E.1-15})$$

Here,  $V_T = V_d$  and a  $h_T$  of  $H/10$  to  $H/12$  is recommended. Hence, if a reasonable estimate of the desirable  $K_T$  for the TADAS device is possible,  $t_T$  can be determined directly from  $h_T$ . In turn,  $b_T$  can be chosen knowing that triangular plates with aspect ratio,  $h_T/b_T$ , between 1 and 1.5 are better energy dissipators, based on experimental results (Tsai et al.,

1993). Finally,  $N$  can then be calculated. Small adjustments to all parameters follow as  $N$  is rounded up to the nearest whole number. Incidentally, many different yet appropriate TADAS systems could be designed within these constraints. Systems with thinner steel plates perform better.

7. Calculate the stiffness of the ductile end-diaphragm by using the equation presented earlier in this appendix. Review the assumed lateral period of the bridge,  $T$ , and update calculation as necessary.
8. For the maximum lateral drift of the bridge at the diaphragm location,  $\delta_{max}$ , check that the maximum ductility capacity of ductile device is not exceeded. For shear links, this is commonly expressed in terms of the maximum link deformation angle,  $\gamma_{max}$  (easily obtained by dividing the maximum relative displacements of link ends by the link length), the maximum drift for the SPS and EBF diaphragms is respectively limited to:

$$\delta_{max} < e\gamma_{max} \quad (E.1-16)$$

$$\delta_{max} < \frac{eH}{L_s} \gamma_{max} \quad (E.1-17)$$

with generally accepted  $\gamma_{max}$  limits of 0.08 (AISC, 1997). Note that, for the SPS dia-

phragms, the following alternative equation accounting for the rotation of bottom beam at the link connection may be more accurate when this factor has an important impact:

$$\delta_{max} < e \left( \gamma_{max} + \frac{V_d L_s (h_l + d_{bb}/2)}{12EI_{bb}} \right) \quad (E.1-18)$$

Should these limits be violated, modify the link's depth and length as well as the stiffness of the EBF or SPS diaphragm as necessary, and repeat the design process. Finally, a maximum drift limit of 2% of the girder height is also suggested here, at least until experimental evidence is provided to demonstrate that higher values are acceptable.

Note that the ductile energy dissipating elements should be laterally braced at their ends to prevent out-of-plane instability. These lateral supports and their connections should be designed to resist 6% of the nominal strength of the beam flange, i.e.  $0.06F_y t_f b_f$  (AISC, 1997). In addition, to prevent lateral torsional buckling of beams in the SPS, EBF, and TADAS end-diaphragms, the unsupported length,  $L_u$ , of these beams shall not exceed  $\frac{200b_f}{\sqrt{F_y}}$ ,

where  $b_f$  is the width of beam flange in meters and  $F_y$  is the yield strength of steel in MPa.



## Appendix F

### DUCTILE END-DIAPHRAGM IN DECK TRUSS BRIDGE

#### F.1 DESIGN PROCEDURE

Similarly to the procedure described in Appendix E, a seismic design strategy that relies on ductile end-diaphragms inserted in the steel superstructure of deck-truss bridges can be, in some instances, an effective alternative to energy dissipation in the substructure. This could be the case, for example, when stiff wall-piers that can, with difficulty, be detailed to have a stable ductile response are used as a substructure. The ductile diaphragms considered in this Article are therefore those that can be specially designed and calibrated to yield before the strength of the substructure is reached (substructural elements, foundation, and bearings are referred generically as “substructure” here).

Seismically generated inertia forces in deck-trusses can follow two possible load paths from the deck to the supports. As a result, to implement the ductile diaphragm strategy in such bridges, it is necessary to locate yielding devices in both the end-cross frames and in the lower end panels adjacent to the supports. This is illustrated in Figure F.1-1. The methodology described in this Appendix is limited to simply supported spans of deck trusses. Until further research demonstrates otherwise, the design concept currently also requires stiffening of the top truss system, which can be achieved by making the concrete deck continuous and composite. This stiffening of the top truss system has two benefits. First, for a given deck lateral displacement at the supports, it reduces mid-span sway, resulting in lower forces in the interior cross-frames. Second, it increases the share of the

total lateral load transferred through the top load path.

Note that the design strategy presented here only provides enhanced seismic resistance and substructure protection for the component of seismic excitation transverse to the bridge, and must be coupled with other devices that constraint longitudinal seismic displacements, such as simple bearings strengthening, rubber bumpers and the likes.

Under transverse earthquake excitation, end-diaphragms are designed to be the only energy dissipation elements in these bridges. The remaining structural components must be designed to remain elastic (i.e., capacity protected). Some restrictions on stiffness are necessary to prevent excessive ductility demands in the panels and excessive drift and deformations in other parts of the superstructure. The engineer must identify the displacement constraints appropriate to specific bridges; these will vary depending on the detailing conditions germane to the particular bridge under consideration. Generally, among those limits of important consequences, the maximum permissible lateral displacement of the deck must not exceed the values at which:

- Unacceptable deformations start to develop in members or connections of the deck-truss, such as inelastic distortion of gusset plates, premature bolt or rivet failures, or damage to structural members;
- $P-\Delta$  effects causes instability of the end verticals during sway of the end panel or damage to the connections of the end verticals;

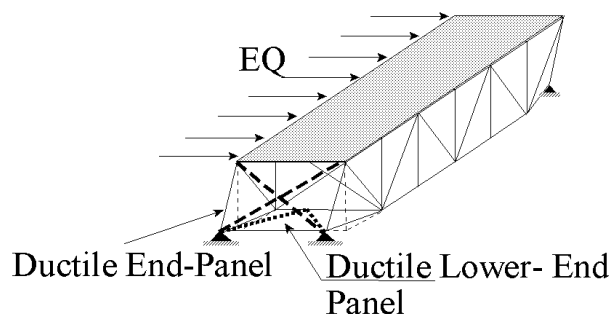


**Figure F.1-1 Ductile Diaphragm Concept in Deck Trusses**

- The energy dissipating devices used in the ductile panels reach their maximum deformation without loss of strength. This requires, for each type of energy dissipating devices considered, engineering judgment and experimental data on the device's ultimate cyclic inelastic performance, often expressed by a consensus opinion. For a given geometry, the ductility demand on the energy dissipating elements is related to the global ductility demand of the deck-truss. Therefore, global stiffness of the structure must be determined so as to keep global ductility and displacement demands within reasonable limits. Stiffness of the ductile devices has a dominant effect on the overall stiffness, and this provides the control necessary for design.

Finally, it is recommended that the stiffness of the ductile panels be kept proportional to their respective capacity, as much as possible, to ensure that yielding in all ductile panels occurs nearly simultaneously. This should enhance energy dissipation capability and minimize the differences in the local ductility demands between the various yielding devices. It also helps prevent sudden changes in the proportion of the load shared between the two load paths, and minimize possible torsion along the bridge axis resulting from the instantaneous eccentricity that can develop when the end ductile panels yield first, while the lower end ductile panels are still elastic.

#### General Design Methodology

Conceptually, any type of ductile energy dissipation system could be implemented in the end panels and lower end panels of the deck-truss, as long as its stiffness, ductility, and strength characteristics satisfy the requirements outlined in this appendix. The design methodology is iterative (initial properties must be assumed), and contains the following general steps.

1. Calculate fundamental period of vibration.

The fundamental period for the transverse mode of vibration is given by:

$$T = 2\pi \sqrt{\frac{M}{K_{Global}}} \quad (F.1-1)$$

where  $M$  is the total mass of the deck, and  $K_{Global}$  is given by:

$$K_{Global} = 2(K_{E,S} + K_{L,S}) \quad (F.1-2)$$

where  $K_{E,S}$  is the stiffness of the ductile end cross-frames, taking into account the contribution to stiffness of the braces, verticals, horizontal, and ductile energy dissipation device/system, and  $K_{L,S}$  is given by:

$$K_{L,S} = \frac{K^* K_{L,E}}{K^* + K_{L,E}} \quad (F.1-3)$$

where  $K_{L,E}$  is the stiffness of the ductile last lower lateral panel, and

$$K^* = \frac{K_{C,B} + \sqrt{K_{C,B}^2 + 4K_{C,B}K_{L,B}}}{2} \quad (F.1-4)$$

where  $K_{L,B}$  represents the lateral stiffness of each panel of the lower lateral system (considering only the contribution of the braces to the panel stiffness) and  $K_{C,B}$  represents the stiffness of the cross bracing panels (considering only the contribution of the braces to the panel stiffness).

The above equations are valid for a truss having at least 6 panels along its length. Otherwise, other equations can be derived following the procedure described in Sarraf and Bruneau (1998a).

2. Determine design forces.

Although use of the capacity spectrum or push-over analysis is recommended for the design of such bridges, design is also possible using the  $R$ -factor approach. In that case, from the elastic seismic base shear resistance,  $V_e$ , for one end of the bridge (half of equivalent static force), it is possible to calculate  $V = V_e / R$ , where  $V$  is the inelastic lateral load resistance of the entire ductile diaphragm panel at the target reduction factor, and  $R$  is the force reduction factor calculated as indicated in Article 7.7.8.3 or 8.7.8.3 of these *Guidelines*. Note that  $\mu$  in that equation represents the ductility capacity of the ductile diaphragm as a whole, not the local ductility of the ductile device that may be implemented in that diaphragm.

3. Determine strength constraints for ductile diaphragms in end panels.

The upper limit for the transverse shear capacity of each end cross-frame panel,  $V_{E,S}$ , can be determined from the following:



$$1.5V_{E,S} \leq \text{Min}\left(\frac{P_{Cr}b}{h}, \frac{T_r b}{h}\right) \quad (\text{F.1-5})$$

where,  $P_{Cr}$ , is the critical buckling load of the end verticals including the effect of vertical gravity as well as vertical inertia force due to earthquake,  $T_r$  is the tensile capacity of the tie down device at each support,  $h$ , and  $b$  are height and width of the end cross-frame panel, respectively, and 1.5 is an overstrength factor.

4. Determine strength constraints for ductile diaphragms in lower end panels.

Analyses showed that the force distribution in the interior cross-frames along the span is non-linear and of a complex shape. The model used to develop the equations presented here gives a conservative value of the lower end panel capacity,  $V_{L,E}$ , i.e. it ensures that  $V_{L,E}$  is reached before any damage develops in any of the interior cross-frame.

The lower end panel capacity shall not exceed the maximum end-panel force attained when the first sway-frame force reaches its strength limit state,  $S_{Cr}$  (corresponding to buckling of its braced members, fracture of a non-ductile connection, or other strength limit states), and defined by:

$$1.5V_{L,E} \leq \frac{\left(\sum_{i=1}^m (1-\xi)^{i-1} - m(1-\xi)^{m-1}\right) S_{Cr}}{1 - (1-\xi)^{m-1}} \quad (\text{F.1-6})$$

where  $m$  is the number of *interior* cross-frames from the support to mid-span, 1.5 is the overstrength factor, and where:

$$\xi = \left( \frac{K_{C,B}}{K_{C,B} + \frac{K^* K_{L,B}}{K^* + K_{L,B}}} \right) \quad (\text{F.1-7})$$

Note that if the total number of interior cross-frames,  $k$ , in a deck-truss is an even number (i.e  $m=(k+1)/2$ , is not an integer),  $m$  can be conservatively taken as  $k/2$ .

Interior cross-frames shall be designed to resist the force  $R'_i$ , given by :

$$R'_i = 1.5V\xi \left(1 - (1-\xi)^{m-1}\right) \quad (\text{F.1-8})$$

where  $V$  is the total seismic force at one end of the deck-truss superstructure.

5. Determine total superstructure capacity.

Given the above limits, the maximum total capacity of the superstructure will be the sum of the capacity of each ductile diaphragm, but not exceeding the substructure capacity, i.e:

$$1.5V_{\max} \leq \left[ \text{Min}\left(2(V_{L,E} + V_{E,S}), 2V_{\text{sub}}\right) \right] \quad (\text{F.1-9})$$

where,  $V_{\text{sub}}$  is the largest shear that can be applied at the top of the abutment without damaging the substructure (connections, wind shoes, etc.), and 1.5 is the overstrength factor. The above equation can be easily modified for bridges having multiple simply-supported spans. Furthermore, a minimum strength,  $V_{\min}$ , must also be provided to resist the winds expected during the life of the structure. Therefore, the yield capacity of the overall deck-truss system,  $R_{\text{total}}$ , should satisfy the following:

$$V_{\min} \leq R_{\text{total}} \leq V_{\max} \quad (\text{F.1-10})$$

6. Distributed total system capacity.

The chosen total capacity of the system can then be divided proportionally between the lower end and end panels according to the following equations, which ensure the same safety margin for both panels.

$$R_{L,E} = \frac{R_{\text{total}}}{V_{\max}} V_{L,E} \quad (\text{F.1-11})$$

$$R_{E,S} = \frac{R_{\text{total}}}{V_{\max}} V_{E,S} \quad (\text{F.1-12})$$

7. Define capacity-based pseudo-acceleration and period limits.

A corresponding *Capacity-Based Pseudo Acceleration*,  $PSa_C$ , can be calculated as:

$$PSa_C = \frac{R_{\text{total}}}{M} \quad (\text{F.1-13})$$

This value can be drawn on a capacity spectrum, or compared with the required design values. Structural period of vibration directly ties this strength to the ductility and displacement demands. For example, in the intermediate period range, the ductility demand of systems having a constant strength decreases as

the period increases (i.e., as stiffness decreases), while their displacement response increases. Therefore, a range of admissible period values can be located along the capacity-based pseudo-acceleration line, based on the permissible values of global ductility and displacement of the system corresponding to a particular ductile system.

Design iterations are required until a compatible set of strength and period are found to provide acceptable ductility and displacement demands. In other words, for a desired structural system strength, a range of limiting periods can be defined by a lower bound to the period,  $T_{min}$ , to limit system ductility demands, and an upper bound,  $T_{max}$ , to limit displacement demands (note that in some instances,  $T_{min}$  may not exist). As a result of these two constraints:

$$T_{min} \leq T \leq T_{max} \quad (F.1-14)$$

Note that it may be more convenient to express these limits in terms of the global stiffness of the entire structural system, or of the end panel. Since:

$$K_{E,S} = \frac{K_{Global}}{\alpha} \quad \text{where } \alpha = 2 \left( 1 + \frac{R_{L,E}}{R_{E,S}} \right) \quad (F.1-15)$$

then:

$$\frac{4\pi^2 M}{T_{max}^2} \leq K_{Global} \leq \frac{4\pi^2 M}{T_{min}^2} \quad (F.1-16)$$

or for the end panel stiffness:

$$\frac{4\pi^2 M}{\alpha T_{max}^2} \leq K_{E,S} \leq \frac{4\pi^2 M}{\alpha T_{min}^2} \quad (F.1-17)$$

This can be used to select proper values of stiffness for the end panel. To calculate the stiffness of the lower end ductile panel,  $K_{L,E}$ , the stiffness of the lower load path system is first determined as:

$$K_{L,S} = \frac{(K_{Global} - 2K_{E,S})}{2} \quad (F.1-18)$$

and  $K_{L,E}$  is given by:

$$K_{L,E} = \frac{K^* K_{L,S}}{K_{L,S} - K^*} \quad (F.1-19)$$

## 8. Design of ductile diaphragm panels.

As indicated in Appendix E, many types of systems capable of stable passive seismic energy dissipation could be used as ductile diaphragms in deck-truss bridges. Among those, eccentrically braced frames (EBF) (e.g., Malley and Popov, 1983; Kasai and Popov, 1986), shear panel systems (SPS) (Fehling et al., 1992; Nakashima, 1995), and steel triangular-plate added damping and stiffness devices (TADAS) (Tsai et al., 1993), popular in building applications, have been studied for bridge applications (Sarraf and Bruneau, 1998a, 1998b). Although concentrically braced frames can also be ductile, they are not admissible in Article 7.7.8.3 or 8.7.8.3 because they can often be stronger than calculated, and their hysteretic curves can exhibit pinching and some strength degradation.

For convenience, the flexibility (i.e. inverse of stiffness) of panels having ductile diaphragms is provided below for a few types of ductile systems.

The flexibility of an eccentrically braced end panel,  $f_{E,S}$ , is expressed by:

$$f_{E,S} = \frac{h^2}{2EIb} \left( \frac{(a+e)^2}{3} - \frac{(b^2 - 2a^2)}{6} \right) + \frac{(a^2 + h^2)^{3/2}}{2EA_b a^2} + \frac{h^3}{2EA_{col} a^2} + \frac{(b-e)}{4EA_l} + \frac{eh^2}{2GA_s ab} \quad (F.1-20)$$

where  $a = (b-e)/2$ ,  $b$  is the panel width,  $h$  is the height,  $A_{col}$  is the cross-sectional area of a vertical panel member,  $A_b$  is the cross-sectional area of a bracing members,  $A_l$ ,  $A_s$ , and  $I$  are respectively the cross-sectional area, shear area, and moment of inertia of the link beam, and  $e$  is the link length.

The flexibility,  $f_{E,S}$ , of a ductile **VSL** panel can be expressed by the following equation:

$$f_{E,S} = \frac{b(s+d/2)^2}{12EI} + \frac{2((h-s-d/2)^2 + b^2/4)^{3/2}}{EA_b b^2} + \frac{2h(h-s-d/2)^2}{EA_{col} b^2} + \frac{b}{4EA_l} + \frac{s}{A_s G} \quad (F.1-21)$$

where,  $s$  is the height of the shear panel,  $I$ , is the bottom beam moment of inertia, and,  $d$ , is the depth of the bottom beam. The other parameters are as previously defined.

The required flexibility of the triangular plates alone for a TADAS system,  $f_T$ , expressed in terms of an admissible flexibility value of the end panel and other panel member properties, is given by:

$$f_T = f_{E,S} - \left( \frac{\frac{b(\eta h + d/2)^2}{12EI} + \frac{2\left(\left((1-\eta)h - d/2\right)^2 + (b/2)^2\right)^{3/2}}{EA_b b^2}}{\frac{2h\left((1-\eta)h - d/2\right)^2}{EA_{col} b^2} + \frac{b}{4EA_I}} \right) \quad (\text{F.1-22})$$

where  $\eta$ , is the ratio of height of triangular plates to the height of the panel and other parameters correspond to the panel members similar to those of VSL panel. Tsai, et.al. (1993) recommended using  $\eta=0.10$ .



## Appendix G

### PARAMETRIC STUDY OF COLUMN DESIGNS

#### G.1 BACKGROUND AND PURPOSE

In support of the NCHRP 12-49 effort to develop the next generation of seismic design provisions for bridges, a parameter study was undertaken to determine the impact of the proposed provisions on the design of bridges in the United States. The proposed provisions are not simply a revision of the current Division I-A seismic provisions of the AASHTO *Standard Specifications for Highway Bridges* or a revision of the seismic provisions in the AASHTO *LRFD Bridge Design Specifications*. Accordingly, the seismic hazard mapping, the design spectrum, the load factors, capacity reduction factors, overstrength factors, and numerous other important design parameters have been changed.

Because the seismic design provisions have, essentially, been rewritten entirely, the purpose of this parameter study was to provide a comprehensive perspective of the impact of the new provisions on typical bridge designs. The uses of the parameter study were two-fold: (1) to benchmark the new provisions' results against those of the existing AASHTO Division I-A seismic provisions and (2) to ascertain the effects of key parameters and fine-tune them relative to good engineering practice.

#### G.2 SCOPE OF THE PARAMETER STUDY

The parameter study was conducted to develop detailed designs of the primary lateral load resisting elements for relatively simple bridge structures. In this context, 'simple' implies, primarily, that the structure can be considered a single-degree-of-freedom (SDOF) system. The results of these simple designs were likewise compared against the results that the Division I-A provisions would produce. The Division I-A provisions were selected as the appropriate benchmark for the parameter study because it was felt that most agencies are using those seismic provisions and not the seismic provisions in the LRFD *Specifications*. Therefore, the best benchmark was judged to be those provisions with which most bridge designers are familiar.

The objective for choosing this approach was to illustrate detailed results for near-actual designs. The detailed designs present a comprehensive view of the resulting member designs and costs for simple structures, although they represent a relatively limited set of data points.

The study includes comparisons for structures founded on concrete columns. The comparisons also included simplified foundation designs for spread footings. Consideration of abutment resistance, particularly in the longitudinal direction, was also performed as part of this study, but is not reported in this summary.

Designs were considered at discrete locations throughout the country. Five locations were used, which represent a broad geographic and seismic hazard range. The sites considered are:

- Seattle, Washington
- Portland, Oregon
- Memphis, Tennessee
- St. Louis, Missouri
- New York, New York

In addition, only Soil Site Class C was included. This is due to the fact that all the designs compared were founded on spread footings, and Type C soil was considered a typical soil on which spread footings would be used.

The 100-year (Expected Earthquake) and 2500-year (Maximum Considered Earthquake) seismic coefficients and soil factors from the proposed next-generation seismic design provisions are included in Table G-1. For comparison, the acceleration coefficients for the Division I-A seismic provisions are included in Table G-2. The site soil factor for Division I-A for all the designs and locations is also included in Table G-2. An overview of the parameters that impact a specific column design for Seattle is shown in Table G-3.

#### G.3 DESCRIPTION OF COLUMN DESIGNS

Simulated viaduct-type bridges were used to study the impact of the proposed seismic design specifications on 4-foot-diameter reinforced concrete columns. The studies included the design of

**Table G-1 Design Spectral Accelerations and Site Class Coefficients (Soil Class C) NCHRP 12-49 Seismic Provisions (Part I of this document)**

Site	100-Year Earthquake				2500-Year Earthquake			
	(50% Prob. of Exceed. in 75 Years)				(3% Prob. of Exceed. in 75 Years)			
	Ss	Fa	S1	Fv	Ss	Fa	S1	Fv
Seattle, WA	0.314	1.2	0.093	1.7	1.60	1.0	0.56	1.3
Portland, OR	0.176	1.2	0.054	1.7	1.05	1.0	0.35	1.46
Memphis, TN	0.067	1.2	0.015	1.7	1.35	1.0	0.41	1.38
St. Louis, MO	0.06	1.2	0.014	1.7	0.59	1.2	0.19	1.61
New York, NY	0.03	1.2	0.007	1.7	0.42	1.2	0.09	1.7

**Table G-2 Design Acceleration Coefficients and Soil Type Factors (Soil Type II) AASHTO Division I-A Seismic Provisions (AASHTO, 1996)**

Site	500-Year Earthquake	
	(10% Prob. of Exceed. in 50 Years)	
	A	S
Seattle, WA	0.32	1.2
Portland, OR	0.16	1.2
Memphis, TN	0.20	1.2
St. Louis, MO	0.10	1.2
New York, NY	0.15	1.2

**Table G-3 Example Calculation of Column Design Forces**

Location: Seattle, WA A = 0.32 Weight: 725 kips S = 1.2 Height: 30 feet $F_v = 0.56$ $P/fcAg$ 0.1 $S_1 = 1.3$ B.C.s: Fixed Top and Bottom				
Division I-A Quantity	Division I-A Result		NCHRP 12-49 Result	NCHRP 12-49 Quantity
	Gross Props.	Effective Props.		
Period, T (sec)	0.58 sec	0.80 sec	0.80 sec	Period, T (sec)
$T_s$	0.44 sec	0.44 sec	0.46 sec	$T_s$
$C_s = 1.2 A S / T^{2/3}$	0.66	0.53	0.91	$SA = F_v S_1 / T$
$V_e = C_s W$	479 kips	388 kips	660 kips	$V_e = SA W$
$M_e = V_e H/2$	7185 kip-ft	5280 kip-ft	9900 kip-ft	$M_e = V_e H/2$
$M_d = M_e / R \phi$	3421 kip-ft	2518 kip-ft	2475 kip-ft	$M_d = M_e / R \phi$
	( R = 3; $\phi = 0.7$ )		( R = 4; $\phi = 1.0$ )	
Ratio of 12-49/I-A	0.72	0.98	--	Ratio of 12-49/I-A

a typical bridge column and spread footing using the existing Division I-A procedures and the proposed NCHRP 12-49 procedures using  $R$ -factors of 2, 4, 6, and 8. Two structure configurations were examined. The first, shown in Figure G-1, included a column type that was fixed for moment at both ends and was assumed to be part of a single-column bent. The second was free to rotate at the top of the column as shown in Figure G-2 and was assumed to be part of a multi-column bent.

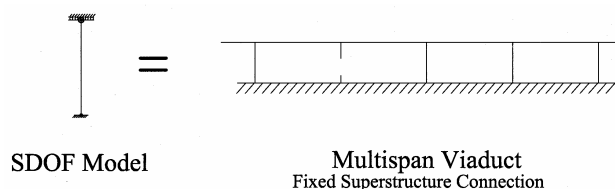


**Figure G-1      SDOF Model for Single-Column Bent Design Study Column Fixed for Moment at Top and Bottom**

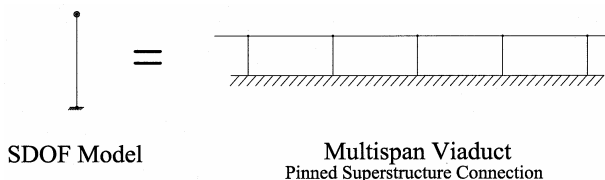


**Figure G-2      SDOF Model for Multi-Column Bent Design Study Column Fixed for Moment at Bottom Only**

Dead load and column length was varied for both structural configurations. Normalized dead load ( $P/f'_c A_g$ ) was varied from 0.05 to 0.20 and was assumed to be 100% effective as mass acting on the columns. Column length varied from 20 to 40 feet. As previously indicated, each structure was designed for five sites: Seattle, Washington; Portland, Oregon; Memphis, Tennessee; St. Louis, Missouri; and New York, New York. These sites were selected to cover a broad range of loading conditions that might be encountered throughout the United States. Concrete strength ( $f'_c$ ) was assumed to be 4000 psi and reinforcing steel was assumed to be Grade 60. To assess the sensitivity of design procedures to column diameter, the studies for multi-column bents were extended to 3-foot-diameter columns in New York and 5-foot-diameter columns in Seattle.

Column design was based on simplified interaction curves constructed by fitting a parabola between the calculated balance point and the maximum column tensile strength. The percentage of longitudinal column reinforcement was determined by interpolating between families of simplified interaction curves. Column design for Division I-A was based on either the minimum steel percentage (0.01) or the calculated moment using the appropriate  $R$ -factor. The moment magnification procedures of the AASHTO Division I provisions, which are intended to account for column slenderness effects, were also included in determining the column design moments. For the proposed NCHRP 12-49 seismic design provisions, design was based on a minimum steel percentage of 0.008, the 2500-year earthquake moments reduced by the appropriate  $R$ -factor, the 100-year earthquake moments reduced by an  $R$ -factor of 1.3, or the minimum column base shear required by the proposed specifications to avoid nonlinear  $P$ - $\Delta$  design. None of the columns studied considered the strength demands of nonseismic load cases or the effect of seismic design in orthogonal directions.

NCHRP 12-49 column designs were evaluated based on their assumed displacements and deformations. Column displacements were adjusted to account for short-period response. Yield displacements were based on the elastic displacements at nominal moment. Column drift, displacement ductility, and plastic rotation were calculated from these assumed displacement values.

The structure was assumed to be supported on square spread footings of a thickness equal to 20% of the plan dimension. Design of these footings was based on a maximum uplift of 50% of the footing or a peak bearing pressure of 20 ksf, whichever controlled. Design moments were the maximum plastic moments generated in the designed column. For Division I-A, this was assumed to be  $1.3M_n$ . A similar simplified method was used for the proposed NCHRP 12-49 criteria except the factor was 1.5 instead of 1.3. A more refined method of calculating  $M_p$ , based on maximum assumed material strengths of  $1.7f'_c$  for concrete and  $1.3f_y$  for reinforcing steel, was also used.

Design of the columns and footings were accomplished within a Microsoft Excel spreadsheet, thus allowing rapid design of a large number of cases (2400). The combinations of parameters used in the study are given in Table G-4.

**Table G-4 Parameter Combinations Used for the Column Design Comparisons**

<b>Column Height</b>	<b>Bridge No.</b>	<b>Gross Weight (kips)</b>	<b><math>P/f_c'A_g</math></b>
20 ft.	1	362	0.05
	2	435	0.06
	3	580	0.08
	4	725	0.10
	5	870	0.12
	6	1015	0.14
	7	1160	0.16
	8	1450	0.20
25 ft.	1A	362	0.05
	2A	435	0.06
	3A	580	0.08
	4A	725	0.10
	5A	870	0.12
	6A	1015	0.14
	7A	1160	0.16
	8A	1450	0.20
30 ft.	1B	362	0.05
	2B	435	0.06
	3B	580	0.08
	4B	725	0.10
	5B	870	0.12
	6B	1015	0.14
	7B	1160	0.16
	8B	1450	0.20
35 ft.	1C	362	0.05
	2C	435	0.06
	3C	580	0.08
	4C	725	0.10
	5C	870	0.12
	6C	1015	0.14
	7C	1160	0.16
	8C	1450	0.20
40 ft.	1D	362	0.05
	2D	435	0.06
	3D	580	0.08
	4D	725	0.10
	5D	870	0.12
	6D	1015	0.14
	7D	1160	0.16
	8D	1450	0.20



## G.4 DISCUSSION OF RESULTS

### G.4.1 Column Strength Control

Column strength, and thus the amount of longitudinal reinforcement, can be controlled by a number of factors in the proposed NCHRP 12-49 seismic design criteria. The column studies demonstrate some interesting trends that are worth noting.

The use of different  $R$ -factors in the proposed NCHRP 12-49 criteria has a surprisingly small impact on a significant number of column designs. For example, a comparison of longitudinal steel requirements for a multi-column bent designed for Seattle using an  $R$ -factor of 4 (Figure G-3) and an  $R$ -factor of 6 (Figure G-4) indicates that no upper limit has been placed on the amount of reinforcement, and that there are only a few column configurations where there is a difference between the longitudinal steel requirements. The reason for this is apparent when the controlling factors for column strength are separated as is done in Figures G-5 through G-7. In Figure G-5, it can be seen that the benefits of an “ $R$ ” value of 6 or 8 are never realized because the steel requirement for the 100-year earthquake is greater than or equal to those for the  $R$ -factor reduced 2500-year earthquake. This is true for larger column heights as well, but as can be seen in Figures G-6 and G-7, column design begins to be dominated by  $P$ - $\Delta$  requirements.

In less seismically active areas, the effect of the 100-year earthquake is diminished, but minimum steel requirements or the  $P$ - $\Delta$  criteria usually govern column design. This is demonstrated in Figure G-8 for Memphis. The breakdown of controlling design factors is shown clearly in Figures G-9 through G-11.

The impact of the  $R$ -factor appears to increase in the single-column bent studies. As shown in Figures G-12 and G-13, reinforcement ratios are significantly less when an  $R$ -factor of 6 was used. However, a close observation of Figures G-14 and G-15 shows that the full benefit of using a higher  $R$ -Factor is never realized due to minimum reinforcement and 100-year earthquake requirements.

The following paragraphs briefly discuss factors affecting column strength.

#### *R-Factors*

It appears that very little benefit can be gained by using high  $R$ -factors. Other column design con-

trols prevent the designer from taking full advantage of these high factors. Based partially on these studies,  $R$ -factors are limited to a value of 6.

#### *100-Year Earthquake*

As illustrated in the Seattle multi-column study, the 100-year earthquake is a major factor in column design in areas of high seismicity, particularly the western United States. In these cases, it often controls over the design for the 2500-year earthquake when a high  $R$ -factor is used. This may present a design problem in certain regions, such as parts of California, but it does not appear to prohibit reasonable column designs elsewhere in the United States. To mitigate unusually strict requirements on column strength, an  $R$ -factor of 1.3 is used with the 100-year earthquake.

#### *P- $\Delta$ Requirements*

The requirements for  $P$ - $\Delta$  are based on avoiding dynamic instability that can result from a biased response of the column in one direction. This could result in a potential “ratcheting over” of the column in an earthquake of long duration. This requirement is critical to column design. Proposed  $P$ - $\Delta$  requirements are similar to requirements given in ATC-32 (ATC, 1996), which are based largely on empirical observations of analytical studies. Further research in this area is necessary to develop a more rational approach to this issue.

#### *Minimum Reinforcement Ratios*

Currently, Division I-A sets the minimum steel percentage at 1%. Even when this percentage is reduced to 0.8%, it still often controls the design. In New York, for example, the design of columns is based entirely on minimum steel requirements as shown in Figure G-16. Because studies have shown that lower steel percentages are still effective, the proposed minimum steel requirement is lowered to 0.8%.

### G.4.2 Column Performance

Column performance, as measured by inelastic demand, appears to be satisfactory in all cases studied. The estimated column plastic rotation never exceeded 0.035, the limit used in the new provisions, for any of the NCHRP 12-49 design columns. Further evaluation using nonlinear push-over analysis is required to confirm this observation.

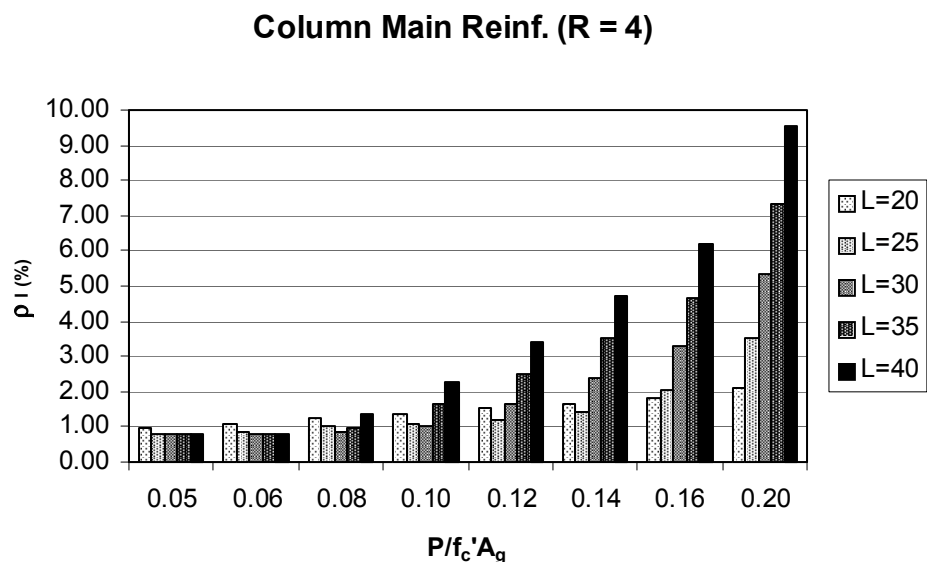


**Figure G-3** Column Main Reinforcement Requirements for 4-Foot-Diameter Multi-Column Bents in Seattle Designed with a R-factor of 4 and Various Column Heights (L).

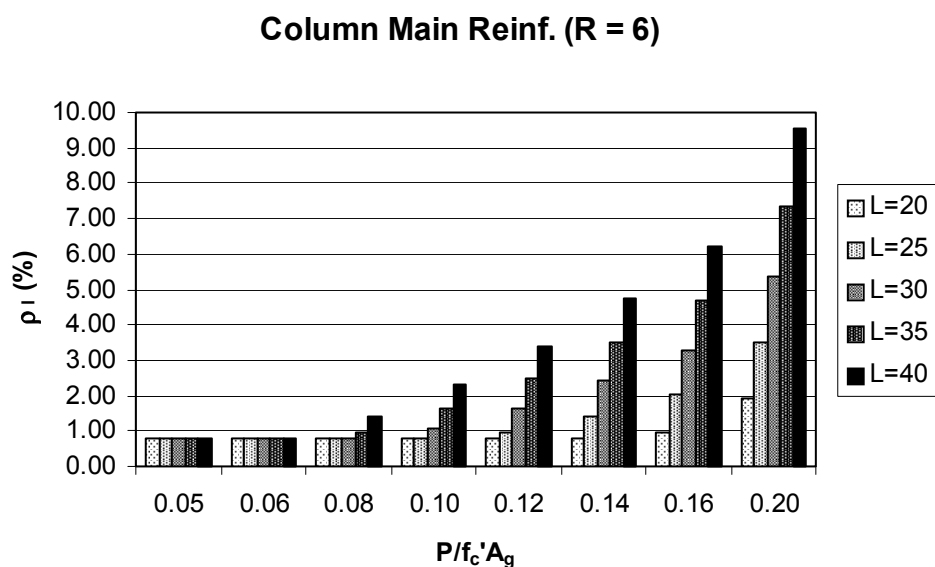


**Figure G-4** Column Main Reinforcement Requirements for 4-Foot-Diameter Multi-Column Bents in Seattle Designed with a R-factor of 6 and Various Column Heights (L).

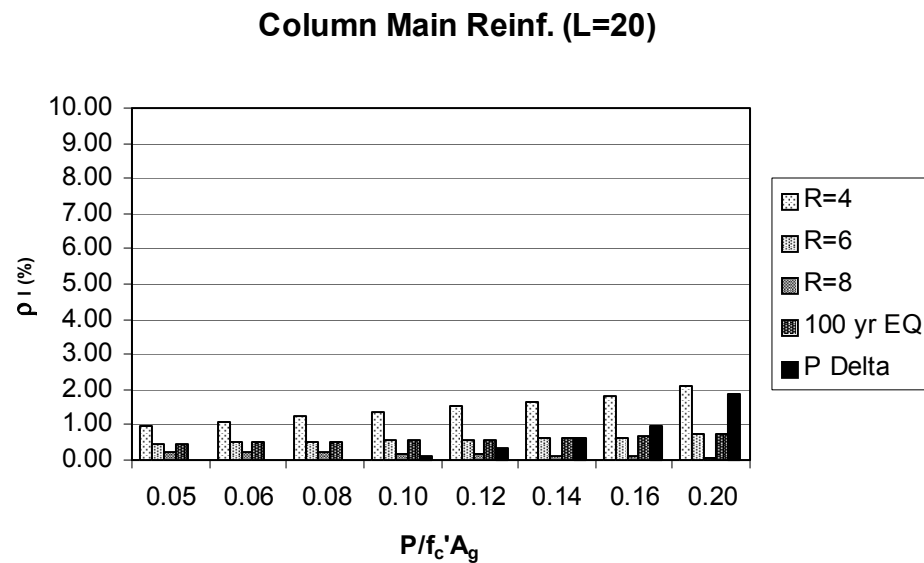


**Figure G-5 Breakdown of Column Main Reinforcement Design Controls for 4-Foot-Diameter 20-Foot-Tall Multi-Column Bents in Seattle**

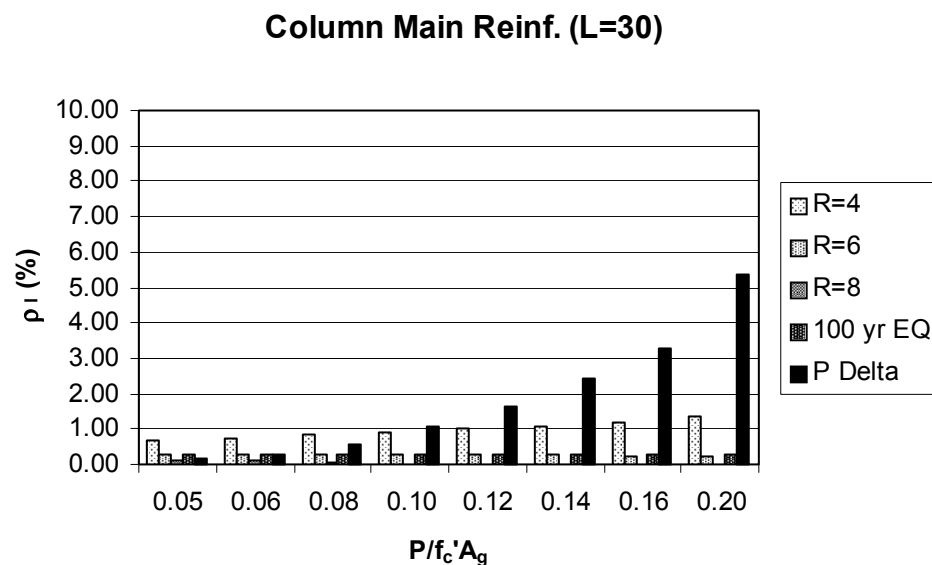


**Figure G-6 Breakdown of Column Main Reinforcement Design Controls for 4-Foot-Diameter 30-Foot-Tall Multi-Column Bents in Seattle**

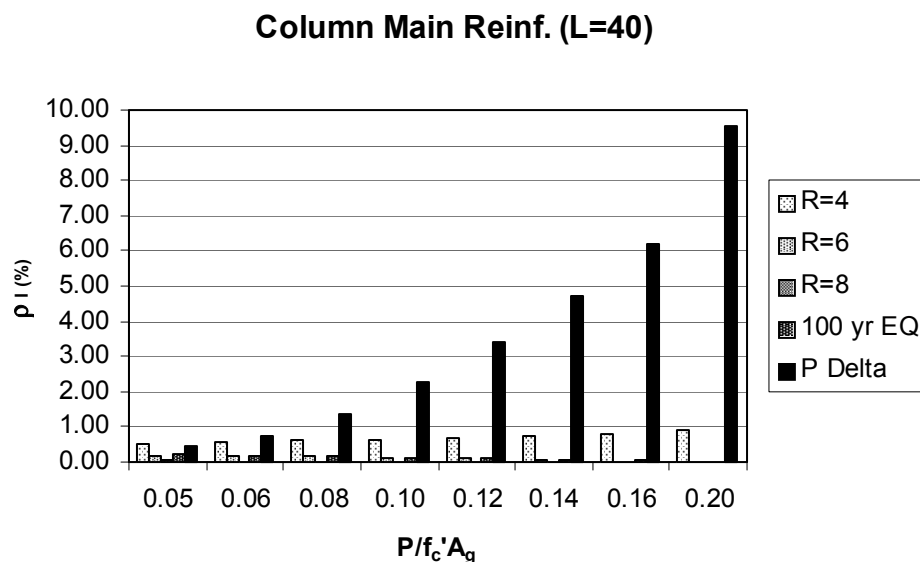


**Figure G-7 Breakdown of Column Main Reinforcement Design Controls for 4-Foot-Diameter 40-Foot-Tall Multi-Column Bents in Seattle**

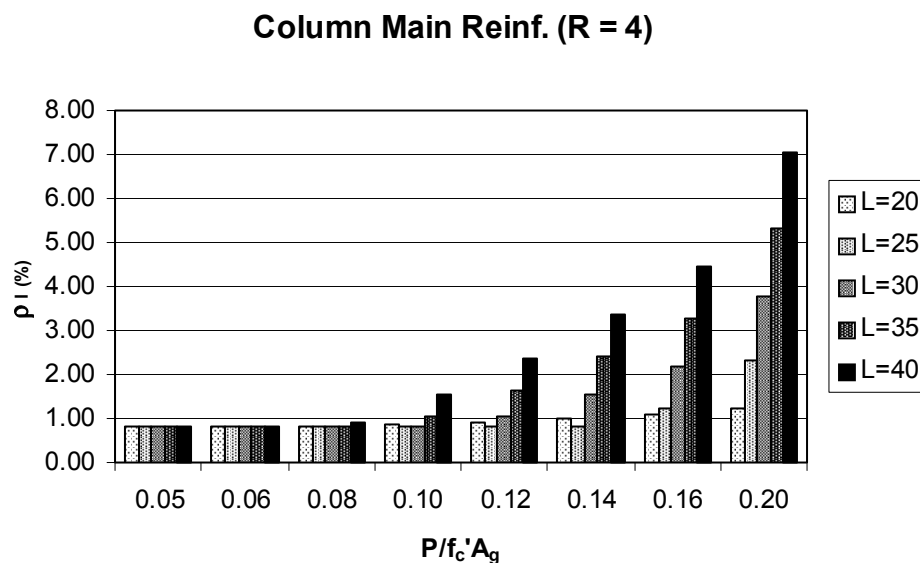


**Figure G-8 Column Main Reinforcement Requirements for 4-Foot-Diameter Multi-Column Bents in Memphis Designed with a R-factor of 4**

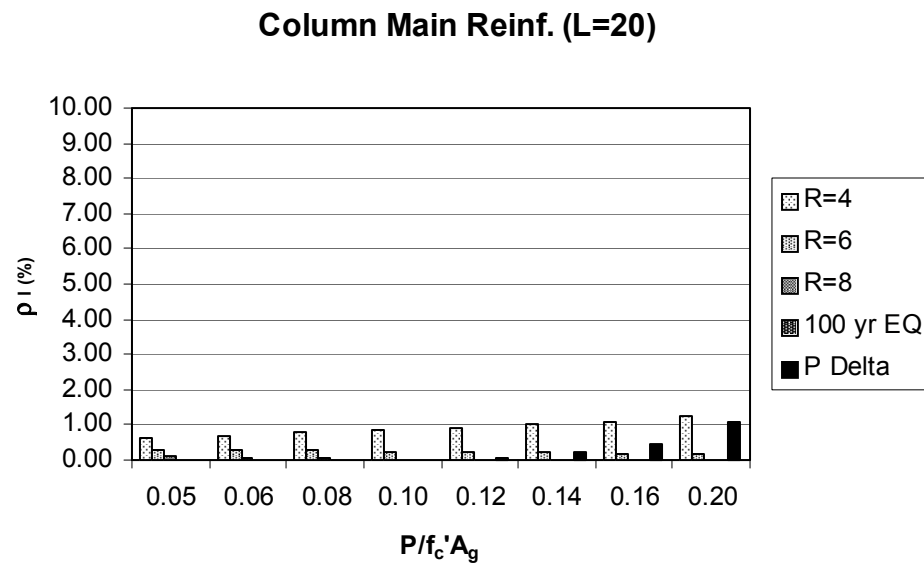


**Figure G-9 Breakdown of Column Main Reinforcement Design Controls for 4-Foot-Diameter 20-Foot-Tall Multi-Column Bents in Memphis**

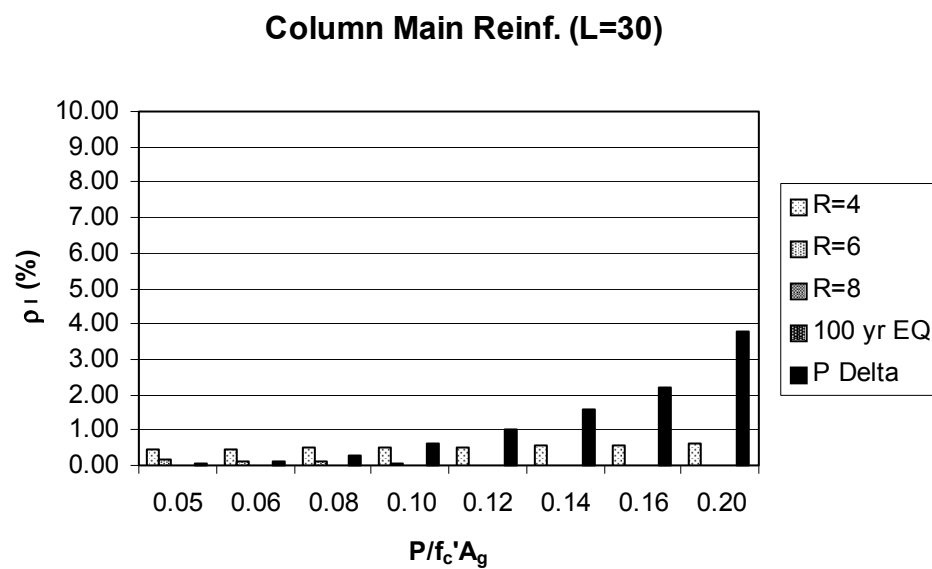


**Figure G-10 Breakdown of Column Main Reinforcement Design Controls for 4-Foot-Diameter 30-Foot-Tall Multi-Column Bents in Memphis**

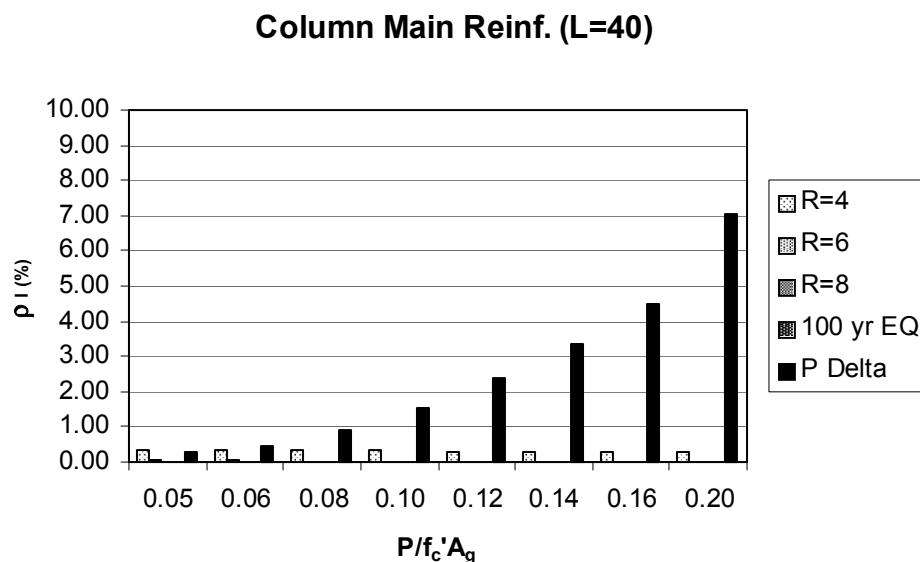


**Figure G-11 Breakdown of Column Main Reinforcement Design Controls for 4-Foot-Diameter 40-Foot-Tall Multi-Column Bents in Memphis**

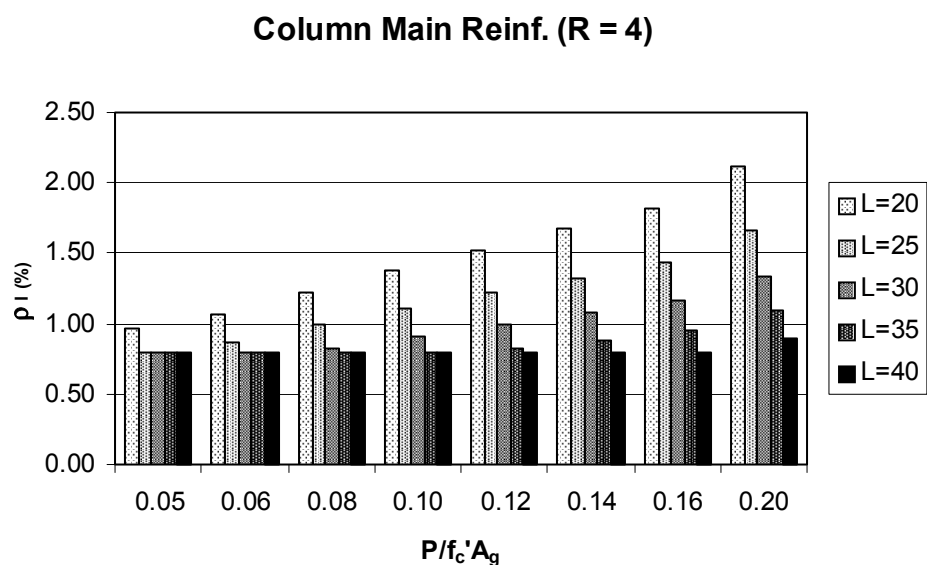


**Figure G-12 Column Main Reinforcement Requirements for 4-Foot-Diameter Single-Column Bents in Seattle Designed with a R-factor of 4**

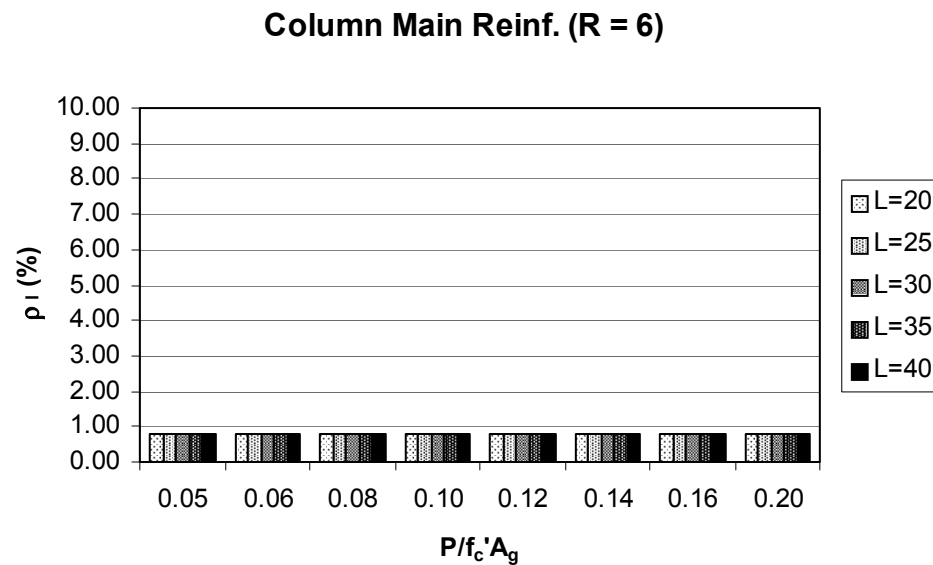


**Figure G-13** Column Main Reinforcement Requirements for 4-Foot-Diameter Single-Column Bents in Seattle Designed with a R-factor of 6

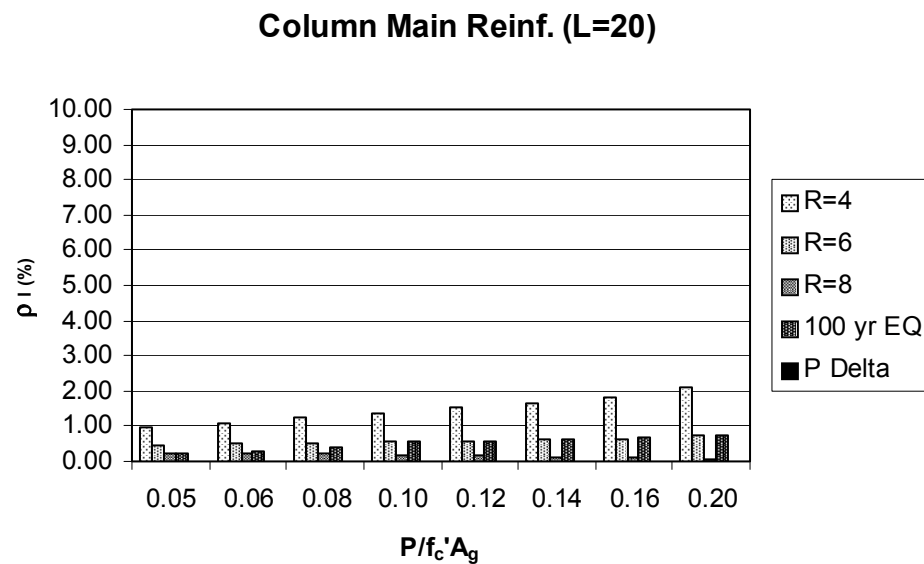


**Figure G-14** Breakdown of Column Main Reinforcement Design Controls for 4-Foot-Diameter 20-Foot-Tall Single-Column Bents in Seattle

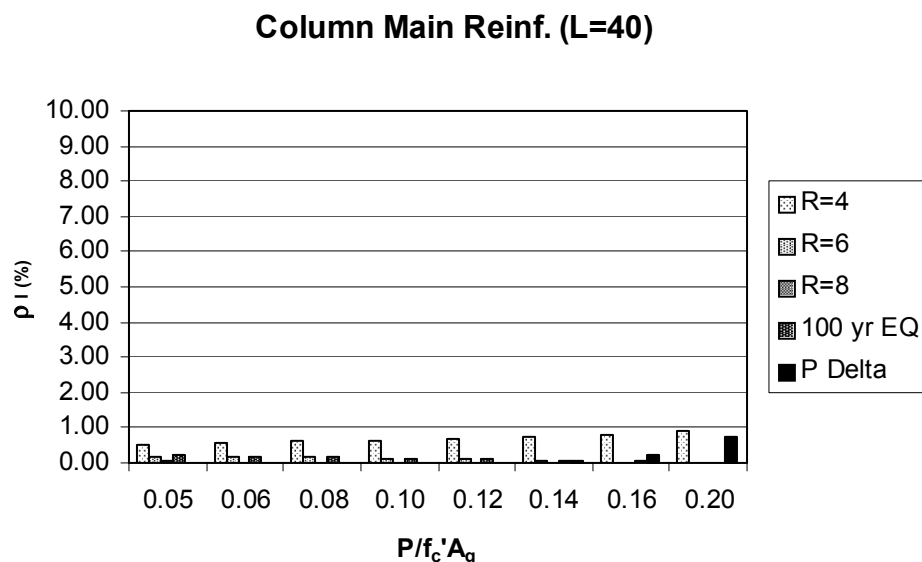


**Figure G-15 Breakdown of Column Main Reinforcement Design Controls for 4-Foot-Diameter 40-Foot-Tall Single-Column Bents in Seattle**

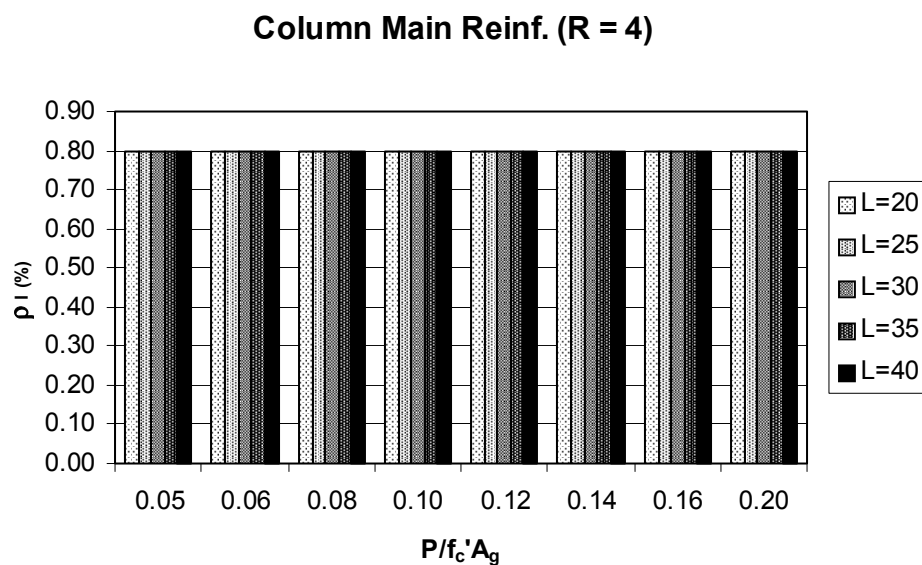


**Figure G-16 Column Main Reinforcement Requirements for 4-Foot-Diameter Multi-Column Bents in New York Designed with a R-factor of 4**



Summaries of column displacements, drift, ductility demands, and plastic rotations are given in Tables G-5 through G-14 for the five cities and for single-column, as well as multi-column bents. These results are all based on designs using an  $R$ -Factor of 4.

### G.4.3 Column Size Effect

The proposed  $P$ - $\Delta$  requirements seem to place a reasonable control on column size. In the Seattle multi-column bent study, high steel percentages in  $P$ - $\Delta$  columns suggested the need for larger column diameter. When column size was increased to 5 feet, the steel percentages were reduced to reasonable levels as shown in Figure G-17. Also, the results of the New York multi-column bent study may tempt a designer to reduce the column size. This would be prevented for heavily loaded tall columns as illustrated in Figures G-18 and G-19 where reinforcement ratios approach or exceed a practical and specified limit of 4% when the column diameter is reduced to 3 feet.

### G.4.4 Column Overstrength

Column overstrength moments have a major impact on footing design. Footing costs tend to be the major contributor to the overall substructure construction cost. Therefore, the use of accurate overstrength moments can have a major cost impact. Because the use of a simplified overstrength factor can often yield overly conservative results, it is recommended that the refined method of calculating overstrength moment be encouraged.

### G.4.5 Cost Impact

Except for a few short, lightly loaded columns, the construction cost of the NCHRP 12-49 de-

signed single-column bents studied tend to be less than their AASHTO (1996) Division 1-A counterparts. This was due to a number of factors, including lower  $R$ -factors, gross section properties used in the AASHTO Division 1-A analysis, AASHTO Division 1-A moment magnification requirements, and lower capacity reduction factors used in the Division I-A designs. Cost ratios for the Seattle designs are illustrated in Figure G-20. Similar plots for the other cities are shown in Figures G-21 through G-24. On the average NCHRP designed substructures with single column bents cost 6% less than their AASHTO Division 1-A counterpart when the simple approach of calculating overstrength moment is used; and 16% less when the refined method of calculating overstrength moment is used.

In the case of NCHRP 12-49 designed multi-column bents, construction costs tend to be higher than these designed using AASHTO Division 1-A in some cases, but on the average, costs are nearly equal. This is partially due to the higher  $R$ -factors used for AASHTO Division 1-A designed multi-column bents, but also due to the  $P$ - $\Delta$  requirements imposed on some of these more flexible columns. The cost ratios for the Seattle designs are shown in Figure G-25. Similar plots for the other cities are shown in Figures G-26 through G-29. On the average NCHRP 12-49 designed substructures with multi-column bents cost 6% more than their AASHTO Division 1-A designed counterpart when the simple approach of calculating overstrength moment is used; and 2% less when the refined method of calculating overstrength moment is used.

**Table G-5 Column Displacement Summary for 4-Foot-Diameter Single-Column Bents in Seattle Designed with a “R” of 4**

<b>NCHRP 12-49</b> <b>Column Design Study</b> <b>Column Performance Evaluation</b> <b>LRFD R=4 (Simple Overstrength Factor)</b>				
<b>Column No.</b>	<b>Displacement (feet)</b>	<b>% Drift</b>	<b>Displacement Ductility</b>	<b>Plastic Rotation (radians)</b>
1	0.16	0.78	3.50	0.006
2	0.18	0.88	3.63	0.007
3	0.21	1.07	3.81	0.009
4	0.25	1.24	3.94	0.010
5	0.28	1.38	4.00	0.011
6	0.30	1.49	4.00	0.012
7	0.32	1.59	4.00	0.013
8	0.36	1.78	4.00	0.015
1A	0.24	0.97	3.93	0.008
2A	0.27	1.09	4.00	0.009
3A	0.31	1.26	4.00	0.010
4A	0.35	1.41	4.00	0.011
5A	0.38	1.54	4.00	0.013
6A	0.42	1.66	4.00	0.014
7A	0.44	1.78	4.00	0.014
8A	0.50	1.99	4.00	0.016
1B	0.33	1.09	4.00	0.009
2B	0.36	1.19	4.00	0.010
3B	0.41	1.38	4.00	0.011
4B	0.46	1.54	4.00	0.012
5B	0.51	1.69	4.00	0.014
6B	0.55	1.82	4.00	0.015
7B	0.58	1.95	4.00	0.016
8B	0.65	2.18	4.00	0.018
1C	0.41	1.18	4.00	0.009
2C	0.45	1.29	4.00	0.010
3C	0.52	1.49	4.00	0.012
4C	0.58	1.66	4.00	0.013
5C	0.64	1.82	4.00	0.015
6C	0.69	1.97	4.00	0.016
7C	0.74	2.10	4.00	0.017
8C	0.82	2.35	4.00	0.019
1D	0.50	1.26	4.00	0.010
2D	0.55	1.38	4.00	0.011
3D	0.64	1.59	4.00	0.013
4D	0.71	1.78	4.00	0.014
5D	0.78	1.95	4.00	0.016
6D	0.84	2.10	4.00	0.017
7D	0.90	2.25	4.00	0.018
8D	1.01	2.51	4.00	0.020

**Table G-6 Column Displacement Summary for 4-Foot-Diameter Single-Column Bents in Portland Designed with a “R” of 4**

<b>NCHRP 12-49</b> <b>Column Design Study</b> <b>Column Performance Evaluation</b> <b>LRFD R=4 (Simple Overstrength Factor)</b>				
<b>Column No.</b>	<b>Displacement (feet)</b>	<b>% Drift</b>	<b>Displacement Ductility</b>	<b>Plastic Rotation (radians)</b>
1	0.11	0.53	3.41	0.004
2	0.12	0.60	3.55	0.005
3	0.15	0.73	3.74	0.006
4	0.17	0.85	3.88	0.007
5	0.19	0.95	3.97	0.008
6	0.21	1.04	4.00	0.009
7	0.22	1.11	4.00	0.009
8	0.25	1.25	4.00	0.010
1A	0.17	0.67	3.86	0.005
2A	0.19	0.75	3.96	0.006
3A	0.22	0.88	4.00	0.007
4A	0.25	0.99	4.00	0.008
5A	0.27	1.08	4.00	0.009
6A	0.29	1.17	4.00	0.010
7A	0.31	1.25	4.00	0.010
8A	0.35	1.39	4.00	0.011
1B	0.23	0.76	4.00	0.006
2B	0.25	0.84	4.00	0.007
3B	0.29	0.97	4.00	0.008
4B	0.32	1.08	4.00	0.009
5B	0.35	1.18	4.00	0.010
6B	0.38	1.28	4.00	0.010
7B	0.41	1.37	4.00	0.011
8B	0.46	1.53	4.00	0.012
1C	0.29	0.82	4.00	0.007
2C	0.32	0.90	4.00	0.007
3C	0.36	1.04	4.00	0.008
4C	0.41	1.17	4.00	0.009
5C	0.45	1.28	4.00	0.010
6C	0.48	1.38	4.00	0.011
7C	0.52	1.47	4.00	0.012
8C	0.58	1.65	4.00	0.013
1D	0.35	0.88	4.00	0.007
2D	0.39	0.97	4.00	0.008
3D	0.45	1.11	4.00	0.009
4D	0.50	1.25	4.00	0.010
5D	0.55	1.37	4.00	0.011
6D	0.59	1.47	4.00	0.012
7D	0.63	1.58	4.00	0.013
8D	0.70	1.76	4.00	0.014

**Table G-7 Column Displacement Summary for 4-Foot-Diameter Single-Column Bents in Memphis Designed with a “R” of 4**

<b>NCHRP 12-49</b> <b>Column Design Study</b> <b>Column Performance Evaluation</b> <b>LRFD R=4 (Simple Overstrength Factor)</b>				
<b>Column No.</b>	<b>Displacement (feet)</b>	<b>% Drift</b>	<b>Displacement Ductility</b>	<b>Plastic Rotation (radians)</b>
1	0.13	0.64	3.57	0.005
2	0.14	0.72	3.70	0.006
3	0.17	0.87	3.87	0.007
4	0.20	1.00	3.99	0.008
5	0.22	1.09	4.00	0.009
6	0.24	1.18	4.00	0.010
7	0.25	1.26	4.00	0.010
8	0.28	1.41	4.00	0.012
1A	0.20	0.79	3.98	0.006
2A	0.22	0.86	4.00	0.007
3A	0.25	1.00	4.00	0.008
4A	0.28	1.11	4.00	0.009
5A	0.31	1.22	4.00	0.010
6A	0.33	1.32	4.00	0.011
7A	0.35	1.41	4.00	0.011
8A	0.39	1.58	4.00	0.013
1B	0.26	0.86	4.00	0.007
2B	0.28	0.95	4.00	0.008
3B	0.33	1.09	4.00	0.009
4B	0.37	1.22	4.00	0.010
5B	0.40	1.34	4.00	0.011
6B	0.43	1.44	4.00	0.012
7B	0.46	1.54	4.00	0.012
8B	0.52	1.73	4.00	0.014
1C	0.33	0.93	4.00	0.008
2C	0.36	1.02	4.00	0.008
3C	0.41	1.18	4.00	0.009
4C	0.46	1.32	4.00	0.011
5C	0.51	1.44	4.00	0.012
6C	0.55	1.56	4.00	0.013
7C	0.58	1.67	4.00	0.013
8C	0.65	1.86	4.00	0.015
1D	0.40	1.00	4.00	0.008
2D	0.44	1.09	4.00	0.009
3D	0.50	1.26	4.00	0.010
4D	0.56	1.41	4.00	0.011
5D	0.62	1.54	4.00	0.012
6D	0.67	1.67	4.00	0.013
7D	0.71	1.78	4.00	0.014
8D	0.80	1.99	4.00	0.016

**Table G-8 Column Displacement Summary for 4-Foot-Diameter Single-Column Bents in St. Louis Designed with a “R” of 4**

<b>NCHRP 12-49</b> <b>Column Design Study</b> <b>Column Performance Evaluation</b> <b>LRFD R=4 (Simple Overstrength Factor)</b>				
<b>Column No.</b>	<b>Displacement (feet)</b>	<b>% Drift</b>	<b>Displacement Ductility</b>	<b>Plastic Rotation (radians)</b>
1	0.07	0.33	3.57	0.003
2	0.08	0.38	3.70	0.003
3	0.09	0.46	3.87	0.004
4	0.11	0.53	3.99	0.004
5	0.12	0.58	4.00	0.005
6	0.12	0.62	4.00	0.005
7	0.13	0.67	4.00	0.006
8	0.15	0.75	4.00	0.006
1A	0.10	0.42	3.98	0.003
2A	0.11	0.46	4.00	0.004
3A	0.13	0.53	4.00	0.004
4A	0.15	0.59	4.00	0.005
5A	0.16	0.65	4.00	0.005
6A	0.17	0.70	4.00	0.006
7A	0.19	0.75	4.00	0.006
8A	0.21	0.83	4.00	0.007
1B	0.14	0.46	4.00	0.004
2B	0.15	0.50	4.00	0.004
3B	0.17	0.58	4.00	0.005
4B	0.19	0.65	4.00	0.005
5B	0.21	0.71	4.00	0.006
6B	0.23	0.76	4.00	0.006
7B	0.25	0.82	4.00	0.007
8B	0.27	0.91	4.00	0.007
1C	0.17	0.49	4.00	0.004
2C	0.19	0.54	4.00	0.004
3C	0.22	0.62	4.00	0.005
4C	0.24	0.70	4.00	0.006
5C	0.27	0.76	4.00	0.006
6C	0.29	0.83	4.00	0.007
7C	0.31	0.88	4.00	0.007
8C	0.35	0.99	4.00	0.008
1D	0.21	0.53	4.00	0.004
2D	0.23	0.58	4.00	0.005
3D	0.27	0.67	4.00	0.005
4D	0.30	0.75	4.00	0.006
5D	0.33	0.82	4.00	0.007
6D	0.35	0.88	4.00	0.007
7D	0.38	0.94	4.00	0.008
8D	0.42	1.06	4.00	0.008

**Table G-9 Column Displacement Summary for 4-Foot-Diameter Single-Column Bents in New York Designed with a “R” of 4**

<b>NCHRP 12-49</b> <b>Column Design Study</b> <b>Column Performance Evaluation</b> <b>LRFD R=4 (Simple Overstrength Factor)</b>				
<b>Column No.</b>	<b>Displacement (feet)</b>	<b>% Drift</b>	<b>Displacement Ductility</b>	<b>Plastic Rotation (radians)</b>
1	0.04	0.19	4.00	0.002
2	0.04	0.21	4.00	0.002
3	0.05	0.24	4.00	0.002
4	0.05	0.27	4.00	0.002
5	0.06	0.29	4.00	0.002
6	0.06	0.31	4.00	0.003
7	0.07	0.34	4.00	0.003
8	0.08	0.38	4.00	0.003
1A	0.05	0.21	4.00	0.002
2A	0.06	0.23	4.00	0.002
3A	0.07	0.27	4.00	0.002
4A	0.07	0.30	4.00	0.002
5A	0.08	0.33	4.00	0.003
6A	0.09	0.35	4.00	0.003
7A	0.09	0.38	4.00	0.003
8A	0.11	0.42	4.00	0.003
1B	0.07	0.23	4.00	0.002
2B	0.08	0.25	4.00	0.002
3B	0.09	0.29	4.00	0.002
4B	0.10	0.33	4.00	0.003
5B	0.11	0.36	4.00	0.003
6B	0.12	0.38	4.00	0.003
7B	0.12	0.41	4.00	0.003
8B	0.14	0.46	4.00	0.004
1C	0.09	0.25	4.00	0.002
2C	0.10	0.27	4.00	0.002
3C	0.11	0.31	4.00	0.003
4C	0.12	0.35	4.00	0.003
5C	0.13	0.38	4.00	0.003
6C	0.15	0.42	4.00	0.003
7C	0.16	0.44	4.00	0.004
8C	0.17	0.50	4.00	0.004
1D	0.11	0.27	4.00	0.002
2D	0.12	0.29	4.00	0.002
3D	0.13	0.34	4.00	0.003
4D	0.15	0.38	4.00	0.003
5D	0.16	0.41	4.00	0.003
6D	0.18	0.44	4.00	0.004
7D	0.19	0.48	4.00	0.004
8D	0.21	0.53	4.00	0.004

**Table G-10 Column Displacement Summary for 4-Foot-Diameter Multi-Column Bents in Seattle Designed with a “R” of 4**

<b>NCHRP 12-49</b> <b>Column Design Study</b> <b>Column Performance Evaluation</b> <b>LRFD R=4 (Simple Overstrength Factor)</b>				
<b>Column No.</b>	<b>Displacement (feet)</b>	<b>% Drift</b>	<b>Displacement Ductility</b>	<b>Plastic Rotation (radians)</b>
1	0.36	1.78	4.00	0.014
2	0.39	1.95	4.00	0.016
3	0.45	2.25	4.00	0.018
4	0.50	2.51	4.00	0.020
5	0.55	2.75	4.00	0.022
6	0.60	2.98	4.00	0.024
7	0.64	3.18	4.00	0.026
8	0.71	3.56	4.00	0.029
1A	0.50	1.99	4.00	0.016
2A	0.54	2.18	4.00	0.017
3A	0.63	2.51	4.00	0.020
4A	0.70	2.81	4.00	0.022
5A	0.77	3.08	4.00	0.025
6A	0.83	3.33	3.86	0.026
7A	0.89	3.56	3.37	0.027
8A	0.99	3.98	2.70	0.027
1B	0.65	2.18	4.00	0.017
2B	0.72	2.39	4.00	0.019
3B	0.83	2.75	4.00	0.022
4B	0.92	3.08	3.75	0.024
5B	1.01	3.37	3.12	0.024
6B	1.09	3.64	2.68	0.024
7B	1.17	3.90	2.34	0.024
8B	1.31	4.36	1.87	0.022
1C	0.82	2.35	4.00	0.019
2C	0.90	2.58	4.00	0.020
3C	1.04	2.98	3.44	0.022
4C	1.16	3.33	2.75	0.022
5C	1.28	3.64	2.30	0.022
6C	1.38	3.94	1.97	0.020
7C	1.47	4.21	1.72	0.019
8C	1.65	4.70	1.38	0.014
1D	1.01	2.51	4.00	0.020
2D	1.10	2.75	3.51	0.021
3D	1.27	3.18	2.64	0.021
4D	1.42	3.56	2.11	0.020
5D	1.56	3.90	1.76	0.018
6D	1.68	4.21	1.51	0.015
7D	1.80	4.50	1.32	0.011
8D	2.01	5.03	1.05	0.003

**Table G-11 Column Displacement Summary for 4-Foot-Diameter Multi -Column Bents in Portland Designed with a “R” of 4**

<b>NCHRP 12-49</b> <b>Column Design Study</b> <b>Column Performance Evaluation</b> <b>LRFD R=4 (Simple Overstrength Factor)</b>				
<b>Column No.</b>	<b>Displacement (feet)</b>	<b>% Drift</b>	<b>Displacement Ductility</b>	<b>Plastic Rotation (radians)</b>
1	0.25	1.25	4.00	0.010
2	0.27	1.37	4.00	0.011
3	0.32	1.58	4.00	0.013
4	0.35	1.76	4.00	0.014
5	0.39	1.93	4.00	0.015
6	0.42	2.09	4.00	0.017
7	0.45	2.23	4.00	0.018
8	0.50	2.49	4.00	0.020
1A	0.35	1.39	4.00	0.011
2A	0.38	1.53	4.00	0.012
3A	0.44	1.76	4.00	0.014
4A	0.49	1.97	4.00	0.016
5A	0.54	2.16	4.00	0.017
6A	0.58	2.33	3.86	0.018
7A	0.62	2.49	3.37	0.019
8A	0.70	2.79	2.70	0.019
1B	0.46	1.53	4.00	0.012
2B	0.50	1.67	4.00	0.013
3B	0.58	1.93	4.00	0.015
4B	0.65	2.16	3.75	0.017
5B	0.71	2.36	3.12	0.017
6B	0.77	2.55	2.68	0.017
7B	0.82	2.73	2.34	0.017
8B	0.92	3.05	1.87	0.015
1C	0.58	1.65	4.00	0.013
2C	0.63	1.81	4.00	0.014
3C	0.73	2.09	3.44	0.016
4C	0.82	2.33	2.75	0.016
5C	0.89	2.55	2.30	0.015
6C	0.97	2.76	1.97	0.014
7C	1.03	2.95	1.72	0.013
8C	1.15	3.30	1.38	0.010
1D	0.70	1.76	4.00	0.014
2D	0.77	1.93	3.51	0.015
3D	0.89	2.23	2.64	0.015
4D	1.00	2.49	2.11	0.014
5D	1.09	2.73	1.76	0.012
6D	1.18	2.95	1.51	0.010
7D	1.26	3.15	1.32	0.008
8D	1.41	3.52	1.05	0.002



**Table G-12 Column Displacement Summary for 4-Foot-Diameter Multi -Column Bents in Memphis Designed with a “R” of 4**

<b>NCHRP 12-49</b> <b>Column Design Study</b> <b>Column Performance Evaluation</b> <b>LRFD R=4 (Simple Overstrength Factor)</b>				
<b>Column No.</b>	<b>Displacement (feet)</b>	<b>% Drift</b>	<b>Displacement Ductility</b>	<b>Plastic Rotation (radians)</b>
1	0.28	1.41	4.00	0.011
2	0.31	1.54	4.00	0.012
3	0.36	1.78	4.00	0.014
4	0.40	1.99	4.00	0.016
5	0.44	2.18	4.00	0.018
6	0.47	2.36	4.00	0.019
7	0.50	2.52	4.00	0.020
8	0.56	2.82	4.00	0.023
1A	0.39	1.57	4.00	0.013
2A	0.43	1.73	4.00	0.014
3A	0.50	1.99	4.00	0.016
4A	0.56	2.23	4.00	0.018
5A	0.61	2.44	4.00	0.019
6A	0.66	2.64	3.86	0.021
7A	0.70	2.82	3.37	0.021
8A	0.79	3.15	2.70	0.021
1B	0.52	1.73	4.00	0.014
2B	0.57	1.89	4.00	0.015
3B	0.66	2.18	4.00	0.017
4B	0.73	2.44	3.75	0.019
5B	0.80	2.67	3.12	0.019
6B	0.87	2.89	2.68	0.019
7B	0.93	3.09	2.34	0.019
8B	1.04	3.45	1.87	0.017
1C	0.65	1.86	4.00	0.015
2C	0.71	2.04	4.00	0.016
3C	0.83	2.36	3.44	0.018
4C	0.92	2.64	2.75	0.018
5C	1.01	2.89	2.30	0.017
6C	1.09	3.12	1.97	0.016
7C	1.17	3.34	1.72	0.015
8C	1.31	3.73	1.38	0.011
1D	0.80	1.99	4.00	0.016
2D	0.87	2.18	3.51	0.016
3D	1.01	2.52	2.64	0.017
4D	1.13	2.82	2.11	0.016
5D	1.24	3.09	1.76	0.014
6D	1.33	3.34	1.51	0.012
7D	1.43	3.57	1.32	0.009
8D	1.59	3.99	1.05	0.002

**Table G-13 Column Displacement Summary for 4-Foot-Diameter Multi -Column Bents in St. Louis Designed with a “R” of 4**

<b>NCHRP 12-49</b> <b>Column Design Study</b> <b>Column Performance Evaluation</b> <b>LRFD R=4 (Simple Overstrength Factor)</b>				
<b>Column No.</b>	<b>Displacement (feet)</b>	<b>% Drift</b>	<b>Displacement Ductility</b>	<b>Plastic Rotation (radians)</b>
1	0.15	0.75	4.00	0.006
2	0.16	0.82	4.00	0.007
3	0.19	0.94	4.00	0.008
4	0.21	1.06	4.00	0.008
5	0.23	1.16	4.00	0.009
6	0.25	1.25	4.00	0.010
7	0.27	1.34	4.00	0.011
8	0.30	1.49	4.00	0.012
1A	0.21	0.83	4.00	0.007
2A	0.23	0.91	4.00	0.007
3A	0.26	1.06	4.00	0.008
4A	0.30	1.18	4.00	0.009
5A	0.32	1.29	4.00	0.010
6A	0.35	1.40	3.86	0.011
7A	0.37	1.49	3.37	0.011
8A	0.42	1.67	2.70	0.011
1B	0.27	0.91	4.00	0.007
2B	0.30	1.00	4.00	0.008
3B	0.35	1.16	4.00	0.009
4B	0.39	1.29	3.75	0.010
5B	0.42	1.42	3.12	0.010
6B	0.46	1.53	2.68	0.010
7B	0.49	1.64	2.34	0.010
8B	0.55	1.83	1.87	0.009
1C	0.35	0.99	4.00	0.008
2C	0.38	1.08	4.00	0.009
3C	0.44	1.25	3.44	0.009
4C	0.49	1.40	2.75	0.009
5C	0.54	1.53	2.30	0.009
6C	0.58	1.65	1.97	0.009
7C	0.62	1.77	1.72	0.008
8C	0.69	1.97	1.38	0.006
1D	0.42	1.05	4.00	0.008
2D	0.46	1.16	3.51	0.009
3D	0.53	1.34	2.64	0.009
4D	0.60	1.49	2.11	0.008
5D	0.65	1.64	1.76	0.007
6D	0.71	1.77	1.51	0.006
7D	0.76	1.89	1.32	0.005
8D	0.84	2.11	1.05	0.001

**Table G-14 Column Displacement Summary for 4-Foot-Diameter Multi -Column Bents in New York Designed with a “R” of 4**

<b>NCHRP 12-49</b> <b>Column Design Study</b> <b>Column Performance Evaluation</b> <b>LRFD R=4 (Simple Overstrength Factor)</b>				
<b>Column No.</b>	<b>Displacement (feet)</b>	<b>% Drift</b>	<b>Displacement Ductility</b>	<b>Plastic Rotation (radians)</b>
1	0.08	0.38	4.00	0.003
2	0.08	0.41	4.00	0.003
3	0.10	0.48	4.00	0.004
4	0.11	0.53	4.00	0.004
5	0.12	0.58	4.00	0.005
6	0.13	0.63	4.00	0.005
7	0.13	0.67	4.00	0.005
8	0.15	0.75	4.00	0.006
1A	0.10	0.42	4.00	0.003
2A	0.12	0.46	4.00	0.004
3A	0.13	0.53	4.00	0.004
4A	0.15	0.59	4.00	0.005
5A	0.16	0.65	4.00	0.005
6A	0.18	0.70	3.86	0.006
7A	0.19	0.75	3.37	0.006
8A	0.21	0.84	2.70	0.006
1B	0.14	0.46	4.00	0.004
2B	0.15	0.50	4.00	0.004
3B	0.17	0.58	4.00	0.005
4B	0.20	0.65	3.75	0.005
5B	0.21	0.71	3.12	0.005
6B	0.23	0.77	2.68	0.005
7B	0.25	0.82	2.34	0.005
8B	0.28	0.92	1.87	0.005
1C	0.17	0.50	4.00	0.004
2C	0.19	0.54	4.00	0.004
3C	0.22	0.63	3.44	0.005
4C	0.25	0.70	2.75	0.005
5C	0.27	0.77	2.30	0.005
6C	0.29	0.83	1.97	0.004
7C	0.31	0.89	1.72	0.004
8C	0.35	0.99	1.38	0.003
1D	0.21	0.53	4.00	0.004
2D	0.23	0.58	3.51	0.004
3D	0.27	0.67	2.64	0.004
4D	0.30	0.75	2.11	0.004
5D	0.33	0.82	1.76	0.004
6D	0.36	0.89	1.51	0.003
7D	0.38	0.95	1.32	0.002
8D	0.43	1.06	1.05	0.001

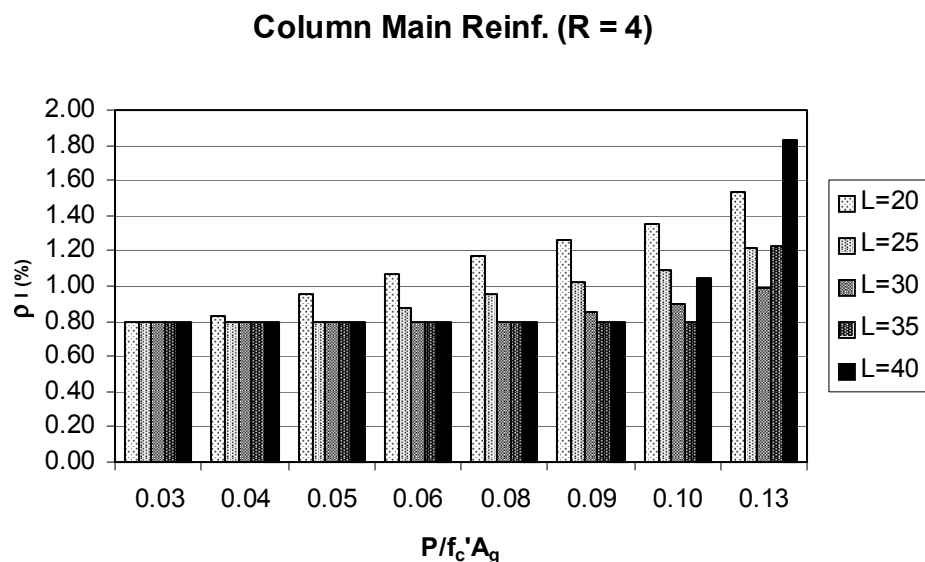


**Figure G-17** Column Main Reinforcement Requirements for 5-Foot-Diameter Multi-Column Bents in Seattle Designed with a R-factor of 4

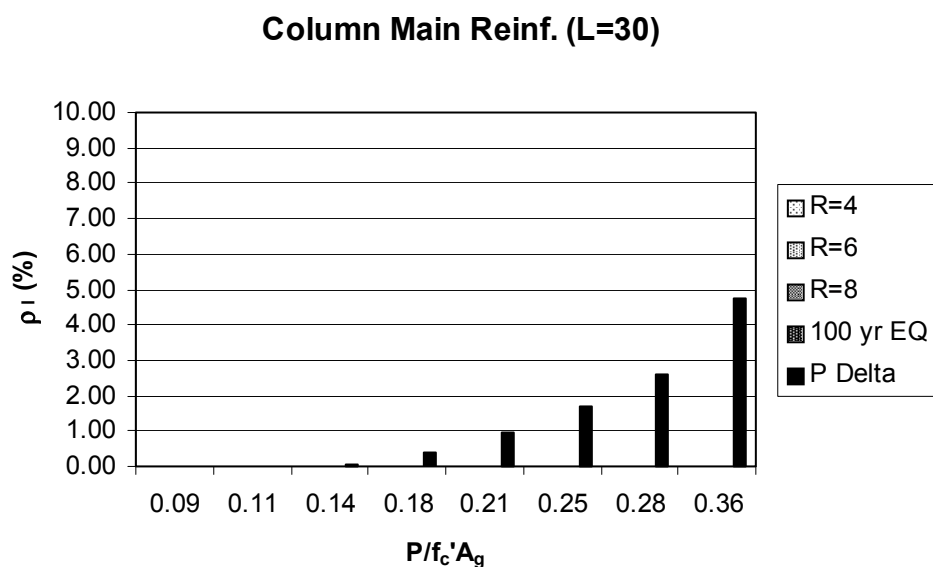


**Figure G-18** Breakdown of Column Main Reinforcement Design Controls for 3-Foot-Diameter 30-Foot-Tall Multi-Column Bents in New York

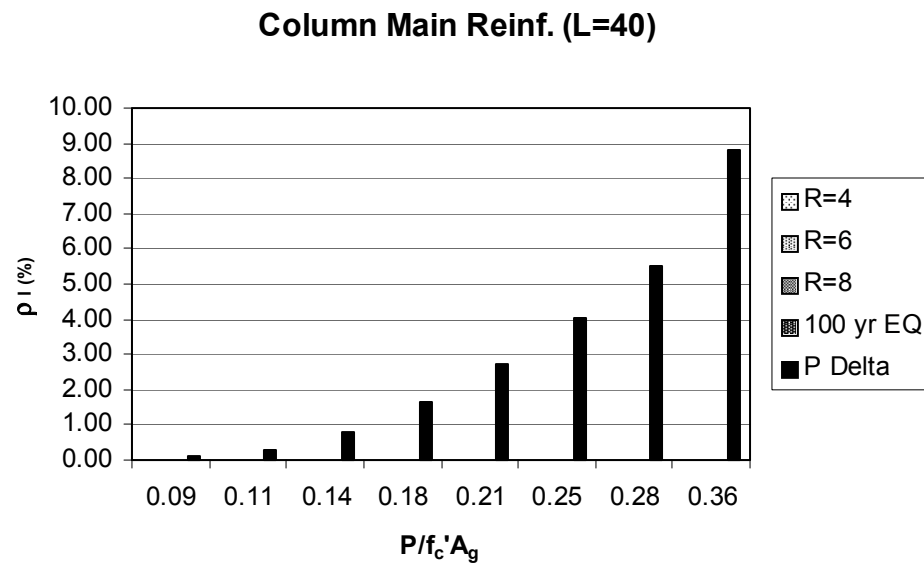


**Figure G-19 Breakdown of Column Main Reinforcement Design Controls for 3-Foot-Diameter 40-Foot-Tall Multi-Column Bents in New York**

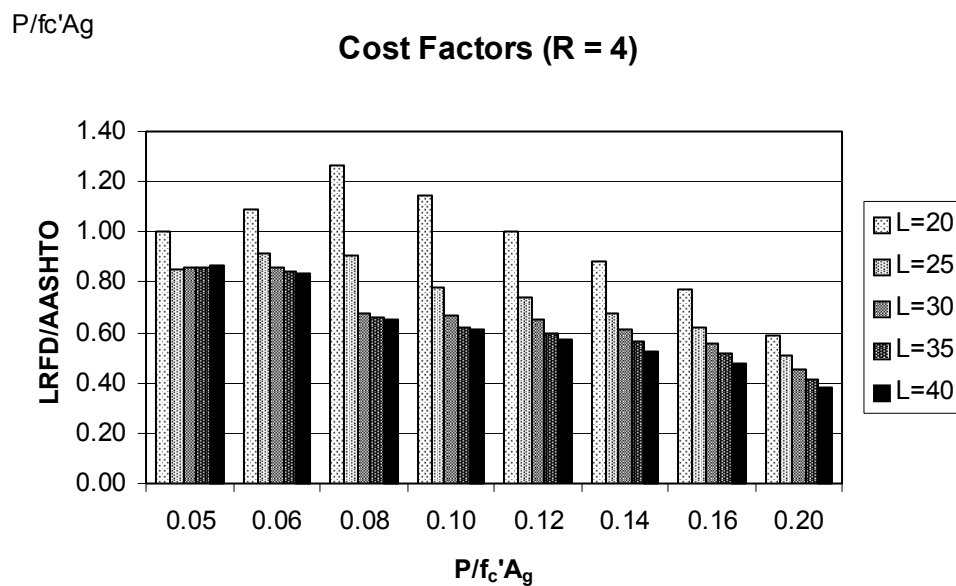


**Figure G-20 Cost Factors (NCHRP 12-49/AASHTO Division 1-A) for 4-Foot-Diameter Single-Column Bents in Seattle Designed with an R-factor of 4**

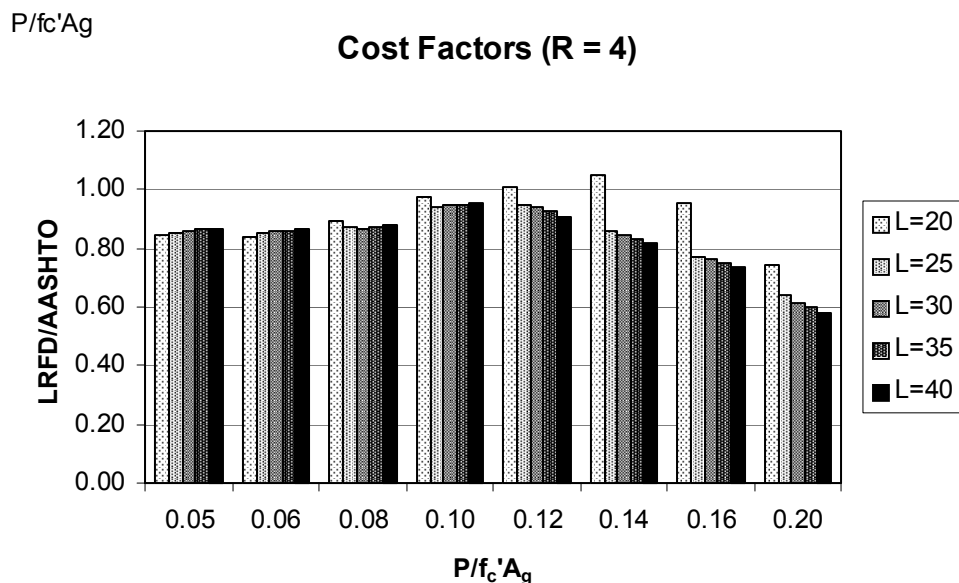


**Figure G-21** Cost Factors (NCHRP 12-49/AASHTO Division 1-A) for 4-Foot-Diameter Single-Column Bents in Memphis Designed with an R-factor of 4

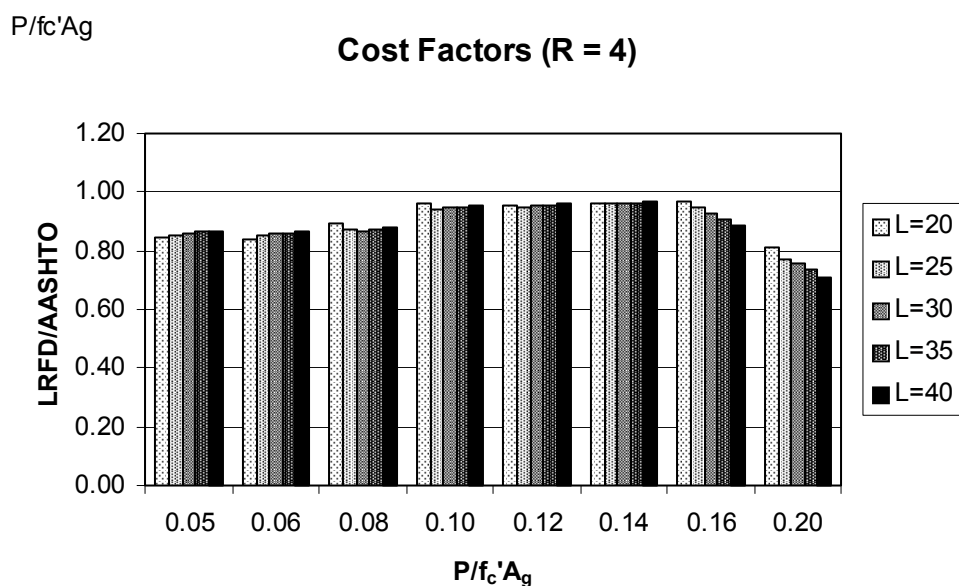


**Figure G-22** Cost Factors (NCHRP 12-49/AASHTO Division 1-A) for 4-Foot-Diameter Single-Column Bents in Portland Designed with an R-factor of 4

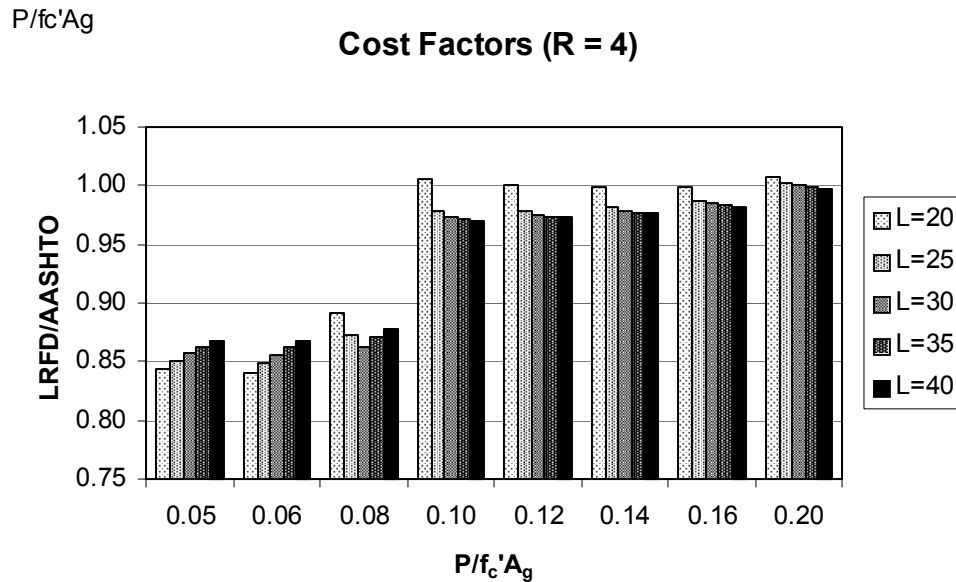


**Figure G-23** Cost Factors (NCHRP 12-49/AASHTO Division 1-A) for 4-Foot-Diameter Single-Column Bents in St. Louis Designed with an R-factor of 4

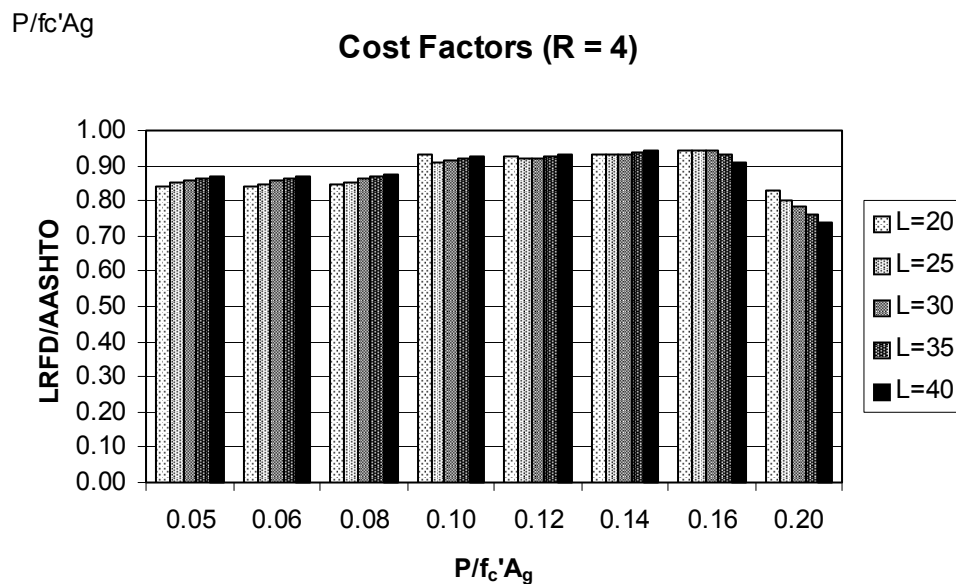


**Figure G-24** Cost Factors (NCHRP 12-49/AASHTO Division 1-A) for 4-Foot-Diameter Single-Column Bents in New York Designed with an R-factor of 4

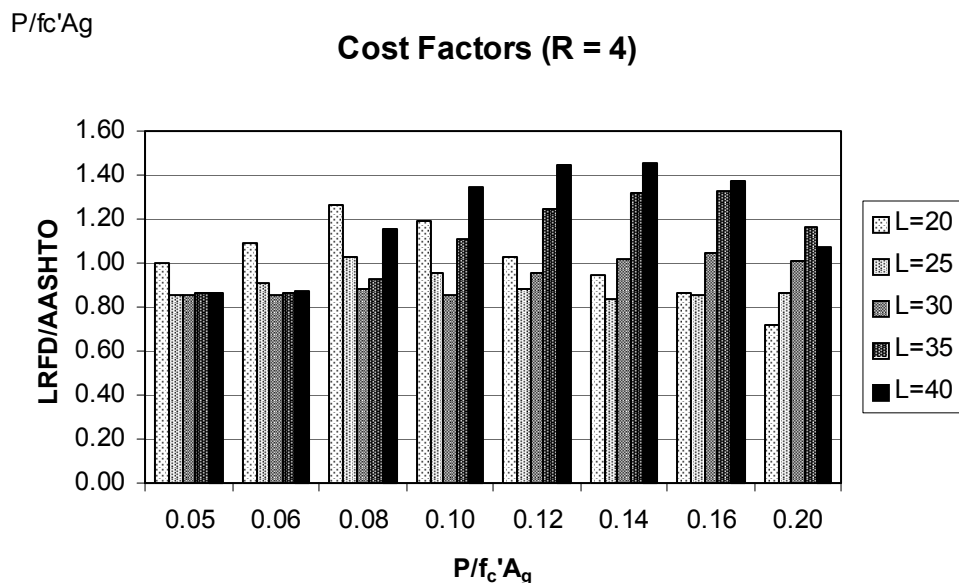


**Figure G-25** Cost Factors (NCHRP 12-49/AASHTO Division 1-A) for 4-Foot-Diameter Multi-Column Bents in Seattle Designed with an R-factor of 4

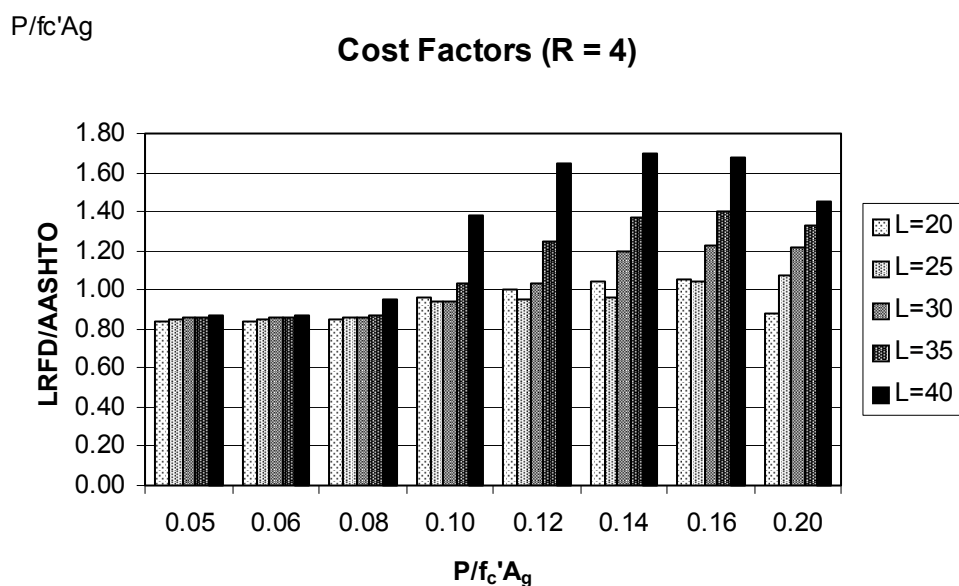


**Figure G-26** Cost Factors (NCHRP 12-49/AASHTO Division 1-A) for 4-Foot-Diameter Multi-Column Bents in Memphis Designed with an R-factor of 4



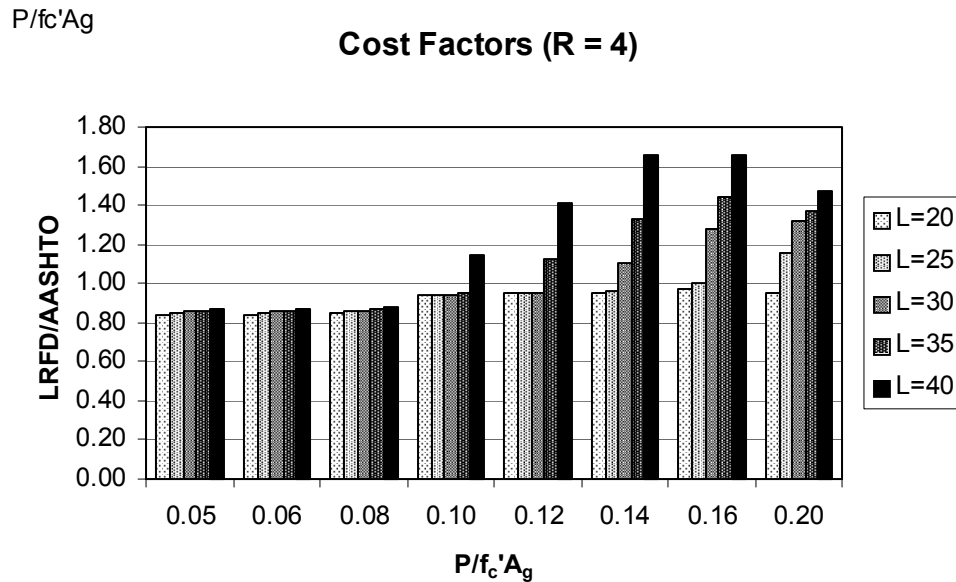


**Figure G-27** Cost Factors (NCHRP 12-49/AASHTO Division 1-A) for 4-Foot-Diameter Multi-Column Bents in Portland Designed with an R-factor of 4

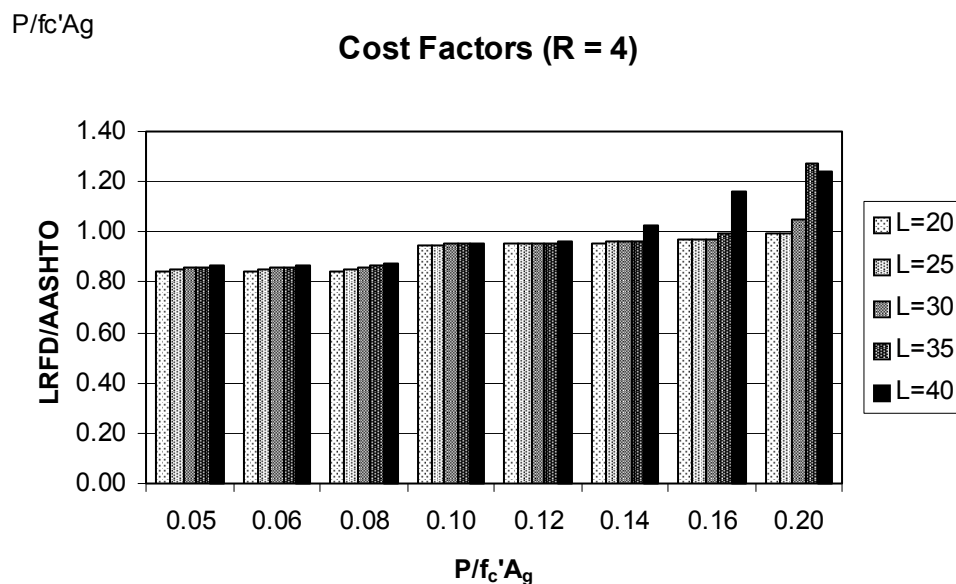


**Figure G-28** Cost Factors (NCHRP 12-49/AASHTO Division 1-A) for 4-Foot-Diameter Multi-Column Bents in St. Louis Designed with an R-factor of 4

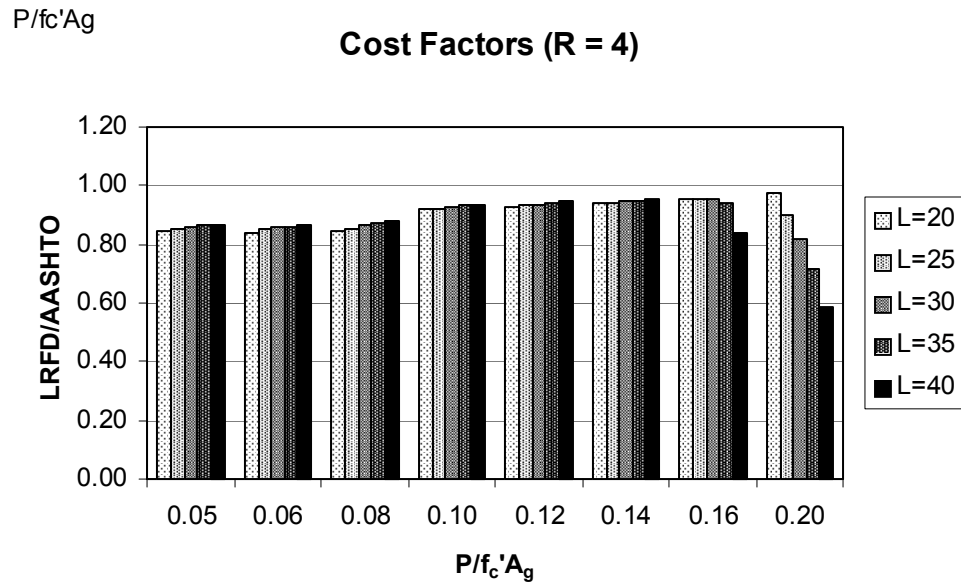


**Figure G-29** Cost Factors (NCHRP 12-49/AASHTO Division 1-A) for 4-Foot-Diameter Multi-Column Bents in New York Designed with an R-factor of 4

## Appendix H

# LIQUEFACTION EFFECTS AND ASSOCIATED HAZARDS

### H.1 PURPOSE AND SCOPE

In support of the NCHRP 12-49 effort to develop the next generation of seismic design provisions for new bridges, a study of the effects of liquefaction and the associated hazards of lateral spreading and flow, was undertaken. This appendix presents a summary of the results of that study (NCHRP 12-49 Liquefaction Study), which is presented in its entirety in the companion MCEER/ATC-49-1 Report, *Liquefaction Study Report, Recommended LRFD Guidelines for the Seismic Design of Highway Bridges* (ATC/MCEER, 2003a)

The motivation for the study was the recommended change in the design return period for ground motions for a rare or “Maximum Considered Earthquake” (MCE) used in the recommended provisions. The recommended provisions are based on using ground motions for the MCE that correspond to a probability of exceedence of 3% in 75 years (2,475-year return period) for most of the United States. In areas near highly active faults, ground motions are bounded deterministically to values that are lower than ground motions for a 2475 year return period. In contrast, the design ground motion hazard in the current AASHTO Division 1-A seismic provisions has a probability of exceedence (PE) of 10% in 50 years (approx. 15% PE in 75 years or 475-year return period). With the increase in return period comes an increase in the potential for liquefaction and liquefaction-induced ground movements. These ground movements could damage bridge structures. Concerns that liquefaction hazards under the recommended provisions may prove to be too costly to accommodate in construction led to this study.

The project team believed that, along with increases in the likelihood or extent of liquefaction at a particular site, there also exists some conservatism in current design practices. If such conservatism exists, then the use of state-of-the-art design procedures could lead to designs that perform satisfactorily in larger earthquakes, and may not be much more expensive than those being currently built.

The scope of the study was limited to two sites in relatively high seismicity locations, one in the western United States in Washington State and one in the central United States in Missouri. The Washington Site is located near the Cascadia subduction zone, and the Missouri site is located near the New Madrid seismic zone. Actual site geologies and bridge configurations from the two states were used as an initial basis for the study. The site geologies were subsequently idealized by providing limited simplification, although the overall geologic character of each site was preserved.

The investigation of the two sites and their respective bridges focused on the resulting response and design differences between the recommended ground shaking level (3% PE in 75 years) and that corresponding to the current AASHTO Division I-A provisions (15% PE in 75 years). The scope of the study for each of the two sites and bridges includes:

1. Development of both 15% PE in 75 year and 3% PE in 75 year acceleration time-histories;
2. Simplified, conventional liquefaction analyses;
3. Nonlinear assessment of the site response to these accelerations including the time history of pore pressure increases;
4. Assessment of stability of abutment end slopes;
5. Estimations of lateral spreading and/or flow conditions at the sites;
6. Design of structural systems to withstand the predicted response and flow conditions;
7. Evaluation of geotechnical mitigation of liquefaction related ground displacement; and
8. Evaluation of cost impacts of the structural and geotechnical mitigation strategies.

The results for the 15% PE in 75 year and 3% PE in 75 year ground motions were compared against one another to assess the implications of using ground motions for the longer return period (lower probability of exceedance level) for design. Additionally, the conduct of the study helped syn-

thesize an overall approach for handling liquefaction-induced movements in the recommended design provisions. The study for the Washington site is described in Articles H.3 through H.8 and for the Missouri site in Article H.9, with lesser detail.

## H.2 DESIGN APPROACH

The design approach used in the study and recommended for the new AASHTO LRFD provisions involves four basic elements:

1. Stability analysis;
2. Newmark sliding block analysis;
3. Assessments of the passive force that can ultimately develop ahead of a pile or foundation as liquefaction induces lateral spread; and
4. Assessment of the likely plastic mechanisms that may develop in the foundations and substructure.

The rationale behind this approach is to determine the likely magnitude of lateral soil movement and assess the structure's ability to both accommodate this movement and/or potentially limit the movement. The approach is based on use of a deep foundation system, such as piles or drilled shafts. Spread footing types of foundations typically will not be used when soil conditions lead to the possibility of liquefaction and associated lateral spreading or settlement.

The concept of considering a plastic mechanism, or hinge, in the piles under the action of spreading forces is tantamount to accepting damage in the foundation. This is a departure from seismic design for structural inertia loading alone, and the departure is felt reasonable for the rare MCE event because it is unlikely that the formation of plastic hinges in the foundation will lead to structure collapse. The reasoning behind this is that lateral spreading is essentially a displacement-controlled process. Thus the estimated soil displacements represent a limit on the structure displacement, excluding the phenomena of buckling of the piles or shafts below grade and the continued displacement that could be produced by large  $P-\Delta$  effects. Buckling should be checked, and methods that include the soil residual resistance should be used. Meyersohn, et al. (1992) provides a method for checking buckling as an example. The effects of  $P-\Delta$  amplification are discussed later in this Appendix.

The fact that inelastic deformations may occur below grade, and that these may be difficult to detect and inspect, should be considered. However, the presence of large ground movements induced by earthquake motions is discernible. Thus, it should be possible to evaluate whether inelastic deformations could have occurred from the post-earthquake inspection information. Additionally, inclinometer tubes could be installed in selected elements of deep foundations to allow quantitative assessment of pile/shaft movement following an earthquake. Also post earthquake investigation using down hole video cameras can be used to assess damage.

A flowchart of the methodology for consideration of liquefaction induced lateral spreading is given in Figure D.4.2-1 and key components of the methodology are numbered in the flowchart and discussed in detail in the commentary to Article D.4.2.2. The figure, together with the commentary, provides a 'roadmap' to the procedure used in this study for the lateral spreading resistance design. The primary feature of the recommended methodology is the use of inelastic action in the piles to accommodate the movement of soil and foundations. If the resulting movements are unacceptable, then mitigation measures must be implemented. Mitigation measures are discussed in Article D.4.3 and are discussed in more detail in the full liquefaction study report (ATC/MCEER, 2003a).

## H.3 SITE SELECTION AND CHARACTERIZATION

Because the purpose of the study was to investigate sites that are realistic, an actual site was chosen as the prototype for a Western U.S. Site and another actual site for a mid-America site. The western site is the primary focus of this Appendix although a brief summary of the results of the Mid-America site are given in Article H.9. The Western site is located just north of Olympia, Washington in the Nisqually River valley<sup>1</sup>. The location is within a large river basin in the Puget Sound area of Washington State, and it is situated

<sup>1</sup> This site was selected and the liquefaction evaluation was completed before the February 2001 Nisqually earthquake. Ground motions associated with the Nisqually earthquake were considerably less than those used in this study. While liquefaction occurred at some locations near the selected site no bridge damage apparently occurred likely because of the limited extent of liquefaction.

near the mouth of the river in the estuary zone. The basin is an area that was over ridden by glaciers during the last ice age and therefore has over-consolidated material at depth. Additionally, the basin contains significant amounts of recently deposited, loose material over the glacially consolidated materials.

Soil conditions for the site were developed from information provided by Washington State Department of Transportation (WSDOT) for another well characterized site located in a geologically similar setting near Seattle. The actual site was moved to the Olympia area to avoid the effects of the Seattle fault. At the prototype site, the material at depths less than 150 feet is characterized by alluvial deposits. At greater depths some estuarine materials exist and below about 200 feet dense glacial materials are found. This then produces a site with the potential for deep liquefiable soils.

For the purposes of this study, the site profile was simplified such that fewer layers exist, and the profile is the same across the entire site. The simplified profile retains features and layering that produce the significant responses of the actual site. The simplified soil profile is given in Figure H-1. This figure also includes relevant properties of the soil layers that have been used for the seismic response assessments and bridge design. Shear wave velocity ( $V_s$ ), undrained shearing strength ( $c_u$ ), soil friction angle ( $\phi$ ), and residual soil strength ( $S_{ur}$ ) were interpreted from the field and laboratory data provided by WSDOT. The cyclic resistance ratio (CRR) was obtained by conducting simplified liquefaction analyses using both the SPT and CPT methods to obtain CRR values. These CRR values are plotted in Figure H-2. Average CRR values were determined for liquefiable materials, and represent clean sand values for a M7.5 event.

The prototype site profile and the structure elevation are shown in Figure H-3. The modified site is a smaller river crossing than the original since the total length of the bridge was substantially shortened for the study. Only enough length was used to illustrate the issues of soil movement and design. In this case the total length of the bridge is 500 feet. The ground surface is shown in Figure H-3 as the 0-foot elevation. As can be seen in the figure, approach fills are present at both ends of the bridge, and in this case, they are relatively tall at 30-feet each.

An approach fill comprised of a relatively clean sandy gravel was assumed at each abutment.

The sandy gravel was assigned a friction angle of 37 degrees.

#### H.4 BRIDGE TYPE

The prototype bridge from which the study data were drawn is a river crossing with several superstructure and foundation types along the structure. Again for the study, the actual structure was simplified. The 500-foot long structure comprises of a 6-foot deep concrete box girder that is continuous between the two abutments. The intermediate piers are two-column bents supported on pile caps and 24-inch steel piles filled with reinforced concrete. The roadway is 40-feet wide. The two 4-foot diameter columns for each pier are approximately 23 feet apart, and due to the relatively large size of the pile caps, a single combined pile cap was used for both columns at each pier. Figure H-4 shows the general arrangement of an intermediate pier.

The centermost pier in this example is located at the deepest point of the river channel, as shown in Figure H-3. While this is somewhat unusual, in that a longer span might often be used to avoid such an arrangement, the river pier was used here for simplicity. The columns of this pier are also relatively slender, and they were deliberately left so to allow any negative seismic effects of the slenderness, for instance  $P-\Delta$ , to be assessed. In a final design, the size of these columns might likely be increased. In fact, non-seismic load combinations/conditions may require the columns to be enlarged.

The abutments are of the overhanging stub abutment type. Figure H-5 shows the transverse and longitudinal elevations of the abutments used for the bridge. For this type of abutment, the backfill is placed directly against the end diaphragm of the superstructure. This has the seismic advantage of providing significant longitudinal resistance for all displacement levels, since the passive resistance of the backfill is mobilized as the superstructure moves. This type of abutment also eliminates the need for expansion joints at the ends of the structure, and for this reason, is limited to the shorter total length structures.

#### H.5 DESIGN RESPONSE SPECTRA AND TIME HISTORIES

The design response spectra for the current AASHTO *Standard Specifications for Highway*

**WASHINGTON SITE**  
**Non-Liquefied Soil Profile**

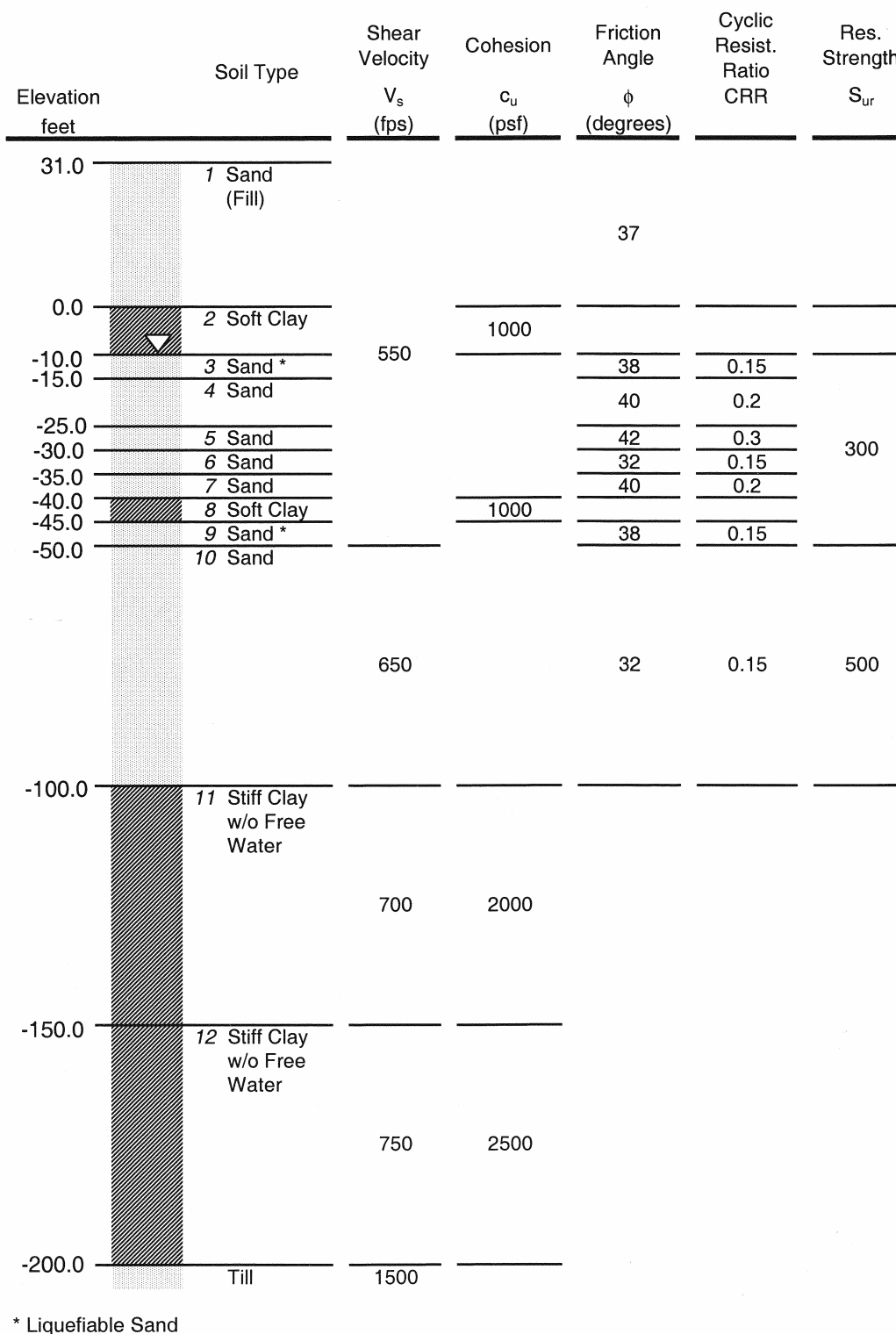


**Figure H-1** Simplified Soil Profile for the Western U.S. (Washington State) Site

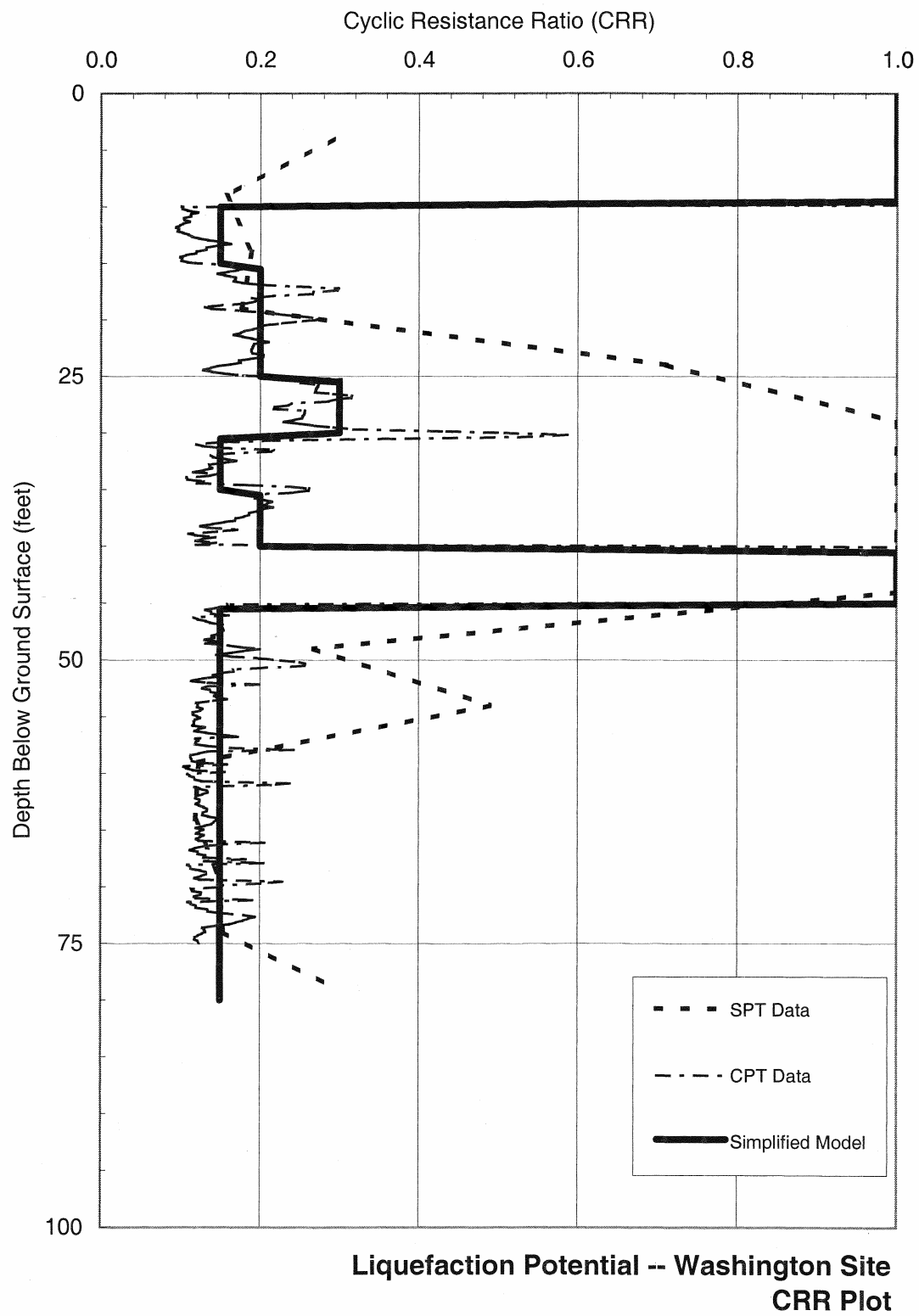


**Figure H-2** Washington State Department of Transportation Location H-13 CRR Plot

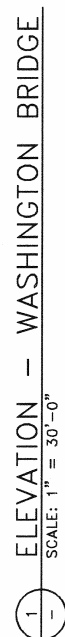


**Figure H-3      Site Profile and Structure Elevation, Washington State Bridge**



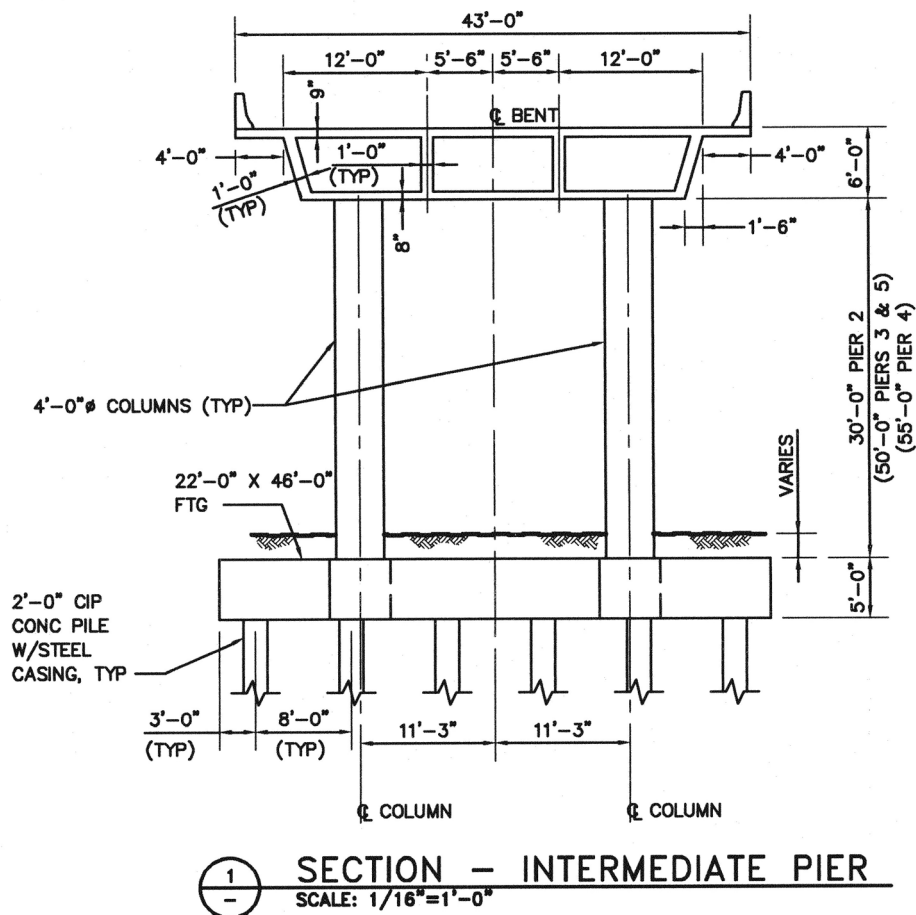


Figure H-4 Elevation of an Intermediate Pier, Washington State Bridge

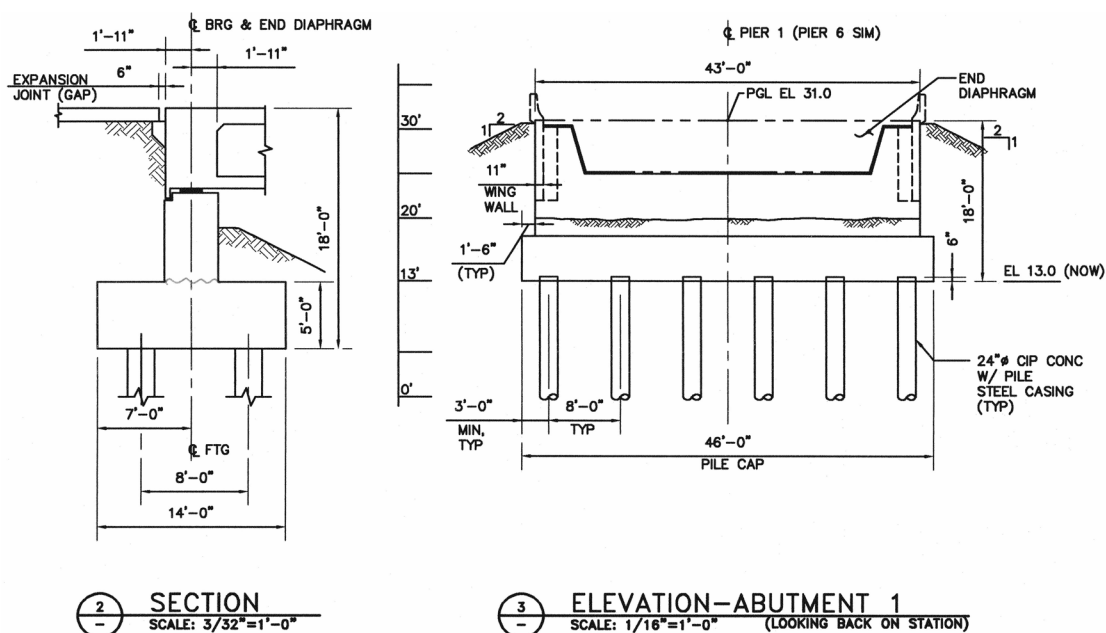


Figure H-5 Elevations of the Abutment, Washington State Bridge

*Bridges* (hereinafter referred to as the current AASHTO *Specifications*) and the NCHRP 12-49 recommended LRFD seismic design provisions were constructed using the procedures and site factors described in the respective specifications. For the current AASHTO *Specifications*, the hazard level of 10% probability of exceedance in 50 years was used. For the recommended LRFD provisions, both the rare earthquake (Maximum Considered Earthquake or MCE) having a probability of exceedance of 3% in 75 years with deterministic bounds near highly active faults, and the frequent earthquake (also termed the Expected Earthquake) having a probability of exceedance of 50% in 75 years, were used as design earthquakes.

Design response spectra based on the current AASHTO *Specifications* were constructed using a (rock) peak ground acceleration (PGA) of 0.24g for the Olympia site. This peak ground acceleration value was determined from the AASHTO map contained in the current AASHTO *Specifications*. Design spectra for the MCE of the recommended LRFD provisions were constructed using rock (Site Class B) spectral accelerations at 0.2-second period and 1.0-second period. These two spectral values were obtained from maps published by the U.S. Geological Survey (USGS). The PGA for the MCE was defined as 0.4 times the spectral acceleration at 0.2 seconds as required by the recommended LRFD provisions. Design spectral accelerations for the Expected Earthquake were obtained from the hazard curves of probabilistic ground motions on the CD-ROM published by the USGS.

Rock spectra based on AASHTO and the recommended LRFD provisions were adjusted for local site soil conditions. According to the AASHTO *Specifications* the site is a Soil Profile III; the recommended LRFD provisions define the site as Class E. Figure H-6 presents the design response spectra for the current AASHTO *Specifications*, on Soil profile Type III, and for the MCE and the frequent earthquake of the recommended LRFD provisions, on Site Class E. These site classifications represent the assessed soil profile below the ground surface where response spectra are defined for structural vibration design and peak ground accelerations are used for simplified liquefaction potential analyses. Note in Figure H-6 that the short-period branch of the AASHTO spectra are assumed to drop from the acceleration plateau at a period of 0.096 second to the peak ground acceleration at 0.02-second period, the same as for the MCE spectra. Also note that, be-

cause the long-period branch of the AASHTO spectra declines more slowly with period than those of the MCE (as  $1/T^{2/3}$  in the current AASHTO *Specifications* compared to  $1/T$  in the recommended LRFD provisions), the AASHTO and MCE spectra come closer together as the period increases.

Acceleration time histories consistent with current AASHTO *Specifications* and with MCE ground motions of the recommended LRFD provisions were developed as firm soil outcropping motions for input to the one dimensional, non-linear site response analyses to assess the liquefaction hazard of the site. These time histories were developed in accordance with the requirements and guidelines of the recommended LRFD provisions. Deaggregation of the probabilistic results for the Olympia site indicates that significant contributions to the ground motion hazard come from three magnitude-distance ranges: (1) magnitude 8 to 9 earthquakes occurring at a distance of 70 to 80 km distance; (2) magnitude 5 to 7 events occurring at a distance of 40 to 70 km distance; and (3) magnitude 5 to 6.5 earthquakes occurring at distances less than 20 km. These three magnitude-distance ranges are associated, respectively, with (1) large-magnitude subduction zone interface earthquakes, (2) moderate magnitude earthquakes occurring within the subducting slab of the Juan de Fuca plate at depth beneath western Washington and in the shallow crust of the North American plate at relatively large distances from the site, and (3) moderate magnitude earthquakes occurring in the shallow crust of the North American plate in the near vicinity of the site. Time histories were developed for each of these earthquake sources. The selected source for (1) was the 1985 Chile earthquake, for (2) it was representative of the events occurring within the subducting slab, of the type that occurred near Olympia in 1949 and the 2001 Nisqually earthquake, and for (3) it was the 1986 North Palm Springs earthquake, a moderate magnitude local shallow crustal earthquake.

## H.6 LIQUEFACTION STUDIES

The liquefaction study for the Washington bridge site involved two phases. In the first, a series of liquefaction analyses were conducted using the SPT and CPT simplified methods. Results of these analyses were used to determine the depths at which liquefaction could occur during the 15% probability of exceedance (PE) in 75 year and 3%

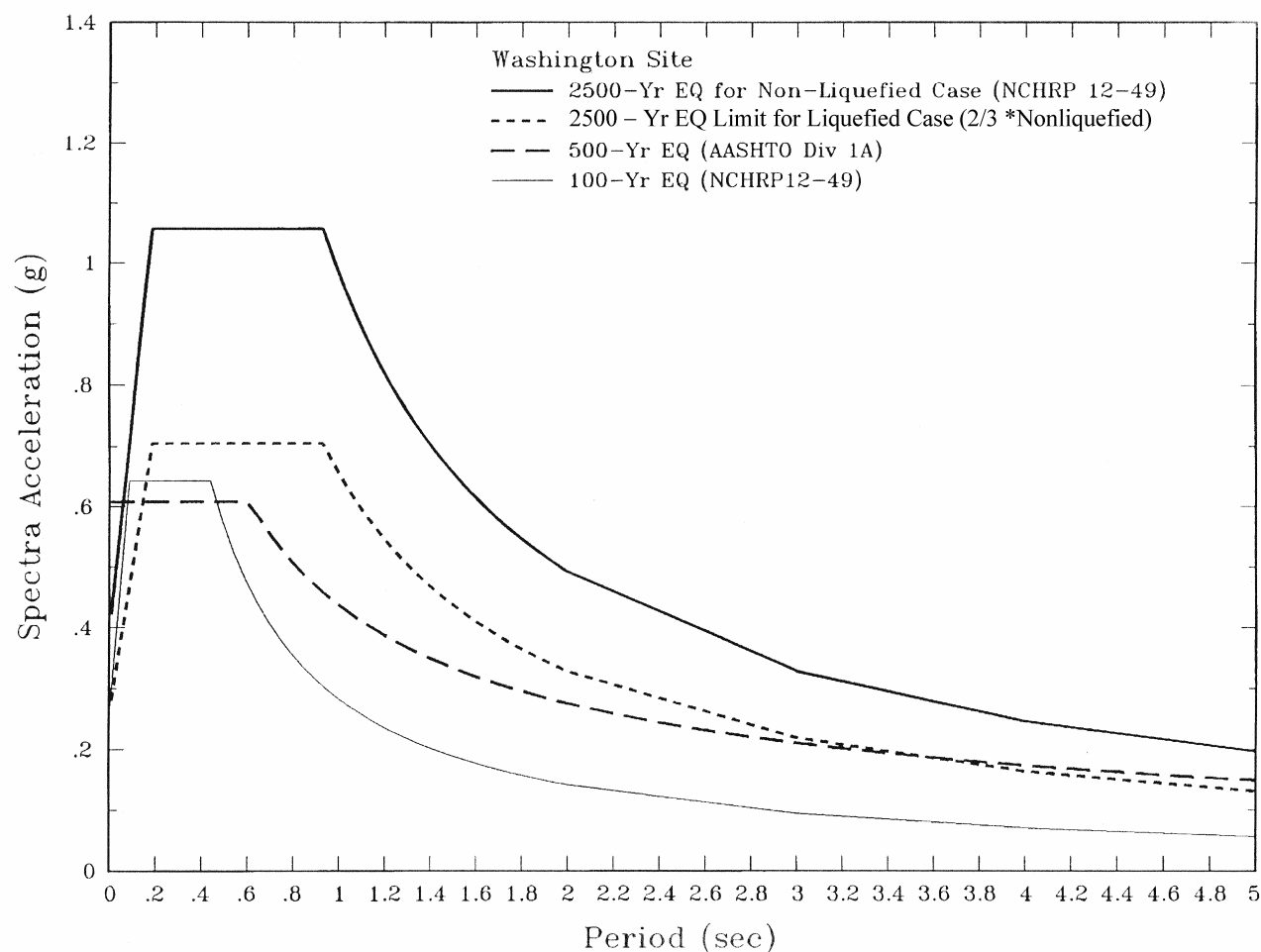


**Figure H-6** Design Response Spectra Based on Current AASHTO *Specifications*, Site Class III, and for the MCE and the Expected Earthquake Events in the Recommended NCHRP 12-49 Design Provisions, Site Class E, Washington Site

PE in 75 year earthquake ground motions. These results were also used as a basis for determining the residual strength of the soil. Concurrent with these analyses, a series of one-dimensional nonlinear, effective stress analyses was conducted to define more explicitly the mechanisms for pore water pressure increase within the soil profile and the changes in ground accelerations and deformations resulting from the development of liquefaction.

#### H.6.1 Simplified Liquefaction Analyses

The first step of the procedure outlined in the commentary to Article D.4.2.2 is to determine whether liquefaction is predicted to occur.

Simplified liquefaction analyses were conducted using the procedures given in Youd and Idriss (1997). Two levels of peak ground accel-

eration (PGA) were used, one representing the acceleration from the current AASHTO *Specifications* with its 10% PE in 50 year ground motion and the other representing the recommended 3% PE in 75 year ground motion. The PGA for the 10% in 50 year ground motion was not adjusted for site effects: this is consistent with the approach recommended in the current AASHTO *Specifications*<sup>2</sup>. Ground motions with a 3% PE in 75 years were adjusted to Site Class E, as recommended in

<sup>2</sup> Common practice is to adjust the PGA for the site soil factors given in Table 2 of Division 1-A of the current AASHTO *Specifications*. While this adjustment may be intuitively correct, these site factors are not explicitly applied to the PGA. If the site coefficient were applied at the Washington site, the PGA would be increased by a factor of 1.5, making it only slightly less than the PGA for the 2,475-year event.

Article 3.4. The resulting PGA values for each case are summarized below.

Input Parameter	10% PE in 50 Years	3% in 75 Years
Peak ground acceleration	0.24g	0.42g
Mean Magnitude	6.5	6.5

The magnitude of the design earthquake was required for the SPT and CPT simplified analyses. Results of deaggregation studies from the USGS database suggest that the mean magnitude for PGA for the 10% PE in 50 year and 3% in 75 year ground motions is 6.5. This mean magnitude reflects contributions from the different seismic sources discussed above. However, common practice within the State of Washington has been to use a magnitude 7.5 event, as being representative of the likely size of a subduction zone event occurring directly below the Puget Sound area. In view of this common practice, a range of magnitudes (6.5, 7.0 and 7.5) was used during the liquefaction analyses.

For these analyses, ground water was assumed to occur 10 feet below the ground surface for the non-fill case. Evaluations were also performed using a simplified model to evaluate the effects of the fill. For the fill model, the soil profile with the associated soil properties was the same as the free-field case. However, an additional 30 feet of embankment was added to the soil profile. This change results in a lower imposed shearing stress (i.e., demand) because of the lower soil flexibility factor ( $R_d$ ). No adjustments were made to the normalized CRR values for the greater overburden. As discussed in Youd and Idriss (1997), the recommended approach for a site where fill is added is to use the pre-fill CRR value, under the assumption that the overburden effects from the fill will not have an appreciable effect on the density of the material.

Factors of safety (FOS) results from the liquefaction evaluations at the three magnitudes (6.5, 7.0 and 7.5) are shown in Figures H-7a and H-7b for the 10% PE in 50 year and 3% PE in 75 year ground motions, respectively, for the case of no approach fill. These results indicate that liquefaction could occur at two depths within the soil profile for the 10% PE in 50 year ground motion, depending somewhat on the assumed earthquake magnitude. For the 3% PE in 75 year ground motions liquefaction is predicted to depths of 75 feet,

regardless of the assumption on the earthquake magnitude<sup>3</sup>.

Results of the liquefaction analyses with the approach fill are compared in the companion *Liquefaction Study Report* (ATC/MCEER, 2003a). The fill case results in somewhat lower liquefaction potential (i.e., higher FOS) due to the lower imposed shearing stress.

## H.6.2 DESRA-MUSC Ground Response Studies

A more detailed and refined approach to assess if liquefaction occurs and the resulting ground motion is to use a nonlinear dynamic effective stress approach. For this assessment, one-dimensional nonlinear effective stress site response analyses were conducted using the program DESRA-MUSC (Martin and Ping, 2000).

The idealized site profile and related soil properties adopted for the response analyses are shown in Figure H-1. Response analyses were performed for the three ground motions, assuming a transmitting boundary input at a depth of 200 feet, corresponding to the till interface. Analyses were conducted for both the 10% PE in 50 year and 3% PE in 75 year ground motions and for site profiles with and without embankment fill. The DESRA-MUSC parameters utilized for analyses for the various soil strata ( $G/G_{max}$  curves, backbone curves and liquefaction strength curves) are documented in the case study report together with the results of response analyses for all cases defined above. A representative set of results for the time history matching the site spectra, but based on the 1985 Chile Earthquake, which has the highest energy levels of the three events used for analyses (representative of a M 8 event), are described below.

<sup>3</sup> The maximum depth of liquefaction was cut-off at 75 feet, consistent with WSDOT's normal practice. There is some controversy whether a maximum depth of liquefaction exists. Some have suggested that liquefaction does not occur beyond 55 feet. Unfortunately, quantitative evidence supporting liquefaction beyond 55 feet on level ground is difficult to find; however, cases of deep liquefaction were recorded in the 1964 Alaskan earthquake. For expediency liquefaction in the simplified analysis was limited to 75 feet.

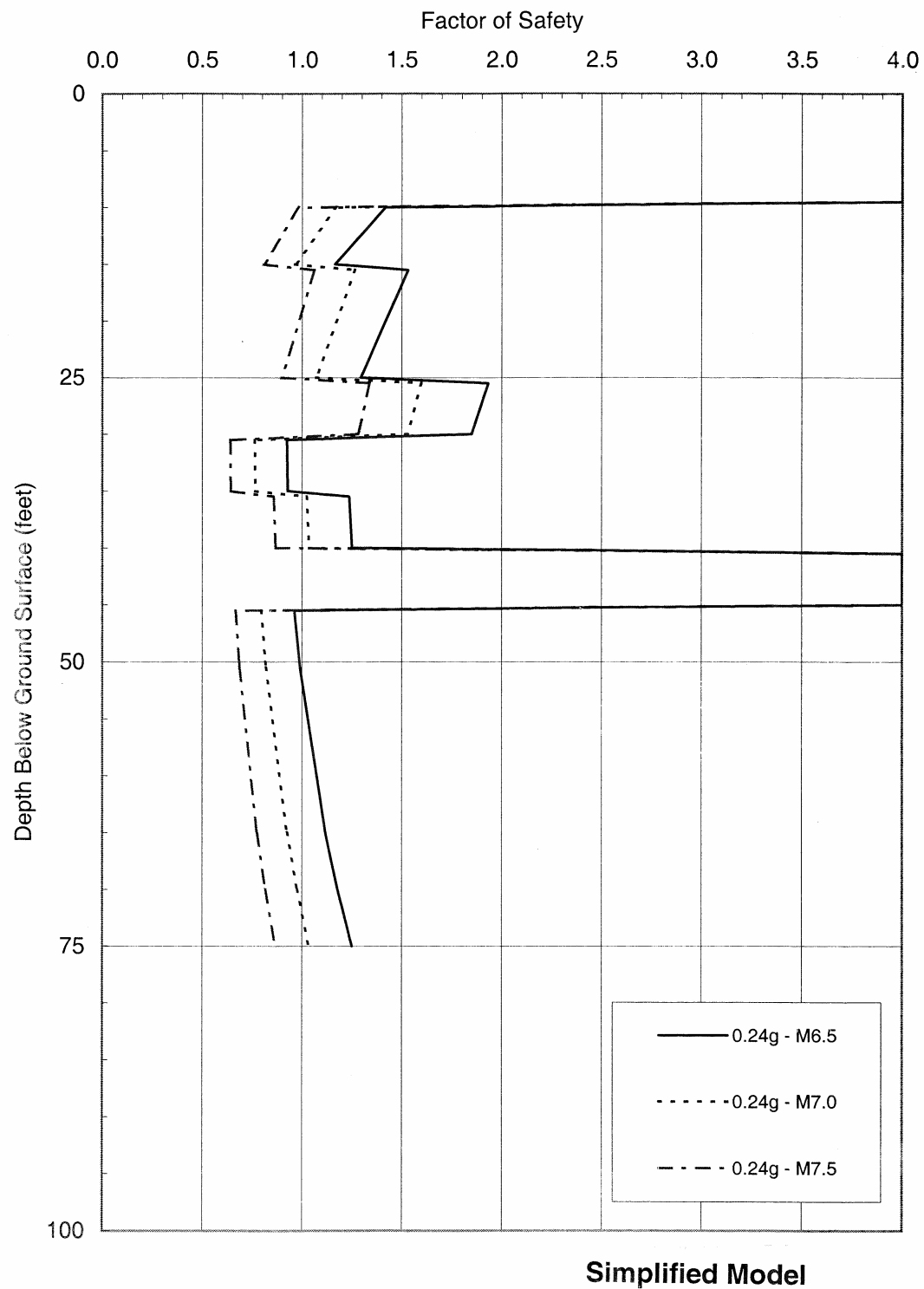


**Figure H-7a** Liquefaction Potential – 475-Year Return Period (10% PE in 50-Year Ground Motion), Washington State Case Study

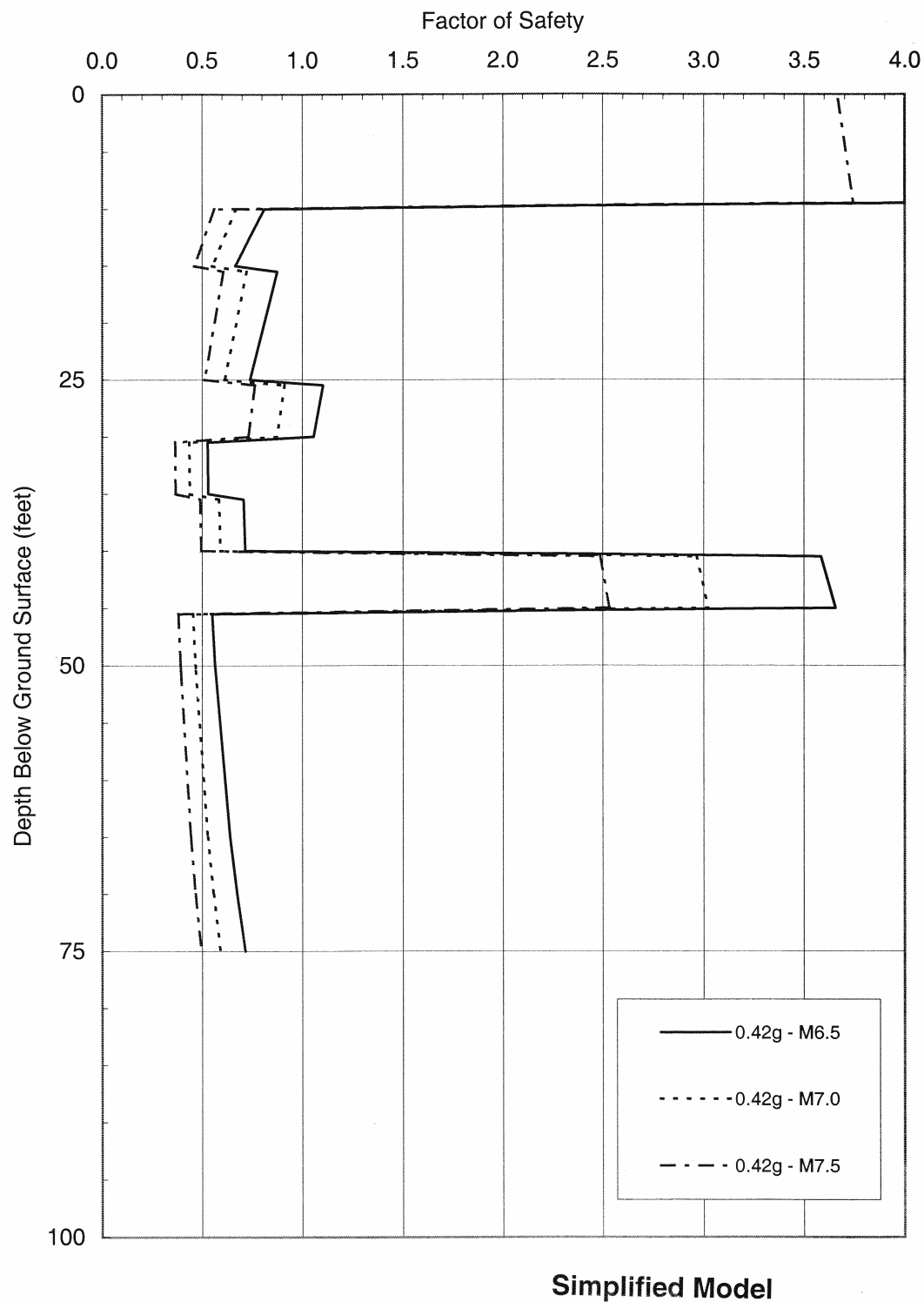


**Figure H-7b** Liquefaction Potential – 2,475-Year Return Period (3% PE in 75-Year Ground Motion), Washington State Case Study

### H.6.2.1 Without Embankment Fill

The site response for the 10% PE in 50-year ground motion is summarized in four figures:

- Figure H-8 – input and output acceleration time histories and response spectra
- Figure H-9 – maximum shear strains induced as a function of depth
- Figure H-10 – time histories of pore water pressure generation at various depths
- Figure H-11 – shear stress-shear strain hysteretic loops at various depths

A similar set of figures summarize data for the 3% PE in 75 year ground motion (see ATC/MCEER, 2003a). The following are key observations from the data plots:

- The pore water pressure time history response and output accelerations are very similar for the 10% PE in 50 year and 3% PE in 75 year cases. The underlying reason for this is the fact that the higher input accelerations for the 3% PE in 75 year case are more strongly attenuated when transmitted through the clayey silts between 100 to 200 feet, such that input accelerations at the 100-foot level for both cases are of the order of 0.25g.
- All liquefiable soils between 10 and 100 feet eventually liquefied for both cases. However liquefaction was first triggered in the 45- to 50-foot layer, which became the focal point for shear distortion and associated ground lurch (see Figures H-9 and H-11). Maximum shear strains of about 6 and 10% for the 10% PE in 50 year and 3% PE in 75 year ground motions, respectively, over the 5-foot depth of this layer, would suggest maximum ground lurches of about 0.3 and 0.5 feet respectively. Liquefaction also occurred at about the same time for the layer between 10 and 20 feet. Maximum shear strains in this and other layers were relatively small, but still sufficient to eventually generate liquefaction. The strong focal point for shear strains for the 45- to 50-foot layer suggests that this layer would also be the primary seat of lateral spread distortion.
- Liquefaction at the 45- to 50-foot depth, which was triggered at about a time of 17 seconds, effectively generated a base isolation layer, subsequently suppressing the transmission of accelerations above that depth, and generating

a much “softer” soil profile. This is graphically illustrated in Figure H-8 which shows suppression of input accelerations and longer period response after about 17 seconds. Such behavior is representative of observations at sites that liquefied during the Niigata and Kobe earthquakes.

Similar trends to those described above were seen for the other two time histories based on the Olympia and Desert Hot Springs earthquakes. However, for the Desert Hot Spring event, more representative of a M6.5 event, liquefaction did not occur at depths greater than 55 feet and only barely occurred at depth between 20 and 30 feet, for the 475-year event, which corresponds to 10% PE in 50 year ground motion.

The above results are generally consistent with the factor of safety calculations using the simplified method. However, one notable difference is the observation that the sand layer between 25 and 30 feet ( $CRR = 0.3$ ) tends to build up pore water pressure and liquefy in a similar manner to the layers above ( $CRR = 0.2$ ) and below ( $CRR = 0.15$ ) due to pore water pressure redistribution effects in DESRA-MUSC, whereas the simplified method which assumes no drainage during earthquake shaking, indicates factors of safety greater than one for 475-year events. The effects of redistribution, also tend to suppress the rate of pore water pressure build up in the layer between 30 and 35 feet.

### H.6.2.2 With Embankment Fill

The site response for the 475- and 2,475-year earthquakes is summarized in a similar manner to the no fill case above. As in the simplified method, the effect of the fill is to suppress the rate of pore water pressure build up in the DESRA-MUSC analyses (or increased factor of safety in the case of the simplified method). However, the overall response is similar for both the 10% PE in 50 year and 3% PE in 75 year cases, as for the no fill case.

Liquefaction was first triggered in the 45 to 50-foot layer, which became the focal point for shear distortion as in the no fill case. Liquefaction also occurred at about the same time for layers between 10 and 20 feet. However, liquefaction was suppressed in layers between 20 and 40 feet. The strong focal point for shear strains for the 45- to 50-foot layers, again suggests that this layer would be the primary seat of lateral spread distortion. Similar trends to those described above were

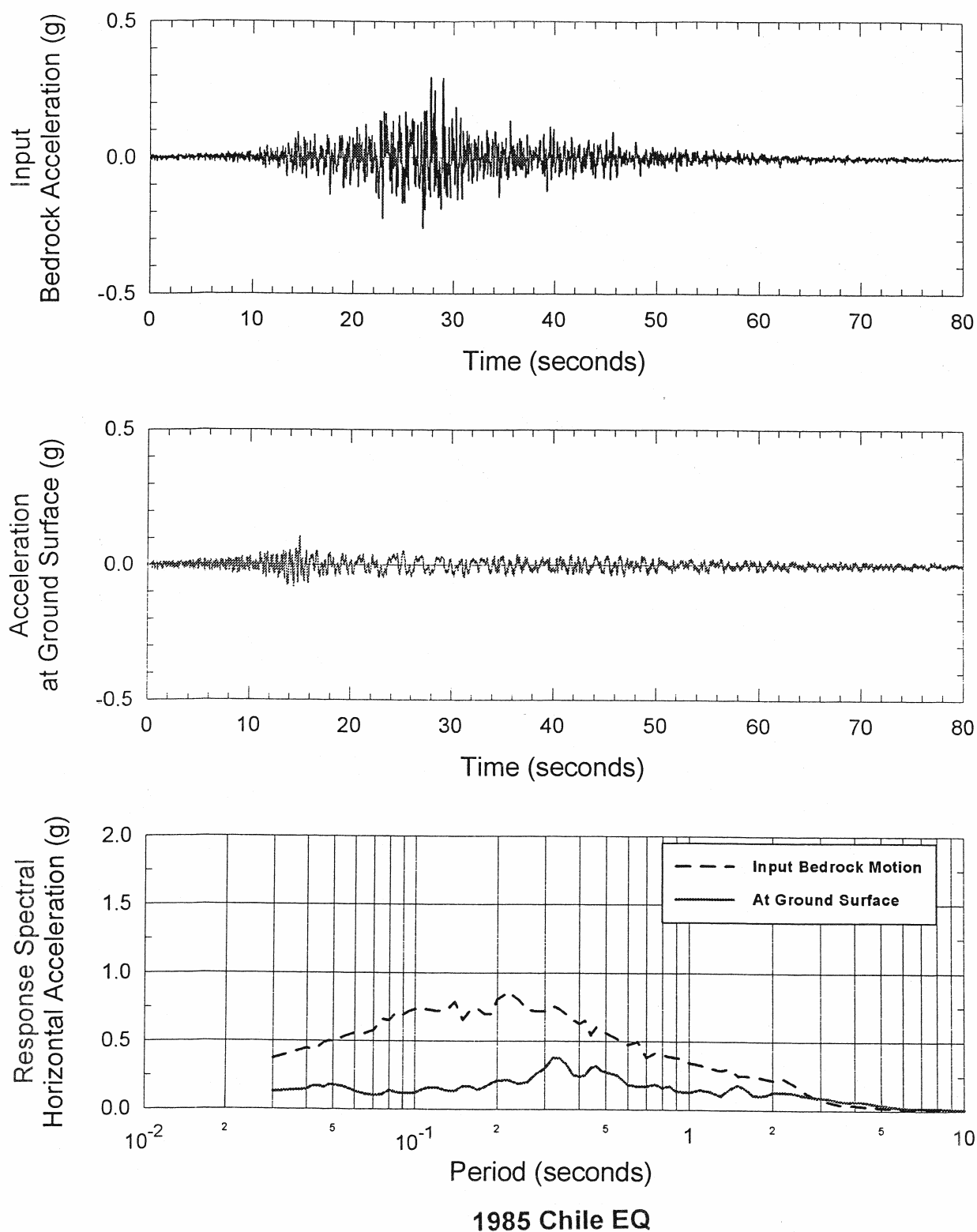


**Figure H-8** Input and Output Acceleration Histories and Response Spectra, 475-Year Earthquake (10% in 50-Year PE Ground Motion) Without Fill, Washington State Case Study



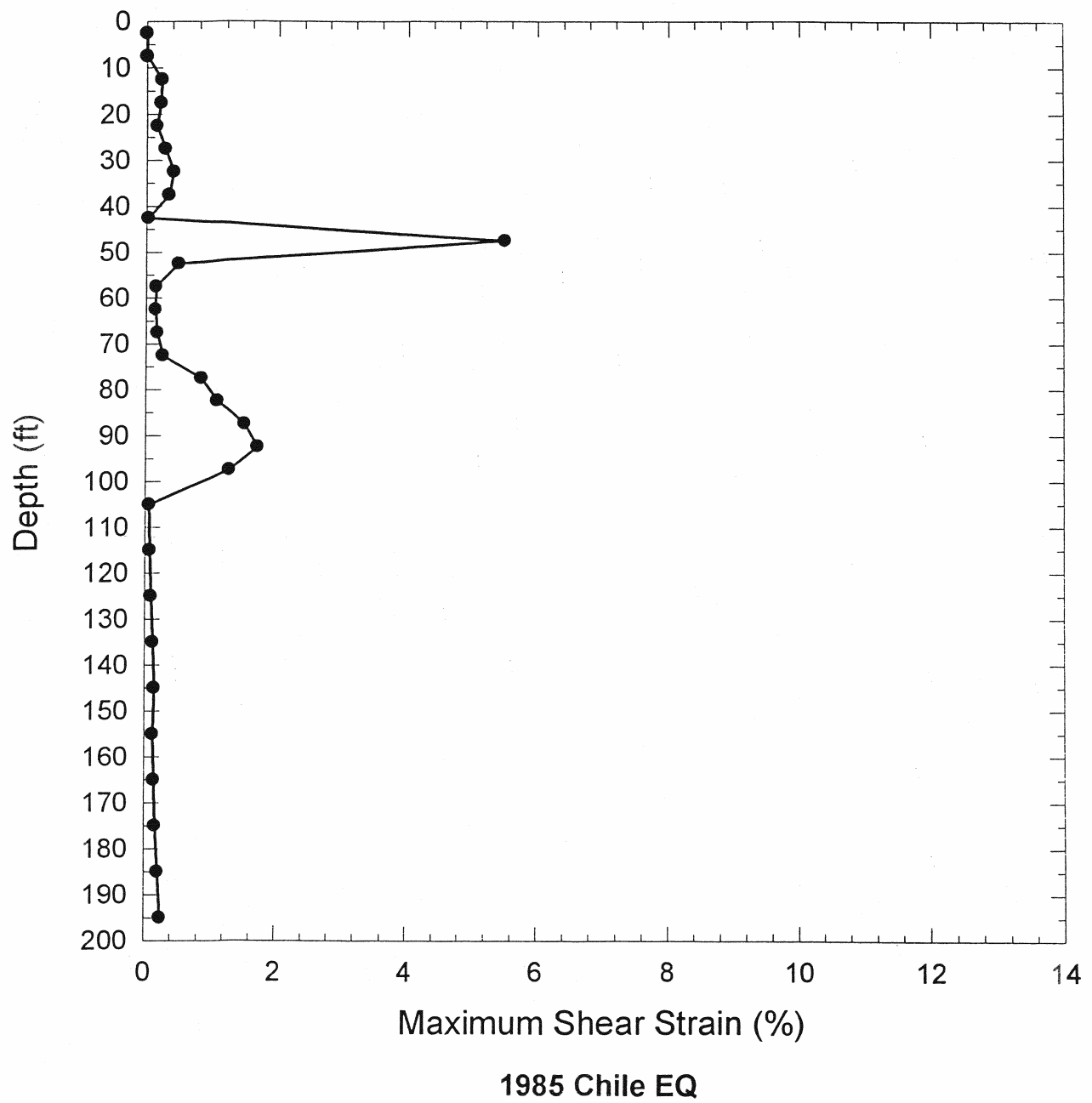
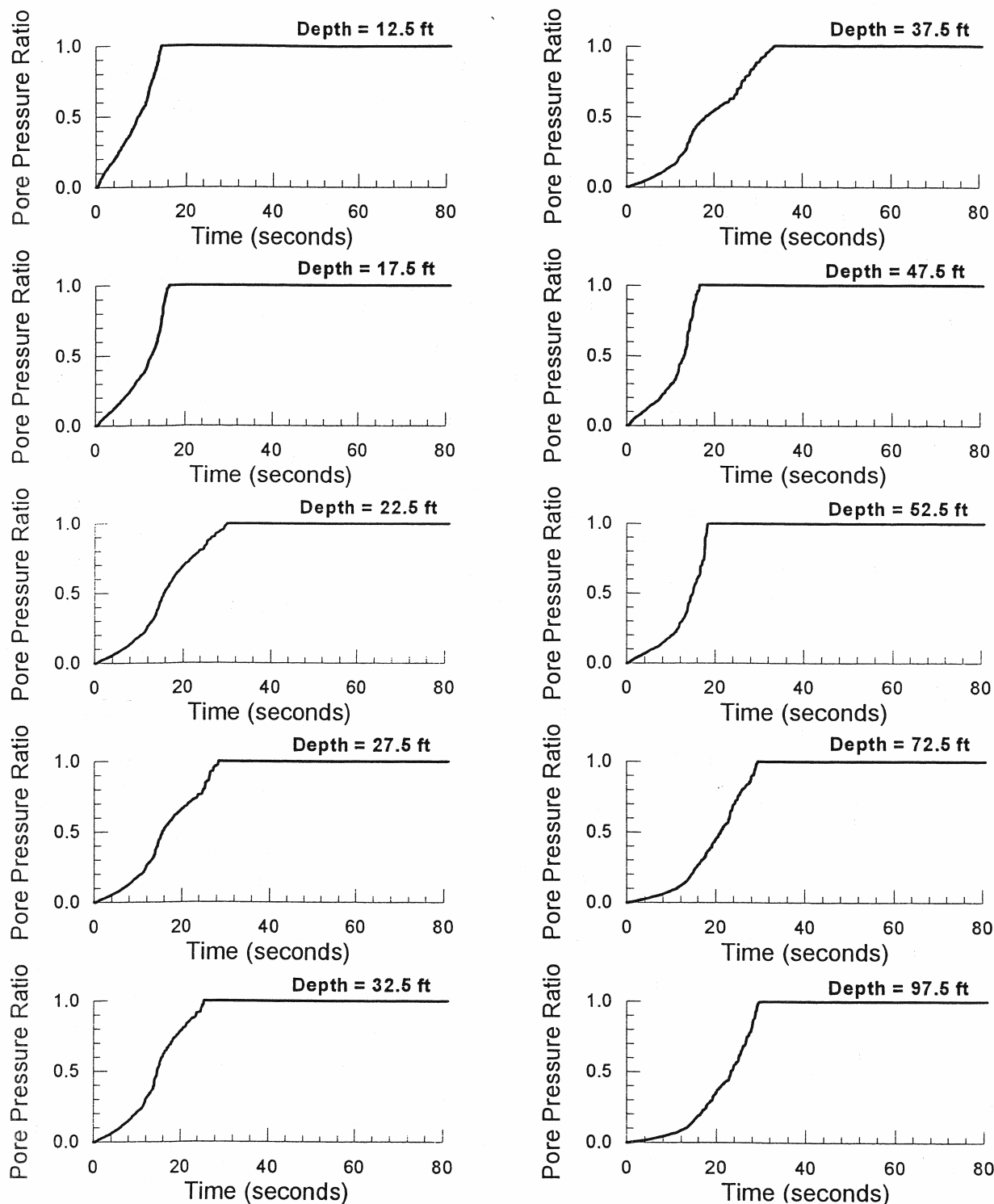
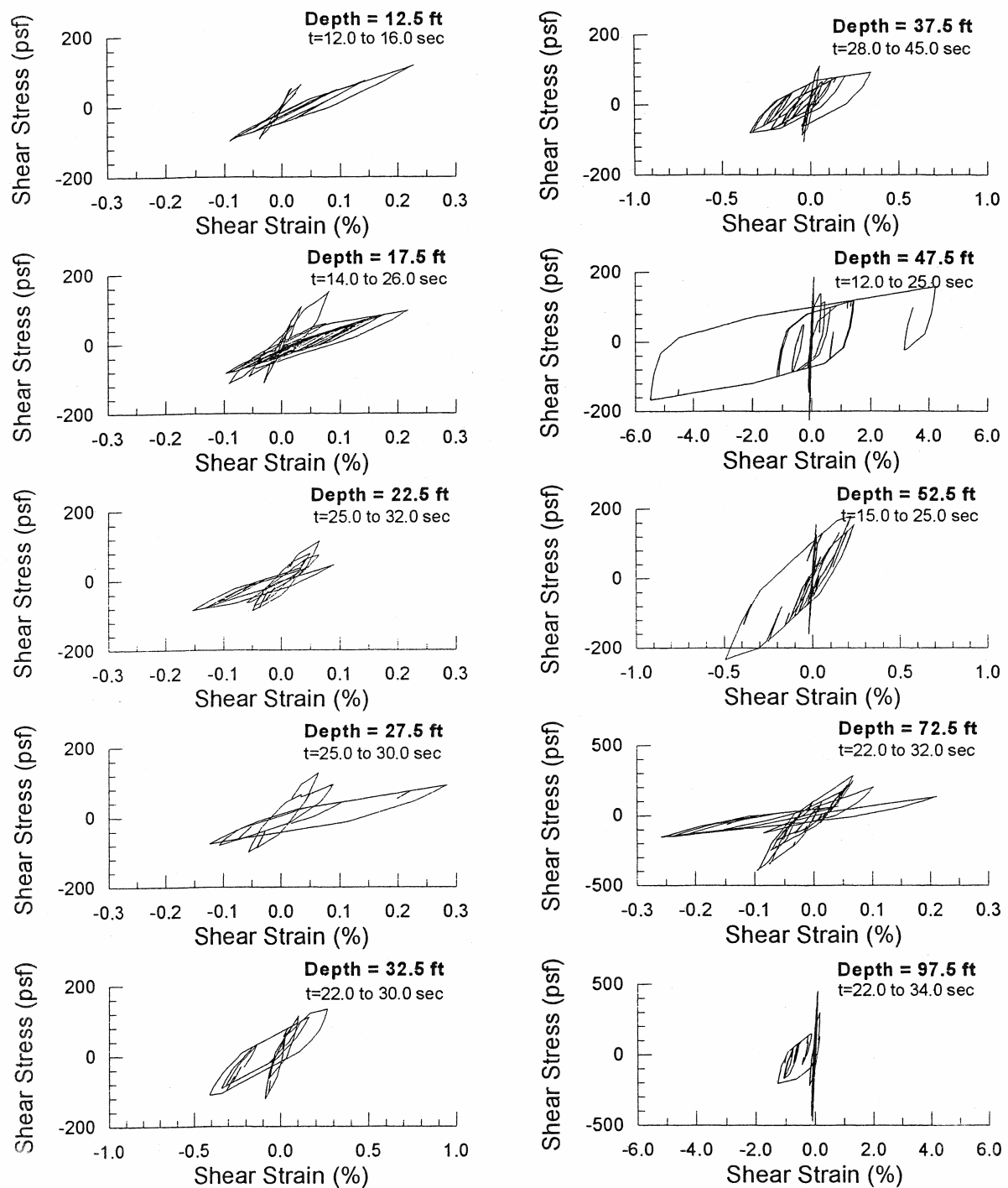


**Figure H-9** Maximum Shear Strains Induced as a Function of Depth, 475-Year Earthquake (10% PE in 50-Year Ground Motion) Without Fill, Washington State Case Study.



### 1985 Chile EQ

**Figure H-10** Time Histories of Pore Pressure Generation at Various Depths, 475-Year Earthquake (10% PE in 50-Year Ground Motion) Without Fill, Washington State Case Study.



### 1985 Chile EQ

**Figure H-11** Shear Stress – Shear Strain Hysteretic Loops at Various Depths, 475-Year Earthquake (10% PE in 50-Year Ground Motion) Without Fill, Washington State Case Study

also seen for the time histories based on the Olympia and Desert Hot Spring earthquakes, although as for the no fill case, liquefaction did not occur at depths greater than 55 feet for the 475-year Desert Hot Springs event.

The above results are again generally consistent with the factor of safety calculations using the simplified method, but with the notable differences that for the 475-year Olympia and Chile events, liquefaction occurred at depths between 70 and 100 feet, whereas factors of safety would have been greater than one based on the simplified method. This reflects the “bottom up” wave propagation used in DESRA-MUSC, versus the “top down” inertial loading from the simplified method.

### H.6.3 Lateral Ground Displacement Assessment

From the results of the simplified liquefaction studies, two liquefiable zones were identified for stability and displacement evaluations. One extends from a depth of 10 feet to 20 feet below the ground surface. The other extends from 45 to 55 feet below the ground surface. The residual strength of these two liquefied zones was selected as 300 psf based on the SPT blow counts in each layer. Soils between 20 and 40 feet below the ground surface and between 55 and 100 feet below the ground surface were assumed to have partial build-up in pore water pressure, resulting in some reduction in the friction angle of the non-liquefied sand layers, as shown in the DESRA-MUSC analyses. For these conditions, the response of the end slope for the approach fill on each side of the channel was estimated by conducting pseudo-static stability evaluations followed by simplified deformation analyses using chart-based Newmark analyses. These correspond to Steps 2 and 3 of the design procedure of Article D. 4.2.2.

#### H.6.3.1 Initial Stability Analyses

Once liquefaction has been determined to occur, a stability analysis is performed to assess the potential for soil movement as indicated in Step 2 of the design procedure.

The computer program PCSTABL was used during these analyses. Most analyses were conducted using a simplified Janbu failure method of analysis with a wedge failure surface. This geometry was believed to be most representative of what would likely develop during a seismic event.

Checks were also performed for a circular failure surface and using the modified Bishop and Spencer methods of analysis. Both pre-liquefaction and post-liquefaction strengths were used during these analyses.

Results of the pre-liquefaction studies indicate that the static FOS for the end slopes on each side of the channel was 1.5 or more, confirming acceptable static conditions. Yield accelerations (accelerations that produce FOS's of 1 on postulated failure surfaces in the pre-liquefaction state) were typically greater than 0.15, suggesting that some deformation would occur within the end slopes, even without liquefaction.

The FOS values dropped significantly when residual strengths were assigned to the two liquefied layers, as summarized in the following table. For these analyses the geometry of the failure surfaces was constrained to force failure through the upper or lower liquefied zone. Results given in the following table are for post-liquefaction conditions; i.e., no seismic coefficient for the right-hand approach fill.

Case	Abutment	Factor of Safety	Comment
Upper Wedge	Right	0.71	Modified Janbu
Lower Wedge	Right	0.79	Modified Janbu
Upper Circle	Right	0.81	Modified Bishop
Lower Circle	Right	0.86	Modified Bishop

Results of the stability analyses for the right-hand abutment indicate that for liquefied conditions and no inertial force in the fill (i.e., after the earthquake), factors of safety range from 0.7 to 0.9 for different assumptions of failure surface location and method of analysis. FOS values less than 1.0 indicate that lateral flow failure of the material is expected during any event that causes liquefaction in the two layers, whether it is associated with the 10% PE in 50 year or 3% PE in 75 year ground motion. The potential for instability is similar for failure surfaces through the upper and lower layers of liquefied soil, suggesting that any mitigation procedure would have to consider displacements through each layer. In other words, it would not be sufficient to improve only the upper 20 feet of soil where the FOS was lower, as a liquefaction-related failure could also occur at deeper depths.

Given the predicted occurrence of a liquefaction-induced flow failure, it would be desirable to quantify the amount of displacement expected dur-

ing this flow, which corresponds to Step 3 of the design procedure. Unfortunately, this is quite difficult when flow failures are predicted to occur. The simplified chart methods or the Newmark time history analysis, cannot be used to compute displacements for flow failures. However, flow displacements could be expected to be large, and such large displacements would indicate mitigation might be needed. More detailed analyses considering both structural pinning effects and ground modifications for mitigation of displacements are discussed in the following section of this Appendix.

#### H.6.3.2 Lateral Spread Implications from DESRA-MUSC Analyses

A key conclusion from the DESRA-MUSC analyses was the strong likelihood that lateral spread deformations would be controlled by a failure zone in the 45- to 50-foot layer. Displacement time histories for a rigid block sliding on this layer (assuming a Newmark sliding block analogy) were generated for a range of yield accelerations, using input acceleration time histories generated at the base of the 50- to 55-foot layer. The analyses were performed using the DISPMNT computer program (Houston et. al., 1987). "Upslope" deformations were suppressed assuming a strong one directional driving force from the embankment. At time zero, drained strengths for the liquefied layer were assumed. Strengths were degraded as a function of pore water pressure increase and reduced to the assumed residual strength of 300 psf when liquefaction was triggered. As would be expected, most of the computed displacements occurred subsequent to triggering.

Results showing displacement time history plots for the 3% PE in 75 year ground motion, based on the Chile earthquake as a function of yield acceleration, are shown in Figure H-12. Total accumulated displacements as a function of yield acceleration are shown in Figure H-13 for the three earthquake records. These plots became a basis for discussion on remediation analyses, as described in Article H.6.3.4. Similar analyses for potential failure surfaces in the depth zone of 10 to 20 feet, gave a maximum displacement of only 0.06 feet.

#### H.6.3.3 Stability Analyses with Mitigation Measures

Since it has been determined that significant soil movements will occur, Step 7 of the design procedure requires an evaluation of measures that will reduce the amount of movement.

Two procedures were evaluated for mitigating the potential for lateral flow or spreading: structural pinning and ground improvement. For these analyses the additional resistance provided by the improved ground or by the structural pinning of the soil was incorporated into the stability analyses described above. If the FOS for the revised analysis was greater than 1.0, the yield acceleration for the mitigated condition was determined, which then allowed displacements to be estimated. If the FOS was still less than 1, then flow would still occur and additional mitigation measures would be required.

For the structural pinning evaluation, shear forces were calculated to be 90 kips per pile for sliding on either the upper or lower failure surfaces. Procedures for determining the amount of pinning force are given in Section H.7.2. The abutment has 12 piles which extend through the sliding zone, resulting in 1,080 kips of additional shear reaction to sliding. Pier 5 of the bridge has 16 piles that produce 1,440 kips of pinning force. The abutment and the columns for Pier 5 are expected to develop reaction forces from passive pressure and column plastic shear. These forces were calculated to be 400 kips and 420 kips, respectively. This reaction occurs over the 48-foot abutment and pile cap widths, resulting in a total resistance of 31 and 70 kips per foot of width (or 1480 kips and 3340 kips, total) for displacement along the upper and lower liquefied zones, respectively.

This reaction force was introduced into the slope stability analysis using two methods:

1. A thin vertical slice the width of the pile group was placed at the location of the pile. This slice was assigned a strength that gives the same total pile resistance per unit width.
2. The resistance per unit width was converted into an equivalent shear strength along the shear plane in the liquefied zone, and this equivalent strength was added to the residual strength of 300 psf. For these analyses the upper failure plane was determined to be 104 feet in length giving an added component to

### Washington Site : Chile EQ - 2475 Year Event

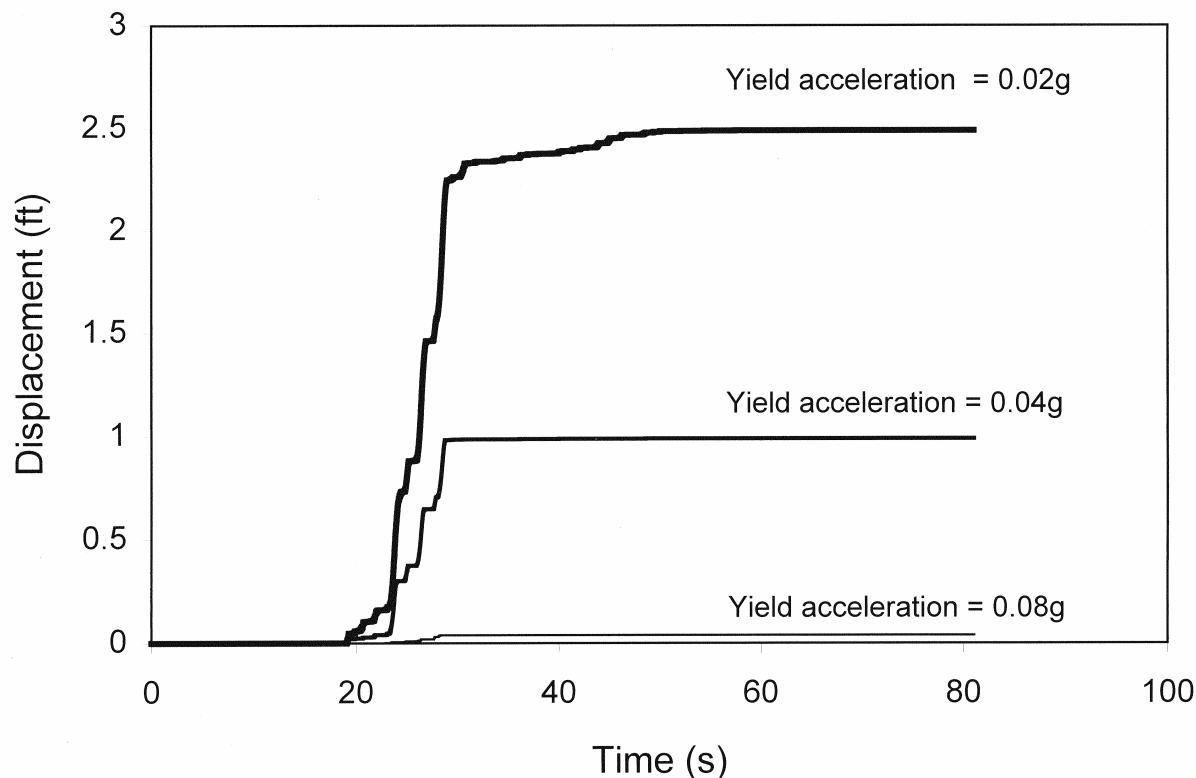


**Figure H-12 Displacement vs. Time for 2475-Year Earthquake (3% PE in 75-Year Ground Motion), Washington State Case Study.**

the liquefied strength of 300 psf. The resulting strength assigned to the liquefied layer was 600 psf (i.e., 300 psf + 300 psf = 600). For the lower zone, the surface is 132 feet in length, resulting in an average pinning resistance of 530 psf and a total resistance of 830 psf.

Both procedures gave generally similar results.

The FOS for the lower surface is greater than 1.0 for the post-liquefaction case, indicating that a post-earthquake flow failure would not occur. However, under the slope inertial loading, displacement of the slope could develop, and this can be assessed using the Newmark sliding block analysis once the yield acceleration is determined. The upper surface has a FOS of 1.0, indicating that a flow failure is on the verge of occurring.

The yield acceleration for the lower surface was determined by varying the seismic coefficient within the slope stability analysis until the factor of safety was 1.0. This analysis resulted in the lower surface yield acceleration given below. For

the upper surface, it was assumed that the yield acceleration was zero, since the FOS was 1.0 without any additional inertial force.

Case	Yield Acceleration (g)
Upper Surface	0
Lower Surface	0.02

For the ground improvement case, different widths of improved ground were used below the abutment. The improved ground extended through each of the liquefied zones. Soil in the improved ground was assigned a friction angle of 45 degrees. This increase in strength was assumed to be characteristic of stone columns or a similar improvement procedure. As with the structural pinning case, two procedures were used to represent the improved zone. One was to model it explicitly; the second involved “smearing” the reaction from the improved strength zone across the failure surface by increasing the strength of the soil in the liquefied zone to give the same reaction. The re-

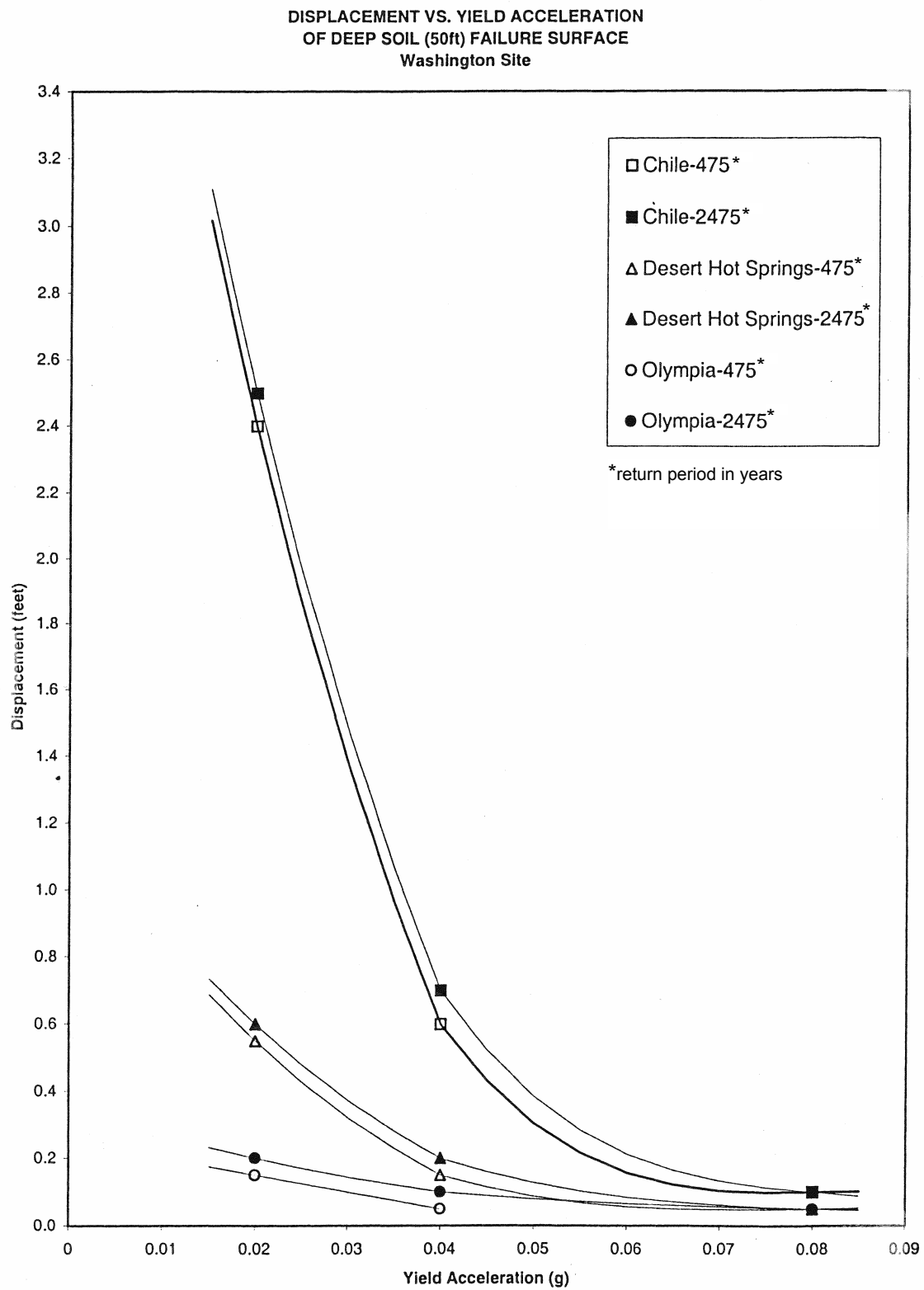


**Figure H-13 Displacement vs. Yield Acceleration for the Deep Sliding Surface of the Washington State Site**

sulting FOS was greater than 1.0 for all cases, indicating that flow would not occur. This allowed yield accelerations to be computed as a function of the width of the improved zone, in order to estimate the displacements that may occur. These values are summarized below.

Width (feet)	Yield Acceleration (g)
30	0.12
50	0.33
70	0.65

#### H.6.3.4 Displacement Estimates from Simplified Methods

Once lateral flow has been prevented, the amount of displacement that occurs from inertial loading on the failure wedge is estimated. This corresponds to Steps 3 and 11 of the design procedure.

Displacements were estimated for the yield accelerations given above using simplified methods. For these estimates, methods recommended by Franklin and Chang (1977), Hynes and Franklin (1984), Wong and Whitman (1982), and Martin and Qiu (1994) were used. All three methods approach the problem similarly. However, the Hynes and Franklin, as well as the Wong and Whitman and Martin and Qiu methods, eliminate some of the conservatism that is implicit to the Franklin and Chang method. For the Franklin and Chang method, it is necessary to define both the peak acceleration and velocity. The ratio of velocity to acceleration was assumed to be 30 for this study based on typical observations from recording of more distant events. For near-source events (epicentral distances less than about 15 km) this ratio can be as high as 60. In the case of the Hynes and Franklin method, displacements can be obtained for the mean, mean plus one standard deviation, and upper bound displacements. The mean displacements are used for this study. The Martin and Qiu study was based on the Hynes and Franklin database, but included the peak ground acceleration as an additional variable in the data regression analyses. Mean values were also used in their regressions. Each of these simplified methods relates displacement to the ratio of yield acceleration to the peak ground acceleration ( $k_{max}$ ). For these evaluations  $k_{max}$  was 0.24g and 0.42g for the 10% PE in 50 and 3% PE in 75-year ground motions, respectively. The resulting displacements for the cases cited above are summarized as follows.

Displacements (inches)				
Case	475-Year Event (10% PE in 50-Year Ground Motion)			
	Franklin & Chang	Hynes & Franklin	Wong & Whitman	Martin & Qiu
1	>36	16	10	28
2	<1	<4	<1	5
3	<1	<4	<1	<1
4	<1	<4	<1	<1
2,475-Year Event (3% PE in 75-Year Ground Motion)				
Case	Franklin & Chang	Hynes & Franklin	Wong & Whitman	Martin & Qiu
1	>36	31	23	42
2	13	<4	3	8
3	<1	<4	<1	<1
4	<1	<4	<1	<1

Table notes: Case 1: Pile Pinning/Lower  
Case 2: Stone Columns – 30 ft  
Case 3: Stone Columns – 50 ft  
Case 4: Stone Columns – 70 ft

It is the recommendation of the new provisions that a designer use the Martin and Qiu results. The Franklin and Chang, and Wong and Whitman, results provide possible upper and lower bound ranges on the displacements, but they are not believed to be as credible as the Hynes and Franklin, and Martin and Qiu, results.

The approximate displacement from the Martin and Qiu method for the 10% PE in 50 year ground motion is 28 inches. For the 3% PE in 75 year ground motion the displacement is 42 inches. (See table above.)

#### H.6.3.5 Displacement Estimates Using Site Response Analysis Results

This section corresponds to Steps 3 and 11 of the design procedure, as they apply to site-specific analysis of potential displacements using the nonlinear, effective stress method.

Similar estimates to the simplified methods described above may be made using the displacement versus yield acceleration curves shown in Figure H-13. As the curves are essentially identical for the 10% PE in 50 year and 3% PE in 75 year ground motions, the displacement estimates



shown in the table below are for both probability levels and for the lower yield surface (45-55-foot depth).

Case	Displacements (inches)		
	Chile	Olympia	Desert Hot Springs
Pile Pinning	29	7	3
Stone Columns (> 30 foot width)	< 1	< 1	< 1

These estimates are generally consistent with the estimates from the simplified methods, although the site-specific results indicate that the event representative of the large mega-thrust subduction zone earthquake (Chile) will produce the largest displacements. The displacements from a moderate magnitude subduction zone intraslab earthquake (Olympia) and a moderate magnitude local shallow crustal earthquake (Desert Hot Springs) produce much more modest displacements that could be accommodated by the foundations.

## H.7 STRUCTURAL ANALYSIS AND DESIGN

The design of bridge structures for liquefaction effects generally has two components. The first is that the bridge must perform adequately with just the liquefaction-induced soil changes. This means that the mechanical properties of the soil that may liquefy are changed to reflect their liquefied values (i.e., properties such as stiffness are reduced). Design for these cases is in reality a design for structural vibration effects, and these are the effects that the code-based procedures typically cover for design. The second component of the design is the consideration of liquefaction-induced ground movements. The potential interaction or combination of these effects must be addressed in the design, and at the present, there is not sufficient understanding of the phenomena to normally warrant performing a combined analysis. Therefore, the recommended methodology is to simply consider the two effects independently; i.e., de-coupled. The reasoning behind this is that it is not likely that the peak vibration response and the peak spreading or flow effect will occur simultaneously. In fact, for most earthquakes the peak vibration response is likely to occur somewhat in advance of the maximum ground movement loading. Furthermore, the de-coupling of response

allows the flexibility to use separate and different performance criteria for design to accommodate the two phenomena. In some areas where extended shaking could result in the two phenomena occurring concurrently, it may be desirable to use more rigorous coupled effective stress computer models to evaluate this.

### H.7.1 Vibration Design

Vibration design was done for both the current AASHTO *Specifications* and for the recommended NCHRP 12-49 LRFD provisions. For the recommended LRFD provisions, both the 3% PE in 75 year and 50% PE in 75 year ground motions were considered. Since the primary objective of the study was to compare the existing and recommended provisions, the designs were more of a preliminary nature, which was felt to be sufficient to highlight the major differences. In this study, the same bridge was evaluated for each of the two specification requirements. Comparisons were then based on the amounts of reinforcing, for example, and in the case where sizes should be altered, recommendations are given. To this end, the designs represent preliminary designs that highlight the differences between the two specifications. A very brief summary follows.

The bridge is comprised of multi-column bents so the existing provisions use an  $R$ -factor of 5, and the recommended provisions allow an  $R$ -factor of 6 provided a nonlinear static displacement check is done. For the 100 year design the proposed provisions allow an  $R$  of 1.3.

For the tallest columns and the recommended LRFD provisions, ground motion for the 2,475-year event required a steel content in the columns of 1.4%, and this was controlled by the 100-year event ground motion. The 100-year event ground motion produced a design moment that was approximately 20% larger than the 2,475-year event. This is due to the relative magnitudes of  $R$  and of the input spectra. For the 475-year event ground motion a design using 1% steel resulted. For Pier 2 the results were similar.

The foundation (piling), used as starting point for both the existing and recommended provisions, was the same. This is because one objective of the study was to evaluate a system that worked for the existing provisions when subject to the effects of the larger design earthquake ground motion.

The pier designs were checked for displacement capacity, using an approximate push over analysis. The assessment considered the super-

structure and the pile caps as rigid restraints against rotation for simplicity. While the check is only required for the recommended provisions, the checks were performed on the designs to the existing provisions, as well. All the columns met the checks (i.e., the displacement capacity exceeded the demands).

The recommended LRFD provisions also require that the displacements be checked for  $P-\Delta$  effects. In other words, the lateral shear capacity of the bents defines a maximum displacement that can occur without suffering problems from displacement amplification due to  $P-\Delta$ . Both piers are adequate as-designed with respect to  $P-\Delta$ .

### H.7.2 Lateral Spreading Structural Design/Assessment

The material in this section generally represents Steps 4, 5, 6, 8, 9 and 12 of the recommended Design Procedure, and the material addresses the structural aspects of the procedure.

In Section H.6.3 the tendency for the soil near Piers 5 and 6 to move during or after a major earthquake was assessed. Once it had been determined that lateral spreading would occur, the next step (Step 7) was to evaluate the beneficial pinning action of the foundation system in the analysis. This section describes the method of determining the pinning force to add to the stability analyses of Section H.6.3, and it describes the process of determining whether flow around the foundation would occur or whether the foundation will move with the soil. This involves Steps 4 and 5 of the design procedure.

#### H.7.2.1 Modes of Deformation

As outlined above there are two potential sliding surfaces during liquefaction for the Pier 5/6 end of the bridge. One is at the base of the upper liquefiable layer, and the other is at the base of the lower liquefiable layer. These potential deformation modes must be determined to evaluate the forces developed by the piles and the structures resistance.

The overall foundation deformation modes may be formally assessed using models that consider both the nonlinear nature of the soil resistance and the nonlinear behavior of the piles and foundations, when subject to prescribed soil displacement profiles. In this study, the deformations and structural behavior have been approximated using assumed displaced structural configurations

that are approximately compatible with the constraints provided by the soil. Examples of these configurations are given in Figures D.4.2-4, D.4.2-5, and H-14. In this example, the abutment foundation will move in a manner similar to that shown in Figure D.4.2-4, because there are sliding bearings at the substructure/superstructure interface. In the figure, the frictional forces transferred through these bearings have been conservatively ignored.

Pier 5 will move similar to the mode shown in Figure D.4.2-5. Under such a displaced shape both the columns and the piles contribute to the lateral resistance of the foundation. The columns contribute because there is an integral connection between them and the superstructure. In the current assessment, the residual displacements have been ignored. There exists some question as to whether this should be included or not. The reductions in resistance due to  $P-\Delta$  effects are likewise given in the figure, but for many of the deformations and column height combinations considered in this study, this reduction is small, and therefore it has not been included in the calculations.

#### H.7.2.2 Foundation Movement Assessment

As described in Step 4 through 6 of the design procedure, an assessment should be made whether the soil will move around the foundation or whether it will move the foundation as it moves. Passive capacities of the various layered soils were extracted from the  $p-y$  curves generated by conducting LPILE analyses<sup>4</sup> for the piles. These forces represent the maximum force that is exerted against the piles as the soil moves around the pile. This then is the upper bound limit state of the soil force that can be developed. Additionally, the maximum passive forces that can be developed against the pile caps and abutment stem wall were developed. Two total forces were developed; one for the shallow-seated soil failure and one for the deep failure. The shallow failure will develop approximately 1100 kips/pile and the deep failure approximately 3500 kips/pile at the point where the soil is moving around the foundation. By comparison, one pile with a clear distance of 30 feet between plastic hinges can develop about 90 kips of shear at the point where a full plastic mechanism has formed in the pile. The conclusion

<sup>4</sup> LPILE is a computer program used to evaluate lateral response of piles subjected to loads and moments at the pile head. This program is similar to COM624.

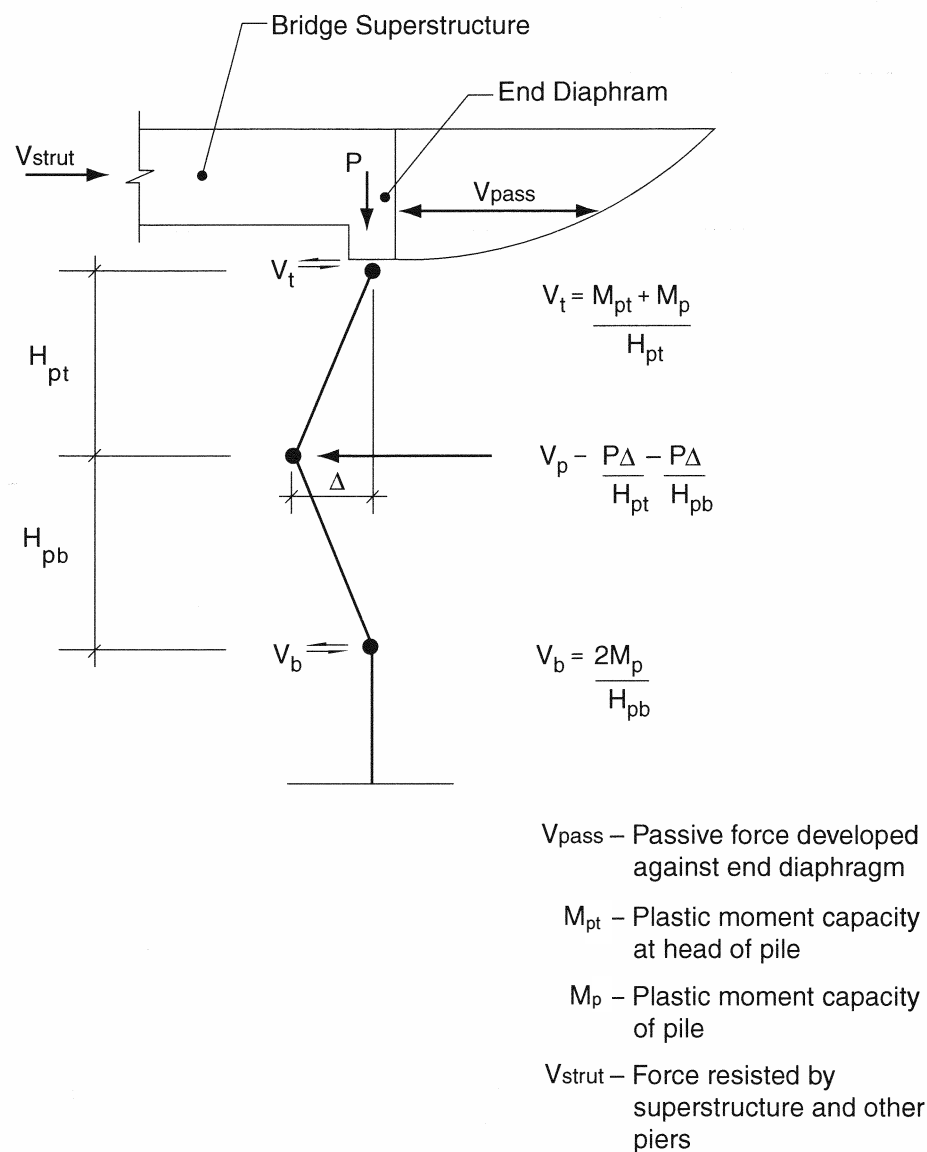


**Figure H-14 Plastic Mechanism for an Integral Abutment Supported on Piles, Washington State Case Study**

from this comparison is that there is no practical likelihood that the soil will move around the piles. Instead the foundations will be pushed along with the soil as it displaces toward the river channel beneath the bridge.

Intuitively, it is only reasonable to expect that soil will move around a pile if there is no crust of non-liquefied material being carried along with the displacing soil (Step 4 of the design procedure). In the case examined here, there are significant (10's of feet) non-liquefied material above the liquefiable material, and it is that material which contributes to the high passive forces. Thus if a

reasonable crust exists, the foundations are likely to move with the soil.

Now the questions to be considered are: (1) can the foundation systems endure the displacement that the soil produces (Step 6), and (2) can the foundations appreciably reduce the soil movement via pinning action (Step 7).

#### H.7.2.3 Pinning Force Calculation

In Article H.6 various pinning forces were discussed and included with the stability analyses to investigate the effectiveness of including the

existing foundation pinning. The following discussion accounts for the development of the force values used.

Figure H-15 illustrates qualitatively the forces developed against the foundations and how they are reacted using the bridge, itself, as a strut. Two soil blocks are shown, Block A on the right and B on the left. Block A represents a postulated deep-seated slide that affects both Piers 5 and 6. The shears,  $V_{p5}$  and  $V_{p6}$ , represent the pinning shear force developed by the piles of Pier 5 and 6, respectively. Shear  $V_{c5}$  is the shear contributed by the Pier 5 columns. Finally,  $V_{pas}$  is the passive resistance provided by the backfill acting against the end diaphragm.

While Block A is the most likely of the two to move, Block B is shown in this example to illustrate where and how the forces transferred into the bridge by Block A are resisted. In this case the bridge acts as a strut. Note that if a significant skew exists, then these forces cannot be resisted without some overall restraint to resist rotation of the bridge about a vertical axis.

Figure H-16 illustrates the pinning forces acting on a soil block sliding on the lower liquefiable layer. In this case, abutment and Pier 5 piles each contribute about 90 kips, the abutment about 400 kips, and the columns at Pier 5 about 420 kips. The total abutment pile resistance is 1080 kips and corresponds to the approximate plastic mechanism shear with 30 feet clear between points of assumed fixity in the piles. This comprises 10 feet of liquefiable material and  $5D$  ( $D$  = pile diameter) to fixity above and below that layer<sup>5</sup>. The upper portion of the soil block is assumed to move essentially as a rigid body, and therefore the piles are assumed to be restrained by the integrity of this upper block. The pile resistance at Pier 5 is determined in a similar manner, and the shear that the Pier 5 piles contribute is 1440 kips. The abutment passive resistance corresponds to half of the prescribed passive capacity of the backfill and is assumed to act against the end diaphragm. The abutment fill is assumed to have slumped somewhat due to the movement of the soil block, and thus half of the nominal resistance was judged to be reasonable. The column resistance at Pier 5 is 420 kips, and this assumes that plastic hinging has occurred at the top and bottoms of the columns at this pier.

<sup>5</sup> Fixity was assumed to develop  $5D$  above the liquefied layer. In an actual design case, a lateral analysis using a computer code such as LPILE could be conducted to be more rigorous about the distance to fixity.

These forces (3360 kips) represent maximum values that occur only after significant plasticity develops. In the case of Pier 5 the approximate displacement limit is 22 inches, which comprises 4 inches to yield and 18 inches of plastic drift. The plastic drift limit is taken as 0.05 radians. The 22-inch displacement limit of Pier 5 is controlled by the piles. Because the piles of Pier 6 are the same, their limit is also 22 inches of displacement.

Because the Pier 5 columns are longer than the distance between hinges of the piles, the column displacement limits are 34 inches total and 7 inches at yield. The fact that the piles control the displacement limit in this case implies that some margin is available in the column to accommodate any residual plastic hinge rotations that remain in the column after strong shaking stops.

Figure H-17 shows the displaced shape of the foundations for a shallow (upper layer) soil failure. In this case, the distance between plastic hinges in the piles is 30 feet, just as with the deeper failure, and thus the plastic shear per pile is 90 kips. The total contributed by the piles is 1080 kips as before.

In Section H.6.3, the estimated displacements for the lower or deeper failure wedge were 28 inches for the 10% PE in 50 year ground motion and 42 inches for the 3% PE in 75 year ground motion. Neither of these are within the plastic capacity of the piles and either additional piles could be added as 'pinch' piles or ground remediation could be used<sup>6</sup>. It will be recalled that the yield acceleration for the upper failure was essentially zero for both the 10% PE in 50 year and 3% PE in 75 year ground motions, which indicates that some remediation would be required to stabilize the fill and its toe for both design ground motions.

## H.8 COMPARISON OF REMEDIATION ALTERNATIVES

The primary intent of these analyses was to determine the potential effects of increasing the seismic design ground motion criteria from its current probability of exceedance of 10% in 50 years to 3% in 75 years. Liquefaction was predicted for both probability of exceedance levels (earthquake return periods), and as a consequence, there is little difference in what remedial work is required

<sup>6</sup> Pinch piles refer to piles driven at close spacing to increase the shear resistance or density of a soil mass. In the Pacific Northwest, these piles are often timber.

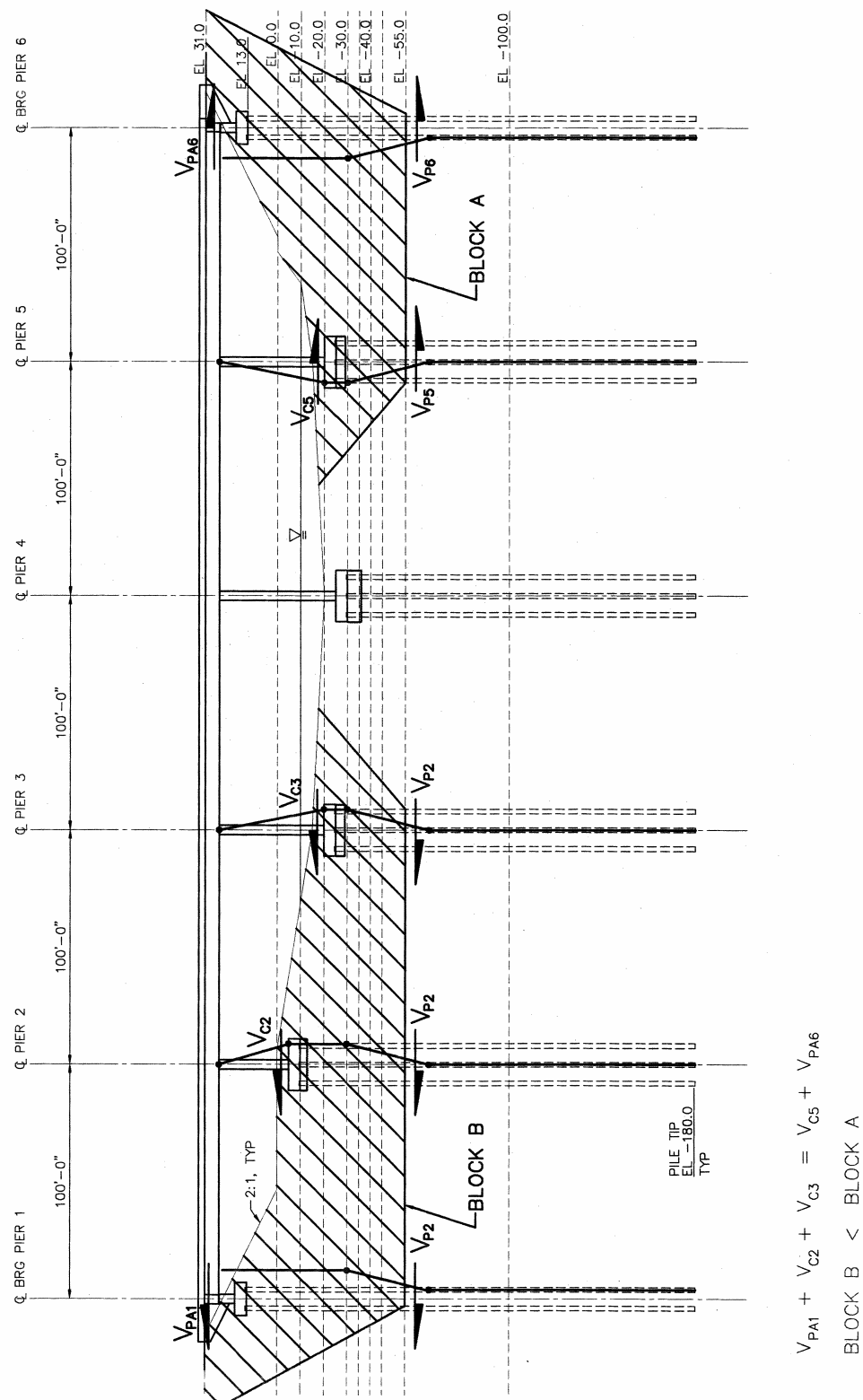


**Figure H-15** Forces Provided by Bridge and Foundation Piling for Resisting Lateral Spreading, Washington State Case Study

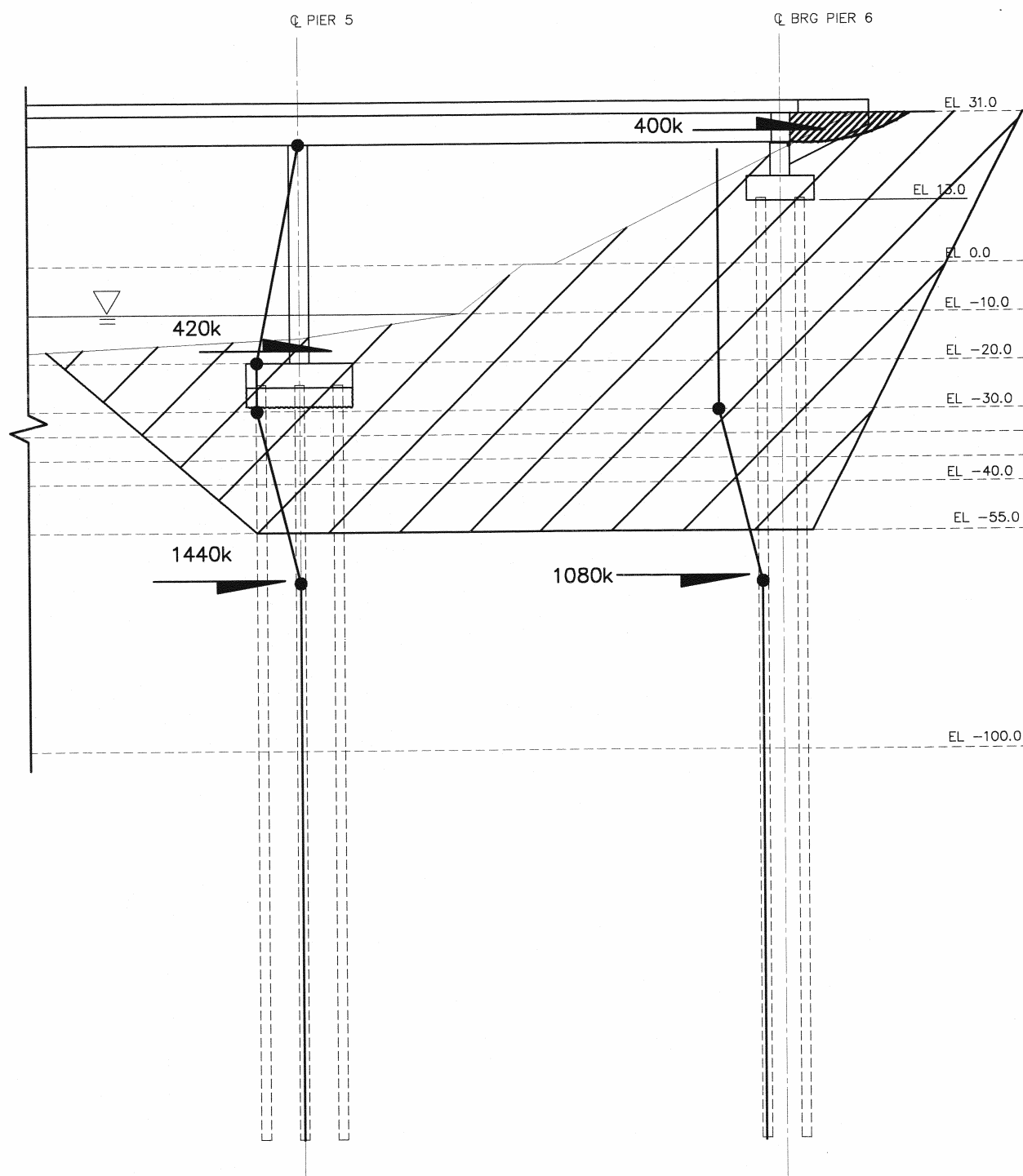


**Figure H-16** Piers 5 and 6 Resisting Lateral Spreading – Deep Wedge, Washington State Case Study

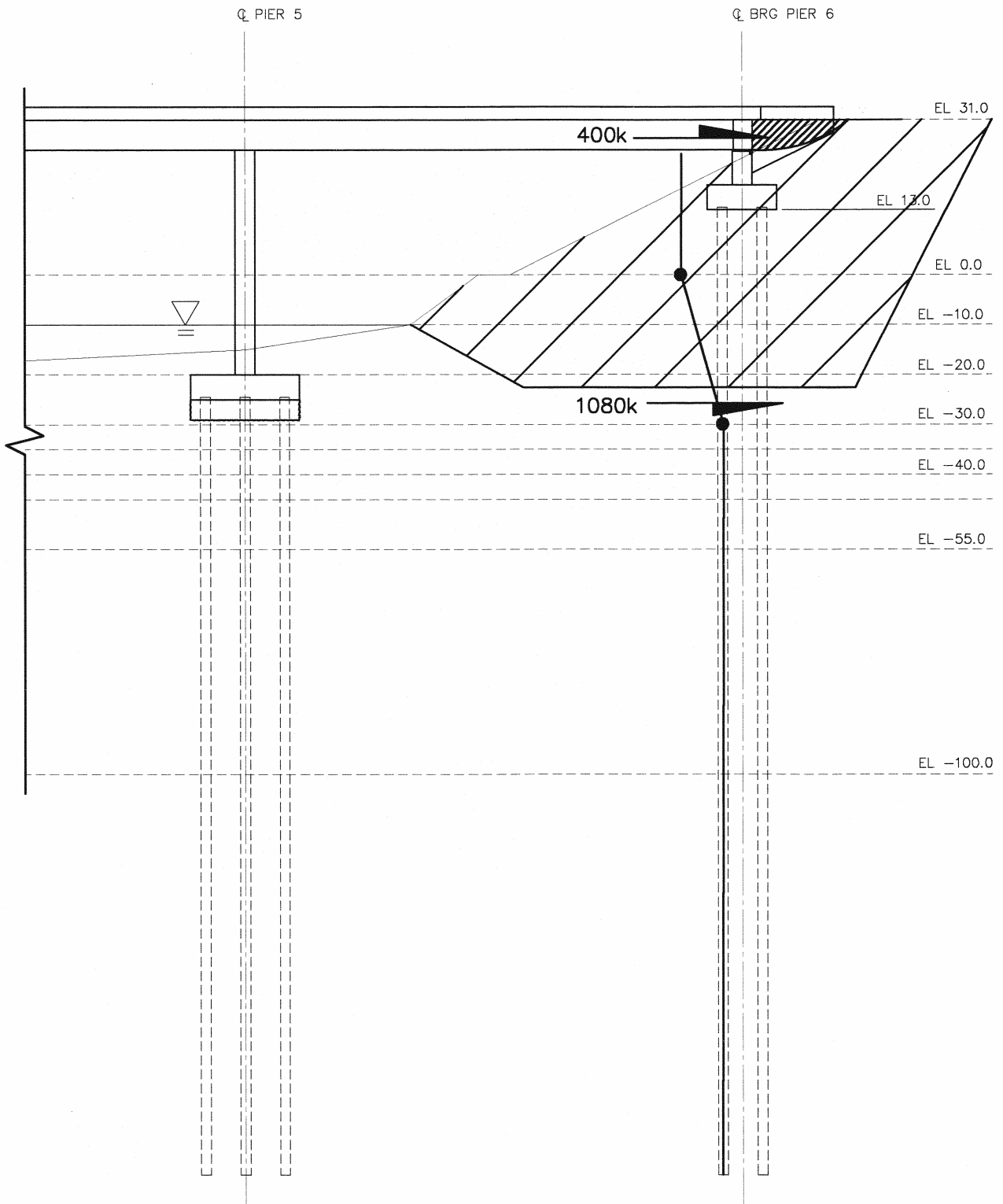


**Figure H-17** Pier 6 Resisting Lateral Spreading – Shallow Wedge, Washington State Case Study

for the two probability of exceedance levels (earthquake return periods).

### H.8.1 Summary of Structural and Geotechnical Options

Mitigation measures are assessed based on the desired performance requirement of the bridge. The first option is to assess the performance in its as-designed configuration. If this results in unacceptable performance, a range of mitigation measures is assessed.

For this example, some form of structural or geotechnical remediation is required at the right-hand abutment because the yield acceleration for the upper failure wedge is zero. This implies that this wedge is unstable under static conditions after the soil liquefies, which it does for both the 3% PE in 75 year ground motion and the 10% in 50 ground motion<sup>7</sup>. Two choices for improving the conditions were considered — use of additional piles or stone columns. Since the yield acceleration for the upper failure surface is so low, the more effective choice of the two was to use stone columns. These provide the combined advantage of increasing the residual shear strength of the sliding interface, and they can reduce pore water pressure build up, thereby postponing or possibly eliminating the onset of liquefaction.

Because the lower failure wedge also has a relatively low yield acceleration, 0.02g, it makes sense to extend the mitigation deep enough to improve the deeper soil layers, as well. This low yield acceleration results in displacements of 28 inches and 42 inches for the 10% PE in 50 year and 3% in 75 year ground motions from the simplified analyses and displacements of approximately 29 inches for both ground motion events for the time history corresponding to the mega thrust subduction zone earthquake for the site-specific Newmark analyses. The decision to improve the deeper layers requires that stone columns extend on the order of 50 feet in depth. The stone column remediation work will provide displacements that are less than 4 inches. This will keep the piles within their elastic range, and this will meet the highest level of operational performance objectives in the foundation system.

<sup>7</sup> The approach fill and ground profile condition for the bridge considered in this study are more severe than that used in the actual bridge that this example was modeled after. Thus, the implication of instability here does not imply instability in the prototype structure.

Although in this example the left-hand abutment was not evaluated in detail because the FOS of the initial stability analyses was greater than 1, a cost/benefit assessment would typically be made to determine if some remediation work on the left-hand abutment would be cost effective. Once a contractor is mobilized on the site, it would make some sense to provide improvement on both sides of the river. It may be that upon more in-depth investigation the stone columns could be spaced further apart or applied over a smaller width on the left-hand bank.

### H.8.2 Comparisons of Costs

As noted above, the remedial work is required for both the 10% PE in 50 year and 3% PE in 75 year ground motions.

The stone column option would likely be applied over a 30-foot length (longitudinal direction of bridge), since that length produced acceptable deflections of less than 4 inches for the site specific results, which is within the elastic capacity of the piles. The width at a minimum would be 50 feet, and the depth also would be about 50 feet. If the columns were spaced roughly on 7-foot centers, then 40 stone columns would be required. At approximately \$30 per lineal foot (plf), the overall cost per approach fill would be on the order of \$60,000, or about \$120,000 for both sides if the left-hand fill were judged to require remediation.

As a rough estimate of the cost of the overall structure, based on square-footage costs of \$100 to \$150 in Washington, the bridge would cost between 2 and 3 million dollars. If the higher cost were used, due to the fact that the bridge is over water and the foundation system is relatively expensive because of its depth, the cost to install stone columns on the right-hand side would run about 2% of the overall cost of the bridge. If both sides were remediated, then the costs would comprise about 4% of the bridge costs. It should be noted that this additional cost will produce a foundation performance level that meets the operational criteria for both ground motion probability of exceedance levels.

If pinch piles were used to augment the piles of the foundations, the pinch piles would not need to be connected to the foundation, and they would not need to extend as deep as the load-bearing foundation piles. The per pile costs for the foundation piles were estimated to be on the order of \$10,000 to \$12,000 each for 180-foot long piles. If shorter piles on the order of 80-feet long were



used, their costs would be about half as much. Thus if pinch piles were used about 10 to 12 piles per side could be installed for the same cost as the stone column remediation option. Although detailed analyses have not been performed with these pinch piles, the amount of movement anticipated would be in the range of 6 to 12 inches, rather than the 4 inches obtained with the stone columns. Therefore, the stone column option would appear the more cost effective in this situation. On a specific project, combinations of the two options would be evaluated in more depth.

It is useful to recognize that in this situation some remediation would be required for both the 10% PE in 50 year and 3% PE in 75 year ground motions because of the predicted instability of the upper failure wedge. In the case of the former, the remediation is required to a depth of 50 feet because the anticipated movement of the lower failure wedge would be on the order of 28 inches for the simplified analyses and 30 inches for the site specific analysis and thus be in excess of the 22 inch limit. For the 3% PE in 75 year ground motion, movement on the order of 42 inches is predicted by the simplified analysis, and 30 inches by the site-specific analyses. Consequently, remediation is required to a depth of 50 feet for both cases. Hence the difference in cost for this site and bridge between the two design earthquakes is minimal.

## H.9 MISSOURI EXAMPLE

The second bridge considered in this study is located in the New Madrid earthquake source zone in the lower southeast corner of Missouri. This general location was selected because this zone is one where a significant seismic hazard occurs, and there are numerous stream crossings and low-lying areas where potential for liquefaction also exists. Additionally, the project team wished to include a non-western site where the effects of different source mechanisms and where the differences in shaking levels between the 475-year and 2,475-year events would be highlighted. Since the design process and procedures used for this example are the same as the Washington example, an abbreviated summary of the key results follows. The details of the work on this bridge can be found in the companion *Liquefaction Study Report* (ATC/MCEER, 2003a).

### H.9.1 Site Characterization and Bridge Type

The site is located in southeastern Missouri along the western edge of the Mississippi River alluvial plane near the New Madrid seismic zone. Soils at this site consist of 20 feet of clay over a 20-foot layer of sand over dense alluvial materials at depths greater than 40 feet. The Missouri Department of Transportation (MoDOT) provided site characterization information for the prototype site, including boring logs with SPT's, CPT soundings, and shear wave velocity data. The geotechnical information was collected by MoDOT for a lifeline earthquake evaluation that they are currently conducting.

The simplified bridge used for the overcrossing is approximately 180 feet long, and comprises three, roughly equal-length spans. There are no horizontal or vertical curves on the bridge, and the bridge has no skew. A general elevation of the bridge and of the ground line is given in Figure H-18. The bridge and site plan have been simplified from that initially provided by MoDOT for illustrative purposes. The configuration of the bridge was selected, in part, due to its common nature. Many states use this type of bridge or variations to this type of bridge. Thus it was felt that the results for such a bridge type would be widely relevant to many other regions around the country.

The bridge structure comprises AASHTO-specified prestressed girders supported on three-column bents. The roadway is approximately 38 feet wide, and five 39-inch girders with a concrete deck form the superstructure. The substructure is formed of 3-foot diameter columns, which support a 40-inch dropped cap-beam. The foundations of the intermediate piers are individual pile caps for each column that are supported on 14-inch steel pipe pile foundations. An elevation of one of the intermediate piers is given in Figure H-19.

The abutments are of the integral type, where the end diaphragm is integrated with the ends of the girders and deck and is directly supported by nine 14-inch-diameter pipe piles. These piles form a single line in the transverse direction to the bridge. An elevation of the abutment is shown in Figure H-20.

The deaggregation results for the Missouri site show that, for both 475-year (10% PE in 50 year ground motion) and 2,475-year (3% PE in 75 year ground motion) return periods and for both short periods and long periods of the response spectrum,

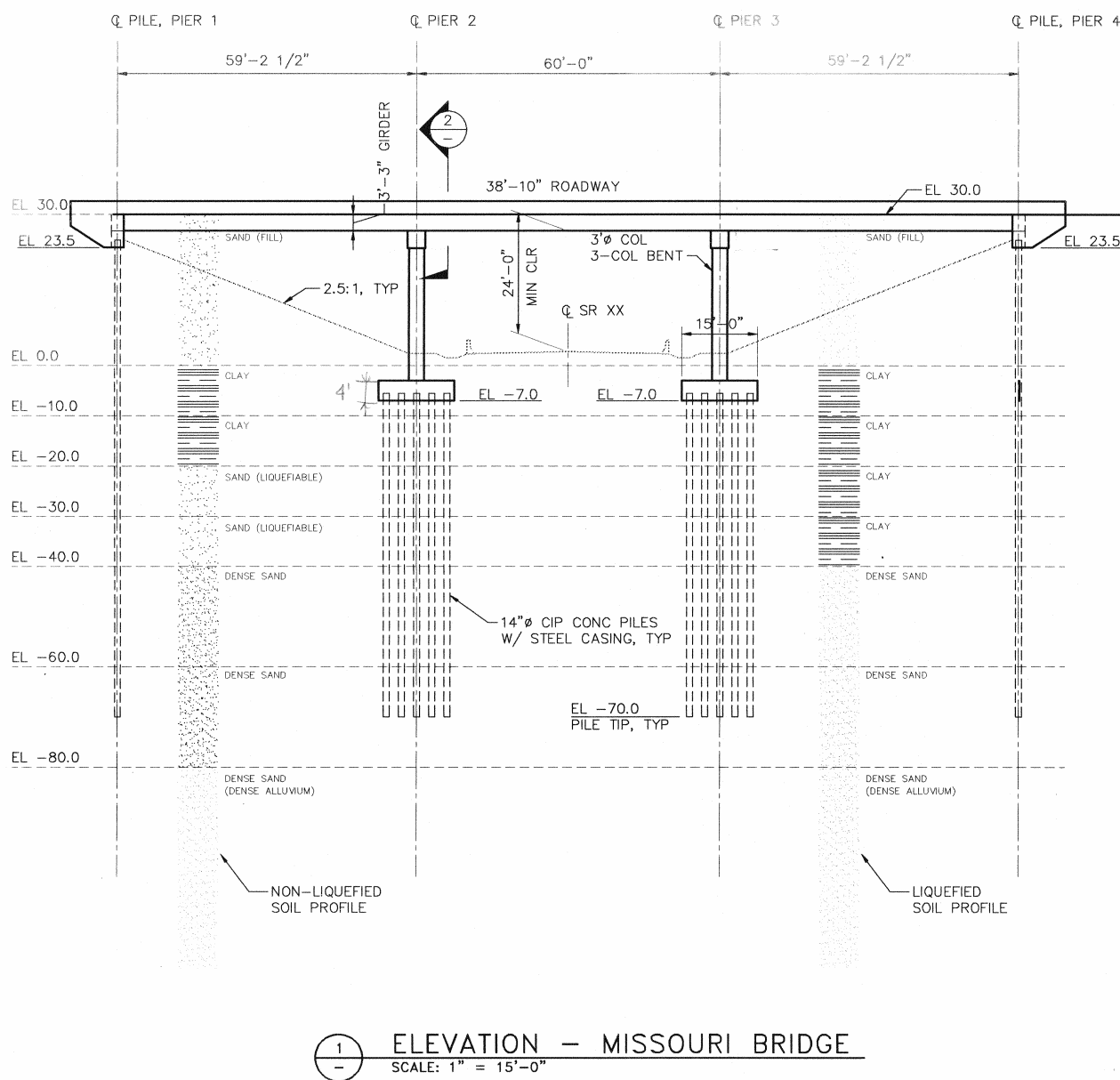


**Figure H-18 Elevation and Ground Profile for the Mid-America (Missouri) Bridge**

the ground motion hazard is dominated by magnitude 8 earthquakes occurring 30 to 80 km from the site. These earthquakes are associated with the New Madrid seismic zone. The range of distances from the New Madrid source reflects the modeling by USGS of the earthquake fault(s) within a relatively broad source zone, since the exact location of the fault(s) within the zone are not known.

The deaggregation results for the Missouri site differ from the results for the Washington site, where three different seismic source types and

magnitude and distance ranges contributed significantly to the ground motion hazard. For the Missouri site a single large magnitude source mechanism dominates the seismic hazard. Three natural recordings were selected from large magnitude earthquakes in Mexico, Chile and Japan to represent the time domain characteristics of the design earthquakes. These records were frequency scaled to be consistent with the design spectra for the site.

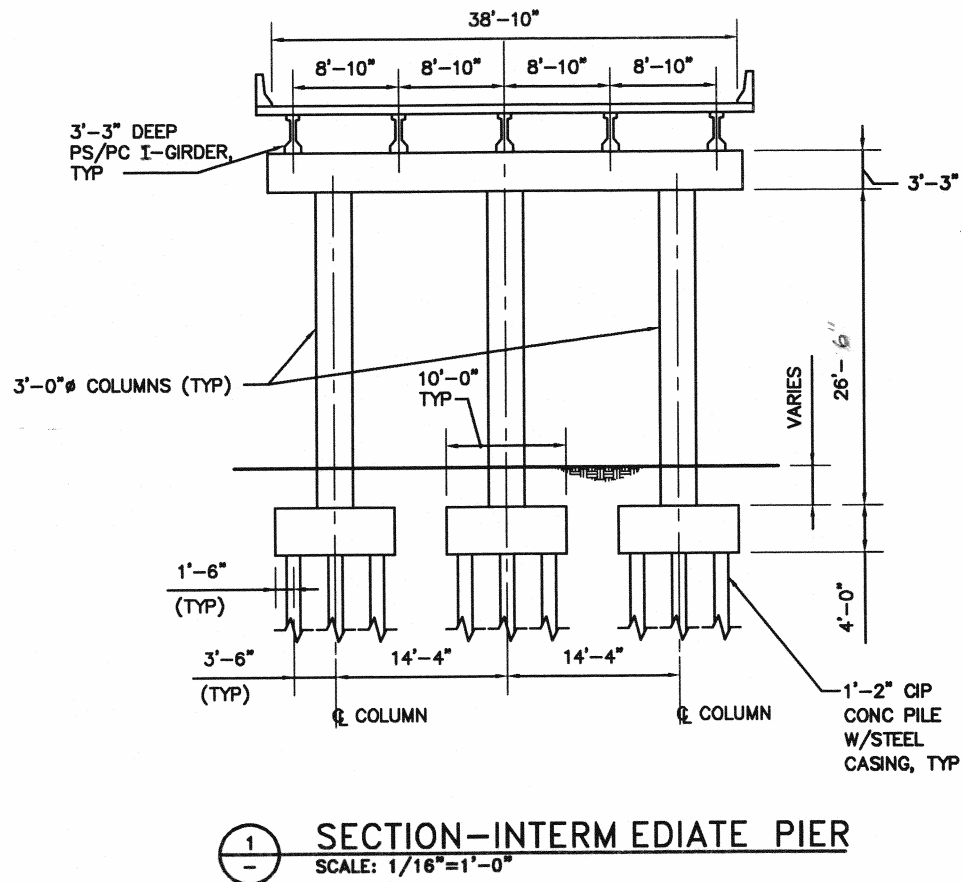


Figure H-19 Elevation of Intermediate Pier, Missouri Bridge

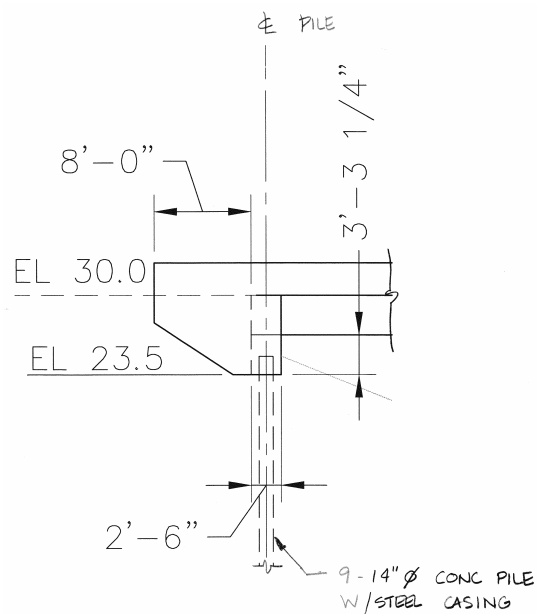


Figure H-20 Elevation of Integral Abutment, Missouri Bridge

### H.9.2 Liquefaction Analyses

The first step of the procedure outlined in Section D.4.2.2 is to determine if liquefaction occurs.

Simplified liquefaction analyses were conducted using the procedures given in Youd and Idriss (1997). Two levels of peak ground acceleration (PGA) were used, one representing the 475-year event within the current AASHTO *Specifications* and the other representing the recommended 2,475-year event. The PGA for the 475-year event was not adjusted for site effects, consistent with the approach recommended in the AASHTO *Specifications*<sup>8</sup>. Ground motions for the 2,475-year event were adjusted to Site Class D, using the procedures given in Section 3 of the recommended LRFD provisions (see companion Part I document). The resulting PGA values for each case are summarized below.

Input Parameter	475-Year Return Period	2,475-Year Return Period
Peak ground acceleration	0.17g	0.53g
Mean Magnitude	6.6	7.5

The magnitude of the design earthquake is required for the SPT and CPT simplified analyses. As discussed previously, results of deaggregation studies from the USGS database for deaggregation suggest that the mean magnitudes for the 475- and 2,475-year events are 6.6 and 7.5, respectively. The mean magnitudes reflect contributions from small to moderate magnitude earthquakes occurring closer to the site. However, the dominant event is the characteristic Magnitude-8 earthquake in the New Madrid seismic zone. For the simplified liquefaction assessment, a range of magnitudes thought to be representative of practice was used in the evaluation. For time history analyses, acceleration time histories representative of the duration of the Magnitude-8 New Madrid earthquake and the levels of ground motion defined by

<sup>8</sup> Common practice is to adjust the PGA for the site factors given in Table 2 of Division 1-A of the current AASHTO *Specifications*. While this adjustment may be intuitively correct, these site factors are not explicitly applied to the PGA. If the site coefficient were applied at the Missouri site, the PGA would be increased by a factor of 1.5, reducing the difference in the ground motions between the 475 year and the 2475 year return-period events.

the current AASHTO *Specifications* spectrum and the MCE spectrum of the recommended NCHRP 12-49 LRFD provisions were developed.

For these analyses ground water was assumed to occur 20 feet below the ground surface for the non-fill case.

Factors of safety (FOS) results from the liquefaction evaluations for the simplified soil model without fill for the three magnitudes are shown in Figure H-21 and Figure H-22 for the 475-year (10% PE in 50-year ground motion) and 2,475-year (3% PE in 75-year ground motion) return periods, respectively. These results indicate that liquefaction may or may not occur for the smaller (475 year return period) event, depending on the assumed magnitude of the earthquake. For the magnitude based on the mean of the deaggregation for the site, liquefaction is not predicted. For the 2,475-year return period event, liquefaction is predicted, regardless of the assumed magnitude.

Ground response analyses were also conducted using DESRA-MUSC, similar to those described in Section H.6.2. Results of these analyses are included in the companion *Liquefaction Study Report* (ATC/MCEER, 2003a). Based on the simplified liquefaction analyses and on the nonlinear effective stress modeling, it was concluded that lateral spread deformations would be distributed over the 20- to 40-foot depth. However, for analysis purposes, in order to compute likely displacement magnitudes of the overlying 20 feet of clay and embankment fill, it was assumed that ground accelerations, at the 40 feet interface depth, would control the displacement, assuming a Newark sliding block analogy.

### H.9.3 Initial Stability Analysis

The first step in the liquefaction evaluation involved an analysis of the post-earthquake stability. In this analysis stability was evaluated for the liquefied condition but without a seismic coefficient. This check was performed to determine if a flow failure would occur in the liquefied state. Results from these analyses show that the FOS dropped significantly when a residual strength was assigned to the liquefied layer; however, the FOS was greater than 1.0, indicating that a flow failure was not expected. This allowed displacements to be estimated using the simplified Newmark method described in Section H.9.2.

Yield accelerations were initially estimated without consideration of the pinning effects of

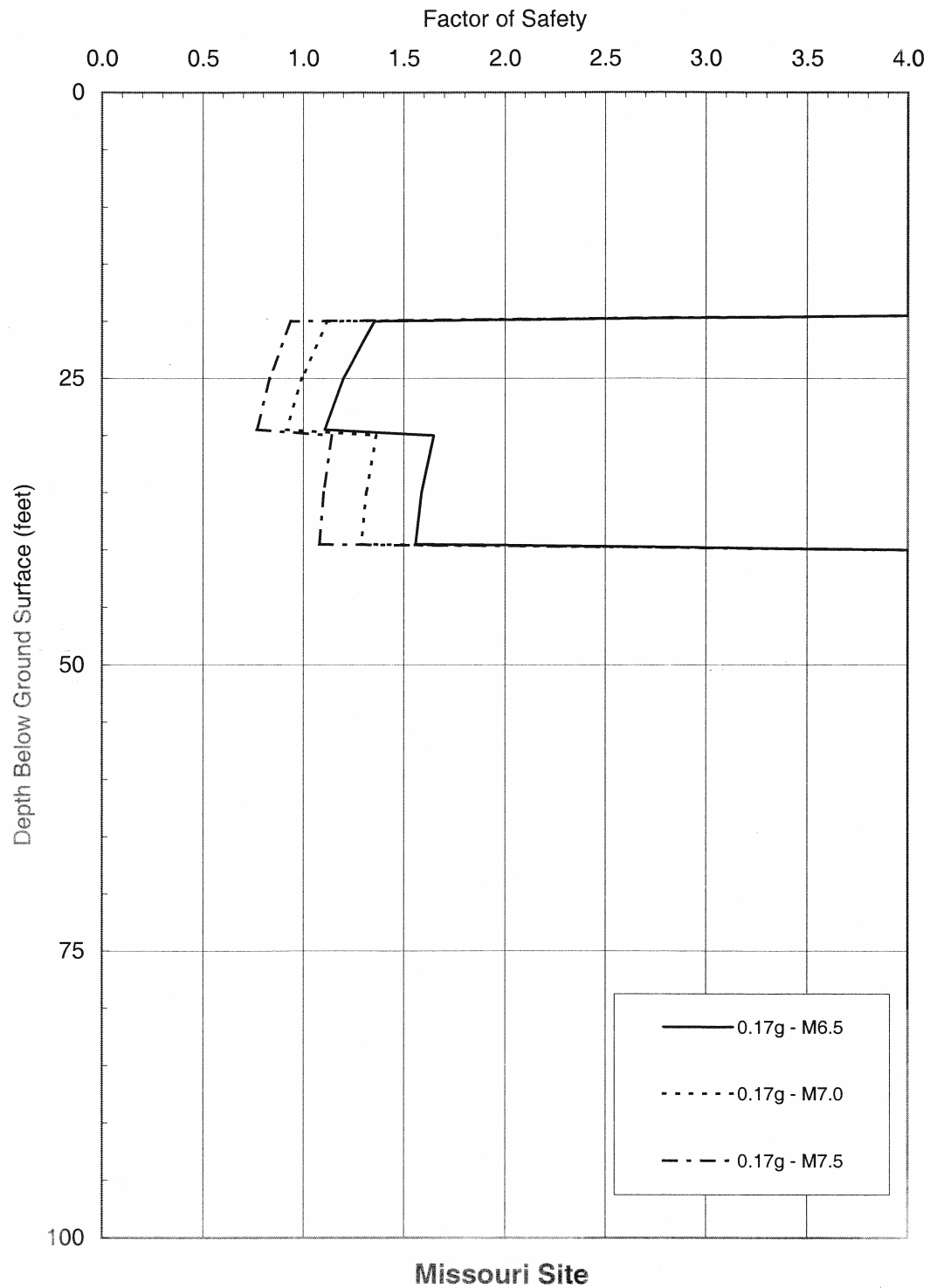


**Figure H-21** Liquefaction Potential – 475-Year Return Period (10% PE in 50-Year Ground Motion), Missouri Case Study.

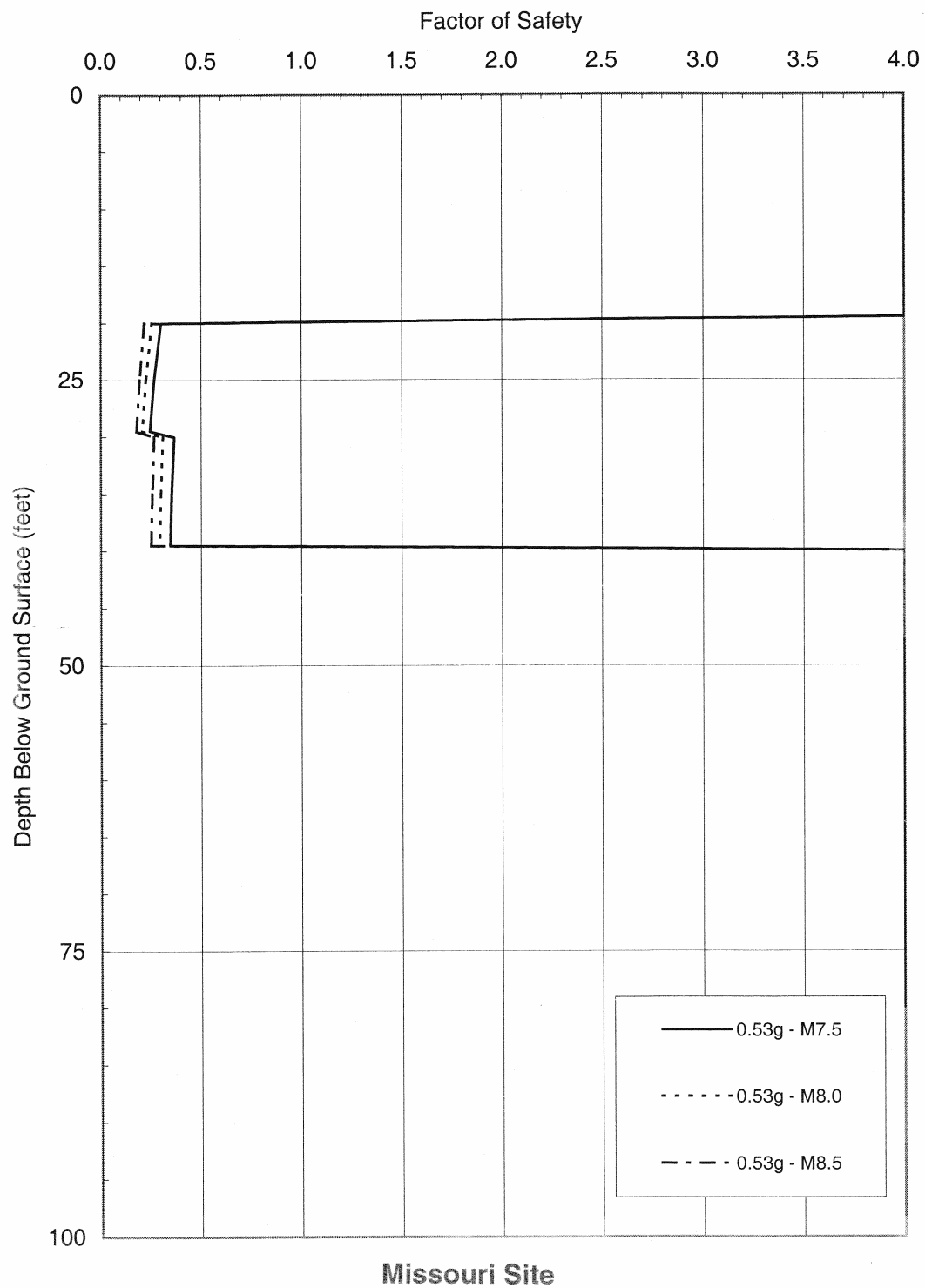


**Figure H-22** Liquefaction Potential – 2,475-Year Return Period (10% PE in 50-Year Ground Motion), Missouri Case Study.

piles by re-running the stability analyses for the liquefied soil profile, with different applied seismic coefficients. The yield acceleration from these analyses is the inertial force required to produce a FOS of 1 and was determined to be approximately 0.02. Displacements were estimated using the same methods and assumptions as presented for the Washington State site, except that the peak ground acceleration and the yield acceleration were those for the Missouri site. The displacements determined for the two return periods are summarized at the table below.

<b>Case: End Slope Displacements (inches)</b>			
<b>Franklin &amp; Chang</b>	<b>Hynes &amp; Franklin</b>	<b>Wong &amp; Whitman</b>	<b>Martin &amp; Qiu</b>
<b>475-Year Event (10% PE in 50-year ground motion):</b>			
>36	>10	5	5
<b>2,475-Year Event (3% PE in 75-year ground motion):</b>			
>36	28	32	32

In these analyses, methods proposed by Franklin and Chang (1977), Hynes and Franklin (1984), Wong and Whitman (1982), and Martin and Qiu (1994) were evaluated. The provisions recommend that mitigation decisions be based on the results from the Martin and Qiu simplified method, which give results of 5 inches and 32 inches for the 475-year (10% PE in 50-year ground motion) and 2,475-year (3% PE in 75-year ground motion) events, respectively. These displacements are large enough, particularly for the 2,475-year return period event, that some mitigation procedures would have to be considered. These mitigation methods could involve structural pinning or ground improvement as described in the next section.

As for the WSDOT site, analyses were also performed using the DISPMNT computer program in combination with DESRA-MUSC results. "Upslope" deformations were suppressed assuming a strong one directional driving force from the embankment. Strengths on the interface were degraded as a function of pore water pressure increases for the 35-40 foot layer, and reduced to the 300 psf residual strength when liquefaction was triggered. Results showing displacement time history plots for the 2,475-year return period Michoacan earthquake, as a function of yield acceleration, are shown in Figure H-23. The input ac-

celeration time histories used at a depth of 40 feet (70 feet with 30 feet of fill) are shown in Figure H-24. The time histories are very similar for the no fill and fill cases. Total accumulated displacements for all earthquake events are shown in Figure H-25, where it may be seen that the 2,475-year (3% PE in 75-year ground motion) events generated significantly larger displacements than the 475-year (10% PE in 50-year ground motion) events, at low values of yield acceleration. These displacements were used as a basis for discussion of remediation analyses, as described in Section H.9.4.

Similar displacement estimates to the simplified methods described above, may be made using the displacement versus yield acceleration curves shown in Figure H-25. The free field displacements without mitigation corresponding to a yield acceleration of 0.02 are summarized below.

<b>Case: End Slope Displacement (inches)</b>		
<b>Michoacan earthquake</b>	<b>Chile earthquake</b>	<b>Tokaji – Oki earthquake</b>
<b>475-year event (10% PE in 50-year ground motion):</b>		
21	21	16
<b>2,475 year event (3% PE in 75-year ground motion):</b>		
180	150	140

#### H.9.4 Stability Analyses with Mitigation Measures

Two procedures were evaluated for reducing the amount of displacement being predicted: structural pinning and ground improvement. For these analyses the additional resistance provided by the improved ground or by the structural pinning of the soil was incorporated into the stability analyses as described previously.

For the structural pinning evaluation, shear forces were calculated for two cases. In the first case, the shear failure occurred at the toe of the end slope in front of Pier 3 (Figure H-26). This gave an increase in resistance of 16 kips/foot for the 43-foot width of the abutment. Both pile pinning and abutment passive resistance are included in this reaction. This reaction occurs over the 35-foot abutment width, resulting in a resistance of 33 to 44 kips/foot of width. This reaction force was introduced into the slope stability analysis using

### Missouri Site : Michoacan EQ - 2475 Year Event

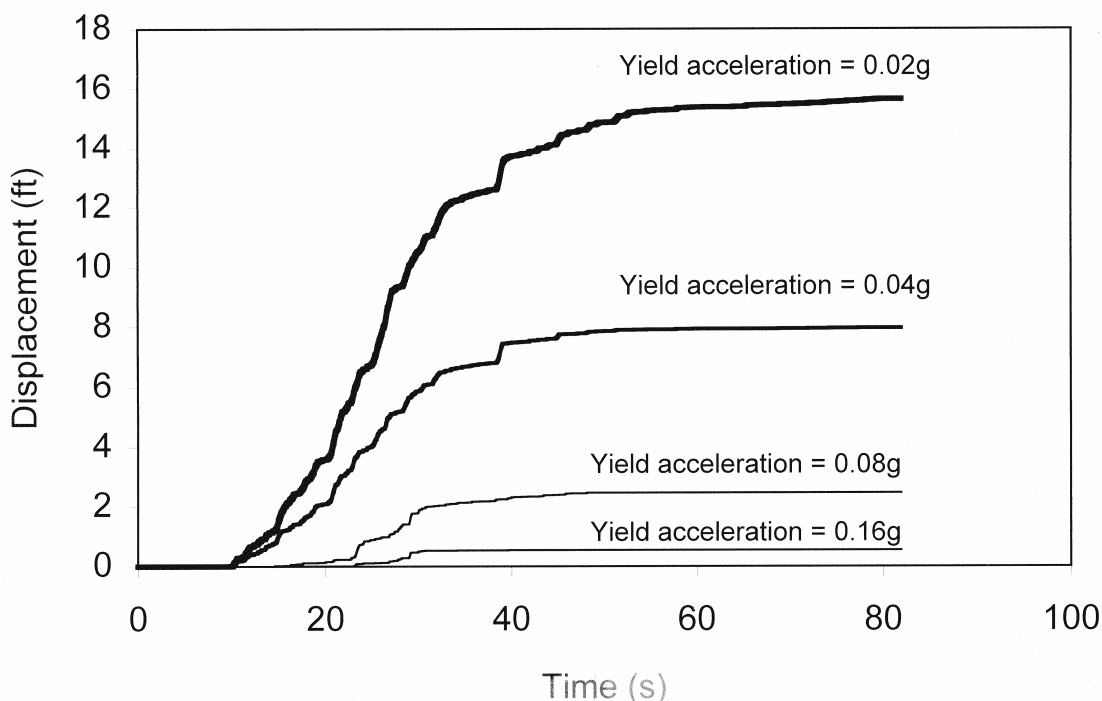


**Figure H-23 Displacement vs. Time for the Missouri Site Failure Surface**

the smearing method described for the Washington State study. For this method the resistance per unit width was converted into an equivalent shear strength along the shear plane in the liquefied zone, and this equivalent strength was added to the residual strength of 300 psf. For these analyses the failure plane was determined to be 90 feet in length, giving an added component to the liquefied strength of 180 psf. The resulting strength assigned to the liquefied layer was 480 psf (i.e., 180 psf + 300 psf = 480 psf).

For the second case, the shear failure was allowed to extend to the opposite embankment, as shown in Figure H-27. The pinning force for this case was 32 kips/foot, resulting in an additional 355 psf of smeared resistance. The resulting assigned strength for the layer was 655 psf (i.e., 355 psf + 300 psf = 655 psf).

Yield accelerations for both cases were determined by varying the seismic coefficient within the slope stability analysis until the factor of safety was 1.0. This analysis gave the following yield accelerations for the two cases.

Case	Yield Acceleration (g)
Toe Wedge	0.12
Deep Wedge	0.10

For the ground improvement case different widths of improved ground were used below the abutment. The improved ground extended through each of the liquefied zones. Soil in the improved ground was assigned a friction angle of 45 degrees. This increase in strength was assumed to be characteristic of stone columns or a similar improvement procedure. As with the ground improvement studies for the Washington State site, two procedures were used to represent the improved zone. One was to model it explicitly<sup>9</sup>; the second involved “smearing” the reaction from the improved strength zone across the failure surface by increasing the strength of the soil in the liquefied zone to give the same reaction. The resulting FOS was greater than 1.0 for all cases. This allowed yield accelerations to be computed as a

<sup>9</sup> The “explicit” case involved modeling the geometry of the correct width of improved ground in the computer. While fundamentally more correct, it is also time consuming to change the geometry of the problem for each width. The smearing technique involved a simple change in strength of the soil layer, which could be accomplished very quickly.



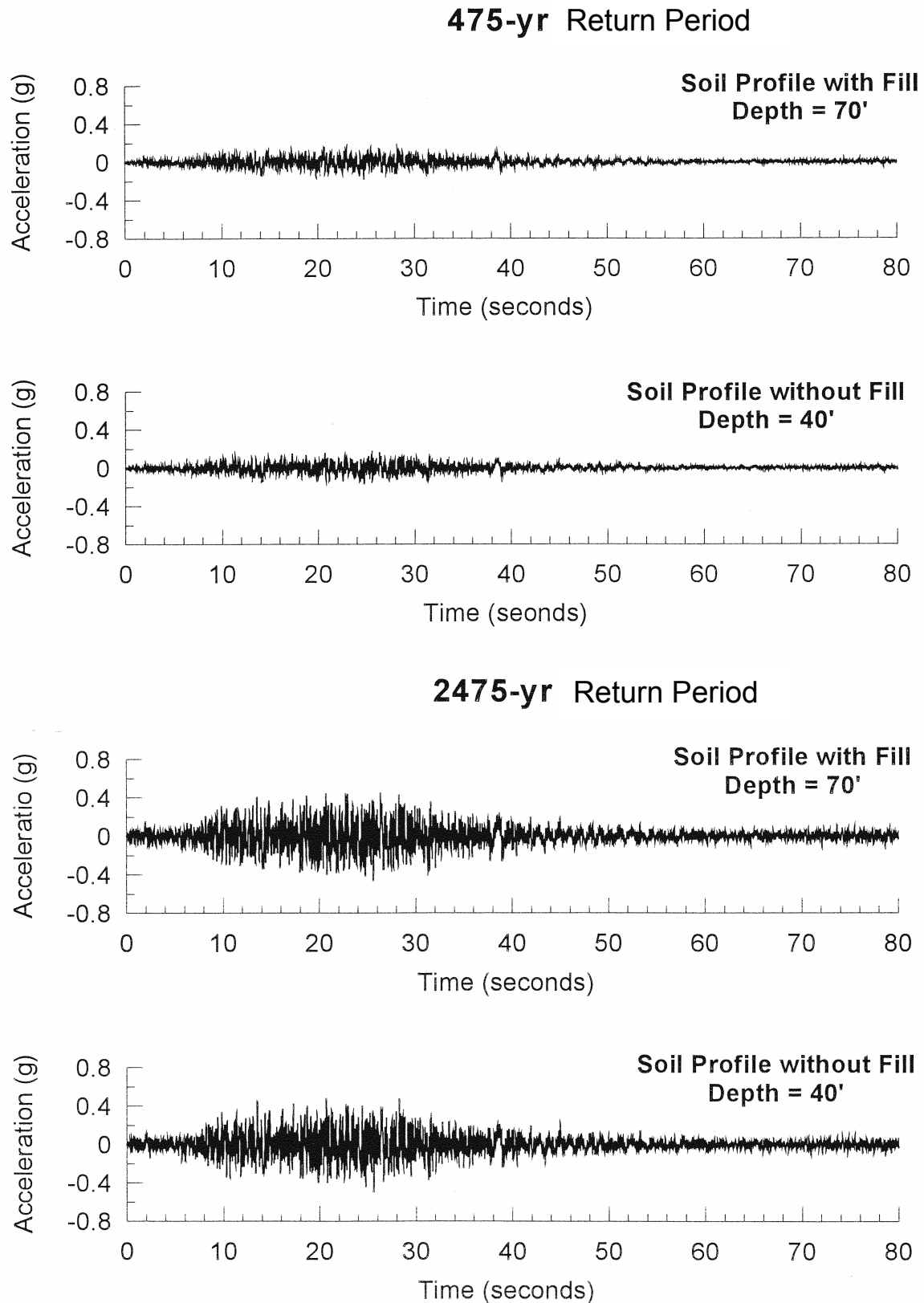


**Figure H-24** Input Acceleration History at Base of Liquefiable Layer, 1985 Michoacan Earthquake, Missouri Case Study

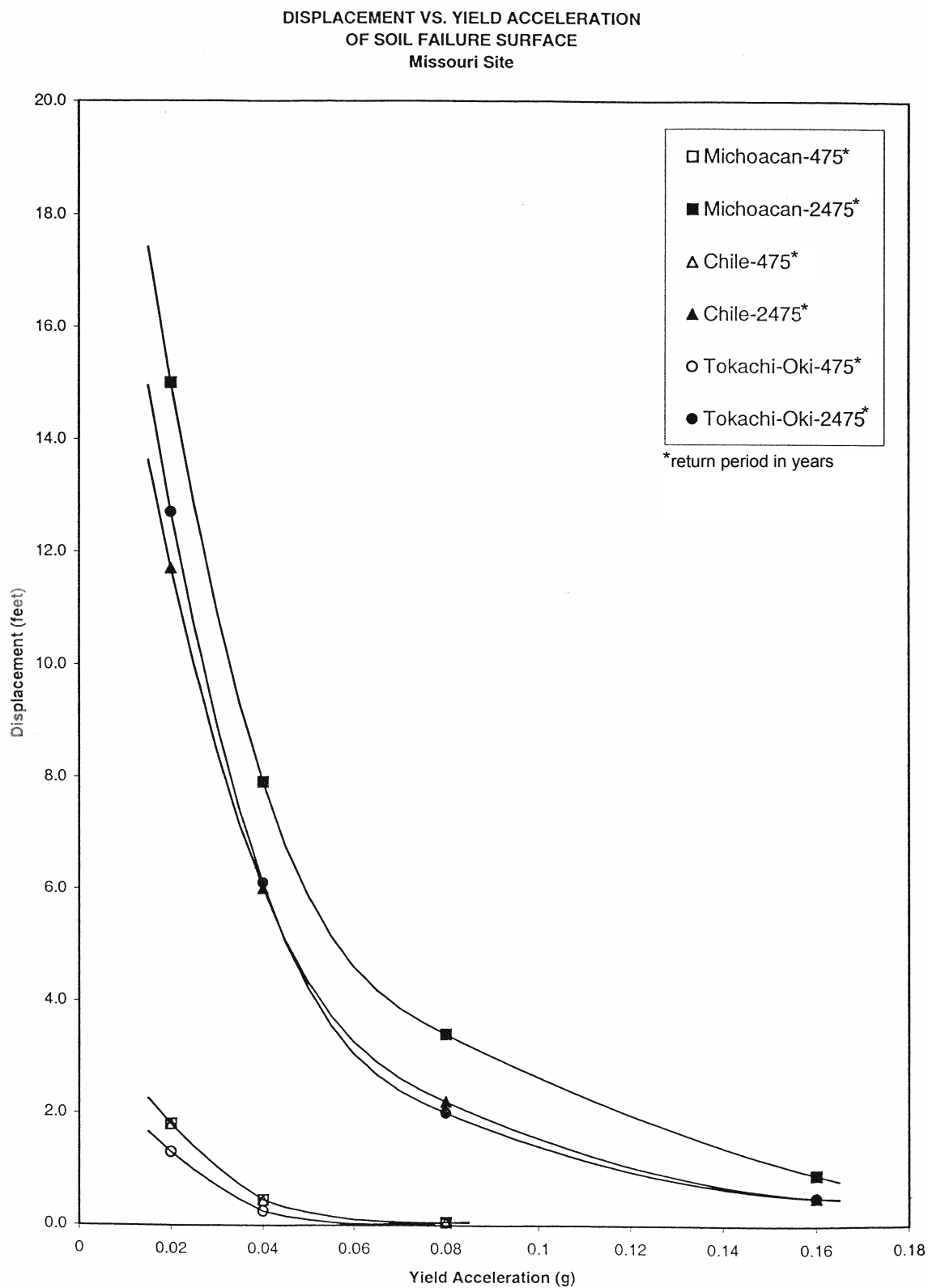


**Figure H-25 Displacement vs. Yield Acceleration of the Soil Failure Surface for the Missouri Site**

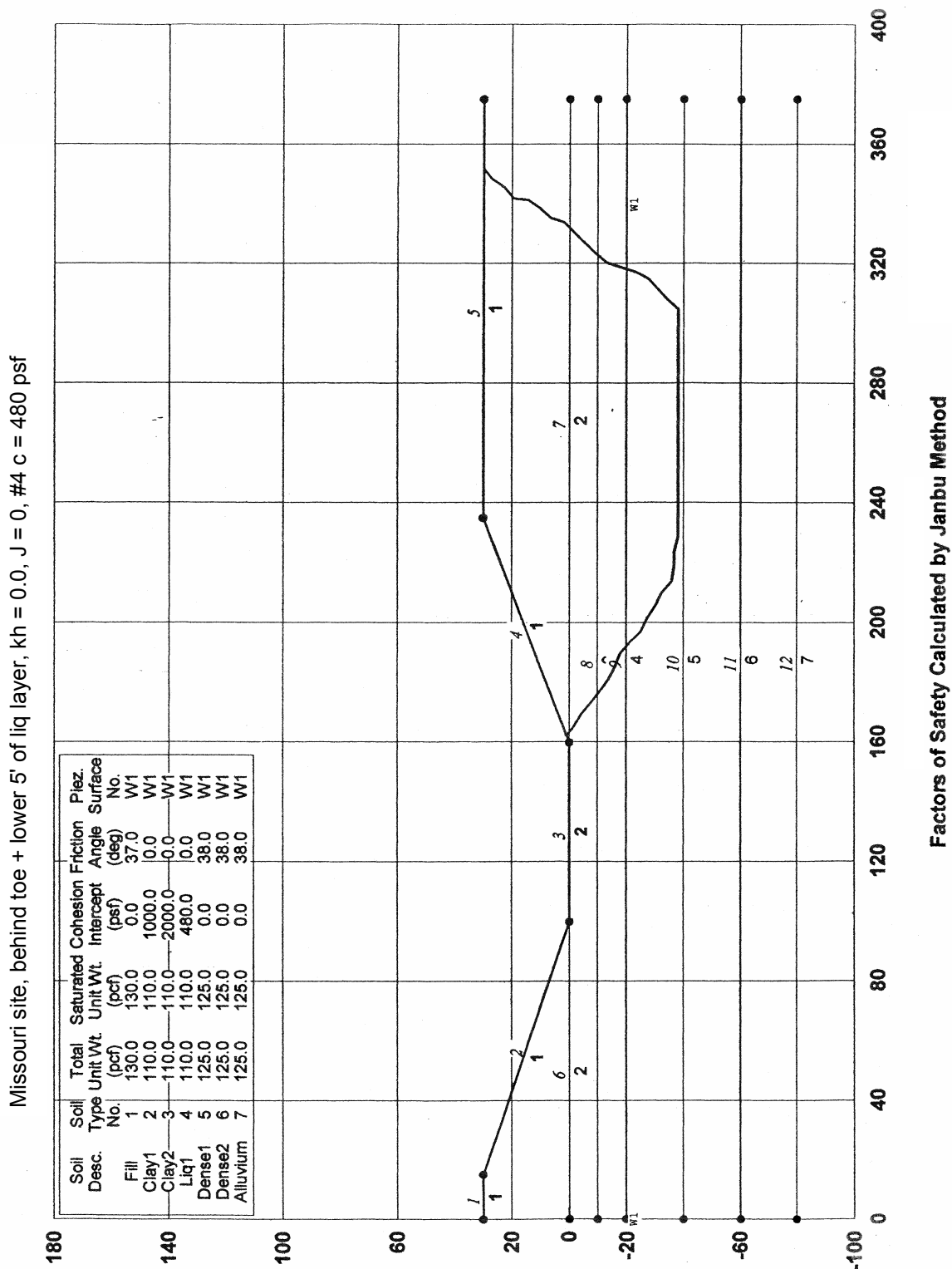


Figure H-26 Geometry of Toe Failure Wedge for Missouri Site

Missouri site, behind toe + lower 5' of liq layer,  $kh = 0.0$ ,  $J = 0$ ,  $a$  &  $p$  pin, #4c = 655

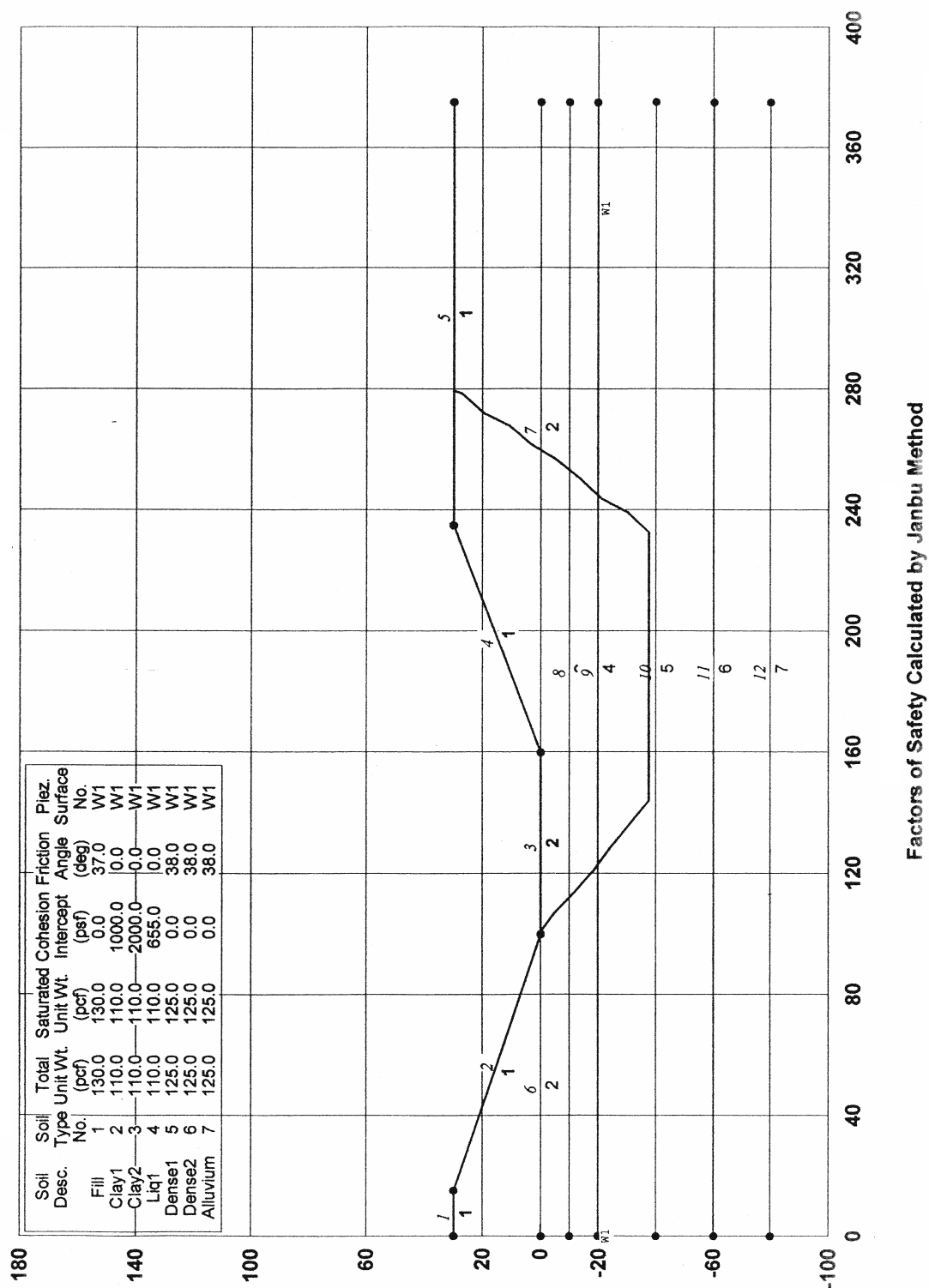


Figure H-27 Geometry of Deep Failure Wedge for Missouri Site

function of the width of the improved zone. These values are summarized as follows.

Width (feet)	Yield Acceleration (g)
10	0.18
30	0.33
50	0.53

### H.9.5 Displacement Estimates from Simplified Methods

Displacements were estimated for each of the yield accelerations given above. In these analyses methods recommended by Franklin and Chang (1977), Hynes and Franklin (1984), Wong and Whitman (1982), and Martin and Qiu (1994) were used. The same assumptions as made for the Washington state site were used during these analyses. The resulting displacements for the cases cited above are summarized in the following.

Displacements (inches)				
475-Year Event (10% PE in 50-year ground motion):				
Case	Franklin & Chang	Hynes & Franklin	Wong & Whitman	Martin & Qiu
1	<1	<4	<1	<1
2	<1	<4	<1	<1
3	<1	<4	<1	<1
4	<1	<4	<1	<1
5	<1	<4	<1	<1
2,475-Year Event (3% PE in 75-year ground motion):				
Case	Franklin & Chang	Hynes & Franklin	Wong & Whitman	Martin & Qiu
1	>36	<4	5	3
2	>36	5	8	5
3	8	<4	2	1
4	<1	<4	<1	1
5	<1	<4	<1	<1

Table notes:

- Case 1: Toe Wedge
- Case 2: Deep Wedge
- Case 3: Stone Columns – 10 ft
- Case 4: Stone Columns – 30 ft
- Case 5: Stone Columns – 50 ft

The estimates for the recommended Martin and Qiu method indicate that for the 475-year (10% PE in 50-year ground motion) event the displacements will be <1 inch for both the toe and deep wedge cases. For the 2,475-year (3% PE in 75-year ground motion) event, the toe wedge case gives 3 inches and the deep wedge 5 inches. Virtually any pinning or ground improvement method will limit displacements to less than about 0.5 feet for the 2,475-year (3% PE in 75-year ground motion) event. (Putting aside the F-C displacements, which are based on a limited database and also reflect an upper bound.)

Similar displacement estimates to the simplified methods described above, may be made using the displacement versus yield acceleration curves shown in Figure H-25. The free field displacements without mitigation corresponding to a yield acceleration of 0.02 are summarized in Section H.9.4.

For the pile pinning and ground remediation yield accelerations described in Section H.9.4, the displacement estimates are summarized in the following.

Displacements (inches):			
	Michoacan earthquake	Chile earthquake	Tokaji – Oki earthquake
475-Year Event (10% PE in 50-year ground motion):			
Case			
1	<1	<1	<1
2	<1	<1	<1
3	<1	<1	<1
4	<1	<1	<1
5	<1	<1	<1
2,475-Year Event (3% PE in 75-year ground motion):			
Case	Michoacan earthquake	Chile earthquake	Tokaji – Oki earthquake
1	24	12	12
2	30	18	18
3	6	4	4
4	<1	<1	<1
5	<1	<1	<1

Table notes:

- 1: Toe Wedge
- 2: Deep Wedge
- 3: Stone Column – 10 ft
- 4: Stone Column – 30 ft
- 5: Stone Column – 50 ft

For the 2,475 earthquake (3% PE in 75-year ground motion) events, the displacements tabulated above are in general less than the Franklin and Chang estimates, but higher than the Hynes and Franklin, the Wong & Whitman, and Martin and Qiu estimates.

### H.9.6 Pinning Force Calculations

As with the Washington State study, the soil movements will induce forces in the superstructure, if either the toe wedge or the deep soil wedge failure develops. The toe wedge only involves the abutment for pinning force, whereas the deep wedge involves both Pier 3 and the abutment. Additionally, the same potential failure modes exist for the left-hand end of the bridge, but since the bridge is symmetric the results for one end apply to the other.

Figure H-28 illustrates the pinning forces acting on the soil block comprising the toe wedge. In this case, the nine piles contribute 105 kips at the bottom of the slide, and they contribute 53 kips at the top. The top force is smaller than the bottom because the top is assumed to be a pinned condition. The location of the central plastic hinge is taken at mid-height of the soil column. The abutment backwall also contributes lateral force that resists the movement of the toe wedge, and that resistance is 520 kips, which is half that available typically. The reduction is taken to recognize the potential for slumping of the backfill due to movement of the toe wedge of soil.

These forces represent maximum values that only occur after significant plasticity develops. In the case of the piles, about 7 to 8 inches of lateral movement occurs at the center plastic hinge shown in the figure before full yield is attained. Subsequent to yielding the maximum deflection that can be tolerated with 0.05 radians of plastic drift is 18 inches. This is the maximum total structural deflection allowed for the toe wedge movement.

Figure H-29 shows the displaced shape when the deep wedge of soil moves. This involves the abutment piles and Pier 3. For the abutment the same resistances and allowable deformations apply as with the toe wedge failure addressed above. For Pier 3 the piles can develop 531 kips of resistance, based on plastic hinges forming  $5D$  above and below the liquefiable layer. This results in about 32 feet of length between plastic hinges in the piles. Additionally, the columns contribute

166 kips to the resistance. The bent was assumed to be connected to the superstructure with a pin connection. This is a reasonable bound for the common details used to connect girder superstructures, provided a full-depth diaphragm is used. The connection typically then behaves as a 'piano hinge'.

The allowable displacements for the deeper wedge failure are approximately 24 inches, which represents total displacement. Pier 3 develops yield at about 6 inches and then can tolerate roughly 18 inches of plastic deformation. However, because both the abutment piles and Pier 3 are moved by the deep wedge, the 18 inch total displacement allowed at the abutment controls. Therefore 18 inches is the allowable displacement.

In Section H.9.5 the estimated deformations for the 475-year (10% PE in 50-year ground motion) event are 7 inches for the deep wedge failure and 5 inches for the toe wedge failure. For the 2,475-year (3% PE in 75-year ground motion) event, including the pinning effect of the substructure, produces displacements of 11 and 14 inches for the toe and deep wedge failures, respectively. This is just in excess of the yield displacements for the piles, but is within their 18-inch plastic capacity, and is thus judged acceptable. This illustrates the potential beneficial effect of considering pinning.

The site-specific predictions of ground motion are given in Figure H-30, and at a yield acceleration of about  $0.1g$ , which applies for the pinning options, the average displacement of the three time histories is about 20 inches. In this case, the site-specific data produces displacements (due mainly to the Michoacan earthquake record) that exceed the simplified methods' predictions, but are close to the plastic capacity of the piles.

The conclusion is that if one wished to be conservative and use the results of the site-specific analysis and not risk displacements close to the capacity of the piles, then some remediation would be desirable to protect the substructure. However, if one used the simplified methods for estimating displacements, then the structure, as designed could withstand the 2,475-year (3% PE in 75-year ground motion) event and the liquefaction that it induces, and the piles would be just beyond their elastic capacity. This range in predicted displacements illustrates the uncertainty associated with the prediction of ground movements.

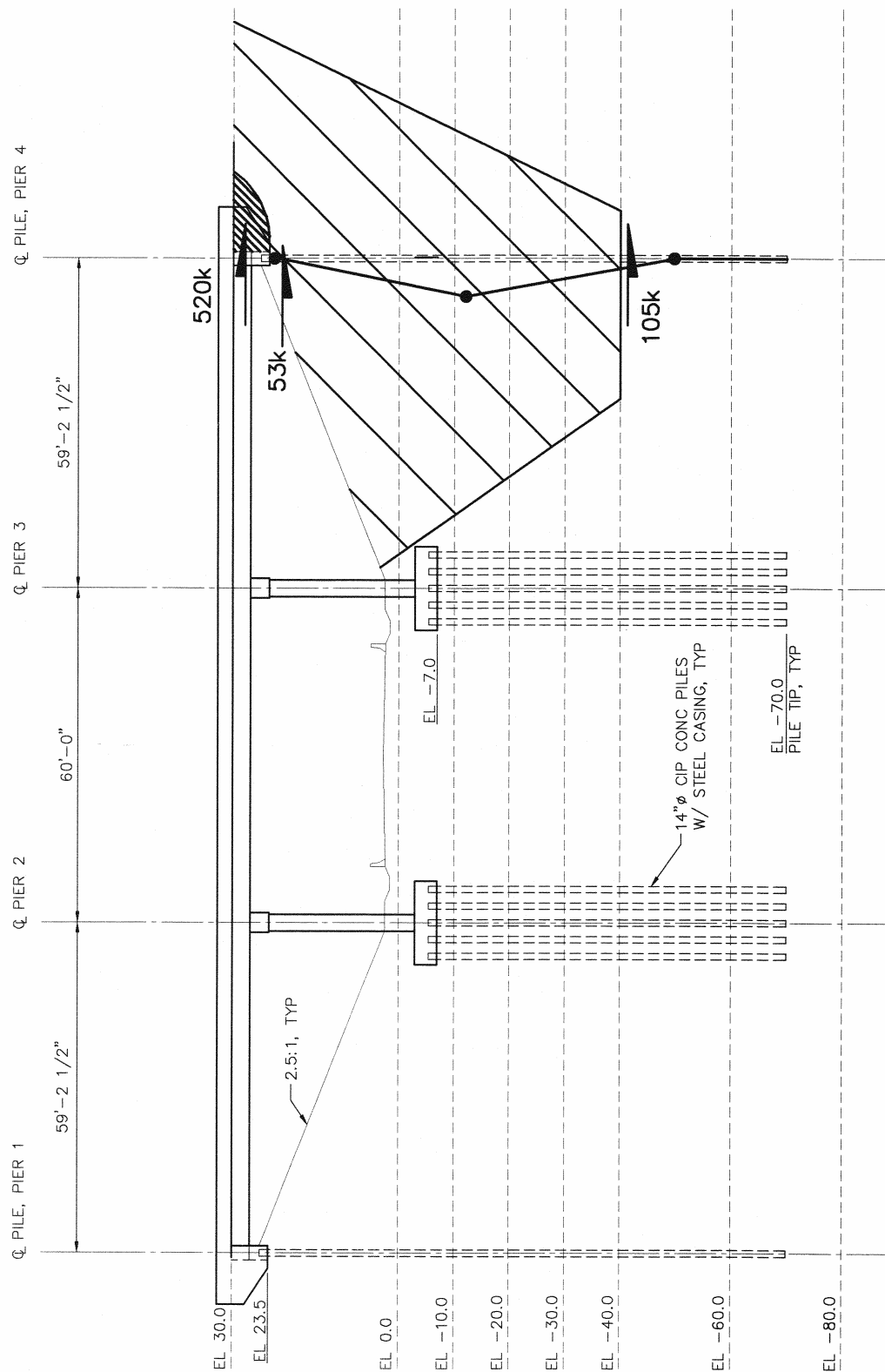


**Figure H-28** Pier 4 Structural Forces Resisting Lateral Spreading, Missouri Case Study

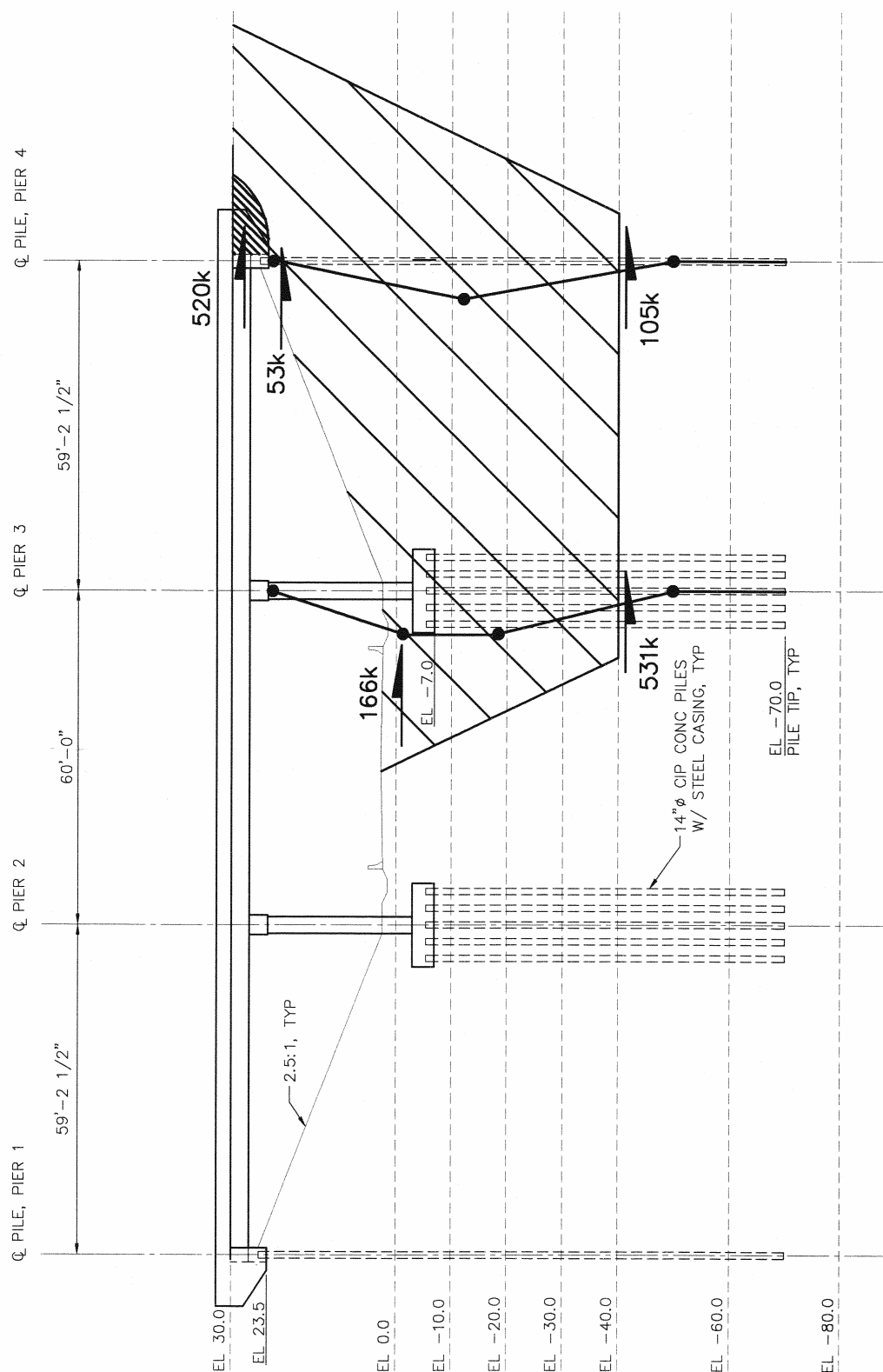
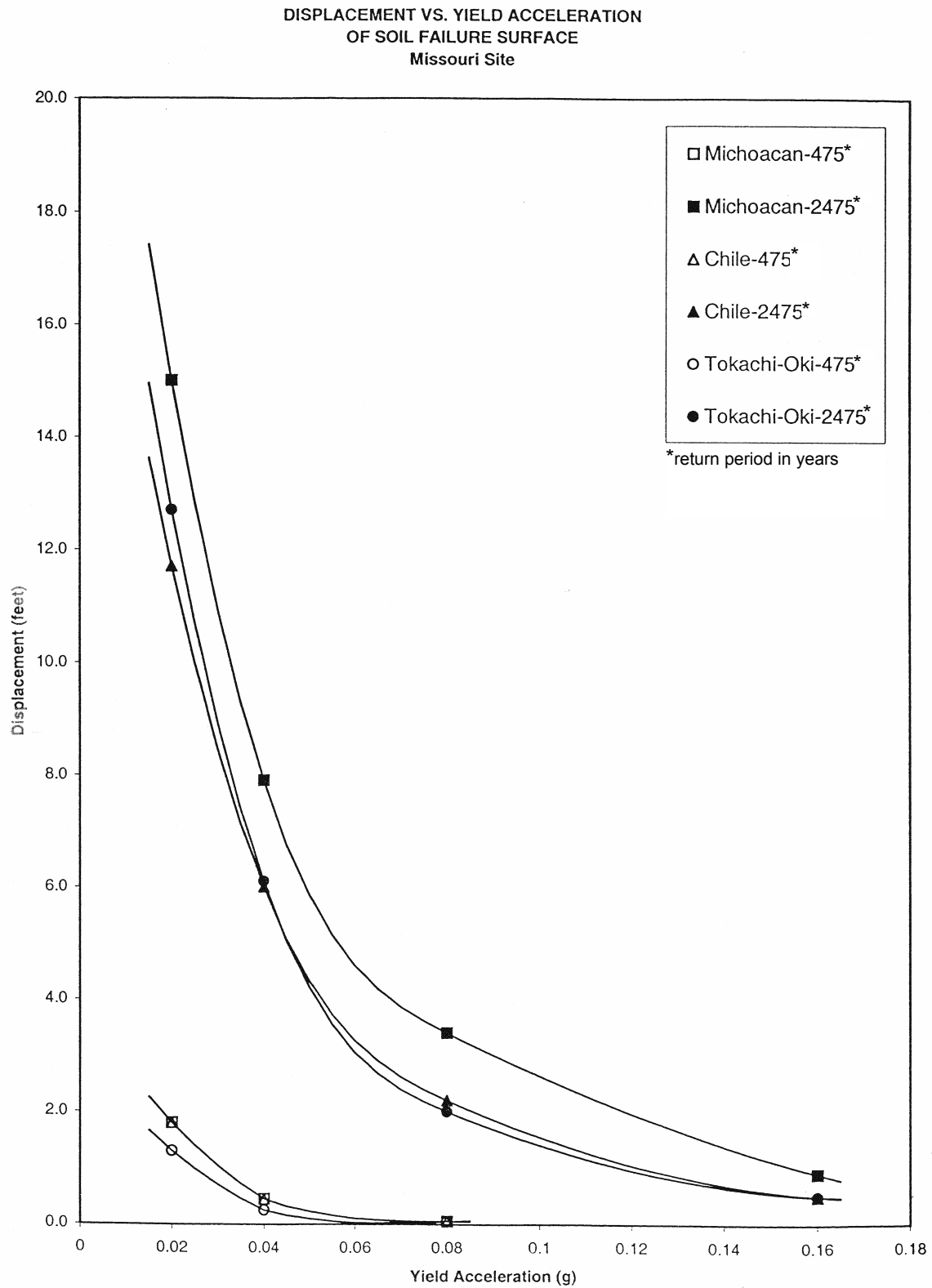


Figure H-29 Pier 3 and Pier 4 Structural Forces Resisting Lateral Spreading, Missouri Case Study





**Figure H-30 Displacement vs. Yield Acceleration of the Soil Failure Surface for the Missouri Site**

### H.9.7 Comparison of Remediation Alternatives

As with the study of the Washington bridge, the intent of the Missouri study was to assess the potential consequences of changing the AASHTO seismic design provisions. This comparison met the objectives by having little if any liquefaction under the 475-year (10% PE in 50-year ground motion) event and large amounts of liquefaction and associated ground movements during the 2,475-year (3% PE in 75-year ground motion) event. It is clear that the structure, as designed, is capable of resisting the lateral spreading associated with the liquefaction without the need for any additional expenditure of funds.

Because the estimated performance under the 2,475-year (3% PE in 75-year ground motion) event produces spreading displacements that will exceed the elastic capacity of the piles, it was worthwhile to investigate mitigation measures that would produce higher levels of performance, so that the piles can remain within their elastic capacity.

Stone columns can be used to limit the displacement of the toe and deep soil wedges. In Section H.9.5, 10-foot, 30-foot, and 50-foot wide buttresses of stone columns were considered. The calculated displacements were all less than about 4 inches for the 2,475-year (3% PE in 75-year ground motion) event when the stone columns were employed, and this provides the operational performance level for the foundations. This displacement ensures the piles remain within their yield displacement.

It is evident that mitigation, if it is deemed necessary to meet higher performance levels, is only required for the longer return period (2,475-year) ground motion. All the displacements for the 475-year (10% PE in 50-year ground motion) event, when pinning is considered, are acceptable.

If additional piles are considered for limiting the overall soil displacements, then the objective would likely be to install enough to reduce the estimated displacements down to values that would be tolerable for the substructure. This would likely require a large number of piles since the existing restraint at the superstructure level currently provides over 50% of the pinning resistance. Thus the inference is that if the deformations need to be limited beyond that which the foundation pinning alone can produce, then stone columns appears to be the rational choice.

There are no additional costs necessary in order to meet the life-safety performance requirements of the 2,475-year (3% PE in 75-year ground motion) event. In this example, spreading displacements of the order of less than 14 inches would be estimated, and these can be accommodated in the piles. If a higher level of performance is desired, such that the piles remain within their elastic limits and spreading displacements are desired to be less than 4 inches, then some remediation work is necessary for the 2,475-year (3% PE in 75-year ground motion) event.

The stone column option would likely only need to be applied over a 10-foot length (longitudinal direction of bridge), since that length produced acceptable deflections of 4 inches or less in the Newmark analysis. The width at a minimum would be 50 feet, and the depth also would be about 40 feet. If the columns were spaced roughly on 7-foot centers (the width would grow to 14 feet), then about 20 stone columns would be required. At approximately \$30 plf, the overall cost per abutment would be on the order of \$24,000 or about \$50,000 for both abutments.

As a rough estimate of the cost of the overall structure, based on square-footage costs of \$80 to \$100, the bridge would cost between about \$600,000 and \$800,000. Thus, the cost to install stone columns would run about 6 to 8% of the overall cost of the bridge. This expenditure would ensure the highest operational level of performance of the structure because foundation movements would be less than the yield level of the piles.

If pinch piles were used to augment the piles of the foundations, the piles would not need to be connected to the foundation, and they would not need to extend as deep as the load-bearing foundation piles. The per pile costs for the foundation piles were estimated to be on the order of \$2500 each for 70-foot long piles. If shorter piles on the order of 40-feet long were used, their costs would be roughly \$1500 each. Thus if pinch piles were used, about 15 piles per side could be installed for the same cost as the stone column remediation option. It is not likely that this number of piles would be as effective in limiting soil movement as the stone columns, although they would produce an acceptable level of performance. Therefore, the stone column option would appear the most cost effective in this situation.

## H.10 SUMMARY AND CONCLUSIONS

These recommendations apply when liquefaction at a site has been determined to be likely as a result of the 2,475-year (3% PE in 75-year ground motion) earthquake. The specific criteria are given in Section 3.10.5 of the recommended LRFD provisions (see *Part I*).

There are two phenomena that must be considered in the design of a bridge on a liquefiable site. The first is the traditional vibration design based effectively on the response spectra for the site. This corresponds to the design cases dealt with in Division I-A of the current AASHTO *Specifications*. The second phenomenon is lateral forces induced by flow sliding or lateral spreading if these potential consequences of liquefaction are predicted to occur. Flow sliding describes the condition where a soil mass is statically unstable after liquefaction-induced weakening of the soil occurs. Such an unstable condition can lead to quite large deformations. Lateral spreading describes deformations that progressively occur during ground shaking due to the combined static plus transient inertial forces exceeding the resistance of the liquefied soil. Deformations due to lateral spreading typically are smaller than those due to flow sliding.

For the Maximum Considered Earthquake (MCE) event, when the recommended performance objective is life-safety, inelastic deformation is allowed in the foundation for the lateral spreading or flow spreading case. Mitigation measures are able to achieve higher levels of performance when desired, so that piles remain within their elastic capacity. The vibration cases are designed, as they always are, for inelastic response above ground and at inspectable locations. It is believed that allowing some inelastic action in the presence of large spreading movements during the MCE event is necessary. Because spreading-induced deformations are ‘displacement-controlled’, instability of the system is unlikely even though some damage may exist in the foundations. The implication of this decision is that a bridge and its foundations may need to be replaced after a MCE event, but it avoids a significant expenditure of funds to prevent the displacement from occurring.

The design for vibration and lateral spreading is split into two independent activities, as coupling of the vibration load case and the spreading load case is not usually warranted. The vibration design is considered separately from the spreading design, because it is unlikely that the maximum

vibration effect and the maximum lateral spreading forces occur simultaneously. The de-coupled approach is considered reasonable with respect to the current state of the art.

The approach recommended is to determine the likely ground movements that may occur at the site, including the effects of altered site configurations such as fills and the beneficial effects of the pinning of piles. This prediction of lateral spreading can be made using either currently accepted simplified methods or site-specific analyses, as outlined in this report. As noted in the two cases studied, there can be a significant variation in the predicted displacements using the different methods, and this indicates that a designer must be aware that there can be a significant range in anticipated movements. Refined accuracy is not warranted. The beneficial resistance of the substructure should be included in the assessment of movements. The substructure is then assessed for the predicted movements, and if it can not tolerate the predicted displacements, then ground or structural remediation should be used.

It is important to recognize that the two case histories considered in this report are based on conditions whereby lateral spreading is parallel to the superstructure, which typically is one of the strong directions of the bridge. If the spreading effect is skewed with respect to the superstructure, then the skew must be accounted for in determining the likely plastic mechanism that will control.

The conclusions from this study of the effects of liquefaction when the design earthquake return period is increased from the existing AASHTO I-A 475-year return period (10% PE in 50-year ground motion) to 2,475-years (3% PE in 75-year ground motion) are summarized as follows.

- For both the Western (Washington State) and Mid-America (Missouri) examples there were no additional costs required to address the recommended liquefaction requirements when a bridge was designed for the current 475-year (10% PE in 50-year ground motion) earthquake and was then subjected to the 2,475-year (3% PE in 75-year ground motion) earthquake recommended in the LRFD provisions for the life-safety level of performance, despite significant increases in the PGA for the 2,475-year return period event.
- For the Western U.S. example, liquefaction occurred for the 475-year (10% PE in 50-year ground motion) event, and it was necessary to provide stone column mitigation measures in

the upper 30 feet or so. This would also most likely be necessary at both abutments (only one was studied in-depth in this effort). The cost for the stone columns at both abutments was estimated to be about 2.5% of the bridge cost. For the 2,475-year (3% PE in 75-year ground motion) event similar measures were required with the depth of the stone columns extended to 50 feet. The estimated cost of this remediation is of the order of 4% of the bridge cost.

- For the Mid-America example, liquefaction did not occur for the 475-year (10% PE in 50-year ground motion) event; however, the bridge was capable of meeting the liquefaction requirements for the recommended NCHRP 12-49 LRFD provisions for the 2,475-year (3% PE in 75-year ground motion) event, with liquefaction occurring at a depth of 20 to 40 feet, through pinning action of the piles. By allowing some inelastic deformations in the piles, no ground improvement was required.
- For the Mid-America and Western U.S. sites the higher operational level of performance can be achieved in the foundation system (i.e., piles remain in their elastic capacity) for the 2,475-year (3% PE in 75-year ground motion) event by improving the ground using stone columns. This improvement can be achieved for less than 5% additional cost in the case of the Western U.S. site and less than 10% additional cost in the case of the Mid-America site.

This study demonstrates the beneficial effects of considering the resistance that the substructure of the bridge offers to lateral movement of soil, ‘pinning’. These effects can be significant and should be considered in predictions of lateral soil movements. The study also shows the benefit of allowing inelastic behavior in the foundation under the action of lateral ground movement. For many cases relatively large displacements of the ground may be accommodated by the structure without collapse.

There has been considerable advancement in the state of the art in assessing impacts of liquefaction since the current AASHTO *Specifications* (Division I-A provisions) were developed. These have been included in the recommended LRFD provisions and used in the two case studies. They are relatively easy to use, and they permit a much better understanding of the effects of liquefaction

and lateral spreading. A summary of the new enhancements is as follows:

- A better ability to estimate the displacements that may occur as a result of lateral spreading. Currently, this is not always done in liquefaction studies.
- The ability to incorporate the beneficial effects of ‘pinning’ of the piles and ground movement in resisting lateral flow movements.
- The new information available from USGS on the deaggregation of the ground shaking hazard into the contributions of different seismic sources, earthquake magnitude, and distances for a particular site.
- The ability to perform nonlinear stress analysis time-history studies using realistic acceleration histories of ground motion to better understand the sequence of events that occur during liquefaction and the modification in ground motions that occur as a result.

As discussed in Section A.6 there were two global options that were considered for the development of these recommended LRFD provisions. The one that was adopted was to design explicitly for ground motions for a larger event (3% PE in 75 years) but refine the provisions to reduce the conservatism and gain a better understanding of what occurs in a larger event while attempting to keep the costs about the same as the current provisions. Under this scenario, the degree of protection against larger earthquakes is quantified and based on scientific principles and engineering experience. The other option which is the basis of the current AASHTO Division 1-A provisions is to design for a moderate sized event and maintain the current conservative provisions as a measure of protection against larger events. In this scenario the degree of protection is unknown and depends on intuition and engineering judgment. These examples demonstrate the benefits of the designing for and understanding what occurs in a larger event.

The implications of the new LRFD recommendations in going to a 2,475-year return period (3% PE in 75-year ground motion) event is that there is a greater area that now requires more detailed seismic design, including a liquefaction assessment. The specific details of when liquefaction should be considered are covered in Section 3.10.5 of the provisions, but in general, liquefaction is considered for bridges classified as SDR 3

or greater for a site that has a mean magnitude earthquake from deaggregation greater than 6.4. If the mean magnitude is less than 6.0, then liquefaction is not required to be considered. Between a mean magnitude of 6.0 and 6.4, liquefaction may or may not be required to be considered depending on the combinations of soil type and acceleration levels. Although liquefaction must be assessed in certain designs, the Mid-America example has demonstrated that a bridge may meet the recommended performance requirements of the new provisions without any additional expenditure of funds. It is difficult to draw wider implications from this study without additional study.

It should be recognized that the approach recommended here for large, infrequent earthquakes is a departure from the traditional approach of preventing damage in the foundation. For ground movements on the order of those expected, it is felt that often either remediation is necessary or

allowance of some inelastic action in foundation is necessary. It is recognized that only two specific examples were considered in this study, and that with time refinement will be possible as more structures are studied and designed. It is also recognized that the prediction of earthquake-induced ground movement is approximate at best, and much remains to be learned by the profession on how to produce more accurate predictions. Of all the issues, the greatest uncertainty lies in the methods of predicting ground displacements as seen in the variations of the simplified methods and the more precise nonlinear analyses. However, it is felt that the recommended approach is a reasonable beginning to rationally designing for such earthquake-induced hazards. The broader implications of these results deserve additional effort that was not part of this scope of work.



## Appendix I

### ISOLATION DESIGN PARAMETERS

#### I.1 SLIDING ISOLATION SYSTEMS

The  $\lambda$  factors on sliding systems are applied to  $Q_d$ .

##### I.1.1 Factors for Establishing $\lambda_{min}$

$$\lambda_{min} = 1.0$$

##### I.1.2 Factors for Establishing $\lambda_{max}$

###### I.1.2.1 $\lambda_{max,a}$

	Unlubricated PTFE		Lubricated PTFE		Bimetallic Interfaces	
Condition	Sealed	Unsealed	Sealed	Unsealed	Sealed	Unsealed
Environment						
Normal	1.1	1.2	1.3	1.4	2.0	2.2
Severe	1.2	1.5	1.4	1.8	2.2	2.5

**Notes:**

- Values are for 30-year exposure of stainless steel. For chrome-plated carbon steel, multiply values by 3.0.
- Unsealed conditions assumed to allow exposure to water and salt, thus promoting further corrosion.
- Severe environments include marine and industrial environments.
- Values for bimetallic interfaces apply for stainless steel and bronze interfaces.

###### I.1.2.2 $\lambda_{max,v}$

Established by test.

#### CI.1 SLIDING ISOLATION SYSTEMS

Woven PTFE shall be treated as unlubricated PTFE.

###### CI.1.2.1 $\lambda_{max,a}$

The aging factor is based on friction data for rough stainless steel plates with PTFE or other materials. It is assumed that the plate has uniform corrosion, which creates a rougher sliding surface.

For bimetallic interfaces, the factor is based on data for stainless steel and leaded bronze interfaces (Lee, 1993). Increases in friction due to stress effects have been observed in the absence of corrosion.

I.1.2.3  $\lambda_{\max,c}$ 

	Unlubricated PTFE	Lubricated PTFE	Bimetallic Interfaces
Sealed with stainless steel surface facing down	1.0	1.0	1.0
Sealed with stainless steel surface facing up*	1.1	1.1	1.1
Unsealed with stainless steel surface facing down	1.1	3.0	1.1
Unsealed with stainless steel surface facing up	Not Allowed	Not Allowed	Not Allowed

\* Use factor of 1.0 if bearing is galvanized or painted for 30-year lifetime.

CI.1.2.3  $\lambda_{\max,c}$ 

Values shown in the table assume that the sliding interface will not be separated.

Sealed bearings shall have a protective barrier to prevent contamination of the sliding interface. The protective barrier shall remain effective at all service load displacements.

I.1.2.4  $\lambda_{\max,tr}$ 

Cumulative Travel		Unlubricated PTFE*	Lubricated PTFE	Bimetallic Interfaces
ft	m			
<3300	1005	1.0	1.0	To be established by test
<6600	2010	1.2	1.0	To be established by test
>6600	2010	To be established by test	To be established by test	To be established by test

\* Test data based on 1/8-inch sheet, recessed by 1/16 inch and bonded.

I.1.2.5  $\lambda_{\max,t}$ 

Minimum Temp for Design		Unlubricated PTFE	Lubricated PTFE	Bimetallic Interfaces
°F	°C			
70	21	1.0	1.0	
32	0	1.1	1.3	
14	-10	1.2	1.5	
-22	-30	1.5	3.0	



**I.2 ELASTOMERIC BEARINGS**

The  $\lambda$  factors on elastomeric systems are applied to  $K_d$  and  $Q_d$ .

**I.2.1 Factors for Establishing  $\lambda_{min}$** 

$$\lambda_{min} = 1.0$$

**I.2.2 Factors for Establishing  $\lambda_{max}$** **I.2.2.1  $\lambda_{max,a}$** 

The aging factor depends significantly on the rubber compound. As a general rule, it is expected that this factor is close to unity for low-damping natural rubber and to be more for high-damping rubber.

**CI.2 ELASTOMERIC BEARINGS**

Elastomeric bearings are produced in a variety of compounds (particularly high-damping rubber bearings), so that a vast number of experiments are needed to establish the relevant  $\lambda$  factors.

Moreover, available data on the behavior of rubber bearings are limited to a small range of parameters, usually established for a particular application. Even in the case of lead-rubber bearings (which found wide application in bridges), data on the effect of temperature are scarce and include one bearing tested in New Zealand at temperatures of  $-31$ ,  $5$ ,  $64$ , and  $113^\circ\text{F}$  ( $-35$ ,  $-15$ ,  $18$ , and  $45^\circ\text{C}$ ); one tested in the United States (Kim et al., 1996) at temperatures of  $-18$  and  $68^\circ\text{F}$  ( $-28$  and  $20^\circ\text{C}$ ); and one in Japan tested at  $-4$  and  $68^\circ\text{F}$  ( $-20$  and  $20^\circ\text{C}$ ).

The factors listed herein are based on the available limited data. In some cases the factors could not be established and need to be determined by test.

It is assumed that elastomeric bearings are tested when unscragged at temperature of  $70^\circ\text{F} \pm 10^\circ\text{F}$  ( $21^\circ\text{C} \pm 5^\circ\text{C}$ ) to establish the relevant properties. Testing is performed at the design displacement and a frequency less than the inverse of period  $T_{eff}$ . The first cycle loop is used to establish the maximum value of effective stiffness ( $k_{max}$ ) and area under loop ( $A_{max}$ ). The minimum values (as a result of scragging) are established as the average of three cycles to be  $k_{min}$  and  $A_{min}$ .

It is also assumed here that scragging is a reversible phenomenon, that is, rubber recovers after some time its initial, unscragged properties. High-damping rubber bearings may exhibit significant difference between unscragged and scragged properties, although this difference depends entirely on the rubber compound.

**CI.2.2.1  $\lambda_{max,a}$** 

The relationship between aging and scragging was assumed in the table. However, such a relationship has not been verified by testing.

	<b>K<sub>d</sub></b>	<b>Q<sub>d</sub></b>
Low-Damping natural rubber	1.1	1.1
High-Damping rubber with small difference between scragged and unscragged properties	1.2	1.2
High-Damping rubber with large difference between scragged and unscragged properties	1.3	1.3
Lead	–	1.0
Neoprene	3.0	3.0

**Notes:**

- A large difference is one in which the unscragged properties are at least 25 percent more than the scragged ones.

**I.2.2.2  $\lambda_{\max,v}$** 

Established by test.

**I.2.2.3  $\lambda_{\max,c}$** 

$$\lambda_{\max,c} = 1$$

**I.2.2.4  $\lambda_{\max,tr}$** 

Established by test.

**I.2.2.5  $\lambda_{\max,t}$** **CI.2.2.5**

Values for lead-rubber bearings are based on grade 3 natural rubber.

<b>Minimum Temp for Design</b>		<b>Q<sub>d</sub></b>			<b>K<sub>d</sub></b>		
°F	°C	HDRB <sup>1</sup>	HDRB <sup>2</sup>	LDRB <sup>2</sup>	HDRB <sup>1</sup>	HDRB <sup>2</sup>	LDRB <sup>2</sup>
70	21	1.0	1.0	1.0	1.0	1.0	1.0
32	0	1.3	1.3	1.3	1.2	1.1	1.1
14	–10	1.4	1.4	1.4	1.4	1.2	1.1
–22	–30	2.5	2.0	1.5	2.0	1.4	1.3

HDRB = High-Damping Rubber Bearing

LDRB = Low-Damping Rubber Bearing

1. Large difference (at least 25%) between scragged and unscragged properties.
2. Small difference (<25%) between scragged and unscragged properties.

I.2.2.6  $\lambda_{\max, \text{scrag}}$ 

$Q_d$			$K_d$		
LDRB	HDRB with $\beta_{\text{eff}} - 0.15$	HDRB with $\beta_{\text{eff}} > 0.15$	LDRB	HDRB with $\beta_{\text{eff}} - 0.15$	HDRB with $\beta_{\text{eff}} > 0.15$
1.0	1.2	1.5	1.0	1.2	1.8



## REFERENCES AND ACRONYMS

### References Cited

- AASHTO, 1988, *Manual on Subsurface Investigations*, American Association of State Highway and Transportation Officials, Washington, D.C.
- AASHTO, 1996, *Standard Specifications for Highway Bridges*, 16th Edition, American Association of State Highway and Transportation Officials, Washington, D.C.
- AASHTO, 1998, *LRFD Bridge Design Specifications*, 2nd Edition, American Association of State Highway and Transportation Officials, Washington, D.C.
- AASHTO, 1999, *Guide Specifications for Seismic Isolation Design*, 2<sup>nd</sup> Edition, American Association of State Highway and Transportation Officials, Washington, D.C.
- AASHTO, 2001, *A Policy on Geometric Design of Highways and Streets*, (otherwise known as the "Green Book"), American Association of State Highway and Transportation Officials, Washington, D.C.
- Abrahamson, N., A., and Silva, W. J., "Empirical Response Spectral Attenuation Relations for Shallow Crustal Earthquakes," *Seismological Research Letters*, Vol. 68, No. 1, pages 94-127.
- AISC, 1992, *Code of Standard Practice for Steel Buildings and Bridges*, American Institute of Steel Construction, Chicago, Illinois.
- AISC, 1993, *Load and Resistance Factor Design Specification for Structural Steel Buildings*, American Institute of Steel Construction, Chicago, Illinois.
- AISC, 1997, *Seismic Provisions for Structural Steel Buildings*, American Institute of Steel Construction, Chicago, Illinois.
- Alfawahkiri, F., 1997, *Cyclic Testing of Concrete-Filled Circular Tubes*, Thesis presented in partial fulfillment for the degree of Master of Applied Sciences, Dept. of Civil Engineering, University of Ottawa, Ottawa, Ontario, Canada.
- Andrus, R., and Youd, T., 1987, *Subsurface investigation of a Liquefaction-Induced Lateral Spread, Thousand Springs Valley, Idaho*, Paper GL-87-8, U.S. Army Engineer Waterways Experiment Station, Vicksburg, Mississippi.
- Arulanandan, K. and Zeng, X., 1994, "Mechanism of Flow Slide-Experimental Results of Model No. 6," *Verification of Numerical Procedures for the Analysis of Soil Liquefaction Problems, Proceedings of International Conference*, Arulanandan and Scott (eds.), Davis, California, Vol. 2, A. A. Balkema, Rotterdam, The Netherlands, pp. 1543-1551.
- ASCE, 1996, *ASCE Standard for Testing Seismic Isolation Systems, Units and Components*, Draft C, ASCE Standards Committee on Testing of Base Isolation Systems, American Society of Civil Engineers, Reston, Virginia.
- ASCE, 2000, *Prestandard and Commentary for the Seismic Rehabilitation of Buildings*, prepared by the American Society of Civil Engineers for the Federal Emergency Management Agency (FEMA 356 Report), Washington, D.C.
- ASCE CERF, 1996, *Guidelines for the Testing of Seismic Isolation and Energy Dissipation Devices*, CERF Report: HITEC 96-02, American Society of Civil Engineering, Civil Engineering Research Foundation, Highway Innovative Technology Evaluation Center, Washington, D.C.
- Astaneh-Asl, A., Goel, S.C., and Hanson, R.D., 1982, *Cyclic Behavior of Double Angle Bracing Members With End Gusset Plates*, Report No.UMEE 82R7, Department of Civil Engineering, University of Michigan. Ann Arbor, Michigan.
- Astaneh-Asl, A., and Roberts, J., 1996. *Proceedings of the 2nd US Seminar on Seismic Evaluation and Retrofit of Steel Bridges*, San Francisco, Report No. UCB/CEE-Steel-96/09, Department of Civil

- and Environmental Engineering, University of California at Berkeley.
- Astaneh-Asl, A., Shen, J. H., and Cho, S. W., 1993, "Seismic Performance and Design Consideration in Steel Bridges", *Proceedings of the 1st US Seminar on Seismic Evaluation and Retrofit of Steel Bridges*, San Francisco, California.
- Astaneh-Asl, A., Bolt, B., McMullin, K. M., Donikian, R. R., Modjtahedi, D., and Cho, S. W., 1994, *Seismic Performance of Steel Bridges During the 1994 Northridge Earthquake*, UCB report CE-STEEL 94/01, University of California at Berkeley.
- ASTM, 1984, *Standard Test Method for Penetration Test and Split-Barrel Sampling of Soils*, Report No. ASTM D1586, American Society for Testing and Materials, West Conshohocken, Pennsylvania.
- ASTM, 1987, *Standard Test Method for Unconsolidated, Undrained Compressive Strength of Cohesive Soils in Triaxial Compression*, Report No. ASTM D2850, American Society for Testing and Materials, West Conshohocken, Pennsylvania.
- ASTM, 1991, *Standard Test Method for Unconfined Compressive Strength of Cohesive Soil*, Report No. ASTM D2166, American Society for Testing and Materials, West Conshohocken, Pennsylvania.
- ASTM, 1993, *Standard Test Methods for Liquid Limit, Plastic Limit, and Plasticity Index of Soils*, Report No. ASTM D4318, American Society for Testing and Materials, West Conshohocken, Pennsylvania.
- ASTM, 1994, *Standard Test Method for Bearing Capacity of Soil for Static Load and Spread Footings* (Withdrawn 2003), Report No. ASTM D1194, American Society for Testing and Materials, West Conshohocken, Pennsylvania.
- ASTM, 1995, *Standard Test Method for Triaxial Compressive Strength of Undrained Rock Core Specimens Without Pore Pressure Measurements*, Report No. ASTM D2664, American Society for Testing and Materials, West Conshohocken, Pennsylvania.
- ASTM, 1997, *Standard Test Method for In Situ Stress and Modulus of Deformation Using the Flatjack Method*, Report No. ASTM D4729, American Society for Testing and Materials, West Conshohocken, Pennsylvania.
- ASTM, 1998a, *Standard Test Method for Mechanical Cone Penetration Tests of Soil*, Report No. ASTM D3441, American Society for Testing and Materials, West Conshohocken, Pennsylvania.
- ASTM, 1998b, *Standard Test Method for Determining the In Situ Modulus of Deformation of Rock Mass Using the Rigid Plate Loading Method*, Report No. ASTM D4394, American Society for Testing and Materials, West Conshohocken, Pennsylvania.
- ASTM, 1998c, *Standard Test Method for One-Dimensional Consolidation Properties of Soils Using Controlled-Strain Loading*, Report No. ASTM D4186, American Society for Testing and Materials, West Conshohocken, Pennsylvania.
- ASTM, 2000a, *Standard Test Method for Determination of Water (Moisture) Content of Soil by the Microwave Oven Method*, Report No. ASTM D4643, American Society for Testing and Materials, West Conshohocken, Pennsylvania.
- ASTM, 2000b, *Standard Test Method for Prebored Pressuremeter Testing in Soils*, Report No. ASTM D4719, American Society for Testing and Materials, West Conshohocken, Pennsylvania.
- ASTM, 2000c, *Standard Test Method for Permeability of Granular Soils (Constant Head)*, Report No. ASTM D2434, American Society for Testing and Materials, West Conshohocken, Pennsylvania.
- ASTM, 2000d, *Standard Test Methods for Laboratory Compaction Characteristics of Soil Using Standard Effort (12,400 ft-lbf/ft<sup>3</sup> (600 kN-m/m<sup>3</sup>))*, Report No. ASTM D698, American Society for Testing and Materials, West Conshohocken, Pennsylvania.
- ASTM, 2000e, *Standard Classification of Soils for Engineering Purposes (Unified Soil Classification System)*, Report No. ASTM D2487, American Society for Testing and Materials, West Conshohocken, Pennsylvania.
- ASTM, 2000f, *Standard Practice for Description and Identification of Soils (Visual-Manual*

- Procedure*), Report No. ASTM D2488, American Society for Testing and Materials, West Conshohocken, Pennsylvania.
- ASTM, 2001a, *Standard Test Method for Splitting Tensile Strength of Intact Rock Core Specimens*, Report No. ASTM D3967, American Society for Testing and Materials, West Conshohocken, Pennsylvania.
- ASTM, 2001b, *Standard Test Method for Field Vane Shear Test in Cohesive Soil*, Report No. ASTM D2573, American Society for Testing and Materials, West Conshohocken, Pennsylvania.
- ASTM, 2001c, *Standard Test Method for Determining Deformability and Strength of Weak Rock by an In Situ Uniaxial Compressive Test*, Report No. ASTM D4555, American Society for Testing and Materials, West Conshohocken, Pennsylvania.
- ASTM, 2002a, *Standard Test Method for Elastic Moduli of Intact Rock Core Specimens in Uniaxial Compression*, Report No. ASTM D3148, American Society for Testing and Materials, West Conshohocken, Pennsylvania.
- ASTM, 2002b, *Standard Test Method for Unconfined Compressive Strength of Intact Rock Core Specimens*, Report No. ASTM D2938, American Society for Testing and Materials, West Conshohocken, Pennsylvania.
- ASTM, 2002c, *Standard Test Method for Particle-Size Analysis of Soils*, Report No. ASTM D422, American Society for Testing and Materials, West Conshohocken, Pennsylvania.
- ASTM, 2002d, *Standard Test Methods for Specific Gravity of Soil Solids by Water Pycnometer*, Report No. ASTM D854, American Society for Testing and Materials, West Conshohocken, Pennsylvania.
- ASTM, 2002e, *Standard Test Methods for Laboratory Compaction Characteristics of Soil Using Modified Effort (56,000 ft-lbf/ft<sup>3</sup> (2,700 kN-m/m<sup>3</sup>))*, Report No. ASTM D1557, American Society for Testing and Materials, West Conshohocken, Pennsylvania.
- ASTM, 2002f, *Standard Test Method for Determining the In Situ Modulus of Deformation of Rock Mass Using a Radial Jacking Test*, Report No. ASTM D4506, American Society for Testing and Materials, West Conshohocken, Pennsylvania.
- ASTM, 2002g, *Standard Test Method for Consolidated Undrained Triaxial Compression Test for Cohesive Soils*, Report No. ASTM D4767, American Society for Testing and Materials, West Conshohocken, Pennsylvania.
- ASTM, 2002h, *Standard Test Method for In Situ Determination of Direct Shear Strength of Rock Discontinuities*, Report No. ASTM D4554, American Society for Testing and Materials, West Conshohocken, Pennsylvania.
- ASTM, 2003a, *Standard Specification for Chromium and Chromium-Nickel Stainless Steel Plate, Sheet, and Strip for Pressure Vessels and for General Applications*, Report No. ASTM A240, American Society for Testing and Materials, West Conshohocken, Pennsylvania.
- ASTM, 2003b, *Standard Test Method for One-Dimensional Consolidation Properties of Soil*, Report No. ASTM D2435, American Society for Testing and Materials, West Conshohocken, Pennsylvania.
- ASTM, 2003c, *Standard Test Method for Direct Shear Test of Soils Under Consolidated Drained Conditions*, Report No. ASTM D3080, American Society for Testing and Materials, West Conshohocken, Pennsylvania.
- ASTM, 2003d, *Standard Test Method for Direct Shear Test of Soils Under Consolidated Drained Conditions*, Report No. ASTM D3080, American Society for Testing and Materials, West Conshohocken, Pennsylvania.
- ASTM, 2003e, *Standard Specification for Plain and Steel-Laminated Elastomeric Bearings for Bridges*, Report No. ASTM D4014, American Society for Testing and Materials, West Conshohocken, Pennsylvania.
- ASTM, 2004, *Standard Test Method for Determining the In Situ Modulus of Deformation of Rock Mass Using the Flexible Plate Loading Method*, Report No. ASTM D4395, American Society for Testing and Materials, West Conshohocken, Pennsylvania.
- ATC, 1981, *Seismic Design Guidelines for Highway Bridges*, ATC-6 Report, Applied

- Technology Council, Redwood City, California.
- ATC, 1986, *Proceedings of a Seminar and Workshop on Base Isolation and Passive Energy Dissipation*, ATC-17 Report, Applied Technology Council, Redwood City, California.
- ATC, 1993, *Proceedings of Seminar on Seismic Isolation, Passive Energy Dissipation, and Active Control*, ATC-17-1 Report, Applied Technology Council, Redwood City, California.
- ATC, 1996, *Improved Seismic Design Criteria for California Bridges: Provisional Recommendations*, ATC-32 Report, Applied Technology Council, Redwood City, California.
- ATC, 1997, *Seismic Design Criteria for Bridges and Other Highway Structures: Current and Future*, ATC-18 Report, Applied Technology Council, Redwood City, California.
- ATC/MCEER, 2003, *Liquefaction Study Report, Recommended LRFD Guidelines for the Seismic Design of Highway Bridges*, MCEER/ATC-49-1 Report, ATC/MCEER Joint Venture, a partnership of the Applied Technology Council and the Multidisciplinary Center for Earthquake Engineering, Redwood City, California.
- Azizinamini, A., Shahrooz, B., El-Remaily, A., and Astanteh, H., 1999, "Chapter 10: Connections to Composite Members," *Handbook of Structural Steel Connection Design and Details*, McGraw-Hill, New York.
- Baez, J.I., 1995, *A Design Model for the Reduction of Soil Liquefaction by Vibro-Stone Columns*, Ph.D. Dissertation, University of Southern California, Los Angeles, California, p. 207.
- Baez, J.I., 1997, "Vibro-Stone Columns, Soil Improvement – A 20 Year Update," *Ground Improvement, Ground Reinforcement, Ground Treatment Developments 1987-1997*, V.R. Schaefer (Editor), Geotechnical Special Publication No. 69, ASCE, Logan, Utah.
- Balakrishnan, A., Kutter, B.L., and Idriss, I.M., 1998, "Remediation and Apparent Shear Strength of Lateral Spreading Centrifuge Models," *Proceedings, Fifth Caltrans Seismic Research Workshop*, Sacramento, California.
- Ballard, T.A., Krimotat, A., Mutobe, R., and Treyger, S., 1996, "Non-linear Seismic Analysis of Carquinez Strait bridge," *Proceedings of the 2nd U.S. Seminar on Seismic Design, Evaluation and Retrofit of Steel Bridges*, San Francisco, Report No. UCB/CEE-Steel-96/09, Department of Civil and Environmental Engineering, University of California, Berkeley, pp.359-368.
- Bartlett, S. F. and Youd, T. L., 1992, *Empirical Analysis of Horizontal Ground Displacement Generated by Liquefaction Induced Lateral Spreads*, Technical Report. NCEER 92-0021, National Center for Earthquake Engineering Research, SUNY-Buffalo, New York.
- Billings, I.J., Kennedy, D.W., Beamish, M.J., Jury, R., Marsh, J., 1996, "Auckland Harbour Bridge Seismic Assessment", *Proceedings of the 2nd U.S. Seminar on Seismic Design, Evaluation and Retrofit of Steel Bridges*, San Francisco, Report No. UCB/CEE-Steel-96/09, Department of Civil and Environmental Engineering, University of California, Berkeley, pp.275-293.
- Bolt, B.A., and Gregor, N.J., 1993, *Synthesized Strong Ground Motions for the Seismic Condition Assessment of the Eastern Portion of the San Francisco Bay Bridge*, Earthquake Engineering Research Center, Berkeley, Report UCB/EERC-93.12, University of California at Berkeley.
- Boulanger, R.W., and Hayden, R.F., 1995, "Aspects of Compaction Grouting of Liquefiable Soil," *Journal of Geotechnical Engineering*, ASCE, Vol. 121, No. 12, pp. 844-855.
- Bruneau, M., and Marson, J., 1999, *Cyclic Testing of Concrete-Filled Circular Steel Tube Bridge Column Having Encased Fixed Based Detail*, Report OCEERC-99-22, Ottawa Carleton Earthquake Engineering Research Centre, Ottawa, Ontario, Canada.
- Bruneau, M., Uang, C.M., and Whittaker, A., 1997, *Ductile Design of Steel Structures*, McGraw-Hill, New York, NY, 480 pages.
- Bruneau, M., Wilson, J.W., and Tremblay, R., 1996, "Performance of Steel Bridges During the 1995 Hyogoken-Nanbu (Kobe, Japan) Earthquake", *Canadian Journal of Civil Engineering*, Vol.23, No.3, pp.678-713.



- BSI, 1979, *Commentary on Corrosion at Bimetallic Contacts and Its Alleviation*. BSI Standards PD 6484, British Standards Institution, London.
- BSI, 1983, *BS5400 – Steel, Concrete and Composite Bridges: Part 9, Bridge Bearings*, British Standards Institution, London.
- BSSC, 1995, *1994 Edition NEHRP Recommended Provisions for Seismic Regulations for New Buildings*, Reports FEMA-222A and FEMA-223A, prepared by the Building Seismic Safety Council for the Federal Emergency Management Agency, Washington, D.C.
- BSSC, 1998, *1997 Edition NEHRP Recommended Provisions for Seismic Regulations for New Buildings and Other Structures*, FEMA-302 and FEMA-303 Reports, prepared by the Building Seismic Safety Council for the Federal Emergency Management Agency, Washington, D.C.
- Buckle, I.G., Mayes, R.L., and Button, M.R., 1987, *Seismic Design and Retrofit Manual for Highway Bridges*, Report FHWA-IP-87-6, Federal Highway Administration, Washington D.C., 312 pp.
- Button, M.R. Cronin, C.J., and Mayes, R.L., 1999, *Effect of Vertical Ground Motions on the Structural Response of Highway Bridges*, Technical Report MCEER-99-0007, State University of New York at Buffalo.
- California Department of Transportation, 1999, *Caltrans Seismic Design Criteria*, Version 1.1, Sacramento, California.
- CSABAC, 1999, *Seismic Soil-Foundation-Structure Interaction*, Final report, Caltrans Seismic Advisory Board Ad Hoc Committee on Soil-Foundation-Structure Interaction (CSABAC), prepared for California Department of Transportation, Sacramento, California.
- Campbell, K.W., and Bozorgnia, Y., 2000, *Vertical Ground Motion: Characteristics, Relationship With Horizontal Component, and Building Code Implications*, prepared for California Division of Mines and Geology, Strong Motion Instrumentation Program, California Geological Survey, Sacramento, California.
- Caquot, A., and Kerisel, R., 1948, “Tables for the Calculation of Passive Pressure, Active Pressure and Bearing Capacity of Foundations,” Reported in *NavFac DM7.2, Foundations and Earth Structures, Design Manual*, p. 182, Gauthier-Villars, Paris.
- CEN, 1995, “European Standard on Structural Bearings,” *Eurocode EN1337*, Comite European de Normalization, Brussels.
- Chang, C.-Y., Mok, C.M., Power, M.S., and Tang, Y.K., 1991, *Analysis of Ground Response at Lotung Large-Scale Soil-Structure Interaction Experiment Site*, Report No. NP-7306-SL, Electric Power Research Institute, Palo Alto, California.
- Chang, G.A. and Mander, J.B., 1994a, *Seismic Energy Based Fatigue Damage Analysis of Bridge Columns: Part I - Evaluation of Seismic Capacity*, Technical Report NCEER-94-0006, National Center for Earthquake Engineering Research, State University of New York at Buffalo, New York.
- Chang, G.A. and Mander, J.B., 1994b, *Seismic Energy Based Fatigue Damage Analysis of Bridge Columns: Part II - Evaluation of Seismic Demand*, Technical Report NCEER-94-0013, National Center for Earthquake Engineering Research, State University of New York at Buffalo, New York.
- Cheng, C-T. and Mander, J.B., 1997, *Seismic Design of Bridge Columns Based on Control and Repairability of Damage*, Technical Report NCEER-97-0013, Multidisciplinary Center for Earthquake Engineering Research, University at Buffalo, New York.
- Clough, R.W. and Penzien, J., 1993, *Dynamics of Structures*, 2<sup>nd</sup> edition, McGraw-Hill, Inc., New York, New York.
- Constantinou, M.C., Tsopelas, P., Kasalanati, A., and Wolff, E.D., 1999, *Property Modification Factors for Seismic Isolation Bearings*. Technical Report MCEER-99-0012, Multidisciplinary Center for Earthquake Engineering Research, Buffalo, New York.
- Cooke, H. G., and Mitchell, J. K., 1999, *Guide to Remedial Measures for Liquefaction Mitigation at Existing Highway Bridge Sites*, Technical Report MCEER-99-015, Multidisciplinary Center for Earthquake

- Engineering Research, Buffalo, New York, 176 pp.
- CSA, 2001, *Limit States Design of Steel Structures*, Canadian Standards Association, Rexdale, Ontario, Canada.
- Dameron, R.A., Sobash, V.P., and Parker, D.R., 1995, *Seismic Analysis of the Existing San Diego-Coronado Bay Bridge*, Report prepared for the California Department of Transportation, Anatech Consulting Engineers, 800 pages.
- Das, B. M., 1999, *Principles of Foundation Engineering*, 4<sup>th</sup> Edition, PWS-KENT, Publishing Co.
- Department of Environment, 1976, "Design Recommendations for Elastomeric Bridge Bearings," *Technical Memorandum BE 1/76*, Highways Directorate, Great Britain.
- Dicleli, M., and Bruneau, M., 1995a, "Seismic Performance of Multispan Simply Supported Slab-on-Girder Highway Bridges," *Engineering Structures*, Vol. 17, No. 1, pp. 4-14.
- Dicleli, M., and Bruneau, M., 1995b, "Seismic Performance of Simply Supported and Continuous Slab-on-Girder Steel Bridges," *Structural Journal of the American Society of Civil Engineers*, Vol. 121, No. 10, pp. 1497-1506.
- Dietrich, A.M., and Itani, A.M, 1999, *Cyclic Behavior of Laced and Perforated Members on the San Francisco-Oakland Bay Bridge*, Center for Civil Engineering Earthquake Research, Report No. CCER-99-09, University of Nevada, Reno, 194 pp.
- DM7, 1982, *Design Manual 7.0, Foundations & Earth Structures*, Naval Facilities Engineering Command, Alexandria, Virginia.
- Dobry, R., 1995, "Liquefaction and Deformation of Soils and Foundations Under Seismic Conditions," State-of-the-Art Paper, *Proceedings, Third Intl. Conf. on Recent Advances in Geotechnical Earthquake Engineering and Soil Dynamics*, S. Prakash (ed.), St. Louis, Missouri, Vol. III, pp. 1465-1490.
- Donikian, R., Luo, S., Alhuraibi, M., Coke, C., Williams, M., and Swatta, M., 1996, "The Global Analysis Strategy for the Seismic Retrofit Design of the San Rafael and San Mateo Bridges", *Proceedings of the 2nd U.S. Seminar on Seismic Design, Evaluation and Retrofit of Steel Bridges*, Report No. UCB/CEE-Steel-96/09, Department of Civil and Environmental Engineering, University of California at Berkeley, pp.405-415.
- Dutta, A., and Mander, J.B., 1998, *Capacity Design and Fatigue Analysis of Confined Concrete Columns*, Multidisciplinary Center for Earthquake Engineering Research, Technical Report MCEER-98-0007, State University of New York at Buffalo.
- Mander, J.B., Panthaki, F.D., and Kasalanati, A., 1994, "Low-Cycle Fatigue Behavior of Reinforcing Steel", *ASCE Journal of Materials in Civil Engineering*, Vol. 6, No. 4, Nov. 1994, Paper No. 6782, pp. 453-468.
- EERI, 1990, "Loma Prieta Earthquake Reconnaissance Report," *Earthquake Spectra*, Supplement to Vol. 6, Earthquake Engineering Research Institute, Oakland, California.
- Egan, J. A. and Wang, Z-L., 1991, "Liquefaction-Related Ground Deformation and Effects on Facilities at Treasure Island, San Francisco, During the 17 October 1989 Loma Prieta Earthquake," *Proceedings of the 3<sup>rd</sup> Japan-U.S. Workshop on Earthquake Resistant Design of Lifeline Facilities and Countermeasures for Soil Liquefaction*, San Francisco, California.
- EPRI, 1993, *Guidelines for Determining Design Basis Ground Motions*, Report No. EPRI TR-102293, Electric Power Research Institute, Palo Alto, California.
- Fehling, E., Pauli, W., and Bouwkamp, J.G., 1992, "Use of vertical shear-links in eccentrically braced frames," *Proceedings 10th World Conference on Earthquake Engineering*, Madrid, vol. 9, pp. 4475-4479.
- Fiegel, G.L. and Kutter, B.L., 1994, "Liquefaction-Induced Lateral Spreading of Mildly Sloping Ground," *Journal of Geotechnical Engineering*, ASCE, Vol. 120, No. 12, pp. 2236-2243.
- Finn, W.D.L., 1991, "Assessment of Liquefaction Potential and Post Liquefaction Behavior of Earth Structures: Developments 1981-1991," State-of-the-Art Paper, *Proc. of the Second Intl. Conf. on Recent Advances in*

- Geotechnical Earthquake Engineering and Soil Dynamics*, S. Prakash (ed.), St. Louis, Missouri, Vol. II, pp. 1833-1850.
- Frankel, A.D., and Leyendecker, E.V., 2001, *Seismic Hazard Curves and Uniform Hazard Response Spectra for the United States*, Open-File Report 01-436 (CD-ROM), U.S. Geological Survey, Golden, Colorado.
- Frankel, A., Mueller, C., Barnhard, T., Perkins, D., Leyendecker, E., Dickman, N., Hanson, S., and Hooper, M., 1996, *National Seismic Hazard Maps: Documentation June 1996*, U.S. Geological Survey Open-File Report 96-532, 110 pp.
- Frankel, A., Mueller, C., Barnhard, T., Perkins, D., Leyendecker, E., Dickman, N., Hanson, S., and Hooper, M., 1997a, *Seismic Hazard Maps For The Conterminous United States*, U.S. Geological Survey Open-File Report 97-131, 12 maps.
- Frankel, A., Mueller, C., Barnhard, T., Perkins, D., Leyendecker, E., Dickman, N., Hanson, S., and Hooper, M., 1997b, *Seismic Hazard Maps For California, Nevada, and Western Arizona/Utah*, U.S. Geological Survey Open-File Report 97-130, 12 maps.
- Frankel, A., Harmsen, S., Mueller, C., Barnhard, D., Leyendecker, E.V., Perkins, D., Hanson, S., Dickman, M., and Hooper, M., 1997c, "U.S. -Geological Survey National Seismic Hazard Maps: Uniform Hazard Spectra, Deaggregation, and Uncertainty," *Proceedings of the FHWA/NCEER Workshop on the National Representation of Seismic Ground Motion for New and Existing Highway Facilities*: National Center for Earthquake Engineering Research Technical Report NCEER-97-0010, pp. 39-73.
- Frankel, A., Mueller, C.S., Barnard, T.P., Leyendecker, E.V., Wesson, R.L., Harmsen, S.C., Klein, F.W., Perkins, D.M., Dickman, N.C., Hanson, S.L., and Hopper, H.G., 2000, "USGS National Seismic Hazard Maps," *Earthquake Spectra*, Vol. 16, No. 1, pp. 1-19.
- Franklin, A.G. and Chang, F.K., 1977, *Earthquake Resistance of Earth and Rock-Fill Dams; Permanent Displacements of Earth Embankments by Newmark Sliding Block Analysis*, Miscellaneous Paper S-71-17, Report 5, U.S. Army Waterways Experiment Station, CE, Vicksburg, Mississippi.
- Friedland, I.F., Power, M.S., and Mayes, R.L., eds., 1997, *Proceedings of the FHWA/NCEER Workshop on National Representation of Seismic Ground Motion for New and Existing Highway Facilities*, Multidisciplinary Center for Earthquake Engineering Research, Buffalo, New York.
- Gasparini, D., and Vanmarcke, E.H., 1976, *SMIQKE: A Program For Artificial Motion Generation*, Department of Civil Engineering, Massachusetts Institute of Technology, Cambridge.
- Gates et al., 1995, *Proceedings of the First National Seismic Conference on Bridges and Highways*, San Diego, California
- Gulkan, P. and Sozen, M., 1974, "Inelastic Response of Reinforced Concrete Structures to Earthquake Motions," *ACI Journal*, December, American Concrete Institute, Farmington Hills, Michigan.
- Hamburger, R.O., and Hunt, R.J., 1997, "Development of the 1997 NEHRP Provisions Ground Motion Maps and Design Provisions," *Proceedings of the FHWA/NCEER Workshop on the National Representation of Seismic Ground Motions for New and Existing Highway Facilities*, Technical Report, NCEER-97-0010, National Center for Earthquake Engineering Research, State University of New York, Buffalo, New York, pp. 75-92.
- Hayden, R.F., and Baez, J.I., 1994, "State of Practice for Liquefaction Mitigation in North America," *Proceedings of the 4th U.S.-Japan Workshop on Soil Liquefaction, Remedial Treatment of Potentially Liquefiable Soils*, PWRI, Tsukuba City, Japan.
- Hose, Y.D., Silva, P.F., and Seible, F., 2000, "Development of a Performance Evaluation Database for Concrete Bridge Components and Systems under Simulated Seismic Loads," *Earthquake Spectra*, Vol. 16, No. 2, Earthquake Engineering Research Institute, Oakland, California, pp. 413-442.
- Houston, S.L., Houston, W.N. and Padilla, J.M., 1987, "Microcomputer-Aided Evaluation of Earthquake-Induced Permanent Slope

- Displacements,” *Microcomputers in Civil Engineering*, Vol. 2, pp. 207-222.
- Hynes, M.E. and Franklin, A.G., 1984, *Rationalizing the Seismic Coefficient Method*, Miscellaneous Paper GL-84-13, U.S. Army Waterways Experiment Station, Vicksburg, Mississippi, 21 pp.
- Idriss, I.M., and Sun, J.I., 1992, *User’s Manual for SHAKE91*, Center for Geotechnical Modeling, Department of Civil and Environmental Engineering, University of California, Davis, California, 13 pp. (plus Appendices).
- Imbsen, R., Davis, F.V., Chang, G.S., Pecchia, D., and Liu, W.D., 1997, “Seismic Retrofit of I-40 Mississippi River Bridges”, *Proceedings of National Seismic Conference on Bridges and Highways – Progress in Research and Practice*, Sacramento, California, pp. 457-469.
- Ingham, T.J., Rodriguez, S., Nader, M.N., Taucer, F., and Seim, C., 1996. “Seismic Retrofit of the Golden Gate Bridge”. *Proceedings of the 2nd U.S. Seminar on Seismic Design, Evaluation and Retrofit of Steel Bridges*, Report No. UCB/CEE-Steel-96/09, Department of Civil and Environmental Engineering, University of California at Berkeley, pp.145-164.
- International Code Council, Inc. (ICC), 2000, *International Building Code*, Building Officials and Code Administrators International Inc., International Conference of Building Officials, and Southern Building Code Congress International, Inc., Birmingham, Alabama.
- Ishihara, K., 1993, “Liquefaction and Flow Failure During Earthquakes,” 33<sup>rd</sup> Rankine Lecture, *Geotechnique*, Vol. 43, No. 3.
- Itani, A.M., Vesco, T.D., and Dietrich, A.M., 1998a, *Cyclic Behavior of “As-Built” Laced Members With End Gusset Plates on the San Francisco-Oakland Bay Bridge*, Center for Civil Engineering Earthquake Research, Report No. CCER-98-01, University of Nevada, Reno, 187 pp.
- Itani, A., Douglas, B., and Woodgate, J., 1998b. *Cyclic Behavior of Richmond-San Rafael Retrofitted Tower Leg*, Center for Civil Engineering Earthquake Research, Department of Civil Engineering, Report No. CCEER-98-5, University of Nevada, Reno.
- Itasca, 1998, *Fast Lagrangian Analysis of Continua*, Itasca Consulting Group, Minneapolis, Minnesota.
- Jibson, R.W., 1993, “Predicting Earthquake-Induced Landslide Displacements Using Newmark’s Sliding Block Analysis,” *Transportation Research Record 1411*, National Research Council, 17 pp.
- Jones, M.H., Holloway, L.J., Toan, V., and Hinman, J., 1997. “Seismic Retrofit of the 1927 Carquinez Bridge by a Displacement Capacity Approach”, *Proceedings of National Seismic Conference on Bridges and Highways – Progress in Research and Practice*, Sacramento, California, pp. 445-456.
- Kasai, K. and Popov, E.P., 1986, “Cyclic web buckling control for shear link beams,” *J. Struct. Engrg.*, ASCE, Vol. 112, No. 3, pp. 505-523.
- Kim, J-H., and Mander, J.B., 1999, *Truss Modeling of Reinforced Concrete Shear-Flexure Behavior*, Multidisciplinary Center for Earthquake Engineering Research, Buffalo NY, Technical Report MCEER-99-0005, State University of New York at Buffalo.
- Kim, D.K., Mander, J.B., and Chen, S.S., 1996, “Temperature and Strain Rate Effects on the Seismic Performance of Elastomeric and Lead-Rubber Bearings,” *Proceedings, 4th World Congress on Joint Sealing and Bearing Systems for Concrete Structures*, American Concrete Institute, Publication SP-164, Vol. 1.
- Klein, F., Frankel, A., Mueller, C., Wesson, R., and Okubo, P., 1999, “Seismic Hazard Maps for Hawaii,” *U.S. Geological Survey Geologic Investigation Series*, (maps also on Website at <http://geohazards.cr.usgs.gov/eq/>).
- Kompfner, T.A., Tognoli, J.W., Dameron, R.A., and Lam, I.P., 1996, “The San Diego - Coronado Bay Bridge Seismic Retrofit Project”, *Proceedings of the 2nd US Seminar on Seismic Evaluation and Retrofit Of Steel Bridges*, Report No. UCB/CEE-Steel-96/09, Department of Civil and Environmental Engineering, University of California at Berkeley, pp.73-93.
- Kramer, S.L., 1996, *Geotechnical Earthquake Engineering*, Prentice Hall, New Jersey.

- Kramer, S.L., Sivaswaran, N., and Tucker, K., 1995, *Seismic Vulnerability of the Alaska Way Viaduct: Geotechnical Engineering Aspects*, Washington State Transportation Center (TRAC), University of Washington.
- Lam, I.P., and Law, H., 1994, "Soil-Foundation-Structure Interaction - Analytical Considerations by Empirical p-y Methods," *Proceedings, 4<sup>th</sup> CALTRANS Seismic Research Workshop*, California Department of Transportation, Sacramento.
- Lam, I.P. and Martin, G.R., 1986, "Seismic Design of Highway Bridge Foundations," *Design Procedures and Guidelines*, FHWA/RD-86/102, Vol.2, FHWA, U.S. Department of Transportation, 181 pp.
- Lam, I.P., Kapuska, M., Chaudhuri, D., 1998, *Modeling of Pile Footing and Drilled Shafts for Seismic Design*, Technical Report MCEER-98-0018, Multidisciplinary Center for Earthquake Engineering Research, State University of New York at Buffalo, New York, 117 pp.
- Lee, D. D., 1993, "The Base Isolation of Koeberg Nuclear Power Station 14 Years After Installation," *Post-SMIRT Conference on Isolation, Energy Dissipation and Control of Vibration of Structures*, Capri, Italy.
- Lee, M.K.W., and Finn, W.D.L., 1978, "DESRA-2, Dynamic Effective Stress Response Analysis of Soil Deposits With Energy Transmitting Boundary Including Assessment of Liquefaction Potential," *Soil Mechanics*, Series No. 36, Department of Civil Engineering, University of British Columbia, Vancouver, Canada, 60 pp
- Li, X.S., Wang, Z.L., and Shen, C.K., 1992, *SUMDES, A Nonlinear Procedure for Response Analysis of Horizontally-Layered Sites Subjected to Multi-Directional Earthquake Loading*, Department of Civil Engineering, University of California, Davis, California.
- Lilhanand, K., and Tseng, W.S., 1988, "Development and Application of Realistic Earthquake Time-Histories Compatible with Multiple-Damping Design Spectra," *Proceedings of the 9th World Conference on Earthquake Engineering*, Tokyo-Kyoto:
- Japan Association for Earthquake Disaster Prevention.
- Leyendecker, E.V., Hunt, R.J., Frankel, A.D., and Rukstales, K.S., 2000, "Development of Maximum Considered Earthquake Ground Motion Maps," *Earthquake Spectra*, Vol. 6, No. 1, Earthquake Engineering Research Institute, Oakland, California, pp. 21-40.
- Leyendecker, E.V., Frankel, A.D., and Rukstales, K. S., 2001, *Seismic Design Parameters*, Open-File Report 01-437 (CD-ROM), U.S. Geological Survey, Golden, Colorado.
- Luehring, R., Dewey, B., Mejia, L., Stevens, M. and Baez, J., 1998, "Liquefaction Mitigation of Silty Dam Foundation Using Vibro-Stone Columns and Drainage Wicks – A Test Section Case History at Salmon Lake Dam," *Proceedings of the 1998 Annual Conference Association of State Dam Safety Officials*, Las Vegas, Nevada
- MacRae, G.A., 1994, "P- $\Delta$  Effects on Single Degree-of-Freedom Structures in Earthquakes," *Earthquake Spectra*, Vol. 10, No. 3, Earthquake Engineering Research Institute, Oakland, California, pp. 539-568.
- Mahin, S.A., and Boroschek, R., 1991, *Influence of Geometric Non-linearities on the Seismic Response and Design of Bridge Structures*, Report to the California Department of Transportation.
- Makdisi, F.I. and Seed, H.B., 1978, "Simplified Procedure for Estimating Dam and Embankment Earthquake-Induced Deformations," *Journal of Geotechnical Engineering*, ASCE, Vol. 104, No. 7, pp. 849-867.
- Malley, J. O. and Popov, E.P., 1983, *Design considerations for shear links in eccentrically braced frames*, EERC report 83-24, Univ. of Calif., Berkeley, California.
- Mander, J.B., and Cheng, C-T., 1999, "Replaceable Hinge Detailing for Bridge Columns," *Seismic Response of Concrete Bridges*, American Concrete Institute, Special Publication SP-187.
- Mander, J.B., Dutta, A. and Goel, P., 1998, *Capacity Design of Bridge Piers and the Analysis of Overstrength*, Report No.MCEER-98-0003, Multidisciplinary Center for

- Earthquake Engineering Research, University at Buffalo, New York.
- Mander, J.B., Panthaki, F.D., and Kasalanati, A., 1994, "Low-Cycle Fatigue Behavior of Reinforcing Steel," *ASCE Journal of Materials in Civil Engineering*, Vol. 6., No. 4, Paper No. 6782, pp. 453-468.
- Maroney, B., 1996, "Seismic retrofit of the east spans of the San Francisco-Oakland bay bridge," *Proceedings of the 2nd US Seminar on Seismic Evaluation and Retrofit Of Steel Bridges*, Report No. UCB/CEE-Steel-96/09, Department of Civil and Environmental Engineering, University of California at Berkeley, pp.17-34.
- Martin, G.R., ed., 1994, *Proceedings of the 1992 NCEER/SEAOC/BSSC Workshop on Site Response During Earthquakes and Seismic Code Provisions*, University of Southern California, Los Angeles, November 18-20, 1992, National Center for Earthquake Engineering Research Special Publication NCEER-94-SP01, Buffalo, New York.
- Martin, G.R., 1998, *Development of Liquefaction Mitigation Methodologies: Ground Densification Methods*, National Center for Earthquake Engineering Research, Technical Report, Buffalo, New York.
- Martin, G.R. and Dobry R., 1994, "Earthquake Site Response and Seismic Code Provisions," *NCEER Bulletin*, Vol. 8, No. 4, National Center for Earthquake Engineering Research, State University of New York at Buffalo.
- Martin, G.R. and Qiu, P., 2000, *Site Liquefaction Evaluation: The Application of Effective Stress Site Response Analyses*, NCEER Task Number 106-E-3.1 (A), Multidisciplinary Center for Earthquake Engineering Research, University at Buffalo, New York.
- Martin, G.R. and Qiu, P., 1994, "Effects of Liquefaction on Vulnerability Assessment," *NCEER Highway Project on Seismic Vulnerability of New and Existing Highway Construction*, Year One Research Tasks – Technical Research Papers.
- Martin, G.R. and Qiu, P., 2000, *Site Liquefaction Evaluation: The Application of Effective Stress Site Response Analyses*, NCEER Task Number 106-E-3.1 (A), Multidisciplinary Center for Earthquake Engineering Research, Buffalo, New York.
- Martin, G.R., Tsai, C-F., and Arulmoli, K., 1991, "A Practical Assessment of Liquefaction Effects and Remediation Needs," *Proceedings, 2<sup>nd</sup> International Conference on Recent Advances in Geotechnical Earthquake Engineering and Soil Dynamics*, St. Louis, Missouri.
- Matasovic, N., 1993, *Seismic response of composite horizontally-layered soil deposits*, Ph.D. Dissertation, Civil and Environmental Engineering Department, University of California, Los Angeles, 452 pp.
- McCallen, D.B., and Astaneh-Asl, A., 1996, "Seismic Response of Steel Suspension Bridge," *Proceedings of the 2nd US Seminar on Seismic Evaluation and Retrofit of Steel Bridges*, Report No. UCB/CEE-Steel-96/09, Department of Civil and Environmental Engineering, University of California at Berkeley, pp.335-347.
- MCEER, 2000, *Seismic Retrofitting Manual for Highway Structure: Part II – Retraining Structures, Slopes, Tunnels, Culverts, and Pavements*, Multidisciplinary Center for Earthquake Engineering Research, NCEER Task Number 106-G-3.2, Buffalo, New York.
- Meyersohn, W.D., O'Rourke, T.D., and Miura, F., 1992, Lateral Spread Effects on Reinforced Concrete Pile Foundations, *Proceedings, Fifth U.S.-Japan Workshop on Earthquake Disaster Prevention for Lifeline Systems*, Tsukuba, Japan.
- Miranda, E. and Bertero, V., 1994, "Evaluation of Strength Reduction Factors for Earthquake-Resistant Design," *Earthquake Spectra*, Vol. 10, No. 2, Earthquake Engineering Research Institute, Oakland, California.
- Miranda, E. and Bertero, V., 1996, "Seismic Performance of an Instrumented Ten-Story Reinforced Concrete Building," *Earthquake Engineering and Structural Dynamics*, Vol. 25, pp. 1041-1059.
- Mitchell, J. K., Cooke, H. G., and Schaeffer, J. A., 1998, "Design Considerations in Ground Improvement for Seismic Risk Mitigation," *Proc., Geotechnical Earthquake Engineering and Soil Dynamics III, Vol. I*, Geotech. Special

- Pub. No. 75., ASCE, Reston, Virginia, pp. 580-613.
- Nakashima, M., 1995, "Strain-Hardening Behavior of Shear Panels Made of Low-Yield Steel. I: Test.," *J. Struct. Engrg.*, ASCE, Vol. 121, No. 12, pp. 1742-1749.
- Nassar, A.A., and Krawinkler, H., 1991, *Seismic Demands for SDOF and MDOF Systems*, Report No. 95, John A. Blume Earthquake Engineering Center, Stanford University, Stanford, California.
- Newmark, N.M., 1965, "Effects of Earthquakes on Dams and Embankments," *Geotechnique*, Vol. 15, No. 2, pp. 139-160.
- NIST, 1996, *Guidelines for Pre-Qualification, Prototype and Quality Control Testing of Seismic Isolation Systems*, Publication NISTIR 5800, National Institute of Standards and Technology, Building and Fire Research Laboratory, Gaithersburg, Maryland.
- NRC, 1985, *Liquefaction of Soils During Earthquakes*, Report No. CETS-EE-001, Committee on Earthquake Engineering, National Research Council, Washington, D.C.
- O'Rourke, T. D., Gowdy, T. E., Stewart, H. E., and Pease, J. W., 1991, "Lifeline Performance and Ground Deformation in the Marina During 1989 Loma Prieta Earthquake," *Proceedings of the 3<sup>rd</sup> Japan-U.S. Workshop on Earthquake Resistant Design of Lifeline Facilities and Countermeasures for Soil Liquefaction*, NCEER Technical Report NCEER-91-0001, National Center for Earthquake Engineering Research, State University of New York at Buffalo.
- Petersen, M., Bryant, W., Cramer, C., Cao, T., Reichle, M., Frankel, A., Lienkaemper, J., McCorry, P., and Schwartz, D., 1996, *Probabilistic Seismic Hazard Assessment for the State of California*: California Department of Conservation, Division of Mines and Geology Open-File Report 96-08, U.S. Geological Survey Open-File Report 96-706.
- Pfeiffer, T.J., and Higgins, J.D., 1991, *Colorado Rockfall Simulation Program*. (manual and software), Misc. Report No. 39, Colorado Geological Survey, Denver, Colorado, 71 pp.
- Popov, E.P., Bertero, V.V., and Chandramouli, S., 1975, *Hysteretic Behavior of Steel Columns*, Earthquake Engineering Research Center Report UCB/EERC-75-11, University of California, Berkeley.
- Poulos, S.J., Castro, G. and France, W., 1985, "Liquefaction Evaluation Procedure," *Journal of Geotechnical Engineering*, ASCE, Vol. 111, No. 6, pp. 772-792.
- Priestley, M.J.N., Seible, F., Chai, Y.H., and Wong, R., 1992, *Santa Monica Viaduct Retrofit Full-Scale Test on Column Lap Splice with #11 [35 mm] Reinforcement*, SSRP 94/14, Structural Systems Research, University of California, San Diego.
- Priestley M.J.N., Seible, F., and Calvi, G.M., 1996, *Seismic Design and Retrofit of Bridges*, John Wiley & Sons, New York.
- Priestley M.J.N., Verma, R., and Xiao, Y., 1994, "Seismic Shear Strength of Reinforced Concrete Columns," *Journal of Structural Engineering*, ASCE, Vol. 120, no. 8, pp. 2310-2329.
- Prucz, Z., Conway, W.B., Schade, J.E., and Ouyang, Y., 1997, "Seismic Retrofit Concepts and Details for Long-Span Steel Bridges", *Proceedings of National Seismic Conference on Bridges and Highways – Progress in Research and Practice*, Sacramento, California, pp.435-444.
- Pyke, R.M., 1992, *TESS: A Computer Program for Nonlinear Ground Response Analyses*, TAGA Engineering Systems & Software, Lafayette, California.
- Qiu, P., 1998, *Earthquake-Induced Nonlinear Ground Deformation Analyses*, Ph.D. dissertation, University of Southern California, Los Angeles.
- Reese, L.C., Wang, S-T, Arrellaga, J.A., and Hendrix, J., 1997, *Computer Program LPILE Plus*, Ensoft, Inc., Austin, Texas.
- Reese, L.C. and Wang, S.T., 1997, *LPILE 3.0 — A Program for the Analysis of Piles and Drilled Shafts under Lateral Loads*, ENSOFT, Inc., Austin, Texas.
- Reese, L.C., Wang, S.T., Arrellaga, J.S., Hendrix, J., 1998, *LPILE Plus*, ENSOFT, Inc., Austin, Texas.
- Rinne, E.E., 1994, "Development of New Site Coefficients for Building Codes," *Proceedings*

- of the Fifth U.S. National Conference on Earthquake Engineering*, Chicago, Illinois, Vol. III, pp. 69-78.
- Roberts, J. E., 1992, "Sharing California's Seismic Lessons", *Modern Steel Constructions*, pp.32-37.
- Rodriguez, S., and Ingham, T.J., 1996. "Nonlinear Dynamic Analysis of the Golden Gate Bridge". *Proceedings of the 2nd US Seminar on Seismic Evaluation and Retrofit Of Steel Bridges*, Report No. UCB/CEE-Steel-96/09, Department of Civil and Environmental Engineering, University of California at Berkeley, pp.457-466.
- Roeder, C.W., Stanton, J.F., and Taylor, A.W., 1987, *Performance of Elastomeric Bearings*, National Cooperative Highway Research Program, Report 298, Transportation Research Board, Washington, D.C.
- SAC, 1995, *Interim Guidelines: Evaluation, Repair, Modification and Design of Welded Steel Moment Frame Structures*, prepared by the SAC Joint Venture, a partnership of the Structural Engineers Association of California, the Applied Technology Council, and California Universities for Research in Earthquake Engineering, published by the Federal Emergency Management Agency, (FEMA-267 Report), Washington, D.C.
- SAC 1997, *Interim Guidelines Advisory No.1 - Supplement to FEMA-267*, prepared by the SAC Joint Venture, a partnership of the Structural Engineers Association of California, the Applied Technology Council, and California Universities for Research in Earthquake Engineering, published by the Federal Emergency Management Agency (FEMA-267A Report), Washington, D.C.
- SAC, 2000, *Recommended Seismic Design Criteria for New Steel Moment-Frame Buildings*, prepared by the SAC Joint Venture, a partnership of the Structural Engineers Association of California, the Applied Technology Council, and California Universities for Research in Earthquake Engineering, published by the Federal Emergency Management Agency, (FEMA-350 Report), Washington, D.C.
- Sarraf, M. and Bruneau, M., 1998a, "Ductile Seismic Retrofit of Steel Deck-Truss Bridges. I: Strategy and Modeling," *ASCE Journal of Structural Engineering*, Vol. 124, No. 11, pp. 1253-1262.
- Sarraf, M. and Bruneau, M., 1998b, "Ductile Seismic Retrofit of Steel Deck-Truss Bridges. II: Design Applications," *ASCE Journal of Structural Engineering*, Vol.124, No.11, pp. 1263-1271.
- SCEC, 1999, "Recommended Procedures for Implementation of DMG Special Technical Publication 117," *Guidelines for Analyzing and Mitigating Liquefaction in California*, Southern California Earthquake Center, University of Southern California, 63 pp.
- Schamber, R.A., Li, F., Fuller, R.T., and Liu, W.D., 1997, "Seismic Resistance of Steel Bascule Bridges," *Proceedings of National Seismic Conference on Bridges and Highways - Progress in Research and Practice*, Sacramento, California, pp. 381-394.
- Schnabel, P.B., Seed, H.B., and Lysmer, J., 1972, *SHAKE - A Computer Program for Earthquake Response Analysis of Horizontally Layered Sites*, Report No. EERC-72-12, Earthquake Engineering Research Center, University of California, Berkeley, California.
- Schneider, S.P., Roeder, C.W., and Carpenter, J.E., 1992, "Seismic Behavior of Moment-Resisting Steel Frames: Experimental Study," *ASCE Structural Journal*, Vol. 119, No. 6; pp. 1885-1902.
- Seed, H.B., 1987, "Design Problems in Soil Liquefaction," *Journal of the Geotechnical Engineering Division*, ASCE, Vol. 113, No. 8.
- Seed, H.B. and DeAlba, P., 1986, "Use of SPT and CPT Tests for Evaluating the Liquefaction Resistance of Sands," in Clemence, S.P. (editor), *Use of In Situ Tests in Geotechnical Engineering*, ASCE Geotechnical Special Publication No. 6, New York, pp. 281-302.
- Seed, H.B. and Harder, L.F., Jr., 1990, "SPT-Based Analysis of Cyclic Pore Pressure Generation and Undrained Residual Strength," *Proceedings, H. Bolton Seed Memorial Symposium*, BiTech Publishers, Ltd., pp. 351-376.
- Seed, H.B., and Idriss, I.M., 1970, *Soil Moduli and Damping Factors for Dynamic Response Analyses*, Report No. EERC 70-10,



- Earthquake Engineering Research Center,  
University of California, Berkeley.
- Seed, H.B. and Idriss, I.M., 1971, "Simplified Procedure for Evaluating Soil Liquefaction Potential," *Journal of the Soil Mechanics and Foundations Division*, ASCE, Vol. 97, No. SM9, pp. 1249-1273.
- Seed, H.B. and Idriss, I.M., 1982, *Ground Motions and Soil Liquefaction During Earthquakes*, Earthquake Engineering Research Institute Monograph, Oakland, California.
- Seed, H.B., Idriss, I.M., and Arango, I., 1983, "Evaluation of Liquefaction Potential Using Field Performance Data," *Journal of the Geotechnical Engineering Division*, ASCE, Vol. 109, No. 3.
- Seed, H.B., Tokimatsu, K., Harder, L.F., and Chung, R.M., 1985, "Influence of SPT Procedures in Soil Liquefaction Resistance Evaluations," *Journal of the Geotechnical Engineering Division*, ASCE, Vol. 111, No. 12.
- Seed, H.B., Wong, R.T., Idriss, I.M., and Tokimatsu, K., 1986, "Moduli and Damping Factors for Dynamic Analyses of Cohesionless Soils," *Journal of Geotechnical Engineering*, ASCE, Vol. 112, No. 11, pp. 1016-1032.
- Seim, C., Ingham, T. and Rodriguez, S., 1993, "Seismic Performance and Retrofit of the Golden Gate bridge", *Proceedings of the 1st US Seminar on Seismic Evaluation and Retrofit Of Steel Bridges*, San Francisco, California.
- Shama, A.A., Mander, J.B., Blabac, B.B., and Chen, S.S., 2001, *Experimental Investigation and Retrofit of Steel Pile Foundations and Pile Bents Under Cyclic Lateral Loading*, Technical Report, Multidisciplinary Center for Earthquake Engineering Research, University at Buffalo, Buffalo, New York.
- Sherman, D.R., 1976, *Tentative Criteria For Structural Applications Of Steel Tubing And Pipe*, American Iron and Steel Institute, Washington, D.C.
- Shinozuka, M., Saxena, V., and Deodatis, G., 1999, *Effect of Spatial Variation of Ground Motion on Highway Structures*, Draft Final Report for MCEER Highway Project, Submitted to Multidisciplinary Center for Earthquake Engineering Research, Buffalo, New York.
- Shirolé, A. M., and Malik, A. H., 1993, "Seismic Retrofitting of Bridges in New York State", *Proceedings, Symposium on Practical Solutions for Bridge Strengthening & Rehabilitation*, Iowa State Univ., Ames, Iowa, pp. 123-131.
- Seible, F., Priestley, M.J.N., Latham, C.T., and Silva, P., 1994, *Full-Scale Bridge Column/Superstructure Connection Tests Under Simulated Longitudinal Seismic Loads*, SSRP 94/14, Structural Systems Research, University of California, San Diego, California.
- Silva, W., 1997, "Characteristics of Vertical Strong Ground Motions for Applications to Engineering Design, *Proceedings of the FHWA/NCEER Workshop on the National Representation of Seismic Ground Motions for New and Existing Highway Facilities*, National Center for Earthquake Engineering Research, Buffalo, New York, Technical Report NCEER-97-0010, State University of New York at Buffalo, pp. 205-252.
- Silva, W., and Lee, K., 1987, "State-of-the-Art for Assessing Earthquake Hazards in the United States: Report 24," *WES RASCAL Code for Synthesizing Earthquake Ground Motions*, Miscellaneous Paper 5-73-1, U.S. Army Engineer Waterways Experiment Station, Vicksburg, Mississippi.
- Somerville, P.G., 1997, "The Characteristics and Quantification of Near Fault Ground Motion," *Proceedings of the FHWA/NCEER Workshop on the National Representation of Seismic Ground Motion for New and Existing Highway Facilities*, Center for Earthquake Engineering Research, Buffalo, New York, Technical Report 97-0010, State University of New York at Buffalo, pp. 1293-318.
- Somerville, P.G., Smith, N.F., Graves, R.W., and Abrahamson, N.A., 1997, "Modification of Empirical Strong Ground Motion Attenuation Relations to Include the Amplitude and Duration Effects of Rupture Directivity," *Seismological Research Letters*, Vol. 68, pp. 199-222.
- Somerville, P., Krawinkler, H., and Alavi, B., 1999, *Development of Improved Ground*

- Motion Representation and Design Procedures for Near-Fault Ground Motions*, prepared for California Strong Motion Instrumentation Program, California Division of Mines and Geology, Sacramento, California, Draft.
- Sritharan, S., and Priestley, M.J.N., 1994a, *Performance of a T-Joint (IC1) Under Cyclic Loading*, Preliminary Report to Caltrans, University of California, San Diego, California.
- Sritharan, S., and Priestley, M.J.N., 1994b, *Behavior of a Partially Prestressed Cap Beam/Column Interior Joint (Unit IC2) Under Cyclic Loading*, Preliminary Report to Caltrans, University of California, San Diego, California.
- Stark, T. D., and Mesri, G., 1992, "Undrained Shear Strength of Liquefied Sands for Stability Analyses," *Journal of the Geotechnical Engineering Division, ASCE*, Vol. 118, No. 11, pp. 1727-1747.
- Stark, T.D., Olson, S.M., Kramer, S.L., and Youd, T.L., 1998, "Shear Strength of Liquefied Soil," *Proceedings, 1998 ASCE Specialty Conference on Geotechnical Earthquake Engineering and Soil Dynamics*, Seattle, Washington.
- Sun, J.I., Goleorkhi, R., and Seed, H.B., 1988, *Dynamic Moduli and Damping Ratios for Cohesive Soils*, Report No. UBC/EERC-88/15, Earthquake Engineering Research Center, University of California, Berkeley.
- Tang, X., and Goel, S.C., 1987, *Seismic Analysis And Design Considerations Of Braced Steel Structures*, Report No. UMCE 87-4, Department of Civil Engineering, University of Michigan. Ann Arbor, Michigan.
- Tang, M.C., Manzanarez, R., Nader, M., Abbas, S., and Baker, G., 2000, "Replacing the East Bay Bridge," *Civil Engineering Magazine*, American Society of Civil Engineers, Vol. 70, No. 9, pp. 38-43.
- Tokimatsu, K. and Seed, H. B., 1987, "Evaluation of Settlements in Sands Due to Earthquake Shaking," *Journal of the Geotechnical Engineering Division, ASCE*, Vol. 113, No. 8.
- Tsai, K.-C., et al., 1993, "Design of Steel Triangular Plate Energy Absorbers for Seismic-Resistant Construction," *Earthquake Spectra*, Vol. 9, No. 3, Oakland, California, pp. 505-528.
- Uang, C.M., and Bertero, V.V., 1986, *Earthquake Simulation Tests and Associated Studies of a 0.3-Scale Model of a Six-Story Concentrically Braced Steel Structure*, Report No. UCB/EERC-86/10, Earthquake Engineering Research Center, University of California, Berkeley.
- Uang, C.M., Tsai, K.C., and Bruneau, M., 2000, "Seismic Design of Steel Bridges", *Bridge Engineering Handbook*, (Ed. W.F. Chen, L.Duan), CRC Press, Boca Raton, Florida, pp. 39-1 to 39-34.
- Uang, C.M., Bruneau, M., Whittaker, A.S., and Tsai, K.C., 2001, "Seismic Design of Steel Structures," *Seismic Design Handbook*, (Ed. Naeim), Kluwer Academic Publishers, Norwell, Massachusetts, pp. 409-462.
- UIC, 1973, "Use of Rubber Bearings for Rail Bridges," The International Union of Railways (UIC) *Code 772R*, Paris, France.
- U.S. Army Corp of Engineers, 2000, *Time History Dynamic Analysis of Concrete Hydraulic Structures*, USACE Engineering Circular EC1110-2-6051.
- USGS, 1990, *Probabilistic Earthquake Acceleration and Velocity Maps for the United States and Puerto Rico*, by S.T. Algermisson, D.M. Perkins, P.C. Thenhaus, S.L. Hanson, and B.L. Bender, U.S. Geological Survey Miscellaneous Field Studies Map MF-2120, Golden, Colorado.
- Vallee, R. P., and Skryness, R. S., 1980, "Sampling and In-Situ Density of a Saturated Gravel Deposit," *Geotechnical Testing Journal*, Vol. 2, No. 3, pp. 136-142.
- Vincent, J., 1996, "Seismic Retrofit of the Richmond-San Raphael Bridge," *Proceedings of the 2nd US Seminar on Seismic Evaluation and Retrofit Of Steel Bridges*, Report No. UCB/CEE-Steel-96/09, Department of Civil and Environmental Engineering, University of California at Berkeley, pp. 215-232.
- Vincent, J., Abrahamson, T., O'Sullivan, M., Lim, K., Dameron, R., and Donikian, R., 1997, "Analysis and Design for the Inelastic Response of a Major Steel Bridge,"

- Proceedings of the 2nd National Conference on Bridges and Highways*, Sacramento, California, pp. 541-555.
- Vucetic, M., and Dobry, R., 1991, "Effect of Soil Plasticity on Cyclic Response," *Journal of Geotechnical Engineering*, ASCE, Vol. 117, No. 1, pp. 89-107.
- Wells, D.L. and Coppersmith, K.J., 1994, "New Empirical Relationships Among Magnitude, Rupture Length, Rupture Area, and Surface Displacement," *Bulletin of the Seismological Society of America*, Vol. 84, pp. 74-1002.
- Wesson, R.L., Frankel, A.D., Mueller, C.S., and Harmsen, S.C., 1999a, *Probabilistic Seismic Hazard Maps of Alaska*, U.S. Geological Survey Open-File Report 99-36.
- Wesson, R.L., Frankel, A.D., Mueller, C.S., and Harmsen, S.C., 1999b, *Seismic Hazard Maps of Alaska and the Aleutian Islands*, U.S. Geological Survey Investigation Series, map I-2679.
- Wong, C.P. and Whitman, R.V., 1982, *Seismic Analysis and Improved Seismic Design Procedure for Gravity Retaining Walls*, Research Report 82-83, Department of Civil Engineering, Massachusetts Institute of Technology, Cambridge, Massachusetts.
- Wong, C.P. and Whitman, R.V., 1982, *Seismic Analysis and Improved Seismic Design Procedure for Gravity Retaining Walls*, Research Report 82-83, Department of Civil Engineering, Massachusetts Institute of Technology, Cambridge, Massachusetts.
- Youd, T.L., 1995, "Liquefaction-Induced Lateral Ground Displacement," State-of-the-Art Paper, *Proceedings, Third Intl. Conf. on Recent Advances in Geotechnical Earthquake Engineering and Soil Dynamics*, Vol. II, S. Prakash (ed.), St. Louis, Missouri, pp. 911-925.
- Youd, T. L., and Idriss, I.M. (Editors), 1997, *Proceedings of the NCEER Workshop on Evaluation of Liquefaction Resistance of Soils*, Salt Lake City, Utah, NCEER Technical Report NCEER-97-0022, Buffalo, New York.
- Youd, T.L., Hansen, C.M., and Bartlett, S.F., 1999, "Revised MLR Equations for Predicting Lateral Spread Displacement," *Proceedings, 7<sup>th</sup> U.S.-Japan Workshop on Earthquake Resistant Design of Lifeline Facilities and Countermeasures Against Liquefaction*, Technical Report MCEER-99-0019, Multidisciplinary Center for Earthquake Engineering Research, State University of New York at Buffalo, pp. 99-114.
- Zahrai, S.M., and Bruneau, M., 1998, "Impact of Diaphragms on Seismic Response of Straight Slab-on-girder Steel Bridges," *ASCE Journal of Structural Engineering*, Vol. 124, No. 8, pp. 938-947.
- Zahrai, S.M., Bruneau, M., 1999a, "Cyclic Testing of Ductile End-Diaphragms for Slab-on-Girder Steel Bridges," *ASCE Journal of Structural Engineering*, Vol. 125, No. 9, pp. 987-996.
- Zahrai, S.M., Bruneau, M., 1999b, "Ductile End-Diaphragms for the Seismic Retrofit of Slab-on-Girder Steel Bridges," *ASCE Journal of Structural Engineering*, Vol. 125, No. 1, pp. 71-80.

### References Considered but not Cited

- AASHTO, 1998, *LRFD Bridge Construction Specifications*, American Association of State Highway and Transportation Officials, Washington, D.C.
- Abrahamson, N.A., 1992, "Non-stationary Spectral Matching Program," *Seismological Research Letters*, v. 63, no. 1, p. 30.
- Andrus, R. D. and Chung, R. M., 1995, *Ground Improvement Techniques for Liquefaction Remediation Near Existing Lifelines*, National Institute of Standards and Technology Report, NISTIR 5714, Gaithersburg, Maryland, 74 pp.
- ANSI/AASHTO/AWS, 1995, *Bridge Welding Code*, D1.5-95, American National Standards Institute, American Association of State Highway and Transportation Officials, and American Welding Society, Washington, D.C.
- ASCE, 1997, *Ground Improvement, Ground Reinforcement, Ground Treatment, Developments 1987 -1997*, Committee on Soil Improvement and Geosynthetics of the Geo-

- Institute, Geotechnical Special Pub. No. 69, ASCE, New York, 616 pp.
- ASME, 1985, *Surface Texture (Surface Roughness, Waviness and Lay)*, ANSI/ASME B46.1-1985, American Society of Mechanical Engineers, New York, New York.
- ASTM, 1992a, *Specification for Polytetrafluorethylene (PTFE) Molding and Extrusion Materials* (withdrawn in 1996 and replaced by ASTM D4894 and ASTM D4895), Report No. ASTM D1457, American Society for Testing and Materials, West Conshohocken, Pennsylvania.
- ASTM, 1992b, *Standard Test Method for Laboratory Determination of Water (Moisture) Content of Soil and Rock by Mass*, Report No. ASTM D2216, American Society for Testing and Materials, West Conshohocken, Pennsylvania.
- ASTM, 1999, *Standard Specification for Stainless and Heat-Resisting Chromium-Nickel Steel Plate, Sheet, and Strip*, Report No. ASTM A167, American Society for Testing and Materials, West Conshohocken, Pennsylvania.
- ASTM, 2003a, *Standard Specification for Stainless Chromium-Nickel Steel-Clad Plate, Sheet, and Strip*, Report No. ASTM A264, American Society for Testing and Materials, West Conshohocken, Pennsylvania.
- ASTM, 2003b, *Standard Specification for Cold-Formed Welded and Seamless Carbon Steel Structural Tubing in Rounds and Shapes*, Report No. ASTM A500, American Society for Testing and Materials, West Conshohocken, Pennsylvania.
- ASTM, 2003c, *Standard Specification for Carbon and High-Strength Low-Alloy Structural Steel Shapes, Plates, and Bars and Quenched-and-Tempered Alloy Structural Steel Plates for Bridges*, Report No. A709/A709M-03a, American Society for Testing and Materials, West Conshohocken, Pennsylvania.
- ASTM, 2003d, *Standard Specification for Structural Steel Shapes*, Report No. ASTM A992/A992M, American Society for Testing and Materials, West Conshohocken, Pennsylvania.
- ATC/BSSC, 1997, *NEHRP Guidelines for the Seismic Rehabilitation of Buildings*, prepared by the Applied Technology Council for the Building Seismic Safety Council, published by the Federal Emergency Management Agency (FEMA-273 Report), Washington D.C.
- Baez, J.I. and Martin, G.R., 1995, *Permeability and Shear Wave Velocity of Vibro-Replacement Stone Columns, Soil Improvement for Earthquake Hazard Mitigation*, Geotech. Special Pub. No. 49, ASCE 7 66-81.
- Berrill, J. B., Christensen, S. A., Keenan, R. J., Okada, W. and Pettinga, J. R., 1997, "Lateral-spreading Loads on a Piled Bridge Foundation," *Seismic Behavior of Ground and Geotechnical Structures, Proc., Special Technical Session on Earthquake Geotechnical Engineering*, 14<sup>th</sup> ICSMFE, A. A. Balkema, Rotterdam, pp. 173-183.
- BSSC, 1997, *NEHRP Recommended Provisions for Seismic Regulations for New Buildings and Other Structures*, prepared by the Building Seismic Safety Council, published by the Federal Emergency Management Agency (FEMA 302 Report), Washington, D.C.
- BSSC, 2001, 2000 Edition of *NEHRP Recommended Provisions for Seismic Regulations for New Buildings and Other Structures*, prepared by the Building Seismic Safety Council, published by the Federal Emergency Management Agency (FEMA 368 and 369 Reports), Washington, D.C.
- Constantinou, M. C. and Quarshie, J. K., 1998, *Response Modification Factors for Seismically Isolated Bridges*. Technical Report MCEER-98-0014, Multidisciplinary Center for Earthquake Engineering Research, Buffalo, New York.
- Department of Defense, 1976, *Dissimilar Metals*, MIL-STD 889B, Defense Printing Service Detachment Office, Philadelphia, Pennsylvania.
- Egan, J. A., Hayden, R. F., Scheibel, L. L., Otus, M. and Servanti, G.M., 1992, "Seismic Repair at Seventh Street Marine Terminal," *Proceedings of Grouting, Soil Improvement and Geosynthetics*, ASCE Conference, New Orleans, R. H. Borden, R.D. Holtz, and I. Juran (eds), Geotechnical Special Publication No. 30, Vol. 2, pp. 867-878.

- Elgamal, A.W., Dobry, R., Parra, E. and Yang, Z., 1998, "Soil Dilation and Shear Deformations During Liquefaction," *Proceedings of 4<sup>th</sup> Intl. Conf. on Case Histories in Geotechnical Engineering*, S. Prakash (ed.), St. Louis, Missouri.
- Gazettas, G., 1991, "Foundation Vibrations," *Foundation Engineering Handbook*, edited by Fang, H.Y., Van Nostrand Reinhold, New York.
- HITEC, 1996, *Guidelines for the Testing of Seismic Isolation and Energy Dissipation Devices*, CERF Report: HITEC 96-02. Highway Innovative Technology Evaluation Center, Washington, D.C.
- Hoit, M.I. and McVay, M.C., 1996, *FLPIER User's Manual*, University of Florida, Gainesville, Florida.
- ICBO, 1994, *Uniform Building Code: Structural Engineering Design Provisions*, Vol. 2, International Conference of Building Officials, Whittier, California.
- ICBO, 1997, *Uniform Building Code*, International Conference of Building Officials, Whittier, California.
- Ishihara, K. and Cubrinovski, M., 1998, "Problems Associated with Liquefaction and Lateral Spreading During Earthquake," *Geotechnical Earthquake Engineering and Soil Dynamic III*, ASCE, Geotechnical Special Publication, No. 75, Vol. 1, pp. 301-312.
- Jackura, K. A. and Abghari, A., 1994, "Mitigation of Liquefaction Hazards at Three California Bridge Sites," *Proceedings, 5th U.S.-Japan Workshop on Earthquake Resistant Design of Lifeline Facilities and Countermeasures Against Soil Liquefaction*, Technical Report NCEER-94-0026, NCEER, Buffalo, New York, pp. 495-513.
- Kelly, J., 1997, *Earthquake Resistant Design with Rubber*, Earthquake Engineering Research Center, National Information Service for Earthquake Engineering, Springer-Verlag London Limited, 2nd Edition, Richmond, California.
- Mace, N. and Martin, G.R., 2001, *An Investigation of Compaction Grouting for Liquefaction Mitigation*, Technical Report, FHWA Contract No. DTFH61-92-C-00106, Multidisciplinary Center for Earthquake Engineering, Buffalo, New York.
- Martin, G.R., 1989, "Some Observations on the Mechanics of Post-Liquefaction Deformations," *Proceedings of the 2<sup>nd</sup> U.S.-Japan Workshop on Liquefaction, Large Ground Deformation, and their Effects on Lifelines*, NCEER Technical Report NCEER-89-0032, State University of New York, Buffalo, New York and Cornell University, Ithaca, New York.
- Martin, G.R. and Qiu, P., 2001, *Site Liquefaction Evaluation: The Application of Effective Stress Site Response Analyses*, Technical Report, FHWA Contract No. DTFH61-92-C00106, Multidisciplinary Center for Earthquake Engineering Research, Buffalo, New York.
- Mitchell, J. K., Baxter, C. D. P., and Munson, T. C., 1995, "Performance of Improved Ground During Earthquakes," *Soil Improvement for Liquefaction Hazard Mitigation*, Geotech. Special Pub. No. 49, ASCE, 1-36.
- Nakano, O., Nishi, H., Shirono, T., and Kumagai, K., 1992, Temperature-Dependency of Base Isolation Bearings, *Proceedings, Second U.S.-Japan Workshop on Earthquake Protective Systems for Bridges*, Tsukuba, Japan.
- Newmark, N. M. and W. J. Hall, 1982, *Earthquake Spectra and Design*, Earthquake Engineering Research Institute, Oakland, California.
- NPFC, 1999, *Silicone Compound, NATO Code Number S-736*, Report No. MIL-S-8660 (superseded by SAE AS 8660), Naval Publications and Forms Center, Philadelphia, Pennsylvania.
- O'Rourke, T. D., Meyersohn, W. D., Shiba, Y. and Chaudhuri, D., 1994, "Evaluation of Pile Response to Liquefaction-Induced Lateral Spread," *Proceedings, 5th U.S.-Japan Workshop on Earthquake Resistant Design of Lifeline Facilities and Countermeasures Against Soil Liquefaction*, Technical Report NCEER-94-0026, NCEER, Buffalo, New York, pp. 457-478.
- Reaveley and Nordenson, 1992, "Acceptable Damage in Low and Moderate Seismic Zones," *Proceedings, 4th U.S.-Japan Workshop on Improvement of Structural Design and Construction Practices*, ATC-15-3

- Report, Applied Technology Council, Redwood City, California.
- Riemer, M. F., Lok, T. M. and Mitchell, J. K., 1996, "Evaluating Effectiveness of Liquefaction Remediation Measures for Bridges," *Proceedings, 6th U.S.-Japan Workshop on Earthquake Resistant Design of Lifeline Facilities and Countermeasures Against Soil Liquefaction*, Technical Report NCEER-96-0006, NCEER, Buffalo, New York.
- Salgado, R., Boulanger, R. W., and Mitchell, J. V., 1997, "Lateral Stress Effects on CPT Liquefaction Resistance Correlations," *Journal of Geotechnical and Geoenvironmental Engineering*, ASCE.
- Soydemir, C., Zoli, T., LaPlante, K., Kraemer, S., Davidson, W. and McCabe, R., 1997, "Seismic Design of Central Artery Bridges Across Charles River in Boston: Geotechnical/Substructure Aspects," from *NCEER Post Liquefaction ground Deformation Workshop*, University of Southern California, Los Angeles.
- Stanton, J. F. and Roeder, C. W., 1982, *Elastomeric Bearings Design, Construction, and Materials*. National Cooperative Highway Research Program, Report 248, Transportation Research Board Washington, D.C.
- Stanton, J. F., Roeder, C. W., and Campbell, T. I., 1993, *High Load Multi-Rotational Bridge Bearings*, Final Report, National Cooperative Highway Research Program, NCHRP 10-20A, Transportation Research Board, Washington, D.C.
- Stark, T. D. and Mesri, G., 1992, "Undrained Shear Strength of Liquefied Sands for Stability Analyses," *Journal of the Geotechnical Engineering Division*, ASCE, Vol. 118, No. 11, pp. 1727-1747.
- Terzaghi, K., 1955, "Evaluation of Coefficients of Subgrade Reaction," *Geotechnique*, Vol. 5, No. 4, pp. 297-326.
- Wang, S. T. and Reese, L. C., 1998, "Designing Pile Foundations in Liquefied Soils," *Geotechnical Earthquake Engineering and Soil Dynamics III*, ASCE Geotechnical Special Publication, No. 75, Vol. 2, pp. 1331-1343.
- Whalen, T., and E. Simiu, 1998, "Assessment of Wind Load Factors for Hurricane-Prone Regions," *Structural Safety*, No. 20, Elsevier Science Ltd.
- Wilson, D. W., Boulanger, R. W., and Kutter, B. L., 1999, "Lateral Resistance of Piles in Liquefying Sand," *Analysis, Design, Construction, and Testing of Deep Foundation, Proc., Offshore Technology Research Center '99 Conference*, Geotechnical Special Publication No. 88, ASCE, Reston, Virginia, pp. 165-179.
- Xiao, Y., Priestley, M. J. N., Seible, F., and Hamada, N., 1994, *Seismic Assessment and Retrofit of Bridge Footings*, SSRP-94/11, Structural Systems Research, University of California, San Diego, California.

## Acronyms

AASHTO	American Association of State Highway and Transportation Officials	MCE	Maximum Considered Earthquake
ADT	average daily traffic	MCEER	Multidisciplinary Center for Earthquake Engineering Research (MCEER supersedes NCEER)
ADTT	average daily truck traffic	N	number of blows
AISC	American Institute of Steel Construction	NCEER	National Center for Earthquake Engineering Research (superseded by MCEER)
ASTM	American Society for Testing and Materials	NCHRP	National Cooperative Highway Research Program
ATC	Applied Technology Council	NEHRP	National Earthquake Hazard Reduction Program
AWS	American Welding Society	NSF	National Science Foundation
BHT	Becker hammer test	OANR	Owner's Approval Not Required
BSSC	Building Seismic Safety Council	PGA	peak ground acceleration
CDMG	California Division of Mines & Geology	PI	plasticity index
CD-ROM	compact disk, read-only memory	PSHA	probability seismic hazard analysis
CEUS	central and eastern United States	PTFE	polytetrafluoroethylene
CIDH	cast in drilled hole	R-factor	response modification factor
CPT	Core Penetrometer Test	SASW	spectral analysis of surface wave
CQC	complete quadratic combination	SDAP	Seismic Design and Analysis Procedure
CRR	cyclic resistance ratio	SDR	Seismic Detailing Requirement
CSR	cyclic stress ratio	SHL	Seismic Hazard Level
EBF	eccentrically braced frame	SPS	shear panel system
EDC	energy dissipated per cycle	SPT	Standard Penetration Test
EE	Expected Earthquake	SRSS	square root of the sum of the squares
EERI	Earthquake Engineering Research Institute	STU	shock transmission unit
ERE	Earthquake Resisting Element	TADAS	shear triangular plate with added damping and stiffness devices
ERS	Earthquake Resisting System	TSL	type, size, and location (phase)
FHWA	Federal Highway Administration	USCS	Unified Soil Classification System
FS	factor of safety	USGS	U.S. Geological Survey
g	acceleration of gravity	WUS	western United States
HPS	high-performance steel		
HSS	high-strength steel		
IBC	International Building Code		
ICC	International Code Council		
LRFD	Load and Resistance Factor Design		





## PROJECT PARTICIPANTS

### PROJECT MANAGEMENT

Ian Friedland (Principal Investigator)  
Applied Technology Council\*  
1300 Pennsylvania Avenue, NW, Suite 700  
Washington, D.C. 20004

Ronald Mayes (Project Manager)  
Simpson Gumpertz & Heger, Inc.  
The Landmark at One Market Street, Suite 600  
San Francisco, California 94105

### NCHRP MANAGEMENT

David B. Beal (Project Officer)  
Transportation Research Board  
National Research Council  
2101 Constitution Ave. N.W., Room 300  
Washington, DC 20418

### PROJECT ENGINEERING PANEL

Ian Buckle (Co-Chair)  
University of Nevada, Reno  
Civil Engineering Department  
Mail Stop 258  
Reno, Nevada 89557

Paul Liles  
Georgia Department of Transportation  
No. 2 Capitol Square, S.W.  
Atlanta, Georgia 30334

Christopher Rojahn (Co-Chair)  
Applied Technology Council  
201 Redwood Shores Parkway, Suite 240  
Redwood City, California 94065

Brian H. Maroney  
California Dept. of Transportation  
P. O. Box 942874  
Sacramento, California 94274

Serafim Arzoumanidis  
Steinman Boynton Gronquist Birdsall  
110 William Street  
New York, New York 10038

Joseph Nicoletti  
Consulting Structural Engineer  
1185 Chula Vista Drive  
Belmont, California 94002

Mark Capron  
Sverdrup Civil, Inc.  
13723 Riverport Drive  
Maryland Heights, Missouri 63043

Charles Roeder (ATC Board Representative)  
University of Washington  
Department of Civil Engineering  
233B More Hall, FX-10  
Seattle, Washington 98195

Ignatius Po Lam  
Earth Mechanics Inc.  
17660 Newhope Street, Suite E  
Fountain Valley, California 92708

Freider Seible  
University of California at San Diego  
Structural Systems, MC 0085  
La Jolla, California 92093-0085

Theodore Zoli  
HNTB Corporation  
330 Passaic Avenue  
Fairfield, New Jersey 07004

\*Employer during term of NCHRP 12-49 project contract

**CONSULTANTS**

Donald Anderson  
CH2M Hill  
777 108<sup>th</sup> Avenue NE  
Bellevue, Washington 98004

Michel Bruneau  
University at Buffalo  
Multidisciplinary Center for Earthquake  
Engineering Research  
105 Red Jacket Quadrangle  
Buffalo, New York 14260

Gregory Fenves  
University of California at Berkeley  
Civil Engineering Department  
729 Davis Hall, #1710  
Berkeley, California 94720-1710

John Kulicki  
Modjeski & Masters  
4909 Louise Drive  
Mechanicsburg, Pennsylvania 17055

John B. Mander  
University of Canterbury  
Department of Civil Engineering  
Private Bag 4800  
Christchurch 8020 New Zealand

Lee Marsh  
Berger/Abam Engineers, Inc.  
33301 Ninth Avenue South  
Federal Way, Washington 98003

**ATC/MCEER STAFF**

A. Gerald Brady (Technical Editor)  
Applied Technology Council  
201 Redwood Shores Parkway, Suite 240  
Redwood City, California 94065

Peter Mork (Desktop Publishing Services)  
Applied Technology Council  
201 Redwood Shores Parkway, Suite 240  
Redwood City, California 94065

Geoffrey Martin  
University of Southern California  
Civil Engineering Department  
Los Angeles, California 90089

Andrzej Nowak  
University of Michigan  
2340 G.G. Brown Laboratory  
2351 Hayward  
Ann Arbor, Michigan 48109-2125

Richard V. Nutt  
Consulting Structural Engineer  
9048 Hazel Oak Court  
Orangevale, California 95662

Maurice Power  
Geomatrix Consultants, Inc.  
2101 Webster Street, 12<sup>th</sup> Floor  
Oakland, California 94612

Andrei Reinhorn  
University at Buffalo  
Department of Civil Engineering  
231 Ketter Hall  
Buffalo, New York 14260

M. Schwartzbach (Desktop Publishing Services)  
Applied Technology Council  
201 Redwood Shores Parkway, Suite 240  
Redwood City, California 94065

Jane Stoye (Reference Compilation and Review)  
University at Buffalo  
Multidisciplinary Center for Earthquake  
Engineering Research  
105 Red Jacket Quadrangle  
Buffalo, New York 14260



